西北农林科技大学引进人才

聘期考核附件

姓名：吴福勇

所在单位：资源环境学院

填写日期：2018年10月29日

西北农林科技大学党委人才工作部制

荣誉证书

吴福勇教授：

您指导的研究生田凯的学位论文《燃煤电厂周边冬小麦多环芳烃吸收积累特征及其膳食暴露风险评价》被评为 2018 年校级优秀学术型硕士学位论文。

编号：B201814

西北农林科技大学

二〇一八年六月二十日

西北农林科技大学
NORTHWEST A&F UNIVERSITY

荣誉证书

乔圣超 同学：

你的本科毕业论文（设计）《陕西渭河电厂周边农田土壤PAHs分布特征、来源及生态风险评价》被评为我校2017届校级优秀本科毕业论文（设计），特发此证。

西北农林科技大学
教务处
二〇一七年六月

荣誉证书

吴福勇 同志被评为西北农林科技大学2015年度优秀教师。

特发此证。

中共西北农林科技大学委员会
西北农林科技大学
二〇一六年三月一日

发表学术论文情况（限第一作者或通讯作者）

累计以第一作者/通信作者发表SCI文章12篇，中文核心文章5篇，其中中科院二区论文6篇，累计影响影子40.493，单篇他引最高15次。

Science of the Total Environment 649 (2019) 1269–1280

Contents lists available at ScienceDirect

Science of the Total Environment

journal homepage: www.elsevier.com/locate/scitotenv

Mass balance-based inventory of heavy metals inputs to and outputs from agricultural soils in Zhejiang Province, China

Taoran Shi [a,b,c], Jin Ma [b,*], Fuyong Wu [a,c,**], Tienan Ju [b], Yiwei Gong [b], Yunyun Zhang [b], Xiao Wu [b], Hong Hou [b], Long Zhao [b], Huading Shi [b]

[a] *College of Natural Resources and Environment, Northwest A&F University, Yangling 712100, China*
[b] *State Key Laboratory of Environmental Criteria and Risk Assessment, Chinese Research Academy of Environmental Sciences, Beijing 100012, China*
[c] *Key Laboratory of Plant Nutrition and the Agri-environment in Northwest China, Ministry of Agriculture, Yangling 712100, China*

HIGHLIGHTS

- Input and output inventory of heavy metals in agroecosystem of Zhejiang was studied.
- There were great variations of inventory in different regions of Zhejiang.
- Atmospheric deposition and livestock manures were the major sources of heavy metals.
- Crop harvesting and leaching were the main output pathways of heavy metals.
- Cd was suggested to be the priority pollutant.

GRAPHICAL ABSTRACT

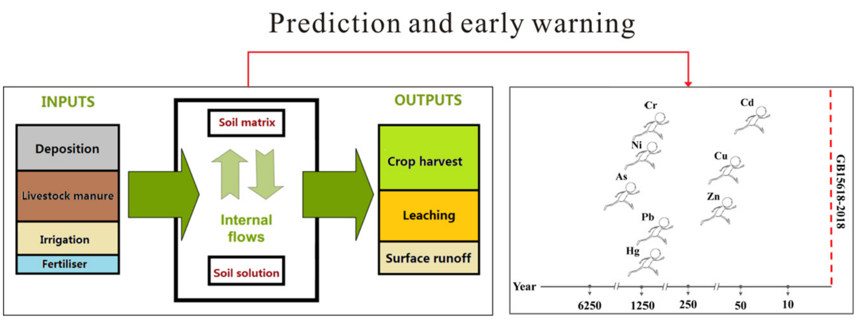

ARTICLE INFO

Article history:
Received 12 June 2018
Received in revised form 28 August 2018
Accepted 29 August 2018
Available online 30 August 2018

Editor: Xinbin Feng

Keywords:
Input and output
Inventory
Heavy metals
Agricultural soil
Zhejiang Province
Prediction and early warning

ABSTRACT

It is important to understand the status and extent of soil contamination with heavy metals to make sustainable management strategies for agricultural soils. Input and output inventory of heavy metals in agricultural soil of Zhejiang Province was systematically studied. The results showed that atmospheric deposition was responsible for 47.88% and 76.87% of the total Cr and Pb inputs, respectively. Livestock manures accounted for approximately 54–85% of the total As, Cu, and Zn inputs. Livestock manure and irrigation were the main sources of Hg, contributed 50.25% and 38.63% of the total inputs, respectively. Ni was derived mainly from atmospheric deposition (57.86%), followed by irrigation (22.69%). As for Cd, the relative contributions of atmospheric deposition, irrigation, and livestock manure were similar. Crop harvesting and leaching were found to be the dominant output pathways of the soil elements Cd, Cu, Hg, and Zn, being responsible for 74.43–83.62% of the total outputs. Surface runoff was the dominant output pathway for As, Cr, Ni, and Pb, accounting for approximately 73.36%, 46.32%, 54.16%, and 48.11% of the total outputs, respectively. According to prediction and early warning, Cd is the priority control pollutant in agricultural soil. This work will assist in developing strategies for reducing heavy metal inputs to agricultural soil and effectively targeting policies to protect soil environment from long-term heavy metal accumulation.

---

[*] Corresponding author.
[**] Correspondence to: F. Wu, College of Natural Resources and Environment, Northwest A&F University, Yangling 712100, China.
E-mail addresses: majin@craes.org.cn (J. Ma), wfy09@163.com (F. Wu).

https://doi.org/10.1016/j.scitotenv.2018.08.414

1. Introduction

Heavy metal contamination of agricultural soil is one of the most pressing environmental concerns worldwide, especially in developing countries such as China (Niu et al., 2013). Such contamination impairs soil function and also threatens the health of the ecosystem and humans (Liu et al., 2006). Heavy metal contamination in soil of the Yangtze River Delta (YRD), one of the most developed regions in China, is much severe. According to the first National Soil Pollution Survey of China, 15% of the agricultural soil in the YRD region is polluted by heavy metals, and pollution is especially severe at the junction of Zhejiang Province, Shanghai City, and Jiangsu Province (Ministry of Environmental Protection, Ministry of Land and Resources of the People's Republic of China, 2014). Lead poisoning incidents in Taizhou and Huzhou in Zhejiang Province in 2011 garnered headlines of local and national media and elicited considerable concern from the public (Shen et al., 2010). Some works has been carried out to evaluate the soil contamination by heavy metals in Zhejiang Province, however, the results were too general to inform specific mitigation measures. Further comprehensive and systematic study is urgently required to identify the biogeochemical cycles of heavy metals in Zhejiang Province. The input and output inventory has been proved to be an effective method for studying heavy metal pollution (Shi et al., 2018). It can be used to accurately assess potential pollution sources and sinks and their contributions. Based on a mass balance model, an inventory can provide a good estimation of the accumulation or depletion of certain elements in selected agroecosystems. To date, studies on heavy metal input and output inventory in China are very limited. Only Hainan Province, Heilongjiang Province, Hunan Province, Tianjin City, the Pearl River Delta region, and Nanjing City have developed inventories to assess the heavy metal balance in agricultural soils (Jiang et al., 2014; Xia et al., 2014; Hou et al., 2013; Zhou et al., 2012; Hu et al., 2013; Yi et al., 2018). In addition, previous studies did not fully address all of the primary input and output pathways when developing their inventories. For example, the impacts of livestock manure on the heavy metal balance in soil at the regional scale were not considered in studies of Hainan and Heilongjiang Province (Jiang et al., 2014; Xia et al., 2014); exportation of heavy metals through leaching and surface runoff was not considered in study of Tianjin City (Hou et al., 2013); loss of heavy metals through leaching was not taken into account in study of Hainan Province (Jiang et al., 2014). It should be noted that, input and output fluxes could be artificially magnified or reduced when the major pathways were not considered overall. In addition, there have been few prediction and early warning of long-term accumulation of heavy metals based on the threshold. This study is the first to systematically assess heavy metal inputs to and outputs from agricultural soils at the provincial scale in Zhejiang Province.

The objectives of this study were to (1) measure soil heavy metal input and output fluxes, (2) determine the dominant soil heavy metal input and output pathways, and (3) perform prediction and early warning forecasting pertaining to the geochemical accumulation of soil heavy metals. This work will help to assess, and inform efforts toward balancing heavy metal inputs and outputs in Zhejiang Province, and would also provide useful guidance for other polluted regions.

2. Materials and methods

2.1. Study area

Zhejiang Province is located in the southern region of the YRD, China (30.5–31.5° N, 120–121°E). It has a continental area of 0.158 billion ha and a cultivated land area of 29.65 million ha, accounting for one-fifth of the total land area of the province. The annual average precipitation is about 2000 mm. As shown in Figs. 1, 81.5% of the total area is farmland, consisting of garden plots (5.5%), forest land (53.5%), grassland (3.8%), and arable land (18.7%), respectively.

2.2. Methods

In the present study, there were four major input pathways of heavy metals, namely total atmospheric deposition, fertilizer application, irrigation water, and livestock manure. Crop harvesting, surface runoff, and leaching water were selected as the three output pathways. Samples collection and chemical analysis as well as data collection were conducted to figure out the heavy metal balance in the agricultural soil of Zhejiang Province. Five typical areas of Zhejiang Province (eastern, western, southern, northern, and central regions) were selected to represent different developmental level and model. Hence, we can distinguish the potential differences in input and output inventory of heavy metals among different areas.

The sampling locations for irrigation water, leaching water, and surface runoff are shown in Fig. 1.

2.3. Sample processing and analysis

2.3.1. Atmospheric deposition

Soil heavy metal input flux data regarding atmospheric deposition (both wet and dry deposition) were collected from Hou et al. (2014).

2.3.2. Fertilizers

Data on the annual consumption of compound fertilizers and their heavy metal concentrations were also collected from literatures (Table 1). The soil input flux of element *i* from fertilization ($Q_{F,i}$) (in mg/m^2/y) was calculated using the following equation:

$$Q_{F,i} = \sum_{j=1}^{n} \left(C_{i,j} \times q_j \right)$$

where $C_{i,j}$ is the analyzed concentration of element *i* in the fertilizer category *j* (mg/kg), q_j is the annual application amount for fertilizer category *j* (kiloton), and n is the number of fertilizer categories at a given sampling point.

2.3.3. Irrigation water

Irrigation water samples were gathered at five sites, as shown in Fig. 1. At each sampling station, five sub-samples were gathered and then mixed together to obtain a representative sample. The irrigation water samples were collected into 500 mL high-density polyethylene (HDPE) bottles with plug screws. The soil input flux of element *i* from irrigation ($Q_{I,i}$) (in mg/m^2/y) was calculated using the following equation:

$$Q_{I,i} = \sum_{j=1}^{n} (C_{i,j} \times W_j)$$

where $C_{i,j}$ is the analyzed concentration of element *i* in the irrigation water of crop *j* (μg/L), W_j is the irrigation consumption of crop *j* (m^3/y), and n is the number of crop categories at a given sampling point.

2.3.4. Livestock manure

Livestock manure, the most commonly used organic waste, is applied either in raw or composted form (i.e., humification under controlled conditions). The soil input flux of element *i* from livestock manure ($Q_{M,i}$) (in mg/m^2/y) was calculated using the following equation:

$$Q_{M,i} = \sum_{i=1}^{3} C_{i,j} \times W \times R_i \times a_i \times (1-w) \times f/T$$

where $C_{i,j}$ is the concentration of element *i* in livestock manure (mg/kg), W is the livestock breeding stock (number), R_i is the amount of manure excreted by livestock (kg/a), a_i is manure utilization (%), w is manure

Fig. 1. Sampling locations of irrigation water, leaching water, surface runoff of agro-ecosystems in Zhejiang Province, China.

moisture (%), f is the heavy metal load of livestock manure (%), and T is the area of cropland (khm^2).

2.3.5. Crop harvest

According to our investigation, cereal and rape are the dominant crops in Zhejiang Province. We collected data on the heavy metal concentrations of cereal and rape and then estimated the heavy metal fluxes of their harvest. The sum of the heavy metal concentrations in canola seed, shoot, and root was taken as the concentration in canola.

Table 1

Average concentrations of heavy metals in fertilizer (mg/kg) (Zhou et al., 2007) and consumption of fertilizers (kiloton) in different areas of Zhejiang Province.

Area	As	Cd	Cr	Cu	Hg	Ni	Pb	Zn	Consumption of fertilizers
Taizhou	3.07	0.23	29.77	8.48	0.172	5.02	3.22	28.55	2.664
Quzhou	3.851	0.26	27.07	4.16	0.114	3.05	2.92	58.56	1.704
Lishui	3.318	0.12	7.7	7.34	0.074	3.38	2.07	21.1	1.811
Huzhou	3.032	0.16	20.71	4.67	0.089	2.07	2.42	213.9	1.213
Jinhua	3.318	0.12	7.7	7.34	0.074	3.38	2.07	21.1	3.141

The soil output flux of element *i* ($Q_{C,i}$) (in mg/m^2/y) from the crop harvest was calculated using the following equation:

$$Q_{C,i} = \sum_{j=1}^{n} (C_{i,j} \times Y_j / S_j)$$

where $C_{i,j}$ is the concentration of element *i* in the crop *j* (mg/kg), Y_j is the annual output of crop *j* (t/y), n is the number of crop categories at a sampling point, and S_j is the sown area of crop *j* (khm^2).

2.3.6. Leaching water

Samples of leaching water were gathered at five sites, as shown in Fig. 1. At each sampling station, five sub-samples were collected and mixed together to obtain a representative sample. MacroRhizon devices for collecting soil leaching water samples were buried in the soil beneath the plow layer (20 cm deep) for two months, from June to July of 2017. The volume of the leaching water was measured and the water was subsequently used for heavy metal analysis. The soil output flux of element i ($Q_{L,i}$) (in mg/m^2/y) from soil leaching water was calculated using the following equation:

$$Q_{L,i} = V_s / A_s \times C_i \times P_h / P_2$$

where V_s is the volume of the leaching water (L), A_s is the mouth area of the device (mm^2), C_i denotes the concentration of element *i* in the leaching water sample (μg/L), and P_2 and P_h denote the precipitation of the sampling point during June–July and during the whole year (2017), respectively (mm). The two precipitation parameters were used to extrapolate the flux for the 2-month period to that of the whole year.

2.3.7. Surface runoff

Surface runoff samples were gathered at five sites, as shown in Fig. 1. At each sampling station, five sub-samples were gathered and mixed together to obtain a representative sample. The samples were collected directly into 500 mL polyethylene plastic bottles with plug screws after rainfall. The soil output flux of element *i* ($Q_{S,i}$) (in $mg/m^2/y$) from surface runoff was calculated using the following equation:

$$Q_{S,i} = C_i \times I_j \times (1 - w)$$

where C_i is the concentration of element *i* in the surface runoff sample (μg/L), I_j is the irrigation quota of the representative crop (m^3/hm^2), and w is the water consumption rate (%). Irrigation water consumption was not measured directly, and the data was collected from statistical yearbook of Zhejiang Province (http://www.zjagri.gov.cn/programs/database).

Water samples, including irrigation water, leaching water, and surface runoff water, were filtered through a 0.45 μm filter membrane and analyzed by inductively coupled plasma-mass spectrometry (ICP-MS) (Agilent 7500a; Agilent, Santa Clara, CA, USA) to quantify target heavy metals.

2.4. Quality control

Three repetitions were performed for each sample, and the relative errors were confined to <10%. The precision and accuracy of the analyses were ensured by inspection of the national standard reference GBW08603 and GBW08608 with the recoveries between 65 and 107%; all samples met the quality requirements.

2.5. Data manipulation

Basic data processing and analysis were performed using SPSS software (ver. 13.0; SPSS Inc., Chicago, IL, USA). Spatial analysis and cartography were performed using ArcGIS software (ver. 10.1; ESRI, Redlands, CA, USA).

3. Results and discussion

3.1. Inventory of heavy metal inputs

3.1.1. Atmospheric deposition

Input fluxes of heavy metals from atmospheric deposition to soil in the five representative areas of Zhejiang are shown in Fig. 2a. The highest input flux from atmospheric deposition was seen for Zn, followed by Pb, Cr, and Cu. The input flux from atmospheric deposition of Zn in Taizhou (272.9 $mg/m^2/y$) was significantly higher than that in the other regions and also exceeded the national average (64.7 $mg/m^2/y$) (Luo et al., 2009). The relatively higher flux of Zn in Taizhou might be attributable to the presence of an electronic and electric waste recycling industry (Zhou and Xu, 2012). Since the 1990s, large amounts of electronic and electric waste have been dismantled in Taizhou, which is a well-known electronic and electric waste recycling centre in China (Tang et al., 2010). Contamination by Pb is probably due to exhaust emissions from vehicles and the metal smelting industry (Han et al., 2018). Although phase-out of leaded gasoline started in the 1990s in China, and then spread nationwide in 2000 (Cai et al., 2017), Pb levels in the atmosphere remained high because it is the main element, along with Zn, produced by mining (Cui and Du, 2011). The input fluxes of heavy metals in Taizhou and Huzhou were higher than those in Quzhou, Lishui and Jinhua. Input fluxes varied greatly among the different regions, which may be related to the differences in industrial and agricultural production, as well as in atmospheric conditions. For example, Engine exhaust, biomass burning, kitchen emissions and e-waste dismantling activities were important emission sources in Taizhou (Gu et al., 2010). Enrichment of heavy metals in Huzhou can be attributed to excessive use of nitrogen and phosphorus fertilizers, as well as surface irrigation and natural soil formation (Chen et al., 2015).

Compared with atmospheric deposition in other regions in China, based on our data (Table 2), the annual deposition fluxes of Cu and Pb were below the 25th percentile, while that of Ni was near the 25th percentile; As and Cd fluxes were within the 25th–50th percentile, that of Hg was around the 50th percentile, and those of Cr and Zn were within the 50th–75th percentile. The heavy metal inputs from atmospheric deposition were highly variable among different regions in China, which is probably indicative of local differences in conditions and amounts released into the atmosphere (Wang et al., 2017). According to SEPAC (2006), the most important sources of heavy metals in atmosphere mainly included electric power, non-metal minerals related plants, black metal smelters, and chemical plants. Actually, most of the industries mentioned above are closely related to coal combustion. Northern China is subject to large quantities of emissions.

3.1.2. Fertilization

The soil input fluxes of heavy metals from fertilization in the five representative areas of Zhejiang are shown in Fig. 2b. Heavy metal inputs to agricultural soils via fertilizers in Zhejiang Province (mean values of the five representative areas) followed the decreasing order of Zn > Cr > Cu > Ni > As > Pb > Cd > Hg. The input fluxes of heavy metals through fertilizer application varied greatly among the different regions. The Cr flux in Taizhou was higher than that in the other regions, as were the Zn fluxes in Huzhou and Taizhou versus the other regions. The heavy metal contents of the fertilizers varied greatly among regions, which can be explained by the fact that the fertilizers applied in the different regions were probably derived from different habitats or species (Liu et al., 2012). According to our analysis, the Zn concentration in the fertilizer collected from Huzhou was much higher than that in the fertilizer gathered from the other regions (Table 1). Chen et al. (2015) also found that phosphate fertilizers were the major source of Zn contamination in the agricultural soils of Huzhou. Moreover, nutrient elements in soil are distributed unequally in Zhejiang Province (Huang et al., 2013). Therefore, the amount of fertilizer that needs to be applied to agricultural soil varies among regions in Zhejiang Province. For example, the highest Zn fluxes, which were observed in Taizhou, may be due to high fertilizer application amounts per unit area, according to the statistical yearbook data for Zhejiang Province.

3.1.3. Irrigation water

The average heavy metal concentrations in irrigation water, and the annual irrigation consumption amounts, are listed in Table 3. The soil input fluxes of heavy metals from irrigation in the five representative areas of Zhejiang are shown in Fig. 2c. The input fluxes were highest for Zn in all five regions. There was also significant spatial variation in heavy metal input fluxes from irrigation water (in decreasing order of Taizhou > Lishui > Quzhou > Jinhua > Huzhou). The soil input fluxes from irrigation water in this study were compared with those from other regions in China (Table 4). The irrigation fluxes of most heavy metals in Zhejiang were higher than the national average level (Luo et al., 2009). The Cd input (0.225 $mg/m^2/y$) was approximately one order of magnitude higher than the national average level (0.02 $mg/m^2/y$) (Luo et al., 2009), being ranked behind only the Pearl River Delta (0.37 $mg/m^2/y$) (Zhou et al., 2012) and Hunan Province (0.255 $mg/m^2/y$) (Yi et al., 2018). Our results are in agreement with a

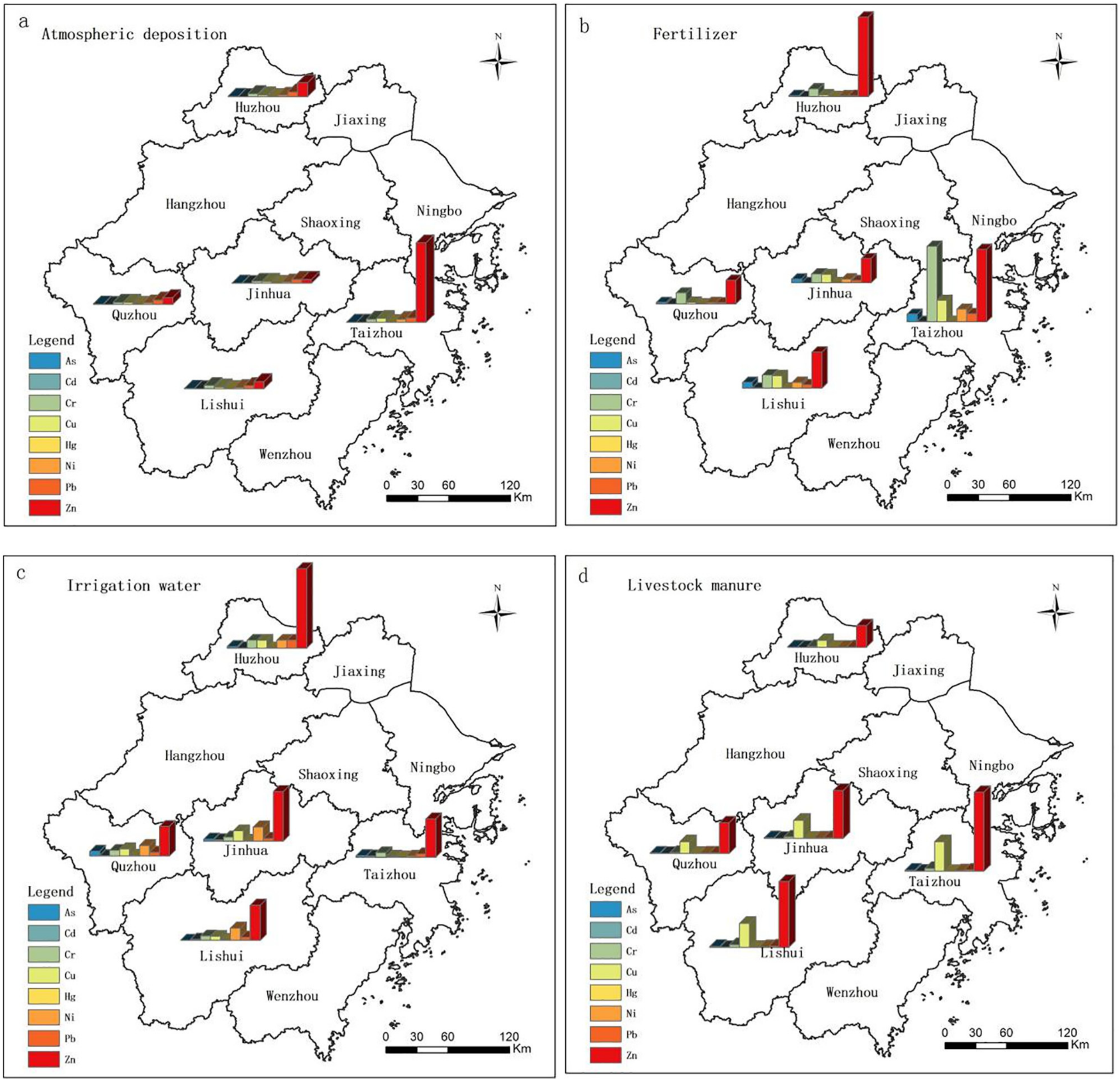

Fig. 2. Soil input fluxes (mg/m^2/y) of heavy metals from atmospheric deposition (a), fertilizer (b), irrigation (c) and livestock manure (d) in five typical areas of Zhejiang Province.

previous report stating that Cd contamination was greatest in farmland soils in central, southwestern, and eastern China (Niu et al., 2013). It has been suggested that sewage irrigation may have contributed to the Cd contamination in Zhejiang Province (Liu et al., 2006).

3.1.4. Livestock manure

In this research, the concentrations of heavy metals in livestock (pig, cattle, and sheep) manures were collected and listed in Table 5. The soil input fluxes of heavy metals from livestock manure in the five

Table 2
Comparison of atmospheric deposition fluxes of heavy metals (mg/m^2/y) among Zhejiang and other regions in China.

Location	As	Cd	Cr	Cu	Hg	Ni	Pb	Zn	Reference
Zhejiang	1.076	0.244	9.425	7.893	0.02	6.091	14.14	76.45	This study
Beijing	4.49	0.475	6.295	15.95	/	6.965	20.65	76.25	Pan and Wang, 2015
Hebei	4.73	0.665	7.855	20.85	/	6.26	31.5	115.7	
Tianjin	4.32	0.53	10.99	16.1	/	12.42	34.2	176.1	
Hainan	0.61	0.091	4.5	6.9	0.015	/	16	29	Jiang et al., 2014
Heilongjiang	4.61	0.36	20.33	16.93	0.03	/	19.18	96.52	Xia et al., 2014
Hunan	9.95	1.665	5.351	/	0.015	/	18.24	/	Yi et al., 2018
Pearl River Delta	/	0.07	6.43	18.6	/	/	12.7	104	Wong et al., 2003
Yangtze River Delta	0.95	0.266	11.19	7.72	0.019	/	15.51	68.22	Hou et al., 2014
Shanghai	0.91	0.175	9.568	8.45	0.02	/	12.46	39.07	
China	2.8	0.4	6.1	10.8	0.14	5.8	20.2	64.7	Luo et al., 2009

Table 3
Average heavy metal concentrations in irrigation water samples (μg/L) and annual irrigation consumption (m^3/m^2).

Area	As	Cd	Cr	Cu	Hg	Ni	Pb	Zn	Irrigation consumption
Taizhou	2.545	0.09	0.5	11.8	0.038	0.3	2.7	12.2	0.91
Quzhou	3.02	0.186	5.714	6.55	0.108	2.529	4.045	32.84	0.795
Lishui	1.78	0.104	5.841	2.76	0.015	0.914	3.67	38.61	0.835
Huzhou	0.4	0.1	2	2	0.05	2	2	20	1.038
Jinhua	3.02	0.186	5.714	3.55	0.019	2.529	3.35	32.84	1.008

Table 4
Comparison of irrigation fluxes of metals ($mg/m^2/y$) among Zhejiang and other regions in China.

Location	As	Cd	Cr	Cu	Hg	Ni	Pb	Zn	Reference
Zhejiang	0.511	0.225	1.368	1.57	0.136	2.389	1.075	12.11	This study
Hainan	47	0.11	7	3.6	2.99	/	0.03	7.1	Jiang et al., 2014
Heilongjiang	0.03	<0.01	0.126	<0.5	0.0006	0.02	<0.1	<0.5	Xia et al., 2014
Hunan	0.43	0.255	0.189	/	0.002	/	0.214	/	Yi et al., 2018
Pearl River Delta	2	0.37	13.21	25.92	0.03	10.44	6.44	206.7	Zhou et al., 2012
China	0.18	0.02	0.04	1.21	0.001	0.19	0.15	3.6	Luo et al., 2009

representative areas of Zhejiang Province are shown in Fig. 2d. Among the various types of livestock manure, we only collected data on pig, sheep, and cattle manures for the shortness of data. Taizhou and Lishui had larger heavy metal inputs than the other three regions due to large-size livestock farming and less arable land for recycling animal manure. The input fluxes of Cu and Zn from livestock manure were higher than those of the other heavy metals in all five representative areas, as shown in Table 5. The most important factor influencing heavy metal inputs was the heavy metal concentration of the input material. The mean concentrations of Cu and Zn in organic fertilizer are significantly higher than those in inorganic fertilizer (Qian et al., 2016), resulting in a high total heavy metal input from organic fertilizer. Commercial feeds are often enriched with essential elements, such as Cu and Zn, to promote optimum growth and confer antimicrobial properties (Wang et al., 2013). Previous research has shown that higher mean concentrations of exchangeable Cu and Zn are found in soils fortified with organic fertilizers (Xu and Zhang, 2017). Due to the potential hazards and accumulated characteristics of Cu and Zn in agricultural land, livestock manures must be applied with great caution, and it is necessary to adhere strictly to the limits on heavy metal levels in fertilizers used in China, to protect soils from heavy metal accumulation via this major source.

3.1.5. Relative contributions to heavy metal amounts of the different input pathways

As mentioned above, there were multiple heavy metal input pathways to soil in the study area. However, the contributions of these input pathways differed to different element, as shown in Fig. 3. Cr and Pb were derived mainly from atmospheric deposition, followed by livestock manure, although manure is the main source in countries with less industrial activity, such as France (Belon et al., 2012). In contrast, As, Cu, and Zn were mainly derived from livestock manure, followed by atmospheric deposition. Previous research has shown that high Cu concentrations in agricultural soil come from Cu-based agrochemicals related to specific agronomic practices in Hangzhou (Chen et al., 2009). Zn was associated with total P in vegetable soil of Hangzhou, which was closely related with fertilizer applications (Chen et al., 2009). Hg imported mainly from livestock manure (average 50.25%) and irrigation (average 38.63%). Ni was derived mainly from atmospheric deposition, followed by irrigation. For Cd, approximately 34% of the input was from atmospheric deposition, while 31% was from irrigation and 31% from livestock manure. Atmospheric deposition of Cd originated from coal combustion is recognized as the major factor for the increasing trend of Cd in the agricultural soil in Zhejiang Province (Shao et al., 2016).

The relative contributions of the various input pathways varied greatly among the different regions. Atmospheric deposition accounted for a higher proportion of the input flux of As in Huzhou, while livestock manure was the main pathway for this element in the other four areas, and for the province as a whole. The high value spots of heavy metal in Huzhou are associated with the discharge of industrial sewage and the dropping in atmosphere (Liu et al., 2006). Overall, atmospheric deposition and livestock manure were the dominant sources of agricultural soil heavy metals in the five representative regions of Zhejiang Province, and for the province as a whole. This is consistent with Heilongjiang and Hunan Province, in which atmospheric deposition was shown to be the dominant source of agricultural soil heavy metals (Xia et al., 2014; Yi et al., 2018). In addition, atmospheric deposition and livestock manure are the predominant sources of heavy metals in agricultural soils for China as a whole (Luo et al., 2009). It should be noted that there are marked differences in input pathways among the different regions of China. For example, irrigation water was found to be the most important heavy metal input pathway to soil on the island of Hainan (Jiang et al., 2014). In Hainan Island, the emissions of sanitary sewage and industrial wastewater are identified as the main sources of heavy metals in irrigation water (Jiang et al., 2014). Furthermore, it may be that at the large regional scale, atmospheric deposition has been identified as the principal source of metals entering soils, whereas fertilizer or irrigation is more significant in some local regions (Huang et al., 2015).

3.2. Inventory of heavy metal outputs

3.2.1. Crop harvesting

The parameters used to inform the calculation of soil output fluxes of heavy metals from crop harvesting are listed in Table 6. Soil-to-plant transfer of heavy metals is the major pathway of human exposure to contaminated soil. The output fluxes of elements associated with

Table 5
Average heavy metal concentrations in livestock manure samples (mg/kg) (Qin et al., 2015).

Livestock manure	As	Cd	Cr	Cu	Hg	Ni	Pb	Zn	Emission factor	Moisture content	Pollution load	Utilization
Pig manure	21.58	1.735	37.06	514.7	0.48	9.77	19.79	1313	398	0.72	0.3	0.625
Cattle manure	5.56	0.63	21.27	114.9	0.48	4.19	12.47	337.4	7300	0.763	0.3	0.625
Sheep manure	0.59	0.28	22.19	22.66	2.39	4.46	1.74	215.4	950	0.75	0.3	0.75

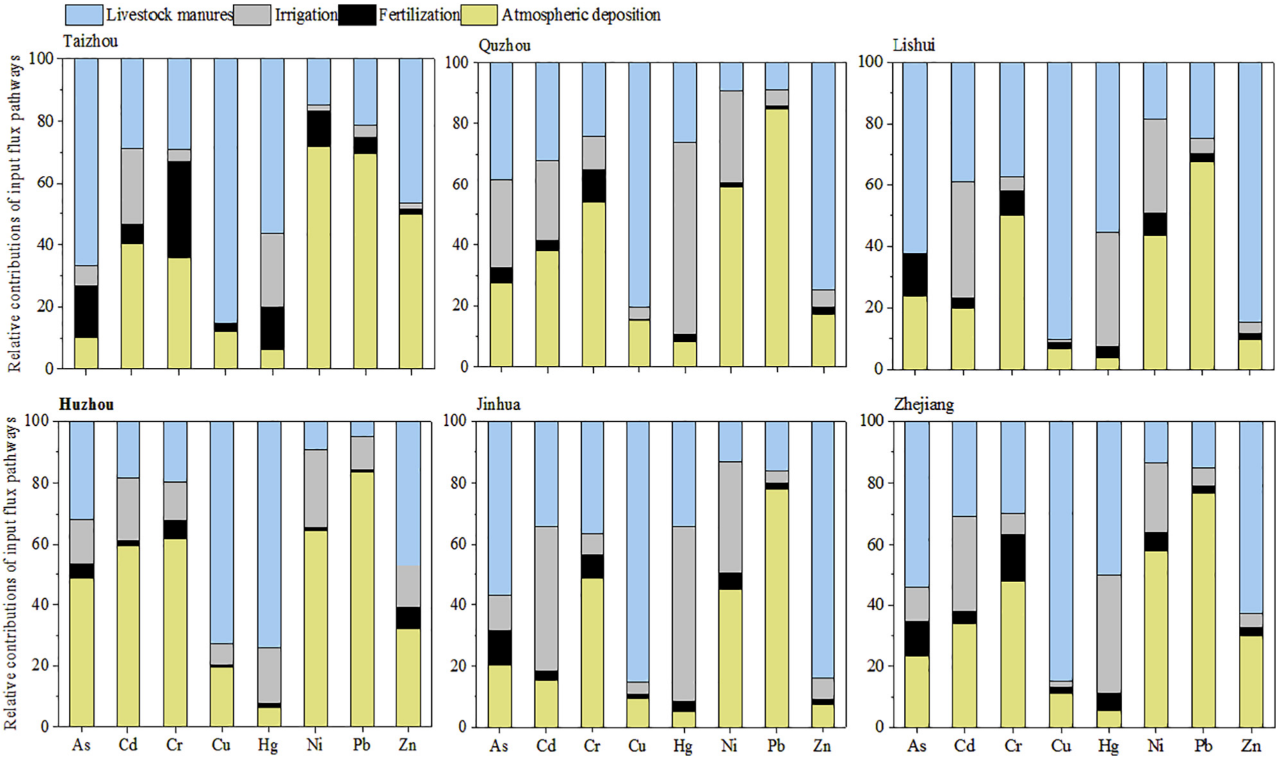

Fig. 3. Relative contributions (%) of different input flux pathways of heavy metals in Zhejiang Province.

harvesting of the dominant plants (cereal and canola) in the study area are shown in Fig. 4a. The output fluxes of Cu and Zn associated with crop harvesting were much higher than those of the other heavy metals, which may be attributed to their high concentrations in crops (Table 6). Heavy metal transfer from soil to plants is largely dependent on plant species, soil organic matter, and soil pH (Ye et al., 2015). Due to limited data, in this study crop harvesting fluxes were calculated under the assumption that there was no variation in As or Hg concentration among the five representative areas of Zhejiang Province (Table 6). Following this assumption, the output flux in an individual area was largely dependent on the crop yields and sown area. Despite our best efforts to collect all necessary data, uncertainties still existed in the estimations of the output fluxes associated with crop harvesting. The effects of crop harvesting include only two representative plants, with the effects of other crop rotations not taken into account. The paucity of data on crop harvesting is the main source of estimation uncertainty.

3.2.2. Leaching water

It has been suggested that heavy metals can accumulate in soil and then dissolve into groundwater via leaching, resulting in contamination of both groundwater and surface water (Bonten et al., 2008). Table 7 shows the heavy metal concentrations in leaching water in this study.

In this study, the fluxes of the elements derived from soil leaching water were calculated, and the results are shown in Fig. 4b. Among the five representative areas, the average Zn output due to leaching was largest in Taizhou. This might be attributed to the high soil Zn concentrations in Taizhou and different values of soil pH (Li et al., 2014). Large amounts of Pb/Zn mine tailings lied in Sanmen County, Taizhou (Li et al., 2011), but at the same time brought the improper treatment of waste emissions. Moreover, the average Zn output due to leaching was the second largest in Huzhou and Quzhou. It could be attributed to intensive agriculture activity (3895 km^2 area used for agriculture in total of 5815 km^2) in Huzhou (Chen et al., 2015) and industrial pollutants emitted from 921 heavy industries in total of 1407 in Quzhou (Zhang et al., 2017). The output flux via soil leaching water found in this study was much lower than that reported in Heilongjiang (Xia et al., 2014). It has also been shown that the leaching of certain heavy metals is largely dependent on pH, with mobility being higher at lower pH and lower when the pH is neutral to slightly alkaline (Zou et al., 2015). Leaching fluxes are based either on model calculations using sorption models and site-specific soil properties, or on measured or estimated dissolved metal concentrations (Cambier et al., 2014). Therefore, heavy metal output inventories are not only related to the concentrations of heavy metals in soil, but also to the methods used for flux assessment.

Table 6
Heavy metal content in cereal and rape stems (mg/kg).

Area	Crop category	As	Cd	Cr	Cu	Hg	Ni	Pb	Zn	Reference
Taizhou	Cereal	0.08	0.008	0.436	2.256	0.005	0.223	0.02	24.77	Cheng et al., 2007
Quzhou		0.08	0.055	0.374	2.633	0.005	0.223	0.145	25.09	Li et al., 2014
Lishui		0.08	0.072	0.158	3.09	0.005	0.221	0.06	20.69	Cao et al., 2014
Huzhou		0.08	0.008	0.482	2.332	0.005	0.125	0.024	22.73	
Jinhua		0.08	0.092	0.078	2.98	0.005	0.353	0.06	22.41	
Zhejiang	Canola seed	0.003	0.047	0.379	5.52	0.003	1.78	0.142	53.8	Yu et al., 2012
	Canola shoot	0.13	0.168	0.483	8.87	0.021	0.76	0.416	45.67	
	Canola root	0.334	0.31	2.2	20.69	0.019	2.37	1.45	70.15	

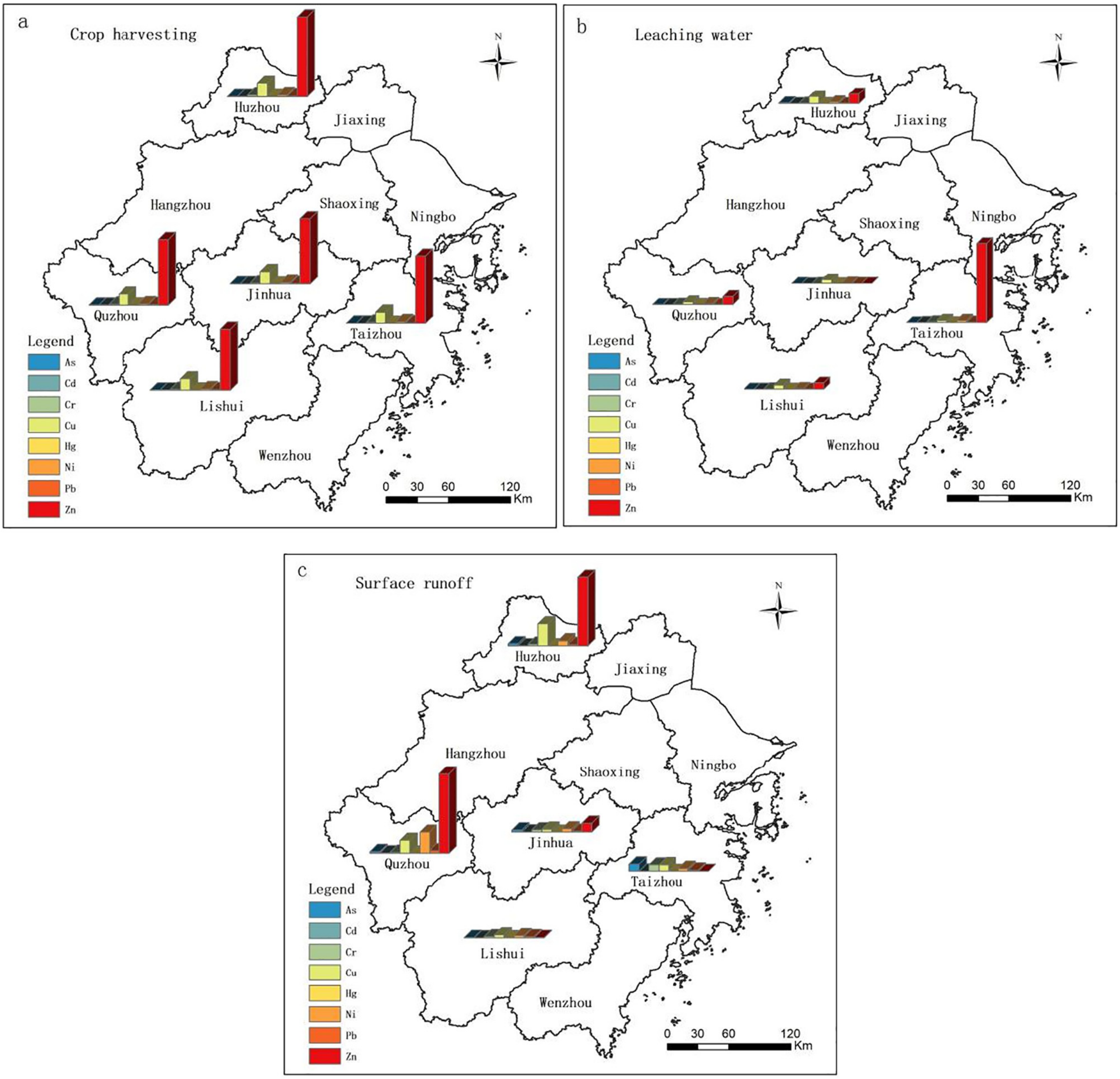

Fig. 4. Soil output fluxes (mg/m^2/y) of heavy metals from crop harvesting (a), leaching water (b) and surface runoff (c) in five typical areas in Zhejiang Province.

3.2.3. Surface runoff

Soil elements are released from a thin layer of surface soil that interacts with rainfall and runoff water. Table 8 lists the heavy metal concentrations in surface runoff, and the output fluxes of heavy metals in each region are shown in Fig. 4c. The output fluxes of Cu, Zn, and Ni from surface water runoff in Huzhou and Quzhou were relatively large. The output flux for surface runoff in Lishui was relatively small compared to those in other regions. The soil OM in Huzhou (0.597%) is the lowest, the pH values of the soil in Quzhou (5.0) is the lowest among all cities in Zhejiang according our research (Unpublished data). Dowdy and Volk (1983) suggested that the movement of heavy metals in soils could occur in sandy, acid, low organic matter soil if subjected to heavy rainfall or irrigation. Heavy metal loss through surface runoff is a very complex process, being controlled by heavy metal concentrations

Table 7
Heavy metal concentrations in leaching water (μg/L).

Area	As	Cd	Cr	Cu	Hg	Ni	Pb	Zn
Taizhou	0.012	0.6	2.213	5.428	0	5.226	1.3	196.2
Quzhou	1.393	0.5806	1.629	18.06	27.53	6.201	0.891	52.03
Lishui	0.404	0.101	1.482	16.06	74.06	2.812	0.955	25.15
Huzhou	3.037	0.128	1.891	26.95	76.74	7.155	0.893	37.29
Jinhua	0.322	0.043	1.325	23.79	1.093	2.83	0.838	1.261

Table 8
Heavy metal concentrations in surface runoff water (μg/L).

Area	As	Cd	Cr	Cu	Hg	Ni	Pb	Zn
Taizhou	7.328	0.188	6.533	6.757	240.6	2.925	1.248	0
Quzhou	1.989	3.224	1.131	14.96	58.79	24.36	2.999	92.02
Lishui	0.399	0.146	1.457	3.252	145.5	2.551	1.413	0.438
Huzhou	1.907	0.113	1.459	19.58	58.25	4.505	1.26	60.76
Jinhua	2.073	0.132	2.149	2.591	47.56	3.069	0.884	8.159

in rain, rainfall intensity and other factors (Elrashidi et al., 2007). Higher rainfall intensity can result in a decrease in total concentrations of heavy metals. The Cd, Cu, Ni, Pb, and Zn losses due to runoff in Nebraska, USA were 0.061, 5.2, 2.13, 0.140, and 3.74 mg/m^2/y, respectively (Elrashidi et al., 2007). With the exception of Cu, the output fluxes by soil runoff in this study area were higher than those reported for Nebraska. At present the large differences in output fluxes from surface water runoff in agricultural soil among different countries/regions are difficult to identify. Thus, further research is needed to identify the runoff losses of heavy metals especially water-soluble and exchangeable fractions in agricultural soils.

3.2.4. Relative contributions of heavy metal output pathways

There were several output pathways for the elements assessed in this study, including crop harvesting, leaching water, and surface runoff. However, for each element, the different output pathways made a differential contribution to the total output, as shown in Fig. 5. As, Ni, Cr, and Pb were exported mainly through surface runoff, accounting for 46.32–73.36% of the total output fluxes. The amounts of Cd, Cu, and Zn removed by crop harvesting were 39.18%, 44.41%, and 51.15%, respectively. For Hg, 43.38% of the total output was derived from leaching; this was followed by crop harvesting, at 39.52%.

The relative influence of the output pathways varied greatly among the different regions. Crop harvesting was an important soil element output pathway in Lishui and Jinhua. Soil elements were also removed by surface water runoff except harvesting in Quzhou and Huzhou. Leaching water was the dominant soil output pathway in Taizhou. Overall, harvesting and leaching were the predominant output pathways of heavy metals in the whole province. Crop harvesting, one of the major sinks, has been observed and evaluated. It is well-known that the accumulation of heavy metals in plants, particularly for hyperaccumulators, is in accordance with a potential risk of transferring them to people (Zhang et al., 2018). Intensively cultivated agricultural soils always have a high potential for losses of water and nutrients by leaching. Therefore, leaching may be an important pathway for soil heavy metal output, which may be related to precipitation (Dobson et al., 2012). Compared with the other typical districts in China, crop harvesting was the main output pathway of soil elements in Hunan Province (Yi et al., 2018). Almost 100% of the heavy metal output in southern Heilongjiang Province was from leaching water (Xia et al., 2014). Due to the natural geographic conditions of the island of Hainan, only surface runoff and harvesting were taken into account in a previous study (Jiang et al., 2014). The output flux of runoff accounted for 58% of the total output in the PRD, without considering leaching (Zhou et al., 2012). It is essential to consider all primary input and output pathways when developing an inventory of heavy metals in agricultural soil.

3.3. Heavy metal balance

Within the biogeochemical cycle of heavy metals, the element concentrations in soil are in a state of dynamic balance. In this study, the total balance amount (Q_i) of element *i* was calculated using the following equation (Bergkvist et al., 1989):

$$Q_i = \sum \text{input}_i - \sum \text{ouput}_i$$

The concentration of a heavy metal in soil is enriched when the input exceeds the output, and depleted when the output exceeds the input. Fig. 6 provides maps showing the differences in inputs and outputs of the heavy metals.

The heavy metals all had positive Q_i values i.e., the input fluxes exceeded the output fluxes, except for Ni in Quzhou. Given the present input and output fluxes, heavy metals selected may be in the state of enrichment in agricultural soil in Zhejiang Province. The heavy metals all had higher Q_i values in Taizhou than in the other areas, indicating that considerable amounts of heavy metals were being deposited into the soil. These results could promote awareness of the hazards posed by the current e-waste recycling activity occurring in Taizhou. Hg and Cd had low-positive Q_i values, with a varied range of 0.24–0.41 mg/m^2/y and 0.04–0.72 mg/m^2/y, respectively. Although they showed slow

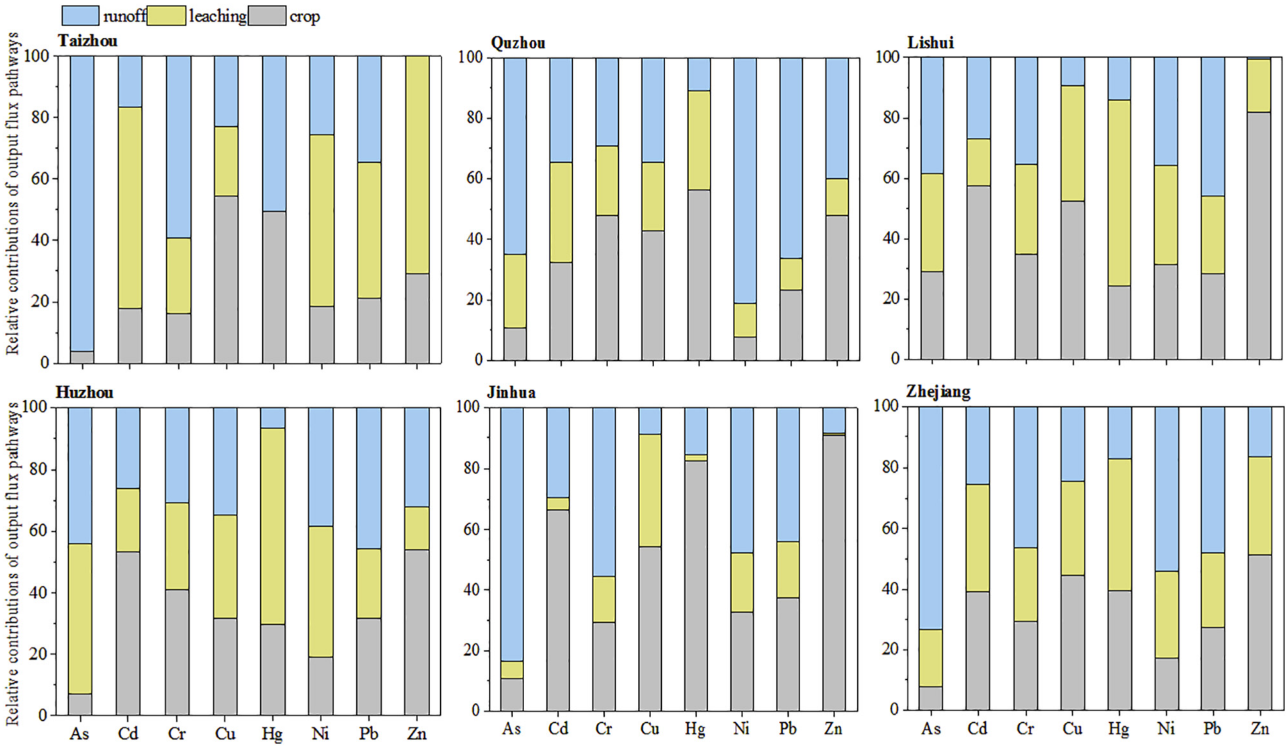

Fig. 5. Relative contributions (%) of different output flux pathways of heavy metals in Zhejiang Province.

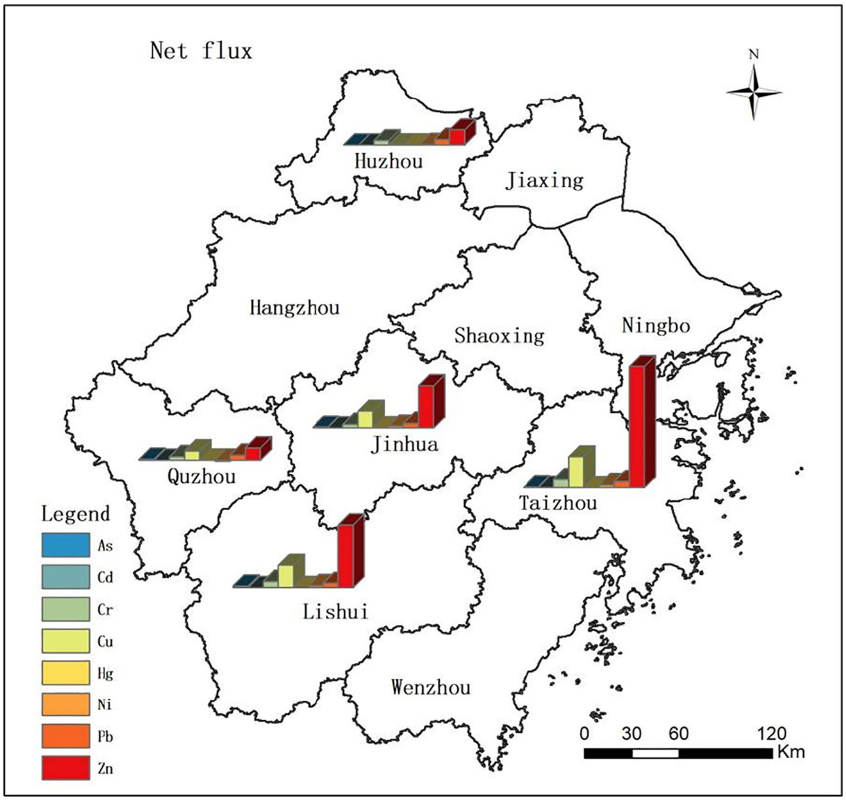

Fig. 6. Net flux (mg/m^2/y) of heavy metals in five typical areas of Zhejiang Province.

accumulation rates, Hg and Cd are elements of the prior concern for agricultural soil because of their lower safety thresholds.

3.4. Prediction and early warning

The difference in input and output of heavy metals in agricultural soils influences the dynamic balance, i.e., whether there is accumulation or depletion (Salman et al., 2017). Without considering the other input and output ways, as well as the change of the increment per year, the environmental risks posed by heavy metals in soil can be evaluated.

Table 9
The annual net input fluxes of heavy metals and predicted time in which heavy metal concentrations accumulated to the limit values in different areas.

	As	Cd	Cr	Cu	Hg	Ni	Pb	Zn
Taizhou (mg/m^2/y)	2.599	0.724	26.45	99.31	0.393	9.541	19.84	391.5
Quzhou (mg/m^2/y)	2.974	0.045	11.71	30.24	0.235	−3.135	16.30	39.86
Lishui (mg/m^2/y)	4.950	0.553	20.56	72.32	0.407	7.432	14.77	202.7
Huzhou (mg/m^2/y)	0.583	0.277	14.31	1.027	0.241	2.036	17.95	49.15
Jinhua (mg/m^2/y)	3.142	0.402	12.45	54.65	0.338	6.696	15.80	137
Background value (mg/kg)[a]	8.47	0.2	67.29	27.88	0.13	27.14	33.14	87.66
Maximum permissible limits (mg/kg)[b]	40	0.3	150	50	1.8	70	90	200
Time required (year)								
Taizhou	2790	32	719	51	978	1033	659	66
Quzhou	2438	512	1625	168	1631	/	802	648
Lishui	1465	42	925	70	943	1326	885	127
Huzhou	12,440	83	1329	4955	1591	4842	729	526
Jinhua	2308	57	1528	93	1137	1472	828	189

[a] Soil environment background values of Zhejiang province (Cheng et al., 2007).
[b] Soil environmental quality standard of China (GB15618–2018) (CNEPA, 2018).

The concentration of element *i* in soil is a temporal variable given by the following equation:

$$C_{t,i} = C_{0,i} + t \times \Delta C_i$$

where $C_{t,i}$ (mg/kg) is the concentration of element *i* at the temporal point *t*, $C_{0,i}$ (mg/kg) is the initial concentration, and ΔC_i (mg/kg) is the change in the quantity of the soil element concentration, *i*. ΔC_i is calculated as.

$$\Delta C_i = Q_i \div (W_{soil} + W_{dry})$$

where W_{soil} is the weight of the soil plow layer and W_{dry} is the increased average weight of dry matter (mg/m^2), calculated as.

$$W_{dry} = A_i + F_i + M_i$$

where A_i is the annual amount of dry atmospheric deposition (mg/m^2), F_i is the annual amount of fertilizer actually applied (mg/m^2), and M_i is the annual amount of manure actually applied (mg/m^2).

Suppose that all of the heavy metal inputs from external sources are within a 20 cm region of cultivated soil; then, the soil volume weight is 1.15 t/m^3 and the calculated value of W_{soil} is 2.3×10^8 mg/m^2 (Luo et al., 2009). Compared with W_{soil}, the calculated A_i, F_i, and M_i are relatively small, so these dry matter inputs can be ignored in the analysis. Hence, in this study W_{dry} was considered to be zero, and the weight of the soil plow layer (0–20 cm) was assumed to be constant.

The current rates of increase in heavy metal concentrations in soil were used to estimate the time (in years) required to increase topsoil concentrations from the background values ($C_{0,i}$) (Cheng et al., 2007) to the environmental quality standard GB15618–2018 ($C_{t,i}$) (China SEPA, 2018). The details of the result are shown in Table 2. Cd is the element of most concern for agricultural soil in Zhejiang, followed by Cu and Zn. With the rates of increase calculated herein, it would take about 32 and 42 years for the average concentration of Cd in Taizhou and Lishui to reach their safety limits, respectively (Table 9). Therefore, greater regulatory efforts against Cd contamination of the agricultural soils in Taizhou and Lishui are required. As, Cr, Hg, Ni, and Pb pose little threat to the environment in the next few years. However, it should be noted that soil heavy metal concentrations are influenced by various processes and factors. Therefore, it is very difficult, or even impossible, to predict their concentrations accurately because the complex influencing parameters vary unpredictably over time. Nevertheless, the results of this study have significance for assessments of local environmental risk.

4. Conclusion

This study observed and assessed the annual input and output fluxes of heavy metals in agricultural soil, and developed a heavy metal inventory for Zhejiang Province. The inventory showed that atmospheric deposition and livestock manure were the predominant sources of heavy metals entering into agricultural soil, and crop harvesting and leaching were important soil element output pathways. Based on the mass balance model, heavy metals may be in a state of enrichment in agricultural soils in Zhejiang Province. For prediction and early warning, control of Cd concentrations should be prioritized. Stricter regulatory strategies may be needed at the provincial level to control and reduce Cd inputs. In future work, other possible heavy metal sources and sinks (e.g., wind erosion, evaporation, and leakage) should be considered to more accurately calculate a complete mass balance to improve the establishment of heavy metal inventories.

Acknowledgment

This work was supported by the National Key Research and Development Program of China (2016YFD0800302), Central Level, Scientific Research Institutes for Basic R&D Special Fund Business (2016YSKY032).

References

Belon, E., Boisson, M., Deportes, I.Z., Eglin, T.K., Feix, I., Bispo, A.O., Guellier, C.R., 2012. An inventory of trace elements inputs to French agricultural soils. Sci. Total Environ. 439, 87–95.

Bergkvist, B., Folkeson, L., Kleja, B.D., 1989. Fluxes of Cu, Zn, Pb,Cd, Cr and Ni in temperate forest ecosystems. A literature review. Water Air Soil Pollut. 47, 217–286.

Bonten, L.T.C., Romkens, P.F.A.M., Brus, D.J., 2008. Contribution of heavy metal leaching from agricultural soils to surface water loads. Environ. Forensic 9, 252–257.

Cai, J., Wang, J., Zhang, Y., Tian, H., Zhu, C., Gross, D.S., Hu, M., Hao, J., He, K., Wang, S., Zheng, M., 2017. Source apportionment of Pb-containing particles in Beijing during January 2013. Environ. Pollut. 226, 30–40.

Cambier, P., Pot, V., Mercier, V., Michaud, A., Benoit, P., Revallier, A., Houot, S., 2014. Impact of long-term organic residue recycling in agriculture on soil solution composition and trace metal leaching in soils. Sci. Total Environ. 499, 560–573.

Cao, F., Wang, R., Cheng, W., Zeng, F., Ahmed, I.M., Hu, X., Zhang, G., Wu, F., 2014. Genotypic and environmental variation in cadmium, chromium, lead and copper in rice and approaches for reducing the accumulation. Sci. Total Environ. 496, 275–281.

Chen, T., Liu, X.M., Li, X., Zhao, K.L., Zhang, J.B., Xu, J.M., Shi, J.C., Dahlgren, R.A., 2009. Heavy metal sources identification and sampling uncertainty analysis in a field-scale vegetable soil of Hangzhou, China. Environ. Pollut. 157, 1003–1010.

Chen, J., Zheng, J., Gao, L.H., 2015. Sources and ecological risk assessment of heavy metal (loid)s in agricultural soils of Huzhou, China. Soil Sediment Contam. 24, 437–453.

Cheng, J.L., Shi, Z., Zhu, Y.W., 2007. Assessment and mapping of environmental quality in agricultural soils of Zhejiang Province, China. J. Environ. Sci. 19, 50–54.

China SEPA, 2018. Ministry of Ecology and Environment of the People's Republic of China: soil environmental quality, Risk control standard for soil contamination of agricultural land (GB15618-2018).

CNEPA, 2018. Ministry of Ecology and Environment of the People's Republic of China: soil environmental quality, Risk control standard for soil contamination of agricultural lamd (GB15618-2018).

Cui, Y., Du, X., 2011. Soil heavy-metal speciation and wheat phytotoxicity in the vicinity of an abandoned lead-zinc mine in Shangyu City, Eastern China. Environ. Earth Sci. 62, 257–264.

Dobson, P.F., Ghezzehei, T.A., Cook, P.J., Rodríguez-Pineda, J.A., Villalba, L., la Garza, R.D., 2012. Heterogeneous seepage at the Nopal I natural analogue site, Chihuahua, Mexico. Hydrogeol. J. 20, 155–166.

Dowdy, R.H., Volk, V.V., 1983. Movement of heavy metals in soils. In: Nelsen, D.W., et al. (Eds.), Chemical Mobility and Reactivity in Soil Systems. SSSA Spec. Publ. 11. SSSA, Madison, WI, pp. 229–240.

Elrashidi, M.A., Hammer, D., Fares, A., Seybold, C.A., Ferguson, R., Peaslee, S.D., 2007. Loss of heavy metals by runoff from agricultural watersheds. Soil Sci. 172, 876–894.

Gu, Z.P., Feng, J.L., Han, W.L., Wu, M.H., Fu, J.M., Sheng, G.Y., 2010. Characteristics of organic matter in PM2.5 from an e-waste dismantling area in Taizhou, China. Chemosphere 80, 800–806.

Han, L.F., Gao, B., Hao, H., Zhou, H.D., Lu, J., Sun, K., 2018. Lead contamination in sediments in the past 20 years: a challenge for China. Sci. Total Environ. 640–641, 746–756.

Hou, J.Y., Shen, Y., Cao, S.P., Cheng, X.J., Wang, W.X., 2013. Heavy metal flux research in Tianjin suburb vegetable farmland. J. Anhui Agric. Sci. 41, 5764–5773 (in Chinese).

Hou, Q., Yang, Z., Ji, J., Yu, T., Chen, G., Li, J., Xia, X., Zhang, M., Yuan, X., 2014. Annual net input fluxes of heavy metals of the agroecosystem in the Yangtze River delta, China. J. Geochem. Explor. 139, 68–84.

Hu, W.Y., Huang, B., Shi, X.Z., Chen, W.P., Zhao, Y.C., Jiao, W.T., 2013. Accumulation and health risk of heavy metals in a plot-scale vegetable production system in a peri-urban vegetable farm near Nanjing, China. Ecotoxicol. Environ. Saf. 98, 303–309.

Huang, L.D., Wang, H.Y., Li, Y.X., Lu, S.G., 2013. Spatial distribution and risk assessment of phosphorus loss potential in urban–suburban soil of Lishui, China. Catena 100, 42–49.

Huang, Y., Li, T.Q., Wu, C.X., He, Z.L., Japenga, J., Deng, M.H., Yang, X.E., 2015. An integrated approach to assess heavy metal source apportionment in pen-urban agricultural soils. J. Hazard. Mater. 299, 540–549.

Jiang, W., Hou, Q.Y., Yang, Z.F., Yu, T., Zhong, C., Yang, Y., Fu, Y.R., 2014. Annual input fluxes of heavy metals in agricultural soil of Hainan Island, China. Environ. Sci. Pollut. Res. 21, 7876–7885.

Li, J., Jin, Z., Gu, Q., 2011. Effect of plant species on the function and structure of the bacterial community in the rhizosphere of lead-zinc mine tailings in Zhejiang, China. Can. J. Microbiol. 57 (7), 569–577.

Li, W.L., Xu, B.B., Song, Q.J., Liu, X.M., Xu, J.M., Brookes, P., 2014. The identification of 'hotspots' of heavy metal pollution in soil–rice systems at a regional scale in eastern China. Sci. Total Environ. 472, 407–420.

Liu, X., Wu, J., Xu, J., 2006. Characterizing the risk assessment of heavy metals and sampling uncertainty analysis in paddy field by geostatistics and GIS. Environ. Pollut. 141, 257–264.

Liu, Z., Yang, J., Yang, Z., Zou, J., 2012. Effects of rainfall and fertilizer types on nitrogen and phosphorus concentrations in surface runoff from subtropical tea fields in Zhejiang, China. Nutr. Cycl. Agroecosyst. 93, 297–307.

Luo, L., Ma, Y.B., Zhang, S.Z., Wei, D.P., Zhu, Y.G., 2009. An inventory of trace element inputs to agricultural soils in China. J. Environ. Manag. 90, 2524–2530.

Ministry of Environmental Protection, Ministry of Land and Resources of the People's Republic of China, 2014. Report on the national general survey of soil contamination. Available at. http://wwwcenewscomcn/sylm/jsxw/201404/t20140418_772973htm.

Niu, L.L., Yang, F.X., Xu, C., Yang, H.Y., Liu, W.P., 2013. Status of metal accumulation in farmland soils across China: from distribution to risk assessment. Environ. Pollut. 176, 55–62.

Pan, Y.P., Wang, Y.S., 2015. Atmospheric wet and dry deposition of trace elements at 10 sites in Northern China. Atmos. Chem. Phys. 14, 951–972.

Qian, M.R., Wu, H.Z., Wang, J.M., Zhang, H., Zhang, Z.L., Zhang, Y.Z., Lin, H., Ma, J.W., 2016. Occurrence of trace elements and antibiotics in manure-based fertilizers from the Zhejiang Province of China. Sci. Total Environ. 559, 174–181.

Qin, L.X., Ma, J.W., Sun, W.C., Wang, F., Lu, H., Yu, Q.G., 2015. Characteristics of heavy metal and nutrient contents in livestock manure in Zhejiang Province. Acta Agric. Zhejiangensis 27, 604–610 (in Chinese).

Salman, S.A., Elnazer, A.A., Nazer, H.A.E., 2017. Integrated mass balance of some heavy metals fluxes in Yaakob village, South Sohag, Egypt. Int. J. Environ. Sci. Technol. 14, 1011–1018.

Shao, D.W., Zhan, Y., Zhou, W.J., Zhu, L.Z., 2016. Current status and temporal trend of heavy metals in farmland soil of the Yangtze River Delta Region: field survey and meta-analysis. Environ. Pollut. 219, 329–336.

Shen, H., Ding, G., Han, G., Wang, X., Xu, X., Han, J., Lou, X., Xu, C., Cai, D., Song, Y., Lu, W., 2010. Distribution of PCDD/Fs, PCBs, PBDEs and organochlorine residues in children's blood from Zhejiang, China. Chemosphere 80, 170–175.

Shi, T.R., Ma, J., Wu, X., Ju, T.N., Lin, X.L., Zhang, Y.Y., Li, X.H., Gong, Y.W., Hou, H., Zhao, L., Wu, F.Y., 2018. Inventories of heavy metal inputs and outputs to and from agricultural soils: a review. Ecotoxicol. Environ. Saf. 164, 118–124.

State Environmental Protection Administration of China (SEPAC), 2006. China Environmental Yearbook 2005. China Environmental Sciences Press, Beijing.

Tang, X.J., Shen, C.F., Shi, D.Z., Cheema, S.A., Khan, M.I., Zhang, C.K., Chen, Y.X., 2010. Heavy metal and persistent organic compound contamination in soil from Wenling: an emerging e-waste recycling city in Taizhou area, China. J. Hazard. Mater. 173, 653–660.

Wang, H., Dong, Y.H., Yang, Y.Y., Toor, G.S., Zhang, X.M., 2013. Changes in heavy metal contents in animal feeds and manures in an intensive animal production region of China. J. Environ. Sci. 25, 2435–2442.

Wang, M.M., Yuan, M.Y., Su, D.C., 2017. Characteristics and spatial-temporal variation of heavy metals in atmospheric dry and wet deposition of China. China Environ. Sci. 37, 4085–4096 (in Chinese).

Wong, C.S.C., Li, X.D., Zhang, G., Qi, S.H., Peng, X.Z., 2003. Atmospheric deposition of heavy metals in the Pearl River Delta, China. Atmos. Environ. 37, 767–776.

Xia, X.Q., Yang, Z.F., Cui, Y.J., Li, Y.S., Hou, Q.Y., Yu, T., 2014. Soil heavy metal concentrations and their typical input and output fluxes on the southern Song-nen Plain, Heilongjiang Province, China. J. Geochem. Explor. 139, 85–96.

Xu, Q.T., Zhang, M.K., 2017. Source identification and exchangeability of heavy metals accumulated in vegetable soils in the coastal plain of eastern Zhejiang province, China. Ecotoxicol. Environ. Saf. 142, 410–416.

Ye, X.Z., Xiao, W.D., Zhang, Y.Z., Zhao, S.P., Wang, G.J., Zhang, Q., Wang, Q., 2015. Assessment of heavy metal pollution in vegetables and relationships with soil heavy metal distribution in Zhejiang province, China. Environ. Monit. Assess. 187, 378.

Yi, K.X., Fan, W., Chen, J.Y., Jiang, S.H., Huang, S.J., Peng, L., Zeng, Q.R., Luo, S., 2018. Annual input and output fluxes of heavy metals to paddy fields in four types of contaminated areas in Hunan Province, China. Sci. Total Environ. 634, 67–76.

Yu, R.L., Ji, J.F., Yuan, X.Y., Song, Y.X., Wang, C., 2012. Accumulation and translocation of heavy metals in the canola (*Brassica napus* L.)—soil system in Yangtze River Delta, China. Plant Soil 353, 33–45.

Zhang, Y.M., Fu, X.M., Zhou, J., 2017. Investigation and suggestion on activity level of atmospheric inventory: case study on Quzhou City. Recycl. Resour. Circ. Econ. 10, 42–44 (in Chinese).

Zhang, J.R., Li, H.Z., Zhou, Y.Z., Dou, L., Cai, L.M., Mo, L.P., You, J., 2018. Bioavailability and soil-to-crop transfer of heavy metals in farmland soils: a case study in the Pearl River Delta, South China. Environ. Pollut. 235, 710–719.

Zhou, L., Xu, Z.M., 2012. Response to waste electrical and electronic equipments in China: legislation, recycling system, and advanced integrated process. Environ. Sci. Technol. 46, 4713–4724.

Zhou, Y., Lu, R.H., Dong, Y.Y., Yao, X.G., 2007. Quality investigation of organic fertilizers, inorganic-organic compound fertilizers and compound fertilizers in Zhejiang province. Plant Nutr. Fertil. Sci. 13, 148–154 (in Chinese).

Zhou, Y.Z., Shen, W.J., Li, Y., Dou, L., Li, W.S., Lai, Q.H., Du, H.Y., Zhong, L.L., Liang, T., 2012. A study of prediction and early-warning forecast on geochemical accumulation of soil heavy metals based on flux model in Pearl River delta Economic zone (China). Adv. Earth Science 27, 1115–1125 (in Chinese).

Zou, L., Wang, S.X., Liu, L., Hashmi, M.Z., Tang, X.J., Shi, J.Y., 2015. Multi-element pollution in soil, ground and surface water from abandoned chromate chemical plants: a case study in Hangzhou, China. Environ. Earth Sci. 74, 2861–2870.

Ecotoxicology and Environmental Safety 164 (2018) 118–124

Contents lists available at ScienceDirect

Ecotoxicology and Environmental Safety

journal homepage: www.elsevier.com/locate/ecoenv

Review

Inventories of heavy metal inputs and outputs to and from agricultural soils: A review

Taoran Shi[a,b,c], Jin Ma[b,*], Xiao Wu[b], Tienan Ju[b], Xianglong Lin[b], Yunyun Zhang[b], Xinhong Li[b], Yiwei Gong[b], Hong Hou[b], Long Zhao[b], Fuyong Wu[a,c,**]

[a] College of Natural Resources and Environment, Northwest A&F University, Yangling 712100, China
[b] State Key Laboratory of Environmental Criteria and Risk Assessment, Chinese Research Academy of Environmental Sciences, Beijing 100012, China
[c] Key Laboratory of Plant Nutrition and the Agri-environment in Northwest China, Ministry of Agriculture, Yangling 712100, China

ARTICLE INFO

Keywords:
Inventory
Heavy metals
Agricultural soil
Fluxes
Atmospheric deposition

ABSTRACT

Heavy metal pollution of agricultural soils is an important issue around the world. To understand the overall pollution process, accurate determination of every input and output pathway of heavy metals to and from soils is essential. Hence, input and output inventory, a quantitative analysis method of heavy metals balance in agricultural soils, has been widely used. However, due to differences in geography, climate, socioeconomic factors, industrial and agricultural production, substantial variation exists among existing input and output inventories for different countries and regions. In this study, we systematically analyzed these differences and the findings will improve the compilation of inventories worldwide.

1. Introduction

The accumulation of heavy metals in agricultural soil has become an important issue around the world (Bigalke et al., 2017). Great efforts have been made to alleviate heavy metal pollution in agricultural soils. First, accurate determination of the input and output pathways of heavy metals to and from soil is needed. Heavy metals can enter an agroecosystem through natural and anthropogenic processes. The application of fertilizers, agrochemicals and irrigation water, as well as atmospheric deposition are recognized as main anthropogenic heavy metal sources to agricultural soils (Hou et al., 2014). In addition, heavy metals in soils have several output pathways, such as biomass exportation, leaching and surface water runoff (Salman et al., 2017). To accurately quantify heavy metal inputs and outputs to and from agricultural soils, the concept of an inventory was developed. An inventory is a method of source apportionment that can be used in conjunction with source (i.e., diffusion) and receptor models. The main areas studied in inventory research include heavy metal inputs to agricultural soils (Nicholson et al., 2003; Luo et al., 2009; Jiang et al., 2014), inputs of heavy metals into soils by atmospheric deposition, fertilizer application, organic waste disposal (Lopes et al., 2011), heavy metal balances of agroecosystems (Moolenaar and Lexmond, 1998), and an emission inventory of heavy metals from the iron and steel industries (Wang et al., 2016a).

The quantification of an inventory can provide a cheap, quick and early diagnosis of agricultural soil contamination by heavy metals (Steiger and Obrist, 1993). The first such inventory was established in the Netherlands to periodically record environmental pollution in 1974 (Misseyer and Van der Most, 1993). Much of the subsequent research has been conducted in European nations, such as France and Germany (Belon et al., 2012), in the United States (Mcgrath et al., 1994) and in China (Luo et al., 2009). An inventory of heavy metal inputs and outputs gives a good indication of the accumulation or depletion of certain elements in selected agroecosystems. It also provides a valuable knowledge base for the improvement of agricultural soil management and development of policy recommendations. Physical geography, climate, economic development, industrial production and citizens' lifestyles differ markedly among countries and regions, resulting in differences in heavy metal inventories and the relative contributions of the input and output pathways to and from soils. However, limited information about these differences in soil inventories among countries and regions is available. In this research, we retrieved totally 260 concerned literatures corresponding to the keywords: inventory, heavy metals, agricultural soil, fluxes, mass balance from databases like web of science, Elsevier ScienceDirect (SDOL), Science Online, Chinese periodical full text, China national knowledge infrastructure (CNKI).

In this research, scattered literatures were utilized to answer the

---

[*] Corresponding author.
[**] Corresponding author at: College of Natural Resources and Environment, Northwest A&F University, Yangling 712100, China.
E-mail addresses: majin@craes.org.cn (J. Ma), wfy09@163.com (F. Wu).

https://doi.org/10.1016/j.ecoenv.2018.08.016
Received 7 November 2017; Received in revised form 24 July 2018; Accepted 3 August 2018

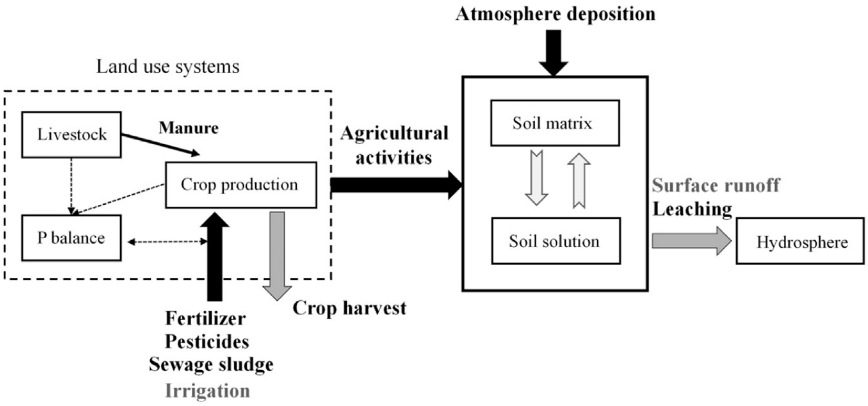

Fig. 1. General scheme for the regional metal balance model PROTERRA-S (Irrigation and Surface runoff are complementary to the PROTERRA-S model).

following questions: How to establish an inventory? How are inventory studies going? Are there differences in main input and output pathways of heavy metals among different regions or countries? What needs to be improved of inventory in the future? To our knowledge, this review is the first to examine heavy metal input and output inventories for agricultural soils.

2. Inventory methodology

2.1. Determine input and output pathways

In order to develop a quantitative inventory, firstly, we need to determine the main input and output pathways. It is need to determine the scale and relative importance of different sources and sinks of heavy metals. Dominant soil heavy metal input and output pathways in agroecosystem as shown in Fig. 1.

Heavy metal inputs into agricultural soils occur due to atmospheric deposition; the application of commercial fertilizers, animal manure and irrigation water; and the use of sewage sludge and other wastes as soil amendments. Pesticides containing Hg and As were banned in the United Kingdom since 1983 (Nicholson et al., 2006). The agricultural use of Hg-, As- and Pb-containing pesticides has been totally prohibited in China since 2002, and only a small number of approved pesticides contain other trace elements such as Cu and Zn (Luo et al., 2009). So the dominant soil heavy metal input pathways exclude pesticides in some studies.

Atmospheric deposition of particles to agroecosystems occurs via wet and dry processes. Heavy metal inputs by atmospheric deposition are obtained by direct collection using various sampling devices or indirect calculation with models (Dulac et al., 1989). The application of fertilizer can be a significant contributor of potentially hazardous heavy metals (Belon et al., 2012). For example, phosphate fertilizers are generally the major sources of trace metals among all inorganic fertilizers, and much attention has been given to the concentration of cadmium (Cd) in phosphate fertilizers (Bigalke et al., 2017). For agricultural soil to which sufficient nutrients cannot be supplied with commercial fertilizers alone, livestock manure is often used (Nicholson et al., 2003). Sewage sludge is also identified as a significant source of heavy metals where the material is excessively applied (Nicholson et al., 2006). Industrial byproducts and composts have often been neglected in soil inventories due to the lack of required information. Some other potential sources of heavy metal inputs to agricultural soil (e.g., flooding events, accumulating waste and spray) have been identified as being of local importance, but were not included in the previous inventories because of difficulties in estimating their contributions to overall heavy metal inputs.

Pathways of soil heavy metal outputs mainly include crop harvesting, leaching water and surface runoff (Fig. 1). Crop harvesting, one of the major sinks, has been observed and evaluated. It is well-known that the accumulation of heavy metals in plants, particularly for hyperaccumulators, is in accordance with a potential risk of transferring them to people. Cd contamination in rice in Hunan, China is a major environmental health concern (Wang et al., 2016b). Moreover, with end uses of harvested residues (such as straw) as fertilizers, animal feed, building material and fuel, they play an important role in heavy metal cycling within arable land systems with resulting consequences for human exposure (Williams et al., 2009). The heavy metal output through crop harvesting has included the grazing of agricultural soil in some studies (Ahmadi et al., 2016). Generally, plant samples from a specific area can be sampled and chemically analyzed to calculate their output fluxes (Xia et al., 2014). The soil output fluxes of heavy metal from harvesting can be calculated by summing the heavy metal stocks in the seedling and seed parts of each sample, with that of the root excluded as in Vries and Mclaughlin (2013). Intensively cultivated agricultural soils always have a high potential for losses of water and nutrients by leaching. Therefore, leaching may be an important pathway for soil heavy metal output, which may be related to precipitation (Dobson et al., 2012). Soil heavy metals can also be removed by surface water runoff, with levels calculated by consideration of the dissolved and particulate forms (Dorioz, 2013).

2.2. Data collection

Secondly, in order to develop a quantitative inventory, we need to collect relevant data. The compilation of an inventory depends on the availability of appropriate data and its robustness. Databases used to develop inventories have been obtained from statistical yearbooks, scientific literature, regional agricultural statistics, soil information systems and model calculations. The data typically collected include the area of cultivated land, consumption of chemical fertilizers, precipitation, sown area of crops, irrigation volume, and output of major farm products in the target areas. Data for heavy metal concentrations in crops, fertilizers and manures are typically obtained from previous studies and reports, or by sample analysis. Data sources for input and output pathways differ primarily with respect to the spatial scale, which influences the precision of the simulation results. When developing inventories, such differentiation has to been typically processed. To make the estimates comparable, all input and output fluxes are given as rates per unit area of arable land for the entire study region.

2.3. Principal models applied in establishing inventories

Various models have been proposed to assess heavy metal balances in agricultural soils. Steiger and Obrist (1993) developed PROTERRA model to assess phosphorus and heavy metal balances in regional agroecosystems. Keller et al. (2001) extended this model to incorporate the leaching of heavy metals and to establish PROTERRA-S model. We extended this model incorporating irrigation and surface runoff of heavy metals in this research. Fig. 1 presents the input, internal and output flows that are generally considered in heavy metal balances of the PROTERRA-S model at a regional scale. The basic units of the balances are land use systems defined by livestock composition and cultivated crops (left portion of Fig. 1). The change of a heavy-metal content in soil is influenced by agricultural activities (left portion of Fig. 1), atmospheric deposition (the middle part of Fig. 1), leaching and surface runoff (right portion of Fig. 1). As shown in left portion of Fig. 1, the regional phosphorus (P) requirements of crops were mainly supplied by animal manure, fertilizers, pesticides, sewage sludge, irrigation and crop. Heavy metal inputs through P fertilizer are determined from the P fertilizer inputs and from the ratios between metal and P concentrations of the fertilizers. More accurate pollution assessment can be attained by comparing model results with inventory-determined metal balances.

Moreover, some input and output fluxes were often based on model calculations instead of sample analysis. The process-oriented model SOACAS was developed to describe the fate of heavy metal in one completely mixed soil compartment using Freundlich isotherm and analytical equations (Duddridge and Wainwright, 1981). Models of the transfer of chemicals from the soil to plants, including sorption, leaching and plant uptake in the root zone, have also been designed (Peng et al., 2016). Some models (e.g., the Probability Kriging model) have been constructed to estimate future heavy metal concentrations.

3. Research advances

As mentioned previously, the first soil heavy metal inventory was established in the Netherlands to periodically record environmental pollution in 1974 (Misseyer and Van der Most, 1993). Moolenaar and Lexmond (1998) studied heavy metal balances in different agroecosystems in the Netherlands. Inventories of the main input pathways, such as the inventories of heavy metals into agroecosystems by atmospheric deposition in Korea, New Zealand, Japan and India at the regional or national scale, have been established (Yun et al., 2002; Gray et al., 2003; Sharma et al., 2008). The UK, China and France have established inventories of heavy metal inputs to agricultural soils at the national scale (Nicholson et al., 2006; Luo et al., 2009; Belon et al., 2012). Recently, a global release inventory for heavy metals in the period 2000–2014 was compiled for the estimation of toxic releases from the application of manure to agricultural soils (Leclerc and Laurent, 2017).

3.1. Inventories of heavy metal inputs

There are great differences in the input inventories among different countries and regions. The use of organic waste (i.e., compost, sludge or manure) as agricultural fertilizers was considered when developing an inventory of heavy metal inputs to agricultural soils in Europe and the US (Lopes et al., 2011). Heavy metal inputs via fertilizers are similar to or even larger than Cd, arsenic (As) and chromium (Cr) inputs via atmospheric deposition in French agricultural soils (Belon et al., 2012). It was also found that for agricultural zinc (Zn) inputs into soils and crops in central Iran resulting from mineral fertilizers, sewage sludge and compost, studies have ignored the contribution of atmospheric deposition (Karami et al., 2014).

In contrast to the situation in European countries, such as France (Belon et al., 2012), atmospheric deposition and livestock manure are the predominant sources of heavy metals entering agricultural soils in China (Luo et al., 2009).

3.2. Inventories of heavy metal outputs

Similarly, great differences are also observed in the output inventories from different countries and regions. Outside of China, inventories of outputs from agricultural soils have concentrated mainly on heavy metal leaching and surface runoff losses from soil to surface waters. Heavy metal leaching from soil has become a significant source for heavy metals in surface waters (Bonten et al., 2008). Estimates of the contribution of leaching to the heavy metal loads of surface waters are difficult to obtain because various important factors that control the magnitude of the leaching flux are unknown (Bengtsson et al., 2006). Leaching fluxes were either based on model calculations using sorption models and site-specific soil properties, or on measured or estimated dissolved metal concentrations (Cambier et al., 2014). Leaching losses have sometimes been calculated indirectly, using a mass balance model, in which the surplus amounts of elements not accounted for have been assumed to be available for water runoff (Godlinski et al., 2011). Other model calculations, such as those in the hydrological soil models and Freundlich adsorption isotherm models have also been performed to quantify heavy metal leaching from agricultural soils to surface waters (Bengtsson et al., 2006; Bonten et al., 2008). There are many hydrological models such as empirical model, the facies-separation model and the holistic model in vertical migration as well as soil and water assessment tools (SWAT) and the migration model with the wind in lateral transfer. Freundlich adsorption isotherm model is used to calculate the distribution between heavy metals in the soil solid phase and the soil solution. Parameters of the Freundlich sorption isotherm model are Freundlich coefficient, soil properties, leaching rate coefficient, heavy metal concentration and so on.

In China, the inventories of heavy metal outputs to agricultural soils assess the contributions of leaching, crop harvesting and surface runoff (Luo et al., 2009). Almost 100% of the heavy metal output was from leaching in southern Heilongjiang (Xia et al., 2014). Output fluxes following the crop harvesting of agricultural soil have also been observed and evaluated (Xia et al., 2014). However, the effects of crop harvesting include only certain representative plants, with the effects of other crop rotations not taken into account. The paucity of data on crop harvesting is the main source of estimation uncertainty. Outputs other than those occurring during crop harvesting are minor, and include grazing and the direct foraging of livestock on fields. Actually, the output fluxes of heavy metals through crop residues, crop harvesting and weeding are quite weak compared with the atmospheric deposition input flux (Xiong et al., 2016). Subsurface flow and surface runoff were found to be the main pathways of heavy metal outputs in soils used for vegetable cultivation in city suburbs (Hou et al., 2013; Xiong et al., 2016).

In China, much effort has also been made through theoretical and experimental studies to quantify the fluxes across interface of heavy metal, such as those from soils or plants to the atmosphere, especially for mercury (Hg) (Luo et al., 2015), as well as to evaluate the characteristics and factors influencing the exchange flux (Liu et al., 2014). A dynamic flux chamber and mercury analyzer have been used to observe Hg exchange fluxes in the field (Liu et al., 2014).

3.3. Heavy metal balances

It is important to clarify the mass balance of the heavy metals between input and output fluxes. A general mass flux assessment model has been used to determine the contributions of different input and output fluxes to the resulting accumulation of heavy metals, with respect to a unit area of the agroecosystem: g/ha/year. The differences in the input and output of heavy metals into agricultural soils influence the state of the dynamic balance, i.e., enrichment or depletion.

Outside of China, mass flux balance studies have been performed for heavy metals in agricultural soils across a wide variety of scales (national, regional, field and farm) (Keller and Schulin, 2003). National conditions and specific policies, such as the use of massive amounts of fertilizer in intensive animal and vegetable production in Poland and the Netherlands, influence the heavy metal balance at the national scale

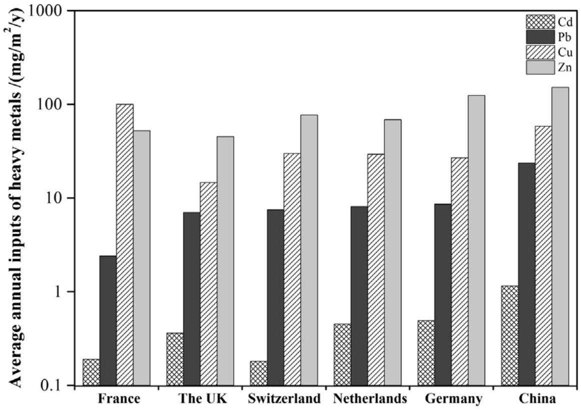

Fig. 2. *Average annually inputs of heavy metals in European countries and China (mg/m^2/yr)* (France: Belon et al., 2012; The UK: Eckel et al., 2005; Switzerland, Netherlands, and Germany: Nicholson et al., 2003; China: Luo et al., 2009).

(Bach and Starmans, 2005). New European regulations concerning heavy metal contents in animal feeding stuffs were implemented in 2003 (European Community, 2003), and may have resulted in changes in heavy metal concentrations in manure. At the regional scale, livestock manure and crop removal data are the main sources of estimation uncertainty (Ahmadi et al., 2016). At the field and farm scales, crop rotation and the choice of fertilizers influence the heavy metal balance of arable farming systems. Furthermore, the role of farm management is very important, but the effects on the heavy metal balance are not always straightforward. Due to the internal cycling of feedstuff and manure, fewer inputs are required, and thus the import of heavy metals containing raw materials and products is minimized. Vertical migration of heavy metals in contaminate soils potentially leading to deterioration of groundwater quality is a major environmental problem. The rates of vertical migration depend on heavy metal species and soil property (Maskall et al., 1996). Very little data on leaching below the plough layer and rooting depths are available, which can result in a large degree of uncertainty in field balances for heavy metals (Bengtsson et al., 2006).

In China, the prediction and provision of early warnings about geochemical accumulations of heavy metals in agricultural soils can be conducted according to the standards for soil environmental quality and the net flux of soil heavy metals based on mass balance model (Zhou et al., 2012).

4. Assessment of previous inventories

4.1. Comparison among inventories

A lot of countries, including England, Wales and Switzerland, have developed input inventories to assess the major sources of heavy metals in agricultural soils (Bvon et al., 1998; Nicholson et al., 2006). No further discussion was given for inventories on a macroscopic standpoint in the following research, neither inventories for one input or output pathway of heavy metals. Representative literatures related to inventory were listed in Table S1, which were necessary for the understanding of the concept and field applicability of inventory. Typical and comprehensive inventories with data for input and/or output pathways were further elaborated. Heavy metal inputs and outputs to and from agricultural soils of selected countries are presented in Table S2.

England and Wales also established an inventory of heavy metal inputs based on detailed sources, and their total inputs are therefore far better quantified than those in other countries (Nicholson et al., 2003). The relative importance of the diverse sources of heavy metals may differ significantly among nations. Atmospheric deposition was the main source of heavy metals entering agricultural land, with livestock manures and sewage sludge also important sources for Zn and Cu across the whole agricultural land area in the England and Wales inventory (Nicholson et al., 2003). Phosphate fertilizers were the main source of Cd, lead (Pb) and Cr in south Sohag, Egypt (Salman et al., 2017). Zn deposition was far higher in New Zealand than in England and Wales. One possible explanation for this difference is the large number of houses with roofs galvanized with a Zn oxide coating in New Zealand (Gray et al., 2003). As mentioned above, it can also be found that previous researches related to inventories focused mostly on the input pathways of heavy metals into agroecosystems compared with output pathways (Table S2). Therefore, to fully evaluate long-term accumulation of heavy metals in agricultural soils, more researches should be conducted on soil heavy metal output fluxes.

As mentioned above, compared to other countries/regions, Europe and China have conducted more inventory studies, accumulated valuable research data. In addition, there are great differences in the level of development, industrial and agricultural production mode, natural environment, etc. between Europe and China. Hence, comparison of inventories between Europe and China could give us meaningful information. As shown in Fig. 2, according to the national-scale inventories for France, the UK, Switzerland, the Netherlands and Germany, heavy metal inputs to agricultural soils can be ranked as follows: Zn > Cu > Pb > Cd; however, the input fluxes showed obvious spatial variability among regions. The inputs of Zn, Cu, Pb and Cd in these five countries were lower than the corresponding figures in China, with the input of Cd being approximately one order of magnitude lower than that in China. The differences were probably linked to adverse natural conditions in some regions, as well as anthropogenic factors, including industrial and agricultural activities and rapid urbanization in China (Belon et al., 2012).

In China, inventories of the annual inputs and outputs of heavy metals to and from agricultural soils at the regional and national scales have been compiled (Luo et al., 2009; Jiang et al., 2014). Soil input and output fluxes of heavy metals from each pathway in provinces and cities in China are listed in Table S3.

Input pathways include atmospheric deposition, fertilizer and pesticide applications, irrigation and seed sowing. Atmospheric deposition is the dominant source of heavy metals to agricultural soils in most areas of China, especially for Cu, Zn and Pb. Hainan is an exception, with irrigation being the main source of heavy metal inputs (Jiang et al., 2014). At the large regional scale, atmospheric deposition has been identified as the principal source of metals entering soils, whereas fertilizer or irrigation is more significant in some local regions (Huang et al., 2015). Pesticide heavy metal input fluxes in the Pearl River Delta (Zhou et al., 2012) and Pb input fluxes from sowing seeds in Chongqing (Xiong et al., 2016) were far lower than the other fluxes considered in selected studies.

The output pathways listed in Table S3 include crop harvesting (vegetable, rice and fruit), leaching, surface runoff, and removal of crop residues and weeding. The output pathways account for different proportions of the total output. Almost 100% of Cd, Pb, Cu and Zn output is from leaching in southern Heilongjiang (Xia et al., 2014). The output flux for surface runoff accounts for 58% of the total output in the Pearl River Delta without considering leaching (Zhou et al., 2012). Due to the natural geographical conditions of Hainan Island, instead of leaching losses, only the surface runoff and crop harvesting were taken into account (Jiang et al., 2014). The exportation of heavy metals via leaching and surface runoff were not considered in Tianjin (Hou et al., 2013). Up to now, researches on heavy metals input and output inventory are very limited in China. The comparison of inventories among different regions of China is difficult. The differences in inventory are not only linked to the selection of dominant input and output pathways but also to the methods used for fluxes assessment. Hence, it is important to fully address all of the primary input and output pathways when developing an inventory of heavy metal balance

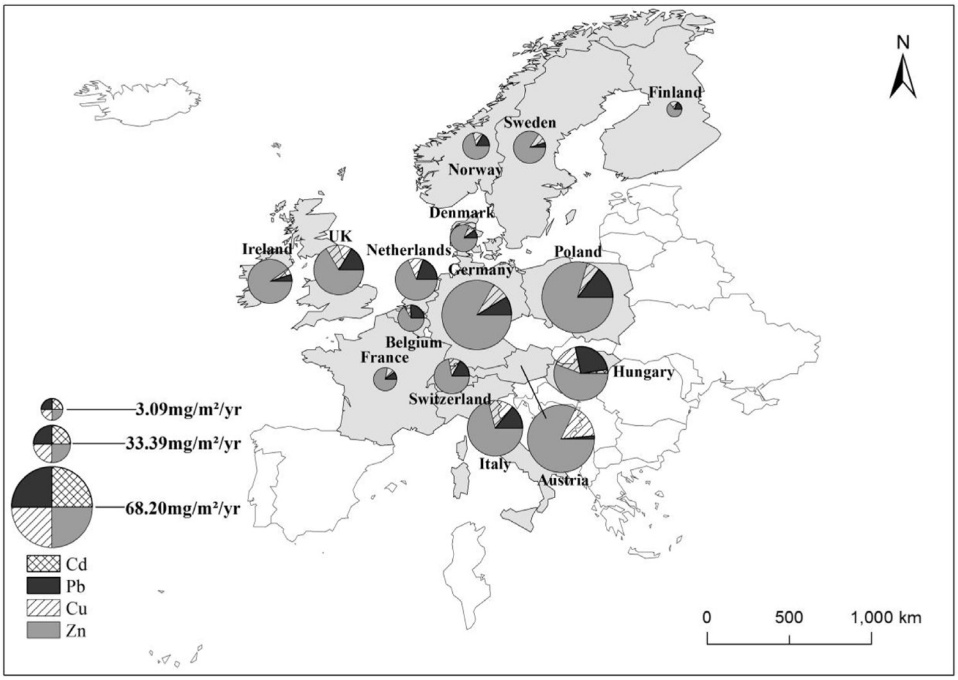

Fig. 3. *Flux of heavy metals from atmospheric deposition in several European countries* (Austria, Belgium, Denmark, Finland, Germany, Hungary, Ireland, Italy, Norway, Poland, Sweden, Switzerland, Netherlands: Nicholson et al., 2003; France: Belon et al., 2012; The UK: Eckel et al., 2005).

in agricultural soil. The guideline for building inventories should be established as soon as possible.

4.2. Atmospheric deposition-one of the predominant sources

Atmospheric deposition has been identified as an important source of heavy metals entering agricultural soil, and became one of the important concerns throughout the world. The characterization of total atmospheric depositions of heavy metals is relevant in order to identify their variabilities and sources. So we highlight exclusively the input pathways of atmospheric deposition.

Information regarding the atmospheric deposition of heavy metals in different countries in Europe (Fig. 3) has indicated that Zn is the element deposited in soil in the largest amounts. The greatest Cd deposition (0.99 $mg/m^2/yr$) was found in Hungary compared to those in other countries ranged from 0.01 to 0.33 $mg/m^2/yr$. It may be due to industrial activities, the use of phosphate fertilizers in agricultural activity, or the effect of long-range atmospheric transport in Hungary (Otvös et al., 2003). The total depositions of Cd, Cu, Pb and Zn in Poland, Germany and Austria have been shown to be higher than that in other countries in Europe. Industrial processes are likely an important source of heavy metals, with Poland, Germany and Austria located in central Europe, where is an industrialized region (Harmens et al., 2010).

Zn was also found to be the most abundant anthropogenic metal in the atmospheric deposition in selected provinces in China, except for Jiangxi (Fig. 4). Jiangxi Province is the largest copper mining, smelting and processing base in China. The increase in mining activity has strongly influenced the excess input of heavy metals (specifically Cu) in soils (Guo et al., 2012). The atmospheric deposition fluxes of Cd, Cu and Pb were much more variable than that for Zn, differed by up to an order of magnitude, and are probably indicative of local differences in conditions and releases to the atmosphere. Because of the limited availability of data on atmospheric deposition (e.g., from one-third of the provinces in China), these values are not considered to be representative of the country as a whole.

Through a direct comparison of Fig. 3 and Fig. 4, annual atmospheric inputs of heavy metals (Cd, Cu, Pb and Zn) in European countries are approximately one order of magnitude lower than that in Chinese provinces. The reasons for this apparent discrepancy are unclear. Direct comparison of deposition rates is complicated, given differences in methods of collecting and measuring deposited materials, as well as in the environments where samples were collected (e.g., urban, rural or remote) (Kondo et al., 2016). At the national scale, annual atmospheric input of Cd, Cu, Pb and Zn to agricultural soils in China was 0.4, 10.67, 20 and 64.08 $mg/m^2/yr$, respectively, totalling 95.15 $mg/m^2/yr$ (Luo et al., 2009). Flux of heavy metals from atmospheric deposition in European countries ranged from 3.09 $mg/m^2/yr$ in Finland to 68.2 $mg/m^2/yr$ in Poland. Comparisons between European countries and China at the national scale reflected larger atmospheric deposition of heavy metals in China raising concerns over the potential long-term environmental and health implications of excessive atmospheric deposition of heavy metals.

4.3. Uncertainty

Previous inventories provide the basic information to control heavy metal accumulation in agricultural soils and effectively manage agroecosystem. Nevertheless, there will still be a number of uncertainties in heavy metal balances researches.

Data limitations and the complexity of soil environmental management, as well as non-consideration of various factors (e.g., wind erosion, leakage, seeds as fodder transformed into animal manure) affecting input fluxes, can artificially magnify or reduce heavy metal accumulations. Moreover, data sources for input and output pathways differ primarily with respect to the spatial scale as mentioned earlier. Data regarding leaching, erosion and crop harvesting are available at the field scale; however, data regarding atmospheric deposition, fertilizer and irrigation are available at the regional scale. Thus, uncertainty is present when a nationwide inventory is used for small or specific regions due to the variation in agricultural amendments and the spatial and temporal heterogeneity of heavy metal sources.

Industrial structural adjustments, changes in farming practices, policy, land use, management measures and environmental conditions

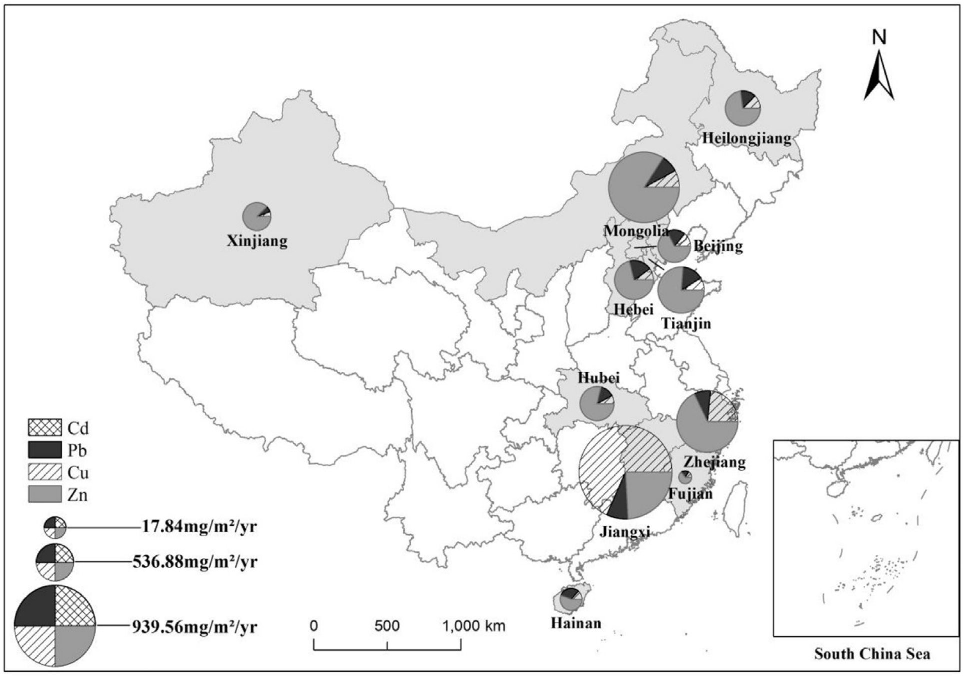

Fig. 4. *Flux of heavy metals from atmospheric deposition in several provinces of China* (Beijing, Tianjin, Hebei: Pan and Wang, 2015; Fujian: Wu et al., 2006; Hainan: Jiang et al., 2014; Heilongjiang: Xia et al., 2014; Hubei: Xu et al., 2015; Jiangxi: Tao et al., 2014; Mongolia: Yin et al., 2014; Xinjiang: Wei et al., 2013; Zhejiang: Huang et al., 2011.).

have caused some inventories to become outdated. The phase-out of leaded gasoline started in the 1990s and spread nationwide in 2000 in China (Xu et al., 2012). The ban of leaded gasoline use can greatly reduce emissions of lead into the atmosphere (Miller and Friedland, 1994). Sewage irrigation has been widely used in China since 1972 (Meng et al., 2016), but it containing heavy metals in agricultural production was first banned on January 28, 2013 (Meng et al., 2016). Therefore, there will be an uncertainty for inputs of heavy metals to agricultural soils via atmospheric deposition and sewage sludge in the inventory (Luo et al., 2009). The atmospheric deposition flux data were collected from 1999 to 2006, and sewage sludge data were based on the published data in 2000s in currently the only inventory of heavy metal inputs to agricultural soils in China (Luo et al., 2009). Therefore, a timely updated inventory of heavy metal inputs to agricultural soils in China is an urgent task to better identify the sources of heavy metals.

5. Conclusions

Input and output inventory has been proved to be an effective method for evaluating heavy metal accumulation in soil. More and more countries/regions have conducted inventory studies, it is interesting to find that inventories varied greatly among different countries/regions due to the temporal and spatial scales, economic development, industrial and agricultural activities, geography, and soil properties. As for China, atmospheric deposition is the most important pathway of heavy metal input to agricultural soil, while animal manure, mineral fertilizers and pesticides are the predominant sources in European countries. It should be noted that there are still many aspects that need further improvement. For examples, the selection of dominant input and output pathways should be more accurate according to actual investigation; More concerns should be paid to fundamental works related to other possible sources and sinks, which would be greatly helpful for update of inventories; In addition, when we assess fluxes using formula calculation and model-based estimation, the differentiation of data need to be processed, which would seriously influence the precision of the result.

Acknowledgement

This work was supported by the National Key Research and Development Program of China (2016YFD0800302), Central Level, Scientific Research Institutes for Basic R&D Special Fund Business (2016YSKY032).

Appendix A. Supplementary material

Supplementary data associated with this article can be found in the online version at doi:10.1016/j.ecoenv.2018.08.016.

References

Ahmadi, D.S., Karami, M., Afyuni, M., 2016. Regional-scale fluxes of zinc, copper, and nickel into and out of the agricultural soils of the Kermanshah province in western Iran. Environ. Monit. Assess. 188 (4), 1–18.

Bach, J., Starmans, D., 2005. Heavy metals balance in Polish and Dutch agronomy: actual state and previsions for the future. Agr. Ecosyst. Environ. 107 (4), 309–316.

Belon, E., Boisson, M., Deportes, I.Z., Eglin, T.K., Feix, I., Bispo, A.O., Galsomies, L., Leblond, S., Guellier, C.R., 2012. An inventory of trace elements inputs to French agricultural soils. Sci. Total. Environ. 439 (22), 87–95.

Bengtsson, H., Alvenäs, G., Nilsson, S.I., Hultman, B., Öborn, I., 2006. Cadmium, copper and zinc leaching and surface run-off losses at the Öjebyn farm in Northern Sweden—Temporal and spatial variation. Agr. Ecosyst. Environ. 113 (1), 120–138.

Bigalke, M., Ulrich, A., Rehmus, A., Keller, A., 2017. Accumulation of cadmium and uranium in arable soils in Switzerland. Environ. Pollut. 221, 85–93.

Bonten, L.T.C., Romkens, P.F.A.M., Brus, D.J., 2008. Contribution of heavy metal leaching from agricultural soils to surface water loads. Environ. Forensics 9 (2–3), 252–257.

Bvon, S., Keller, A., Schulin, R., 1998. Regional mass flux balancing for controlling gentle soil remediation operations. Nutr. Cycl. Agroecosys. 50 (1–3), 303–306.

Cambier, P., Pot, V., Mercier, V., Michaud, A., Benoit, P., Revallier, A., Houot, S., 2014. Impact of long-term organic residue recycling in agriculture on soil solution composition and trace metal leaching in soils. Sci. Total Environ. 499 (15), 560–573.

Dobson, P.F., Ghezzehei, T.A., Cook, P.J., Rodríguez-Pineda, J.A., Villalba, L., la Garza, R.D., 2012. Heterogeneous seepage at the Nopal I natural analogue site, Chihuahua, Mexico. Hydrogeol. J. 20 (1), 155–166.

Dorioz, J.M., 2013. Mechanisms and control of agricultural diffuse pollution: the case of phosphorus. BMC Ophthalmol. 15 (1), 1–8.

Duddridge, J.E., Wainwright, M., 1981. Heavy metals in river sediments—calculation of metal adsorption maxima using Langmuir and Freundlich isotherms. Environ. Pollut. 2 (5), 387–397.

Dulac, F., Buat-Ménard, P., Ezat, U., Melki, S., Bergametti, G., 1989. Atmospheric input of trace metals to the western Mediterranean: uncertainties in modelling dry deposition from cascade impactor data. Tellus B. 41B (3), 362–378.

Eckel, H., Roth, U., Döhler, H., Nicholson, F., Unwin, R., 2005. Assessment and reduction of heavy metal input into agro-ecosystems. KTBL Publisher.

European Community, 2003. Commission regulation (EC) No 1334/2003 of 25 July 2003 amending the conditions for authorization of a number of additives in feeding stuffs belongs to the group of trace elements. Off. J. Eur. Union L187, 11–15 (26 July

2003).

Godlinski, F., Aust, M.O., Travis, G., Hao, X.Y., Thiele-Bruhn, S., McAllister, T.A., Leinweber, P., 2011. Phosphorus and trace metal distribution under confined cattle feeding operations in Southern Alberta. Landbauforsch. Volk. 61 (3), 249–260.

Gray, C.W., Mclaren, R.G., Roberts, A.H.C., 2003. Atmospheric accessions of heavy metals to some New Zealand pastoral soils. Sci. Total. Environ. 305 105–115 (1–3).

Guo, S., Zhao, Y.Y., Qu, H.C., Wu, D.X., Xu, H., Li, C., Liu, Y., Zhu, X.Y., Wang, Z.K., 2012. Geological characteristics and ore-forming time of the Dexing porphyry copper ore mine in Jiangxi Province. Acta Geol. Sin. 86 (3), 691–699.

Harmens, H., Norris, D.A., Steinnes, E., Kubin, E., Piispanen, J., Alber, R., 2010. Mosses as biomonitors of atmospheric heavy metal deposition: spatial patterns and temporal trends in Europe. Environ. Pollut. 158 (10), 3144–3156.

Hou, J.Y., Shen, Y., Cao, S.P., Cheng, X.J., Wang, W.X., 2013. Heavy metal flux research in Tianjin suburb vegetable farmland. Journal of Anhui Agricultural Sciences, 41 (13) 5764–5773 in Chinese.

Hou, Q., Yang, Z., Ji, J., Yu, T., Chen, G., Li, J., Xia, X., Zhang, M., Yuan, X., 2014. Annual net input fluxes of heavy metals of the agroecosystem in the Yangtze River delta, China. J. Geochem. Explor. 139 (1), 68–84.

Huang, C.L., Song, J.Q., Pan, W.F., 2011. Impact of dry and wet atmospheric deposition on content of heavy metals in soils along coastal areas of eastern Zhejiang Province. Geol. Bull. China 30 (9), 1434–1441 (in Chinese).

Huang, Y., Li, T.Q., Wu, C.X., He, Z.L., Japenga, J., Deng, M.H., Yang, X.E., 2015. An integrated approach to assess heavy metal source apportionment in pen-urban agricultural soils. J. Hazard. Mater. 299, 540–549.

Jiang, W., Hou, Q.Y., Yang, Z.F., Yu, T., Zhong, C., Yang, Y., Fu, Y.R., 2014. Annual input fluxes of heavy metals in agricultural soil of Hainan Island, China. Environ. Sci. Pollut. Res. 21 (13), 7876–7885.

Karami, M., Amini, M., Afyuni, M., Khoshgoftarmanesh, A.H., Keller, A., Abdia, A., Schulin, R., 2014. Agricultural zinc fluxes into soils and crops of central Iran at regional scale. Arch. Agron. Soil Sci. 60 (3), 437–456.

Keller, A., Schulin, R., 2003. Modelling regional-scale mass balances of phosphorus, cadmium and zinc fluxes on arable and dairy farms. Eur. J. Agron. 20 (1–2), 181–198.

Keller, A., Steiger, B.V., van der Zee, S.E.A.T.M., Schulin, R., 2001. A stochastic empirical model for regional heavy-metal balances in agroecosystems. J. Environ. Qual. 30 (6), 1976–1989.

Kondo, M.C., Sharma, R., Plante, A.F., Yang, Y., Burstyn, I., 2016. Elemental concentrations in urban green stormwater infrastructure soils. J. Environ. Qual. 45 (1), 107–118.

Leclerc, A., Laurent, A., 2017. Framework for estimating toxic releases from the application of manure on agricultural soil: national release inventories for heavy metals in 2000–2014. Sci. Total Environ. 590–591, 452–460.

Liu, F., Cheng, H.X., Yang, K., Zhao, C.D., Liu, Y.H., Peng, M., Li, K., 2014. Characteristics and influencing factors of mercury exchange flux between soil and air in Guangzhou City. J. Geochem. Explor. 139 (1), 115–121.

Lopes, C., Herva, M., Franco-Uría, A., Roca, E., 2011. Inventory of heavy metal content in organic waste applied as fertilizer in agriculture: evaluating the risk of transfer into the food chain. Environ. Sci. Pollut. Res. 18 (6), 918–939.

Luo, L., Ma, Y.B., Zhang, S.Z., Wei, D.P., Zhu, Y.G., 2009. An inventory of trace element inputs to agricultural soils in China. J. Environ. Manage. 90. pp. 2524–2530.

Luo, Y., Duan, L., Xu, G., Hao, J., 2015. Inhibition of mercury release from forest soil by high atmospheric deposition of Ca^{2+} and $SO_4$2-. Chemosphere 134, 113–119.

Maskall, J., Whitehead, K., Gee, C., Thornton, I., 1996. Long-term migration of metals at historical smelting sites. Appl. Geochem. 11 (1), 43–51.

Mcgrath, S.P., Chang, A.C., Page, A.L., Witter, E., 1994. Land application of sewage sludge: scientific perspectives of heavy metal loading limits in Europe and the United States. Environ. Rev. 2 (1), 108–118.

Meng, W., Wang, Z., Hu, B., Wang, Z., Li, H., Goodman, R.C., 2016. Heavy metals in soil and plants after long-term sewage irrigation at Tianjin China: a case study assessment. Agr. Water Manag. 171, 153–161.

Miller, E.K., Friedland, A.J., 1994. Lead migration in forest soils: response to changing atmospheric inputs. Environ. Sci. Technol. 28 (4), 662–669.

Misseyer, M.P., Van der Most, P.F.J., 1993. Decision support systems for environmental impact assessment: addressing the industrial need. Work. Conf. Comput. Support Environ. Impact Assess. 301–310.

Moolenaar, S.W., Lexmond, T.M., 1998. Heavy-metal balances of agro-ecosystems in the Netherlands. Neth. J. Agr. Sci. 46 (2), 171–192.

Nicholson, F.A., Smith, S.R., Alloway, B.J., Carlton-Smith, C., Chambers, B.J., 2003. An inventory of heavy metals inputs to agricultural soils in England and Wales. Sci. Total Environ. 311 (1–3), 205–219.

Nicholson, F.A., Mciwem, S.R.S., Alloway, B.J., Carlton-Smith, C., Chambers, B.J., 2006. Quantifying heavy metal inputs to agricultural soils in England and wales. Water Environ. J. 20, 87–95.

Otvös, E., Pazmandi, T., Tuba, Z., 2003. First national survey of atmospheric heavy metal deposition in Hungary by the analysis of mosses. Sci. Total Environ. 309 (1), 151–160.

Pan, Y.P., Wang, Y.S., 2015. Atmospheric wet and dry deposition of trace elements at 10 sites in Northern China. Atmos. Chem. Phys. 14 (2), 951–972.

Peng, C., Wang, M.E., Chen, W.P., 2016. Modelling cadmium contamination in paddy soils under long-term remediation measures: model development and stochastic Simulations. Environ. Pollut. 216, 146–155.

Salman, S.A., Elnazer, A.A., Nazer, H.A.E., 2017. Integrated mass balance of some heavy metals fluxes in Yaakob village, south Sohag, Egypt. Int. J. Environ. Sci. Technol. 14 (5), 1011–1018.

Sharma, R.K., Agrawal, M., Marshall, F.M., 2008. Atmospheric deposition of heavy metals (Cu, Zn, Cd and Pb) in Varanasi City, India. Environ. Monit. Assess. 142 (1–3), 269–278.

Steiger, B.V., Obrist, J., 1993. Available databases for the assessment of regional mass balances in agricultural land. Birkhäuser Basel. 35–46.

Tao, M.J., Zhou, J., Liang, J.N., Cui, H.B., Xu, L., Zhu, Z.Q., 2014. Atmospheric deposition of heavy metals in farmland area around a copper smelter. J. Agro-Environ. Sci. 33 (7), 1328–1334 (in Chinese).

Vries, W.D., Mclaughlin, M.J., 2013. Modeling the cadmium balance in Australian agricultural systems in view of potential impacts on food and water quality. Sci. Total Environ. 240 (7), 461–462.

Wang, M., Chen, W., Peng, C., 2016b. Risk assessment of Cd polluted paddy soils in the industrial and township areas in Hunan, southern China. Chemosphere 144, 346–351.

Wei, Z.S., Tu, Q.J., Zhang, X.M., Zhao, X.J., 2013. A study of heavy metal elements fluxes and sources from dry atmospheric deposition in the area of Urumqi and Changji. Xinjiang Geol. 31, 36–40 (in Chinese).

Williams, P.N., Ming, L., Sun, G.X., Huang, Q., Ying, L., Deacon, C., Meharg, A.A., Zhu, Y.G., 2009. Occurrence and partitioning of cadmium, arsenic and lead in mine impacted paddy rice: hunan, China. Environ. Sci. Technol. 43 (3), 637–642.

Wu, C.X., Qi, S.H., Fang, M., Su, Q.K., 2006. Precipitation characteristics of heavy metal in dustfall to Quanzhou Bay of Fujian Province. Res. Environ. Sci. 19 (6), 27–30 (in Chinese).

Xia, X.Q., Yang, Z.F., Cui, Y.J., Li, Y.S., Hou, Q.Y., Yu, T., 2014. Soil heavy metal concentrations and their typical input and output fluxes on the southern Song-nen Plain, Heilongjiang Province, China. J. Geochem. Explor. 139 (1), 85–96.

Xiong, A.Q., Chen, Y.C., DaiY., Hou, J.H., Yi, T.H., 2016. Study on Lead Flux in Vegetable-based Soil in Chongqing Suburb Based on Heavy Metals Flow. Environ. Impact Assess. 38 (6), 92–96 in Chinese.

Xu, H.L., Li, D.Y., Yang, J., Zhang, X., Zhu, L.L., 2015. Preliminary study on flux of atmospheric dry and wet deposition of heavy metal elements in Yunmeng county, Hubei province. Resour. Environ. Eng. 29 (6), 816–821 (in Chinese).

Xu, H.M., Cao, J.J., Ho, K.F., Ding, H., Han, Y.M., Wang, G.H., Chow, J.C., Watson, J.G., Khol, S.D., Qiang, J., Li, W.T., 2012. Lead concentrations in fine particulate matter after the phasing out of leaded gasoline in Xi'an, China. Atmos. Environ. 46 (46), 217–224.

Yin, L.L., Jia, K.L., Shi, X.H., Zhao, S.N., Yang, F., Wu, Y., 2014. Atmospheric deposition characteristics and fluxes of heavy metals in Lake Ulansuhai. J. Lake Sci. 26 (6), 931–938 (in chinese).

Yun, H.J., Yi, S.M., Kim, Y.P., 2002. Dry deposition fluxes of ambient particulate heavy metals in a small city, Korea. Atmos. Environ. 36 (35), 5449–5458.

Science of the Total Environment 618 (2018) 777–784

Contents lists available at ScienceDirect

Science of the Total Environment

journal homepage: www.elsevier.com/locate/scitotenv

Residuals, bioaccessibility and health risk assessment of PAHs in winter wheat grains from areas influenced by coal combustion in China

Kai Tian [a,b], Huanyu Bao [a,b], Xuechen Zhang [a,b], Taoran Shi [a,b], Xueping Liu [c], Fuyong Wu [a,b,]*

[a] *College of Natural Resources and Environment, Northwest A&F University, Yangling 712100, Shaanxi, PR China*
[b] *Key Laboratory of Plant Nutrition and the Agri-environment in Northwest China, Ministry of Agriculture, Yangling 712100, Shaanxi, PR China*
[c] *School of Municipal and Environment Engineering, Henan University of Urban Construction, Pingdingshan 467036, PR China*

HIGHLIGHTS

- The winter wheat grains from the PAHs-contaminated areas were seriously contaminated with PAHs.
- The bioaccessibility of PAHs in the winter wheat grains was apparently higher than that in animal-based foods and in fish.
- The values of ILCR based on total PAHs were higher than 10^{-6} and some even fell the range of 10^{-5}–10^{-4}.

GRAPHICAL ABSTRACT

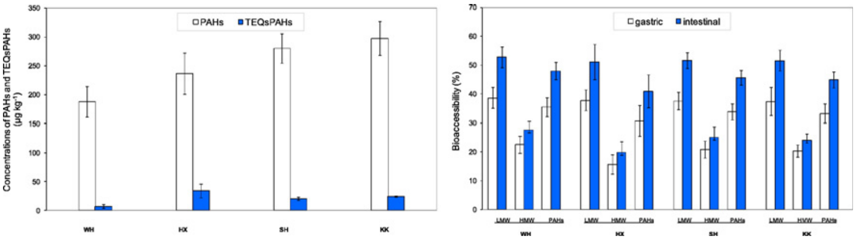

ARTICLE INFO

Article history:
Received 25 April 2017
Received in revised form 16 August 2017
Accepted 16 August 2017
Available online 25 October 2017

Editor: Adrian Covaci

Keywords:
Polycyclic aromatic hydrocarbons
Residual level
Cereal
Gastrointestinal digestion model
Bioaccessibility

ABSTRACT

Polycyclic aromatic hydrocarbons (PAHs) contamination in atmospheric and soil was serious, which is mainly due to high level of emission of PAHs in China resulted from the predominating use of coal in energy consumption and continuous development of economy and society for years. However, the status of PAHs in winter wheat grains from the areas influenced by coal combustion in China was still not clear. During harvest season, the winter wheat grains were collected from agricultural fields surrounding coal-fired power plants located in Shaanxi and Henan Provinces. This study found that the mean concentrations of 15 priority PAHs ranged from 69.58 to 557.0 μg kg^{-1}. Three-ring PAHs (acenaphthene, acenaphthylene, fluorene, phenanthrene and anthracene) were dominant in the grains, accounting for approximately 70–81% of the total PAHs. The bioaccessibility of low molecular weight (LMW, 2–3 ring) PAHs (51.1–52.8%), high molecular weight (HMW, 4–6 ring) PAHs (19.8–27.6%) and total PAHs (40.9–48.0%) in the intestinal condition was significantly ($p < 0.001$) higher than that (37.4–38.6%; 15.6–22.5%; 30.7–35.5%) in the gastric condition, respectively. Based on total PAHs, the values of incremental lifetime cancer risk (ILCR) for children, adolescents, adults and seniors were all higher than the baseline value (10^{-6}) and some even fell in the range of 10^{-5}–10^{-4}, which indicated that most grains from the areas affected by coal combustion possessed considerable cancer risk. The present study also indicated that the children were the age group most sensitive to PAHs contamination. The pilot research provided relevant information for the regulation of PAHs in the winter wheat grains and for the safety of the agro-products growing in the PAHs-contaminated areas.

1. Introduction

Polycyclic aromatic hydrocarbons (PAHs) are ubiquitous organic pollutants that raise environmental concerns because of their being

---

* Corresponding author at: College of Natural Resources and Environment, Northwest A&F University, Yangling 712100, Shaanxi, PR China.
E-mail addresses: fuyongwu@nwsuaf.edu.cn, wfy09@163.com (F. Wu).

https://doi.org/10.1016/j.scitotenv.2017.08.174
0048-9697/

toxic, mutagenic, and carcinogenic, which are chief byproducts of incomplete combustion of fossil fuels and biomass and pyrosynthesis of organic materials (Mastral and Callen, 2000). As semi volatile chemicals, PAHs can be transported in the atmosphere over long distances and deposited on land and water surfaces through dry or wet deposition (Srogi, 2007). Mainly due to the predominating use of coal in energy consumption and continuous development of economy and society, emission of PAHs in China has maintained high level for years. The annual PAHs emission of China was up to 106,000 tons in 2007, accounting for 21% of the global total emission (Shen et al., 2013), which has resulted in seriously PAHs contamination in atmospheric and soil. According to recent nationwide surveys, 1.4% of soil samples were contaminated with PAHs based on China's soil environmental quality limits (The Ministry of Environmental Protection, 2014). The status of soils in areas surrounding metal smelting, thermal power, urban heating and oil refining plants is especially serious (Xu et al., 2006). Because energy consumption structure being given priority to coal will not change significantly in the coming decades, severe PAHs contamination in China is expected to continue. Therefore, there is urgent need to pay more attention to the safety of the agro-products growing in the PAHs-contaminated areas.

China is one of the primary winter wheat producing countries, with a total cultivated area of 24.1 million ha in 2011 (China Statistical Yearbook, 2016). Central, north and northwest China including Hebei, Shandong, Henan and Shaanxi Provinces not only are main producing areas of the winter wheat, but also are the predominant areas of coal production and consumption. Thousands of hectares of agricultural soils are planted with winter wheat surrounding plenty of coal combustion enterprises such as coal-fired power plants, coking plants and urban heating plants. Previous investigations showed that PAHs concentrations in the winter wheat grains from Taiyuan and Tianjin China were far higher than those in Catalonia, Spain (Martí-Cid et al., 2008; Li, 2007; Xia et al., 2010). Generally, dietary intake is the main (>70%) way of exposure to PAHs for nonsmokers and non-occupationally exposed populations (Phillips, 1999; Alomirah et al., 2011; Ma and Harrad, 2015), with cereals and vegetables showing the greatest contribution. A number of epidemiological studies have shown that a large proportion of human cancers are attributable, at least in part, to dietary exposure to PAHs (Harris et al., 2013; Abid et al., 2014; Muscaritoli et al., 2016). Wheat is a staple food in north China and in the central plains. Therefore, it is critical to investigate the status of PAHs in the wheat grains from the areas influenced by coal combustion in China.

The oral bioaccessibility is defined as the fraction of a compound that is released from its matrix in the gastrointestinal tract, and thus becomes available for intestinal absorption (Oomen et al., 2000). Using total extractable PAHs from contaminated foods for health risk assessment may result in an over estimation of the amount of contaminants absorbed via dietary intake (Harris et al., 2013). Based on in vivo studies, it was observed that the absorption rate of benzo(a)pyrene was only 33% in pigs (Laurent et al., 2002) and 12% in lactating goats (Grova et al., 2002). Therefore, for assessing human health risks posed by PAHs, bioavailability should be taken into consideration. Although ingestion of PAHs through diet far exceeds the amount accidentally ingested through soil, much of focus is so far centered on PAHs bioaccessibility in soil (Ruby et al., 2016). Few studies have been conducted on the bioaccessibility of PAHs in fishes and animal-based foods, respectively (Wang et al., 2010; Yu et al., 2012). However, there is a lack of information concerning the bioaccessibility of PAHs in cereals.

We hypothesized that the winter wheat from areas affected by coal combustion might have been contaminated to some degree with PAHs, and the winter wheat grains would pose differential health risks via accumulation of different PAHs. The major objectives of the present study were: (1) to determine concentrations and bioaccessibility of PAHs in the winter wheat grains from areas affected by coal combustion and; (2) to evaluate the potential health risks of the collected grains to the local residents.

2. Materials and methods

2.1. Wheat grain sample collection

During the harvest season of the winter wheat (from 27 May to 10 June 2015), whole plants were collected from agricultural fields surrounding coal-fired power plants, including the Weihe power plant (WH) and the second power plant of Hu county (HX) in Xi'an City, Shaanxi Province, the Sanhe thermal power plant (SH) and the pithead power plant (KK) in Pingdingshan City, Henan Province (Fig. S1). A global positioning system (GPS) was utilized in identification of the precise location of each site. The whole plants were sampled according to Fig. S2. The plant samples at each point were collected from at least one plot (5 × 5 m). Each plot was sampled from three random points. Along the same direction, there were 50 m between two neighboring sampling points. After sampling and transportation to the laboratory, the grains were manually harvested and thoroughly washed with running tap water to remove airborne dust and soil particles. The grains were air-dried, weighed to determine the biomass, and milled to pass through a 70-mesh sieve. All samples were kept frozen at −18 °C before PAHs analysis.

2.2. PAHs analyses

Each samples (about 4 g) were Soxhlet extracted for 16–18 h with 120 mL of acetone and dichloromethane (DCM) mixture (1:3, *v*/v) (USEPA, 1996a). The concentrated extracts were clean up using a florisil column (15 cm silica gel, and 1.0 cm anhydrous sodium sulfate from bottom up, pre-eluted with 20 mL n-hexane) with 70 mL hexane/DCM mixture (1:1) as elution solvent (USEPA, 1996b). The silica gel was baked at 450 °C for 6 h, activated at 300 °C for 12 h, and deactivated with deionized water (3%, *w*/w) prior to use. The anhydrous sodium sulfate was baked at 450 °C for 8 h. The eluants were then evaporated and exchanged with methanol to a final volume of 2.0 mL.

PAHs in samples were analyzed using HPLC (Shimadzu, LC-20A) equipped with a ultraviolet detector (SPD-20A) and a fluorescence detector (PF-20A). The UV detector was operated at fixed wave lengths of 290 and 254 nm, and the in-series fluorescence spectrophotometer wavelength programmed according to elution time. The analytical system included a PAH-specific reverse column (Φ3.0 × 250 mm Intersil ODS-SP column, 3 μm, Shimadzu, Kyoto, Japan) and a mixture of methanol and ultrapure water as the mobile phase. A flow rate of 0.6 mL min^{-1} was maintained at 40 °C and the equilibration time was set at 5 min. The elution profile employed as follows: 0–3 min 90% methanol; 3–12 min 90–97% methanol; constant 97% methanol for 23 min; 35–40 min 80% methanol. Sixteen US EPA priority PAHs were measured in the present study: naphthalene (NAP), acenaphthylene (ACY), acenaphthene (ACE), fluorene (FLO), phenanthrene (PHE), anthracene (ANT), fluoranthene (FLA), pyrene (PYR), benzo(a)anthracene (BaA), chrysene (CHR), benzo(b)fluoranthene (BbF), benzo(k)fluoranthene (BkF), benzo(a)pyrene (BaP), indeno(1,2,3-c,d)pyrene (IcdP), dibenzo(a,h)-anthracene (DahA) and benzo(g,h,i)perylene (BghiP).

2.3. Oral bioaccessibility of PAHs in the winter wheat grains

Determination of the digestible fraction of PAHs in the winter wheat grains followed the method described by Wang et al. (2010) with slight modification. Briefly, about 4.0 g of air-dried samples were first placed in a 50 mL capped centrifuge tube with 30 mL of synthetic gastric juice (5.0% *w*/*v* pepsin in 0.15 M NaCl, acidified with HCl to pH 1.8) and shaken at 100 rpm for 1 h at 37 °C in the dark. After gastric digestion, the mixtures were centrifuged (15 min, at 37 °C and 1500 rpm), and all suspensions were transferred to new tubes for further cleanup and PAHs analyses. Twenty milliliters of artificial intestinal juice (1.5%, *w*/*v* pancreatin, 0.5%, w/v amylase, and 0.3% w/v bile salts, in 0.15 M

NaCl, pH 6.8) was added into the residues, and the mixture was resuspended and shaken at 30 rpm and 37 °C for 6 h in the dark. Finally, the tubes were centrifuged at 1500 rpm and 37 °C for 15 min to separate supernatant and solid. Both gastric and intestinal supernatants were extracted using liquid-liquid shaking method, with 50 mL of hexane twice and with 50 mL of DCM once, respectively. All of the extracts were concentrated to 2.0 mL using a rotary evaporator (IKA-RV8, Germany) and passed through a florisil column for purification according to the method previously used. The eluants were solvent exchanged to methanol for PAHs analyses. Blanks were prepared by containing the enzyme treatment in series without wheat samples. The bioaccessibility (% BA) of PAHs in gastric or intestinal juice was calculated as the ratio of the amount of PAHs in liquid phase to that in the grains (Eq. 1).

$$\%\mathrm{BA} = (\text{extratable PAHs in the gastric or intestinal juice}/\text{total PAHs}) \times 100 \tag{1}$$

2.4. QA/QC

QA/QC was conducted by performing method blanks, standard reference material recoveries, standard spiked recoveries and HPLC detection limits. The limit of detection (LOD) using the present method was determined as the concentrations of analyzes in a sample that gave rise to a peak with a signal-to-noise ratio (S/N) of 3, which ranged from 0.06 to1.41 μg kg^{-1}. The recoveries of individual PAHs ranged from 80.76.% for DahA to 192.04% for Nap. For each batch of 12 samples, a method blank (solvent), a spiked blank (standards spiked into solvent), a sample duplicate, and a standard reference material (NIST SRM 2977) sample were processed. PAHs were identified on the basis of retention times relative to five deuterated internal standards (naphthalene-d_8, acenaphthene-d_{10}, phenanthrene-d_{10}, chrysene-d_{12} and perylene-d_{12}). The variation coefficients of PAHs concentrations between duplicate samples were <10%. The levels of PAHs in digestion blank were less than the LOD.

2.5. Risk assessment of dietary exposure

The incremental lifetime cancer risk (ILCR) of PAHs through the consumption of winter wheat grains was calculated as follows:

$$\mathrm{BEC} = \textstyle\sum_{i=1}^{n} (C_i \times \mathrm{TEF}_i) \tag{2}$$

where BEC (μg kg^{-1}) is the potency equivalent concentration of PAHs; TEF_i and C_i are the toxic equivalency factor (TEF) and concentration (μg kg^{-1}) of an individual PAH congener, respectively. The toxicity equivalent concentrations of PAHs (TEQs) are based on the TEF with respect to BaP values (Nisbet and LaGoy, 1992).

The population of local residents including city and countryside were divided into eight groups according to age and gender: children (4–10 years), adolescents (11–17 years), adults (18–60 years) and seniors (61–70 years) of male as well as the above groups of female. The daily dietary PAH exposure level (E_D) through the winter wheat grains for each group was calculated as follows:

$$E_D = \mathrm{BEC} \times \mathrm{IR} \tag{3}$$

where BEC = B[*a*]P equivalent concentration of PAHs in the winter wheat grains (ng g^{-1}); IR = ingestion amount of wheat grains per day (g d^{-1}). Ingestion amount of foods by each group was obtained from survey on the Chinese national health and nutrition II conducted by Zhai and Yang (2006). We treated BEC and IR, which followed log-normal and normal distribution, respectively, in Eq. (3).

$$\mathrm{ILCR} = (E_D \times \mathrm{EF} \times \mathrm{ED} \times \mathrm{SF} \times \mathrm{CF})/(\mathrm{BW} \times \mathrm{AT}) \tag{4}$$

where E_D = the daily dietary PAH exposure level (ng d^{-1}); EF = the exposure frequency (365 d y^{-1}); ED = exposure duration (y) (for children: ED = 7; for adolescents: ED = 7; for adults: ED = 43; for seniors: ED = 10) (Xia et al., 2010); SF = oral cancer slope factor of BaP (4.5, 5.9, 9.0 and 11.7, with a geometric mean of 7.3 per [(mg kg^{-1}) d^{-1}] (Brune et al., 1981; USEPA, 1991a, 1991b, 2001); CF = conversion factor (10^{-6} mg ng^{-1}); BW = body weight (kg), body weight of each group was obtained from the Survey on the Chinese national health and nutrition II conducted by Zhai and Yang (2006); AT = average lifespan for carcinogens (25,550 days). We treated ED, SF and BW, which obeyed log-normal, log-normal and normal distributions, respectively, in Eq. (4).

2.6. Data analyses

NAP was not included in the total PAHs reported in the present study because of its higher recovery (>100%) and higher percentage in the total PAHs. Statistical analyses were conducted using SPSS 19.0 (SPSS Inc., USA). Means of different groups were compared using one-way ANOVA test. Prior to one-way ANOVA, the data was log transformed to meet the normality assumption. Unless otherwise indicated, all treatment means were tested for significant difference at $p < 0.05$.

3. Results and discussion

3.1. Levels of PAHs in the winter wheat grains

The mean concentrations of PAHs (sum of the 3–6 ring PAHs) ranged from 69.58 to 557.0 μg kg^{-1} in the winter wheat grains collected form areas affected by coal combustion located in Shaanxi and Henan Provinces, with an average of 187.7 μg kg^{-1} (WH), 236.4 μg kg^{-1} (HX), 280.3 μg kg^{-1} (SH) and 297.3 μg kg^{-1} (KK) as shown in Table 1. There were insignificant variations in concentrations of PAHs among the four sites. The level of 15 priority PAHs (mean 245.5 μg kg^{-1}) in the winter wheat grains in the present study were apparently higher than those from market of Taiyuan (161.5 μg kg^{-1}) (Xia et al., 2010), Tianjin (177 μg kg^{-1}) of China (Li, 2007), Catalonia of Spain (27.9 μg kg^{-1}) (Martí-Cid et al., 2008) and Rothamsted experimental station of England (4–46 μg kg^{-1}) (Jones et al., 1989). PAHs can enter into the winter wheat via foliar uptake and soil-root uptake (Tao et al., 2009). The higher PAHs in the winter wheat grains should be attributed to heavily PAHs contamination in air and soil of the planted area affected by coal combustion. It was estimated that China was the country with the highest PAH emissions in the global in 2007 (Shen et al., 2013). The mean particulate phase PAHs concentration in the North China Plain was 346 ng m^{-3} in the winter of 2005, which is 8.9 times of London and 4.9 times of Chicago, respectively (Liu et al., 2007; Dimashki et al., 2001; Sun et al., 2006). Up to 1665 μg kg^{-1} PAHs has been recorded in the soils from a coke production base in Shanxi Province, China (Duan et al., 2015). The present study showed that the status of the wheat grains was serious from areas affected by coal combustion. The levels of BaP in the grains from WH, HX, SH and KK were 5.75, 6.44, 18.98 and 22.57 times of the maximum levels (1.0 μg kg^{-1}) suggested by the commission regulation (EC No 1881, 2006), respectively. These implied that levels of PAHs, especially BaP, in the wheat grains from the areas affected by coal combustion posed a significant threat to human health. Wheat, which was most consumed by residents of Shaanxi and Henan Provinces, also had high level of total PAHs (245.5 μg kg^{-1}) in comparison with rice (86.3 μg kg^{-1}) and vegetables (5.97–56.9 μg kg^{-1}) (Xia et al., 2010). It was investigated that Taiyuan residents in China suffered from heavy risk of dietary exposure to PAHs and the winter wheat accounted for 48.3–53.5% of the total dietary intake of PAHs (Xia et al., 2010). Thus, minimizing the transfer of PAHs from soil and air to the wheat grains is a top priority around the sampled area.

Table 1
Summary of measured PAHs in grains of the winter wheat collected from agricultural fields surrounding coal-fired power plants, including the Weihe power plant (WH) and the second power plant of Hu county (HX) in Xi'an City, Shaanxi province, the Sanhe thermal power plant (SH) and the pithead power plant (KK) in Pingdingshan City, Henan province.

Compounds	Aromatic ring	WH ($n = 16$)					HX ($n = 11$)					SH ($n = 13$)					KK ($n = 11$)				
		Mean	SD	Median	Min	Max	Mean	SD	Median	Min	Max	Mean	SD	Median	Min	Max	Mean	SD	Median	Min	Max
ACE	3	85.0	39.6	75.7	24.1	187	74.9	60.1	72.0	5.39	218.2	70.8	35.2	72.1	2.68	153	77.7	40.5	76.4	6.27	285
ACY	3	15.3	4.84	15.7	6.25	27.3	25.4	3.70	24.7	17.4	41.04	36.1	6.82	35.6	23.3	56.2	30.6	5.43	30.0	18.7	41.8
FLO	3	17.8	5.71	19.0	7.32	26.5	26.8	4.79	26.8	2.64	39.71	40.5	4.96	40.4	29.1	54.3	42.8	5.05	41.9	36.2	59.8
PHE	3	31.4	24.0	27.3	7.96	113	33.3	26.4	23.2	12.4	125.2	65.7	38.1	66.6	8.92	176	69.9	36.4	66.9	4.74	264
ANT	3	4.04	0.83	4.19	2.40	5.22	4.94	0.46	4.90	3.69	6.88	5.22	0.56	5.26	4.06	6.71	5.22	0.83	5.17	3.66	9.56
FLA	4	8.59	1.76	8.94	5.48	11.5	10.7	1.56	10.6	5.51	14.85	13.5	3.35	12.9	9.21	33.1	13.2	4.21	12.3	9.00	30.6
PYR	4	9.39	2.15	9.07	6.78	17.7	7.74	4.14	9.35	0.00	13.05	13.4	3.06	12.6	10.7	32.3	14.9	5.90	13.2	9.90	38.7
BaA	4	2.50	1.30	2.21	0.95	8.07	1.76	0.84	1.49	1.04	4.86	1.83	0.63	1.70	0.52	4.23	1.91	0.82	1.57	0.75	3.80
CHR	4	2.50	1.68	2.22	0.22	8.47	2.74	1.69	2.60	n.d.	8.11	6.57	2.06	6.26	4.87	18.5	7.98	3.66	7.11	5.27	26.4
BbF	5	3.91	1.10	3.76	1.92	7.24	3.00	1.52	2.71	n.d.	9.19	5.69	10.0	1.99	0.00	40.7	8.78	14.4	1.70	0.00	50.6
BkF	5	1.56	1.04	2.16	n.d.	2.96	0.30	0.77	0.00	n.d.	2.26	0.81	0.48	0.83	0.00	3.61	0.87	0.16	0.86	0.28	1.26
BaP	5	5.75	6.06	2.69	n.d.	17.5	6.44	6.99	3.13	n.d.	29.60	19.0	4.94	18.9	2.38	35.7	22.6	2.22	22.0	16.6	28.1
DahA	5	n.d.	n.d.	n.d.	n.d.	0.00	26.7	26.3	11.9	n.d.	66.88	n.d.	n.d.	n.d.	n.d.	n.d.	n.d.	n.d.	n.d.	n.d.	n.d.
IcdP	6	n.d.	n.d.	n.d.	n.d.	n.d.	n.d.	n.d.	n.d.	n.d.	n.d.	n.d.	n.d.	n.d.	n.d.	n.d.	n.d.	n.d.	n.d.	n.d.	n.d.
BghiP	6	n.d.	n.d.	n.d.	n.d.	0.00	11.7	8.43	10.4	n.d.	29.82	1.31	1.34	0.95	n.d.	6.01	0.86	0.51	0.69	0.48	2.92
LMWPAHs[a]		154	47.7	154	48.5	253	165	69.6	162	78.4	322.8	218	49.4	202	149	347	226	51.5	221	164	449
HMWPAHs[b]		34.2	8.72	34.21	20.3	47.5	71.1	32.1	57.0	26.8	122.9	62.1	14.2	59.7	30.7	123	71.0	19.0	59.9	47.9	110
$\sum$ PAHs[c]		188	52.6	188	69.6	295	236	71.3	230	107.6	378.5	280	51.0	273	191	406	297	59.3	291	225	557
TEQs-PAHs[d]		6.79	6.12	4.08	0.64	18.5	34.0	23.7	19.3	7.19	70.7	20.2	5.09	20.0	2.71	37.3	24.1	2.70	24.0	17.3	29.1

n.d. indicating that it is not detectable

[a] Low molecular weight 2–3 ring PAHs.

[b] High molecular weight 4–6 ring PAHs.

[c] ΣPAHs concentrations excluding NAP.

[d] Total TEQs-PAH concentrations, PAH toxic equivalency factor with respect to BaP (Nisbet and LaGoy, 1992).

3.2. Composition profiles of PAHs

The composition profiles of 15 PAHs in the winter wheat grains were comparable among WH, SH and KK (Fig. 1). However, a significantly ($p < 0.01$) higher percentage of six-ring PAHs (BghiP) was observed in the wheat grains from HX (5.0%) than those from WH (0%), SH (0.47%) and KK (0.29%), respectively. Most PAHs detected were low molecular weight (LMW, 2–3 ring) ones. Three-ring PAHs (ACE, ACY, FLO, PHE and ANT) were dominant in the grains, accounting for approximately 70–81% of the total PAHs (Fig. 1). Among PAHs detected, ACE was predominant, accounting for 25.3–45.3% of the total PAHs, followed by PHE (14.1–23.5%) (Table 1). The LMW PAHs in the winter grains was greater mainly due to their higher solubility. Similarly, Xia et al. (2010) also found that 2–3 ring PAHs were dominant in the winter grains collected from the market of Taiyuan, China. Four-ring PAHs (FLA, PYR, BaA and CHR) accounted for 9.7–12.8% of the total PAHs, and those with five-ring (BbF, BkF, BaP and DahA) accounted for 6.0–15.4%. In addition, DahA was only detected in the wheat grains from HX. Except IcdP, 5–6 ring PAHs were detected in the wheat grains from areas affected by coal combustion (Table 1). The present results suggest that 3-ring PAHs had the highest tendency to be taken up by the grains whereas 5–6 ring PAHs had the lowest likelihood of being taken up. The 5–6 ring PAHs accounted for a small part of sum PAHs in the grains, implying that the ones are more difficult to be absorbed and translocated to the grains. Jones et al. (1989) also reported the detection of 2–6 ring PAHs in wheat grains under field conditions. However, Li and Ma (2016) found that no 5–6 ring PAHs were detected in the wheat grains from a soil-wheat system with amendments of sewage sludge. Generally, plants uptake PAHs via two pathways: air-plant pathway (foliar uptake) and air-soil-plant pathway (root uptake) (Desalme et al., 2013). Because of their high hydrophobicity, five to six ring PAHs are generally assumed to be tightly bound to soil particles and weakly bioavailable even for the most water-soluble PAHs which demonstrate high sorption to organic matter in soil and low desorption capacity (Amellal et al., 2006; Pilon-Smits, 2005). Therefore, it is assumed that the 5–6 ring PAHs entered into the winter wheat grains mainly via air-plant pathway and detailed process need to further investigate.

3.3. Oral bioaccessibility of PAHs

Fig. 2 shows that the bioaccessibility of LMW PAHs (51.1–52.8%), the high molecular weight (HMW, 4–6 ring) PAHs (19.8–27.6%) and total PAHs (40.9–48.0%) in the intestinal condition was significantly ($p < 0.001$) higher than those (37.4–38.6%; 15.6–22.5% and 30.7–35.5%) in the gastric condition, respectively. This could be possibly due to the

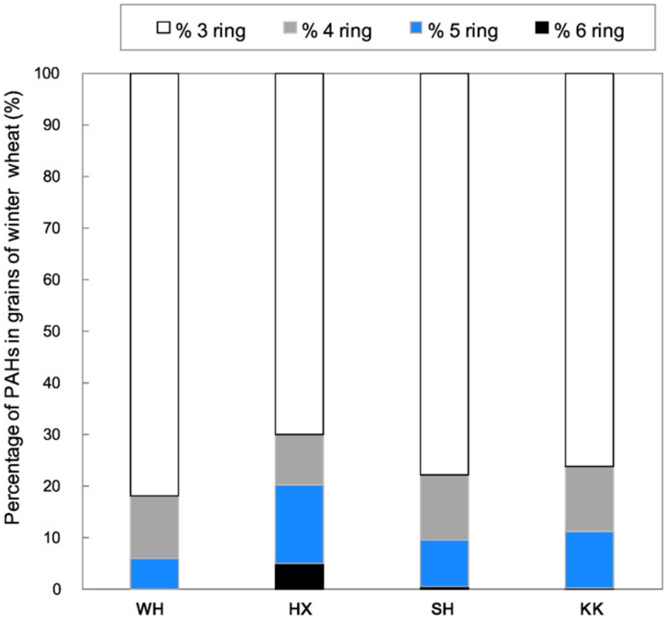

Fig. 1. Percentage contribution of different molecular weight PAHs groups in the winter wheat grains from agricultural fields surrounding coal-fired power plants, including the Weihe power plant (WH) and the second power plant of Hu county (HX) in Xi'an City, Shaanxi Province, the Sanhe thermal power plant (SH) and the pithead power plant (KK) in Pingdingshan City, Henan Province.

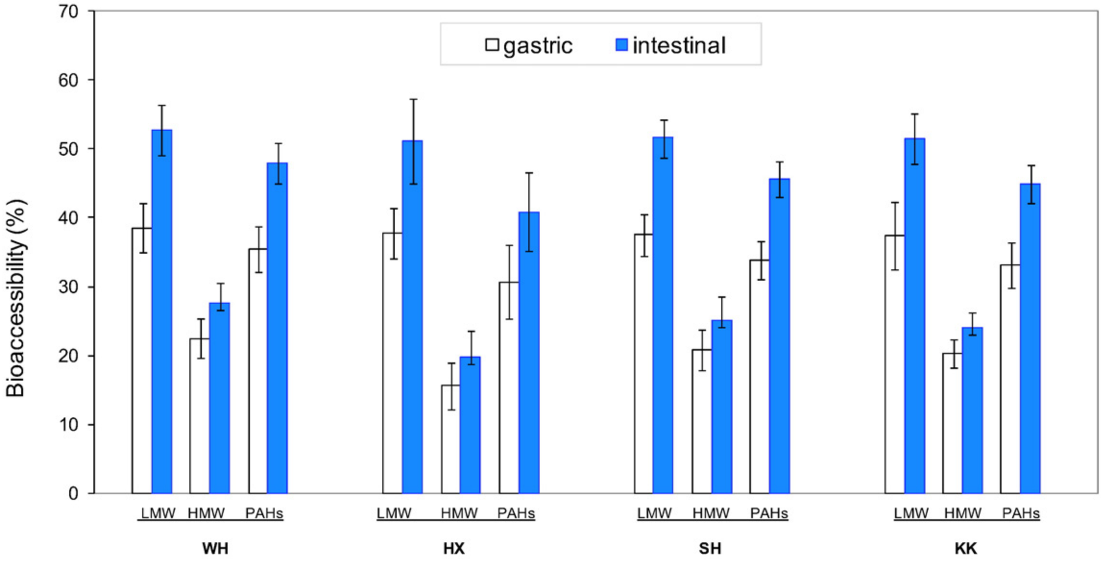

Fig. 2. Bioaccessibilities of different molecular weight PAHs in the winter wheat grains from agricultural fields surrounding coal-fired power plants, including the Weihe power plant (WH, n = 16) and the second power plant of Hu county (HX, n = 11) in Xi'an City, Shaanxi Province, the Sanhe thermal power plant (SH, n = 13) and the pithead power plant (KK, $n = 11$) in Pingdingshan City, Henan Province in gastric and intestinal conditions.

formation of micelles in the aqueous suspensions by bile constituents (Tang et al., 2006). Wang et al. (2010) also found that the bioaccessibility of total PAHs in fishes in the intestinal condition (12.6–42.6%, mean of 31.1%) was significantly ($p < 0.01$) higher than that in the gastric condition (12.1–37.9%, mean of 24.3%). As expected, the bioaccessibility of LMW PAHs in the wheat grains was significantly ($p < 0.001$) higher than HMW PAHs in both gastric and intestinal conditions. For PAH congeners, the oral bioaccessibility ranged from 8.0 (BghiP) to 51.3% (ACY) in gastric condition and from 10.7 (BghiP) to 63.7% (ACY) in intestinal condition (Fig. 3). No significant ($p > 0.05$) difference of bioaccessibility among the four sites was observed in both gastric and intestinal conditions. PAHs are generally lipophilic. Besides their physicochemical properties including molecular weight (MW), water solubility, octanol water partition coefficients (K_{OW}), and octanol-air partition coefficient (K_{OA}), lipid contents in foods also influenced the bioaccessibility of PAHs (Wang et al., 2010). The mean bioaccessibility of PAHs in the winter wheat grains (78.7%) was higher than that in animal-based foods (29.0–61.2%) and in fish (55.4%), primarily due to the lower lipid

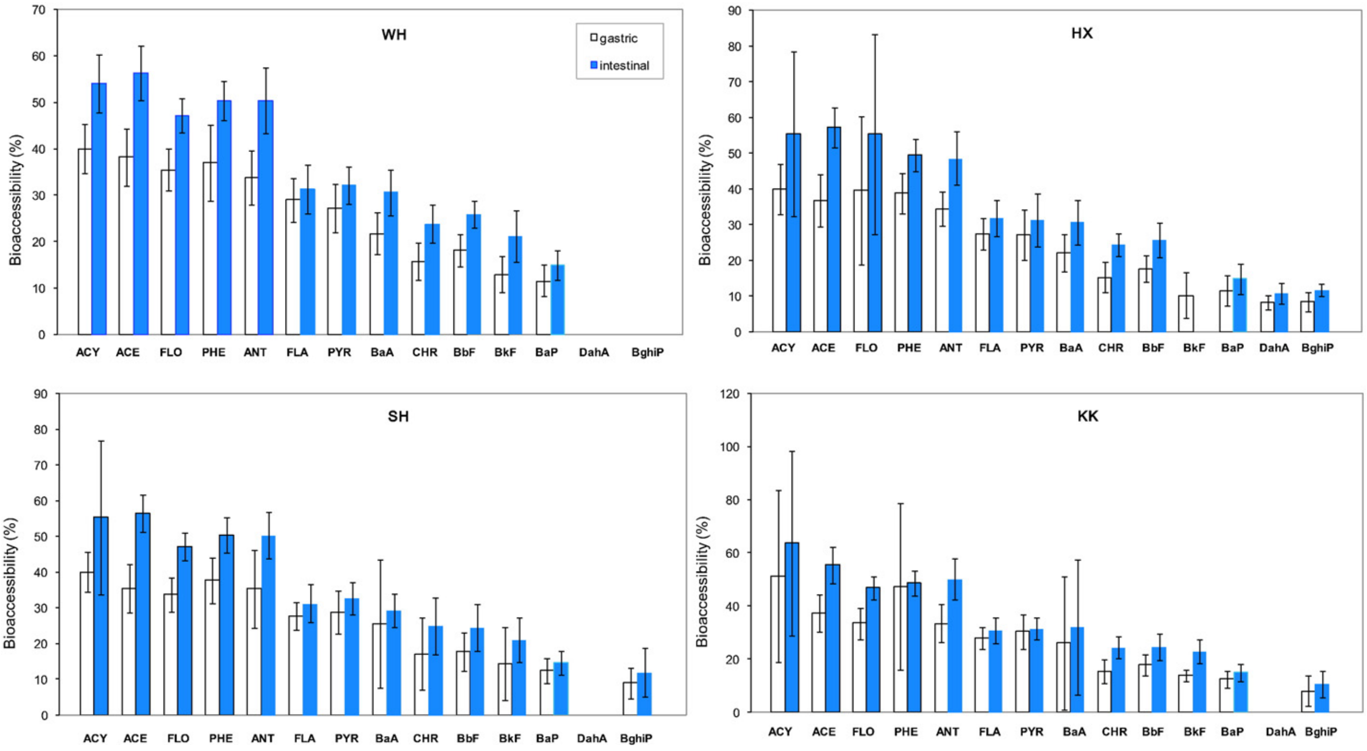

Fig. 3. Average bioaccessibility of grain PAH congeners of the winter wheat from agricultural fields surrounding coal-fired power plants, including the Weihe power plant (WH) and the second power plant of Hu county (HX) in Xi'an City, Shaanxi Province, the Sanhe thermal power plant (SH) and the pithead power plant (KK) in Pingdingshan City, Henan Province in gastric and intestinal conditions.

Table 2

Incremental lifetime cancer risk (ILCR) values for PAHs in grains of the winter wheat collected from agricultural fields surrounding coal-fired power plants, including the Weihe power plant (WH) and the second power plant of Hu county (HX) in Xi'an City, Shaanxi province, the Sanhe thermal power plant (SH) and the pithead power plant (KK) in Pingdingshan City, Henan province.

Site	Age	Gender	WH (n = 16)				HX (n = 11)				SH (n = 13)				KK (n = 11)			
			Mean	Median	Min	Max	Mean	Median	Min	Max	Mean	Median	Min	Max	Mean	Median	Min	Max
Based on the total PAHs in wheat grains																		
City	Children	Male	1.5E-05	9.1E-06	1.4E-06	4.1E-05	3.1E-04	1.4E-04	3.6E-05	7.5E-04	4.5E-05	4.4E-05	6.0E-06	8.3E-05	5.4E-05	5.3E-05	3.8E-05	6.5E-05
		Famale	1.5E-05	8.9E-06	1.4E-06	4.0E-05	3.1E-04	1.4E-04	3.5E-05	7.4E-04	4.4E-05	4.4E-05	5.9E-06	8.1E-05	5.3E-05	5.2E-05	3.8E-05	6.3E-05
	Adolescents	Male	1.2E-05	7.1E-06	1.1E-06	3.2E-05	2.5E-04	1.1E-04	2.8E-05	5.9E-04	3.5E-05	3.5E-05	4.7E-06	6.5E-05	4.2E-05	4.2E-05	3.0E-05	5.1E-05
		Famale	1.0E-05	6.2E-06	9.6E-07	2.8E-05	2.1E-04	9.5E-05	2.4E-05	5.1E-04	3.0E-05	3.0E-05	4.1E-06	5.6E-05	3.6E-05	3.6E-05	2.6E-05	4.4E-05
	Adults	Male	6.5E-05	3.9E-05	6.1E-06	1.8E-04	1.4E-03	6.0E-04	1.6E-04	3.3E-03	1.9E-04	1.9E-04	2.6E-05	3.6E-04	2.3E-04	2.3E-04	1.7E-04	2.8E-04
		Famale	6.1E-05	3.6E-05	5.7E-06	1.7E-04	1.3E-03	5.6E-04	1.4E-04	3.0E-03	1.8E-04	1.8E-04	2.4E-05	3.3E-04	2.2E-04	2.1E-04	1.5E-04	2.6E-04
	Seniors	Male	1.4E-05	8.6E-06	1.3E-06	3.9E-05	3.0E-04	1.3E-04	3.4E-05	7.2E-04	4.3E-05	4.2E-05	5.7E-06	7.9E-05	5.1E-05	5.1E-05	3.7E-05	6.1E-05
		Famale	1.4E-05	8.7E-06	1.4E-06	4.0E-05	3.0E-04	1.3E-04	3.5E-05	7.2E-04	4.3E-05	4.3E-05	5.8E-06	8.0E-05	5.1E-05	5.1E-05	3.7E-05	6.2E-05
Countryside	Children	Male	1.9E-05	1.2E-05	1.8E-06	5.3E-05	4.0E-04	1.8E-04	4.6E-05	9.7E-04	5.8E-05	5.7E-05	7.8E-06	1.1E-04	6.9E-05	6.9E-05	5.0E-05	8.3E-05
		Famale	2.1E-05	1.2E-05	1.9E-06	5.6E-05	4.3E-04	1.9E-04	4.9E-05	1.0E-03	6.1E-05	6.1E-05	8.2E-06	1.1E-04	7.3E-05	7.3E-05	5.2E-05	8.8E-05
	Adolescents	Male	1.6E-05	9.4E-06	1.5E-06	4.3E-05	3.2E-04	1.4E-04	3.7E-05	7.8E-04	4.7E-05	4.6E-05	6.3E-06	8.6E-05	5.6E-05	5.6E-05	4.0E-05	6.7E-05
		Famale	1.5E-05	9.2E-06	1.4E-06	4.2E-05	3.2E-04	1.4E-04	3.6E-05	7.6E-04	4.5E-05	4.5E-05	6.1E-06	8.4E-05	5.4E-05	5.4E-05	3.9E-05	6.5E-05
	Adults	Male	8.7E-05	5.3E-05	8.2E-06	2.4E-04	1.8E-03	8.1E-04	2.1E-04	4.4E-03	2.6E-04	2.6E-04	3.5E-05	4.8E-04	3.1E-04	3.1E-04	2.2E-04	3.7E-04
		Famale	8.0E-05	4.8E-05	7.5E-06	2.2E-04	1.7E-03	7.4E-04	1.9E-04	4.0E-03	2.4E-04	2.3E-04	3.2E-05	4.4E-04	2.8E-04	2.8E-04	2.0E-04	3.4E-04
	Seniors	Male	2.0E-05	1.2E-05	1.8E-06	5.4E-05	4.1E-04	1.8E-04	4.7E-05	9.8E-04	5.9E-05	5.8E-05	7.9E-06	1.1E-04	7.0E-05	7.0E-05	5.0E-05	8.4E-05
		Famale	1.8E-05	1.1E-05	1.7E-06	4.8E-05	3.7E-04	1.6E-04	4.2E-05	8.8E-04	5.3E-05	5.2E-05	7.1E-06	9.7E-05	6.3E-05	6.3E-05	4.5E-05	7.6E-05
Based on the digestible PAHs in wheat grains																		
City	Children	Male	4.7E-06	3.3E-06	7.7E-07	1.2E-05	5.9E-05	3.1E-05	7.5E-06	1.8E-04	1.3E-05	1.3E-05	1.7E-06	2.8E-05	1.5E-05	1.5E-05	8.3E-06	2.3E-05
		Famale	4.6E-06	3.2E-06	7.5E-07	1.2E-05	5.8E-05	3.1E-05	7.3E-06	1.7E-04	1.3E-05	1.3E-05	1.7E-06	2.8E-05	1.5E-05	1.5E-05	8.1E-06	2.2E-05
	Adolescents	Male	3.7E-06	2.6E-06	6.0E-07	9.6E-06	4.6E-05	2.5E-05	5.9E-06	1.4E-04	1.0E-05	1.0E-05	1.4E-06	2.2E-05	1.2E-05	1.2E-05	6.5E-06	1.8E-05
		Famale	3.2E-06	2.2E-06	5.2E-07	8.3E-06	4.0E-05	2.1E-05	5.1E-06	1.2E-04	8.9E-06	8.7E-06	1.2E-06	1.9E-05	1.1E-05	1.0E-05	5.6E-06	1.5E-05
	Adults	Male	2.0E-05	1.4E-05	3.3E-06	5.3E-05	2.6E-04	1.4E-04	3.2E-05	7.6E-04	5.7E-05	5.5E-05	7.5E-06	1.2E-04	6.7E-05	6.7E-05	3.6E-05	9.8E-05
		Famale	1.9E-05	1.3E-05	3.1E-06	4.9E-05	2.4E-04	1.3E-04	3.0E-05	7.0E-04	5.3E-05	5.1E-05	7.0E-06	1.1E-04	6.2E-05	6.2E-05	3.3E-05	9.0E-05
	Seniors	Male	4.4E-06	3.1E-06	7.3E-07	1.2E-05	5.6E-05	3.0E-05	7.1E-06	1.7E-04	1.2E-05	1.2E-05	1.6E-06	2.7E-05	1.5E-05	1.5E-05	7.9E-06	2.1E-05
		Famale	4.5E-06	3.1E-06	7.4E-07	1.2E-05	5.7E-05	3.0E-05	7.2E-06	1.7E-04	1.3E-05	1.2E-05	1.7E-06	2.7E-05	1.5E-05	1.5E-05	8.0E-06	2.2E-05
Countryside	Children	Male	6.0E-06	4.2E-06	9.9E-07	1.6E-05	7.6E-05	4.0E-05	9.6E-06	2.3E-04	1.7E-05	1.6E-05	2.2E-06	3.6E-05	2.0E-05	2.0E-05	1.1E-05	2.9E-05
		Famale	6.3E-06	4.4E-06	1.0E-06	1.7E-05	8.1E-05	4.3E-05	1.0E-05	2.4E-04	1.8E-05	1.7E-05	2.4E-06	3.8E-05	2.1E-05	2.1E-05	1.1E-05	3.1E-05
	Adolescents	Male	4.8E-06	3.4E-06	8.0E-07	1.3E-05	6.2E-05	3.2E-05	7.8E-06	1.8E-04	1.4E-05	1.3E-05	1.8E-06	2.9E-05	1.6E-05	1.6E-05	8.6E-06	2.3E-05
		Famale	4.7E-06	3.3E-06	7.8E-07	1.2E-05	6.0E-05	3.2E-05	7.6E-06	1.8E-04	1.3E-05	1.3E-05	1.7E-06	2.8E-05	1.6E-05	1.6E-05	8.4E-06	2.3E-05
	Adults	Male	2.7E-05	1.9E-05	4.5E-06	7.1E-05	3.4E-04	1.8E-04	4.3E-05	1.0E-03	7.6E-05	7.4E-05	1.0E-05	1.6E-04	9.0E-05	8.9E-05	4.8E-05	1.3E-04
		Famale	2.5E-05	1.7E-05	4.1E-06	6.5E-05	3.1E-04	1.7E-04	4.0E-05	9.3E-04	6.9E-05	6.7E-05	9.2E-06	1.5E-04	8.2E-05	8.1E-05	4.4E-05	1.2E-04
	Seniors	Male	6.1E-06	4.3E-06	1.0E-06	1.6E-05	7.7E-05	4.1E-05	9.8E-06	2.3E-04	1.7E-05	1.7E-05	2.3E-06	3.7E-05	2.0E-05	2.0E-05	1.1E-05	2.9E-05
		Famale	5.5E-06	3.8E-06	9.0E-07	1.4E-05	6.9E-05	3.7E-05	8.8E-06	2.1E-04	1.5E-05	1.5E-05	2.0E-06	3.3E-05	1.8E-05	1.8E-05	9.7E-06	2.6E-05

contents in the wheat grains (1.3%) than those in animal-based foods (1.0–6.7%) and fishes (1.1–12.7%) (Kobayashi et al., 2007; Wang et al., 2010; Yu et al., 2012). It was observed that lipids may decrease the intake of BaP in vitro model in everted intestinal segments from channel catfish (Weber and Lanno, 2001). Similarly, Xing et al. (2008) also observed that high-lipid food may have a much lower bioaccessibility of polychlorinated biphenyls (PCBs) than low-lipid food, for which lipid is difficult to digest and PCBs are more difficult to be released from the food matrix.

3.4. Health risk assessment of the winter wheat grains

The ILCR was used to assess the potential health hazards to residents exposed to PAHs contamination in the wheat grains from areas affected by coal combustion. According to the US EPA, one in a million chance of additional human cancer over a 70 year lifetime ($\text{ILCR} = 10^{-6}$) is considered acceptable or inconsequential, while additional lifetime cancer risk of one in ten thousand or greater ($\text{ILCR} = 10^{-4}$) is considered serious and there is high priority for paying attention to such health problem (USEPA, 1996c). Based on total and digestible PAHs in the wheat grains, the ILCR of total cancer risk for children, adolescents, adults and seniors in the areas affected by coal combustion are presented in Table 2. The mean values of ILCR based on total PAHs for all population groups were higher than the baseline value of acceptable risk (10^{-6}) and some even fell in the range of 10^{-5}–10^{-4}. When the bioaccessibility of PAHs was considered, the ILCR values for most residents still fell in the range of 10^{-6}–10^{-5}. These suggested that most grains from areas affected by coal combustion possessed significant cancer risk. The ILCR values in the present results were apparently higher than dietary health risk assessment for PAHs in Taiyuan and the Yangtze River Delta region of China (Xia et al., 2010; Wang et al., 2017). Due to the fact that air, soil and other foods such as vegetables form the sampled area must be contaminated with PAHs, the present risk assessment might somewhat underestimate the actual risk. It was investigated that the ILCR values for residents induced by soils were higher than the acceptable risk level (10^{-6}) in industrial areas of the Yangtze River Delta region of China (Wang et al., 2017). Therefore it is urgent to take appropriate measures to control the health risk due to dietary PAH exposure via wheat grains in the areas affected by coal combustion.

Depending on the potency equivalent concentration of PAHs in the wheat grains, the highest ILCR was found in HX, followed by KK, SH and WH (Table 2). The values of ILCR for residents was up to 1.81×10^{-3} in HX, where the wheat grains possessed significantly ($p < 0.01$) higher percentage of 6-ring PAHs (BghiP) than those from WH, SH and KK (Fig. 1). Generally, the residents in countryside possessed higher ILCR values than those in city. With respect to gender, males (9.51×10^{-5}, 7.47×10^{-5} and 4.12×10^{-4}) showed a little higher ILCR values than females (9.32×10^{-5}, 6.47×10^{-5} and 3.82×10^{-4}) in groups of children, adolescents and adults, which was in accordance with dietary intake of wheat grains (Table S1). According to age, the ranking of ILCR in decreasing order was adults > children > seniors > adolescents for both males and females (Table 2). Considering exposure duration for children (7 years) was much higher for adults (43 years), the present study indicated that the children were the age group most sensitive to PAH contamination. Although the dietary exposure of PAHs via the wheat grains for the children was less than that of both the adolescents and the seniors, the body weight of children was much lower (Table S1), resulting in higher ILCR value than adolescents and seniors. In addition, due to their hand-to mouth activity, the dietary exposure of PAHs via soils or dusts for the children was more than those for the adults, adolescents and seniors (Wang et al., 2011, 2017). Furthermore, early development of organ, nervous, and immune systems could probably enhance the carcinogens sensitivity in children (Maertens et al., 2008). Thus, the health risk for the children exposed to PAHs in the wheat grains should be paid enough attention.

4. Conclusion

This paper attempted to report a pilot research on levels and health risk assessment of PAHs in the winter wheat grains from areas influenced by coal combustion in China. The present study showed that the winter wheat grains were seriously contaminated with PAHs with concentrations in the range of 69.6–557 μg kg^{-1}. The bioaccessibility of PAHs in the winter wheat grains (78.7%) was apparently higher than that in animal-based foods (29.0–61.2%) and in fish (55.4%), respectively. The present study indicated that most grains from areas affected by coal combustion possessed significant cancer risk and the children were the age group most sensitive to PAH contamination. Finally, the results of this investigation provide relevant information for the regulation of PAHs in the wheat grain and for the safety of the agro-products growing in the PAHs-contaminated areas.

Acknowledgement

We sincerely thank Dr. Mukesh Kumar Awasthi from Northwest A&F University for improving the manuscript. The financial support from National Natural Science Foundation of China (41571456), Program for Science & Technology Innovation Talents in Universities of Henan Province (14HASTIT048) and the Scientific Research Foundation for the Introduction of Talent, Northwest A&F University, China (2014) is gratefully acknowledged.

Appendix A. Supplementary data

Supplementary data to this article can be found online at https://doi.org/10.1016/j.scitotenv.2017.08.174.

References

Abid, Z., Cross, A.J., Sinha, R., 2014. Meat, dairy, and cancer. Am. J. Clin. Nutr. 100, 386S–393S.

Alomirah, H., Al-Zenki, S., Al-Hooti, S., Zaghloul, S., Sawaya, W., Ahmed, N., Kannan, K., 2011. Concentrations and dietary exposure to polycyclic aromatic hydrocarbons (PAHs) from grilled and smoked foods. Food Control 22, 2028–2035.

Amellal, S., Boivin, A., Ganier, C.P., Schiavon, M., 2006. High sorption of phenanthrene in agricultural soils. Agron. Sustain. Dev. 26, 99–106.

Brune, H., Deutsch-Wenzel, R.P., Habs, M., Ivankovic, S., Schmahl, D., 1981. Investigation of the tumorigenic response to benzo[a]pyrene in aqueous caffeine solution applied orally to Sprague–Dawley rats. J. Cancer Res. Clin. Oncol. 102, 153–157.

China Statistical Yearbook, 2016. Beijing: China Statistical Press p. (475-390).

Desalme, D., Binet, P., Chiapusio, G., 2013. Challenges in tracing the fate and effects of atmospheric polycyclic aromatic hydrocarbon deposition in vascular plants. Environ. Sci. Technol. 47, 3967–3981.

Dimashki, M., Lim, L.H., Harrison, R.M., Harrad, S., 2001. Temporal trends, temperature dependence, and relative reactivity of atmospheric polycyclic aromatic hydrocarbons. Environ. Sci. Technol. 35, 2264–2267.

Duan, Y., Shen, G., Tao, S., Hong, J., Chen, Y., Xue, M., Li, T., Su, S., Shen, H., Fu, X., Meng, Q., Zhang, J., Zhang, B., Han, X., Song, K., 2015. Characteristics of polycyclic aromatic hydrocarbons in agricultural soils at a typical coke production base in Shanxi, China. Chemosphere 127, 64–69.

EC No 1881, 2006. Setting maximum levels for certain contaminants in foodstuffs. Off. J. Eur. Union.

Grova, N., Feidt, C., Laurent, C., Rychen, G., 2002. [C-14] Milk, urine and faeces excretion kinetics in lactating goats after an oral administration of [C-14] polycyclic aromatic hydrocarbons. Int. Dairy J. 12, 1025–1031.

Harris, K.L., Banks, L.D., Mantey, J.A., Huderson, A.C., Ramesh, A., 2013. Bioaccessibility of polycyclic aromatic hydrocarbons: relevance to toxicity and carcinogenesis. Expert Opin. Drug Metab. Toxicol. 9, 1465–1480.

Jones, K.C., Grimmer, G., Jacob, J., Johnston, A.E., 1989. Changes in the polynuclear aromatic hydrocarbon content of wheat grain and pasture grassland over the last century from one site in the U.K. Sci. Total Environ. 78, 117–130.

Kobayashi, R., Cahill, T.M., Okamoto, R.A., Maddalena, R.L., Kado, N.Y., 2007. Controlled exposure chamber study of uptake and clearance of airborne polycyclic aromatic hydrocarhons by wheat grain. Environ. Sci. Technol. 41, 7934–7940.

Laurent, C., Feidt, C., Grova, N., Mpassi, D., Lichtfouse, E., Laurent, F., Rychen, G., 2002. Portal absorption of C-14 after ingestion of spiked milk with C-14-phenanthrene, C-14-benzo[a]pyrene or C-14-TCDD in growing pigs. Chemosphere 48, 843–848.

Li, X.R., 2007. Spatial distribution pattern of emission, dispersion and exposure of polycyclic aromatic hydrocarbons in Tianjin, China. Thesis of PhD. Peking University, Beijing, China, p. 152.

Li, H.L., Ma, Y.B., 2016. Field study on the uptake, accumulation, translocation and risk assessment of PAHs in a soil-wheat system with amendments of sewage sludge. Sci. Total Environ. 560, 55–56.

Liu, S.Z., Tao, S., Liu, W.X., Liu, Y.N., Dou, H., Zhao, J.Y., Wang, L.G., Wang, J.F., Tian, Z.F., Gao, Y., 2007. Atmospheric polycyclic aromatic hydrocarbons in north China: a wintertime study. Environ. Sci. Technol. 41, 8256–8261.

Ma, Y., Harrad, S., 2015. Spatiotemporal analysis and human exposure assessment on polycyclic aromatic hydrocarbons in indoor air, settled house dust, and diet: a review. Environ. Int. 17, 7–16.

Maertens, R.M., Yang, X.F., Zhu, J.P., Gagne, R.W., Douglas, G.R., White, P.A., 2008. Mutagenic and carcinogenic hazards of settled house dust I: polycyclic aromatic hydrocarbon content and excess lifetime cancer risk from preschool exposure. Environ. Sci. Technol. 42, 1747–1753.

Martí-Cid, R., Llobet, J.M., Castell, V., Domingo, J.L., 2008. Evolution of the dietary exposure to polycyclic aromatic hydrocarbons in Catalonia, Spain. Food Chem. Toxicol. 46, 3163–3171.

Mastral, A.M., Callen, M.S., 2000. A review on polycyclic aromatic hydrocarbon (PAH) emission from energy generation. Environ. Sci. Technol. 34, 3051–3057.

Muscaritoli, M., Amabile, M.I., Molfino, A., 2016. Foods and their components promoting gastrointestinal cancer. Curr. Opin. Clin. Nutr. Metab. Care 19, 377–381.

Nisbet, I.C.T., LaGoy, P.K., 1992. Toxic equivalency factors (TEFs) for polycyclic aromatic hydrocarbons (PAHs). Regul. Toxicol. Pharmacol. 16, 290–300.

Oomen, A.G., Sips, A., Groten, J.P., Sijm, D., Tolls, J., 2000. Mobilization of PCBs and lindane from soil during in vitro digestion and their distribution among bile salt micelles and proteins of human digestive fluid and the soil. Environ. Sci. Technol. 34, 297–303.

Phillips, D.H., 1999. Polycyclic aromatic hydrocarbons in the diet. Mutat. Res. 443, 139–147.

Pilon-Smits, E., 2005. Phytoremediation. Annual Review of Plant Biology. vol. 56. Annual Reviews, Palo Alto, pp. 15–39.

Ruby, M.V., Lowney, Y.W., Bunge, A.L., Roberts, S.M., Gomez-Eyles, J.L., Ghosh, U., Kissel, J.C., Tomlinson, P., Menzie, C., 2016. Oral bioavailability, bioaccessibility, and dermal absorption of PAHs from soil-state of the science. Environ. Sci. Technol. 50, 2151–2164.

Shen, H.Z., Huang, Y., Wang, R., Zhu, D., Li, W., Shen, G.F., Wang, B., Zhang, Y.Y., Chen, Y.C., Lu, Y., Chen, H., Li, T.C., Sun, K., Li, B.G., Liu, W.X., Liu, J.F., Tao, S., 2013. Global atmospheric emissions of polycyclic aromatic hydrocarbons from 1960 to 2008 and future predictions. Environ. Sci. Technol. 47, 6415–6424.

Srogi, K., 2007. Monitoring of environmental exposure to polycyclic aromatic hydrocarbons: a review. Environ. Chem. Lett. 5, 169–195.

Sun, P., Blanchard, P., Brice, K.A., Hites, R.A., 2006. Trends in polycyclic aromatic hydrocarbon concentrations in the Great Lakes atmosphere. Environ. Sci. Technol. 40, 6221–6227.

Tang, X.Y., Tang, L., Zhu, Y.G., Xing, B.S., Duan, J., Zheng, M.H., 2006. Assessment of the bioaccessibility of polycyclic aromatic hydrocarbons in soils from Beijing using an in vitro test. Environ. Pollut. 140, 279–285.

Tao, Y.Q., Zhang, S.Z., Zhu, Y.G., Christie, P., 2009. Uptake and acropetal translocation of polycyclic aromatic hydrocarbons by wheat (*Triticum aestivum* L.) grown in field-contaminated soil. Environ. Sci. Technol. 43, 3556–3560.

The Ministry of Environmental Protection, 2014. The Ministry of Land and Resources Report on the national soil contamination survey. http://www.mep.gov.cn/gkml/hbb/qt/201404/t20140417_270670.htm, Accessed date: 27 August 2014.

USEPA, 1991a. Dose–response Analysis of Ingested Benzo[a]pyrene (CAS No. 50-32-8). Human Health Assessment Group, Office of Health and Environmental Assessment, Washington, DC (EPA/600/R-92/045).

USEPA, 1991b. Drinking water criteria document for PAH. Prepared by the Office of Health and Environmental Assessment, Environmental Criteria and Assessment Office, Cincinnati. OH for the Office of Water Regulations and Standards, Washington, DC.

USEPA, 1996a. Method 3540C: Soxhlet Extraction. US Environmental Protection Agency, Washington, DC.

USEPA, 1996b. Method 3620B: Florisil Cleanup. US Environmental Protection Agency, Washington, DC.

USEPA, 1996c. Soil Screening Guidance: User's Guide. second ed. http://nepis.epa.gov/Exe/ZyPURL.cgi?Dockey=100027WI.txt.

USEPA, 2001. Integrated Risk Information System (IRIS): Benzo [a] pyrene (BaP) (CASRN 50-32-8).

Wang, H.S., Man, Y.B., Wu, F.Y., Zhao, Y.G., Wong, C.S.C., Wong, M.H., 2010. Oral bioaccessibility of polycyclic aromatic hydrocarbons (PAHs) through fish consumption, based on an in vitro digestion model. J. Agric. Food Chem. 58, 11517–11524.

Wang, W., Huang, M.J., Kang, Y., Wang, H.S., Leung, A.O.W., Cheung, K.C., Wong, M.H., 2011. Polycyclic aromatic hydrocarbons (PAHs) in urban surface dust of Guangzhou, China: status, sources and human health risk assessment. Sci. Total Environ. 409, 4519–4527.

Wang, J., Zhang, X.F., Ling, W.T., Liu, R., Liu, J., Kang, F.X., Gao, Y.Z., 2017. Contamination and health risk assessment of PAHs in soils and crops in industrial areas of the Yangtze River Delta region, China. Chemosphere 168, 976–987.

Weber, L.P., Lanno, R.P., 2001. Effect of bile salts, lipid, and humic acids on absorption of benzo[a]pyrene by isolated channel catfish (*Ictalurus punctatus*) intestine segments. Environ. Toxicol. Chem. 20, 1117–1124.

Xia, Z.H., Duan, X.L., Qiu, W.X., Liu, D., Wang, B., Tao, S., Jiang, Q.J., Lu, B., Song, Y.X., Hu, X.X., 2010. Health risk assessment on dietary exposure to polycyclic aromatic hydrocarbons (PAHs) in Taiyuan, China. Sci. Total Environ. 408, 5331–5337.

Xing, G.H., Yang, Y., Chan, J.K.Y., Tao, S., Wong, M.H., 2008. Bioaccessibility of polychlorinated biphenyls in different foods using an in vitro digestion method. Environ. Pollut. 156, 1218–1226.

Xu, S.S., Liu, W.X., Tao, S., 2006. Emission of polycyclic aromatic hydrocarbons in China. Environ. Sci. Technol. 40, 702–708.

Yu, Y.X., Chen, L., Yang, D., Pang, Y.P., Zhang, S.H., Zhang, X.Y., Yu, Z.Q., Wu, M.H., Fu, J.M., 2012. Polycyclic aromatic hydrocarbons in animal-based foods from shanghai: bioaccessibility and dietary exposure. Food Addit. Contam., Part A 29, 1465–1474.

Zhai, F.Y., Yang, X.G., 2006. Survey on the Chinese National Health and Nutrition II: the National Diet and Nutrition in 2002. Peoples Medical Publishing House, Beijing, pp. 145–146 (in Chinese).

Science of the Total Environment 512–513 (2015) 194–200

Contents lists available at ScienceDirect

Science of the Total Environment

journal homepage: www.elsevier.com/locate/scitotenv

Levels of $PM_{2.5}$/PM_{10} and associated metal(loid)s in rural households of Henan Province, China

Fuyong Wu [a,b,c,d,*], Wei Wang [b,c], Yu Bon Man [b,c], Chuen Yu Chan [e], Wenxin Liu [f], Shu Tao [f], Ming Hung Wong [b,c,**]

[a] College of Natural Resources and Environment, Northwest A&F University, Yangling 712100, PR China
[b] Consortium on Health, Environment, Education and Research (CHEER), The Hong Kong Institute of Education, Tai Po, Hong Kong SAR, PR China
[c] Department of Science and Environmental Studies, The Hong Kong Institute of Education, Tai Po, Hong Kong SAR, PR China
[d] School of Municipal and Environment Engineering, Henan University of Urban Construction, Pingdingshan 467036, PR China
[e] Faculty of Environmental Science and Engineering, Sun Yat-sen University, Guangzhou 510275, PR China
[f] Laboratory for Earth Surface Processes, College of Urban and Environmental Science, Peking University, Beijing 100871, PR China

HIGHLIGHTS

- PM and associated metal(loid)s exhibited seasonal variability.
- Using coal could result in more severe indoor air pollutants.
- Using electricity would effectively improve indoor air quality in rural China.

ARTICLE INFO

Article history:
Received 13 October 2014
Received in revised form 14 January 2015
Accepted 16 January 2015
Available online xxxx

Editor: P. Kassomenos

Keywords:
Indoor air pollution
Solid biomass fuel
PM
Trace element
Rural area

ABSTRACT

Although a majority of China's rural residents use solid fuels (biomass and coal) for household cooking and heating, clean energy such as electricity and liquid petroleum gas is becoming more popular in the rural area. Unfortunately, both solid fuels and clean energy could result in indoor air pollution. Daily respirable particulate matter ($PM \leq 10\ \mu m$) and inhalable particulate matter ($PM \leq 2.5\ \mu m$) were investigated in kitchens, sitting rooms and outdoor area in rural Henan during autumn (Sep to Oct 2012) and winter (Jan 2013). The results showed that PM ($PM_{2.5}$ and PM_{10}) and associated metal(loid)s varied among the two seasons and the four types of domestic energy used. Mean concentrations of $PM_{2.5}$ and PM_{10} in kitchens during winter were 59.2–140.4% and 30.5–145.1% higher than those during autumn, respectively. Similar with the trends of $PM_{2.5}$ and PM_{10}, concentrations of As, Pb, Zn, Cd, Cu, Ni and Mn in household $PM_{2.5}$ and PM_{10} were apparently higher in winter than those in autumn. The highest mean concentrations of $PM_{2.5}$ and PM_{10} (368.5 and 588.7 $\mu g\ m^{-3}$) were recorded in sitting rooms in Baofeng during winter, which were 5.7 and 3.9 times of corresponding health based guidelines for $PM_{2.5}$ and PM_{10}, respectively. Using coal can result in severe indoor air pollutants including PM and associated metal(loid)s compared with using crop residues, electricity and gas in rural Henan Province. Rural residents' exposure to $PM_{2.5}$ and PM_{10} would be roughly reduced by 13.5–22.2% and 8.9–37.7% via replacing coal or crop residues with electricity. The present study suggested that increased use of electricity as domestic energy would effectively improve indoor air quality in rural China.

1. Introduction

Over the past decades, much attention has been placed on investigating, monitoring and regulating air pollution in the outdoor environment. There seems to be a general misconception that air pollution is only an outdoor phenomenon. A number of studies noted that indoor air can be many times more contaminated than outdoor air (Jiang and Bell, 2008; Wong et al., 2004). Indoor air pollution derived from solid fuels is the single largest environmental risk factor in China (Smith et al., 2004). Approximately 420,000 premature deaths occur annually due to use of solid fuels in Chinese households, which is 40% more than premature deaths (300,000) attributed to outdoor air pollution in Chinese cities (Cohen et al., 2004). It has been estimated that 4–5% of deaths in developing countries and approximately 3.5 million deaths per year in China

---

* Correspondence to: F. Wu, College of Natural Resources and Environment, Northwest A&F University, Yangling 712100, PR China.
** Correspondence to: M. H. Wong, Consortium on Health, Environment, Education and Research (CHEER), The Hong Kong Institute of Education, Tai Po, Hong Kong SAR, PR China.
E-mail addresses: wfy09@163.com (F. Wu), mhwong@hkbu.edu.hk (M.H. Wong).

http://dx.doi.org/10.1016/j.scitotenv.2015.01.041
0048-9697/

result from indoor air pollution (Mestl et al., 2007; Smith and Mehta, 2003). Moreover, people (especially women and children) spend majority of their time indoors and thus the potential health risks posed by indoor air pollutants are of great concern. Therefore, it is critical to characterize profiles and concentrations of health-damaging pollutants in rural households.

An overwhelming majority of China's rural residents use solid fuels (mainly including biomass and coal) for household cooking and heating (Smith et al., 2004). The pollutants produced from combustion of solid fuels include suspended particulates (PM_{10} and $PM_{2.5}$), carbon monoxide (CO), carbon dioxide (CO_2), nitrogen oxides (NO_x), sulfur dioxide (SO_2) and heavy metals (Clark et al., 2013). Combustion of biomass and coal is the dominant source of indoor air pollution in China (Ding et al., 2012; Zhang and Smith, 2007). The rural residents generally experienced a higher exposure to particular matter (PM) in indoor air than the urban residents, even though the outdoor air particulate levels in rural areas are much lower than in urban areas (Mestl et al., 2007). Adverse health effects resulted from household air pollution due to combustion of biomass and coal included respiratory illnesses, lung cancer, chronic obstructive pulmonary disease, weakening of the immune system, and reduction in lung function in China (Zhang and Smith, 2007).

With the rapid development of the economy and society, commercial energies such as electricity and liquid petroleum gas (gas) are becoming more popular in Chinese rural households. In 2010, 23% of rural households were reported to use clean fuels (gas or electricity) as their main cooking fuel (NBS, 2012). The use of multi-fuels is a common feature of domestic energy in rural China mainly due to fuel availability. There may be day-to-day or seasonal changes in emissions of indoor air pollutants because of changes in energy use patterns or housing conditions in rural China. It is recognized that understanding the patterns of exposure to PM and associated metal(loid)s is required to evaluate and design environmental health interventions, but only limited studies have been conducted to investigate the levels and temporal patterns of indoor air pollutants using different types of domestic energy in rural China.

Jiang and Bell (2008) indicated that levels of PM_{10} in rural kitchens are three times higher than those in urban kitchens during cooking in Liaoning Province. Compared with Guizhou and Shaanxi Provinces using coal as the primary domestic energy, both Inner Mongolia and Gansu Provinces using biomass as the primary fuel had the highest PM_4 concentrations (Jin et al., 2005). As the 3rd largest provincial population (94.06 million), Henan Province is also the 5th highest producer and consumer (283.7 million tons) of coal and produces the largest yield of winter wheat (31.77 million tons) in China (China Energy Statistical Yearbook, 2012; China Statistical Yearbook, 2013). For many years, both coal and crop residues have been, and still are the primary domestic energy in rural Henan Province. Unfortunately, the status of indoor air pollution in rural households in this province is still not clear. It is hypothesized that the levels of household $PM_{2.5}/PM_{10}$ and associated metal(loid)s (As, Pb, Zn, Cd, Cu, Ni and Mn) in rural households of Henan Province exceed China's indoor air quality standards and that there are seasonal variations of PM and the associated metal(loid)s in rural households using different types of domestic energy in the province.

The main objectives of the present work were to: (1) characterize $PM_{2.5}/PM_{10}$ and associated metal(loid)s (As, Pb, Zn, Cd, Cu, Ni and Mn) in rural households of Henan Province; and (2) investigate differences in $PM_{2.5}/PM_{10}$ and associated metal(loid)s among four types of domestic energy (crop residues, coal, liquid petroleum gas and electricity).

2. Materials and methods

2.1. Characteristics of the sampling houses

The present investigations were conducted in nine households in a village of Baofeng County (BF) and in three households in another village of Fangcheng County (FC), both from Henan Province (Fig. 1). The two villages are around 110 km apart. The selection of households was based on the following criteria: (i) Houses possess similar structures (number and layout of rooms) that are typical in the selected village; (ii) the stoves in the selected households are representative in the village. Coal is a primary fuel used by nearly all households for heating and by a majority of households for cooking in Baofeng County, which is mainly dependent on coal-mine exploitation and agricultural production. Crop residues are commonly used for cooking and heating in Fangcheng County, mainly dependent on agricultural production. Two kinds of clean fuels including liquid petroleum gas (gas) and electricity are also used in few rural households of Baofeng County for cooking recently. Representative households using the four types of domestic energy: crop residues, coal, electricity and gas were selected for sampling.

The structure of selected households in the two villages is similar, which is one-story consisting of a kitchen and living areas (with a sitting room, two bed rooms and a storage room), and a yard with area of about 40–50 m^2. Kitchens and living areas are usually separated and around 3–5 m apart. The sitting room has a door open to outside and is also connected with the two bed rooms by entrance. The average area of kitchen and sitting room is about 10–15 m^2 and 15–20 m^2, respectively. Cooking activities are usually limited in the kitchen. The cooking stoves using coal have no chimneys, while the cooking stoves using crop residues have chimneys. Ventilation in the kitchens is generally based on natural draft. There is also a heating stove with a chimney in the sitting room, which only operates in winter.

2.2. Collection of household $PM_{2.5}$ and PM_{10}

To ensure that the samples are representative of the rural households in Henan Province, three households were selected for each type of domestic energy used. At each of the households, four stationary active samplers (7388MAS aerosol sampler, Zhongshan SLC Environmental Technology Corp., China) were deployed, with two ($PM_{2.5}$ and PM_{10}) each in the kitchen and sitting room. In addition, two stationary active samplers were also deployed in outdoor in one of the three households which used the same domestic energy. A low volume air sampler was used, with a flow rate of 5.0 L min^{-1} (±5%). The sampler was placed at least 1.0 m away from the wall or windows and approximately 1.0 m from the stove in the kitchen and sitting room. Levels of outdoor $PM_{2.5}$ and PM_{10} were measured in the yard of rural households, approximately 1.0 m from the main house. Other criteria for selecting the sampling positions included the accessibility to electricity, the safety and stabilization of the samplers and avoidance of interference with household activities. All stationary monitors were placed on a flat surface at a height of approximately 1.2 m. During autumn (Sep to Oct 2012), the stationary sampling was conducted for nine consecutive days and the filters ($PM_{2.5}$ and PM_{10}) were changed and collected every three days, while during winter (Jan 2013), the sampling was done for six consecutive days and the filters ($PM_{2.5}$ and PM_{10}) were changed and collected every two days (Table 1). One sample of field blank was taken for each sampling day. During sampling period, people lived as usual except that they were asked not to smoke in the sampling room. The flow rate of the sampler was checked and recalibrated by adjusting the flow meter before and after sampling. All samplings were conducted during days with no precipitation and wind speed was less than 3 m s^{-1}.

The filters ($PM_{2.5}$ PTFE membrane, 46.2 mm in diameter, Whatman; PM_{10} QM-A quartz fiber filter, 47 mm in diameter, Whatman) were desiccated at 25 °C and relative humidity (40–50%) for at least 24 h and then weighed (0.001 mg precision, Sartious Micro, Japan) before and after sampling, respectively. The 24-h PM concentrations were calculated by dividing the blank-corrected increase in filter mass by the total air volume sampled. All of the sampled filters were sealed in a petri dish with parafilm and stored at −25 °C in dark until chemical analyses.

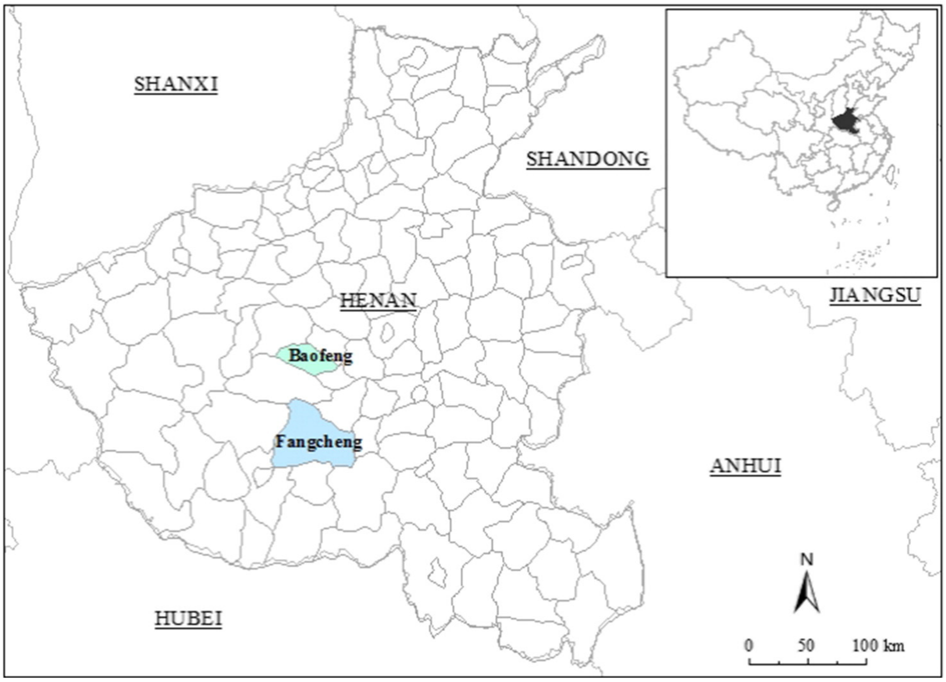

Fig. 1. Map of study area showing Baofeng County and Fangcheng County, Henan Province.

The filter blanks were treated in the same way as the samples for quality control.

2.3. Digestion and analyses of heavy metals in $PM_{2.5}$ and PM_{10}

Half of the sampled filters was digested by the acid mixture (6 mL of conc. HNO_3 and 1.5 mL $HClO_4$), using a microwave accelerated reaction system. Concentrations of As, Pb, Zn, Cd, Cu, Ni and Mn of the solutions were determined with inductively coupled plasma mass spectrometry (ICP-MS, Perkin-Elmer, Elan 9000). Blanks and standard reference (indoor dust, SRM 2584) obtained from the US National Institute of Standards and Technology were used for quality assurance. The recovery rates of As, Pb, Zn, Cd, Cu, Ni and Mn in the standard reference were within 79–105%.

2.4. Data analyses

Statistical analyses were conducted using SPSS 19.0 (SPSS Inc., USA). Means of different groups were compared using one-way ANOVA test. Prior to one-way ANOVA test, the data was log transformed to meet the normality assumption. Unless otherwise indicated, all treatment means were tested for significant difference at $p < 0.05$.

3. Results

3.1. Concentrations of rural household $PM_{2.5}$ and PM_{10} during autumn and winter in Henan Province

There were totally 168 valid $PM_{2.5}$ and PM_{10} samples collected in the two seasons. In Baofeng and Fangcheng, the mean concentrations of $PM_{2.5}$ and PM_{10} were substantially higher in winter than in autumn at all measurement points (Figs. 2–3) (many of the differences were statistically significant at $p < 0.05$). This indicated that winter heating in the study area caused the seasonal variation of indoor air pollution. Among the valid samples, 92.9% $PM_{2.5}$ samples and 87.5% PM_{10} samples exceeded the 24-h health based guidelines for $PM_{2.5}$ (65 μg m^{-3} recommended by U.S. EPA) (USEPA, 1997) and PM_{10} (150 μg m^{-3} recommended by China) (GB/T, 18883–2002), respectively (Figs. 2–3). During winter, the highest mean concentrations of $PM_{2.5}$ and PM_{10} (368.5 and 588.7 μg m^{-3}) were recorded in sitting

Table 1
Sampling periods for $PM_{2.5}$ and PM_{10}.

Locations	House	Venue	Main types of domestic energy		Sampling period	
			Kitchen	Sitting room	Autumn	Winter
FW	A	Kitchen, sitting room, outdoor	Crop	Crop	11–20 Oct 2012	23–29 Jan 2013
	B	Kitchen, sitting room			11–20 Oct 2012	23–29 Jan 2013
	C	Kitchen, sitting room			11–20 Oct 2012	23–31 Jan 2013
BF	A	Kitchen, sitting room, outdoor	Coal	Coal	1–10 Sep 2012	1–7 Jan 2013
	B	Kitchen, sitting room			1–10 Sep 2012	1–7 Jan 2013
	C	Kitchen, sitting room			2–11 Sep 2012	1–9 Jan 2013
	D	Kitchen, sitting room, outdoor	Gas	Coal	10–19 Sep 2012	8–14 Jan 2013
	E	Kitchen, sitting room			10–19 Sep 2012	8–14 Jan 2013
	F	Kitchen, sitting room			11–20 Sep 2012	9–15 Jan 2013
	G	Kitchen, sitting room, outdoor	Electricity	Coal	19–28 Sep 2012	15–21 Jan 2013
	H	Kitchen, sitting room			20–29 Sep 2012	15–23 Jan 2013
	J	Kitchen, sitting room			19–28 Sep 2012	15–21 Jan 2013

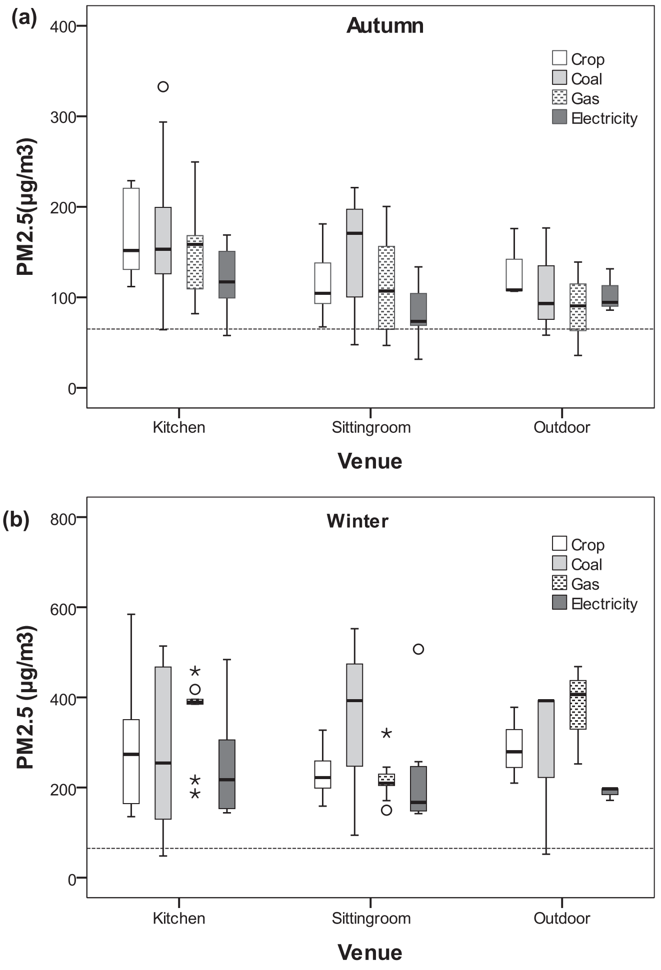

Fig. 2. Box plots of daily average $PM_{2.5}$ concentrations in rural households of Henan Province used different domestic energy during autumn (a) and winter (b). Three households each were used to estimate $PM_{2.5}$ concentrations for kitchens and sitting rooms and one household for outdoor. The sampling was conducted for nine consecutive days and $PM_{2.5}$ were collected every three days in autumn and was done for six consecutive days and $PM_{2.5}$ were collected every two days in winter.

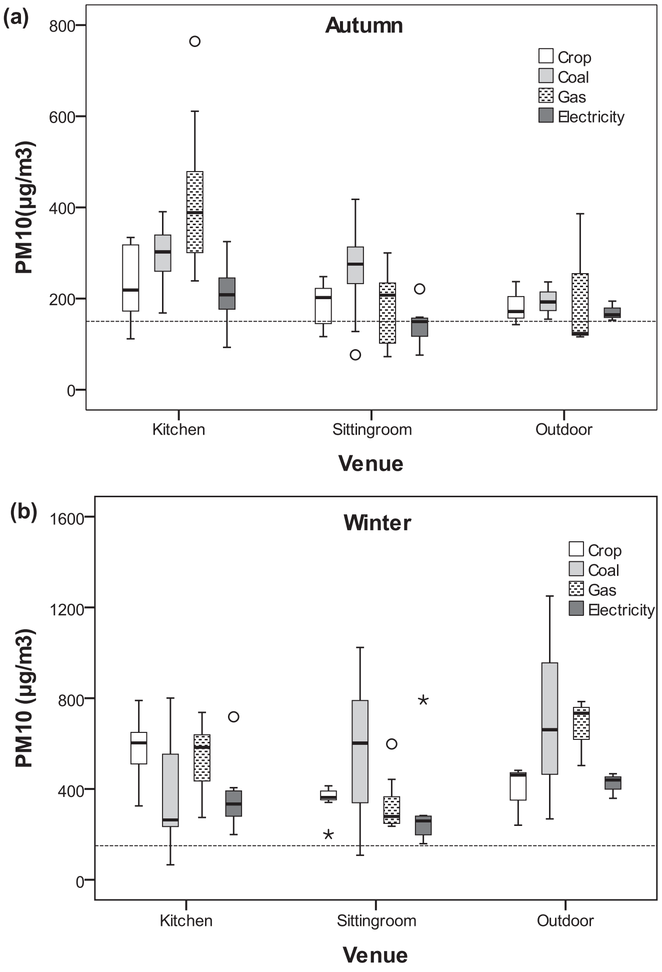

Fig. 3. Box plots of daily average PM_{10} concentrations in rural households of Henan Province used different domestic energy during autumn (a) and winter (b). Three households each were used to estimate PM_{10} concentrations for kitchens and sitting rooms and one household for outdoor, respectively. The sampling was conducted for nine consecutive days and PM_{10} were collected every three days in autumn and was done for six consecutive days and PM_{10} were collected every two days in winter.

rooms in Baofeng, which were 5.7 and 3.9 times of corresponding health based guidelines for $PM_{2.5}$ and PM_{10}, respectively. These implied that levels of household $PM_{2.5}$ and PM_{10} in rural Henan Province, especially during winter, posed a significant threat to human health. Furthermore, the average indoor ratios of $PM_{2.5}/PM_{10}$ in winter (0.65 in kitchens and 0.71 in sitting rooms) were apparently higher than those in autumn (0.59 in kitchens and 0.61 in sitting rooms), indicating that PM_{10} comprised a large fraction of fine particles in the winter.

3.2. Variations of rural household $PM_{2.5}$ and PM_{10} by types of domestic energy used in Henan Province

Figs. 2–3 show that there were obvious variations of indoor $PM_{2.5}$ and PM_{10} among four types of domestic energy used in rural Henan. As expected, using coal resulted in significantly ($p < 0.05$) higher $PM_{2.5}$ and PM_{10} than those using the other three types of domestic energy in sitting rooms. Using electricity resulted in lower levels of indoor $PM_{2.5}$ and PM_{10} than using crop residues, coal and gas. $PM_{2.5}$ concentrations in kitchens using electricity were 122.2 and 246.9 μg m^{-3} in and winter, which were 71.0%, 67.8% and 81.8% in autumn and 89.0%, 73.4% and 50.2% in winter of those using crop residues, coal and gas, respectively. Surprisingly, using another clean energy, gas, resulted in apparently higher kitchen $PM_{2.5}$ in winter and significantly ($p < 0.01$) higher kitchen PM_{10} in autumn than using crop residues, coal and electricity, respectively.

3.3. Variations of rural household $PM_{2.5}$ and PM_{10} concentrations in kitchens, sitting rooms and outdoors in Henan Province

The present studies show that there are obvious spatial variations of household $PM_{2.5}$ and PM_{10} in different microenvironments of rural Henan (Figs. 2–3). In autumn, the samples collected in kitchens had higher $PM_{2.5}$ and PM_{10} concentrations than those collected in sitting rooms and outdoors, indicating that combustion of crop residues, coal or gas and cooking are the main sources of indoor air pollution. However, the levels of $PM_{2.5}$ and PM_{10} in winter varied among kitchens, sitting rooms and outdoors and among the four types of domestic energy. The highest level of $PM_{2.5}$ and PM_{10} in the microenvironments was recorded in kitchens (306.6 and 581.8 μg m^{-3}) using crop residues, in sitting rooms (368.5 and 588.7 μg m^{-3}) using coal and in outdoors (406.6 and 661.1 μg m^{-3}) using gas, respectively. In autumn, outdoor $PM_{2.5}$ concentrations in Fangcheng (130.3 μg m^{-3}) were apparently higher than in Baofeng (100.6 μg m^{-3}). In winter, outdoor PM_{10} concentrations in Fangcheng (394.7 μg m^{-3}) were apparently lower than in Baofeng (607.5 μg m^{-3}). In addition, $PM_{2.5}$ levels were significantly ($p < 0.05$) correlated with PM_{10} loadings with correlation coefficients (R^2) of 0.57 for kitchens, 0.84 for sitting rooms and 0.72 for outdoors in rural

Henan (Fig. 4a–c). This indicated that $PM_{2.5}$ and PM_{10} came from similar particulate emission sources.

3.4. Concentrations of As, Pb, Zn, Cd, Cu, Ni and Mn in household $PM_{2.5}$ and PM_{10}

Tables 2–3 shows the mass concentrations of As, Pb, Zn, Cd, Cu, Ni and Mn in household $PM_{2.5}$ and PM_{10} of rural Henan Province. Zn, Pb and Mn were the most abundant elements in both $PM_{2.5}$ and PM_{10}, of which Zn had the highest concentration, and then Pb, while Cd and Ni were the lowest. The highest concentrations of As (143.5 pg m^{-3}) and Zn (1039 pg m^{-3}) in PM_{10} were recorded in sitting rooms using coal during winter, and the lowest concentrations of As (7.70 pg m^{-3}), Zn (61.13 pg m^{-3}) and Pb (54.21 pg m^{-3}) in PM_{10} in sitting rooms using electricity during autumn. Similar to the changing trend of $PM_{2.5}$ and PM_{10}, levels of As, Pb, Zn, Cd, Cu, Ni and Mn in household $PM_{2.5}$ and PM_{10} were substantially higher in winter than in autumn at all measurement points (Tables 2–3) (mostly significantly different at $p < 0.05$). In autumn, the levels of As, Pb and Zn in $PM_{2.5}$ and PM_{10} from kitchens and sitting rooms using coal were significantly ($p < 0.05$) higher than those using crop residues, gas and electricity. In winter, the levels of As, Pb and Zn in $PM_{2.5}$ and PM_{10} from kitchens and sitting rooms using crop residues were significantly ($p < 0.05$) lower than those using coal, gas and electricity.

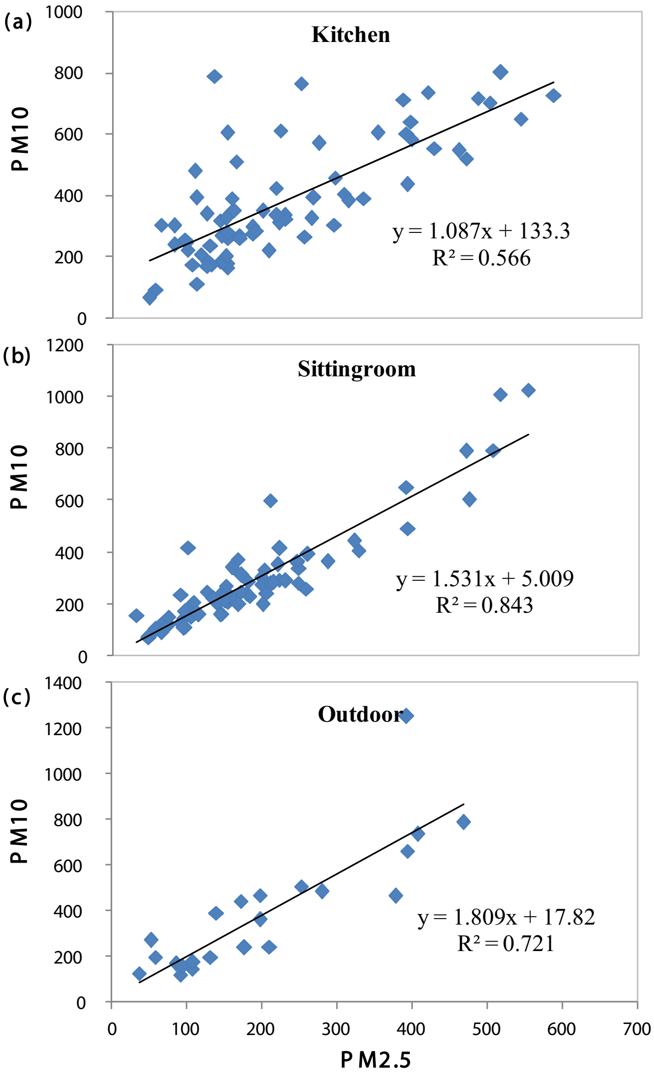

Fig. 4. Relationship between PM_{10} and $PM_{2.5}$ concentrations (μg m^{-3}) in kitchen (a), sitting room (b) and outdoor (c).

4. Discussion

The present study shows that higher levels of $PM_{2.5}$ and PM_{10} and associated metal(loid)s in rural Henan Province were recorded in winter. Either in indoors or in outdoors, the mean concentrations of $PM_{2.5}$ and PM_{10} in the two counties of Henan Province exceeded the health-based standards for $PM_{2.5}$ and PM_{10} in ambient (outdoor) environment (GB/T, 18883–2002; USEPA, 1997). It can be observed that mean concentrations of $PM_{2.5}$ and PM_{10} in kitchens during winter were 59.2–140.4% and 30.5–145.1% higher than during autumn, respectively. The average $PM_{2.5}$ concentration of kitchen using crop residues during winter was 306.6 μg m^{-3} in rural Henan, which was 1.71 times higher than that in rural Tibet (178.89 μg m^{-3}) (Gao et al., 2009). The present study added to the growing body of evidence that solid fuel (crop residues and coal) can result in highly elevated levels of indoor air pollution, which in turn can contribute to adverse health effects. Epidemiology surveys showed that long-term exposure to PM_{10} is associated with an increased risk of lung cancer (Beeson et al., 1998; Pope et al., 2002). The Chinese population suffers from a high health burden of lung disease and respiratory disease, which are primary causes of death in rural China (Schmidt, 2002). It is vital for in-depth studies of the current status of indoor air pollution and their health effects in households of rural China, and then based on these, to enhance the design of policies and interventions for addressing this pressing problem.

The present study also showed that there were apparent spatial variations of household $PM_{2.5}$ and PM_{10} concentrations in rural Henan (Figs. 2–3). The highest concentrations of $PM_{2.5}$ and PM_{10} were recorded in kitchens among the three microenvironments (kitchen, sitting room and outdoor) of rural Henan in autumn. Daily average $PM_{2.5}$ concentrations in kitchens, sitting rooms and outdoors were 156.0 μg m^{-3}, 116.4 μg m^{-3} and 108.0 μg m^{-3} in autumn, respectively. In winter, the highest $PM_{2.5}$ (368.5 μg m^{-3}) and PM_{10} (588.7 μg m^{-3}) were recorded in sitting rooms. This indicated that heating practice is a prominent determinant of indoor air quality in rural Henan, similar to other studies conducted in other rural areas (Inner Mongolia, Gansu, Shaanxi, and Guzhou) of China (Fischer and Koshland, 2007; He et al., 2005; Jin et al., 2005). In Baofeng, the outdoor PM_{10} concentrations in winter were not as low as expected and even higher than in kitchens and sitting rooms, which might be due to the coal mine activities close to the village. Henan Province is one of the highest producers and consumers of coal in China (China Energy Statistical Yearbook, 2012). Moreover, it can be observed that the outdoor levels of $PM_{2.5}$ in Fangcheng (130.3 μg m^{-3}) were 30% higher than those in Baofeng (100.6 μg m^{-3}) in autumn, which might be due to the open burning of maize stalk close to the village in Fangcheng. Yan et al. (2006) indicated that the open burning of agricultural residues occurred frequently during harvest seasons in several provinces, including Henan, Hebei, Shandong, Jiangsu, and Anhui, based on satellite pictures from the FY-1 earth observation satellite. The average $PM_{2.5}$ emission factor from maize stove is 11.7 ± 1.0 g kg^{-1} of biomass (dry basis) (Li et al., 2007).

The present study indicated that higher levels of $PM_{2.5}$ and PM_{10} were recorded in households using crop residues and coal than using electricity in rural Henan (Tables 2–3). Household $PM_{2.5}$ concentrations (231.4–306.6 μg m^{-3}) using crop residues in Henan were significantly lower than PM_4 concentrations in Inner Mongolia (>700 μg m^{-3}) and Gansu (351–661 μg m^{-3}) where biomass is the primary fuel (Jin et al., 2005). The lower concentrations of $PM_{2.5}$ in Henan reflect its warmer temperature and lower heating hours in winter. In addition, household $PM_{2.5}$ concentrations (286.9–368.5 μg m^{-3}) using coal in Henan were comparable with PM_4 concentrations in Guizhou (301–352 μg m^{-3}) and Shaanxi (187–329 μg m^{-3}) where coal is the primary fuel (Jin et al., 2005).

Table 2
Mass concentrations of heavy metals in PM_{25} at different monitoring sites in rural households of Henan Province used different domestic energy during autumn and winter (pg m^{-3}, mean ± SD, n = 9 for kitchen and sitting room, n = 3 for outdoor).

Venue	Energy	As	Pb	Zn	Cd	Cu	Ni	Mn
Autumn								
Kitchen	Crop	5.41 ± 3.78 b	62.33 ± 28.67 b	121.3 ± 79.68 a	2.41 ± 1.28 a	8.77 ± 5.22 b	2.43 ± 1.35 a	33.26 ± 15.03 ab
	Coal	15.30 ± 10.38 a	128.8 ± 99.21 a	203.7 ± 157.4 a	2.67 ± 1.95 a	15.03 ± 9.39 a	1.94 ± 0.89 ab	23.88 ± 7.41 b
	Gas	12.86 ± 12.56 ab	38.92 ± 28.91 b	179.4 ± 223.4 a	3.66 ± 4.46 a	7.48 ± 3.33 b	1.42 ± 0.70 b	24.26 ± 8.98 b
	Electricity	6.90 ± 3.74 b	54.80 ± 26.27 b	101.2 ± 67.92 a	1.45 ± 0.73 a	10.04 ± 3.63 ab	1.92 ± 0.40 ab	37.78 ± 11.15 a
Sitting room	Crop	5.35 ± 2.36 b	47.18 ± 19.34 b	99.17 ± 53.32 b	2.21 ± 0.84 ab	8.38 ± 3.40 a	1.82 ± 1.12 a	27.54 ± 11.21 a
	Coal	16.30 ± 13.44 a	113.0 ± 98.13 a	245.3 ± 264.3 a	2.78 ± 1.56 ab	11.92 ± 5.62 a	2.10 ± 0.46 a	26.60 ± 10.82 a
	Gas	9.29 ± 5.32 ab	107.9 ± 85.74 ab	137.6 ± 72.29 ab	3.75 ± 3.21 a	9.97 ± 6.15 a	2.15 ± 1.77 a	30.30 ± 12.43 a
	Electricity	4.72 ± 3.24 b	46.52 ± 23.94 b	75.82 ± 42.77 b	1.69 ± 0.73 b	8.07 ± 2.68 a	1.35 ± 0.45 a	29.35 ± 9.23 a
Outdoor	Crop	6.92 ± 3.96 a	67.20 ± 39.25 a	160.7 ± 113.7 a	2.54 ± 1.31 a	10.80 ± 6.11 a	2.14 ± 0.92 ab	40.66 ± 27.80 a
	Coal	14.46 ± 8.46 a	94.50 ± 38.81 a	187.1 ± 142.4 a	2.00 ± 0.94 a	14.28 ± 10.05 a	2.30 ± 0.62 ab	42.39 ± 6.34 a
	Gas	11.60 ± 3.92 a	66.43 ± 13.91 a	132.0 ± 15.65 a	1.96 ± 0.63 a	10.91 ± 6.35 a	1.23 ± 0.10 b	34.39 ± 9.65 a
	Electricity	9.00 ± 6.87 a	63.03 ± 36.70 a	127.6 ± 70.30 a	1.64 ± 0.90 a	10.45 ± 5.62 a	3.31 ± 1. 19 a	37.78 ± 8.25 a
Winter								
Kitchen	Crop	26.95 ± 7.60 b	181.6 ± 54.13 b	278.5 ± 57.83 b	10.03 ± 15.78 a	28.28 ± 9.48 a	7.82 ± 6.15 a	33.88 ± 11.61 b
	Coal	50.90 ± 33.19 a	400.3 ± 240.6 a	609.7 ± 455.5 ab	5.82 ± 2.34 a	34.13 ± 17.21 a	2.88 ± 1.32 b	72.99 ± 31.23 a
	Gas	47.28 ± 23.25 ab	280.9 ± 115.5 ab	872.5 ± 847.0 a	13.71 ± 18.49 a	39.40 ± 5.23 a	5.10 ± 0.70 ab	79.54 ± 13.90 a
	Electricity	40.14 ± 21.31 ab	291.9 ± 141.9 ab	629.0 ± 303.8 ab	6.87 ± 3.62 a	39.72 ± 21.29 a	5.32 ± 3.29 ab	82.38 ± 46.42 a
Sitting room	Crop	22.66 ± 7.22 c	133.7 ± 29.52 b	243.6 ± 74.19 b	4.27 ± 1.39 b	25.33 ± 7.82 bc	3.85 ± 1.02 ab	31.28 ± 9.37 c
	Coal	30.55 ± 19.31 bc	345.6 ± 272.1 a	310.8 ± 3.94 ab	3.94 ± 2.41 b	17.32 ± 16.23 c	2.33 ± 1.80 b	51.05 ± 38.55 bc
	Gas	55.99 ± 26.18 a	374.6 ± 139.2 a	628.4 ± 236.9 a	6.62 ± 3.26 ab	35.87 ± 12.11 ab	4.47 ± 2.51 a	74.53 ± 51.45 ab
	Electricity	43.98 ± 24.91 ab	265.8 ± 178.0 ab	647.0 ± 456.5 a	7.46 ± 3.99 a	40.19 ± 17.17 a	4.47 ± 2.18 a	91.41 ± 41.77 a
Outdoor	Crop	30.40 ± 6.74 ab	191.2 ± 21.60 ab	382.1 ± 26.47 ab	4.68 ± 0.56 ab	28.65 ± 1.56 b	6.51 ± 0.91 a	50.68 ± 0.55 ab
	Coal	17.84 ± 7.78 b	186.1 ± 65.35 ab	457.8 ± 257.8 ab	3.38 ± 1.66 ab	15.50 ± 5.74 c	2.79 ± 1.38 b	80.36 ± 24.80 a
	Gas	35.74 ± 9.42 a	278.9 ± 62.62 a	578.2 ± 74.43 a	5.41 ± 1.37 a	37.32 ± 3.26 a	5.43 ± 0.91 a	83.10 ± 19.53 a
	Electricity	17.39 ± 7.28 b	94.45 ± 49.69 b	250.5 ± 78.84 b	2.55 ± 1.25 b	7.28 ± 4.66 d	2.67 ± 1.43 b	33.67 ± 27.53 b

Different letters within the same column indicate significant difference between different domestic energy used at the level of $p < 0.05$.

The present study suggested that replacing crop residues or coal with cleaner energy like electricity would improve indoor air quality, and exposure to $PM_{2.5}$ and PM_{10} by rural residents with a reduction of 13.5–22.2% and 8.9–37.7%, respectively. However, $PM_{2.5}$ concentrations in kitchens using another cleaner energy (gas) were comparable with using crop residues and coal, and the corresponding PM_{10} concentrations were significantly ($p < 0.05$) higher in autumn than using crop residues and coal (Figs. 2–3). Fischer and Koshland (2007) also observed that the use of "improved" fuel (gas) for cooking was associated with significantly worse air quality on both peak and daily measures of CO and PM. The present results were inconsistent with the results noted by Gao et al. (2009), which indicated that using methane (a cleaner energy) resulted in lower $PM_{2.5}$ concentrations in kitchens than using dry dung cake and fuel wood in rural Tibet in winter. The main reasons may

Table 3
Mass concentrations of heavy metals in PM_{10} at different monitoring sites in rural households of Henan Province used different domestic energy during autumn and winter (pg m^{-3}, mean ± SD, n = 9 for kitchen and sitting room, n = 3 for outdoor).

Venue	Energy	As	Pb	Zn	Cd	Cu	Ni	Mn
Autumn								
Kitchen	Crop	10.68 ± 3.84 b	84.73 ± 33.09 b	141.5 ± 68.97 ab	2.47 ± 1.04 b	16.61 ± 23.61 a	2.53 ± 1.67 a	52.76 ± 31.46 a
	Coal	32.15 ± 29.58 a	259.9 ± 224.2 a	263.2 ± 216.0 a	3.63 ± 2.01 ab	18.39 ± 16.01 a	2.85 ± 2.39 a	57.62 ± 10.59 a
	Gas	24.26 ± 10.78 ab	122.4 ± 39.07 b	203.9 ± 130.6 ab	4.85 ± 3.16 a	9.93 ± 6.96 a	1.38 ± 0.81 a	61.45 ± 27.18 a
	Electricity	11.91 ± 4.77 b	69.22 ± 20.15 b	81.95 ± 32.86 b	2.65 ± 2.16 b	10.49 ± 2.77 a	2.81 ± 0.64 a	67.59 ± 10.68 a
Sitting room	Crop	11.75 ± 4.94 b	75.76 ± 37.45 b	142.3 ± 95.24 b	2.57 ± 1.23 bc	16.91 ± 18.86 a	4.79 ± 8.06 a	57.55 ± 44.05 ab
	Coal	29.72 ± 16.55 a	190.9 ± 117.3 a	256.9 ± 148.5 a	5.00 ± 2.17 a	16.50 ± 9.16 a	2.93 ± 2.64 a	81.42 ± 26.97 a
	Gas	16.67 ± 10.98 b	119.5 ± 79.99 b	139.0 ± 65.54 b	3.81 ± 1.79 ab	16.13 ± 10.62 a	2.56 ± 1.92 a	50.06 ± 28.75 b
	Electricity	7.70 ± 3.82 b	54.$_{21}$ ± 21.14 b	61.13 ± 34.70 b	1.41 ± 0.49 c	7.32 ± 1.58 a	2.08 ± 0.84 a	49.04 ± 11.26 b
Outdoor	Crop	12.84 ± 6.31 b	91.98 ± 60.90 b	152.2 ± 117.5 a	2.46 ± 1.43 a	9.73 ± 11.19 a	3.38 ± 0.79 b	48.80 ± 29.24 b
	Coal	26.76 ± 6.48 a	154.4 ± 33.01 a	223.9 ± 114.2 a	3.04 ± 1.20 a	13.65 ± 14.21 a	5.05 ± 2.72 a	73.34 ± 15.61 a
	Gas	17.30 ± 9.34 b	83.85 ± 34.92 b	112.7 ± 67.06 a	2.62 ± 1.17 a	16.60 ± 11.03 a	2.80 ± 0.49 b	64.01 ± 5.71 b
	Electricity	13.58 ± 10.27 b	87.49 ± 50.32 b	94.66 ± 89.27 a	2.49 ± 2.28 a	12.62 ± 4.35 a	3.05 ± 0.56 b	86.67 ± 9.81 ab
Winter								
Kitchen	Crop	31.30 ± 4.53 b	215.3 ± 28.01 b	211.3 ± 51.20 b	7.49 ± 4.29 a	25.24 ± 8.67 c	5.34 ± 1.69 b	83.80 ± 31.08 b
	Coal	69.56 ± 24.96 a	408.9 ± 244.9 ab	536.3 ± 344.2 a	7.49 ± 2.42 a	35.73 ± 16.39 bc	10.14 ± 4.69 a	79.38 ± 32.83 b
	Gas	77.05 ± 40.73 a	328.9 ± 223.7 ab	608.1 ± 456.4 a	10.04 ± 6.39 a	39.72 ± 9.60 b	7.43 ± 2.03 ab	89.76 ± 23.82 b
	Electricity	64.57 ± 24.14 a	553.5 ± 339.2 a	713.1 ± 316.0 a	9.05 ± 3.27 a	55.18 ± 14.57 a	6.92 ± 2.59 b	130.6 ± 54.36 a
Sitting room	Crop	28.79 ± 6.54 c	191.7 ± 40.52 b	213.5 ± 52.96 c	4.96 ± 1.27 b	26.29 ± 10.65 a	5.92 ± 2.04 b	83.61 ± 22.94 a
	Coal	143.5 ± 73.24 a	378.5 ± 282.0 ab	1039 ± 624.3 a	9.37 ± 3.22 a	42.49 ± 29.25 a	13.68 ± 6.42 a	84.11 ± 34.02 a
	Gas	73.47 ± 32.75 b	440.1 ± 229.7 a	476.5 ± 278.5 bc	7.42 ± 3.55 ab	36.88 ± 11.24 a	9.11 ± 2.80 b	92.08 ± 42.90 a
	Electricity	55.24 ± 29.22 bc	406.7 ± 239.3 a	589.2 ± 286.8 b	7.41 ± 3.86 ab	41.85 ± 24.45 a	7.27 ± 2.35 b	112.9 ± 53.50 a
Outdoor	Crop	35.42 ± 10.56 b	235.2 ± 30.26 b	312.2 ± 93.87 a	5.64 ± 1.13 a	32.64 ± 5.12 a	5.77 ± 2.02 b	128.6 ± 20.46 a
	Coal	54.25 ± 19.42 ab	246.3 ± 115.9 ab	520.8 ± 238.8 a	8.66 ± 5.36 a	31.16 ± 25.25 a	12.91 ± 4.53 ab	190.1 ± 110.4 a
	Gas	86.31 ± 36.35 a	479.9 ± 142.4 a	721.4 ± 207.1 a	11.74 ± 4.21 a	59.13 ± 18.12 a	17.44 ± 5.44 a	139.9 ± 31.49 a
	Electricity	53.39 ± 16.09 ab	365.5 ± 172.9 ab	494.7 ± 301.0 a	6.79 ± 4.67 a	25.86 ± 16.85 a	8.01 ± 3.09 b	96.04 ± 28.51 a

Different letters within the same column indicate significant difference between different domestic energy used at the level of $p < 0.05$.

be due to both the architectural style and living habits of the residents in Tibet are quite different from Henan. Moreover, Mestl et al., 2007 indicated that the indoor air pollution levels are generally influenced by other sources such as cooking oil fumes, incense burning and smoking.

The present study demonstrated that concentrations of As, Pb and Zn associated with $PM_{2.5}$/PM_{10} in kitchens using coal were substantially higher than using crop residues, gas and electricity (Tables 2–3). Unlike biomass, many coals in China contain toxic trace elements such as Ni, Cr, As, F, Pb, Zn and Hg mainly due to epigenetic mineralization (Finkelman et al., 1999; Liu et al., 2007). These metal(loid)s could not be destroyed during combustion, but are released into air in their original or oxidized form. By contrast, concentrations of As, Pb and Zn in $PM_{2.5}$/PM_{10} in kitchens using crop residues were substantially lower than using coal, gas and electricity, especially in winter (Tables 2–3). These indicated that metal(loid)s concentrations in household $PM_{2.5}$ and PM_{10} in rural Henan varied among the four types of domestic energy. In addition, concentrations of As, Pb, Zn, Cd, Cu, Ni and Mn in household $PM_{2.5}$ and PM_{10} exhibited seasonal variations, similar with the trend of $PM_{2.5}$ and PM_{10}. Zn, Pb and Mn were the most abundant elements in both $PM_{2.5}$ and $PM_{10,}$ during both autumn and winter. Hu et al. (2012) also observed that Zn, Pb, Mn and Cu were the most abundant elements among the studied metal(loid)s in both outdoor TSP and $PM_{2.5}$ in Nanjing, China. It has been shown that oxidative damage caused by both indoor and outdoor PM_{10} at Hutou village, Xuan Wei, the village with the highest lung cancer rate (or incidence), was obviously higher than that in Xize village, Xuan Wei, China. Furthermore, the levels of water-soluble As, Cd, Cs, Pb, Sb, Tl and Zn in PM_{10} could be the most important components responsible for the higher oxidative capacity of indoor PM_{10} in Hutou Village (Shao et al., 2013). The present study indicated that As, Pb and Zn in $PM_{2.5}$ and PM_{10} from kitchens and sitting rooms using coal were apparently higher than those using crop residues. These suggested that oxidative damage caused by indoor PM_{10} using coal was obviously higher than that using crop residues. However, further investigations are essential before a more concrete conclusion can be drawn.

5. Conclusion

In the present study, multiple pollutants, including $PM_{2.5}$, PM_{10} and associated metal(loid)s (As, Pb, Zn, Cd, Cu, Ni and Mn) were investigated in rural households using four types of domestic energy in Henan Province. The results showed that particulate matter ($PM_{2.5}$ and PM_{10}) and associated metal(loid)s varied among the two seasons and the four types of domestic energy used. Mean concentrations of $PM_{2.5}$ and PM_{10} in kitchens in winter were 59.2–140.4% and 30.5–145.1% higher than those in autumn, respectively. Using coal can result in severe increase of indoor air pollutants including PM and associated metal(loid)s compared with using crop residues, electricity and gas in rural Henan. The concentrations of $PM_{2.5}$ and PM_{10} taken in by rural residents would be roughly reduced by 13.5–22.2% and 8.9–37.7% when using electricity, leading to a significant improvement in indoor air quality.

Acknowledgment

Financial support from the National Natural Science Foundation of China/Hong Kong Research Grants Council Joint Research Scheme (NFSC/RGC N_HKBU210/11) and the Pingdingshan City Science and Technology Innovation Fund for Distinguished Young Scholars (2012063) are gratefully acknowledged.

References

Beeson, W.L., Abbey, D.E., Knutsen, S.F., 1998. Long-term concentrations of ambient air pollutants and incident lung cancer in California adults: results from the AHSMOG study. Environ. Health Perspect. 106, 813–823.

China Energy Statistical Yearbook. China Statistics Press, Beijing, p. 87.

China Statistical Yearbook. China Statistics Press, Beijing, p. 98, 453.

Clark, M.L., Peel, J.L., Balakrishnan, K., Breysse, P.N., Chillrud, S.N., Naeher, L.P., Rodes, C.E., Vette, A.F., Balbus, J.M., 2013. Health and household air pollution from solid fuel use: the need for improved exposure assessment. Environ. Health Perspect. 121, 1120–1128.

Cohen, A.J., Anderson, H.R., Ostro, B., Pandey, K.D., Krzyzanowski, M., Künzil, N., 2004. Urban air pollution. In: Ezzati, M., Rodgers, A., Lopez, A., Murry, C. (Eds.), Comparative Quantification of Health Risks: Global and Regional Burden of Disease Attributable to Selected Major Risk Factors. World Health Organization, Geneva, Switzerland, pp. 1353–1433.

Ding, J., Zhong, J., Yang, Y., Li, B., Shen, G., Su, Y., Wang, C., Li, W., Shen, H., Wang, B., Wang, R., Huang, Y., Zhang, Y., Cao, H., Zhun, Y., Simonich, S.L.M., Tao, S., 2012. Occurrence and exposure to polycyclic aromatic hydrocarbons and their derivatives in a rural Chinese home through biomass fuelled cooking. Environ. Pollut. 169, 160–166.

Finkelman, R.B., Belkin, H.E., Zheng, B.S., 1999. Health impacts of domestic coal use in China. Proc. Natl. Acad. Sci. 96, 3427–3431.

Fischer, S., Koshland, C., 2007. Daily and peak 1 h indoor air pollution and driving factors in a rural Chinese village. Environ. Sci. Technol. 41, 3121–3126.

Gao, X., Yu, Q., Gu, Q., Chen, Y., Ding, K., Zhu, J., Chen, L., 2009. Indoor air pollution from solid biomass fuels combustion in rural agricultural area of Tibet, China. Indoor Air 19, 198–205.

GB/T 18883–2002. Indoor air quality standard in P. R. China.

He, G., Ying, B., Liu, J., Gao, S., Shen, S., Balakrishnan, K., Jin, Y.L., Liu, F., Tang, N., Shi, K., Baris, E., Ezzati, M., 2005. Patterns of household concentrations of multiple indoor air pollutants in China. Environ. Sci. Technol. 39, 991–998.

Hu, X., Zhang, Y., Ding, Z.H., Wang, T.J., Lian, H.Z., Sun, Y.Y., Wu, J.C., 2012. Bioaccessibility and health risk of arsenic and heavy metals (Cd, Co, Cr, Cu, Ni, Pb, Zn and Mn) in TSP and PM2.5 in Nanjing, China. Atmos. Environ. 57, 146–152.

Jiang, R.T., Bell, M.L., 2008. A comparison of particulate matter from biomass-burning rural and non-biomass-burning urban households in northeastern China. Environ. Health Perspect. 116, 907–914.

Jin, Y.L., Zhou, Z., He, G.L., Wei, H.Z., Liu, J., Liu, F., Tang, N., Ying, B., Liu, Y.C., Hu, G.H., Wang, H.W., Balakrishnan, K., Watson, K., Baris, E., Ezzati, M., 2005. Geographical, spatial, and temporal distributions of multiple indoor air pollutants in four Chinese provinces. Environ. Sci. Technol. 39, 9431–9439.

Li, X., Wang, S., Duan, L., Hao, J., Li, C., Chen, Y., Yang, L., 2007. Particulate and trace gas emissions from open burning of wheat straw and corn straw in China. Environ. Sci. Technol. 41, 6052–6058.

Liu, G.J., Zheng, L.G., Zhang, Y., Qi, C.C., Chen, Y.W., Peng, Z.C., 2007. Distribution and mode of occurrence of As, Hg and Se and sulfur in coal Seam 3 of the Shanxi Formation, Yanzhou Coalfield, China. Int. J. Coal Geol. 71, 371–385.

Mestl, H.E., Aunan, K., Seip, H.M., Wang, S., Zhao, Y., Zhang, D., 2007. Urban and rural exposure to indoor air pollution from domestic biomass and coal burning across China. Sci. Total Environ. 377, 12–26.

NBS (National Bureau of Statistics), 2012. Tabulation on the 2010 Population Census of the People's Republic of China. Population Census Office of the State Council and Population and Employment Statistics Department, National Bureau of Statistics of China, China Statistics Press.

Pope III, C.A., Burnett, R.T., Thun, M.J., Calle, E.E., Krewski, D., Ito, K., Thurston, G.D., 2002. Lung cancer, cardiopulmonary mortality, and long-term exposure to fine particulate air pollution. J. Am. Med. Assoc. 287, 1132–1141.

Schmidt, C.W., 2002. Economy and environment: China seeks a balance. Environ. Health Perspect. 110, A516–A522.

Shao, L.Y., Hu, Y., Wang, J., Hou, C., Yang, Y.Y., Wu, M.Y., 2013. Particle-induced oxidative damage of indoor PM10 from coal burning homes in the lung cancer area of Xuan Wei, China. Atmos. Environ. 77, 959–967.

Smith, K.R., Mehta, S., 2003. The burden of disease from indoor air pollution in developing countries: comparison of estimates. Int. J. Hyg. Environ. Health 206, 279–289.

Smith, K.R., Mehta, S., Maeusezahl-Feuz, M., 2004. Indoor air pollution from household solid fuel use. In: Ezzati, M., Lopez, A.D., Rodgers, A., Murray, C.J.L. (Eds.), Comparative Quantification of Health Risks: Global and Regional Burden of Disease Attributable to Selected Major Risk Factors. World Health Organization, Geneva, Switzerland, pp. 1435–1493.

USEPA, 1997. Office of air and radiation, office of air quality planning and standards, fact sheet. EPA's Revised Particulate Matter StandardsUnited States Environmental Protection Agency.

Wong, G.W.K., Ko, F.W.S., Hui, D.S.C., Fok, T.F., Carr, D., von Mutius, E., Zhong, N.S., Chen, Y.Z., Lai, C.K.W., 2004. Factors associated with difference in prevalence of asthma in children from three cities in China: multicentre epidemiological survey. BMJ 329, 486–488.

Yan, X., Ohara, T., Akomoto, H., 2006. Bottom-up estimate of biomass burning in mainland China. Atmos. Environ. 40, 5262–5273.

Zhang, J.J., Smith, K.R., 2007. Household air pollution from coal and biomass fuels in China: measurements, health impacts, and interventions. Environ. Health Perspect. 115, 848–855.

Science of the Total Environment 536 (2015) 840–846

Contents lists available at ScienceDirect

Science of the Total Environment

journal homepage: www.elsevier.com/locate/scitotenv

Characterization of particulate-bound PAHs in rural households using different types of domestic energy in Henan Province, China

Fuyong Wu [a,b,c,*], Xueping Liu [c], Wei Wang [b], Yu Bon Man [b], Chuen Yu Chan [d], Wenxin Liu [e], Shu Tao [e], Ming Hung Wong [b,**]

[a] *Key Laboratory of Plant Nutrition and the Agri-environment in Northwest China, Ministry of Agriculture, and College of Natural Resources and Environment, Northwest A&F University, Yangling, 712100 Shaanxi, PR China*
[b] *Department of Science and Environmental Studies, The Hong Kong Institute of Education, Tai Po, Hong Kong SAR, PR China*
[c] *School of Municipal and Environment Engineering, Henan University of Urban Construction, Pingdingshan 467036, PR China*
[d] *Faculty of Environmental Science and Engineering, Sun Yat-sen University, Guangzhou 510275, PR China*
[e] *Laboratory for Earth Surface Processes, College of Urban and Environmental Science, Peking University, Beijing 100871, PR China*

HIGHLIGHTS

- Particulate-bound PAHs exhibited seasonal variability.
- Particulate-bound PAHs varied among four types of domestic energy used.
- Using liquid petroleum gas as a "clean" fuel in rural areas needs further research.

GRAPHICAL ABSTRACT

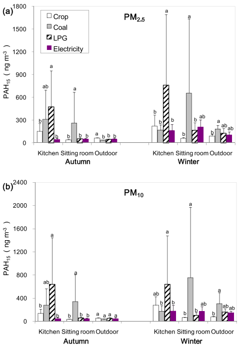

ARTICLE INFO

Article history:
Received 9 December 2014
Received in revised form 15 July 2015
Accepted 22 July 2015
Available online xxxx

Editor: D. Barcelo

Keywords:
Indoor air pollution
Polycyclic aromatic hydrocarbons
Particulate matter
Risk assessment

ABSTRACT

The concentrations and composition of sixteen PAHs adsorbed to respirable particulate matter ($PM_{10} \leq 10$ μm) and inhalable particulate matter ($PM_{2.5} \leq 2.5$ μm) were determined during autumn and winter in rural households of Henan Province, China, which used four types of domestic energy [crop residues, coal, liquid petroleum gas (LPG) and electricity] for cooking and heating. The present results show that there were significantly ($p < 0.05$) seasonal variations of particulate-bound PAHs in the rural households. The daily mean concentrations of particulate-bound PAHs in the kitchens, sitting rooms and outdoors were apparently higher in winter than those in autumn, except those in the kitchens using coal. The present study also shows that there were obvious variations of particulate-bound PAHs among the four types of domestic energy used in the rural households. The households using LPG for cooking can, at least in some circumstances, have higher concentrations of PAHs in the kitchens than using crop residues or electricity. In addition, using coal in the sitting rooms seemed to result in apparently higher concentrations of particulate-bound PAHs than using the other three types of domestic energy during winter. The most severe contamination occurred in the kitchens using LPG in winter, where the daily mean concentrations of $PM_{2.5}$-bound PAHs were up to 762.5 ± 931.2 ng m^{-3}, indicating that there was serious

---

[*] Correspondence to: F. Wu, Key Laboratory of Plant Nutrition and the Agri-environment in Northwest China, Ministry of Agriculture, and College of Natural Resources and Environment, Northwest A&F University, Yangling, 712100 Shaanxi, PR China.
[**] Corresponding author.
E-mail addresses: wfy09@163.com (F. Wu), mhwong@hkbu.edu.hk (M.H. Wong).

http://dx.doi.org/10.1016/j.scitotenv.2015.07.101

health risk of inhalation exposure to PAHs in the rural households of Henan Province. Rural residents' exposure to $PM_{2.5}$-bound PAHs in kitchens would be roughly reduced by 69.8% and 85.5% via replacing coal or crop residues with electricity in autumn. The pilot research would provide important supplementary information to the indoor air pollution studies in rural area.

1. Introduction

More than 70% of China's households rely on solid fuels (mainly wood, crop residues and coal) for domestic energy, especially in rural areas (Smith et al., 2004). The combustion of biomass and coal is the dominant source of indoor air pollution in China and contributes significantly to the total burden of ill health (Zhang and Smith, 2007). Biomass burning, domestic coal combustion and coking industry resulted in 60%, 20% and 16% of the total emission of polycyclic aromatic hydrocarbons (PAHs) in China, respectively (Xu et al., 2006). As an important component of indoor air pollutants resulting from household combustion of the solid fuels, PAHs have partially caused higher risks for lung cancer, especially in developing countries (Straif et al., 2006). Inhalation exposure to ambient air PAHs is estimated to cause 1.6% of total lung cancer morbidity in China (Zhang et al., 2009). Moreover, a number of studies noted that indoor air can be many times more contaminated than outdoor air (Jiang and Bell, 2008; Wong et al., 2004). Given that most people (especially women and children) spend the majority of their time indoors and thus the potential health risks posed by indoor air PAHs are more serious. Therefore, it is critical to investigate levels of PAHs in rural households of China.

Previous studies have investigated indoor air PAHs in urban areas. Gustafson et al. (2008) found that the total PAHs cancer potency was significantly higher (about 4 times) in the wood-burning homes than the reference homes in a Swedish residential area. Masih et al. (2010) showed the spatial trend of total PAHs in the house at urban sites in North India, with kitchen > living room > outdoors. Total concentrations of PAHs ranged from 425 to 36,200 ng m^{-3} in residential air in Hangzhou, China, with the highest concentrations recorded in the kitchens (Zhu et al., 2009). However, there are only limited studies investigating indoor air PAHs in rural China. Furthermore, serious concentrations of PAHs have been recorded in these limited studies (Ding et al., 2012; Lu et al., 2006; Mumford et al., 1990). Up to 3249 ng benzo(a)pyrene m^{-3} was measured in rural households of Xuanwei (Mumford et al., 1990), which was over 3000 times of China's Indoor Air Quality Standards for BaP (1.0 ng m^{-3}) (GB/T, 1883–2002). Generally, PAHs are distributed between vapor and particulate phases in air and harmful PAHs with 5–6 aromatic rings are predominantly found in particulates (Lu and Chen, 2008; Slezakova et al., 2011). Allen et al. (1996) indicated that over 90% of PAHs in atmospheric aerosols are associated with $PM_{2.5}$ (aerodynamic diameter ≤ 2.5 μm). However, PAHs partition between $PM_{2.5}$ and PM_{10} (aerodynamic diameter ≤ 10 μm) is yet unknown in rural China.

Recently, both electricity and liquid petroleum gas (LPG) are becoming more popular in rural China. In 2010, 23% of rural households used clean fuels (LPG or electricity) as their main cooking fuel (NBS, 2012). The use of multi-fuels is a common feature of domestic energy in rural China mainly due to fuel availability. Presumably, there may be day-to-day or seasonal changes in PAH emission resulting from changes in patterns of energy use and/or housing conditions (such as house structure) in rural China. However, spatial and temporal patterns of PAHs in rural households using different types of domestic energy are still unclear in China.

The main objectives of the present study were to: (1) determine the seasonal variation of concentrations and distribution patterns of PAHs associated with $PM_{2.5}$ and PM_{10} in rural households of Henan Province and; (2) investigate differences in particulate-bound PAHs among four types of domestic energy (crop residues, coal, LPG and electricity) used.

2. Materials and methods

2.1. Sampling of $PM_{2.5}$ and PM_{10}

Henan Province is located in central China, where coal and crop residues are the primary domestic energy in rural areas. Two kinds of clean fuels: LPG and electricity, are also used in a few rural households for cooking more recently. Coal is a primary fuel used by nearly all households for heating and by a majority of households for cooking in Baofeng County (BF) of Henan Province, which is mainly dependent on coal-mine exploitation and agricultural production. Crop residues are commonly used for cooking and heating in Fangcheng County (FC) of Henan Province, mainly dependent on agricultural production. During the sampling period, three households of FC and three households of BF were requested to use crop residues or coal only for cooking and heating, respectively. In addition, another six households of BF were requested to use coal only for heating, half of them were requested to use LPG or electricity only for cooking, respectively. Main types of domestic energy used in the sampling houses of Henan Province are summarized in Table 1. At each of the household, four stationary active samplers (7388MAS aerosol sampler, Zhongshan SLC Environmental Technology Corp., China) were deployed, with two ($PM_{2.5}$ and PM_{10}) each in the kitchen and sitting room. In addition, two stationary active samplers were also deployed in outdoor in one of the three households which used the same domestic energy. The stationary sampling was conducted for nine consecutive days and the filters ($PM_{2.5}$ and PM_{10}) were changed and collected every three days during autumn (Sep to Oct 2012), while the sampling was done for six consecutive days and the filters ($PM_{2.5}$ and PM_{10}) were changed and collected every two days during winter (Jan 2013). Totally 168 $PM_{2.5}$ and PM_{10} samples were collected in kitchens, sitting rooms and outdoors from the 12 households. Details of the selection criteria and structure of the sampling households, sampling and the treatment of filters of $PM_{2.5}$ and PM_{10} were previously described (Wu et al., 2015).

Table 1
Main types of domestic energy used in the sampling houses of Henan Province.

Locations	House	Autumn		Winter	
		Kitchen	Sitting room	Kitchen	Sitting room
Fangcheng County (FC)	A	Crop	No energy used for heating	Crop	Crop
	B	Crop		Crop	Crop
	C	Crop		Crop	Crop
	A	Coal	No energy used for heating	Coal	Coal
	B	Coal		Coal	Coal
	C	Coal		Coal	Coal
Baofeng County (BF)	D	Liquid petroleum gas	No energy used for heating	Liquid petroleum gas	Coal
	E	Liquid petroleum gas		Liquid petroleum gas	Coal
	F	Liquid petroleum gas		Liquid petroleum gas	Coal
	G	Electricity	No energy used for heating	Electricity	Coal
	H	Electricity		Electricity	Coal
	J	Electricity		Electricity	Coal

2.2. Extraction and analysis of PAHs

Half of the sampled filters ($PM_{2.5}$ and PM_{10}) were Soxhlet extracted for 16 h with 100 mL of n-hexane/acetone/DCM mixture (1:1:1) (USEPA, 1996). The concentrated extracts were clean up using a florisil column (15 cm silica gel, and 1 cm anhydrous sodium sulfate from bottom up, pre-eluted with 20 mL n-hexane) with 70 mL hexane/DCM mixture (1:1) as elution solvent. The silica gel was baked at 450 °C for 6 h, activated at 300 °C for 12 h, and deactivated with deionized water (3%, w/w) prior to use. The anhydrous sodium sulfate was baked at 450 °C for 8 h. The eluant was concentrated to 1 mL, solvent exchanged to hexane, and spiked with 320 ng deuterated PAHs (naphthalene-d_8, acenaphthene-d_{10}, phenanthrene-d_{10}, chrysene-d_{12} and perylene-d_{12}). PAHs were analyzed using gas chromatographic mass spectrometry (GC, HP 6890, HP 5973, 30 m Agilent DB-5MS UI capillary column) in electron ionization mode. The oven temperature was programmed as the following: initial temperature at 100 °C, increased to 300 °C at a rate of 8 °C/min and held for 20 min, using He as the carrier gas. Data were scanned from 35 to 500 mass units. The target PAHs and their derivatives were identified based on retention time and qualifying ions of the standards in selected ion monitoring mode (SIM). Sixteen US EPA priority PAHs were measured in the present study: naphthalene (NAP), acenaphthylene (ACY), acenaphthene (ACE), fluorene (FLO), phenanthrene (PHE), anthracene (ANT), fluoranthene (FLA), pyrene (PYR), benzo(a)anthracene (BaA), chrysene (CHR), benzo(b)fluoranthene (BbF), benzo(k)fluoranthene (BkF), benzo(a)pyrene (BaP), indeno(1,2,3-c,d)pyrene (IcdP), dibenzo(a,h)-anthracene (DahA), and benzo(g,h,i)perylene (BghiP). BbF and BkF co-eluted and therefore were quantified together.

2.3. Quality control

All the glassware were cleaned using an ultrasonic cleaner and heated to 450 °C for 8 h. Each of the four field blanks were analyzed with the true samples obtained in autumn and winter, respectively. An international standard reference material of house dust (SRM 2585) obtained from the National Institute of Standards and Technology (NIST), USA was used for calibration and analytical control. A method blank, a standard reference material (SRM 2585) and a sample duplicate were analyzed in parallel with each batch of 10 filter samples. The coefficient of variation of PAH concentrations between duplicate samples was less than 10%. PAHs were identified on the basis of retention times relative to five deuterated internal standards (Nap-d_8, Ace-d_{10}, Phe-d_{10}, Chr-d_{10}, and Per-d_{12}). The recoveries based on SRM for individual PAH ranged from 65% to 127%.

2.4. Data analyses

NAP was not included in the total PAHs reported in the present study because of its lower recovery and higher percentage in the total PAHs. Statistical analyses were conducted using SPSS 19.0 (SPSS Inc., USA). Means of different groups were compared using one-way ANOVA test. Prior to one-way ANOVA test, the data was log transformed to meet the normality assumption. Unless otherwise indicated, all treatment means were tested for significant difference at $p < 0.05$.

3. Results

3.1. PAHs in household $PM_{2.5}$ and PM_{10} in rural Henan during autumn and winter

Table 2 shows the geometric mean concentrations of $PM_{2.5}$-bound and PM_{10}-bound PAHs in rural households of Henan Province during autumn and winter. The daily mean concentrations of particulate-bound PAHs in the kitchens, sitting rooms and outdoors in winter were apparently higher than those in autumn, except those in

Table 2
Summary of measured PAHs in $PM_{2.5}$ and PM_{10} in rural households using four types of domestic energy in Henan province during autumn and winter (mean ± S.D., n = 9 for kitchen and sitting room, n = 3 for outdoor, ng m^{-3}).

PM	PAHs	Kitchen				Sitting room				Outdoor			
		Crop	Coal	LPG	Electricity	Crop	Coal	LPG	Electricity	Crop	Coal	LPG	Electricity
$PM_{2.5}$	Autumn												
	LMW PAHs[a]	19.39 ± 11.05 a	3.18 ± 1.51 b	3.21 ± 1.31 b	4.71 ± 1.49 b	15.29 ± 5.47 a	4.84 ± 2.69 b	4.31 ± 1.52 b	4.25 ± 1.29 b	14.52 ± 6.57 a	2.21 ± 0.71 b	3.49 ± 0.71 b	5.20 ± 0.65 b
	HMW PAHs[b]	130.7 ± 95.71 b	308.8 ± 384.4 ab	472.1 ± 476.1 a	40.64 ± 12.90 b	25.33 ± 6.90 b	255.5 ± 407.3 a	48.58 ± 16.91 b	43.05 ± 11.91 b	49.92 ± 10.94 a	32.61 ± 2.14 a	41.07 ± 10.50 a	40.48 ± 15.60 a
	∑ PAHs[c]	150.1 ± 104.8 b	312.0 ± 385.2 ab	475.3 ± 476.2 a	45.35 ± 14.00 b	40.62 ± 10.55 b	260.4 ± 407.2 a	52.89 ± 17.60 b	47.3 ± 11.95 b	64.44 ± 5.75 a	34.82 ± 2.59 b	44.56 ± 10.05 b	45.68 ± 14.99 b
	TEQs-PAHs[d]	27.48 ± 21.92 b	79.88 ± 106.4 ab	111.3 ± 113.0 a	7.75 ± 4.05 b	3.34 ± 1.94 b	66.65 ± 113.8 a	11.3 ± 4.50 b	10.04 ± 3.28 b	9.85 ± 2.92 a	6.63 ± 0.84 a	8.79 ± 2.48 a	7.49 ± 3.05 a
	Winter												
	LMW PAHs	15.70 ± 6.21b	11.61 ± 3.77 b	62.83 ± 81.07 a	14.82 ± 10.45 b	7.36 ± 1.66 b	34.18 ± 47.93 a	26.33 ± 10.51 ab	20.64 ± 8.85 ab	8.70 ± 2.96 a	15.55 ± 2.48 a	16.06 ± 18.22 a	21.87 ± 19.18 a
	HMW PAHs	205.9 ± 138.3 b	154.1 ± 70.64 b	699.6 ± 868.5 a	144.6 ± 74.45 b	52.02 ± 13.58 b	621.4 ± 932.0 a	138.2 ± 106.4 b	190.7 ± 95.66 ab	80.44 ± 19.20 b	166.4 ± 45.64 a	109.9 ± 59.69 ab	82.03 ± 26.52 b
	∑ PAHs	221.6 ± 143.7 b	165.7 ± 73.45 b	762.5 ± 931.2 a	159.4 ± 81.94 b	59.37 ± 14.30 b	655.5 ± 979.7 a	164.6 ± 100.6 b	211.4 ± 94.82 ab	89.13 ± 22.10 b	181.9 ± 47.73 a	125.9 ± 64.12 ab	103.9 ± 42.23 ab
	TEQs-PAHs	30.82 ± 23.47 b	22.44 ± 13.64 b	113.1 ± 147.7 a	25.06 ± 12.20 b	5.65 ± 3.02 b	111.2 ± 185.7 a	22.55 ± 20.18 ab	33.41 ± 17.49 ab	13.30 ± 2.85 a	16.44 ± 6.54 a	14.02 ± 10.05 a	10.67 ± 2.82 a
PM_{10}	Autumn												
	LMW PAHs	4.57 ± 1.08 a	2.79 ± 0.98 b	3.54 ± 1.87 ab	2.97 ± 1.10 b	3.22 ± 1.00 a	2.76 ± 0.60 a	2.92 ± 1.30 a	3.73 ± 1.58 a	4.68 ± 1.62 ab	2.08 ± 0.62 c	3.37 ± 1.05 bc	5.41 ± 0.64 a
	HMW PAHs	131.5 ± 75.05 b	273.9 ± 288.0 ab	637.9 ± 803.3 a	43.09 ± 13.71 b	31.63 ± 5.82 b	340.0 ± 463.0 a	53.43 ± 16.61 b	39.99 ± 14.76 b	49.90 ± 10.94 a	36.65 ± 5.35 a	48.81 ± 18.14 a	38.99 ± 15.86 a
	∑ PAHs	136.0 ± 76.01 b	276.7 ± 287.7 ab	641.4 ± 804.3 a	46.06 ± 14.01 b	34.85 ± 5.51 b	342.8 ± 463.2 a	56.34 ± 16.52 b	43.72 ± 15.21 b	54.58 ± 9.97 a	38.73 ± 5.15 a	52.18 ± 17.10 a	44.4 ± 16.49 a
	TEQs-PAHs	22.14 ± 14.70 b	66.38 ± 79.25 ab	145.5 ± 199.7 a	7.22 ± 3.01 b	3.60 ± 1.84 b	85.32 ± 124.2 a	10.88 ± 5.06 b	6.93 ± 3.69 b	6.67 ± 3.19 a	6.19 ± 0.40 a	9.98 ± 3.78 a	6.48 ± 3.33 a
	Winter												
	LMW PAHs	9.94 ± 5.82 a	8.76 ± 3.50 a	14.99 ± 13.75 a	12.18 ± 3.36 a	6.44 ± 0.87 a	21.85 ± 38.5 a	7.14 ± 1.63 a	8.28 ± 3.69 a	5.83 ± 1.22 b	15.24 ± 7.45 a	11.11 ± 2.41 ab	10.68 ± 2.04 ab
	HMW PAHs	267.8 ± 144.0 ab	164.5 ± 97.29 b	622.2 ± 832.1 a	167.0 ± 92.48 b	58.12 ± 9.48 b	732.3 ± 1181 a	97.78 ± 44.56 b	164.8 ± 77.05 ab	66.84 ± 15.10 b	288.2 ± 183.1 a	147.0 ± 53.00 ab	134.4 ± 26.76 ab
	∑ PAHs	277.8 ± 148.6 ab	173.2 ± 99.75 b	637.2 ± 841.7 a	179.2 ± 94.95 b	64.55 ± 9.31 b	754.1 ± 1220 a	104.9 ± 45.34 b	173.1 ± 76.83 ab	72.67 ± 16.11 b	303.4 ± 190.2 a	158.1 ± 55.36 ab	145.1 ± 27.14 ab
	TEQs-PAHs	38.83 ± 21.73 ab	24.71 ± 17.13 b	95.24 ± 135.4 a	28.23 ± 24.91 ab	5.40 ± 1.69 b	129.0 ± 235.0 a	12.14 ± 7.22 b	26.19 ± 14.00 ab	8.43 ± 3.05 a	34.98 ± 29.02 a	14.47 ± 8 45 a	18.41 ± 6.66 a

[a] Low molecular weight 2–3 ring PAHs; [b] High molecular weight 4–6 ring PAHs; [c] ∑ PAH concentrations excluding NAP; [d] Total TEQs-PAH concentrations, PAH toxic equivalency factor with respect to BaP (Nisbet and LaGoy, 1992).
Different letters within the same row under the same venue indicate significant difference between different types of domestic energy at the level $p < 0.05$.

kitchens using coal. When crop residues were used, concentrations of $PM_{2.5}$-bound PAHs in the kitchens (221.6 ng m^{-3}), sitting rooms (59.4 ng m^{-3}) and outdoors (89.1 ng m^{-3}) in winter were 1.38–1.48 times higher than those in the corresponding microenvironments (150.1, 40.6 and 64.4 ng m^{-3}) in autumn, respectively. The concentrations of PAHs in $PM_{2.5}$ were comparable to those in PM_{10}. Both in winter and autumn, outdoor PAHs concentrations in $PM_{2.5}$ (34.8–64.4 ng m^{-3}) and PM_{10} (38.7–54.6 ng m^{-3}) were apparently lower than the corresponding concentrations in the kitchens (45.4–475.3 ng m^{-3} and 46.1–641.4 ng m^{-3} for $PM_{2.5}$ and PM_{10}, respectively) (many of the differences were statistically significant at $p < 0.05$) (Table 2). The average indoor/outdoor ratios of $PM_{2.5}$-bound PAHs for kitchens (0.99–10.67 and 0.91–6.06) were higher than the corresponding ratios for sitting rooms (0.63–7.48 and 0.67–3.60) in both autumn and winter, respectively, indicating heavy contamination in kitchen air of rural Henan.

3.2. Variations of particulate-bound PAHs in rural households using four types of domestic energy

Fig. 1 shows obvious variations of particulate-bound PAHs among four types of domestic energy used in the rural households of Henan Province. Surprisingly, using LPG in the kitchens resulted in apparently higher concentrations of particulate-bound PAHs than using crop residues or electricity, respectively. Either in autumn or in winter, the highest concentrations of $PM_{2.5}$-bound PAHs (475.3 and 762.5 ng m^{-3}) were recorded in the kitchens using LPG. As expected, using coal in the sitting rooms resulted in significantly ($p < 0.05$) higher concentrations of particulate-bound PAHs than using the other three types of domestic energy in autumn and winter. The concentrations of $PM_{2.5}$-bound PAHs in the sitting rooms using coal as the only household energy were 260.4 and 655.5 ng m^{-3} in autumn and winter, which were 6.41, 4.92 and 5.50 times of those in autumn and 11.04, 3.98 and 3.10 times of those in winter using crop residues, LPG and electricity, respectively.

3.3. Composition profiles of particulate-bound PAHs

The composition profiles of 15 PAHs in particulate phases in the kitchens, sitting rooms and outdoors measured during autumn and winter are shown in Fig. 2 and Tables 2–3. It was found that the composition profiles of particulate-bound PAHs were apparently different among four types of domestic energy used and between autumn and winter. In kitchens, a higher percentage of 2–3 ring PAHs was observed in $PM_{2.5}$ using crop residues (12.9%) and electricity (10.4%), compared with those using coal (1.02%) and LPG (0.67%) in autumn (Fig. 2, Table 2). In sitting rooms and outdoors, a higher percentage of 2–3 ring PAHs was also observed in $PM_{2.5}$ using crop residues (37.6% and 22.5%) compared with those using coal (1.86% and 6.34%), LPG (8.15% and 7.83%) and electricity (8.99% and 11.4%). In general, 4–5 ring PAHs were dominated in $PM_{2.5}$ (55.1–83.8%) and PM_{10} (60.8–97.1%), respectively (Fig. 2). The ratio of high molecular weight (HMW) PAHs (including FLA, PYR, BaA, CHR, B(b + k)F, BaP, IcdP, DahA and BghiP) to total PAHs in $PM_{2.5}$ and PM_{10} in autumn (62.4–99.3% and 87.8–99.5%) was comparable to that in winter (79.0–94.8% and 90.0–97.7%), respectively (Table 2). In addition, the composition profiles of $PM_{2.5}$-bound PAHs were similar with those of PM_{10}-bound PAHs (Table 3). Moreover, daily mean concentrations of BaP in $PM_{2.5}$ or PM_{10} were in excess of Chinese Air Quality Standards (1.0 ng m^{-3}) for indoor air (GB/T, 1883–2002) and the highest concentrations of BaP in $PM_{2.5}$ were up to 39.2 ng m^{-3} recorded in the sitting rooms using coal in winter, imposing serious potential health risks of rural indoor air to inhabitants of Henan Province.

4. Discussion

The present study shows that apparently higher levels of particulate-bound PAHs in the rural households of Henan Province were recorded in winter than in autumn (Fig. 1). The daily mean concentrations of $PM_{2.5}$-bound PAHs in the kitchens ranged from 45.4 to 475.3 ng m^{-3} in autumn and from 165.7 to 762.5 ng m^{-3} in winter, primarily due to minimal ventilation in winter when door and windows in the kitchen were often kept closed. In addition, there was significant ($p < 0.05$) difference in the concentrations of particulate-bound PAHs in the sitting rooms between winter and autumn. Besides minimal ventilation in winter, the higher levels of particulate-bound PAHs in the sitting rooms mainly resulted from combustion of coal or crop residues for heating, respectively. Similarly, Ding et al. (2012) observed that concentrations of particulate phase PAHs in the kitchen were significantly higher in winter (3288 ng m^{-3}) than those in summer (988 ng m^{-3}) in a rural household of northern China. Seasonal variation of particulate phase PAHs in urban air has also been investigated in a number of studies, most of which showed higher concentrations of PAHs in winter than in other seasons (Guo et al., 2003; Ravindra et al., 2006; Sin et al., 2003). In addition, Singh et al. (2011) showed that concentrations of particle-bound PAHs at a site in Delhi (India) varied inversely with temperature i.e., higher concentrations in winter and lower in summer. These suggested that the differences in ventilation and atmospheric temperature between autumn and winter can influence seasonal variation of particulate PAHs in the present study. The minimal ventilation and lower temperature in winter can result in higher levels of particulate-bound

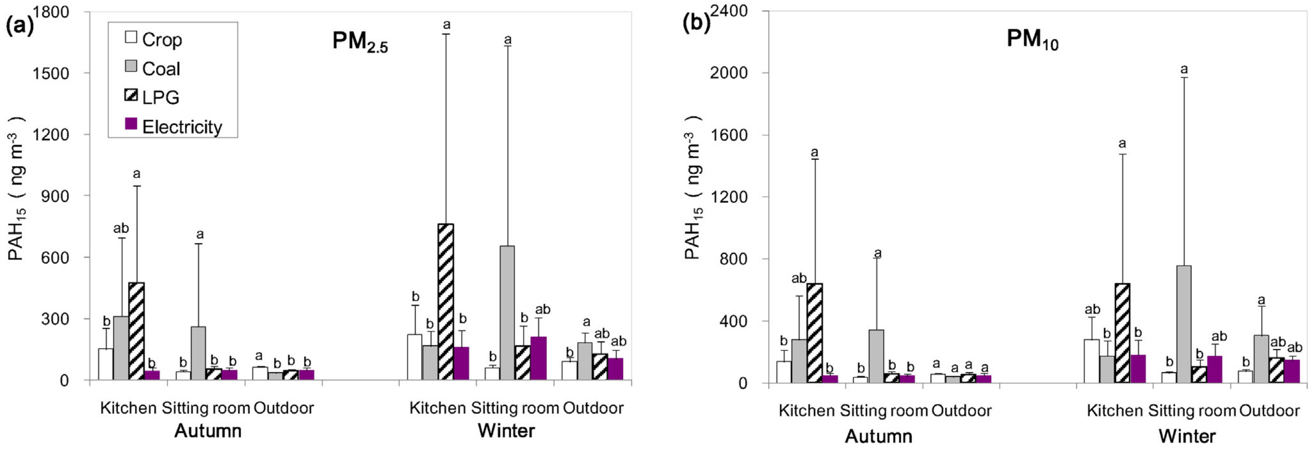

Fig. 1. Daily mean concentrations of PAH_{15} (total of 15 USEPA priority PAHs) in $PM_{2.5}$ (a) and PM_{10} (b) in rural households of Henan Province used four domestic energy during autumn and winter. Bars marked with different letters in the same site are significantly different according to least significant difference (LSD) test ($p < 0.05$) (mean ± S.D., n = 9 for kitchen and sitting room, n = 3 for outdoor).

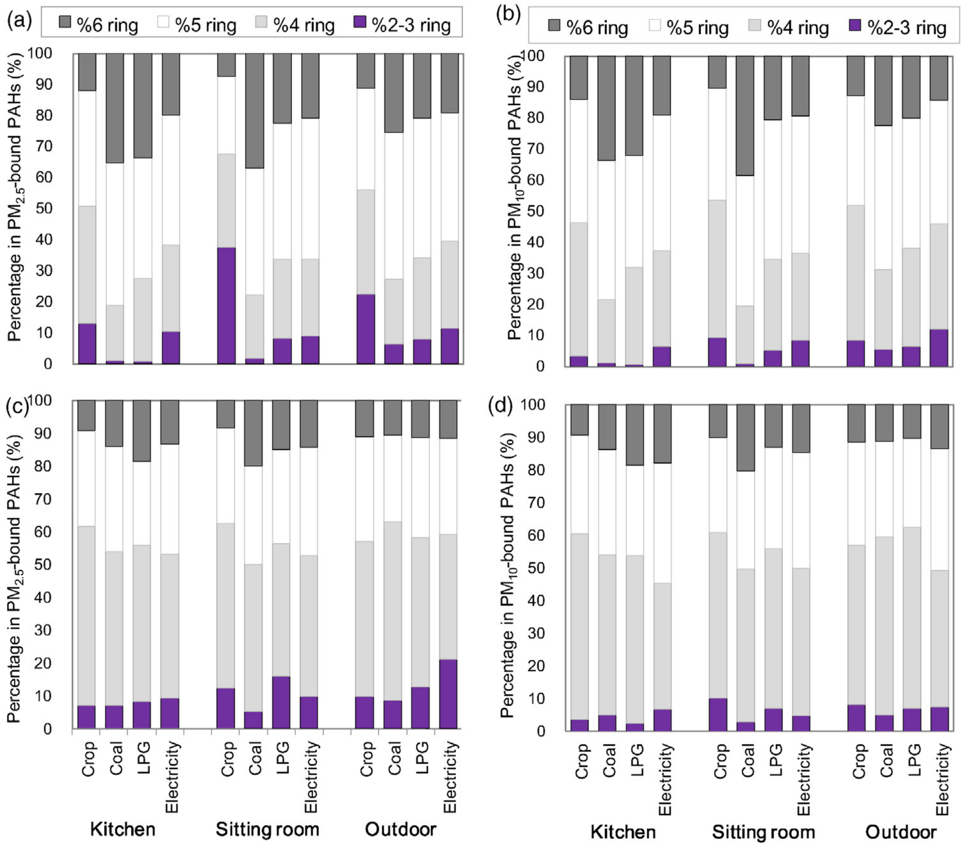

Fig. 2. Percentage contribution of different molecular weight PAHs groups to $PM_{2.5}$-bound (a, c) and PM_{10}-bound (b, d) PAHs in rural households of Henan Province used different domestic energy during autumn (a, b) and winter (c, d).

PAHs and a relatively larger portion of PAHs portioning to the particle phase, respectively.

The present study also shows that there were apparent variations in particulate-bound PAHs among four types of domestic energy used in the rural households of Henan Province. In autumn, the trend of $PM_{2.5}$-bound and PM_{10}-bound PAHs in the kitchens was as follows: LPG > coal > crop residues > electricity. Generally, LPG is often considered as a cleaner energy for cooking. However, the present study indicates that using LPG resulted in the highest concentrations of particulate-bound PAHs in the kitchens in rural Henan in both autumn and winter (Fig. 1). This may be attributed by the following two reasons. Firstly, activities such as frying and roasting in the kitchens using LPG may be more often than using other types of domestic energy mainly due to its being convenient for use, which would contribute to emissions of PAHs. Gao et al. (2009) found that family income has significant influence on cooking energy choice in rural agricultural area of Tibet, China. With living standards improving and getting wealthier in rural area of China, people would like to afford cooking energy which is more convenient and clean and it is a common phenomenon that frying and roasting is more often in the kitchens. Mestl et al. (2007) indicated that the levels of indoor air pollution are generally influenced by other sources such as cooking oil fumes, incense burning and smoking. Zhu and Wang (2003) found that frying and roasting can generate relatively higher concentrations of PAHs, with higher concentrations of BaP in the kitchen air derived from frying (65 ng m^{-3}) and roasting (45 ng m^{-3}). Ding et al. (2012) also showed that the concentrations of PAH_{15} in kitchen when LPG was used as the sole energy source (1400 ± 490 ng m^{-3}) were similar to those when wood was burned (1500 ± 1400 ng m^{-3}). Secondly, comparable or higher concentrations of PM resulted from combustion of LPG were recorded in the kitchens, which could absorb more PAHs. A significant positive correlation was found between PM_{10} concentrations and PM_{10}-bound PAHs in autumn ($r = 0.533$, $p < 0.001$, $n = 36$). Our recent study demonstrated that $PM_{2.5}$ concentrations in kitchens using LPG were comparable with using crop residues and coal, and the corresponding PM_{10} concentrations (421.5 ± 171.3 μg m^{-3}) were apparently higher in autumn than using crop residues (237.4 ± 84.2 μg m^{-3}), coal (288.0 ± 73.8 μg m^{-3}) or electricity (211.4 ± 64.7 μg m^{-3}) in rural Henan (Wu et al., 2015). Further studies are needed to understand emissions of PAHs in kitchens using LPG because increasing rural Chinese households are shifting from the use of biomass and coal to LPG as a “clean” fuel. However, using another clean energy (electricity) would improve kitchen air quality by reducing $PM_{2.5}$-bound and PM_{10}-bound PAHs to 14.5–30.2% and 16.7–33.9% of those using coal and crop residues in autumn, respectively (Fig. 1; Table 2).

The highest concentrations of particulate-bound PAHs generally occurred in the kitchens in rural Henan, except those using coal in winter (Fig. 1). This was mainly due to both the combustion of crop residues or using LPG for cooking and the activities such as frying, stir frying and deep frying food are quite often which may be responsible for generating large amount of PAHs (Koo et al., 1994). In addition, most of the kitchens had no ventilating fans installed and PAHs could not be diluted in time due to the small space of kitchens in rural Henan. The higher concentrations of particulate-bound PAHs in sitting rooms using coal reflected long heating hours in winter. Frequently, cooking and heating take place in the sitting rooms during winter in rural households, making those the main exposure microenvironments.

The present study shows that indoor air quality was a serious problem in rural Henan Province (Table 2). The daily mean concentrations of $PM_{2.5}$-bound PAHs were up to 762.5 ± 931.2 ng m^{-3} in the kitchens in winter. Using coal also resulted in higher particular-bound PAHs in the sitting rooms. Moreover, the domination of 4–5 ring PAHs in $PM_{2.5}$ (55.1–83.8%) and PM_{10} (60.8–97.1%) further aggravated the deterioration of indoor air quality (Fig. 2, Table 3). A previous study also indicated

Table 3

Geometric mean concentrations of PAHs in $PM_{2.5}$ and PM_{10} in rural households using four types of domestic energy in Hean province during autumn and winter (mean, n = 9 for kitchen and sitting room, n = 3 for outdoor, ng m^{-3}).

PAHs	$PM_{2.5}$												PM_{10}											
	Kitchen				Sitting room				Outdoor				Kitchen				Sitting room				Outdoor			
	Crop	Coal	LPG	Electricity	Crop	Coal	LPG	Electricity	Crop	Coal	LPG	Electricity	Crop	Coal	LPG	Electricity	Crop	Coal	LPG	Electricity	Crop	Coal	LPG	Electricity
Autumn																								
ACY	0.12	0.03	0.02	0.04	0.08	0.03	0.11	0.06	0.01	0.01	0.03	0.04	0.15	0.03	0.03	0.17	0.09	0.02	0.04	0.03	0.21	0.01	0.02	0.02
ACE	0.04	0.02	0.01	0.04	0.06	0.03	0.04	0.07	0.02	0.01	0.01	0.04	0.06	0.01	0.00	0.01	0.06	0.01	0.01	0.00	0.09	0.03	0.00	0.01
FLO	1.09	0.32	0.33	0.38	0.89	0.39	0.47	0.54	0.73	0.19	0.18	0.48	0.40	0.18	0.21	0.24	0.27	0.25	0.24	0.19	0.47	0.33	0.11	0.35
PHE	17.8	2.65	2.68	4.11	14.1	4.26	3.52	3.42	13.5	1.94	3.20	4.45	3.79	2.47	3.11	2.45	2.68	2.36	2.48	3.41	3.82	1.65	3.14	4.85
ANT	0.33	0.15	0.16	0.14	0.11	0.14	0.17	0.16	0.26	0.06	0.08	0.20	0.17	0.10	0.19	0.10	0.12	0.12	0.15	0.09	0.08	0.07	0.09	0.18
FLA	9.47	3.34	5.35	2.61	3.37	5.11	3.21	2.71	5.46	2.15	2.55	3.40	10.4	4.19	7.19	2.87	4.18	4.33	4.08	2.74	6.49	2.71	3.56	4.15
PYR	8.71	2.37	4.38	1.91	2.31	3.21	3.40	1.97	4.24	1.46	2.02	2.41	10.2	3.86	5.13	2.02	3.39	3.02	3.52	2.11	5.31	1.83	3.05	2.90
BaA	20.0	9.23	24.5	2.77	2.71	9.27	2.30	2.29	5.17	1.29	2.15	2.36	18.5	8.70	44.7	2.75	3.01	10.4	2.81	2.26	4.72	1.81	3.02	2.52
CHR	18.7	40.7	94.2	5.36	3.80	35.3	4.56	4.74	6.78	2.43	5.10	4.72	19.2	39.8	145.4	6.59	4.86	45.8	6.08	5.13	7.10	3.68	6.83	5.43
B(b + k)F	14.3	77.4	100.9	8.24	3.64	53.9	8.50	8.00	5.61	6.42	7.89	8.35	16.6	69.1	118.2	10.3	5.12	77.3	10.4	9.22	6.88	8.34	7.75	9.10
BaP	18.5	28.9	39.8	4.39	1.27	25.5	7.27	6.67	6.45	3.67	5.40	4.32	13.1	23.2	52.6	3.80	1.16	28.0	6.46	3.70	3.32	2.87	6.34	3.68
IcdP	23.1	36.9	43.6	6.35	5.26	26.9	7.52	6.83	8.93	6.33	6.68	6.24	24.5	32.4	59.4	6.01	6.31	39.5	8.41	6.45	9.11	6.72	7.86	4.94
DahA	2.85	37.5	52.6	1.49	0.82	31.2	2.04	1.52	1.28	1.45	1.59	1.34	2.69	31.1	67.9	1.37	0.90	43.2	2.09	1.30	1.13	1.51	1.61	1.03
BghiP	15.0	72.4	106.8	7.52	2.14	65.2	9.76	8.34	6.01	7.41	7.71	7.35	16.1	61.5	137.4	7.36	2.69	88.4	9.56	7.08	5.83	7.17	8.79	5.26
Winter																								
ACY	0.23	0.09	0.14	0.16	0.13	0.13	0.09	0.21	0.10	0.15	0.11	0.08	0.06	0.12	0.07	0.09	0.20	0.07	0.05	0.07	0.07	0.15	0.12	0.06
ACE	0.05	0.02	0.06	0.01	0.07	0.04	0.04	0.02	0.01	0.02	0.04	0.01	0.07	0.05	0.03	0.03	0.10	0.04	0.03	0.02	0.01	0.03	0.04	0.01
FLO	1.10	0.66	1.98	0.68	0.83	1.25	0.98	0.92	0.95	0.81	0.75	0.63	0.56	0.38	0.49	0.41	0.66	0.46	0.40	0.36	0.48	0.66	0.48	0.23
PHE	13.1	10.3	57.2	13.4	6.17	31.2	24.9	18.7	7.19	13.6	15.1	20.9	8.44	7.84	13.1	11.2	5.34	19.9	6.39	7.57	5.02	13.7	10.2	10.2
ANT	1.25	0.52	3.47	0.57	0.16	1.58	0.32	0.79	0.45	0.98	0.11	0.23	0.81	0.37	1.30	0.41	0.13	1.39	0.27	0.27	0.26	0.70	0.25	0.17
FLA	35.6	21.4	44.2	19.7	9.51	38.7	13.7	22.8	11.2	32.7	15.4	11.3	45.6	23.7	41.1	19.4	10.4	52.4	12.7	19.3	10.3	55.9	28.3	14.6
PYR	30.3	15.9	38.9	15.5	6.23	32.1	10.4	17.5	10.4	23.9	11.2	7.94	40.9	18.1	36.1	14.9	7.21	43.0	9.44	14.7	7.92	40.3	19.6	11.2
BaA	27.7	12.5	58.4	12.1	5.61	50.3	11.5	15.6	8.95	13.8	9.17	6.42	35.6	12.9	52.0	11.0	5.63	58.3	8.20	12.9	6.79	22.3	10.7	9.95
CHR	27.4	28.2	221.5	22.8	8.46	172.6	31.0	35.2	11.8	28.8	21.6	14.2	36.0	29.9	198.7	23.5	9.49	199.0	21.2	31.2	10.5	46.9	29.0	24.9
B(b + k)F	18.7	21.6	101.3	19.3	6.37	98.8	19.6	26.8	7.87	20.9	16.1	13.5	25.4	22.3	91.3	28.8	7.58	113.2	15.1	26.2	8.18	35.2	19.1	25.3
BaP	19.3	11.4	38.4	15.8	2.12	39.2	11.4	19.2	8.38	6.55	7.13	4.68	24.6	13.5	31.1	12.8	1.58	45.6	5.00	13.9	4.19	19.1	6.55	8.21
IcdP	26.8	20.0	55.6	18.6	8.80	58.2	16.1	23.9	12.0	20.6	15.1	12.0	33.9	20.3	53.5	24.8	9.73	68.4	12.5	21.2	10.6	34.6	17.4	20.6
DahA	3.63	5.14	49.8	3.82	1.31	48.6	5.87	6.91	1.80	3.84	2.48	2.51	4.06	5.14	41.6	8.44	1.35	56.3	3.21	5.75	1.47	5.83	2.71	4.17
BghiP	16.5	18.0	91.6	17.1	3.61	82.8	18.6	22.7	8.10	15.3	11.6	9.51	21.8	18.6	76.9	23.3	5.10	96.1	10.5	19.8	6.87	28.1	13.7	15.5

seriously high concentrations of PAHs being recorded in rural households of Yunnan and Hebei Province, respectively (Ding et al., 2012; Mumford et al., 1990). The daily mean concentrations of BaP associated with $PM_{2.5}$ or PM_{10} were exceeded the Chinese Air Quality Standards (1.0 ng m^{-3}) for indoor air (GB/T, 1883–2002) in autumn and winter. In addition, the sampled households in the present study also suffered serious levels of $PM_{2.5}$ and PM_{10} (Wu et al., 2015). Ohura et al. (2005) indicated that the combination of $PM_{2.5}$ with carcinogenic PAHs could impose harmful effects on human health and can predispose people to respiratory disease. The present study further confirms the serious health risk of inhalation exposure to PAHs in rural households of Henan Province.

5. Conclusion

This paper attempts to report a pilot research on PAH concentrations associated with different types of domestic energy used in rural areas. Although the present study did not uncover a full picture of indoor air pollution, it did provide new information on PAH concentrations in rural Henan. Based on the limited $PM_{2.5}$ and PM_{10} samples collected in the two seasons, high concentrations of $PM_{2.5}$-bound and PM_{10}-bound PAHs were detected in the rural households using four types of domestic energy in Henan Province. The most severe contamination occurred in the kitchens in winter, where the daily mean concentrations of $PM_{2.5}$-bound PAHs were up to 762.5 ± 931.2 ng m^{-3}, indicating that there was serious health risk of inhalation exposure to PAHs in rural households of Henan Province. The present results also show that particulate-bound PAHs in rural households exhibited a large variability between the two seasons and among four types of domestic energy used. Significantly higher levels of particulate-bound PAHs in rural Henan Province were recorded in winter than in autumn. Surprisingly, using LPG resulted in the highest concentrations of particulate-bound PAHs in the kitchens in rural Henan. However, using electricity would significantly improve indoor air quality by reducing $PM_{2.5}$-bound and PM_{10}-bound PAHs.

Acknowledgment

The financial support from the National Natural Science Foundation of China/Hong Kong Research Grants Council Joint Research Scheme (NFSC/RGC N_HKBU210/11), Program for Science&Technology Innovation Talents in Universities of Henan Province (14HASTIT048) and the Scientific Research Foundation for the Introduction of Talent, Northwest A&F University, China (2014) is gratefully acknowledged.

References

Allen, J.O., Dookeran, N.M., Smith, K.A., Sarofim, A.F., Taghizadeh, K., Lafleur, A.L., 1996. Measurement of polycyclic aromatic hydrocarbons associated with size-segregated atmospheric aerosols in Massachusetts. Environ. Sci. Technol. 30, 1023–1031.

Ding, J.N., Zhong, J.J., Yang, Y.F., Li, B.G., Shen, G.F., Su, Y.H., Wang, C., Li, W., Shen, H.Z., Wang, B., Wang, R., Huang, Y., Zhang, Y.Y., Cao, H.Y., Zhun, Y., Simonich, S.L.M., Tao, S., 2012. Occurrence and exposure to polycyclic aromatic hydrocarbons and their derivatives in a rural Chinese home through biomass fuelled cooking. Environ. Pollut. 169, 160–166.

Gao, X., Yu, Q., Gu, Q., Chen, Y., Ding, K., Zhu, J., Chen, L., 2009. Indoor air pollution from solid biomass fuels combustion in rural agricultural area of Tibet, China. Indoor Air 19, 198–205.

GB/T, 1883–2002. Indoor Air Quality Standard in P.R. China.

Guo, H., Lee, S.C., Ho, K.F., Wang, X.M., Zou, S.C., 2003. Particle-associated polycyclic aromatic hydrocarbons in urban air of Hong Kong. Atmos. Environ. 37, 5307–5317.

Gustafson, P., Ostman, C., Sallsten, G., 2008. Indoor levels of polycyclic aromatic hydrocarbons in homes with or without wood burning for heating. Environ. Sci. Technol. 42, 5074–5080.

Jiang, R.T., Bell, M.L., 2008. A comparison of particulate matter from biomass-burning rural and non-biomass-burning urban households in northeastern China. Environ. Health Perspect. 116, 907–914.

Koo, L.C., Matsushita, H., Ho, J.H.C., Wong, M.C., Shimizu, H., Mori, T., Matsuki, H., Tominago, S.C., 1994. Carcinogens in the indoor air of Hong-Kong homes — levels, sources, and ventilation effects on 7 polynuclear aromatic-hydrocarbons. Environ. Technol. 15, 401–418.

Lu, H., Chen, S., 2008. Pollution level, phase distribution and health risk of polycyclic aromatic hydrocarbons in indoor air at public places of Hangzhou, China. Environ. Pollut. 152, 569–575.

Lu, C.G., Gao, X., Yu, Q., Li, C.L., Chen, L.M., 2006. Indoor air polycyclic aromatic hydrocarbons in rural tibetan residence and the depositions on human respiratory tract. J. Fudan. Univ. 45, 714–718.

Masih, J., Masih, A., Kulshrestha, A., Singhvi, R., Taneja, A., 2010. Characteristics of polycyclic aromatic hydrocarbons in indoor and outdoor atmosphere in the North central part of India. J. Hazard. Mater. 177, 190–198.

Mestl, H.E., Aunan, K., Seip, H.M., Wang, S., Zhao, Y., Zhang, D., 2007. Urban and rural exposure to indoor air pollution from domestic biomass and coal burning across China. Sci. Total Environ. 377, 12–26.

Mumford, J.L., Helmes, C.T., Lee, X., Seidenberg, J., Nesnow, S., 1990. Mouse skin tumorigenicity studies of indoor coal and wood combustion emissions from homes of residents in Xuan Wei, China with high lung cancer mortality. Carcinogenesis 11, 397–403.

NBS (National Bureau of Statistics), 2012. Tabulation on the 2010 Population Census of the People's Republic of China. Population Census Office of the State Council and Population and Employment Statistics Department, National Bureau of Statistics of China China, Statistics Press.

Nisbet, I.C.T., LaGoy, P.K., 1992. Toxic equivalency factors (TEFs) for polycyclic aromatic hydrocarbons (PAHs). Regul. Toxicol. Pharmacol. 16, 290–300.

Ohura, T., Noda, T., Amagai, T., Fusaya, M., 2005. Prediction of personal exposure to PM2.5 and carcinogenic polycyclic aromatic hydrocarbons by their concentrations in residential microenvironments. Environ. Sci. Technol. 39, 5592–5599.

Ravindra, K., Bencs, L., Wauters, E., de Hoog, J., Deutsch, F., Roekens, E., Bleux, N., Berghmans, P., Grieken, R., 2006. Seasonal and site-specific variation in vapour and aerosol phase PAHs over Flanders (Belgium) and their relation with anthropogenic activities. Atmos. Environ. 40, 771–785.

Sin, D.W.M., Wong, Y.C., Choi, Y.Y., Lam, C.H., Louie, P.K.K., 2003. Distribution of polycyclic aromatic hydrocarbons in the atmosphere of Hong Kong. J. Environ. Monit. 5, 989–996.

Singh, D.P., Gadi, R., Mandal, T.K., 2011. Characterization of particulate-bound polycyclic aromatic hydrocarbons and trace metals composition of urban air in Delhi, India. Atmos. Environ. 45, 7653–7663.

Slezakova, K., Castro, D., Delerue-Matos, C., Alvim-Ferraz, M.C., Morais, S., Pereira, M.C., 2011. Air pollution from traffic emissions in Oporto, Portugal: health and environmental implications. Microchem. J. 99, 51–59.

Smith, K.R., Mehta, S., Maeusezahl-Feuz, M., 2004. Indoor air pollution from household solid fuel use. In: Ezzati, M., Lopez, A.D., Rodgers, A., Murray, C.J.L. (Eds.), Comparative Quantification of Health Risks: Global and Regional Burden of Disease Attributable to Selected Major Risk Factors. World Health Organization, Geneva, Switzerland, pp. 1435–1493.

Straif, K., Baan, R., Grosse, Y., Secretan, B., El Ghissassi, F., Cogliano, V., 2006. Carcinogenicity of household solid fuel combustion and of high-temperature frying. Lancet Oncol. 7, 977–978.

USEPA, 1996. Method 3540C: Soxhlet Extraction. US Environmental Protection Agency, Washington, DC.

Wong, G.W.K., Ko, F.W.S., Hui, D.S.C., Fok, T.F., Carr, D., von Mutius, E., Zhong, N.S., Chen, Y.Z., Lai, C.K.W., 2004. Factors associated with difference in prevalence of asthma in children from three cities in China: multicentre epidemiological survey. Br. Med. J. 329, 486–488.

Wu, F.Y., Wang, W., Man, Y.B., Chan, C.Y., Liu, W.X., Tao, S., Wong, M.H., 2015. Levels of PM2.5/PM10 and associated metal(loid)s in rural households of Henan Province, China. Sci. Total Environ. 512–513, 194–200.

Xu, S.S., Liu, W.X., Tao, S., 2006. Emission of polycyclic aromatic hydrocarbons in China. Environ. Sci. Technol. 40, 702–708.

Zhang, J.J., Smith, K.R., 2007. Household air pollution from coal and biomass fuels in China: measurements, health impacts, and interventions. Environ. Health Perspect. 115, 848–855.

Zhang, Y.X., Tao, S., Shen, H.Z., Ma, J.M., 2009. Inhalation exposure to ambient polycyclic aromatic hydrocarbons and lung cancer risk of Chinese population. Proc. Natl. Acad. Sci. U. S. A. 106, 21063–21067.

Zhu, L.Z., Wang, J., 2003. Sources and patterns of polycyclic aromatic hydrocarbons pollution in kitchen air, China. Chemosphere 50, 611–618.

Zhu, L.Z., Lu, H., Chen, S.G., Amagai, T., 2009. Pollution level, phase distribution and source analysis of polycyclic aromatic hydrocarbons in residential air in Hangzhou, China. J. Hazard. Mater. 162, 1165–1170.

Effects of mycorrhizal inoculation of upland rice on uptake kinetics of arsenate and arsenite

Fuyong Wu[1,2,3]*, **Xueping Liu**[2], **Shengchun Wu**[4], and **Ming Hung Wong**[3,4]

[1] Key Laboratory of Plant Nutrition and the Agri-environment in Northwest China, Ministry of Agriculture, and College of Natural Resources and Environment, Northwest A&F University, Yangling 712100, Shaanxi, PR China
[2] School of Municipal and Environment Engineering, Henan University of Urban Construction, Pingdingshan, 467036, Henan, PR China
[3] Croucher Institute for Environmental Sciences, and Department of Biology, Hong Kong Baptist University, Kowloon Tong, Hong Kong SAR, PR China
[4] School of Environmental and Resource Sciences, Zhejiang Agricultural and Forestry University, Linan, Zhejiang, PR China

Abstract

We assessed the effect of mycorrhizal inoculation on short-term uptake kinetics of arsenate and arsenite by excised roots of upland rice (*Oryza sativa* L. cv. Zhonghan 221). A concentration of 0.01–0.05 mM arsenic (As) differentially affected the influx rates of both arsenate and arsenite into rice roots non-inoculated or inoculated with *Glomus mosseae* and *G. versiforme*. While V_{max} for arsenate uptake by non-mycorrhizal roots was 1.02 μmol g^{-1} fresh weight h^{-1}, it was reduced by a factor of 2.4 for mycorrhizal roots (about 0.42 μmol g^{-1} fresh weight h^{-1}) in the high-affinity uptake system. However, at high concentrations of 0.5–2.5 mM As only *G. versiforme* was able to reduce As influx. The results show that mycorrhizal effects on As uptake of upland rice are both concentration and species-specific.

Key words: AM fungi / inorganic arsenic / *Oryza sativa* / upland rice

Accepted January 27, 2015

1 Introduction

Arsenic (As) contamination is of growing concern in many regions of Asia (*Meharg*, 2004). Excessive accumulation of As in soils not only results in environmental contamination but also affects food safety. Inorganic As (arsenate and arsenite) is the predominant form of As in soils, and both arsenite and arsenate are easily taken up by rice roots (*Abedin* et al., 2002; *Chen* et al., 2005). Concentrations of up to 1.8 mg kg^{-1} As have been reported in rice grain originating from As-contaminated soils in Bangladesh (*Meharg* and *Rahman*, 2003). Human As intake from consumption of rice can be substantial and in some cases exceeds that from drinking water (*Williams* et al., 2006; *Zavala* et al., 2008). Hence, mitigation measures to reduce As concentrations in rice grain are urgently needed.

Arbuscular mycorrhizal (AM) fungi can not only significantly enhance the phosphate acquisition by host plants (*Smith* and *Smith*, 2011) but may also significantly decrease As grain concentrations of upland rice, growing on As-spiked soils (own preliminary investigations). Thus, AM fungi may alleviate adverse effects on rice caused by arsenate in soils (*Wu* et al., 2014). However, *Li* et al. (2011b) showed that AM effects on grain As concentrations tend to differ between rice/AM combinations. The mechanisms by which AM fungi influence As uptake of upland rice are still largely unknown.

Arsenate is the main As species under aerobic soil conditions, while arsenite dominates in anaerobic environments such as flooded paddy soils (*Smith* et al., 1998; *Xu* et al., 2008). Depending on the redox status of the soil, arsenate and arsenite are inter-convertible. Due to the fact that arsenate acts as a phosphate analogue (*Abedin* et al., 2002) and is transported across plasma membranes *via* phosphate transport systems (*Poynton* et al., 2004), it is expected that AM enhance not only the uptake of P but also that of As. However, it has been shown that AM fungi can have contradictory effects on P and As acquisition by alfalfa and upland rice grown under aerobic soil conditions (*Chen* et al., 2007; *Wu* et al., 2014). In addition, arsenate and arsenite are taken up by different transporters in rice (*Abedin* et al., 2002). Preliminary physiological (*Meharg* and *Jardine*, 2003) and molecular studies (*Ma* et al., 2008) suggested that arsenite may be transported by aquaporins in rice. Thus, our present knowledge of the mechanisms of AM fungi on plant arsenate uptake cannot be extrapolated to arsenite. The present work investigated (1) the effects of AM fungi on the arsenate and arsenite uptake kinetics of excised roots of upland rice, and (2) the variation in As uptake by different AM species.

2 Material and methods

2.1 Cultivation of rice seedlings

Seeds of upland rice (*Oryza sativa* L. cv. Zhonghan 221) were obtained from the National Rice Research Institute (CNRRI), Hangzhou, China. The seeds were sterilized with 20% H_2O_2 for 30 s, washed thoroughly with deionized water,

---

* Correspondence: F. Y. Wu ; e-mail: wfy09@163.com

then incubated in petri dishes with moistened filter papers and placed into a 30°C incubator for 3 d. Seedlings were transferred to 20% Hoagland–Arnon nutrient solution (*Hoagland* and *Arnon*, 1938): 0.2 mM KH_2PO_4, 1.0 mM KNO_3, 1.0 mM $Ca(NO_3)_2$, 0.4 mM $MgSO_4$, 9 μM H_3BO_3, 1.8 μM $MnCl_2$, 0.15 μM $ZnSO_4$, 0.07 μM $CuSO_4$, 0.03 μM H_2MoO_4, 4 μM Fe-EDTA. The nutrient solution was changed twice per week. After 2 weeks, the seedlings of uniform height (about 15 cm) were used for the following plant inoculation.

2.2 Plant inoculation

Soil was collected from a farm in Tai Po, Hong Kong, and its attributes have been described by *Wu* et al. (2014). After passing through a 2 mm sieve, the soils were autoclaved at 121°C for 2 h and air-dried. Both *Glomus mosseae* BGC GD01A and *G. versiforme* BGC GD01B had been isolated previously from the rhizosphere of the As hyper-accumulator species *Pteris vittata* L. (*Wu* et al., 2009). Pots, containing 1.5 kg soil and four rice seedlings, were inoculated with 50 g AM fungi, consisting of spores, colonized root fragments, and external mycelium. Sterilized inoculum (50 g) and mycorrhizal fungal-free filtrate (50 mL) from the suspension were added to the soils serving as non-mycorrhizal control treatments. There were ten replications per treatment. The plants were watered with deionized water every other day to maintain 80% water-holding capacity, and with 20% Hoagland–Arnon nutrient solution (*Hoagland* and *Arnon*, 1938) once per week. Plants were cultivated in a greenhouse with 28/23°C, day/night temperatures. Natural sunlight was supplemented by cool-white fluorescent lamps to achieve a photon flux density of 350 $\mu mol\ m^{-2}\ s^{-1}$ for 12 $h\ d^{-1}$.

2.3 Concentration-dependent kinetics of arsenate and arsenite uptake

After 8 weeks of growth, roots of upland rice were washed with deionized water to remove adhering soil, excised at the basal node, and incubated for 20 min in a pretreatment solution containing 0.5 mM $Ca(NO_3)_2$ and 10 mM 2-(*N*-morpholino) ethanesulfonic acid (MES), adjusted to a pH of 5.0. Excised roots (0.4–0.6 g fresh weight) were transferred into an aerated test solution amended with different concentrations of arsenate (Na_2HAsO_4) or arsenite ($NaAsO_2$), ranging from 0 to 0.0532 mM for the high-affinity and from 0 to 2.5 mM for the low-affinity uptake experiments, respectively, using three replications. After 20 min, the excised roots were rinsed with deionized water and incubated in an ice-cold, As-free medium (containing 10 mM MES, 0.5 mM $Ca(NO_3)_2$ and 1 mM Na_2HPO_4) for 15 min to remove apoplastic As. The roots were blotted dry, weighed and oven-dried before being ground.

Sub-samples of fine roots were collected and clarified in 10% (w/w) KOH at 90°C for 1 h, rinsed three times, bleached with fresh alkaline H_2O_2 solution (30 mL 10% H_2O_2 + 3 mL of NH_4OH + 567 mL deionized water) for 20 min to 1 h, acidified with 1% HCl (1–4 min) and stained with 0.05% Trypan Blue (modified method of *Phillips* and *Hayman*, 1970). The AM colonization was quantified on fifty 1-cm-long fine root segments using the slide-length method (*Giovannetti* and *Mosse*, 1980) and examined under a stereomicroscope (Nikon) at 100× magnification. Length of roots of infected cortex was assessed in millimeters for each root piece, averaged for 50 pieces, and expressed as a percentage AM colonization, using four replications.

2.4 Chemical analyses

The As and P contents in plant tissues were analyzed after acid digestion [conc. HNO_3 + conc. $HClO_4$ (85 : 15, v/v)] with Inductively Coupled Plasma Mass Spectroscopy (ICP-MS, Perkin–Elmer, Elan 9000). Blanks and a standard reference (Tomato leaves, SRM 1573a) from the U.S National Institute of Standards and Technology were used for quality assurance. The recovery rates of As were within 91 ± 7.9%.

2.5 Statistical analyses

The differences in As and P concentrations in plants were tested using Fisher's protected least significant difference (LSD) after analysis of variance (ANOVA). Curve fitting was done using SigmaPlot. All statistical procedures including Pearson's partial correlation analysis were carried out using SAS 8.1. Unless otherwise indicated, all treatment means were tested for significant difference at $P < 5\%$.

3 Results

3.1 Mycorrhizal colonization

Moderate colonization was recorded in roots of rice roots inoculated with *G. mosseae* and *G. versiforme* ranging from 26 to 31%, while roots of control plants remained largely uncolonized (< 1%). There were insignificant differences in AM colonization rates of roots between the two species of AM fungi.

3.2 Effects of AM fungi on uptake kinetics of arsenate and arsenite

As expected, inoculation significantly increased P concentrations (0.53 ± 0.10 $g\ kg^{-1}$) of non-mycorrhizal roots to 1.08 ± 0.22 of roots inoculated with *G. mosseae* and 1.03 ± 0.37 with *G. versiforme*. Regardless of the AM fungi, influx of arsenate and arsenite into upland rice followed a hyperbolic trend with increasing concentrations of As in solution (Fig. 1). While the uptake of arsenate was significantly larger by non-mycorrhizal than that by both AM-inoculated roots at 0.01–0.05 mM, only *G. versiforme* was able to significantly reduce the uptake of arsenite. Also at low As concentrations in the solution, inoculation with both AM fungi reduced the arsenate and the arsenite uptake by roots (Table 1) with concentration-dependent influx fitting Michaelis–Menten kinetics (Table 2).

However, the kinetics for arsenate differed considerably between mycorrhizal and non-mycorrhizal roots. Thus, the V_{max} of 1.02 $\mu mol\ g^{-1}$ fresh weight h^{-1} for the arsenate uptake by non-mycorrhizal roots was 2.4-fold higher than that of mycorrhizal roots with 0.43 and 0.41 $\mu mol\ g^{-1}$ fresh weight h^{-1} for

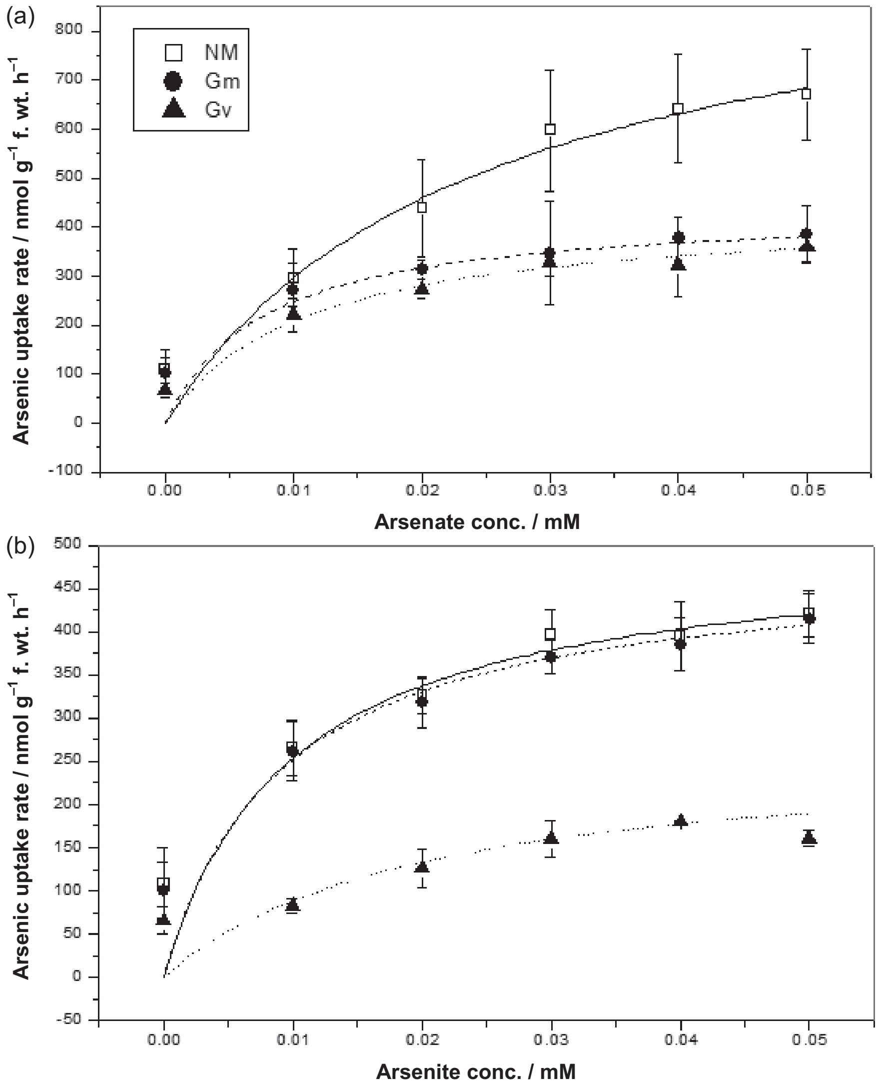

Figure 1: Concentration-dependent kinetics for high-affinity root arsenate (a) and arsenite (b) uptake of upland rice (cv. Zhonghan 221) without inoculation (NM) orinoculated with *Glomus mosseae* (Gm) or *G. versiforme* (Gv). Error bars are mean ± SD of three replicates.

Table 1: Analysis of covariance for arsenate and arsenite uptake for the high affinity and low affinity.

	df	**Arsenate**		**Arsenite**	
		F	**P**	**F**	**P**
High-affinity					
AMF treatment	2	43.88	< 0.0001	355.08	< 0.0001
Concentrations	4	13.02	< 0.0001	41.02	< 0.0001
AMF x Conc.	8	2.28	< 0.05	1	< 0.4591
Low-affinity					
AMF treatment	2	62.3	< 0.001	263.19	< 0.0001
Concentrations	4	34.03	< 0.001	212.65	< 0.0001
AMF x Conc.	8	3.01	< 0.05	11.71	< 0.0001

Table 2: Kinetic parameters for arsenate and arsenite uptake into roots of upland rice uninoculated (NM) / inoculated with *Glomus mosseae* or *G. versiforme*. Kinetic parameters were calculated from mean As uptake ($n = 3$) using Michaelis–Menten function (nonlinear regression) and linear regression model.

As treatment	Inoculation treatment	Nonlinear regression			Linear regression		
		V_{max} / µmol g^{-1} fresh weight h^{-1}	K_m / mM	R^2	a (slope)	b (intercept)	R^2
Arsenate	*High-affinity*						
	NM	1.02	0.024	0.98	9.50	0.24	0.91
	Gm	0.43	0.007	0.97	2.94	0.25	0.95
	Gv	0.41	0.009	0.96	3.27	0.20	0.91
	Low-affinity						
	NM	7.17	1.057	0.98	1.33	1.96	0.93
	Gm	4.41	0.453	0.96	0.70	2.16	0.94
	Gv	3.46	0.479	0.95	0.06	1.65	0.93
Arsenite	*High-affinity*						
	NM	0.49	0.009	0.96	3.79	0.25	0.88
	Gm	0.48	0.009	0.98	3.73	0.24	0.95
	Gv	0.25	0.019	0.98	2.28	0.07	0.89
	Low-affinity						
	NM	1.36	2.053	0.96	2.32	1.98	0.99
	Gm	12.50	2.179	0.94	2.08	1.71	0.98
	Gv	5.34	0.939	0.94	0.99	1.61	0.98

G. mosseae and *G. versiforme*, respectively. The corresponding K_m values were 24 µM in non-mycorrhizal and 6.5 and 9.3 µM in mycorrhizal roots. As for V_{max}, K_m values did not differ significantly between AM species, suggesting (1) that the uptake carriers had a lower affinity and/or (2) that mycorrhizal colonization down-regulated the expression of P transporters. In the case of arsenite, the kinetic parameters (V_{max} and K_m) of non-mycorrhizal roots were comparable to those inoculated with *G. mosseae* but were reduced by a factor of 2 in the case of *G. versiforme* (0.25 µmol g^{-1} fresh weight h^{-1} and 19 µM, respectively). These results suggest that AM fungi species differentially affected arsenite uptake by the high-affinity system.

On the other hand, at 0.5 and 1.0 mM the arsenite uptake rate decreased linearly by 33.1 and 42.7% compared to the non-mycorrhizal treatment. The concentration-dependent uptake for arsenate followed Michaelis–Menten kinetics (Table 2). The V_{max} and K_m for arsenate uptake were almost 2.0 times higher for non-mycorrhizal than in mycorrhizal roots. In the case of arsentite, V_{max} and K_m values were two times higher with G. mosseae than with G. versiforme suggesting a high AM species dependence of arsenite uptake by the low-affinity uptake system (Fig.2).

4 Discussion

The present study suggests that the concentration-dependent uptake isotherms for both arsenate and arsenite uptake by mycorrhizal and non-mycorrhizal roots may involve an active process that requires energy and selective binding sites and transporters (Figs. 1 and 2, Table 2) as suggested for rice by *Li* et al. (2011a) and for maize by *Yu* et al. (2009). Both *G. mosseae* and *G. versiforme* reduced arsenate uptake, which has been hypothesized to be related to changes in root architecture with AM inoculation (*Gutjahr* et al., 2009). Thus, *Price* et al. (1989) demonstrated that inoculation with *G. etunicatum* and *G. margarita* reduced the production of fine lateral roots of cotton. *Gutjahr* et al. (2009) found that *G. intraradices* preferentially colonized and induced the formation of large lateral roots. The As uptake by non-mycorrhizal roots may thus be related to higher numbers of fine lateral roots. *Deng* et al. (2010) also showed that As uptake by non-mycorrhizal rice (Gui Chao-2) increased mainly due to an increased number of lateral roots and a higher specific root surface area under flooded than under aerobic conditions. Inoculation with AM fungi enhances the expression of P transporters in rice (*Paszkowski* et al., 2002; *Chen* et al., 2013) and arsenate and phosphate share the same transporters (*Abedin* et al.,

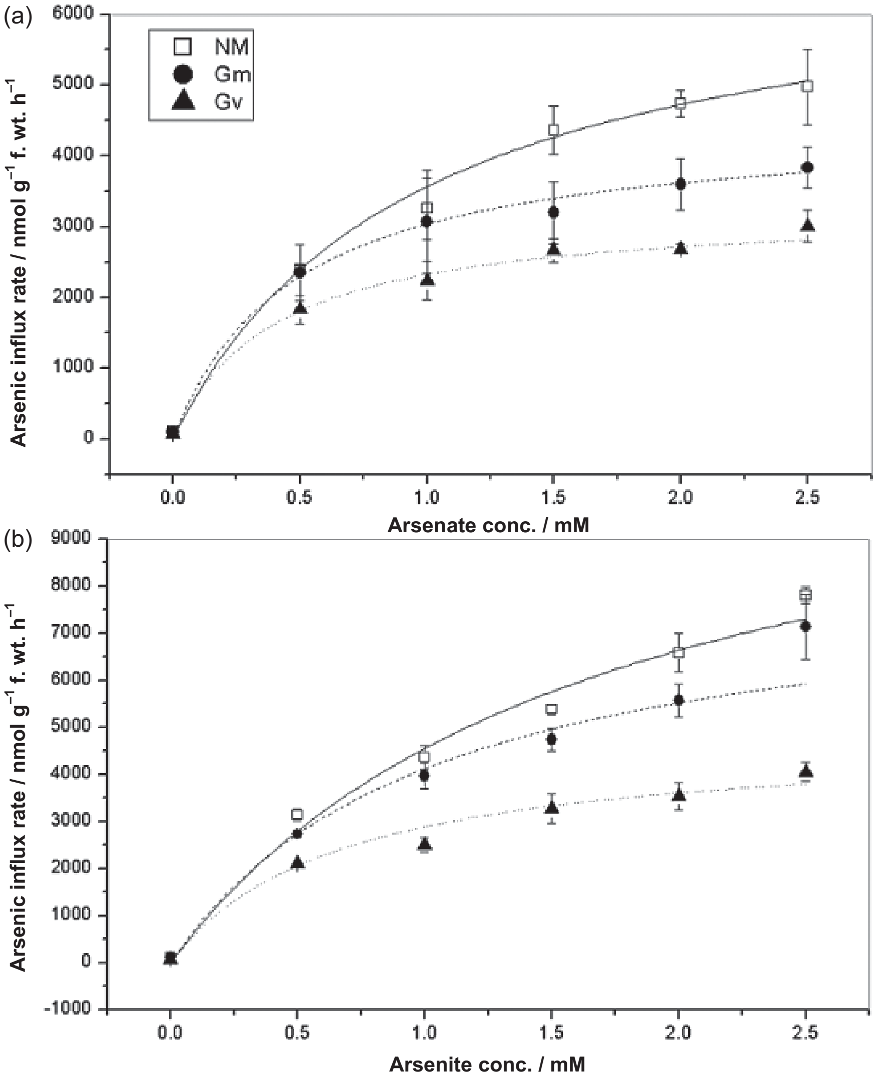

Figure 2: Concentration-dependent kinetics for low-affinity root arsenate (a) and arsenite (b) uptake of upland rice (cv. Zhonghan 221) without inoculation (NM) or inoculated with *Glomus mosseae* (Gm) or *G. versiforme* (Gv). Error bars are mean ± SD of three replicates.

2002; *Poynton* et al., 2004). These findings are contradictory to the observation that *G. intraradices* increased the expression of OsPT11 but decreases that of OsPT2. As a result, AM inoculation increased P uptake while reducing arsenate concentrations in rice tissues (*Chen* et al., 2013).

Arsenite, on the other hand, shares the same transporters (Lsi1 and Lsi2) as silicon in lowland rice (*Ma* et al., 2008). *Chen* et al. (2012) showed that *G. intraradices* down-regulated the expression of Lsi1 and Lsi2 and consequently led to a decrease of arsenite uptake per unit of root dry mass of lowland rice. While both AM species in the present study reduced the root uptake of arsenite, there were distinct differences between AM species (Table 1, Fig. 2). Thus, *G. versiforme* reduced arsenite uptake mainly at low As concentrations, while *G. mosseae* was more effective in reducing arsenite at higher concentrations (Table 1, Fig. 2). This is in agreement with the results of *Yu* et al. (2009), who showed that *G. mosseae* had no effect on arsenite uptake by maize roots at 0–0.10 mM arsenite in the solution. It remains still unclear why the two species of AM fungi differentially affected the arsenite uptake by upland rice.

5 Conclusion

We conclude that changes of morphological (root architecture, specific root area, and root length) and physiological (phosphate and Si transporters) attributes in response to AM colonization may differentially influence the uptake of arsenate and arsenite and that the extent of such effects differs by AM species

Acknowledgments

We sincerely thank Ms. *Sue Fung* (Hong Kong Baptist University) for improving the manuscript. This study was supported by *Talent Foundation of Northwest Agriculture and Forestry University*, China, and by *Program for Science & Technology Innovation Talents in Universities of Henan Province* (*14HASTIT048*).

References

Abedin, M. J., *Feldmann, J.*, *Meharg, A. A.* (2002): Uptake kinetics of arsenic species in rice plants. *Plant Physiol.* 128, 1120–1128.

Chen, B., *Xiao, X.*, *Zhu, Y.-G.*, *Smith, F. A.*, *Xie, Z. M.*, *Smith, S. E.* (2007): The arbuscular mycorrhizal fungus *Glomus mosseae* gives contradictory effects on phosphorus and arsenic acquisition by *Medicago sativa* Linn. *Sci. Total. Environ.* 379, 226–334.

Chen, X., *Li, H.*, *Chan, W. F.*, *Wu, C.*, *Wu, F.*, *Wu, S.*, *Wong, M. H.* (2012): Arsenite transporters expression in rice (*Oryza sativa* L.) associated with arbuscular mycorrhizal fungi (AMF) colonization under different levels of arsenite stress. *Chemosphere* 89, 1248–1254.

Chen, X. W., *Wu, F. Y.*, *Li, H.*, *Chan, W. F.*, *Wu, C.*, *Wu, S. C.*, *Wong, M. H.* (2013): Phosphate transporters expression in rice (*Oryza sativa* L.) associated with arbuscular mycorrhizal fungi (AMF) colonization under different levels of arsenate stress. *Environ. Exp. Bot.* 87, 92–99.

Chen, Z., *Zhu, Y.-G.*, *Liu, W.-J.*, *Meharg, A. A.* (2005): Direct evidence showing the effect of root surface iron plaque on arsenite and arsenate uptake into rice (*Oryza sativa*) roots. *New Phytol.* 165, 91–97.

Deng, D., *Wu, S.-C.*, *Wu, F.-Y.*, *Deng, H.*, *Wong, M.-H.* (2010): Effects of root anatomy and Fe plaque on arsenic uptake by rice seedlings grown in solution culture. *Environ. Pollut.* 158, 2589–2595.

Giovannetti, M., *Mosse, B.* (1980): An evaluation of techniques to measure vesicular-arbuscular infection in roots. *New Phytol.* 84, 489–500.

Gutjahr, C., *Casieri, L.*, *Paszkowski, U.* (2009): *Glomus intraradices* induces changes in root system architecture of rice independently of common symbiosis signaling. *New Phytol.* 182, 829–837.

Hoagland, D. R., *Arnon, D. I.* (1938): The water culture method for growing plants without soil. *Calif. AES Circ.* 347, 1–39.

Li, H., *Wu, C.*, *Ye, Z. H.*, *Wu, S. C.*, *Wu, F. Y.*, *Wong, M. H.* (2011a): Uptake kinetics of different arsenic species in lowland and upland rice colonized with *Glomus intraradices*. *J. Hazard. Mater.* 194, 414–421.

Li, H., *Ye, Z. H.*, *Chan, W. F.*, *Chen, X. W.*, *Wu, F. Y.*, *Wu, S. C.*, *Wong, M. H.* (2011b): Can arbuscular mycorrhizal fungi improve grain yield, As uptake and tolerance of rice grown under aerobic conditions? *Environ. Pollut.* 159, 2537–2545.

Ma, J. F., *Yamaji, N.*, *Mitani, N.*, *Xu, X.-Y.*, *Su, Y.-H.*, *McGrath, S. P.*, *Zhao, F.-J.* (2008): Transporters of arsenite in rice and their role in arsenic accumulation in rice grain. *P. Natl. Acad. Sci. USA* 105, 9931–9935.

Meharg, A. A. (2004): Arsenic in rice-understanding a new disaster for South-East Asia. *Trends Plant Sci.* 9, 415–417.

Meharg, A. A., *Rahman, M.* (2003): Arsenic contamination of Bangladesh paddy field soils: implications for rice contribution to arsenic consumption. *Environ. Sci. Technol.* 37, 229–234.

Meharg, A. A., *Jardine, L.* (2003): Arsenite transport into paddy rice (*Oryza sativa*) roots. *New Phytol.* 157, 39–44.

Paszkowski, U., *Kroken, S.*, *Roux, C.*, *Briggs, S. P.* (2002): Rice phosphate transporters include an evolutionarily divergent gene specifically activated in arbuscular mycorrhizal symbiosis. *P. Natl. Acad. Sci. USA* 99, 13324–13329.

Phillips, J. M., *Hayman, D. S.* (1970): Improved procedures for clearing and staining parasitic and vesicular-arbuscular mycorrhizal fungi for rapid assessment of infection. *Trans. Brit. Mycol. Soc.* 55, 158–161.

Poynton, C. Y., *Huang, J. W. W.*, *Blaylock, M. J.*, *Kochian, L. V.*, *Elless, M. P.* (2004): Mechanisms of arsenic hyperaccumulation in Pteris species: root as influx and translocation. *Planta* 219, 1080–1088.

Price, N., *Roncadori, R.*, *Hussey, R.* (1989): Cotton root growth as influenced by phosphorus nutrition and vesicular-arbuscular mycorrhizas. *New Phytol.* 111, 61–66.

Smith, E., *Naidu, R.*, *Alston, A. M.* (1998): Arsenic in the soil environment: a review. *Adv. Agron.* 64, 149–195.

Smith, S. E., *Smith, F. A.* (2011): Roles of arbuscular mycorrhizas in plant nutrition and growth: new paradigms from cellular to ecosystem scales. *Ann. Rev. Plant Biol.* 62, 227–250.

Williams, P. N., *Islam, M. R.*, *Adomako, E. E.*, *Raab, A.*, *Hossain, S. A.*, *Zhu, Y. G.*, *Feldmann, J.*, *Meharg, A. A.* (2006): Increase in rice grain arsenic for regions of Bangladesh irrigating paddies with elevated arsenic in groundwaters. *Environ. Sci. Technol.* 40, 4903–4908.

Wu, F. Y., *Hu, J. L.*, *Wu, S. C.*, *Wong, M. H.* (2014): Grain yield and arsenic uptake of upland rice inoculated with arbuscular mycorrhizal fungi in As-spiked soils. *Environ. Sci. Pollut. Res.* DOI: 10.1007/s11356-012-1440-9.

Wu, F. Y., *Ye, Z. H.*, *Wong, M. H.* (2009): Intraspecific differences of arbuscular mycorrhizal fungi in their impacts on arsenic accumulation by *Pteris vittata L. Chemosphere* 76, 1258–1264.

Xu, X. Y., *McGrath, S. P.*, *Meharg, A. A.*, *Zhao, F. J.* (2008): Growing rice aerobically markedly decreases arsenic accumulation. *Environ. Sci. Technol.* 42, 5574–5579.

Yu, Y., *Zhang, S.*, *Huang, H.*, *Luo, L.*, *Wen, B.* (2009): Arsenic accumulation and speciation in maize as affected by inoculation with arbuscular mycorrhizal fungus *Glomus mosseae*. *J. Agric. Food Chem.* 57, 3695–3701.

Zavala, Y. J., *Gerads, R.*, *Gürleyük, H.*, *Duxbury, J. M.* (2008): Arsenic in rice: II. Arsenic speciation in USA grain and implications for human health. *Environ. Sci. Technol.* 42, 3861–3866.

Do arsenate reductase activities and oxalate exudation contribute to variations of arsenic accumulation in populations of Pteris vittata?

Fuyong Wu, Feifei Xu, Xiaona Ma, Wanqing Luo, Laiqing Lou & Ming Hung Wong

Journal of Soils and Sediments

ISSN 1439-0108
Volume 18
Number 11

J Soils Sediments (2018) 18:3177-3185
DOI 10.1007/s11368-018-1987-2

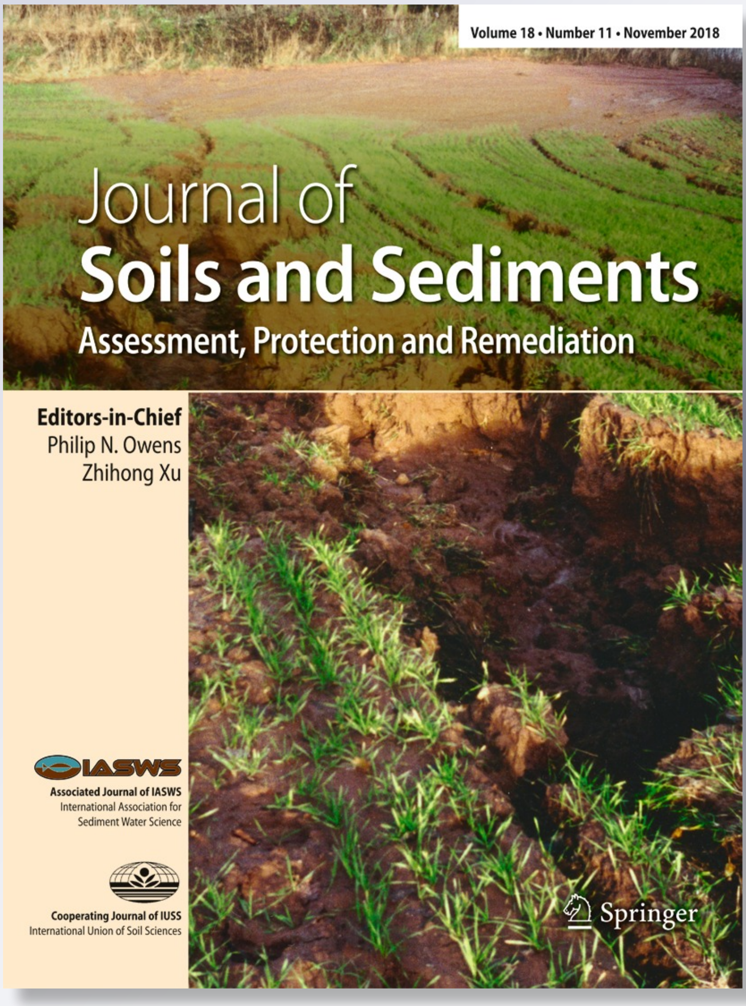

Volume 18 • Number 11 • November 2018

Journal of
Soils and Sediments
Assessment, Protection and Remediation

Editors-in-Chief
Philip N. Owens
Zhihong Xu

IASWS
Associated Journal of IASWS
International Association for
Sediment Water Science

Cooperating Journal of IUSS
International Union of Soil Sciences

Springer

Springer

Journal of Soils and Sediments (2018) 18:3177–3185
https://doi.org/10.1007/s11368-018-1987-2

SOILS, SEC 1 • SOIL ORGANIC MATTER DYNAMICS AND NUTRIENT CYCLING • RESEARCH ARTICLE

Do arsenate reductase activities and oxalate exudation contribute to variations of arsenic accumulation in populations of *Pteris vittata*?

Fuyong Wu[1,2] • Feifei Xu[1,2] • Xiaona Ma[1,2] • Wanqing Luo[1,2] • Laiqing Lou[3] • Ming Hung Wong[4]

Received: 20 January 2018 / Accepted: 27 March 2018 / Published online: 11 April 2018

Abstract

Purpose Although arsenic (As) hyperaccumulation is a constitutive property for *Pteris vittata*, there is intraspecific variation in As accumulation among metallicolous (from As-contaminated soils) and nonmetallicolous populations (from uncontaminated soils) and the related mechanisms is still not clear.

Materials and methods Pot trials, hydroponic culture, and manual simulation were conducted to investigate the roles of arsenate reductase and root exudates in accumulating As in *P. vittata*, which were collected from two uncontaminated sites including Sun Yat-sen University campus, Guangdong Province (ZD), and a botanical garden in Guangxi Academy of Forestry Sciences, Nanning City, Guangxi Province (NN), and two As and Pb/Zn mining and/or smelting sites located in Shaoguan of Guangdong Province (SG) and Guiyang of Hunan Province (GY).

Results and discussion The nonmetallicolous populations (ZD and NN) possessed more efficient uptake of arsenate and arsenite than the metallicolous populations (SG and GY). There were significant ($p < 0.05$) difference in arsenate reductase activities in roots among the four populations of *P. vittata* and that the higher arsenate reductase activities were recorded in the nonmetallicolous populations (110 nkat mg^{-1} protein for ZD, 160 nkat mg^{-1} protein for NN) compared with the metallicolous populations (62.9 nkat mg^{-1} protein for SG, 78.1 nkat mg^{-1} protein for GY). Root exudates from the nonmetallicolous population (NN) and the metallicolous population (GY) of *P. vittata* contained similar compositions of organic acids including oxalic, malic, and succinic acids, of which oxalate were dominant (> 67%). The NN population exuded 4.23 times more oxalate than the SG population. Root exudates from the NN population mobilized significantly ($p < 0.05$) more As from As-contaminated soils than those from the SG population, of which oxalate had the most effective in As mobilization.

Conclusions The present study suggests that higher arsenate reductase activities and oxalate exudation in the nonmetallicolous populations may play an important role in increasing their efficiency in phytoremediation of As-contaminated soils.

Keywords Arsenate reductase · Arsenic species · Chinese brake fern · Intraspecific variation · Oxalate secretion

---

Responsible editor: Xilong Wang

Electronic supplementary material The online version of this article (https://doi.org/10.1007/s11368-018-1987-2) contains supplementary material, which is available to authorized users.

✉ Fuyong Wu
wfy09@163.com; fuyongwu@nwsuaf.edu.cn

[1] College of Natural Resources and Environment, Northwest A&F University, Yangling 712100, Shaanxi, People's Republic of China

[2] Key Laboratory of Plant Nutrition and the Agri-environment in Northwest China, Ministry of Agriculture, Yangling 712100, Shaanxi, People's Republic of China

[3] College of Life Sciences, Nanjing Agricultural University, Nanjing 210095, People's Republic of China

[4] Consortium on Health, Environment, Education and Research (CHEER), Education University of Hong Kong, Tai Po, Hong Kong, SAR, People's Republic of China

1 Introduction

Arsenic (As) is not only ubiquitous in the natural condition but also an environmental and food chain contaminant (Zhao et al. 2010). The first As hyperaccumulator identified, *Pteris vittata*, has offered hope that As-contaminated soils widely present could be coped with using efficient, environmentally friendly, cost-effective phytoextraction technology (Ma et al. 2001). However, in spite of important progress made in recent years, the complexity of hyperaccumulation is far from being understood (Rascio and Navari-Izzo 2011) and potential use of hyperaccumulators in phytoremediation is limited.

P. vittata has received considerable attention for years. Arsenic is mainly distributed (78–96%) in fronds of *P. vittata* (Ma et al. 2001), and is mainly stored in the vacuoles (Lombi et al. 2002; Pickering et al. 2006). Over 85% As in fronds are in the form of arsenite [As(III)], and the remaining mostly as arsenate [As(V)], minimum as dimethylarsinic acid (DMAA) and monomethylarsonic acid (MMAA) (Ma et al. 2001; Wang et al. 2002). *P. vittata* has effective reduction of As(V) to As(III) to detoxify As once taken into the plant (Poynton et al. 2004; Su et al. 2008). After 1 h of exposure to As(V), As(III) could be determined in *P. vittata* (Su et al. 2008). Arsenate reductase in roots plays an important role in the detoxification of As in the fern (Duan et al. 2005; Liu et al. 2009). Recently, two arsenate reductase proteins including PvACR2 and Pv2.5–8 have been identified from sporophytes and gametophytes of *P. vittata*, respectively (Cesaro et al. 2015). *P. vittata* could be present in many countries and regions (Ma et al. 2001; Chen et al. 2002; Zhao et al. 2002; Visoottiviseth et al. 2002; Wu et al. 2007). There is intraspecific variation in As accumulation among populations of *P. vittata*, although As hyperaccumulation is a constitutive property (Wu et al. 2009; Wan et al. 2013). Our previous work indicated that nonmetallicolous populations (from uncontaminated soils) of *P. vittata* possessed more effective As accumulation than metallicolous populations (from As-contaminated soils) (Wu et al. 2015). However, it is not clear whether the metallicolous and nonmetallicolous populations of *P. vittata* from contrasting conditions possess similar or different mechanisms of arsenate reduction.

Plants generally release root exudates to response to nutrient deficiencies, inorganic ion stresses, or interact with neighbors in rhizosphere soil (Ryan et al. 2001). Root exudation represents a significant carbon cost to the plant, with young seedlings typically exuding about 30–40% of their fixed carbon as root exudates (Whipps 1990). Among root exudates, organic acids are the most common and important due to their ability to mobilize nutrients and heavy metals (Bais et al. 2006). It has been suggested that the organic acids secreted from the roots of *P. vittata* were highly efficient in solubilize As in soils and apparently enhanced As accumulation by the fern (Tu et al. 2004; Liu et al. 2016). However, the role of organic acids in metal accumulation in hyperaccumulators remains controversial. Zhao et al. (2001) found that root exudates of *Noccaea caerulescens* (a Zn/Cd hyperaccumulator) were not involved in Zn and Cd hyperaccumulation. Therefore, the contribution of root exudates to As accumulation in *P. vittata* need further research.

The main objectives of the present study were to (1) investigate the variation of As accumulation and arsenate reductase activities among four populations of *P. vittata*, (2) determine the differences in organic acids secreted from roots of the nonmetallicolous and metallicolous populations of *P. vittata*, and (3) quantify the ability of root exudates to As mobilization in soils.

2 Materials and methods

2.1 Spores of *P. vittata* collection

From November to December 2014, spores of *P. vittata* and corresponding rhizosphere soils were collected from two uncontaminated sites including Sun Yat-sen University campus, Guangdong Province (ZD), and a botanical garden in Guangxi Academy of Forestry Sciences, Nanning City, Guangxi Province (NN), and two As and Pb/Zn mining and/or smelting sites located in Shaoguan of Guangdong Province (SG) and Guiyang of Hunan Province (GY). The spores and soil samples at each site were collected from at least four plots (5 × 5 m). Each plot was sampled from three random points. The spores were air-dried and reserved for the following plant culture. Both SG and GY were heavily contaminated by As (24,618 and 28,933 mg kg^{-1}), Pb (6339 and 3273 mg kg^{-1}), and Zn (5791 and 10,424 mg kg^{-1}), while the corresponding metal concentrations at ZD and NN were below the class II standards of Chinese soil environmental quality (GB15618–1995) (Table S1, Electronic Supplementary Material).

2.2 Plant culture

The spores of each population of *P. vittata* were sprinkled on arable land soils in a plastic tray, respectively. The tray was covered with plastic cling film to maintain moisture. After germination, the sporelings were fertilized biweekly with 20% Hoagland's nutrient solution (Hoagland and Arnon 1938): 0.2 mM KH_2PO_4, 1.0 mM KNO_3, 1.0 mM $Ca(NO_3)_2\cdot 4H_2O$, 0.4 mM $MgSO_4\cdot 7H_2O$, 9 μM H_3BO_3, 1.8 μM $MnCl_2\cdot 4H_2O$, 0.15 μM $ZnSO_4\cdot 7H_2O$, 0.07 μM $CuSO_4\cdot 5H_2O$, 0.03 μM $H_2MoO_4\cdot H_2O$, and 4 μM Fe-EDTA. Two-month-old sporelings (with two to three fronds) of *P. vittata* were transplanted to another plastic tray for further growth and the following experiments. Both spore germination and plant culture were performed in a greenhouse with temperature control (28/23 °C, day/

night). In addition to natural sunlight, a 12-h photon flux density of 380 μmol m^{-2} s^{-1} was supplied via an assembly of cool-white fluorescent lamps.

2.3 Pot trial

As-contaminated soils were collected from abandoned rice fields located in Shantou City, Guangdong Province. Their selected physical and chemical properties were as follows: pH = 7.49 (soil:deionized water = 1:5) and 251 mg As kg^{-1}, 125 mg Pb kg^{-1}, and 144 mg Zn kg^{-1}.The soils were air-dried and sieved through a 2-mm mesh. Two three-month-old sporelings of each of the four populations (NN, ZD, SG, and GY) of *P. vittata* were transferred to each pot, each of which being filled with 2.0 kg of the soils. The fern were watered with deionized water every 2 days to maintain 70–80% water-holding capacity (WHC) and fertilized with 20% Hoagland's nutrient solution at weekly intervals. After 4 months, fronds and roots of *P. vittata* were harvested separately, washed thoroughly with tap water, and rinsed with deionized water to remove any soil/substrate particles attached. Part of samples was homogenized to powder with liquid nitrogen. The frozen powder was stored at − 80 °C for analysis of arsenate reductase activity and As species. The rest of the samples was oven-dried at 70 °C for 3 days for the analysis of total As.

2.4 Root exudate collection

Three-month-old sporelings (with four to six fronds) of each of the two populations (NN and GY) previously cultured were transplanted to polyethylene pots filled with 2.0 L 20% modified Hoagland's nutrient solution (Hoagland and Arnon 1938). The plants were mounted on floating polyfoam boards with their roots suspended in the solution. To ensure plant uniformity, only sporelings with similar fresh weight (1–2 g) and root length (8–12 cm) were selected for the experiments. The pH of the nutrient solution was adjusted to 6.0 (using dilute HCl or NaOH), aerated vigorously, and renewed twice per week to prevent depletion of metals and nutrients. After growing in hydroponic systems for 6 weeks, the sporelings of each population of *P. vittata* were exposed to 20% Hoagland's nutrient solution subjected to 0, 200, or 2000 μM As(V) ($Na_2HAsO_4 \cdot 7H_2O$) or As(III) ($NaAsO_2$). There were two sporelings in each pot and four replicates for each treatment. After 2 days of exposure, root exudates were collected according to methods described by Tu et al. (2004). Briefly, plant roots were soaked in 30 mg L^{-1}chloramphenicol for 2 h to minimize microbial growth and washed with sterile Milli-Q water. The sporelings were subsequently transferred to 500 mL of sterile Milli-Q water to collect root exudates for 6 h. The root exudate was immediately filtered, lyophilized to 25 mL, and stored at − 80 °C for further analysis.

After collection of root exudates, the fern were divided into fronds and roots and rinsed with tap water. The roots were then incubated in an ice-cold phosphate buffer [containing 1 mM Na_2HPO_4, 10 mM2-(N-morpholino) ethanesulfonic acid (MES) and 0.5 mM $Ca(NO_3)_2$] for 10 min to ensure desorption of As from surface and free space of the roots. Plant tissues were oven-dried at 70 °C for 72 h to constant weight.

2.5 Arsenic mobilization from As-contaminated soils by the root exudates

The As-contaminated soils used in the As mobilization were same as previously used as pot trials. Four milliliters of previously reserved root exudates collected from the fern exposed to 0 As was added to a centrifuge tube with 100 mg of the As-contaminated soil. Four milliliters of deionized water was used as a control. Fifty microliters of chloroform was added to prevent microbial decomposition of root exudates. The solutions were mechanically shaken at 25 °C for 24 h and centrifuged at 10,000*g* for 15 min. The supernatant was acidified using concentrated HNO_3 (50 μL) for total As determination. The net As mobilization from As-contaminated soil was calculated as follows:

$$\text{Net As-mobilization}\left(\text{mg kg}^{-1}\text{g}^{-1}\right) = \frac{\text{As}_\text{S} - \text{As}_\text{RE} - \text{As}_\text{C}}{\text{M}_\text{Soil} \times \text{Root}} \quad (1)$$

where As_S is the amount of As in the supernatant, As_{RE} is the amount of As contained in root exudates, As_C is the amount of As solubilized by control, M_{Soil} is the soil weight, and Root is the dry weight of roots.

2.6 Arsenic mobilization from As-contaminated soil by organic acids

Based on organic acids identified in the root exudates of the fern, the role of oxalic acid, malic acid, and succinic acid on As mobilization in the As-contaminated soils was investigated. Arsenic dissolution from the As-contaminated soil was carried out in a batch experiment. Into a 10-mL centrifuge tube, 100 mg of the soil was weighed. This was followed by adding 4 mL of oxalic, malic, or succinic acid solution with concentrations ranging from 0 to 10 mM and 50 μL of chloroform to inhibit microbial activity. Deionized water was used as a control. The centrifuge tube was capped, shaken mechanically at room temperature for 24 h, and centrifuged at 10,000*g* for 15 min. The supernatant was removed and acidified with 10 μL of concentrated HNO_3 for total As determination.

2.7 Chemical analysis

2.7.1 As determination in the plant

Analyses of total As in the plant were conducted by digesting the plant tissues with an acid mixture [concentrated HNO_3 + concentrated $HClO_4$ (5:1, *v*/*v*)] and determined with anatomic fluorescence spectrometer (AFS-9780, Beijing Haiguang Instruments Company, China). A standard reference plant material [GBW10023 (GSB-14)] from the National Research Center for Standards, China, was used for quality assurance. Recovery rate of the standard reference materials was within 85 ± 5%. For As(III) and As(V) in the plant, the samples were ground under liquid nitrogen and extracted with methanol:water (1:1 *v*/*v*) under sonication for repeated three times, and the three extracts were combined (Zhang et al. 2002). Total As in the extracts were determined with anatomic fluorescence spectrometer.

2.7.2 Determination of arsenate reductase activity in roots of *P. vittata*

The roots reserved were ground and homogenized with quartz sand in 6 mL buffer solution containing 50 mM3-(N-morpholino) propanesulfonic acid (MOPS) and 50 mM MES, which was adjusted to pH of 6.5 with NaOH. After the homogenate centrifuged at 10,000*g* for 30 min at 4 °C, the supernatant was filtered through filter paper. The filtrate was passed through Sephadex PD-10 desalting columns. Arsenate reductase activity in the roots was assayed using the methods described by Duan et al. (2005) and Liu et al. (2009).

2.7.3 Determination of organic acids in root exudates

Organic acids in root exudates reserved were analyzed by high-performance liquid chromatography (Shimadzu, LC-20A) equipped with a reversed-phase C_{18} anion -exchange analytical column and a multiwavelength UV detector at 210 nm. The mobile phase was 25 mM KH_2PO_4 (adjusted to pH 2.5 with concentrated ortho-phosphoric acid) at a flow rate of 1 mL min^{-1}. Individual organic acids in the root exudates were identified and calibrated by comparing retention times with those of standards prepared with known concentrations of oxalic, malic, succinic, and citric acids. The organic acid concentrations were expressed on a dry root weight (dwt) basis.

2.8 Statistical analysis

The differences in plant biomass, As concentrations, As accumulation, organic acid concentrations, and arsenate reductase activities among populations of *P. vittata* were assessed using Fisher's protected least significant difference after ANOVA. All statistical procedures were carried out using SAS 8.1 software. Unless indicated otherwise, all treatment means were tested for significant difference at $p < 0.05$.

3 Results

3.1 Variations of As accumulation in four populations of *P. vittata*

There was insignificant difference in frond biomass among four populations of *P. vittata* after growing As-contaminated soils for 4 months (Fig. 1a). The metallicolous populations (SG and GY) had significantly ($p < 0.05$) higher root biomass (0.33 and 0.54 g) than the nonmetallicolous populations (ZD and NN) (0.10 and 0.01 g). According to Figs. 1 and 2, there was significant ($p < 0.01$) difference in concentrations of total As, As(III), and As(V) in fronds of the four populations. The present study further showed that the nonmetallicolous populations exhibited a significantly ($p < 0.01$) higher As accumulation in fronds than the metallicolous populations in As-contaminated soils, which was contributed to higher As concentrations in fronds (Fig. 1). Generally, the highest concentrations of As(III) and As(V) in fronds were observed in the nonmetallicolous populations, while the lowest were recorded in the metallicolous populations (Fig. 2). Concentrations of As(III) and As(V) in the fronds of NN population were about 13.7- and 17.2-fold for those of SG population, respectively.

3.2 Arsenate reductase activities in roots of four populations of *P. vittata*

The present study indicated that there were significant ($p < 0.05$) difference in arsenate reductase activities in roots among the four populations of *P. vittata* (Fig. 3). Apparently higher arsenate reductase activities were recorded in the nonmetallicolous populations (110 nkat mg^{-1} protein for ZD, 160 nkat mg^{-1} protein for NN) compared with the metallicolous populations (62.9 nkat mg^{-1} protein for SG, 78.1 nkat mg^{-1} protein for GY). This is consistent with the results that the nonmetallicolous populations possessed higher As(III) concentrations in fronds than those in the metallicolous populations (Fig. 2a).

3.3 Arsenic accumulation in the two populations of *P. vittata* exposed to As(V) and As(III)

Based on the results of previous pot trials, sporelings of *P. vittata* were exposed to 0, 200, or 2000 μM As(V) or As(III) for 2 days in hydroponic culture for further investigating variations of As accumulation in the two populations (NN and SG). Table 1 shows that the nonmetallicolous

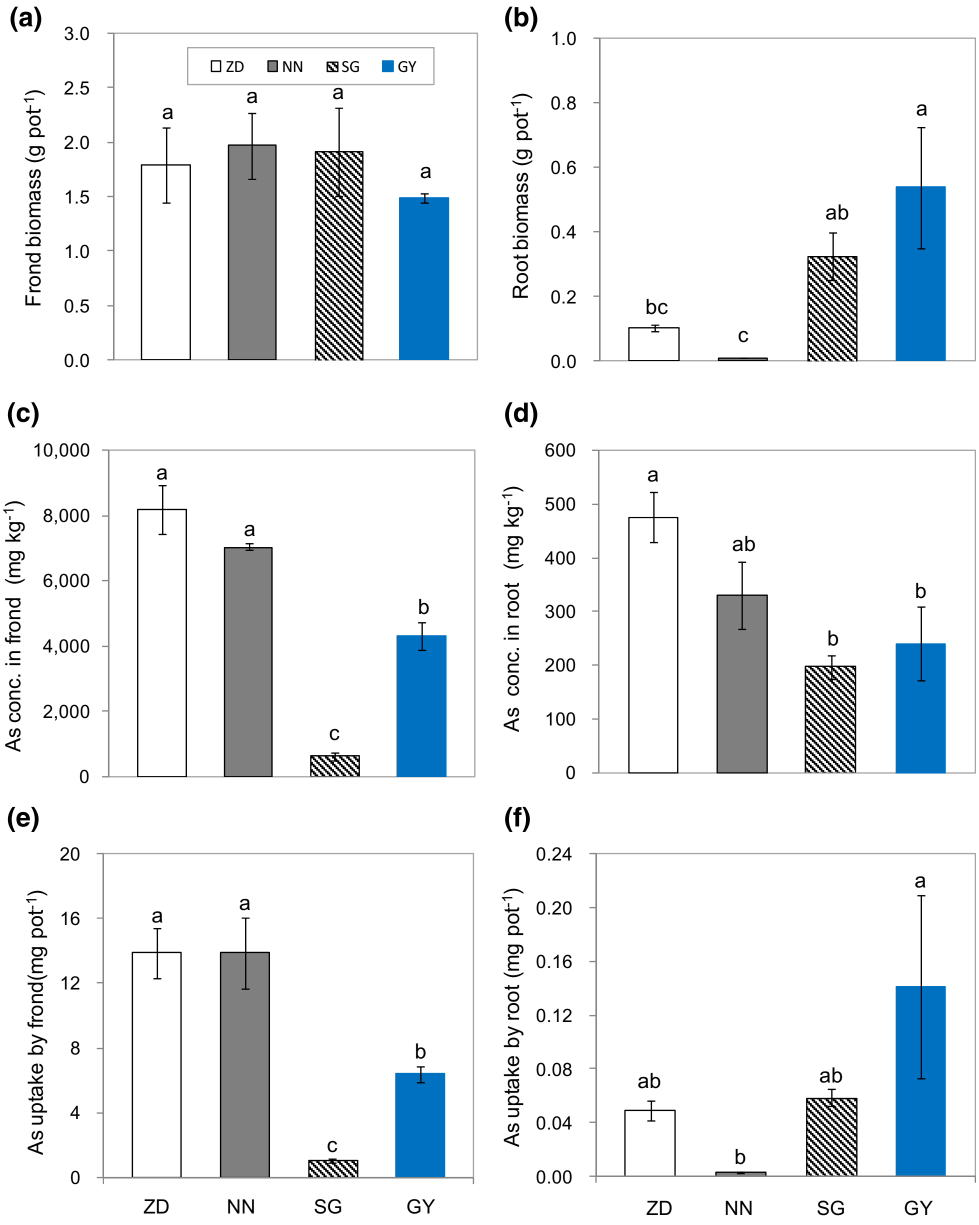

Fig. 1 Frond (**a**) and root (**b**) dry biomass, arsenic concentrations (**c**, **d**), and accumulation (**e**, **f**) in four populations (ZD, NN, SG, and GY) of *Pteris vittata* growing on As-contaminated soils for 4 months. Bars marked with different letters are significantly different among four populations according to least significant difference (LSD) test ($p < 0.05$) (mean ± SE, $n = 4$)

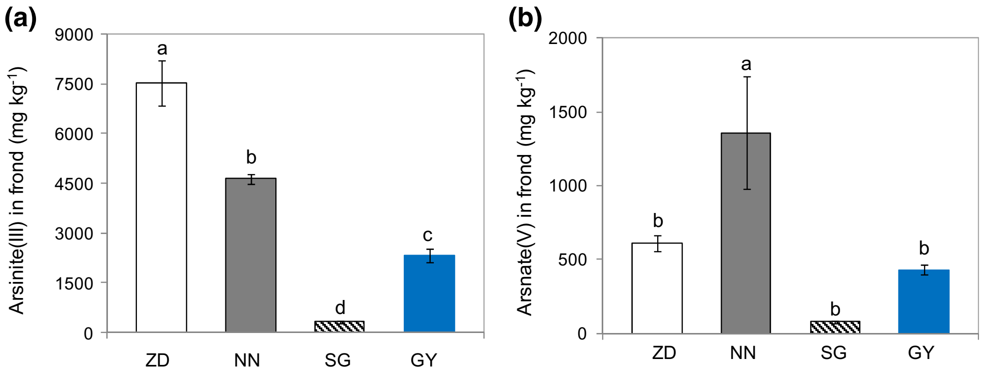

Fig. 2 Arsenite (**a**) and arsenate (**b**) concentrations in fronds of four populations (ZD, NN, SG, and GY) of *Pteris vittata* growing on As-contaminated soils for 4 months. Bars marked with different letters are significantly different among four populations according to least significant difference (LSD) test ($p < 0.05$) (mean ± SE, $n = 4$)

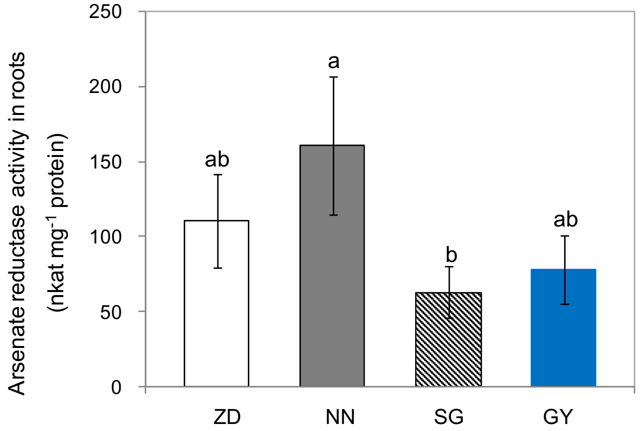

Fig. 3 Arsenate reductase activity in the roots of four populations (ZD, NN, SG, and GY) of *Pteris vittata* growing on As-contaminated soils for 4 months. Bars marked with different letters are significantly different among four populations according to least significant difference (LSD) test ($p < 0.05$) (mean ± SE, $n = 4$)

population (NN) possessed apparently higher frond As concentrations than the metallicolous population (SG) under any of As treatment. After exposure to 2000 μM As(V) or As(III), frond As concentrations in the NN population were significantly ($p < 0.01$) higher than those in the SG population. In addition, frond As concentrations under As(III) treatments (707–2258 mg kg^{-1}) were comparable with those under As(V) treatments (751–1366 mg kg^{-1}). These results further demonstrated that the nonmetallicolous population of *P. vittata* had a apparently higher accumulation capacity for As than the metallicolous populations, regardless of exposed to As(V) or As(III).

3.4 Pattern of root exudates

As shown in Table 1, root exudates from the two populations of *P. vittata* contained similar compositions of organic acids including oxalic, malic, and succinic acids. Oxalate was the predominant organic acid in the root exudates of the two populations of *P. vittata*, accounted for 67.2–97.7% of total organic acid secreted (Table 1). As expected, oxalate concentrations increased with increasing As concentrations in nutrient solution. For example, oxalate concentrations in root exudates of NN were 68.7 mg kg^{-1} under the control, which increased to 90.4 mg kg^{-1} under 2000-μM As(V) treatment (Table 1). Although As(III) is more toxic than As(V),the species of As seemed to have insignificant effects on oxalate secretion from fern plants (Table 1). The oxalate concentrations in root exudates of the NN population were significantly ($p < 0.05$) higher than those in the GY population, except those exposed to 2000-μM As(III) treatment. The oxalate concentrations in root exudates of the NN population (90.4 mg kg^{-1}) were 5.23 times of those in the SG population (17.3 mg kg^{-1}) under 2000-μM As(V) treatment, suggesting that oxalate exudation was related to efficiency of As accumulation in the former populations.

3.5 Arsenic mobilization from As-contaminated soils by root exudates and exogenous supply of organic acids

Root exudates from the NN population mobilized significantly ($p < 0.01$) more As from As-contaminated soils than those from the GY population (Fig. 4a), suggesting that the former

Table 1 Arsenic concentrations in fronds, oxalic acid, malic acid, and succinic acid concentrations in root exudates of the two populations (NN and GY) of *Pteris vittata* after growing for 2 days in 0.2-strength Hoagland solution containing 0, 200, or 2000 μM arsenate ($Na_2HAsO_4{\bullet}7H_2O$) or arsenite ($NaAsO_2$) (mean ± SE, $n = 4$)

Level (μM)	Population	As concentration in frond (mg kg^{-1})	Oxalic acid concentration (mg kg^{-1} d.wt)	Malic acid concentration (mg kg^{-1} d.wt)	Succinic acid concentration (mg kg^{-1} d.wt)
Arsenate					
0	NN	15.5 ± 3.27 a	68.7 ± 10.0 a	2.93 ± 1.21 a	0.66 ± 0.05 b
	GY	10.4 ± 3.14 ab	26.5 ± 4.96 b	3.83 ± 1.31 a	1.74 ± 0.16 a
200	NN	775 ± 44.8 a	86.6 ± 8.13 a	2.04 ± 0.00 ab	n.d.
	GY	751 ± 80.7 a	32.3 ± 5.99 b	4.19 ± 1.65 a	2.49 ± 0.48
2000	NN	1724 ± 118 a	90.4 ± 7.71 a	4.00 ± 0.09 a	1.33 ± 0.49 ab
	GY	1366 ± 73.1 b	17.3 ± 1.69 b	5.40 ± 1.66 a	3.04 ± 1.06 a
Arsenite					
200	NN	1005 ± 93.0 a	96.9 ± 3.08 a	4.12 ± 0.36 b	0.53 ± 0.03 b
	GY	707 ± 160 a	33.0 ± 10.4 b	7.15 ± 0.86 a	2.34 ± 0.43 a
2000	GY	2258 ± 15.4 a	59.5 ± 14.1 a	3.58 ± 0.56 a	0.41 ± 0.02
	NN	941 ± 91.1 b	34.8 ± 1.17 a	3.27 ± 0.65 a	n.d.

Different letters within the same column indicate significant difference between inoculated treatments at the level of $p < 0.05$

n.d. not detectable

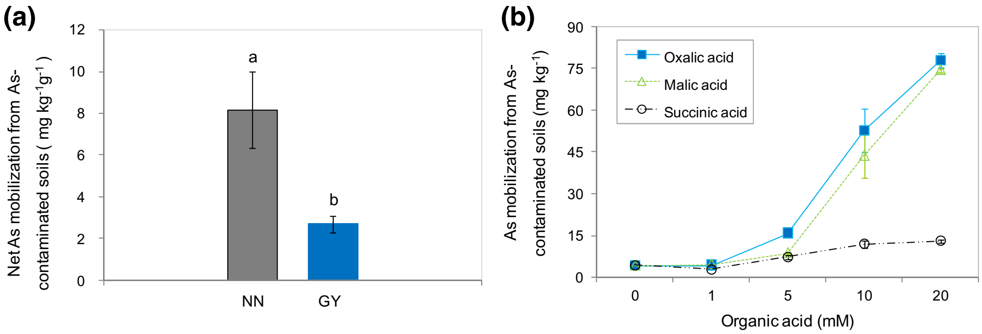

Fig. 4 Arsenic mobilization from As-contaminated soils by root exudates (**a**) collected from the two populations (NN and GY) of *Pteris vittata* growing in 0.2-strength Hoagland solution for 2 days and exogenous supply of organic acids (**b**) including oxalic acid, malic acid, and succinic acid. Bars marked with different letters are significantly different among four populations according to least significant difference (LSD) test ($p < 0.05$) (mean ± SE, $n = 4$)

possesses greater ability to solubilize As than the later. Oxalic, malic, and succinic acids were the three organic acids identified in the root exudates of *P. vittata* (Table 1). Therefore, the role of the three organic acids on As mobilization in soils was examined. As expected, net As mobilization from As-contaminated soils increased with increasing concentrations of organic acids (Fig. 4b). Among the three organic acids, oxalic acid was the most effective in As mobilization and succinic acid was the least.

4 Discussion

Based on the results of pot trials (Fig. 1) and hydroponic culture (Table 1), the present study showed that the nonmetallicolous populations of *P. vittata* possessed significantly higher As accumulation in the fronds than the metallicolous populations. This is in line with Wu et al. (2015), who showed that the nonmetallicolous populations of *P. vittata* possessed more effective As accumulation than the metallicolous populations. The nonmetallicolous populations exhibit apparent advantage for enhancing phytoextration of As-contaminated soils and the advantage need to investigate under field conditions. Furthermore, the present study indicated that the nonmetallicolous populations of *P. vittata* could uptake more As(III) compared to the nonmetallicolous populations. The As(III) influx fitted well with Michaelis–Menten kinetics in both nonmetallicolous and metallicolous populations of *P. vittata*, and higher value of V_{max} for As(III) was recorded in the nonmetallicolous populations (Wu et al. 2015). An aquapor in PvTIP4;1 mainly expressed in roots may be involved in As(III) uptake by *P. vittata* (He et al. 2016). Halimaa et al. (2014) found that expression of genes with possible contribution to Zn, Cd, and Ni hyperaccumulation and hypertolerance was difference between *Noccaea caerulescens* ecotypes. Molecular mechanisms of intravariations in As accumulation of *P. vittata* need further investigation.

The majority (> 67%) of As species in fronds was As(III) either in the nonmetallicolous or in the metallicolous populations, in line with the previous works (Wang et al. 2002; Su et al. 2008). Zhang et al. (2002) showed that conversion of As(V) to As(III) is an essential process for As detoxification in *P. vittata* because As(III) may be stored and sequestered in vacuoles to inhibit its toxicity to the plant (Lombi et al. 2002). In addition, the rate of As(III) to total As in fronds of the nonmetallicolous populations were apparently higher than that in the metallicolous populations (data not shown). Higher arsenate reductase activities were recorded in the nonmetallicolous populations compared with the metallicolous populations, which indicated that the former populations may be possess more effective capacity for conversion of As(V) to As(III) (Fig. 3). Su et al. (2008) found that roots are the main location of As(V) reduction in *P. vittata*. As(V) can be directly reduced to As(III) by arsenate reductase in roots of *P. vittata* (Duan et al. 2005). The present study demonstrated that metallicolous and nonmetallicolous populations of *P. vittata* from contrasting conditions (As-contaminated soils vs clean soils) possess similar mechanisms for As(V) reduction.

The composition of root exudates of *P. vittata* in the present study was consistent with Lou et al. (2010). Oxalate was the predominant organic acid in the root exudates of nonmetallicolous or metallicolous populations of *P. vittata*. Oxalate is typical organic acid in plant root exudates (Li et al. 2003; Zhu et al. 2011). Tao et al. (2016) also found that oxalate was the dominant organic acid in the root exudates of a Cd hyperaccumulator, *Sedum alfredii*. Phytic acid was not detected in root exudates of *P. vittata* in the present study, which was in line with Lou et al. (2010) and Das et al. (2017). However, Tu et al. (2004) and Liu et al. (2016) found that phytic acid was the predominant organic acid in the root exudates of *P. vittata*. The inconsistent composition of root exudates of *P. vittata* may be due to difference in the age of an individual plant and external factors like biotic and abiotic stressors. Valentinuzzi et al. (2015) found that the growth stage of the plant and different trap solutions to collect root exudates markedly influenced the composition and concentration of organic acids in root exudates.

The present study showed that significant ($p < 0.05$) higher oxalate concentrations were recorded in the NN population, except 2000-μM As(III) treatment (Table 1). Similarly, Tao et al. (2016) observed variations in oxalate secretion between genotypes of the same plant species. They found that hyperaccumulating ecotype of *S. alfredii* had nearly 2-fold higher oxalate secretion than nonhyperaccumulating ecotype. Garcia et al. (2001) showed that root exudation is positively correlated with root growth of two Lupinus cultivars, which means that actively growing root systems secrete more exudates. Our previous study found that the nonmetallicolous populations of *P. vittata* possessed higher biomass and more actively growing roots than the metallicolous populations (Wu et al. 2015), which seemed to be resulted in higher oxalate secretion in the nonmetallicolous populations. Moreover, manual simulation indicated that root exudates from the NN population mobilized apparent more As from As-contaminated soils than that from the GY population, of which oxalic acid possessed the most effective in As mobilization (Fig. 4). It has been reported that oxalate could mobilize Cd and Al (Dytrtova et al. 2011; Morita et al. 2011). As discussed formerly, there were higher frond As concentrations and more amounts of oxalic acid recorded in the nonmetallicolous population, which suggested that As-stimulated oxalate secretion increased As uptake and accumulation in the fern and that exogenous oxalate supply maybe promoted As accumulation efficiently. The information obtained in the present study will be very valuable in revealing and explaining the physiology mechanisms of As accumulation and tolerance in *P. vittata*.

5 Conclusions

The present study indicated that the nonmetallicolous populations of *P. vittata* possess more effective capacity for conversion of As(V) to As(III) than the metallicolous populations. The present study identified oxalate as dominant organic acid from both nonmetallicolous and metallicolous populations of *P. vittata*. The nonmetallicolous populations with more As accumulation excreted higher concentrations of oxalate than the metallicolous populations. Our data also clearly showed the role of root exudates in releasing As from As-contaminated. The nonmetallicolous populations of *P. vittata* possessed more effective As accumulation than the metallicolous populations, which was contributed to higher arsenate reductase activities and higher concentrations of oxalate in the roots. Further investigating of intravariations of accumulating As in *P. vittata* and the associated molecular mechanisms may be useful to increase plant uptake of As, which has implication for more efficient phytoextration of As-contaminated soils.

Funding The present work was supported by Natural Science Basic Research Plan in Shaanxi Province of China (Program No. 2016JM4004) and Chinese Universities Scientific Fund (Program No. 2452015179), and the Scientific Research Foundation for the Introduction of Talent, Northwest A&F University, China (2014), is gratefully acknowledged.

References

Bais HP, Weir TL, Perry LG, Gilroy S, Vivanco JM (2006) The role of root exudates in rhizosphere interactions with plants and other organisms. Annu Rev Plant Biol 57:233–266

Cesaro P, Cattaneo C, Bona E, Berta G, Cavaletto M (2015) The arsenic hyperaccumulating *Pteris vittata* expresses two arsenate reductases. Sci Rep 5:14525

Chen TB, Wei CY, Huang ZC, Huang QF, Lu QG, Fan ZL (2002) Arsenic hyperaccumulator *Pteris vittata* L. and its arsenic accumulation. Chin Sci Bull 47:902–905

Das S, Chou ML, Jean JS, Yang HJ, Kim PJ (2017) Arsenic-enrichment enhanced root exudates and altered rhizosphere microbial communities and activities in hyperaccumulator *Pteris vittata*. J Hazard Mater 325:279–287

Duan GL, Zhu YG, Tong YP, Cai C, Kneer R (2005) Characterization of arsenate reductase in the extract of roots and fronds of Chinese brake fern, an arsenic hyperaccumulator. Plant Physiol 138:461–469

Dytrtova JJ, Jakl M, Sestakova I, Zins EL, Schroder D, Navratil T (2011) A new approach to study cadmium complexes with oxalic acid in soil solution. Anal Chim Acta 693:100–105

Garcia JAL, Barbas C, Probanza A, Barrientos ML, Manero FJG (2001) Low molecular weight organic acids and fatty acids in root exudates of two *Lupinus* cultivars at flowering and fruiting stages. Phytochem Anal 12:305–311

Halimaa P, Lin YF, Ahonen VH, Blande D, Clemens S, Gyenesei A, Haikio E, Karenlampi SO, Laiho A, Aarts MGM (2014) Gene expression differences between *Noccaea caerulescens* ecotypes help to identify candidate genes for metal phytoremediation. Environ Sci Technol 48:3344–3353

He ZY, Yan HL, Chen YS, Shen HL, Xu WX, Zhang HY, Shi L, Zhu YG, Ma M (2016) An aquaporin PvTIP4;1 from *Pteris vittata* may mediate arsenite uptake. New Phytol 209:746–761

Hoagland DR, Arnon DI (1938) The water culture method for growing plants without soil. Circ Calif Agric Exp Sta 347:1–39

Li YH, Huang BX, Shan XQ (2003) Determination of low molecular weight organic acids in soil, plants, and water by capillary zone electrophoresis. Anal Bioanal Chem 375:775–780

Liu Y, Wang HB, Wong MH, Ye ZH (2009) The role of arsenate reductase and superoxide dismutase in As accumulation in four Pteris species. Environ Int 35:491–495

Liu X, Fu JW, Guan DX, Cao Y, Luo J, Rathinasabapathi B, Chen Y, Ma LQ (2016) Arsenic induced phytate exudation, and promoted $FeAsO_4$ dissolution and plant growth in as-hyperaccumulator *Pteris vittata*. Environ Sci Technol 50:9070–9077

Lombi E, Zhao FJ, Fuhrmann M, Ma LQ, McGrath SP (2002) Arsenic distribution and speciation in the fronds of the hyperaccumulator *Pteris vittata*. New Phytol 156:195–203

Lou LQ, Ye ZH, Lin AJ, Wong MH (2010) Interaction of arsenic and phosphate on their uptake and accumulation in Chinese brake fern. Int J Phytoremed 12:487–502

Ma LQ, Komar KM, Tu C, Zhang W, Cai Y, Kennelly ED (2001) A fern that hyperaccumulates arsenic. Nature 409:579

Morita A, Yanagisawa O, Maeda S, Takatsu S, Ikka T (2011) Tea plant (*Camellia sinensis* L.) roots secrete oxalic acid and caffeine into medium containing aluminum. Soil Sci Plant Nutr 57:796–802

Pickering IJ, Gumaelius L, Harris HH, Prince RC, Hirsch G, Banks JA, Salt DE, George GN (2006) Localizing the biochemical transformations of arsenate in a hyperaccumulating fern. Environ Sci Technol 40:5010–5014

Poynton CY, Huang JWW, Blaylock MJ, Kochian LV, Elless MP (2004) Mechanisms of arsenic hyperaccumulation in *Pteris* species: root as influx and translocation. Planta 219:1080–1088

Rascio N, Navari-Izzo F (2011) Heavy metal hyperaccumulating plants: how and why do they do it? And what makes them so interesting? Plant Sci 180:169–181

Ryan PR, Delhaize E, Jones DL (2001) Function and mechanism of organic anion exudation from plant roots. Annu Rev Plant Physiol Mol Biol 52:527–560

Su YH, McGrath SP, Zhu YG, Zhao FJ (2008) Highly efficient xylem transport of arsenite in the arsenic hyperaccumulator *Pteris vittata*. New Phytol 180:434–441

Tao Q, Hou DD, Yang XE, Li TQ (2016) Oxalate secretion from the root apex of S*edum alfredii* contributes to hyperaccumulation of cd. Plant Soil 398:139–152

Tu SX, Ma L, Luongo T (2004) Root exudates and arsenic accumulation in arsenic hyperaccumulating *Pteris vittata* and nonhyperaccumulating *Nephrolepis exaltata*. Plant Soil 258:9–19

Valentinuzzi F, Cesco S, Tomasi N, Mimmo T (2015) Influence of different trap solutions on the determination of root exudates in *Lupinus albus* L. Biol Fertil Soils 51:757–765

Visoottiviseth P, Francesconi K, Sridokchan W (2002) The potential of Thai indigenous plant species for the phytoremediation of arsenic contaminated land. Environ Pollut 118:453–461

Wan XM, Lei M, Liu YR, Huang ZC, Chen TB, Gao D (2013) A comparison of arsenic accumulation and tolerance among four populations of *Pteris vittata* from habitats with a gradient of arsenic concentration. Sci Total Environ 442:143–151

Wang JR, Zhao FJ, Meharg AA, Raab A, Feldmann J, McGrath SP (2002) Mechanisms of arsenic hyperaccumulation in *Pteris vittata*. Uptake kinetics, interactions with phosphate, and arsenic speciation. Plant Physiol 130:1552–1561

Whipps JM (1990) Carbon economy. In: Lynch JM (ed) The rhizosphere. John Wiley & Sons Ltd, Essex, pp 59–97

Wu FY, Ye ZH, Wu SC, Wong MH (2007) Metal accumulation and arbuscular mycorrhizal status in metallicolous and nonmetallicolous populations of *Pteris vittata* L. and *Sedum alfredii* Hance. Planta 226:1363–1378

Wu FY, Ye ZH, Wu SC, Leung HM, Wong MH (2009) Variation in arsenic, lead and zinc tolerance and accumulation in six populations of *Pteris vittata* L. from China. Environ Pollut 157:2394–2404

Wu FY, Deng D, Wu SC, Lin XG, Wong MH (2015) Arsenic tolerance, uptake and accumulation between nonmetallicolous and metallicolous populations of *Pteris vittata* L. Environ Sci Pollut Res 22:8911–8918

Zhang W, Cai Y, Tu C, Ma LQ (2002) Arsenic speciation and distribution in an arsenic hyperaccumulating plant. Sci Total Environ 300:167–177

Zhao FJ, Hamon RE, McLaughlin MJ (2001) Root exudates of the hyperaccumulator *Thlaspi caerulescens* do not enhance metal mobilization. New Phytol 151:613–620

Zhao FJ, Dunham SJ, McGrath SP (2002) Arsenic hyperaccumulation by different fern species. New Phytol 156:27–31

Zhao FJ, McGrath SP, Meharg AA (2010) Arsenic as a food chain contaminant: mechanisms of plant uptake and metabolism and mitigation strategies. Annu Rev Plant Biol 61:535–559

Zhu XF, Zheng C, Hu YT, Jiang T, Liu Y, Dong NY, Yang JL, Zheng SJ (2011) Cadmium-induced oxalate secretion from root apex is associated with cadmium exclusion and resistance in *Lycopersicon esulentum*. Plant Cell Environ 34:1055–1064

Environmental Science and Pollution Research (2018) 25:18947–18959
https://doi.org/10.1007/s11356-018-1928-z

Status, sources, and risk assessment of polycyclic aromatic hydrocarbons in urban soils of Xi'an, China

Huanyu Bao[1,2] · **Shaowei Hou**[1,2] · **Hao Niu**[1,2] · **Kai Tian**[1,2] · **Xueping Liu**[3] · **Fuyong Wu**[1,2]

Received: 26 September 2017 / Accepted: 3 April 2018 / Published online: 2 May 2018

Abstract

To identify status, source of polycyclic aromatic hydrocarbons (PAHs) in urban soils and to assess soil environmental quality in Xi'an City, China, total 45 soil samples were collected from surface layer (0–10 cm) in different functional areas. Total concentrations of 16 US EPA priority PAHs ranged from 149.9 to 5770 μg kg^{-1}, with a mean of 1246 μg kg^{-1}. High molecular weight (HMW) PAHs accounted for the majority (42.4–72.2%) of the total PAHs in the urban soils, and phenanthrene (Phe), fluorene (Flo), pyrene (Pyr), benzo(b)fluoranthene (BbF), and chrysene (Chr) were the major compounds. Concentrations of PAHs varied among different functional areas. High level of PAHs was particularly apparent in industrial zones and city road overpass, while low level was recorded in scenic spots and campus. The integration of isomer ratios, principal component analysis (PCA), and positive matrix factor (PMF) indicated that the sources of PAHs in Xi'an urban soils were mainly derived from vehicle emissions and coal combustion. Based on incremental lifetime cancer risks (ILCR) model, the urban soils from the three functional areas (industrial zone, urban road, and city road overpass) posed potential cancer risk, and the cancer risks of direct ingestion for children were apparently higher than that for adolescence and for adult, respectively. Therefore, attention should be paid to the health risk for children exposed to PAHs in the urban soils.

Keywords Polycyclic aromatic hydrocarbons · Source identification · Risk assessment · Urban soil

Introduction

Polycyclic aromatic hydrocarbons (PAHs) are ubiquitous organic pollutants and mainly generated from anthropogenic sources, such as coal and fossil fuel combustion, vehicle emissions, oil refining, industrial processing, chemical manufacturing, and petroleum leakage (Ravindra et al. 2008). Owing to rapid growth in economy and energy consumption, PAH emissions of China have been continuously increasing and are up to 106,000 tons in 2007, accounting for 21% of the global total emission (Shen et al. 2013). Due to their potential toxicity, carcinogenicity, and mutagenicity to human and other organisms, PAHs have been attracted enough attention for years.

As semivolatile chemicals, PAHs can be transported in the atmosphere over long distances and entered into surface soils via wet and/or dry deposition (Desalme et al. 2013). Because of their strong hydrophobicity and resistance to degradation, PAHs are easy to accumulate in soils, which makes soils become the most important sink of PAHs in environmental media, and approximately 90% of the total PAHs retain in surface soils (Ping et al. 2007; Wild and Jones 1995). Given recent rapid urbanization and industrialization, urban soil pollution including PAHs has become a very important issue (Wang et al. 2017b). PAH concentrations vary significantly in various rural and urban environments and are mainly influenced by vehicular and domestic emissions (Ravindra et al. 2008). Generally, soil PAH concentrations in urban areas are much

Responsible editor: Zhihong Xu

Electronic supplementary material The online version of this article (https://doi.org/10.1007/s11356-018-1928-z) contains supplementary material, which is available to authorized users.

✉ Fuyong Wu
wfy09@163.com; fuyongwu@nwsuaf.edu.cn

[1] College of Natural Resources and Environment, Northwest A&F University, Yangling 712100, Shaanxi, People's Republic of China

[2] Key Laboratory of Plant Nutrition and the Agri-environment in Northwest China, Ministry of Agriculture, Yangling 712100, Shaanxi, People's Republic of China

[3] School of Municipal and Environment Engineering, Henan University of Urban Construction, Pingdingshan 467036, People's Republic of China

higher than those in areas far away from the city center. For example, PAH concentrations were 7.4 times higher in industrial areas than in agricultural areas in Delhi, India (Singh et al. 2012) and ten times higher in busy streets than in natural soils (Wilcke 2000). Soils collected from roadside or busy street in Lanzhou of China showed much higher levels of PAHs than those collected from parks and residential areas (Jiang et al. 2016). Xi'an is the capital city of Shaanxi Province and the largest city in Northwest China, with a population of almost 9.0 million. A few studies have reported that high level of PAHs was recorded in fine particulate matter ($PM_{2.5}$), air and urban surface dust in Xi'an (Wei et al. 2015; Wang et al. 2016a, b, 2017a; Xu et al. 2016a), indicating serious pollution of the urban environments. The status of PAHs in proximity of urban soils is of vital importance for local residents because it can affect human health via inhalation, ingestion, or dermal contact (Cachada et al. 2012; Chen et al. 2013). Substantial variation which exists among existing studies focused on urban soil pollution, the status, distribution, and source of PAHs pollution for different regions due to differences in geography, sources, climate, and agricultural production (Wang et al. 2017b). However, the situation of PAHs in urban soils of Xi'an has not been fully investigated, and the health risk of human exposure to PAHs in urban soils from different urban functional districts is also lacking.

The major objectives of the present study were to (1) investigate the level and spatial distribution of PAHs (the 16 US EPA priority PAHs) in urban soils from Xi'an, (2) identify possible sources of PAHs in urban soils from Xi'an, and (3) evaluate health risk of human exposure to PAHs in urban soils from different urban functional districts of Xi'an.

Materials and methods

Collection and preparation of urban soil samples

During December 2016, total 45 soil samples were collected from surface layer (0–10 cm) in different functional areas of Xi'an, including industrial zone (IZ), campus (CP), residential areas (RA), parks (PR), urban road (UR), city road overpass (CRO), and scenic spots (SS) (Fig. 1). For each sampling site, four sub-samples were randomly collected in area of 10 m × 10 m and mixed as one composite sample. All the soil samples were stored in polyethylene sealing bag, placed in a dark environment, and transported to the laboratory for experimental analysis as soon as possible. Part of soil samples was air-dried for 2 weeks, sieved through a 2-mm mesh, and stored at − 80 °C for analysis of total PAHs and soil organic matter (SOM), while the rest was placed at − 80 °C for determination of microbial biomass carbon (MBC).

Extraction and analysis of PAHs

Each samples (about 3.5 g) were Soxhlet extracted for 18 h with 120 mL of acetone and dichloromethane (DCM) mixture (1:3, *v*/*v*) (USEPA 1996a). The sample cleanup and

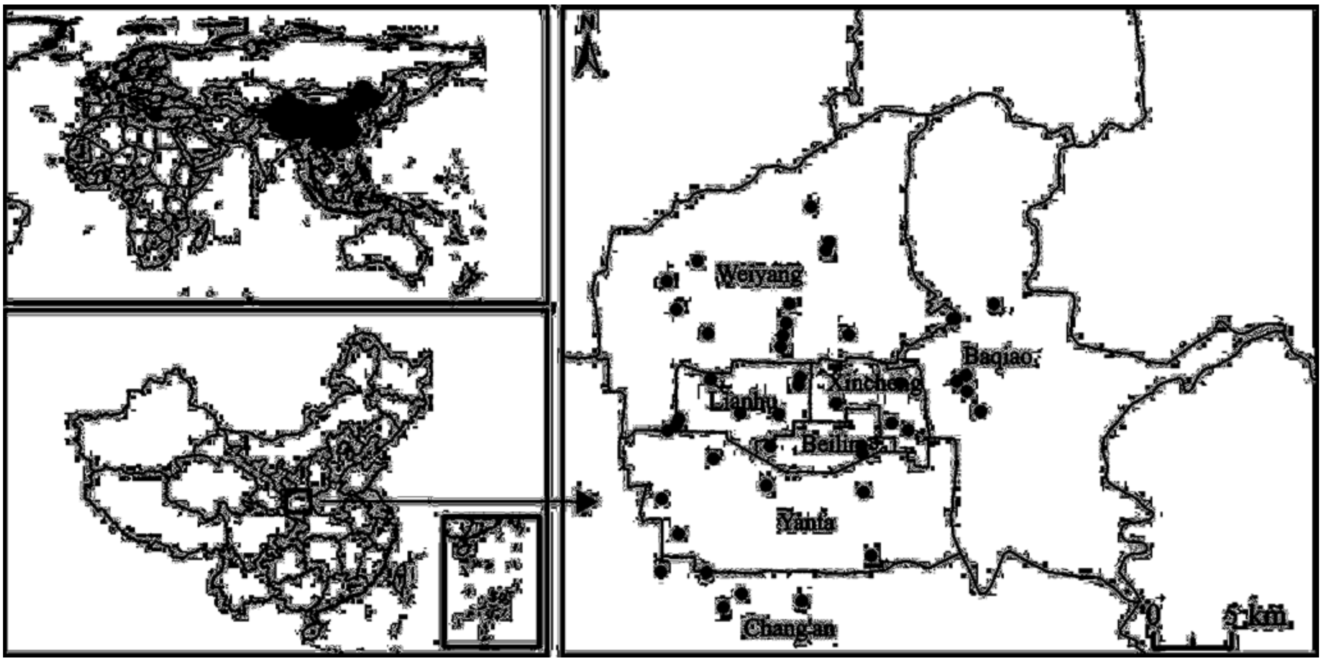

Fig. 1 Schematic showing the geographical locality of sampling sites of urban soils in Xi'an City, China

detection method is described in our previous study (Tian et al. 2018). Briefly, the extracts were concentrated to about 2 mL by a rotary evaporator, then passed through a silica gel column (top layer 2 g anhydrous Na_2SO_4 and sub-layer 2 g silica gel), and eluted with 60 mL hexane and DCM (1:1, *v*/*v*). The extracts were evaporated, exchanged with methanol to 2 mL, and analyzed using HPLC-FLD (Shimadzu, LC-20A) equipped with an ultraviolet detector (PF-20A) and a fluorescence detector (SPD-20A). The HPLC system was fitted with a PAH-specific reverse column (Φ4.6 × 150-mm Intersil ODS-P column, 5 μm, Shimadzu, Kyoto, Japan) and a mixture of methanol and ultrapure water as the mobile phase. Sixteen PAHs were measured in the present study: naphthalene (Nap), acenaphthylene (Acy), acenaphthene (Ace), fluorene (Flo), phenanthrene (Phe), anthracene (Ant), fluoranthene (Fla), pyrene (Pyr), benzo(a)anthracene(BaA), chrysene (Chr), benzo(b)fluoranthene (BbF), benzo(k)fluoranthene (BkF), benzo(a)pyrene (BaP), indeno(1,2,3-c,d)pyrene (IcdP), dibenzo(a,h)-anthracene (DahA), and benzo(g,h,i)perylene (BghiP).

Quality control

A method blank, a standard reference material (SRM 1649b) and a sample duplicate were processed and analyzed in parallel with each batch of 12 soil samples. The standard reference material of urban dust (SRM 1649b) obtained from the National Institute of Standards and Technology (NIST), USA was used for calibration and analytical control for urban soils. PAHs were identified on the basis of retention times relative to five deuterated internal standards (d_8-Nap, d_{10}-Ace, d_{10}-Phe, d_{10}-Chr, and d_{12}- perylene). The limit of detection (LOD) using the present method was determined as the concentrations of analytes in a sample that gave rise to a peak with a signal-to-noise ratio (S/N) of 3, which ranged from 0.07 to 1.41 $\mu g\ kg^{-1}$. The recoveries of individual PAHs in SRM and internal standards ranged from 77.9% for Pyr to 139% for Nap. The variation coefficient of PAH concentrations between duplicate samples was less than 10%.

Determination of SOM and MBC

SOM was determined with the potassium dichromate volumetric method (Lao 1988). MBC was determined with the chloroform fumigation extraction method (Vance et al. 1987). Briefly, fresh soil (12.5 g) was fumigated (ethanol-free chloroform), and an equivalent amount of soil was non-fumigated as blank for 24 h at 25 °C in an evacuated extractor. Both fumigated and non-fumigated soils were extracted with 25 mL of 0.5 mol L^{-1} K_2SO_4 for 1 h, then filtered through 0.45-μm filters. The extracts were preserved in the dark at −20 °C, and organic C in the extracts was determined with a TOC-V_{CPH} analyzer (Shimadzu, Japan).

Cancer risk assessment

Tsai et al. (2004) proposed a method for the evaluation of toxic equivalents based on BaP. BaP is the only known carcinogen slope factor in PAHs, and toxicity equivalency factor (TEF) is used to quantify the concentration of BaP and other carcinogenic PAHs. The total BaP equivalent concentrations were calculated as follows:

$$\mathrm{TEQ_{BaP}} = C_i \times \mathrm{TEF_i}$$

where C_i is the concentration of PAH congener i ($\mu g\ g^{-1}$); $\mathrm{TEF_i}$ is the toxicity equivalency factor of PAH congener i.

In this study, potential cancer risk imposed on townsfolk as a result of being in contact with contaminated soils was assumed to occur via three major exposure pathways including ingestion, dermal contact, and inhalation. Incremental lifetime cancer risks (ILCR) were calculated as a means of quantitatively evaluating the integrated lifetime risks of exposure to PAHs in urban surface soils. The USEPA standard models used in this study were described in Peng et al. (2011). The individual cancer risk was estimated based on the following three equations.

$$\mathrm{ILCR_{Ingestion}} = \frac{\mathrm{SC} \times \left(\mathrm{CSF_{Ingestion}} \times \sqrt[3]{\frac{\mathrm{BW}}{70}}\right) \times \mathrm{IR_{Ingestion}} \times \mathrm{EF} \times \mathrm{ED}}{\mathrm{BW} \times \mathrm{AT} \times 10^6} \tag{1}$$

$$\mathrm{ILCR_{Dermal}} = \frac{\mathrm{SC} \times \left(\mathrm{CSF_{Dermal}} \times \sqrt[3]{\frac{\mathrm{BW}}{70}}\right) \times \mathrm{SA} \times \mathrm{AF} \times \mathrm{ABS} \times \mathrm{EF} \times \mathrm{ED}}{\mathrm{BW} \times \mathrm{AT} \times 10^6} \tag{2}$$

$$\mathrm{ILCR_{Inhalation}} = \frac{\mathrm{SC} \times \left(\mathrm{CSF_{Inhalation}} \times \sqrt[3]{\frac{\mathrm{BW}}{70}}\right) \times \mathrm{IR_{Inhalation}} \times \mathrm{EF} \times \mathrm{ED}}{\mathrm{BW} \times \mathrm{AT} \times \mathrm{PEF}} \tag{3}$$

In these equations, where SC is the sum of converted PAH levels based on toxic equivalents of BaP, CSF is the carcinogenic slope factor $(\mathrm{mg\ kg^{-1}\ day^{-1}})^{-1}$; BW is the average body weight; AT is the average life span; EF is the exposure frequency; ED is the exposure duration; SA is the surface area of the skin that exposure to PAHs; AF is skin factor; ABS is the dermal absorption factor; $IR_{ingestion}$ is the ingestion rate of soil; $IR_{Inhalation}$ is the inhalation rate, and PEF is the particle emission factor. Parameters used for the estimation of ILCR are presented in Table S1.

Data analyses

Positive matrix factorization (PMF) was adopted to identify pollution patterns and the potential sources of PAHs in Xi'an urban soils. PMF calculation was conducted using EPA PMF 5.0. Two input files are required for the PMF 5.0 model: one is for the measured concentrations (C) of PAHs, and the other is for the estimated uncertainty (U) of the concentrations. PAHs concentration below the method detection limits (MDL) was substituted by half the detection limit. The input matrix of uncertainties was calculated by applying MDL for each PAH and measurement uncertainty (MU, %). If the PAH concentration is less than or equal to the MDL, then $U = 5/6$ MDL. Otherwise, $U = [(MU \times C)^2 + (MDL)^2]^{1/2}$. In addition, correlation analyses, principal component analyses (PCA), and other statistical analyses were conducted using SPSS 23.0 and Origin 8.0. The Inverse Distance Weighted (IDW) map showing the spatial distribution of $\sum_{16}$ PAHs was carried out with ArcGIS 9.3.

Results and discussion

Concentrations of PAHs in urban soils from Xi'an

The concentrations of 16 PAHs (Σ_{16}PAHs) in urban soils collected from Xi'an ranged from 149.9 to 5770 μg kg^{-1}, with an average of 1246 μg kg^{-1} (Table 1). According to the contamination classification indicated by Maliszewska–Kordybach (1996), 91.1% of the samples of urban soils in Xi'an were contaminated with PAHs (> 200 μg kg^{-1}). Levels of PAHs in urban soils from Xi'an were much higher than those in

Table 1 Summary of measured PAHs in urban surface soil of Xi'an (μg kg^{-1})

Compounds	Abbreviation	Aromatic ring	TEF[a]	Mean	Minimum	Maximun	Median	SD[b]
Naphthalene	Nap	2	0.001	76.64	nd	481.8	36.20	108.6
Acenaphthylene	Acy	3	0.001	22.16	0.073	169.0	6.396	39.33
Acenaphthene	Ace	3	0.001	33.03	nd	139.8	22.91	34.10
Fluorene	Flo	3	0.001	48.40	4.681	212.9	34.40	44.91
Phenanthrene	Phe	3	0.001	202.4	30.12	950.1	141.9	179.0
Anthracene	Ant	3	0.01	24.58	1.954	163.7	16.01	31.16
Fluoranthene	Fla	4	0.001	143.5	8.941	750.6	77.50	178.1
Pyrene	Pyr	4	0.001	135.3	2.658	988.0	57.47	200.7
Benz(a)anthracene	BaA	4	0.1	79.89	5.852	424.2	40.48	100.2
Chrysene	Chr	4	0.01	116.3	3.923	581.3	57.09	145.3
Benzo(b)fluoranthene	BbF	5	0.1	118.4	5.162	752.2	55.27	166.5
Benzo(k)fluoranthene	BkF	5	0.1	35.95	1.936	293.4	19.42	52.04
Benzo(a)pyrene	BaP	5	1	60.26	2.084	702.9	29.00	109.5
Dibenz(a,h)anthracene	DahA	5	0.1	34.02	nd	241.3	6.541	62.18
Indeno(1,2,3-cd)pyrene	IcdP	6	1	50.30	nd	400.7	23.85	78.29
Benzo(g,h,i)perylene	BghiP	6	0.01	65.16	nd	559.7	28.04	106.5
	LMW PAH$_s$[c]			407.3	58.20	1897	308.9	372.7
	HMW PAH$_s$[d]			839.2	37.47	5153	424.8	1120
	ΣPAH_7[e]			495.2	24.66	3202	245.5	660.0
	ΣPAH_{16}[f]			1246	149.9	5770	662.6	1403

nd indicating that it is not detectable

[a] Toxic equivalency factors

[b] Standard deviation

[c] Low molecular weight 2–3 ring PAHs

[d] High molecular weight 4–6 ring PAHs

[e] Sum of seven carcinogenic PAHs (BaA, Chr, BbF, BkF, BaP, IcdP, and DahA)

[f] Total PAHs concentration

seaside cities, such as Shenzhen (360 μg kg^{-1}), Dalian (796 μg kg^{-1}), and Guiyu (582 μg kg^{-1}) of China; Torino (857 μg kg^{-1}) of Italy; and Bangkok (129 μg kg^{-1}) of Thailand (Table 2). As the capital city of the largest province of coal producer and consumer of China, coal combustion from coal burning power plants, coal-power, and domestic heated in residential areas in winter, as well as coke oven used in the steel industry were assigned as a crucial source of PAHs in Xi'an. The energy consumption in the city was up to 4,905,405 tons of standard coal equivalent, in 2011(Statistics Bureau of Xi'an City 2012). Xi'an also has heavy auto-mobile traffic, and there were more than 2.60 million motor vehicles in 2016 (Hu and Gao 2017). Meanwhile, the concentrations of Σ_{16} PAHs in urban soils were influenced more by meteorological factors such as temperature and wind (Wang et al. 2017a). As an inland city, Xi'an ranks as one of the cities with the worst air quality in China, mainly attributed to industrial pollution and its topography surrounded by Qin Mountain and Loess Plateau hindering the dispersion of air pollutants (Wei et al. 2015). Up to 104.7 ng m^{-3} $PM_{2.5}$-bound PAHs were recorded in Xi'an, China, in summer of 2013 (Xu et al. 2016a). Wang et al. (2017b) suggested that soil temperature is a very important factor in determining the degradation of soil PAHs that decreases with lower temperature. Lower average year temperature in Xi'an compared with Shenzhen, Dalian, and Guiyu of China also contributed to higher level of PAHs in the urban soils because of lower degradation of soil PAHs at lower temperature. On the other hand, the concentrations of Σ_{16} PAHs in Xi'an urban soils were lower than those megacities, such as Beijing (6653 μg kg^{-1}), Nanjing (3330 μg kg^{-1}), and Shanghai (1970 μg kg^{-1}) of China, Bergen of Norway (6780 μg kg^{-1}), Glasgow (11,930 μg kg^{-1}), and London (18,000 μg kg^{-1}) of UK (Table 2), which are large cities with comparatively large population and heavy industries developed. Nam et al. (1999) indicated that there was a positive correlation between population density and soil PAH concentrations. Compared with the data from those reported in urban areas, the level of PAHs in Xi'an urban soil is moderately contaminated with PAHs and should pay enough attention.

Spatial distribution of PAHs

Concentrations of PAHs in urban soils varied greatly among the seven functional areas in Xi'an (Table 3). The mean concentrations ofΣ_{16}PAHs decreased in the following order: IZ > CRO > UR > PR > RA > SS > CP. The PAHs concentrations in IZ were significantly ($p < 0.05$) higher than those in other zones except for CRO, indicating that this functional area has been identified as the primary source of PAHs in Xi'an. Similarly, both Chen et al. (2013) and Jia et al. (2017) found that the highest concentrations of PAHs in urban soils were recorded in roadside areas and industrial areas. The present study also showed that the gradient of PAHs was obvious from the roadside to residential areas. This may be due to that many residential areas were built in recent years and that the parks were generally located in underground in Xi'an, which reduced PAH accumulation in RA soils from vehicular emission. In addition, domestic coal was replaced with electricity, and natural gas widely leading to a lower PAH concentrations in RA(Yang et al. 2017).

The spatial distribution of $\sum_{16}$ PAHs in urban soils from Xi'an is shown using a forecast map (Fig. 2). PAHs concentrations in urban soils were higher in east and west of center of Xi'an city, while those was lower in the south and north of the city. Two sections with hotspots isolated by the predicted mapping plot showed the highest concentrations PAHs in Xi'an urban soils which matched the proximity of major emission sources of PAHs geographically. Both sections A and B are located in the IZ, which have coal-fired power plants and other factories. Owing to the high-temperature and continuous

Table 2 Concentrations of ΣPAHs in topsoil of the in this study and other cities in previous studies

City and country	No. of PAHs	Depth	Mean (μg kg^{-1})	Range (μg kg^{-1})	References
Glasgow, UK	15	0–10	11,930	1487–51,882	Morillo et al.(2007)
Bergen, Norway	16	0–2	6780	nd-200,000	Haugland et al.(2008)
Torino, Italy	15	0–10	857	148–3410	Morillo et al.(2007)
Bangkok, Thailand	20	0–5	129	12–380	Boonyatumanond et al. (2007)
London, UK	16	5–20	18,000	4000–66,000	Vane et al.(2014)
Shenzhen, China	16	0–5	360	2–6745	Zhang et al.(2016a)
Nanjing, China	16	0–5	3330	59–18,000	Wang et al.(2015)
Dalian	15	0–5	796	190–8595	Wang et al.(2006)
Guiyu, China	16	0–20	582	45–3206	Xu et al.(2016b)
Shanghai, China	16	0–20	1970	83–7220	Wang et al.(2013)
Beijing, China	15	0–5	6653	924–44,495	Zhang et al.(2016b)
Xi'an, China	16	0–10	1257	149–5770	This study

Table 3 Effect of functional type on individual PAH concentrations in Xi'an surface soil

	Industrial zone ($n = 8$)		Campus ($n = 6$)		Residential areas ($n = 6$)		Parks ($n = 6$)		Urban road ($n = 9$)		City road overpass ($n = 5$)		Scenic spots ($n = 5$)	
Compounds	Mean	Max	Mean	Max	Mean	Max	Mean	Max	Mean	Max	Mean	Max	Mean	Max
Nap	183.0	481.8	33.14	122.2	35.83	79.25	59.24	225.9	83.78	349.8	83.99	349.8	34.95	84.16
Acy	35.45	159.2	4.544	10.65	6.778	12.18	2.928	6.396	29.93	169.0	28.82	169.0	14.86	55.20
Ace	45.34	139.8	12.88	31.61	27.86	48.92	13.89	30.81	41.96	110.2	41.52	110.2	43.52	132.7
Flo	88.58	212.9	15.45	44.39	38.37	82.74	17.30	27.37	58.15	138.7	55.91	138.7	31.88	47.80
Phe	361.1	950.1	63.82	131.0	87.95	147.9	118.5	202.9	252.7	514.9	251.6	517.3	101.9	179.0
Ant	59.67	163.7	4.218	11.87	17.08	47.62	11.38	22.64	21.98	45.87	23.60	52.89	11.04	16.01
Fla	327.0	750.6	55.52	136.9	57.20	146.6	89.24	201.3	141.5	288.0	140.9	462.6	45.61	65.93
Pyr	347.0	988.0	29.65	65.17	39.89	113.9	65.43	127.9	127.0	376.9	126.3	497.8	28.31	47.06
BaA	188.9	424.2	24.15	46.68	26.11	53.22	38.44	67.24	75.54	175.3	74.34	236.8	22.70	30.78
Chr	244.7	581.3	30.24	64.72	36.65	98.36	54.58	114.6	130.2	254.4	129.1	527.5	26.42	38.77
BbF	297.6	752.2	29.69	55.27	24.94	43.42	53.01	97.66	121.1	276.4	120.1	404.3	21.27	32.43
BkF	91.62	293.4	11.37	21.28	10.13	23.99	19.85	40.17	34.46	77.12	34.82	99.11	6.929	11.34
Bap	162.7	702.9	18.23	32.24	16.28	44.51	30.85	56.72	56.64	121.6	57.87	156.1	12.53	20.50
DahA	48.97	118.5	2.718	5.985	2.211	6.900	3.493	8.800	52.42	241.3	51.49	241.3	3.358	15.61
IcdP	131.2	400.7	10.96	23.39	10.57	23.85	24.17	44.15	49.96	124.9	51.07	167.2	4.871	12.07
BghiP	169.5	559.7	13.62	28.52	11.88	30.54	26.74	55.76	66.16	175.8	65.25	202.4	3.681	8.792
LMW PAHs	773.1	1897	134.0	267.0	213.9	311.7	223.3	488.6	485.5	1309	696.0	1309	238.2	326.1
HMW PAHs	2009	5153	226.1	479.2	235.9	577.7	405.8	804.4	851.2	1801	1605	2966	175.7	246.7
ΣPAH$_7$[a]	1166	3202	127.4	248.6	126.9	286.6	224.4	429.3	518.8	1005	990.7	1803	98.08	142.5
ΣPAH$_{16}$	2782	5770	360.2	691.8	449.7	886.6	629.1	1148	1337	2472	2301	3691	413.8	572.8

[a] Sum of seven carcinogenic PAHs (BaA, Chr, BbF, BkF, BaP, IcdP, and DahA)

combustion processes, large amounts of PAH would be generated. Therefore, these special points should be paid attention seriously.

Composition profile of PAHs in urban soils from Xi'an

The composition profiles of Σ_{16}PAHs in the urban soils from Xi'an were comparable among different functional areas, except for those from SS (2.0%) in which percentage of 6-ring PAHs was apparently lower than those from the other six different functional areas including UR (9.0%), CRO (9.8%), RA (5.0%), PR (8.1%), CP (6.8%), and IZ (10.8%), respectively (Fig. 3). High molecular weight PAHs (HMW PAHs, 4–6 rings) accounted for the majority (62.8–72.2%) of the total PAHs in urban soils from UR, CRO,PR, CP, and IZ, similar with previously studies conducted in many cities (Chung et al. 2007; Ma et al. 2009; Cachada et al. 2012; Wang et al. 2013). These were probably due to the higher persistence of HMWPAHs in soils and the tendency of HMW PAHs accumulating in soils close to emission sources (Chung et al. 2007; Liu et al. 2011). Comparatively, RA and SS were dominated by low molecular weight PAHs (LMWPAHs, 2–3 rings) (47.6% and 57.5). LMW PAHs are deemed to petrogenic origins and usually formed in low-temperature processes, which are easily transported to remote areas and considered as "multi-hop" chemicals due to their high volatility and octanol-water partition coefficient(Gouin et al. 2004). For the individual compounds, Phe, Flu, Pyr, BbF, and Chr were the major compounds, accounting for 16.2, 11.5, 10.9, 9.5, and 9.3% of Σ_{16}PAHs, respectively. As shown in Table 4, the correlation coefficient matrix among the different rings of PAHs reflected that nearly all variables were significantly ($p < 0.01$) inter correlated. The higher correlations represented by r value ($r > 0.6$) were found in individual PAHs between LMW and HMW compounds group. Most of the HMW PAHs were significantly ($p < 0.01$) correlated with one another. However, there was insignificantly correlated between LMW PAHs and HMW PAHs, suggesting that the sources of LMW PAHs were different from the HMW PAHs.

Effects of SOM and MBC on PAHs in urban soils from Xi'an

The present study shows that there were significantly positive correlation between SOM and total PAHs ($r = 0.452$, $p < 0.01$), HMW PAHs ($r = 0.453$, $p < 0.01$), LMW PAHs ($r = 0.341$, $p < 0.05$), and seven kinds of carcinogenic PAHs ($r = 0.417$, $p < 0.01$) in urban soils from Xi'an (Table 4). Previous studies also found a strong correlation between SOM and concentrations of soil PAHs (Jiang et al. 2011; Yu

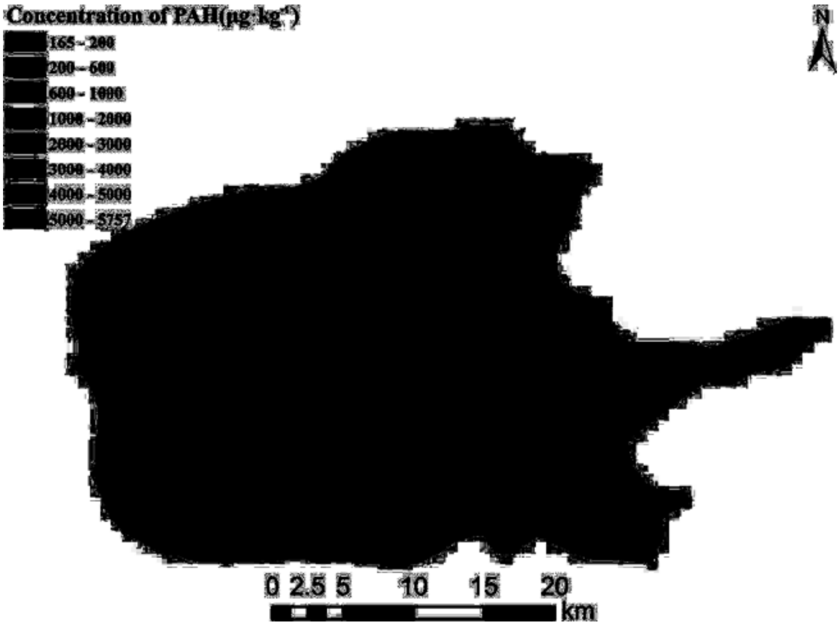

Fig. 2 Composition profile plot of PAHs in urban soils collected from seven functional areas including industrial zone (IZ), campus (CP), residential areas (RA), parks (PR),urban road (UR), city road overpass (CRO), and scenic spots (SS) in Xi'an City, China

et al. 2013). This phenomenon may be attributed to the strong adsorption of PAHs to SOM, especially the allochthonous carbonaceous SOM that exhibits adsorption properties much different from the autochthonous SOM (Dachs and Eisenreich 2000). PAHs in soils could decompose by heterotrophic microorganisms, which use organic carbon as nutrients and energy sources (Chiou et al. 2001). MBC, which drives the decomposition of organic compounds, is often used as a sensitive indicator of the various stresses caused by the disturbance of soil properties in ecosystems (Sun et al. 2016; Wang et al. 2012). However, the present study showed that there were insignificant correlation between MBC and individual PAHs (Table 4), similar with the results done by Hu et al. (2016). MBC is the most active part of soil organic carbon, and it is moving fast and poor stability, and much easier to be changed. The insignificant correlation between MBC and individual PAHs may be due to that soil microbial can mineralize and use PAHs absorbed in soils (Sun et al. 2012). In addition,

Table 4 Correlation coefficients (*r*) among the concentrations of individual PAHs, soil organic matter, and microbial biomass carbon in the soil samples

	2-ring PAHs	3-ring PAHs	4-ring PAHs	5-ring PAHs	6-ring PAHs	LMW PAHs	HMW PAHs	ΣPAH_7	ΣPAH_{16}	SOM[a]	MBC[b]
2-ring PAHs	1.000										
3-ring PAHs	0.708**	1.000									
4-ring PAHs	0.568**	0.738**	1.000								
5-ring PAHs	0.489**	0.684**	0.946**	1.000							
6-ring PAHs	0.365*	0.505**	0.921**	0.945**	1.000						
LMW PAHs	0.838**	0.979**	0.736**	0.670**	0.496**	1.000					
HMW PAHs	0.521**	0.697**	0.989**	0.980**	0.959**	0.690**	1.000				
ΣPAH_7	0.506**	0.709**	0.969**	0.996**	0.945**	0.695**	0.991**	1.000			
ΣPAH_{16}	0.638**	0.816**	0.985**	0.960**	0.897**	0.816**	0.981**	0.976**	1.000		
SOM[a]	0.435**	0.227	0.476**	0.394**	0.435**	0.341*	0.453**	0.417**	0.452**	1.000	
MBC[b]	− 0.157	− 0.200	− 0.153	− 0.160	− 0.191	− 0.200	− 0.164	− 0.153	− 0.184	0.192	1.000

*Correlation is significant at the 0.05 level (2-tailed)

**Correlation is significant at the 0.01 level (2-tailed)

[a] Soil organic matter

[b] Microbial biomass carbon

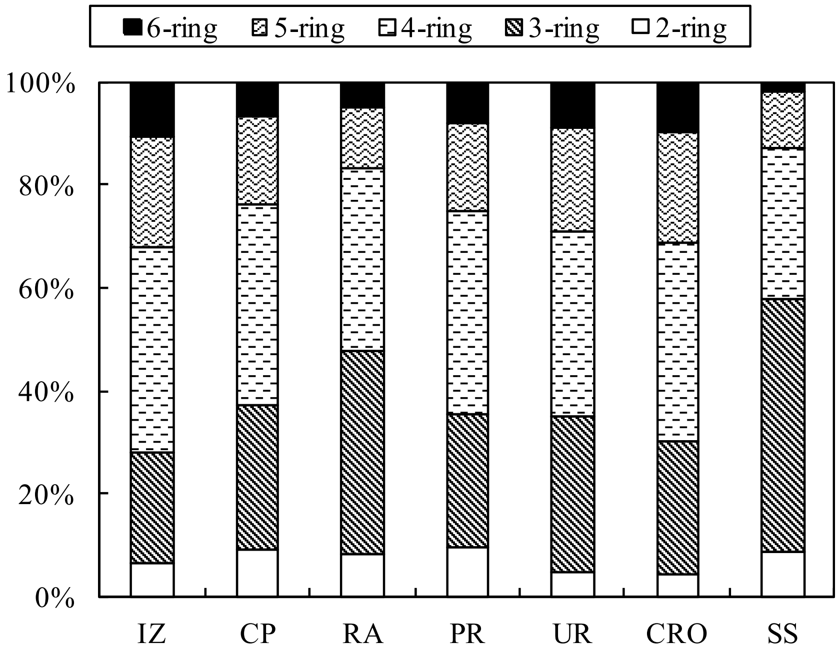

Fig. 3 Spatial distribution of PAHs in urban soils from Xi'an City, China (A and B were the sections isolated with the high-polluted hot spots)

previous studies indicated that there are many factors such as anthropogenic activity, vegetation, and soil property influencing the concentrations of MBC (Xu et al. 2007; Dai et al. 2016). MBC in unban soil may be more susceptible to human activity, which results in the insignificant correlation with PAHs.

Possible source of PAHs in urban soils from Xi'an

There are two main sources of PAHs in soils, including natural and anthropogenic sources (Morillo et al. 2007). It is necessary to identify the source of PAHs in urban soils, which is the key to carry out soil risk assessment and risk management. Up to date, the diagnostic ratio, PCA, and PMF are widely used for the source identification of PAHs in soils (Zhang et al. 2016a). In the present study, diagnostic ratio analysis, PCA, and PMF were used to identify the possible source of PAHs in urban soils from Xi'an.

Isomeric ratios of PAHs

The diagnostic ratio determines the origin of PAHs by comparing the relative concentrations of the individual PAHs. A series PAHs isomeric ratios have been widely used for discriminating the potential sources of PAHs (Budzinski et al. 1997; Yunker et al. 2002). A ratio of Ant/(Ant+Phe) < 0.1 suggests a petroleum source, while a ratio > 0.1 indicates a dominance of combustion products. Meanwhile, a ratio of Fla./(Fla + Pyr) < 0.4 indicates a petroleum input source; 0.4–0.5 implies petroleum combustion and > 0.5 indicates sources from combustion of biomass and coal. The Ant/(Ant+Phe) and the Fla./(Fla + Pyr) of all 45 sampling sites from Xi'an were calculated and plotted in Fig. 4A. The present study showed that the ratio of Ant/(Ant+Phe) and Fla./(Fla + Pyr) was ranged from 0.02 to 0.24 and from 0.06 to 0.85, respectively, indicating that PAHs in urban soils from Xi'an were primarily derived from combustion of biomass, coal, and petroleum as well as petroleum input. The Fla./(Fla + Pyr) value in all RA samplings was above 0.5, indicating the PAHs sources in RA mainly from combustion of biomass and coal. This may due to the low temperature in winter of Xi'an; local residents had boosted demand for coke in heating. Meanwhile, the Fla./(Fla + Pyr) value in part of samplings in IZ was between 0.4 and 0.5, while the rest were beyond 0.5, which suggest that the combustion of biomass, coal, and petroleum was the main source in IZ.

Principal component analysis

To further investigate possible sources of PAH pollution in Xi'an urban soil, PCA was performed by dividing the original variables into several sets of new set variables, then selecting a smaller number of important variables which can reflect as much as possible the original information (Golobočanin et al. 2004). For Xi'an, two principal components (PC1 and PC2) with the eigenvalues > 1were extracted and collectively represented more than 84.20% of the total variance of Σ_{16}PAHs (Fig. 4B). PC1 (67.54% of total variances) was predominated by Fla., Pyr, BaA, Chr, BbF, BkF, and IcdP. BaA, Chr, BbF, BkF, and IcdP are typical tracers of vehicle-related sources (Duval and Friedlander 1981; Hyeok and Sungdeuk 2014), while the Fla. and Pyr are the components of coal combustion (Larsen and Baker 2003). Thus, PC1 apparently represents mixed sources of vehicle sources and coal

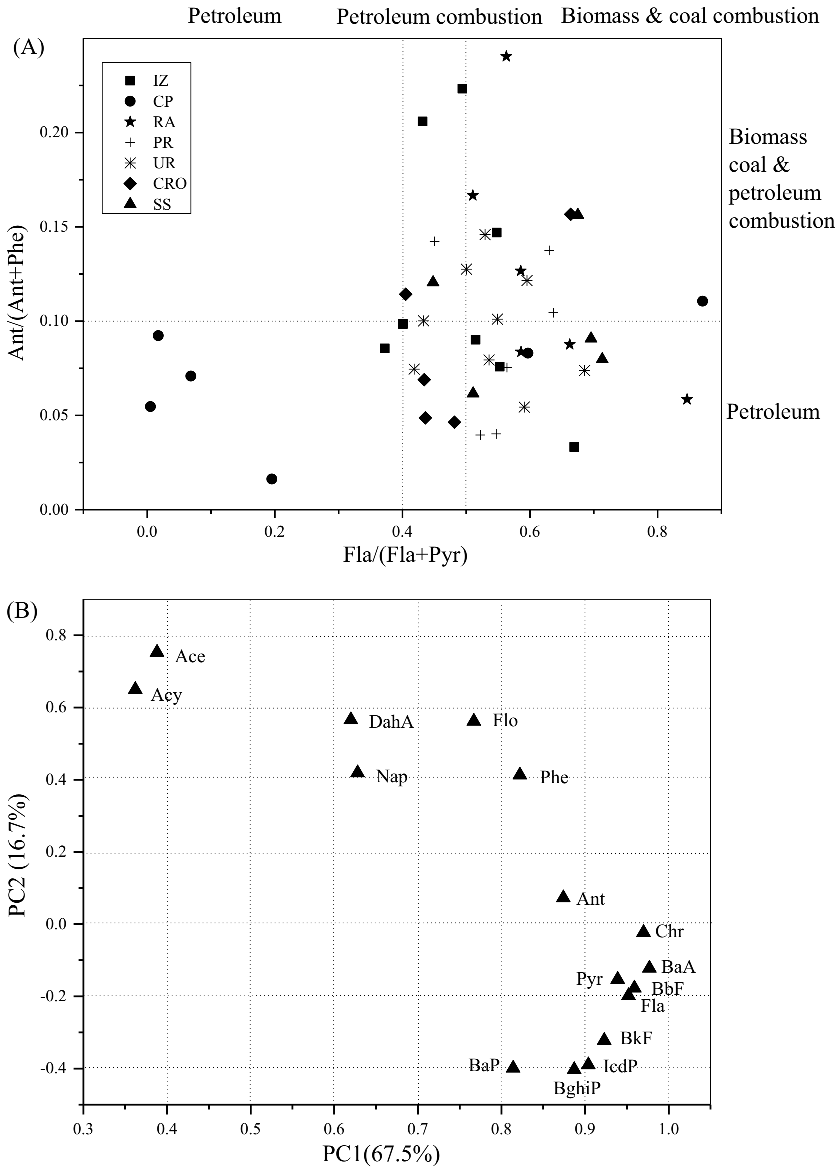

Fig. 4 Ratio analysis of PAHs in urban soils from Xi'an City, China. **a** Cross plot for the isomeric ratios of Ant/(Ant+Phe) vs. Fla./(Fla + Pyr). **b** Factor loadings of16 PAHs on two components

combustion. PC2 (16.66% of variance) was heavily weighted by Ace, reflecting a low-temperature combustion source and indicating a coke source (Steinhauer and Boehm 1992). Thus, the PCA showed that the PAHs originated mainly from vehicle sources and coal combustion as well as petroleum emission.

Positive matrix factorization (PMF)

The isomeric ratio is a qualitative method of source identification. Due to the values of isomeric ratios may vary with travel distance, the results may be under debate for a number of uncertainties (Katsoyiannis and Breivik 2014). In order to assess the contribution of various sources to PAH contamination quantitatively, PMF was adopted to quantitatively assess the proportion of each source associated with urban soil in Xi'an. The source of composition profiles of the 16 PAHs based on a 3-factor solution are depicted in Fig. 5. Factor 1 was mainly loaded by Nap and explained 18% of the total PAHs. Nap was served as markers for petroleum source (Chen et al. 2013). Therefore, factor 1 indicated a petroleum source. Factor 2 was predominantly loaded by Acy, Ace, and Flo, indicating a coke source (Khalili et al. 1995). The relative contributions for factor 3 was 58%, which was dominated by Fla., Pyr, BaA, Chr, BbF, BkF, BaP, DahA, IcdP, and BghiP. Among these PAHs, BghiP, IcdP, BbF, BkF, and Chr are typical tracers of traffic tunnel markers (Nielsen 1996). BaA, Chr, IcdP, and BkF are the components of diesel combustion (Venkataraman et al. 1994; Khalili et al.1995; Larsen and Baker 2003). BbF, IcdP, Chr, Pyr, and BghiP are related to the profile of gasoline engine

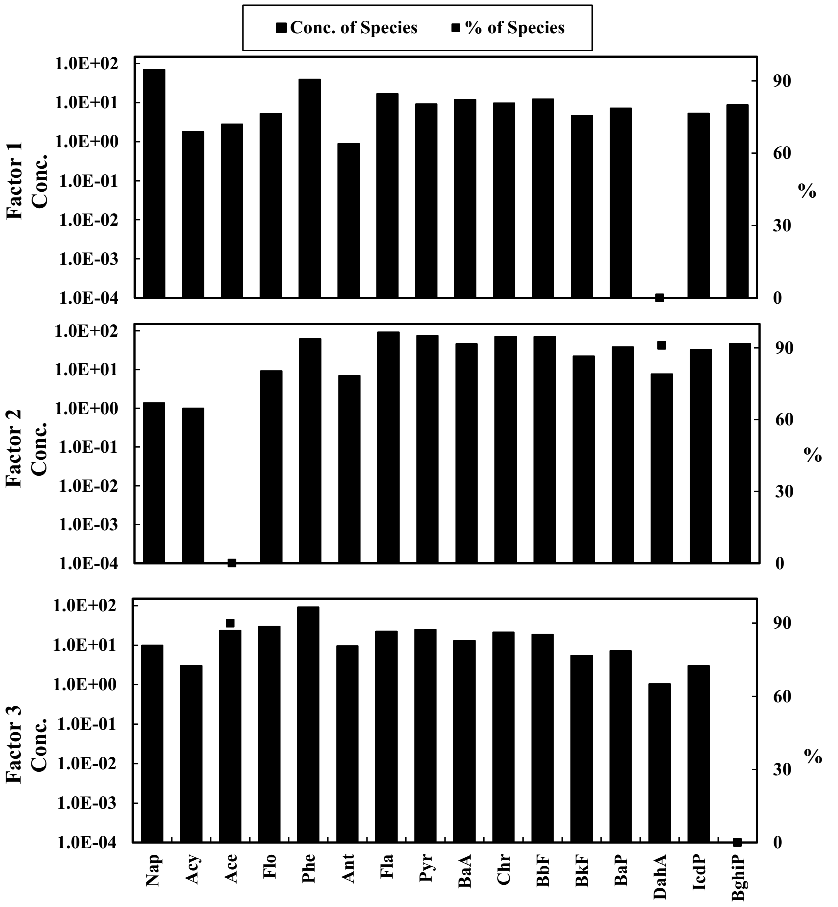

Fig. 5 Source profiles obtained from the positive matrix factorization (PMF) model

emissions (Wang et al. 2009). Fla. and Pyr are the components of coal combustion (Larsen and Baker 2003). Thus, factor 3 indicates contributions from vehicle sources and coal combustion.

Health risk assessment

According to the US EPA, one in a million chance of additional human cancer over a 70-year lifetime (ILCR = 10^{-6}) is considered acceptable or inconsequential, while 10^{-4} is considered serious and is high priority for paying attention to such health problem (USEPA 1996b). Based on total PAHs in urban soils from Xi'an, the ILCR for children, adolescents, and adults via direct ingestion, dermal contacts and inhalation are presented in Table 5. The mean values of ILCR in IZ, UR, and CRO were higher than the acceptable risk level (10^{-6}), indicating that the urban soils from the three functional areas possessed potential cancer risk. The ILCR value in IZ was significantly higher ($p < 0.05$) than that in other functional districts, except for CRO. The present study was similar with results conducted by Wang et al. (2016a), who found that the ILCR value exposed to PAHS in urban surface dust in industrial and traffic district of Xi'an was higher than that in other area. The present results showed that the cancer risk levels (8.52×10^{-8}– 3.17×10^{-6}) through ingestion and dermal contact in all urban soils were 10^3 to10^7 times higher than that through inhalation (2.23×10^{-12}– 1.21×10^{-10}) (Table 5), which indicated the cancer risk of inhalation of urban soils through the mouth and nose was negligible. As shown in Table 5, the ILCR value of direct ingestion for children was apparently higher than that for adolescence and for adult, respectively. Children are the most sensitive subpopulation mainly due to their hand-to-mouth activity and poor hygiene practices. As a result, PAHs-contaminated soils can be readily ingested (Wang et al. 2017c). Moreover, early development of organs, nerves, and immune system may enhance the susceptibility to carcinogens in children (Maertens et al. 2008). Therefore, attention should be paid to the health risk for children exposed to PAHs in the urban soils.

Conclusion

The $\sum_{16}$PAHs concentrations in the urban soil samples ranged from 149.9 to 5770 μg kg^{-1}, with an average of 1246 μg kg^{-1}.HMWPAHs accounted for the majority (42.4–72.2%) of the total PAHs in urban soils. For the individual compounds, Phe, Flu, Pyr, BbF, and Chr were

Table 5 Incremental lifetime cancer risk (ILCR) values for PAHs in Xi'an urban soil collected from different functional districts

Functional areas	Exposure pathways	Childhood		Adolescence		Adulthood	
		Male	Female	Male	Female	Male	Female
Industrial zone (IZ)	Ingestion	1.74E-06	1.80E-06	9.06E-07	9.42E-07	1.63E-06	1.78E-06
	Dermal contact	2.17E-06	2.25E-06	2.26E-06	2.35E-06	2.89E-06	3.17E-06
	Inhalation	3.68E-11	3.81E-11	6.22E-11	6.46E-11	1.10E-10	1.21E-10
	Cancer risk	3.91E-06	4.05E-06	3.17E-06	3.29E-06	4.52E-06	4.95E-06
Campus (CP)	Ingestion	1.76E-07	1.82E-07	9.15E-08	9.51E-08	1.64E-07	1.80E-07
	Dermal contact	2.19E-07	2.27E-07	2.58E-07	2.37E-07	2.92E-07	3.20E-07
	Inhalation	3.72E-12	3.85E-12	6.28E-12	6.53E-12	1.11E-11	1.22E-11
	Cancer risk	3.95E-07	4.09E-07	3.50E-07	3.32E-07	4.56E-07	5.00E-07
Residential areas (RA)	Ingestion	1.64E-07	1.70E-07	8.52E-08	8.86E-08	1.53E-07	1.68E-07
	Dermal contact	2.04E-07	2.11E-07	2.13E-07	2.21E-07	2.72E-07	2.29E-06
	Inhalation	3.47E-12	3.58E-12	5.85E-12	6.08E-12	1.04E-11	1.14E-11
	Cancer risk	3.68E-07	3.81E-07	2.98E-07	3.10E-07	4.25E-07	2.46E-06
Parks (PR)	Ingestion	3.26E-07	3.37E-07	1.69E-07	1.76E-07	3.04E-07	3.33E-07
	Dermal contact	4.06E-07	4.20E-07	4.22E-07	4.39E-07	5.39E-07	5.91E-07
	Inhalation	6.88E-12	7.12E-12	1.16E-11	1.21E-11	2.06E-11	2.26E-11
	Cancer risk	7.32E-07	7.57E-07	5.91E-07	6.15E-07	8.43E-07	9.24E-07
Urban road (UR)	Ingestion	6.65E-07	6.88E-07	3.46E-07	3.59E-07	6.20E-07	6.80E-07
	Dermal contact	8.29E-07	8.57E-07	8.62E-07	8.96E-07	1.10E-06	1.21E-06
	Inhalation	1.41E-11	1.45E-11	2.37E-11	2.47E-11	4.21E-11	4.61E-11
	Cancer risk	1.49E-06	1.55E-06	1.21E-06	1.26E-06	1.72E-06	1.89E-06
07 City road overpass (CRO)	Ingestion	1.15E-06	1.19E-06	5.99E-07	6.23E-07	1.08E-06	1.18E-06
	Dermal contact	1.44E-06	1.49E-06	1.49E-06	1.55E-06	1.91E-06	2.09E-06
	Inhalation	2.23E-12	2.52E-11	4.11E-11	7.30E-11	7.30E-11	8.00E-11
	Cancer risk	2.59E-06	2.68E-06	2.09E-06	2.17E-06	2.99E-06	3.27E-06
Scenic spots (SS)	Ingestion	1.13E-07	1.17E-07	5.88E-08	6.11E-08	1.05E-07	1.16E-07
	Dermal contact	1.41E-07	1.46E-07	1.47E-07	1.52E-07	1.87E-07	2.05E-07
	Inhalation	6.21E-13	6.42E-13	1.05E-12	1.09E-12	1.86E-12	2.04E-12
	Cancer risk	2.54E-07	2.63E-07	2.06E-07	2.13E-07	2.92E-07	3.21E-07

the major compounds. Correlation analysis suggested that SOM affected the accumulation of PAHs in urban soil. Concentrations of PAHs varied in different functional groups, with high PAH contamination observed in IZ and CRO, while low levels were recorded in SS and CP. Vehicle emissions and coal combustion were the primary sources of PAHs in urban soils from Xi'an. Risk assessment based on ILCR model was conducted to evaluate human cancer risk associated with urban soil. The industrial zone and the areas adjacent to roadways should draw considerable attention for their potential human health risk from soil PAHs.

Acknowledgements The study was financially supported by the National Natural Science Foundation of China (41571456), Program for Science & Technology Innovation Talents in Universities of Henan Province (14HASTIT048), and the Scientific Research Foundation for the Introduction of Talent, Northwest A&F University, China (2014).

References

Boonyatumanond R, Murakami M, Wattayakorn G, Togo A, Takada H (2007) Sources of polycyclic aromatic hydrocarbons (PAHs) in street dust in a tropical Asian mega-city, Bangkok, Thailand. Sci Total Environ 384(1–3):420–432

Budzinski H, Jones I, Bellocq J, Piérard C, Garrigues P (1997) Evaluation of sediment contamination by polycyclic aromatic hydrocarbons in the Gironde estuary. Mar Chem 58(1–2):85–97

Cachada A, Pato P, Rocha-Santos T (2012) Levels, sources and potential human health risks of organic pollutants in urban soils. Sci Total Environ 430:184–192

Chen M, Huang P, Chen L (2013) Polycyclic aromatic hydrocarbons in soils from Urumqi, China: distribution, source contributions, and potential health risks. Environ Monit Assess 185(7):5639–5651

Chiou CT, Sheng GY, Manes M (2001) A partition-limited model for the plant uptake of organic contaminants from soil and water. Environ Sci Technol 35(7):1437–1444

Chung MK, Hu R, Cheung KC (2007) Pollutants in Hong Kong soils: polycyclic aromatic hydrocarbons. Chemosphere 67(3):464–473

Dachs J, Eisenreich SJ (2000) Adsorption onto aerosol soot carbon dominates gas-particle partitioning of polycyclic aromatic hydrocarbons. Environ Sci Technol 34:3690–3697

Dai J, Wu H, Chang Z et al (2016) Responses of soil microbial biomass and bacterial community structure to closed-off management (an ecological natural restoration measures): a case study of Dongting Lake wetland, middle China. J Biosci Bioeng 122(3):345–350

Desalme D, Binet P, Chiapusio G (2013) Challenges in tracing the fate and effects of atmospheric polycyclic aromatic hydrocarbon deposition in vascular plants. Environ Sci Technol 47(9):3967–3981

Duval MM, Friedlander SK (1981) Source resolution of polycyclic aromatic hydrocarbons in the Los Angeles atmosphere: application of a chemical species balance method with first order chemical decay. Final report Jan-Dec 80

Golobočanin DD, Škrbić BD, Miljević NR (2004) Principal component analysis for soil contamination with PAHs. Chemom Intell Lab 72(2):219–223

Gouin T, Mackay D, Jones KC, Harner T, Meijer SN (2004) Evidence for the "grasshopper" effect and fractionation during long-range atmospheric transport of organic contaminants. Environ Pollut 128(1–2): 139–148

Haugland T, Ottesen RT, Volden T (2008) Lead and polycyclic aromatic hydrocarbons (PAHs) in surface soil from day care centres in the city of Bergen, Norway. Environ Pollut 153(2):266–272

Hu WT, Gao Y (2017) Xi'an: open the door to "Tucao", crack parking difficult road traffic management 0(4):18–20. (in Chinese)

Hu TP, Zhang JQ, Ye C et al (2016) Status, source and health risk assessment of polycyclic aromatic hydrocarbons (PAHs) in soil from the water-level-fluctuation zone of the three gorges reservoir, China. J Geochem Explor 172:20–28

Hyeok K, Sungdeuk C (2014) Polycyclic aromatic hydrocarbons (PAHs) in soils from a multi-industrial city, South Korea. Sci Total Environ 470-471:1494–1501

Jia JP, Bi CJ, Xue G et al (2017) Characteristics, identification, and potential risk of polycyclic aromatic hydrocarbons in road dusts and agricultural soils from industrial sites in Shanghai, China. Environ Sci Pollut Res 24(1):605–615

Jiang YF, Wang XT, Wu MH, Sheng GY, Fu JM (2011) Contamination, source identification, and risk assessment of polycyclic aromatic hydrocarbons in agricultural soil of Shanghai, China. Environ Monit Assess 183:139–150

Jiang YF, Yves UJ, Sun H, Hu X, Zhan H, Wu Y (2016) Distribution, compositional pattern and sources of polycyclic aromatic hydrocarbons in urban soils of an industrial city, Lanzhou, China. Ecotoxicol Environ Saf 126:154–162

Katsoyiannis A, Breivik K (2014) Model-based evaluation of the use of polycyclic aromatic hydrocarbons molecular diagnostic ratios as a source identification tool. Environ Pollut 184(1):488–494

Khalili NR, Scheff PA, Holsen TM (1995) Pah source fingerprints for coke ovens, diesel and, gasoline engines, highway tunnels, and wood combustion emissions. Atmos Environ 29(4):533–542

Lao JC (1988) Handbook of soil chemical analysis. Agriculture Press, Beijing

Larsen RK, Baker JE (2003) Source apportionment of polycyclic aromatic hydrocarbons in the urban atmosphere: a comparison of three methods. Environ Sci Technol 37:1873–1881

Liu SD, Xia XH, Zhai YW (2011) Blackcarbon (BC) in urban and surrounding rural soils of Beijing, China: spatial distribution and relationship with polycyclic aromatic hydrocarbons (PAHs). Chemosphere 82(2):223–228

Ma WL, Li YF, Sun DZ (2009) Polycyclic aromatic hydrocarbons and polychlorinated biphenyls in topsoils of Harbin, China. Arch Environ Contam Toxicol 57(4):670–678

Maertens RM, Yang XF, Zhu JP, Gagne RW, Douglas GR, White PA (2008) Mutagenic and carcinogenic hazards of settled house dust. I: polycyclic aromatic hydrocarbon content and excess lifetime cancer risk from preschool exposure. Environ Sci Technol 42(5): 1747–1753

Maliszewska-Kordybach B (1996) Polycyclic aromatic hydrocarbons in agricultural soils in Poland: preliminary proposals for criteria to evaluate the level of soil contamination. Appl Geochem 11(1): 121–127

Morillo E, Romero AS, Maqueda C, Madrid L, Ajmone-Marsan F, Grcman H, Davidson CM, Hursthouse AS, Villaverde J (2007) Soil pollution by PAHs in urban soils: a comparison of three European cities. J Environ Monit 9(9):1001–1008

Nam JJ, Sweetman AJ, Jones KC (1999) Polynuclear aromatic hydrocarbons (PAHs) in global background soils. J Environ Monit 11(1):45–48

Nielsen T (1996) Traffic contribution of polycyclic aromatic hydrocarbons in the center of a large city. Atmos Environ 30(20):3481–3490

Peng C, Chen WP, Liao XL, Wang M, Ouyang Z, Jiao W, Bai Y (2011) Polycyclic aromatic hydrocarbons in urban soils of Beijing: status, sources, distribution and potential risk. Environ Pollut 159(3):802–808

Ping LF, Luo YM, Zhang HB, Li QB, Wu LH (2007) Distribution of polycyclic aromatic hydrocarbons in thirty typical soil profiles in the yangtze river delta region, East China. Environ Pollut 147(2):358–365

Ravindra K, Sokhi R, Grieken RV (2008) Atmospheric polycyclic aromatic hydrocarbons: source attribution, emission factors and regulation. Atmos Environ 42(13):2895–2921

Shen H, Huang Y, Wang R, Zhu D, Li W, Shen G, Wang B, Zhang Y, Chen Y, Lu Y, Chen H, Li T, Sun K, Li B, Liu W, Liu J, Tao S (2013) Global atmospheric emissions of polycyclic aromatic hydrocarbons from 1960 to 2008 and future predictions. Environ Sci Technol 47(12):6415–6424

Singh DP, Gadi R, Mandal TK (2012) Levels, sources, and toxic potential of polycyclic aromatic hydrocarbons in urban soil of Delhi, India. Hum Ecol Risk Assess 18(2):393–411

Statistics Bureau of Xi'an City, C (2012) Xi'an statistical yearbook. China Statistics Press, Beijing

Steinhauer MS, Boehm PD (1992) The composition and distribution of saturated and aromatic hydrocarbons in near shore sediments, river sediments, and coastal peat of the Alaskan Beaufort Sea: implications for detecting anthropogenic hydrocarbon inputs. Mar Environ Res 33(4):223–253

Sun GD, Xu Y, Jin JH, Zhong ZP, Liu Y, Luo M, Liu ZP (2012) Pilot scale ex-situ bioremediation of heavily PAHs-contaminated soil by indigenous microorganisms and bioaugmentation by a PAHs-degrading and bioemulsifier-producing strain. J Hazard Mater 233-234(3):72–78

Sun MM, Ye M, Shen FY, Xu J, Ye C, Yu L, Hu F, Li H, Jiang X, Kengara FO (2016) Function of nitrate ion and tea saponin application rates in anerobic PAH dissipation in paddy soil. Clean-Soil Air Water 44(6):667–676

Tian K, Bao HY, Zhang XC, Shi TR, Liu XP, Wu FY (2018) Residuals, bioaccessibility and health risk assessment of PAHs in winter wheat grains from areas influenced by coal combustion in China. Sci Total Environ 618:777–784

Tsai PJ, Shih TS, Chen HL, Lee WJ, Lai CH, Liou SH (2004) Assessing and predicting the exposures of polycyclic aromatic hydrocarbons (PAHs) and their carcinogenic potencies from vehicle engine exhausts to highway Toll Station workers. Atmos Environ 38(2): 333–343

USEPA (1996a) Method 3540C: Soxhlet extraction. US Environmental Protection Agency, Washington, DC

USEPA (1996b) Soil screening guidance: user's guide, seconded. http://nepis.epa.gov/Exe/ZyPURL.cgi?Dockey=100027WI.txt

Vance ED, Brookes PC, Jenkinson DS (1987) An extraction method for measuring soil microbial biomass C. Soil Biol Biochem 19(6):703–707

Vane CH, Kim AW, Beriro DJ, Cave MR, Knights K, Moss-Hayes V, Nathanail PC (2014) Polycyclic aromatic hydrocarbons (PAH) and polychlorinated biphenyls (PCB) in urban soils of greater London, UK. Appl Geochem 51:303–314

Venkataraman C, Lyons JM, Friedlander SK (1994) Size distributions of polycyclic aromatic hydrocarbons and elemental carbon. 1. Sampling, measurement methods, and source characterization. Environ Sci Technol 28(4):555–562

Wang Z, Chen J, Yang P et al (2006) Polycyclic aromatic hydrocarbons in Dalian soils: distribution and toxicity assessment. J Environ Monit 9(2):199–204

Wang D, Yang MH, Zhou L et al (2009) Polycyclic aromatic hydrocarbons in urban street dust and surface soil: comparisons of concentration, profile, and source. Arch Environ Contam Toxicol 56(2): 173–180

Wang K, Zhang J, Zhu ZQ, Huang H, Li T, He Z, Yang X, Alva A (2012) Pig manure vermicompost (PMVC) can improve phytoremediation of Cd and PAHs co-contaminated soil by Sedum alfredii. J Soils Sediments 12(7):1089–1099

Wang XT, Miao Y, Zhang Y, Li YC, Wu MH, Yu G (2013) Polycyclic aromatic hydrocarbons (PAHs) in urban soils of the megacity Shanghai: occurrence, source apportionment and potential human health risk. Sci Total Environ 447(1):80–89

Wang CH, Wu SH, Zhou SL, Wang H, Li B, Chen H, Yu Y, Shi Y (2015) Polycyclic aromatic hydrocarbons in soils from urban to rural areas in Nanjing: concentration, source, spatial distribution, and potential human health risk. Sci Total Environ 527-528:375–383

Wang LJ, Wang L, Tao WD, Smardon RC, Shi X, Lu X (2016a) Characteristics, sources, and health risk of polycyclic aromatic hydrocarbons in urban surface dust: a case study of the city of Xi'an in Northwest China. Environ Sci Pollut Res 23(13):13389–13402

Wang JZ, Ho SSH, Huang RJ et al (2016b) Characterization of parent and oxygenated-polycyclic aromatic hydrocarbons (PAHs) in Xi'an, China during heating period: an investigation of spatial distribution and transformation. Chemosphere 159:367–377

Wang JZ, Xu HM, Guinot B, Li L, Ho SSH, Liu S, Li X, Cao J (2017a) Concentrations, sources and health effects of parent, oxygenated- and nitrated- polycyclic aromatic hydrocarbons (PAHs) in middle-school air in Xi'an, China. Atmos Res 192:1–10

Wang CH, Wu SH, Zhou SL et al (2017b) Characteristics and source identification of polycyclic aromatic hydrocarbons(PAHs) in urban soils: a review. Pedosphere 27(1):17–26

Wang J, Zhang XF, Ling WT, Liu R, Liu J, Kang F, Gao Y (2017c) Contamination and health risk assessment of PAHs in soils and crops in industrial areas of the Yangtze River Delta region, China. Chemosphere 168:976–987

Wei C, Bandowe BA, Han Y et al (2015) Polycyclic aromatic hydrocarbons (PAHs) and their derivatives (alkyl-PAHs, oxygenated-PAHs, nitrated-PAHs and azaarenes) in urban road dusts from Xi'an, Central China. Chemosphere 134:512–520

Wilcke W (2000) Synopsis polycyclic aromatic hydrocarbons (PAHs) in soil—a review. J Plant Nutr Soil Sci 163(3):229–248

Wild SR, Jones KC (1995) Polynuclear aromatic hydrocarbons in the United Kingdom environment: a preliminary source in inventory and budget. Environ Pollut 88(1):91–108

Xu XK, Han L, Wang YS, Inubushi K (2007) Influence of vegetation types and soil properties on microbial biomass carbon and metabolic quotients in temperate volcanic and tropical forest soils. Soil Sci Plant Nutr 53(4):430–440

Xu HM, Ho SSH, Gao ML, Cao J, Guinot B, Ho KF, Long X, Wang J, Shen Z, Liu S, Zheng C, Zhang Q (2016a) Microscale spatial distribution and health assessment of PM2.5-bound polycyclic aromatic hydrocarbons (PAHs) at nine communities in Xi'an, China. Environ Pollut 218:1065–1073

Xu PJ, Tao B, Ye ZQ (2016b) Polycyclic aromatic hydrocarbon concentrations, compositions, sources, and associated carcinogenic risks to humans in farmland soils and riverine sediments from Guiyu, China. J Environ Sci 48:102–111

Yang JY, Yu F, Yu YC, Zhang J, Wang R, Srinivasulu M, Vasenev VI (2017) Characterization, source apportionment, and risk assessment of polycyclic aromatic hydrocarbons in urban soil of Nanjing, China. J Soils Sediments 17(4):1116–1125

Yu BM, Yuan K, Hong SW et al (2013) Cancer risk assessments of Hong Kong soils contaminated by polycyclic aromatic hydrocarbons. J Hazard Mater 261(13):770–776

Yunker MB, Macdonald RW, Vingarzan R, Mitchell RH, Goyette D, Sylvestre S (2002) PAHs in the Fraser River basin: a critical appraisal of PAH ratios as indicators of PAH source and composition. Org Geochem 33(4):489–515

Zhang D, Wang JJ, Zeng H (2016a) Soil polycyclic aromatic hydrocarbons across urban density zones in Shenzhen, China: occurrences, source apportionments, and spatial risk assessment. Pedosphere 26(5):676–686

Zhang J, Wu J, Liu Y (2016b) Polycyclic aromatic hydrocarbons in urban green spaces of Beijing: concentration, spatial distribution and risk assessment. Environ Monit Assess 188(9):511

Environmental Science and Pollution Research (2018) 25:23780–23790
https://doi.org/10.1007/s11356-018-2456-6

RESEARCH ARTICLE

Accumulation and distribution of PAHs in winter wheat from areas influenced by coal combustion in China

Kai Tian[1,2] · Huanyu Bao[1,2] · Xueping Liu[3] · Fuyong Wu[1,2]

Received: 15 January 2018 / Accepted: 30 May 2018 / Published online: 6 June 2018

Abstract
In order to investigate level and potential sources of polycyclic aromatic hydrocarbons (PAHs) in wheat fields affected by coal combustion in Henan and Shaanxi Provinces and to investigate distribution and transfer of PAHs in winter wheat grown in the areas, various tissues of the crop and the corresponding rhizosphere soils were collected during the harvest season of winter wheat. The mean concentrations of USEPA 15 priority PAHs (sum of the three- to six-ring PAHs) ranged from 486 to 1117 μg kg^{-1} in the rhizosphere soils, indicating serious PAH contamination. Based on both the isomeric ratios of PAHs and a principal component analysis (PCA), the main sources of PAHs in the agricultural soils were from combustion of biomass, coal and petroleum, and petroleum. $\sum_{15}$PAHs were significantly ($p < 0.001$) higher in the roots (287–432 μg kg^{-1}) than those in aerial tissues (221–310 μg kg^{-1}). There were two decreasing gradients of PAH concentrations, one from roots, stems to leaves, and the other from glumes to grains. Regardless of sampling sites, most PAHs detected in the roots and in the aerial tissues were three-ring PAHs (acenaphthene, acenaphthylene, fluorene, phenanthrene, and anthracene) and the percentages of three-ring PAHs were much higher in the aerial tissues (72.5–82.7%) than in the roots (49.5–74.0%) and in the rhizosphere soils (36.3–65.7%). The distribution of PAHs with different ring numbers in the stems, leaves, and glumes was quite similar to each other but was significantly different from that of the roots and rhizosphere soils. Combined with significant results from partial correlation and linear regression models, the present study suggested that partial three- to four-ring PAHs in the aerial tissues are derived from root-soil uptake and that six-ring PAHs may come from the air-to-leaf pathway, although the quantity contribution of foliar uptake and root uptake was yet to be further studied.

Keywords Polycyclic aromatic hydrocarbons · Cereal · *Triticum aestivum* L. · Accumulation

Introduction

Mainly resulted from incomplete combustion of biomass or fossil fuels including coal and petroleum, polycyclic aromatic hydrocarbons (PAHs) are ubiquitous organic pollutants and possess carcinogenic, mutagenic, and genotoxic potential to human. As a "coal kingdom," coal has been as the majority (> 70%) of energy in China for years (China Energy Statistical Yearbook 2015). China became the largest coal consumer in the world and annual consumption of coal was 2794 million tons in 2014 (China Energy Statistical Yearbook 2015). Consequently, PAH emission of China was 106,000 tons in 2007, accounting for 21% of the global total (Shen et al. 2013), which has resulted in high level of PAHs in air and soils. Up to 346 ng m^{-3} PAHs was recorded in ambient air in the North China Plain, which was 8.9 times of London and 4.9 times of Chicago, respectively (Dimashki et al. 2001; Sun et al. 2006; Liu et al. 2007). Due to their strong hydrophobicity and resistance to degradation, PAHs are easy to accumulate in soils and approximately 90% of total PAHs retain in surface soils (Wild and Jones 1995). Based on China's soil environmental quality limits (BaP < 100 μg kg^{-1}), 1.4% of soil samples were contaminated with PAHs and the area influenced by industry activities including metal smelting, thermal power,

Responsible editor: Philippe Garrigues

Electronic supplementary material The online version of this article (https://doi.org/10.1007/s11356-018-2456-6) contains supplementary material, which is available to authorized users.

✉ Fuyong Wu
wfy09@163.com; fuyongwu@nwsuaf.edu.cn

[1] College of Natural Resources and Environment, Northwest A&F University, Yangling 712100, Shaanxi, People's Republic of China

[2] Key Laboratory of Plant Nutrition and the Agri-environment in Northwest China, Ministry of Agriculture, Yangling 712100, Shaanxi, People's Republic of China

[3] School of Municipal and Environment Engineering, Henan University of Urban Construction, Pingdingshan 467036, People's Republic of China

urban heating, and oil refining plants was more serious (The Ministry of Environmental Protection 2014). Approximately 60% of the soil samples were heavily polluted with PAHs (> 600 μg kg^{-1}), which were collected from area around a coke production base in Shanxi Province, China (Duan et al. 2015). The average concentrations of 16 USEPA priority PAHs in surface soils in industrial areas of the Yangtze River Delta region of China were 471 μg kg^{-1} (Wang et al. 2017). Considering energy consumption structure being given priority to coal will not change significantly in the coming decades, severe PAH contamination in China is expected to continue for years. Therefore, there is urgent need to investigate level and source of PAHs in agricultural systems of China.

PAH contamination has become one of the main obstacles affecting the safety of agricultural products. PAH contamination in crops has been reported worldwide, including the edible part of vegetables (1298 μg kg^{-1}) and rice grains (352 μg kg^{-1}) from industrial areas in the Yangtze River Delta region of China (Wang et al. 2017) and vegetables (186,000 μg kg^{-1}) from Abia State, Nigeria (Nwaichi et al. 2014). Generally, dietary intake is the main (> 70%) way of exposure to PAHs for nonsmokers (Phillips 1999). The total values of incremental lifetime cancer risk (ILCR) of crops from industrial areas in the Yangtze River Delta region of China for all groups ranged from 10^{-6} to 10^{-3}, with an average of 1.75×10^{-5} which was apparently higher than the acceptable risk level (10^{-6}) (Wang et al. 2017). Therefore, more attention should be paid to the safety of the agro-products growing in the PAH-contaminated areas.

China has the highest global wheat production and the total cultivated area was up to 24.2 million ha in 2011 (China Statistical Yearbook 2017). The majority of winter wheat cultivation within China is concentrated in specific key areas, such as Henan, Hebei, Shandong, and Shaanxi Provinces. Henan Province is the highest province of winter wheat production and making up 27% of total wheat production in China (China Statistical Yearbook 2017). Henan and Shaanxi Provinces are also regarded as the heartland of Chinese coal mining, where wheat fields and coal combustion enterprises such as coal-fired power plants, coking plants, and urban heating plants coexist. Levels of PAHs in ambient air during the maturity time of wheat and in surface soil of wheat fields near a large steel-smelting manufacturer in northern China are serous (Liu et al. 2017). PAHs can enter into the winter wheat via foliar uptake and soil-root uptake (Tao et al. 2009; Shi et al. 2017). Previous works have confirmed that PAHs can move into roots of the winter wheat via both passive and active transport (Zhan et al. 2010, 2012, 2015). It has been shown that PAH concentrations in grains of the winter wheat from market of Taiyuan (162 μg kg^{-1}) and Tianjin 177 μg kg^{-1}), China, were far higher than those (27.9 μg kg^{-1}) in Catalonia, Spain (Li 2007; Martí-Cid et al. 2008; Xia et al. 2010). Our recent study showed that the winter wheat grains from areas affected by coal combustion were seriously contaminated with PAHs and possessed significant cancer risk to local residents (Tian et al. 2018). However, level, distribution, and transfer of PAHs in tissues of winter wheat from the areas influenced by coal combustion in China have not been adequately addressed.

The major objectives of the present study were (1) to investigate concentrations, profiles, and potential sources of PAHs in agricultural soils from areas affected by coal combustion in Henan and Shaanxi Provinces and (2) to investigate transfer of PAHs and their distribution in tissues of winter wheat grown in the areas. The results of this investigation would provide valuable information for identification of the sources of PAHs in agricultural systems and minimization of crop contamination and human health risks in these areas.

Materials and methods

Plant and soil sample collection

During the harvest season of the winter wheat (from 27 May to 10 June 2015), whole plants and rhizosphere soils were collected from agricultural fields surrounding coal-fired power plants, including the Weihe power plant (WH, 34° 25′ 55″ N, 108° 54′ 26″ E) and the second power plant of Hu county (HX, 34° 04′ 42″ N, 108° 37′ 11″ E) in Xi'an City, Shaanxi Province, the Sanhe thermal power plant (SH, 33° 42′ 25″ N, 113° 23′ 16″ E) and the pithead power plant (KK, 33° 47′ 07″ N, 113° 12′ 07″ E) in Pingdingshan City, Henan Province. The location of sampling sites and the sampling method of plants were described in our previous study (Tian et al. 2018). There were about 150–1050 m from the sampling point to the coal-fired power plants. The plant and soil samples at each point were collected from at least one plot (5 × 5 m) and each plot was sampled from three random points. Along the same direction, there were 50 m between two neighboring sampling points. The majority of bulk soils were manually removed from the roots. Soil samples were taken from the rhizosphere of the responding plant and only those closely attached to the root systems were sampled. Totally, there were total 51 valid plant samples and 51 responding rhizosphere soil samples collected, of which 16 samples were from WH, 11 samples from HX, 13 samples from SH, and 11 samples from KK, respectively. After transportation to the laboratory, the whole plants thoroughly were washed with running tap water to remove airborne dust and soil particles and were divided into various tissues including grains, glumes, leaves, stems, and roots (Fig. 1). The sub-samples of the plant were air-dried, weighed to determine the biomass, and milled to pass through a 70-mesh sieve. All samples were kept frozen at − 18 °C before PAH analysis.

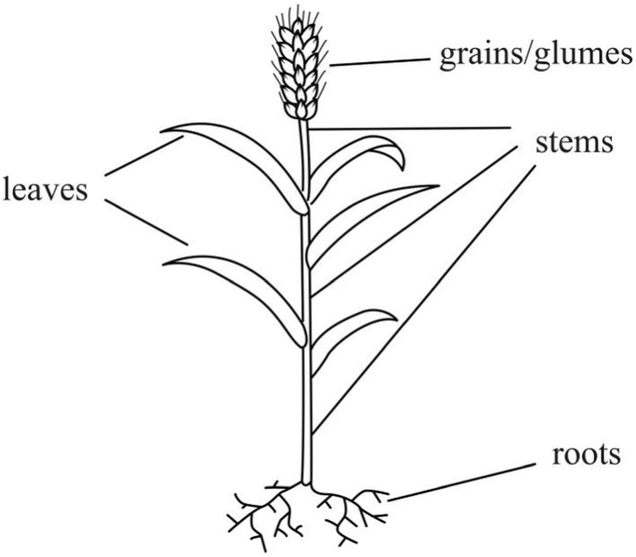

Fig. 1 Schematic diagram of various tissues of winter wheat

PAH analyses

Soil or plant samples (about 4.0 g) were Soxhlet extracted for 18–20 h with 120 mL of acetone and dichloromethane (DCM) mixture (1:3, *v*/*v*) (USEPA 1996). The sample cleanup and detection method is described in our previous study (Tian et al. 2018). Briefly, the extracts were concentrated to about 2 mL by a rotary evaporator, then passed through a silica gel column (top layer 2 g anhydrous Na_2SO_4 and sub-layer 2 g silica gel), and eluted with 60 mL hexane and DCM (1:1, *v*/*v*). The extracts were evaporated, exchanged with methanol to 2 mL, and analyzed using HPLC-FLD (Shimadzu, LC-20A) equipped with an ultraviolet detector (PF-20A) and a fluorescence detector (SPD-20A). The HPLC system was fitted with a PAH-specific reverse column ($\Phi 4.6 \times 150$-mm Intersil ODS-P column, 5 μm, Shimadzu, Kyoto, Japan) and a mixture of methanol and ultrapure water as the mobile phase. Sixteen US EPA priority PAHs were measured in the present study: naphthalene (NAP), acenaphthylene (ACY), acenaphthene (ACE), fluorene (FLO), phenanthrene (PHE), anthracene (ANT), fluoranthene (FLA), pyrene (PYR), benzo(a)anthracene (BaA), chrysene (CHR), benzo(b)fluoranthene (BbF), benzo(k)fluoranthene (BkF), benzo(a)pyrene (BaP), indeno(1,2,3-c,d)pyrene (IcdP), dibenzo(a,h)-anthracene (DahA), and benzo(g,h,i)perylene (BghiP).

QA/QC

QA/QC was conducted by performing method blanks, standard reference material recoveries, standard spiked recoveries, and HPLC detection limits. The limit of detection (LOD) using the present method was determined as the concentrations of analyses in a sample that gave rise to a peak with a signal-to-noise ratio (S/N) of 3, which ranged from 0.08 to1.53 μg kg^{-1}. The recoveries of individual PAHs ranged from 76.7% for DahA to 178.1% for Nap. For each batch of 12 samples, a method blank (solvent), a spiked blank (standards spiked into solvent), a sample duplicate, and a standard reference material (NIST SRM 2977) sample were processed. PAHs were identified on the basis of retention times relative to five deuterated internal standards (naphthalene-d_8, acenaphthene-d_{10}, phenanthrene-d_{10}, chrysene-d_{12}, and perylene-d_{12}). The variation coefficients of PAH concentrations between duplicate samples were < 10%. The levels of PAHs in digestion blank were less than the LOD.

Data analyses

NAP was not included in the total PAHs reported in the present study because of its higher recovery (> 100%) and higher percentage in the total PAHs. Means of different groups were compared using one-way ANOVA test. Concentration PAHs in soils and plants were log-transformed before analysis. Statistical analyses including Pearson's partial correlation analysis were conducted using SPSS 19.0 (SPSS Inc., USA). Unless otherwise indicated, all treatment means were tested for significant difference at $p < 0.05$.

Results and discussion

Levels of PAHs in the rhizosphere soils of winter wheat from field conditions

As shown in Table 1, the mean concentrations of USEPA 15 priority PAHs ($\sum_{15}$PAHs, sum of the three- to six-ring PAHs) ranged from 486 to 1117 μg kg^{-1} in the rhizosphere soils of winter wheat collected from the areas affected by coal combustion located in Shaanxi and Henan Provinces, with an average of 676 μg kg^{-1} (WH), 477 μg kg^{-1} (HX), 792 μg kg^{-1} (SH), and 933 μg kg^{-1} (KK). There were significant ($p <$ 0.001) variations in concentrations of PAHs in the rhizosphere soils among the four sites. The concentrations of PAHs in the rhizosphere soils are affected by anthropogenic factors (such as emission intensity of PAHs and history of coal-fired power plants) and by non-anthropogenic factors (such as soil property including organic carbon, climate). The soils near older coal-fired power plants have been receiving emissions for longer periods of time and high levels of PAHs were recorded as the result of long-term accumulation. Based on the contamination classification proposed by Maliszewska-Kordybach (1996), all the rhizosphere soils could be considered as PAH-contaminated, which 29.4% were weakly contaminated (> 200 μg kg^{-1}), 68.6% contamination (600–1000 μg kg^{-1}), and 2.0% heavy contamination (> 1000 μg). The level of $\sum_{15}$PAHs (mean 720 μg kg^{-1}) in the rhizosphere soils in the present study was far higher than those in the soil-wheat

Table 1 Summary of measured PAHs in rhizosphere soils of the winter wheat collected from agricultural fields surrounding coal-fired power plants, including the Weihe power plant (WH) and the second power plant of Hu county (HX) in Xi'an City, Shaanxi province, the Sanhe thermal power plant (SH) and the pithead power plant (KK) in Pingdingshan City, Henan province (μg kg^{-1})

Compounds	Aromatic ring	WH (*n* = 64)					HX (*n* = 44)					SH (*n* = 52)					KK (*n* = 44)				
		Mean	SD	Median	Min	Max	Mean	SD	Median	Min	Max	Mean	SD	Median	Min	Max	Mean	SD	Median	Min	Max
ACY	3	54.1	17.8	55.5	12.7	95.8	73.7	10.41	73.7	45.6	96.4	71.8	10.7	72.0	48.2	92.7	76.7	9.36	78.1	59.1	93.6
ACE	3	17.5	14.0	13.4	5.84	73.3	6.99	2.41	7.31	2.33	14.7	5.35	2.96	4.84	1.62	19.4	7.40	3.80	6.83	2.05	17.5
FLO	3	66.3	15.9	65.0	24.6	110	49.3	11.7	47.6	24.7	90.1	48.9	13.5	48.0	5.15	75.7	65.0	18.5	65.0	9.38	100
PHE	3	166	28.5	172	112	237	165	26.1	160	121	235	170	26.3	170	104	224	186	23.4	189	121	239
ANT	3	20.5	6.64	18.1	12.7	46.2	18.3	3.58	17.8	12.9	26.7	22.6	14.6	19.9	7.84	74.9	3.91	1.20	3.90	1.83	7.11
FLA	4	65.8	19.6	59.8	41.0	116	29.4	10.2	27.2	10.4	65.0	79.7	24.2	79.2	37.5	120	44.6	11.2	43.2	22.8	66.7
PYR	4	42.6	23.5	32.8	17.6	111	10.8	6.36	8.76	4.81	35.0	36.5	11.7	35.6	17.0	63.9	70.4	13.6	69.4	42.6	102
BaA	4	29.5	13.4	25.8	11.5	75.4	14.5	5.43	12.6	5.30	27.8	40.5	14.6	39.7	18.3	83.4	56.0	16.8	52.8	14.4	94.6
CHR	4	51.5	15.1	48.7	28.4	86.8	25.9	8.9	22.7	7.8	49.6	85.7	19.6	86.9	43.0	119	86.1	17.6	89.3	28.9	111
BbF	5	41.2	22.8	31.7	21.9	121	24.7	11.2	21.6	8.9	67.8	56.2	11.4	55.0	35.7	80.5	72.7	10.9	71.8	54.0	109
BkF	5	15.3	6.6	13.5	5.7	32.1	9.88	3.24	8.75	4.70	16.3	27.6	14.8	24.5	11.9	99.4	58.4	16.0	59.8	22.5	89.6
BaP	5	21.0	10.9	19.7	9.0	58.8	10.5	4.69	8.00	4.85	24.8	33.5	16.6	29.7	5.26	79.7	63.6	17.8	64.8	3.3	99.8
DahA	5	18.6	17.0	12.5	4.9	93.8	11.2	3.88	10.9	4.80	22.7	19.4	6.34	18.7	8.13	32.6	48.8	10.9	49.4	25.5	81.6
BghiP	6	35.9	20.1	31.8	5.8	96.0	11.4	3.76	10.4	6.15	23.2	55.6	27.8	48.3	15.2	108	42.2	7.56	42.	18.4	63.5
IcdP	6	30.6	15.6	24.9	12.8	97.9	15.6	5.15	14.0	5.84	28.0	38.9	16.8	35.9	17.0	90.4	51.7	8.77	52.0	32.6	77.3
LMW PAHs[a]		324	44.9	324	236	434	314	39.9	308	245	447	318	42.2	324	232	413	339	37.3	341	231	410
HMW PAHs[b]		352	95.4	340	196	597	164	51.6	146	71.2	284	474	103	489	286	658	594	50.2	596	484	714
ΣPAHs[c]		676	116	655	486	990	477	81.5	460	317	731	792	121	811	556	1020	933	76.5	932	736	1117
TEQs-PAHs[d]		52.8	25.6	45.7	24.6	125	29.1	9.91	24.8	17.3	58.7	71.3	22.3	69.1	34.4	126	138	25.8	140	64.5	197

[a] Low molecular weight two- to three-ring PAHs

[b] High molecular weight four- to six-ring PAHs

[c] ΣPAH concentrations excluding NAP

[d] Total TEQ-PAH concentrations, PAH toxic equivalency factor with respect to BaP (Nisbet and LaGoy 1992)

systems from Henan Province, China (6.91–72.4 μg kg^{-1}, mean 24.3 μg kg^{-1}) (Feng et al. 2017) and those in agricultural soils from the Huanghuai plain (15.7–1248 μg kg^{-1}, mean 130 μg kg^{-1}) (Yang et al. 2012). Moreover, the concentrations of $\sum_{15}$PAHs in the rhizosphere soils were comparable with those collected from area around a coke production base in Shanxi Province (247–1410 μg kg^{-1}, mean 691 μg kg^{-1}) (Duan et al. 2015) and higher than those from the coal production area surrounding Xinzhou in Shanxi Province (n.d. 782 μg kg^{-1}, mean 202 μg kg^{-1}) (Zhao et al. 2014) and from industrial areas of the Yangtze River Delta region, China (104–744 μg kg^{-1}, mean 341 μg kg^{-1}) (Wang et al. 2017). The main PAH sources in soils from the latter were determined to be the combustion of coal and petroleum (Wang et al. 2017). These indicated that the status of soil contamination in the areas affected by coal combustion is serious and that the safety of the agro-products growing in the areas needs to be paid more attention.

Possible source of PAHs in the rhizosphere soils of winter wheat

Isomeric ratios of PAHs

The diagnostic ratios of ANT/(ANT+PHE), FLA/(FLA+PYR), IcdP/(IcdP+BghiP), and BaP/BghiP were applied to identify PAH sources in the rhizosphere soils of winter wheat collected form areas affected by coal combustion located in Shaanxi and Henan Provinces (Fig. 2). The ratio of ANT/(ANT+PHE) < 0.1 suggests a petroleum source, while a ratio > 0.1 indicates a pyrogenic source of biomass, coal, and petroleum combustion (Pies et al. 2008). The ratio of FLA/(FLA+PYR) < 0.4 indicates a petroleum source, while 0.4–0.5 implies petroleum combustion and > 0.5 indicates sources from combustion of biomass and coal (Yunker et al. 2002). The ratio of IcdP/(IcdP + BghiP) < 0.2 likely implies a petroleum source, while 0.2–0.5 indicates liquid fossil fuel (vehicle and crude oil) combustion and > 0.5 indicates grass, wood, and coal combustion (Yunker et al. 2002). In addition, the ratio of BaP/BghiP > 0.6 indicates traffic emissions, while < 0.6 indicates non-traffic emissions (Katsoyiannis et al. 2007). The present study showed that the ratio of ANT/(ANT+PHE) is from 0.01 to 0.24, 66.7% of which are less than 0.1; the ratio of FLA/(FLA+PYR) is from 0.17 to 0.71, 64.7% of which are less than 0.4; the ratio of IcdP/(IcdP+BghiP) is from 0.25 to 0.67, 64.7% of which are higher than 0.5; and the ratio of BaP/BghiP is from 0.18 to 2.87, 62.7% of which are higher than 0.6. These revealed that combustion of biomass, coal and petroleum, and petroleum input contribute significantly to PAHs in the agricultural soils from areas affected by coal combustion located in Shaanxi and Henan Provinces.

Principal component analysis

In order to investigate possible sources of PAH pollution in four coal-fired power plants soils, principal component analysis (PCA) was performed by using a mathematical linear transformation and picking out fewer number of important variables to reflect more information of the original variables (Golobocanin et al. 2004). As shown in Fig. 3, four principal components (eigenvalue > 1) were extracted for the accumulated variance contribution rates above 80.04%. PC1 explained 44.83% of the total variance and was characterized by high loadings of PAHs with four to six rings, including

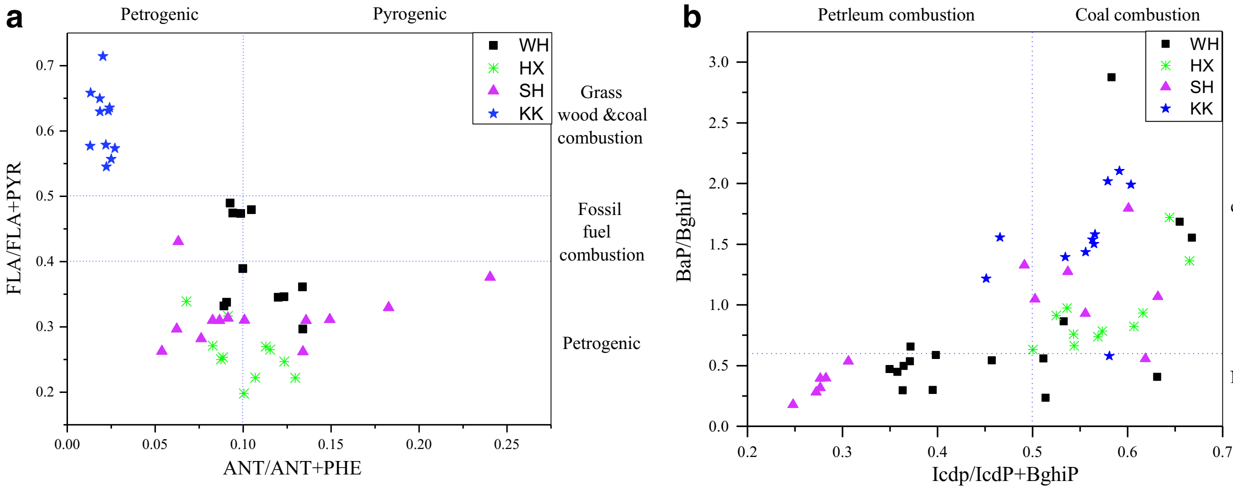

Fig. 2 Cross plots for the isomeric ratios of ANT/(ANT+PHE) vs FLA/(FLA+PYR) (**a**) and IcdP/(IcdP+BghiP) vs BaP/BghiP (**b**) in the soils collected from agricultural fields surrounding coal-fired power plants, including the Weihe power plant (WH) and the second power plant of Hu county (HX) in Xi'an City, Shaanxi Province, the Sanhe thermal power plant (SH) and the pithead power plant (KK) in Pingdingshan City, Henan Province

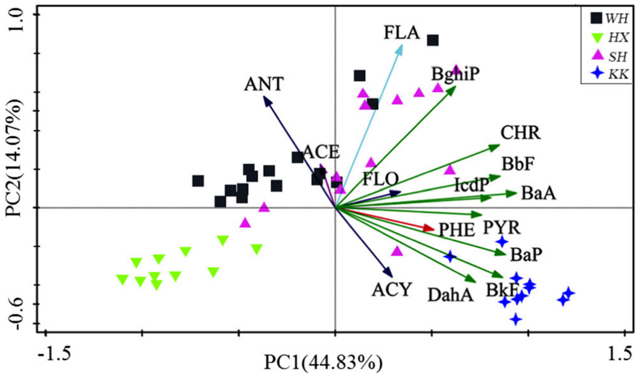

Fig. 3 Score plot for PCA analysis in the soils collected from agricultural fields surrounding coal-fired power plants, including the Weihe power plant (WH) and the second power plant of Hu county (HX) in Xi'an City, Shaanxi Province, the Sanhe thermal power plant (SH) and the pithead power plant (KK) in Pingdingshan City, Henan Province

PYR, BaA, CHR, BbF, BkF, BaP, DahA, and IcdP. PYR, BaA, CHR, and BaP are the component of coal combustion (Simcik and Lioy 1999; Larsen and Baker 2003), while IcdP is typical tracer for gasoline engine emissions (Kavouras et al. 2001). In addition, DahA, BbF, and BkF are associated with traffic emission of diesel vehicle (Khalili et al. 1995). The source of China's electric energy most relies heavily on coal combustion. The large amount of coal consumption in coal-fired power plants makes it the primary contributor of PAHs in the nearby environment. Besides, heavy automobile traffic around power plants for coal transportation is also a major contributor of PAHs pollution. Consequently, PC1 indicated that PAHs were primarily derived from fossil fuel combustion sources in four coal-fired power plants soils. From the distribution of sampling points (Fig. 3), different scores were observed at four sites, suggesting that PAHs in the four sites soils were derived from different sources. PC2 accounted for 14.07% of the total variance and was loaded only with FLA, reflecting a coal combustion sources (Simcik and Lioy 1999). PC3 (13.16% of variance) and PC4 (7.99% of variance) were load with ACE and PHE, representing biomass and coal combustion, respectively.

Accumulation and distribution of PAHs in the roots and aerial tissues of winter wheat

The total concentrations of $\sum_{15}$PAHs in the roots and aerial tissues of winter wheat collected form areas affected by coal combustion located in Shaanxi and Henan Provinces are shown in Fig. 4. The concentrations of $\sum_{15}$PAHs ranged from 208 to 552 μg kg^{-1} for the roots, from 164 to 387 μg kg^{-1} for the straws, from 149 to 355 μg kg^{-1} for the leaves, and from 123 to 577 μg kg^{-1} for the glumes, respectively. There were significant ($p < 0.001$) variations in concentrations of PAHs in the roots and in the aerial tissues among the four sites and the highest concentrations of PAHs in the plant were recorded in KK (Fig. 4), which was consistent with the highest concentrations of PAHs in the corresponding rhizosphere soils (Table 1). PAH concentrations in the roots (208–552 μg kg^{-1}) and straws (164–387 μg kg^{-1}) of winter wheat in the present study were far higher those (root 50.9 μg kg^{-1}, straw 38.9 μg kg^{-1}) from Henan Province, China (Feng et al. 2017), which were consistent with the far higher concentrations of PAHs in the rhizosphere soils (477–933 vs 6.91–72.4 μg kg^{-1}) as previously described.

The distribution of PAHs with different ring numbers in the roots of winter wheat was comparable among WH, HX, SH, and KK (Fig. 5(b)). Regardless of sampling sites, most PAHs detected in the roots were three-ring PAHs (ACE, ACY, FLO, PHE, and ANT), accounting for approximately 49.5–74.0% of the total PAHs (Table S1). Among PAHs detected, PHE was predominant, accounting for 28.4–27.6% of the total PAHs, followed by ACE (12.9–23.1%) (Table S1). Three-ring PAHs in the roots were greater mainly due to their higher solubility and higher concentrations in the corresponding rhizosphere soils (Table 1). Four-ring PAHs (FLA, PYR, BaA, and CHR) accounted for 19.3–33.2% of the total PAHs, and those with five-ring (BbF, BkF, BaP, and DahA) accounted for 6.2–16.2% (Fig. 5(b)). Six-ring PAHs accounted for a small part (0.46–1.4%) of sum PAHs in the roots and were apparently lower than those (5.6–11.9%) in the rhizosphere soils (Fig. 5(a, b)), implying that the ones are more difficult to be absorbed to the roots. Because of their high hydrophobicity, five- to six-ring PAHs are generally assumed to be tightly bound to soil particles, high sorption to organic matter in soil and low desorption capacity and thus weakly bioavailable (Pilon-Smits 2005; Amellal et al. 2006). The concentrations of three-, four-, five-, and six-ring PAHs in the roots significantly ($r = 0.68$–0.96, $p < 0.001$) positive correlated with the corresponding concentrations of PAHs in the rhizosphere soils (Table 2). The present results suggested that PAHs in roots of winter wheat are derived from root-soil uptake, in line with Tao et al. (2009) conducted in the growth chamber.

The distribution of PAHs with different ring numbers in the stems, leaves, and glumes was quite similar to each other but was significantly different from that of the roots and rhizosphere soils (Fig. 5). The distribution of PAHs in the aerial tissues were comparable among WH, SH, and KK, while a significantly ($p < 0.01$) higher percentage of six-ring PAHs was recorded in the stems (7.9%), leaves (9.3%), and glumes (4.5%) of winter wheat from HX than those from WH (0–0.5%), SH (0.4–0.6%), and KK (0.3–0.6%), respectively (Fig. 5). Our previous study also observed that the grains of winter wheat from HX possessed a significantly ($p < 0.01$) higher percentage of six-ring PAHs than those from WH, SH, and KK (Tian et al. 2018). The percentages of three-ring PAHs were much higher in the aerial tissues (72.5–82.7%) than in the roots (49.5–74.0%) and in the rhizosphere soils (36.3–65.7%). Similar with those in the roots, three-ring

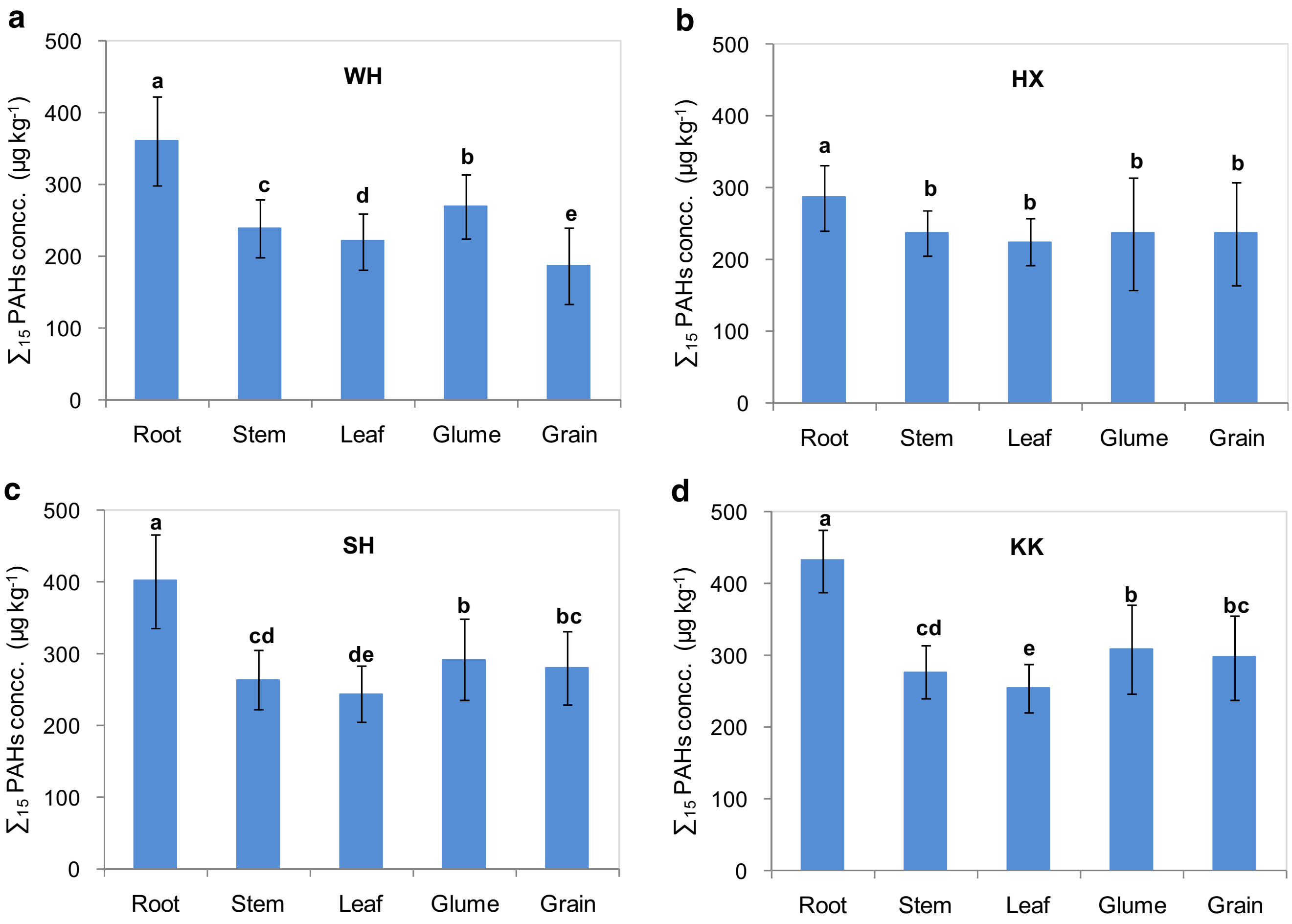

Fig. 4 Concentration of PAHs in root, stem, leaf, glume, and grain of winter wheat from agricultural fields surrounding coal-fired power plants, including the Weihe power plant (WH, $n = 64$) (**a**) and the second power plant of Hu county (HX, $n = 44$) (**b**) in Xi'an City, Shaanxi Province, the Sanhe thermal power plant (SH, $n = 52$) (**c**) and the pithead power plant (KK, $n = 44$) (**d**) in Pingdingshan City, Henan Province. Concentration of PAHs in grain was referred to Tian et al. (2018)

PAHs were dominant in the stems, leaves, and glumes, accounting for approximately 72.5–80.2, 73.1–79.7, and 77.5–82.7% of the total PAHs, respectively (Fig. 5, Table S1). Three-ring PAHs in the aerial tissues were greater mainly due to their higher solubility. Shi et al. (2017) showed that the concentration PAHs in leaves of winter wheat were positively ($p < 0.05$) correlated with the water solubility of the six selected PAHs (PHE, ANT, PYR, BaA, BaP, and BghiP). The concentrations of $\sum_{15}$ PAHs especially three- to four-ring PAHs in the aerial tissues significantly ($r = 0.32$–0.64, $p < 0.001$) positive correlated with the concentrations of PAHs in the corresponding rhizosphere soils (Table 2), suggesting that partial three- to four-ring PAHs in the aerial tissues are derived from root-soil uptake. Gao and Zhu (2004) found that transport of PHE and PYR from roots to shoots was the major pathway of shoot accumulation. However, the percentages of five- to six-ring PAHs were much lower in the aerial tissues (2.2–8.7%; 0–0.75%) than in the roots (6.2–16.2%; 1.1–1.4%) and the rhizosphere soils (11.8–26.1%; 5.6–11.9%), respectively, except those from HX. The concentrations of six-ring PAHs in the aerial tissues significantly ($r = 0.46$–0.58, $p < 0.001$) negative correlated with the corresponding concentrations of PAHs in the rhizosphere soils and significantly ($r = 0.75$–1.00, $p < 0.001$) positive correlated with the concentrations of PAHs in the adjacent tissues (Table 2). These indicated that a proportion of six-ring PAHs in aerial tissues may come from the air-to-leaf pathway, although the quantity contribution of foliar uptake of coal-fired power plants is still not clear.

Bioconcentration and translocation of PAHs in roots and aerial tissues of winter wheat

The RCF was defined as the ratio of the PAH concentrations in roots to those in soil on a dry weight basis (Hulster et al. 1994). The average RCFs for three-, four-, and five to six-ring PAHs were 0.87, 0.61, 0.32, and 0.06, respectively (Fig. 6). Goodin and Webber (1995) also found that roots can absorb PAHs from the soil directly, but PAH concentrations for vegetation are typically less than those for the soil

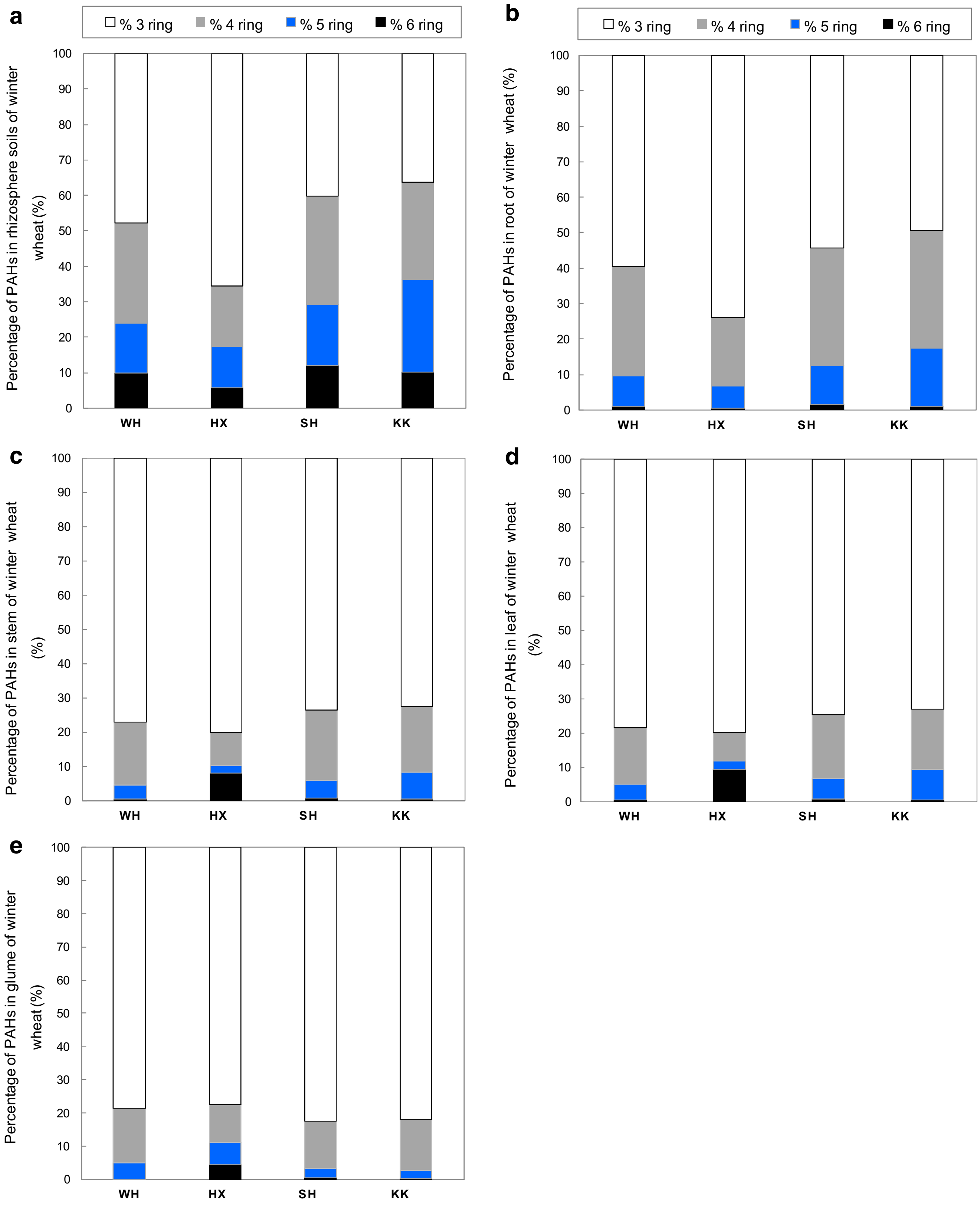

Fig. 5 Percentage distribution profiles of PAHs in soils, stems, leaves, and glumes of winter wheat from agricultural fields surrounding coal-fired power plants, including the Weihe power plant (WH) and the second power plant of Hu county (HX) in Xi'an City, Shaanxi Province, the Sanhe thermal power plant (SH) and the pithead power plant (KK) in Pingdingshan City, Henan Province

Table 2 Pearson correlation coefficients between concentrations of PAHs in root, stem, leaf, glume, grain in winter wheat, and rhizosphere soils ($n = 204$)

	3-ring PAH						4-ring PAH				
	Soil	Root	Stem	Leaf	Glume		Soil	Root	Stem	Leaf	Glume
3-ring PAH						4-ring PAH					
Root	0.68***					Root	0.95***				
Stem	0.66***	0.85***				Stem	0.93***	0.98***			
Leaf	0.67**	0.88**	0.95***			Leaf	0.93***	0.98***	0.99***		
Glume	NS	NS	NS	NS		Glume	0.33***	0.31***	0.29***	0.31***	
Grain[a]	NS	NS	0.18**	0.13*	0.74***	Grain[a]	0.39***	0.32***	0.29***	0.30***	0.38***
	5-ring PAH						6-ring PAH				
	Soil	Root	Stem	Leaf	Glume		Soil	Root	Stem	Leaf	Glume
5-ring PAH						6-ring PAH					
Root	0.96***					Root	0.95***				
Stem	0.96***	0.99***				Stem	−0.58***	−0.53***			
Leaf	0.95***	0.98***	0.99***			Leaf	−0.58***	−0.53***	1.00***		
Glume	− 0.39***	− 0.41***	− 0.41***	− 0.42***		Glume	− 0.46***	− 0.44***	0.76***	0.75***	
Grain[a]	0.12*	NS	NS	NS	0.22**	Grain[a]	− 0.46***	− 0.44***	0.76***	0.76***	1.00***
	ΣPAHs										
	Soil	Root	Stem	Leaf	Glume						
ΣPAHs											
Root	0.90***										
Stem	0.64***	0.81***									
Leaf	0.59***	0.79***	0.96***								
Glume	0.32***	0.29***	0.20**	0.13*							
Grain[a]	0.32***	0.23***	0.27***	0.25***	0.65***						

Significant levels: NS indicates no significance, $*p < 0.05$, $**p < 0.01$, $***p < 0.001$

[a] Tian et al. (2018)

where they grow, with accumulation factors for plants range between 0.001 and 0.4. The three-ring PAHs (ACY, ACE, FLO, and ANT) showed higher RCF values than other PAHs, of which ACE showed the maximum RCF value (Fig. 6). The five- to six-ring PAHs (BbF, BkF, DahA, BghiP, and IcdP) had lower RCF values. The present study suggested that three-ring PAHs had the highest tendency to be taken up by wheat roots whereas five- to six-ring PAHs had the lowest likelihood of being taken up. There were negative significant ($r = 0.879$, $p < 0.01$) relationship between RCF and log K_{ow} (Octanol-Water Partition Coefficient, K_{ow}) of PAHs (Fig. 6). However, Lin et al. (2006) observed that there was a positive linear relationship between log RCF and log K_{ow} for the uptake of NAP, ACY, FLO, PHE, and PYR by tea plants grown in hydroponic solution. These may be mainly due to the difference in growth conditions. In hydroponic culture, PAHs only partitioned between roots and solution and their uptake by roots depended solely on the hydrophobicity of PAHs and root lipids. Under field conditions, not only there is a sorption-desorption equilibrium of PAHs on soil particles but also properties of the organic compounds and soil characteristics could influence root uptake of PAHs.

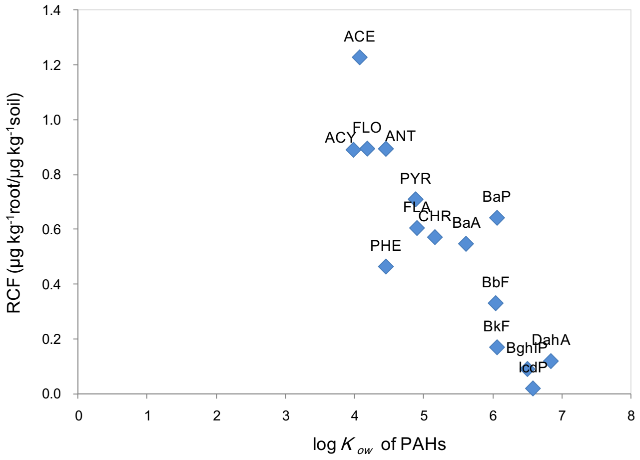

Fig. 6 Relationship between RCF (the ratio of the PAH concentration in roots of winter wheat to that in soil on a dry weight basis) and K_{ow} of PAHs

PAHs were significantly ($p < 0.001$) higher in the roots than in aerial tissues (Fig. 4). There were a decreasing gradient of PAH concentrations from roots, stems, and leaves. Similar with other organic pollutants, PAHs enter into plants mainly from the air through respiration (foliar uptake) and from soil via transpiration (root uptake) (Desalme et al. 2013). PAHs in the aerial tissues of winter wheat are derived from two pathways: uptake from the atmosphere and translocation from roots with the transpiration stream. For plants grown in PAH-contaminated soils, main PAHs (53.6–72.6%) in the shoots of winter wheat were translocated from the roots (Tao et al. 2009). Acropetal translocation depends primarily on the transpiration stream flow of the plant (Verkleij et al. 2009). The gradient of transpiration pull from stems and leaves maybe resulted in decreasing gradient of PAH concentrations from roots, stems, and leaves and the underlying mechanisms need further investigate.

Among those plant tissues exposed to air, elevated PAH concentrations occur in the glumes and grains (Fig. 4). Grain is the main nutritional organs of winter wheat and more than 80% mineral nutrition and carbohydrates of the whole plant will be transferred to the organ during ripening period. Along with mineral nutrition and carbohydrates, it was assumed that PAHs retained in stems or leaves were also transferred to glumes and grains. The concentrations of $\sum_{15}$ PAHs in the glumes and grains significantly correlated with the corresponding concentrations of PAHs in the leaves ($r = 0.13$, $p < 0.05$) and glumes ($r = 0.65$, $p < 0.001$) (Table 2), suggesting that partial PAHs in the grains are translocated from leaves and glumes, respectively. PAHs were apparently higher in the glumes than in the grains (Fig. 4). The grains are protected by glumes and have significantly less of a chance of direct contact with the environment than glumes. Similarly, Tao et al. (2006) also found that PAH concentrations for grains were much lower than those for other tissues of the rice plants and were more than one order of magnitude lower than those reported for the roots.

Conclusion

The rhizosphere soils of winter wheat were seriously contaminated with PAHs in the range of 486 to 1117 $\mu g\ kg^{-1}$, which collected from areas affected by coal combustion located in Shaanxi and Henan Provinces. The main sources of the PAHs in agricultural soils were from combustion of biomass, coal and petroleum, and petroleum. There were significant ($p < 0.001$) variations in concentrations of PAHs in the roots and in the aerial tissues among the four sites and the highest concentrations of PAHs in the plant were recorded in KK. Regardless of sampling sites, most PAHs detected in the roots were three-ring PAHs (ACE, ACY, FLO, PHE, and ANT), accounting for approximately 49.5–74.0% of the total PAHs. PAHs were significantly ($p < 0.001$) higher in the roots than in aerial tissues. The distribution of PAHs with different ring numbers in the stems, leaves, and glumes was quite similar to each other but was significantly different from that of the roots and rhizosphere soils. The present indicated that a proportion of six-ring PAHs in aerial tissues may come from the air-to-leaf pathway.

Funding information This study was supported by the National Natural Science Foundation of China (41571456) and Program for Science & Technology Innovation Talents in Universities of Henan Province (14HASTIT048).

References

Amellal S, Boivin A, Ganier CP, Schiavon M (2006) High sorption of phenanthrene in agricultural soils. Agron Sustain Dev 26:99–106

China Energy Statistical Yearbook (2015) China Statistics Press, Beijing, p 56

China Statistical Yearbook (2017) China Statistics Press, Beijing, p 381–410

Desalme D, Binet P, Chiapusio G (2013) Challenges in tracing the fate and effects of atmospheric polycyclic aromatic hydrocarbon deposition in vascular plants. Environ Sci Technol 47:3967–3981

Dimashki M, Lim LH, Harrison RM, Harrad S (2001) Temporal trends, temperature dependence, and relative reactivity of atmospheric polycyclic aromatic hydrocarbons. Environ Sci Technol 35:2264–2267

Duan YH, Shen GF, Tao S, Hong JP, Chen YC, Xue M, Li TC, Su S, Shen HZ, Fu XF (2015) Characteristics of polycyclic aromatic hydrocarbons in agricultural soils at a typical coke production base in Shanxi, China. Chemosphere 127:64–69

Feng JL, Li XY, Zhao JH, Sun JH (2017) Distribution, transfer, and health risks of polycyclic aromatic hydrocarbons (PAHs) in soil-wheat systems of Henan Province, a typical agriculture province of China. Environ Sci Pollut Res Int 24:18195–18203

Gao YZ, Zhu LZ (2004) Plant uptake, accumulation and translocation of phenanthrene and pyrene in soils. Chemosphere 55:1169–1178

Golobocanin DD, Skrbic BD, Miljevic NR (2004) Principal component analysis for soil contamination with PAHs. Chemom Intell Lab Syst 72:219–223

Goodin JD, Webber MD (1995) Persistence and fate of anthracene and benzo(a)pyrene in municipal sludge treated soil. J Environ Qual 24:271–278

Hulster A, Muller JF, Marschner H (1994) Soil-plant transfer polychlorinated dibenzo-p-dioxins and dibenzofurans to vegetables of the cucumber family (Cucurbitaceae). Environ Sci Technol 28:1110–1115

Katsoyiannis A, Terzi E, Cai QY (2007) On the use of PAH molecular diagnostic ratios in sewage sludge for the understanding of the PAH sources. Is this use appropriate? Chemosphere 69:1337–1339

Kavouras IG, Koutrakis P, Tsapakis M, Lagoudaki E, Stephanou EG, Von Baer D, Oyola P (2001) Source apportionment of urban particulate aliphatic and polynuclear aromatic hydrocarbons (PAHs) using multivariate methods. Environ Sci Technol 35:2288–2294

Khalili NR, Scheff PA, Holsen TM (1995) PAH source fingerprints for coke ovens, diesel and, gasoline engines, highway tunnels, and wood combustion emissions. Atmos Environ 29:533–542

Larsen PK, Baker JE (2003) Source apportionment of polycyclic aromatic hydrocarbons in the urban atmosphere: a comparison of three methods. Environ Sci Technol 37:1873–1881

Li XR (2007) Spatial distribution pattern of emission, dispersion and exposure of polycyclic aromatic hydrocarbons in Tianjin, China. Thesis of PhD, Beijing, China: Peking University, p 152

Lin DH, Zhu LZ, He W, Tu YT (2006) Tea plant uptake and translocation of polycyclic aromatic hydrocarbons from water and around air. J Agric Food Chem 54:3658–3662

Liu SZ, Tao S, Liu WX, Liu YN, Dou H, Zhao JY, Wang LG, Wang JF, Tian ZF, Gao Y (2007) Atmospheric polycyclic aromatic hydrocarbons in north China: a wintertime study. Environ Sci Technol 41: 8256–8261

Liu WJ, Wang YL, Chen YC, Tao S, Liu WX (2017) Polycyclic aromatic hydrocarbons in ambient air, surface soil and wheat grain near a large steel-smelting manufacturer in northern China. J Environ Sci 57:93–103

Maliszewska-Kordybach B (1996) Polycyclic aromatic hydrocarbons in agricultural soils in Poland: preliminary proposals for criteria to evaluate the level of soil contamination. Appl Geochem 11:121–127

Martí-Cid R, Llobet JM, Castell V, Domingo JL (2008) Evolution of the dietary exposure to polycyclic aromatic hydrocarbons in Catalonia, Spain. Food Chem Toxicol 46:3163–3171

Nisbet ICT, LaGoy PK (1992) Toxic equivalency factors (TEFs) for polycyclic aromatic hydrocarbons (PAHs). Regul Toxicol Pharmacol 16:290–300

Nwaichi EO, Wegwu MO, Nwosu UL (2014) Distribution of selected carcinogenic hydrocarbon and heavy metals in an oil-polluted agriculture zone. Environ Monit Assess 186:8697–8706

Phillips DH (1999) Polycyclic aromatic hydrocarbons in the diet. Mutat Res 443:139–147

Pies C, Hoffmann B, Petrowsky J, Yang Y, Ternes TA, Hofmann T (2008) Characterization and source identification of polycyclic aromatic hydrocarbons (PAHs) in river bank soils. Chemosphere 72:1594–1601

Pilon-Smits E (2005) Phytoremediation. Annu Rev Plant Biol 56:15–39

Shen HZ, Huang Y, Wang R, Zhu D, Li W, Shen GF, Wang B, Zhang YY, Chen YC, Lu Y, Chen H, Li TC, Sun K, Li BG, Liu WX, Liu JF, Tao S (2013) Global atmospheric emissions of polycyclic aromatic hydrocarbons from 1960 to 2008 and future predictions. Environ Sci Technol 47:6415–6424

Shi TR, Tian K, Bao HY, Liu XP, Wu FY (2017) Variation in foliar uptake of polycyclic aromatic hydrocarbons in six varieties of winter wheat. Environ Sci Pollut Res Int 24:27215–27224

Simcik M, Lioy PS (1999) Source apportionment and sourcesink relationships of PAHs in the coastal atmosphere of Chicago and Lake Michigan. Atmos Environ 33:5071–5079

Sun P, Blanchard P, Brice KA, Hites RA (2006) Trends in polycyclic aromatic hydrocarbon concentrations in the Great Lakes atmosphere. Environ Sci Technol 40:6221–6227

Tao S, Jiao XC, Chen SH, Liu WX, Coveney RM, Zhu LZ, Luo YM (2006) Accumulation and distribution of polycyclic aromatic hydrocarbons in rice (*Oryza sativa*). Environ Pollut 140:406–415

Tao YQ, Zhang SZ, Zhu YG, Christie P (2009) Uptake and acropetal translocation of polycyclic aromatic hydrocarbons by wheat (*Triticum aestivum* L.) grown in field-contaminated soil. Environ Sci Technol 43:3556–3560

The Ministry of Environmental Protection (2014) The Ministry of Land and Resources Report on the national soil contamination survey. http://www.mep.gov.cn/gkml/hbb/qt/201404/t20140417_270670.htm

Tian K, Bao HY, Zhang XC, Shi TR, Liu XP, Wu FY (2018) Residuals, bioaccessibility and health risk assessment of PAHs in winter wheat grains from areas influenced by coal combustion in China. Sci Total Environ 618:777–784

USEPA (1996) Method 3540C: Soxhlet extraction. US Environmental Protection Agency, Washington, DC

Verkleij JAC, Golan-Goldhirsh A, Antosiewisz DM, Schwitzguebel JP, Schroder P (2009) Dualities in plant tolerance to pollutants and their uptake and translocation to the upper plant parts. Environ Exp Bot 67:10–22

Wang J, Zhang XF, Ling WT, Liu R, Liu J, Kang FX, Gao YZ (2017) Contamination and health risk assessment of PAHs in soils and crops in industrial areas of the Yangtze River Delta region, China. Chemosphere 168:976–987

Wild SR, Jones KC (1995) Polynuclear aromatic hydrocarbons in the United Kingdom environment: a preliminary source in inventory and budget. Environ Pollut 88:91–108

Xia ZH, Duan XL, Qiu WX, Liu D, Wang B, Tao S, Jiang QJ, Lu B, Song YX, Hu XX (2010) Health risk assessment on dietary exposure to polycyclic aromatic hydrocarbons (PAHs) in Taiyuan, China. Sci Total Environ 408:5331–5337

Yang B, Xue ND, Zhou LL, Li FS, Cong X, Han BL, Li HY, Yan YZ, Liu B (2012) Risk assessment and sources of polycyclic aromatic hydrocarbons in agricultural soils of Huanghuai Plain, China. Ecotoxicol Environ Saf 84:304–310

Yunker MB, Macdonald RW, Vingarzan R, Mitchell RH, Goyette D, Sylvestre S (2002) PAHs in the Fraser River basin: a critical appraisal of PAH ratios as indicators of PAH source and composition. Org Geochem 33:489–515

Zhan XH, Ma HL, Zhou LX, Liang JR, Jiang TH, Xu GH (2010) Accumulation of phenanthrene by roots of intact wheat (*Triticum acstivnm* L.) seedlings: passive or active uptake? BMC Plant Biol 10:52

Zhan XH, Zhang XB, Yin XM, Ma HL, Liang JR, Zhou LX, Jiang TH, Xu GH (2012) H+/phenanthrene symporter and aquaglyceroporin are implicated in phenanthrene uptake by wheat (*Triticum aestivum* L.) roots. J Environ Qual 41:188–196

Zhan XH, Yi X, Yue L, Fan XR, Xu GH, Xing BS (2015) Cytoplasmic pH-stat during phenanthrene uptake by wheat roots: a mechanistic consideration. Environ Sci Technol 49:6037–6044

Zhao L, Hou H, Shangguan YX, Cheng B, Xu YF, Zhao RF, Zhang YG, Hua XZ, Huo XL, Zhao XF (2014) Occurrence, sources, and potential human health risks of polycyclic aromatic hydrocarbons in agricultural soils of the coal production area surrounding Xinzhou, China. Ecotoxicol Environ Saf 108:120–128

Environ Sci Pollut Res (2017) 24:27215–27224
DOI 10.1007/s11356-017-0312-8

Variation in foliar uptake of polycyclic aromatic hydrocarbons in six varieties of winter wheat

Taoran Shi[1,2] · **Kai Tian**[1,2] · **Huanyu Bao**[1,2] · **Xueping Liu**[3] · **Fuyong Wu**[1,2]

Received: 19 July 2017 / Accepted: 21 September 2017 / Published online: 30 September 2017

Abstract To investigate intraspecific variations of foliar uptake of polycyclic aromatic hydrocarbons (PAHs) of winter wheat (*Triticum aestivum* L.), leaves of six varieties including Changwu 521 (CW), Hedong TX-006 (HD), Jiaomai 266 (JM), Xiaoyan 22 (XY), Yunong 949 (YN), and Zhongmai 175 (ZM) were exposed to three levels of (0, 0.25, and 1.5 mg L^{-1}) mixture of six selected PAHs (phenanthrene, anthracene, pyrene, benz[a]anthracene, benzo[a]pyrene, and benzo[g,h,i]perylene). After 10 consecutive days of application, all the six selected PAHs (Σ_6 PAHs) were determined in the leaves of the six varieties of the winter wheat. There were apparent intraspecific differences in foliar uptake of PAHs in the winter wheat. The highest concentrations of Σ_6 PAHs in the leaves of YN variety (64.6 mg kg^{-1}) were approximate two times of the lowest concentrations in the leaves of HD variety (29.6 mg kg^{-1}). Both individual PAHs and Σ_6 PAHs in the cuticular waxes were significantly ($p < 0.01$) higher than those in leaves and far higher than those in roots, indicating that the cuticular waxes could play significant role in foliar uptake of PAHs. The present results also showed that the concentrations PAHs in leaves were positively ($p < 0.05$) correlated with the water solubility of the six selected PAHs. In addition, the present study suggested that there was basipetal translocation of PAHs in the winter wheat after foliar application of PAHs, although the mechanism was yet to be further studied.

Keywords PAHs · Foliar uptake · Intraspecific variation · Basipetal translocation

Introduction

Polycyclic aromatic hydrocarbons (PAHs) are a large class of mutagenic, carcinogenic, and teratogenic organic pollutants, which mainly originate from incomplete combustion of biomass or fossil fuels (Wild and Jones 1995). Mainly due to being ubiquitous in environments and heavily toxic to human, PAHs have been attracted considerable attentions for years. For non-smokers and non-occupationally exposed populations, dietary intake is generally the main (> 70%) way of human exposure to PAHs (Phillips 1999; Ma and Harrad 2015), with cereals and vegetables showing the greatest contribution. Therefore, understanding plant uptake and accumulation of PAHs from the environment has significant implications for human risk assessments.

Similar with other organic pollutants, PAHs may enter into plants via two pathways, one from the atmosphere by gas-phase and particle-phase deposition onto the waxy cuticle of the leaf or by uptake through the stomata (foliar uptake), the other from contaminated soil or water to the root and translocating in the vegetation by the xylem (root uptake) (Desalme et al. 2013). Foliar uptake is assumed to be the major contributing pathway for plant accumulation of PAHs when plants grow in non-polluted soils (Kipopoulou et al. 1999; Lehndorff and Schwark 2004), which mainly depends on atmospheric concentrations of PAHs, environmental

Responsible editor: Philippe Garrigues

✉ Fuyong Wu
wfy09@163.com

[1] College of Natural Resources and Environment, Northwest A&F University, Yangling 712100, Shaanxi, People's Republic of China

[2] Key Laboratory of Plant Nutrition and the Agri-environment in Northwest China, Ministry of Agriculture, Yangling 712100, Shaanxi, People's Republic of China

[3] School of Municipal and Environment Engineering, Henan University of Urban Construction, Pingdingshan 467036, People's Republic of China

variables and leaf properties (Desalme et al. 2013). Based on field investigation, Tao et al. (2006) found that surface area appeared to be an important factor controlling PAHs levels in various exposed tissues of rice. Plant roots can take up organic contaminants via passive diffusive partitioning and/or active process, depending on the plant species and the properties of the organic contaminant, such as molecular structure, solubility, and Henry's law constant (Collins et al. 2006). Zhan et al. (2013a, b) indicated that there was significantly positive correlation between root uptake of phenanthrene and specific surface area and lipid of crop roots, respectively. Although there have been some significant advances in our understanding of the processes of plant uptake of PAHs in recent years, mechanisms for PAHs uptake by crop still remain unclear.

Wheat is a major component of diet for most of the Chinese population with a total cultivated area of 24.1 million ha in 2011 (China statistical yearbook 2016). Although PAH levels in cereals are often low, the large amounts consumed make grains a significant source of PAHs for human beings. Xia et al. (2010) found that citizens in Taiyuan of China possess high potential carcinogenic risk of dietary intake of PAHs, of which wheat gave the greatest contribution (48.30–53.47%). PAHs can enter into the winter wheat via foliar uptake and soil-root uptake (Tao et al. 2009). Recently, some researchers have investigated PAHs uptake by roots of winter wheat (Zhan et al. 2010, 2013a, b; Yin et al. 2014). Wheat roots may take up phenanthrene via active process (Zhan et al. 2010). Tao et al. (2009) indicated that PAHs uptake by roots of winter wheat could be translocated to shoot and that the acropetal translocation of PAHs depended on their chemical properties. However, the mechanism of foliar uptake of PAHs by winter wheat is little understood.

The aim of the present study was to: (1) investigate variations of foliar uptake of PAHs of six varieties of winter wheat, phenanthrene (PHE), anthracene (ANT), pyrene (PYR), benz[a]anthracene (BaA), benzo[a]pyrene (BaP), and benzo[g,h,i]perylene (BghiP) as representatives and; (2) assess PAHs translocation and distribution in different parts of wheat seedlings via foliar uptake.

Materials and methods

Precultivation of winter wheat seedlings

Seeds of six varieties of winter wheat (*Triticum aestivum* L.) were obtained from the Shaanxi Long Feng seed company of China, including Changwu 521 (CW), Hedong TX-006 (HD), Jiaomai 266 (JM), Xiaoyan 22 (XY), Yunong 949 (YN), and Zhongmai 175 (ZM). The seeds were surface-sterilized in 3% H_2O_2 for 15 min, rinsed and germinated in a cultivation dish by placing them on moist filter paper in the dark. Fifteen to eighteen pre-germinated seeds were sown in a plastic pot with sands (< 2 mm) and thinned to 10 seedlings. The seedlings were fixed through a drilled hole in an aluminum foil. For air-sealed, the vaseline was smeared over the hole. The experimental setup was illustrated in Fig. 1. The seedlings were watered daily and fertilized weekly with full-strength Hoagland's nutrient solution (Hoagland and Arnon 1938): 1.0 mM KH_2PO_4, 5.0 mM KNO_3, 5.0 mM $Ca(NO_3)_2·4H_2O$, 2.0 mM $MgSO_4·7H_2O$, 45 μM H_3BO_3, 9.0 μM $MnCl_2·4H_2O$, 0.75 μM $ZnSO_4·7H_2O$, 0.35 μM $CuSO_4·5H_2O$, 0.15 μM $H_2MoO_4·H_2O$, 20 μM Fe-EDTA. The pH of the nutrient solution was adjusted to 5.5 using dilute HCl or NaOH. Plant culture was performed in a greenhouse with temperature control (28/23 °C, day/night). In addition to natural sunlight, a 12-h photon flux density of 380 $\mu mol\ m^{-2}\ s^{-1}$ was supplied via an assembly of cool-white fluorescent lamps.

Foliar uptake of PAHs

Six kinds of PAHs (PHE, ANT, PYR, BaA, BaP, and BghiP) were obtained from Aldrich Chemical with a purity of > 98%. To prepare the application solution of mixture of the six kinds of PAHs, 0.25 or 1.5 mg of each compound was dissolved in 1.0 mL acetone and filled up with distilled water to 1000 mL. At three-leaf stage of the seedlings, 100 μL of the corresponding solution per seedling was applied to the leaves with a micropipette at 9:00 a.m. The solutions were applied on both leaf side before the drip point was reached. The care was taken for abaxial and adaxial placement not to overlap on the leaf. Control seedlings were applied with the same amount of distilled water containing 0.1% acetone. The moisture content of the substrate was maintained at approximately 70% of gravimetric water capacity and fertilized weekly with full-strength Hoagland's nutrient solution. After 10 days, phloem sap was collected with an EDTA-facilitated exudation method (Palmer et al. 2014). All the plants from each treatment were sampled, rinsed thoroughly with deionized water, and separated into leaves, stems, and roots. Partial leaves were reserved for determination of cuticular wax. The rest of the leaves, stems, and

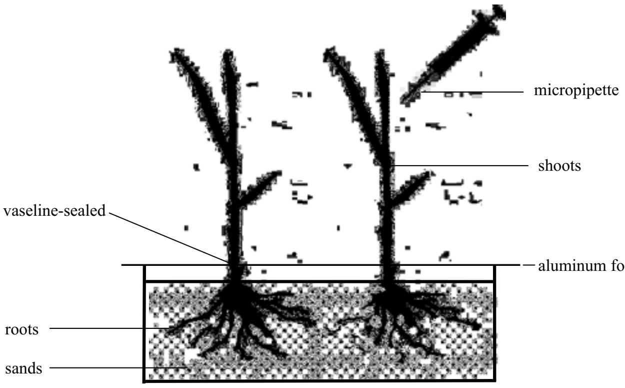

Fig. 1 Schematic diagram of simulation device for winter wheat seedlings exposure to PAHs

roots were homogenized to powder with liquid nitrogen, respectively. The frozen powder was stored at − 80 °C for PAHs analysis.

Determination of cuticular wax

Fresh leaves of winter wheat were extracted with dichloromethane (DCM) (150 mL) and mechanically shaken at 100 r min^{-1} for 2 min. The solution was filtered through a 0.45-μm Millipore membrane, followed by a second extraction with DCM (50 mL) for interception of leaves for 2 min. Two parts of extracts were collected, mixed, and diluted to 200 mL. Partial extracts (50 mL) were condensed in a rotary evaporator to approximately 2 mL, subsequently dried under a stream of nitrogen, weighed as cuticular wax. The remained 150 mL extracts were condensed to approximately 2 mL and exchanged with methanol to a final volume of 2.0 mL for determining PAHs concentrations in the cuticular wax.

PAHs analyses

The plant samples were Soxhlet extracted for 16–18 h with 120 mL of acetone and DCM mixture (1:3, *v*/*v*) (USEPA 1996a). The concentrated extracts were cleaned up using a florisil column (15 cm silica gel, and 1.0 cm anhydrous sodium sulfate from bottom up, pre-eluted with 20 mL n-hexane) with 70 mL hexane/DCM mixture (1:1, *v*/*v*) as elution solvent (USEPA 1996b). The silica gel was baked at 450 °C for 6 h, activated at 300 °C for 12 h, and deactivated with deionized water (3%, *w*/*w*) prior to use. The anhydrous sodium sulfate was baked at 450 °C for 8 h. The eluants were then evaporated and exchanged with methanol to a final volume of 2.0 mL. The detection method of PAHs was described in our previous study (Tian et al. 2017). Briefly, the extracts were analyzed using HPLC-FLD (Shimadzu, LC-20A) equipped with an ultraviolet detector (PF-20A) and a fluorescence detector (SPD-20A). The HPLC system was fitted with a PAH-specific reverse column (Φ4.6 × 150-mm Intersil ODS-P column, 5 μm, Shimadzu, Kyoto, Japan) and a mixture of methanol and ultrapure water as the mobile phase. The six kinds of PAHs (PHE, ANT, PYR, BaA, BaP, and BghiP) were measured in the present study.

QA/QC

QA/QC was conducted by performing method blanks, standard reference material recoveries, standard spiked recoveries, and HPLC detection limits. The limit of detection (LOD) using the present method was determined as the concentrations of analytes in a sample that gave rise to a peak with a signal-to-noise ratio (S/N) of 3, which ranged from 0.08 to1.51 μg kg^{-1}. For each batch of 12 samples, a method blank (solvent), a spiked blank (standards spiked into solvent), a sample duplicate, and a standard reference material (NIST SRM 2977) sample were processed. PAHs were identified on the basis of retention times relative to five deuterated internal standards (naphthalene-d_8, acenaphthene-d_{10}, phenanthrene-d_{10}, chrysene-d_{12}, and perylene-d_{12}). The variation coefficients of PAH concentrations between duplicate samples were < 10%. The PAH levels of digestion blank were less than the LOD. Recovery of PAHs was investigated by spiking plant samples with standards at fortification levels of 40 μg kg^{-1}. The recoveries of individual PAHs ranged from 77.9% for BghiP to 103% for PHE.

Data analyses

The differences in plant biomass and PAHs concentrations among varieties of winter wheat were assessed using Fisher's protected least significant difference after ANOVA. All statistical procedures were carried out using SAS 8.1 software. Unless indicated otherwise, all treatment means were tested for significant difference at $p < 0.05$.

Results and discussion

Foliar uptake of PAHs in six varieties of winter wheat

In the present study, applying mixed PAHs solutions onto the leaf surface of winter wheat simulated the possible mechanisms of foliar uptake, which atmospheric deposition followed by penetration via cuticular waxes. After 10 consecutive days of exposure, all the six selected PAHs (Σ_6 PAHs) were recorded in the leaves of the six varieties of winter wheat (Table 1). With increasing concentrations of the applying solutions, there was apparent increasing concentrations of PAHs in the leaves. Lin et al. (2007) also found that above-ground parts of maize directly accumulate PAHs from air in proportion to exposure levels. Under 1.5 mg L^{-1} of PAHs treatment, Σ_6 PAHs in the leaves were significantly ($p < 0.001$) different among the six varieties. The highest concentrations of Σ_6 PAHs in the leaves of YN variety (64.6 mg kg^{-1}) were approximate two times of the lowest concentrations in the leaves of HD variety (29.6 mg kg^{-1}), indicating that there were apparent intraspecific differences in foliar uptake of PAHs in the wheat winter. Filed investigations also showed that there were highly variable in PAH concentrations of plant shoots among plant species (Howsam et al. 2000; Ratola et al. 2012). Besides the physicochemical properties of the compound and environmental conditions, foliar uptake of organic contaminants is determined by the plant properties (Bakker et al. 1999; Dias et al. 2016). Bakker et al. (1999) indicated that plant

Table 1 Concentrations of PAHs in leaves of six varieties of winter wheat including Changwu 521 (CW), Hedong TX-006 (HD), Jiaomai 266 (JM), Xiaoyan 22 (XY), Yunong 949 (YN), and Zhongmai 175 (ZM) under applying different level of mixed PAHs solutions onto the leaf surface for 10 days (mean±SD, $n = 3$)

Applying level (mg L^{-1})	Wheat variety	PHE (mg kg^{-1})	ANT (mg kg^{-1})	PYR (mg kg^{-1})	BaA (mg kg^{-1})	BaP (mg kg^{-1})	BghiP (mg kg^{-1})	Σ_6 PAHs (mg kg^{-1})
0	CW	1.49 ± 0.75 ab	1.14 ± 0.48 a	nd	0.21 ± 0.002 a	nd	nd	2.85 ± 0.61 a
	HD	0.28 ± 0.10 bc	nd	nd	0.23 ± 0.012 a	nd	nd	0.51 ± 0.11 b
	JM	0.25 ± 0.28 bc	0.35 ± 0.02 c	nd	0.20 ± 0.002 a	nd	nd	0.80 ± 0.26 b
	XY	0.43 ± 0.39 bc	0.65 ± 0.04 bc	nd	0.20 ± 0.001 a	nd	nd	1.28 ± 0.42 b
	YN	0.10 ± 0.08 c	0.74 ± 0.17 b	nd	0.20 ± 0.001 a	nd	nd	1.05 ± 0.11 b
	ZM	2.02 ± 1.57 a	0.82 ± 0.12 ab	nd	0.29 ± 0.118 a	nd	nd	3.12 ± 1.51 a
0.25	CW	18.9 ± 7.79 b	1.67 ± 0.12 ab	2.00 ± 0.28 a	0.75 ± 0.09 a	0.56 ± 0.02 a	0.40 ± 0.04 a	24.3 ± 8.28 ab
	HD	19.2 ± 12.4 b	1.91 ± 0.80 a	1.67 ± 0.50 abc	0.72 ± 0.06 a	0.51 ± 0.06 a	0.37 ± 0.12 a	24.4 ± 13.9 ab
	JM	25.1 ± 12.8 ab	1.20 ± 0.10 b	1.34 ± 0.40 bc	0.58 ± 0.07 a	0.45 ± 0.03 a	0.29 ± 0.02 a	28.9 ± 13.3 ab
	XY	9.52 ± 2.34 b	1.54 ± 0.26 ab	1.26 ± 0.11 c	0.75 ± 0.11 a	0.56 ± 0.14 a	0.47 ± 0.25 a	14.1 ± 2.77 b
	YN	35.6 ± 3.26 a	1.42 ± 0.32 ab	1.91 ± 0.43 ab	0.72 ± 0.01 a	0.48 ± 0.06 a	0.32 ± 0.08 a	40.5 ± 3.27 a
	ZM	20.9 ± 9.32 ab	1.43 ± 0.24 ab	1.73 ± 0.10 abc	0.69 ± 0.05 a	0.53 ± 0.05 a	0.35 ± 0.05 a	25.6 ± 9.10 ab
1.5	CW	22.6 ± 2.26 c	2.48 ± 0.28 ab	2.52 ± 0.09 a	0.79 ± 0.11 a	1.23 ± 0.09 b	0.72 ± 0.06 b	30.3 ± 2.24 c
	HD	22.2 ± 0.99 c	2.16 ± 0.26 b	2.60 ± 0.15 a	0.70 ± 0.03 a	1.17 ± 0.13 b	0.80 ± 0.12 b	29.6 ± 1.36 c
	JM	24.6 ± 4.79 c	2.56 ± 0.18 ab	1.67 ± 0.13 c	0.78 ± 0.14 a	1.15 ± 0.07 b	0.87 ± 0.07 b	31.7 ± 4.65 c
	XY	24.9 ± 0.76 c	4.03 ± 2.18 a	2.15 ± 0.20 b	0.76 ± 0.03 a	1.21 ± 0.06 b	1.07 ± 0.10 a	34.1 ± 3.19 c
	YN	56.3 ± 7.85 a	2.37 ± 0.08 b	2.49 ± 0.06 a	0.79 ± 0.12 a	1.45 ± 0.14 a	1.16 ± 0.18 a	64.6 ± 7.51 a
	ZM	35.5 ± 1.66 b	2.29 ± 0.17 b	1.54 ± 0.15 c	0.72 ± 0.04 a	1.13 ± 0.08 b	0.74 ± 0.11 b	42.0 ± 1.44 b

Different letters within the same row indicating significant difference among different varieties of winter wheat at the level of $p < 0.05$

architecture, leaf surface area, amount of leaf hairs played significant roles in determining the partitioning of PAHs between plants and the atmosphere. Leaf surfaces, leaf overlap, leaf area, wax cuticle, surface roughness, the number and distribution of stomata, leaf hairs, and water repellence varied greatly among plant species (Neinhuis and Barthlott 1997; Barthlott and Neinhuis 1997). Jouraeva et al. (2002) suggested that leaves with higher specific leaf area had a greater ability to accumulate PAHs. The growth conditions of wheat varieties were

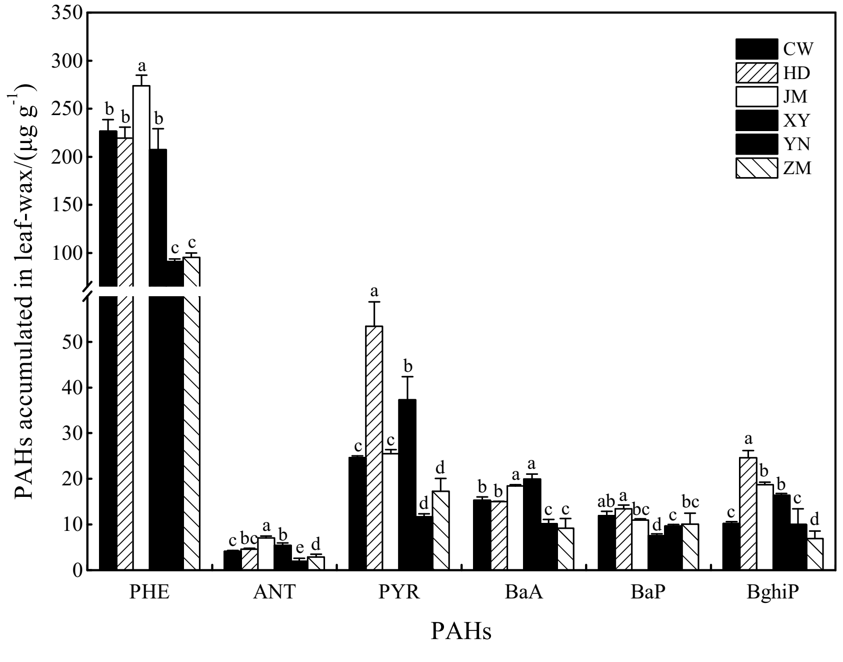

Fig. 2 PAHs in leaf wax of six varieties (CW, HD, JM, XY, YN, and ZM) of winter wheat under applying mixed PAHs solutions (0.25 mg L^{-1}) onto the leaf surface for 10 days. Bars marked with different letters in the same soils treatment are significantly different according to least significant difference (LSD) test ($p < 0.05$) (mean±SE, $n = 3$)

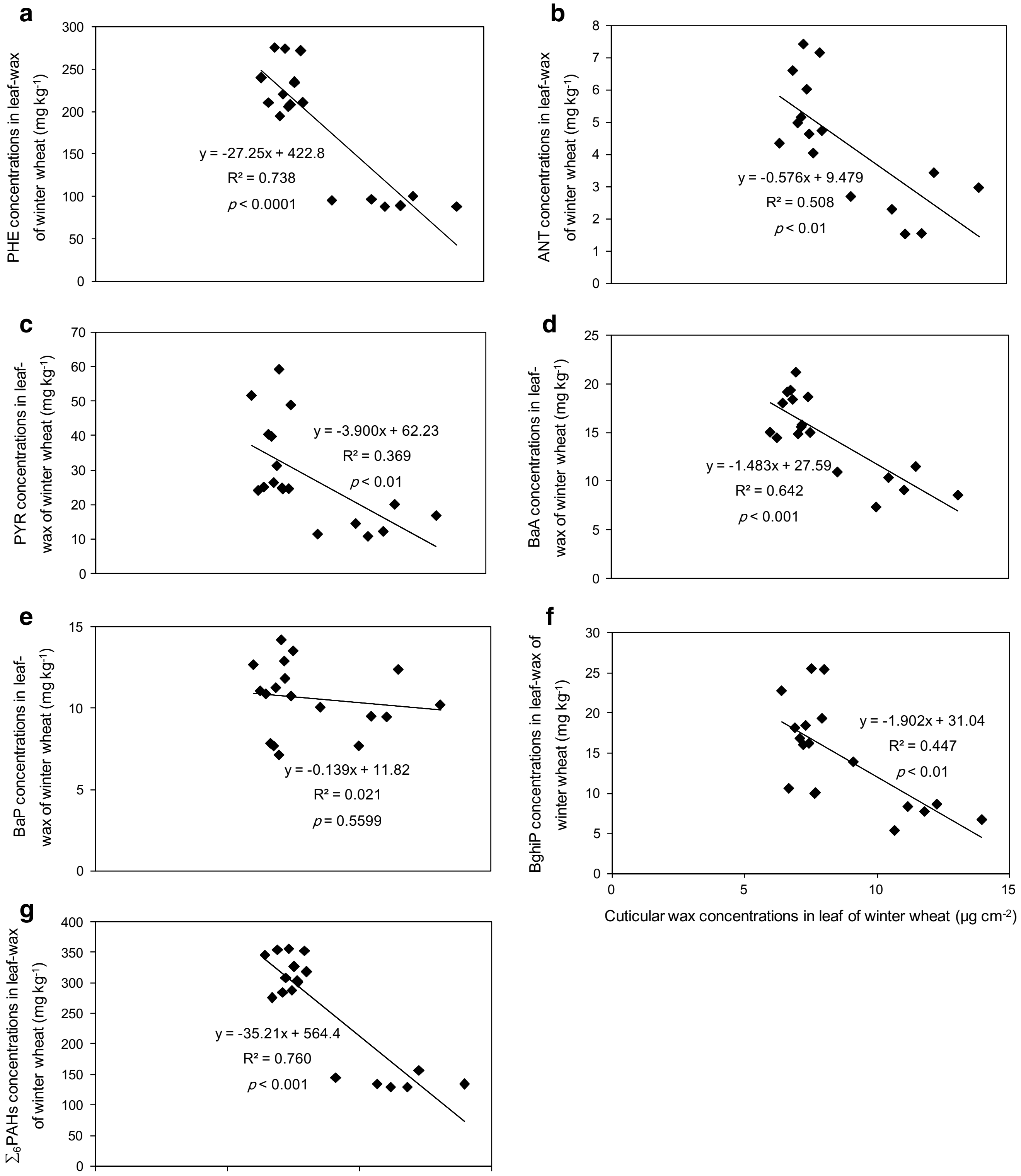

Fig. 3 Relationship between PAHs concentrations in leaf wax and cuticular wax concentrations in leaves of six varieties (CW, HD, JM, XY, YN, and ZM) of winter wheat under applying mixed PAHs solutions (0.25 mg L^{-1}) onto the leaf surface for 10 days

identical in the present study. Thus, the variation of foliar uptake of Σ_6 PAHs among the six varieties of winter wheat would come from disparity of leaf properties and detailed mechanisms need further research.

Table 2 Concentrations of PAHs in roots of six varieties of winter wheat including Changwu 521 (CW), Hedong TX-006 (HD), Jiaomai266 (JM), Xiaoyan 22 (XY), Yunong 949 (YN), and Zhongmai 175 (ZM) under applying different level of mixed PAHs solutions onto the leaf surface for 10 days (mean±SD, $n = 3$)

Applying level (mg L^{-1})	Wheat variety	PHE (mg kg^{-1})	ANT (mg kg^{-1})	PYR (mg kg^{-1})	BaA (mg kg^{-1})	BaP (mg kg^{-1})	BghiP (mg kg^{-1})	Σ_6 PAHs (mg kg^{-1})
0	CW	nd	nd	nd	nd	nd	nd	nd
	HD	nd	nd	nd	nd	nd	nd	nd
	JM	nd	nd	nd	nd	nd	nd	nd
	XY	nd	nd	nd	nd	nd	nd	nd
	YN	nd	nd	nd	nd	nd	nd	nd
	ZM	nd	nd	nd	nd	nd	nd	nd
0.25	CW	1.12 ± 0.17 b	0.18 ± 0.07 b	1.40 ± 0.51 c	0.74 ± 0.10 b	0.37 ± 0.06 b	0.42 ± 0.04 b	4.23 ± 0.58 cd
	HD	1.40 ± 0.99 b	0.34 ± 0.09 ab	2.59 ± 1.06 b	0.66 ± 0.33 b	0.40 ± 0.14 b	0.45 ± 0.12 b	5.83 ± 1.90 bc
	JM	0.24 ± 0.03 c	0.20 ± 0.09 b	1.87 ± 0.64 bc	0.75 ± 0.22 b	0.38 ± 0.05 b	0.45 ± 0.10 b	3.89 ± 0.99 d
	XY	0.96 ± 0.08 b	0.39 ± 0.08 a	2.90 ± 1.04 b	0.93 ± 0.09 b	0.51 ± 0.09 ab	0.58 ± 0.13 ab	6.27 ± 1.37 b
	YN	1.12 ± 0.14 b	0.22 ± 0.07 b	2.04 ± 0.31 bc	0.99 ± 0.07 ab	0.42 ± 0.06 b	0.51 ± 0.13 ab	5.30 ± 0.56 bcd
	ZM	3.73 ± 0.34 a	0.47 ± 0.21 a	4.21 ± 0.88 a	1.36 ± 0.51 a	0.73 ± 0.36 a	0.67 ± 0.13 a	11.2 ± 1.75 a
1.5	CW	4.97 ± 0.67 a	0.25 ± 0.09 a	2.27 ± 0.39 ab	0.82 ± 0.18 a	0.36 ± 0.01 c	0.41 ± 0.03 b	9.09 ± 1.30 a
	HD	3.46 ± 2.28 abc	0.34 ± 0.07 a	2.25 ± 0.85 ab	0.80 ± 0.06 a	0.43 ± 0.07 ab	0.50 ± 0.07 a	7.79 ± 2.84 ab
	JM	1.62 ± 0.61 c	0.33 ± 0.07 a	2.69 ± 0.12 a	0.92 ± 0.10 a	0.42 ± 0.05 b	0.48 ± 0.06 ab	6.46 ± 0.33 b
	XY	2.44 ± 1.26 bc	0.36 ± 0.01 a	1.72 ± 0.51 b	0.92 ± 0.15 a	0.49 ± 0.02 a	0.55 ± 0.05 a	6.47 ± 0.99 b
	YN	4.32 ± 1.98 ab	0.30 ± 0.06 a	2.15 ± 0.22 ab	0.90 ± 0.06 a	0.44 ± 0.01 ab	0.50 ± 0.01 a	8.62 ± 2.21 ab
	ZM	4.03 ± 1.14 ab	0.29 ± 0.11 a	2.29 ± 0.32 ab	0.90 ± 0.18 a	0.41 ± 0.04 bc	0.47 ± 0.08 ab	8.38 ± 1.49 ab

Different letters within the same row indicating significant difference among different varieties of winter wheat at the level of $p < 0.05$

PAHs in cuticular wax of wheat leaves

Figure 2 shows concentrations of PAHs in cuticular wax of the six varieties of winter wheat applying 0.25 mg L^{-1} of PAHs for 10 consecutive days. Both individual PAHs and Σ_6 PAHs in the cuticular waxes were significantly ($p < 0.001$) different among the six varieties and were significantly ($p < 0.01$) higher than those in leaves (Table 1). Besides having significantly higher ($p < 0.001$) levels of Σ_6 PAHs in leaves, the two varieties (YN and ZM) possess significantly ($p < 0.001$) higher cuticular wax concentrations than the other four varieties (CW, HD, JM, and XY). This indicated that cuticular wax of wheat leaves had a higher capacity to absorb PAHs. The cuticular wax is the main storage location of POPs in the leaf (Wang et al. 2008) and is considered to be a critical interface of PAHs cycling between the atmosphere and leaf inner tissues (Keyte et al. 2009; Wild et al. 2005). In addition, there was a significantly ($p < 0.01$) negative linear relationship between concentrations of cuticular wax and concentrations of Σ_6 PAHs or individual of the five selected PAHs (PHE, ANT, PYR, BaA, and BghiP) in the cuticular waxes (Fig. 3). The present results are consistent with previous field investigation, which showing a negative correlation between the wax contents and Σ_{16} PAHs concentrations in the cuticular wax of in *Cinnamomum camphora* leaves collected from Shanghai, China (Yang et al. 2017) (Table 2).

Composition profiles of PAHs in cuticular waxes, leaves and roots

Figure 4 shows the profiles of six individual PAH in cuticular waxes, leaves, and roots of winter wheat after applying 0.25 mg L^{-1} of PAHs for 10 consecutive days. The distribution of PAHs with different ring numbers in cuticular waxes was similar to that of leaves but was significantly different from that of the roots. The similar distribution patterns of PAHs between cuticular wax and leaves indicated that PAHs came from the same source. The percentages of 3-ring PAHs were much higher in cuticular waxes and leaves than in roots, whereas the percentages of 4- and 5–6-ring PAHs were much lower in cuticular waxes and leaves than in roots. Similarly, Xia et al. (2010) also found that 2–3-ring PAHs were dominant in the winter grains collected from the market of Taiyuan, China. PHE was predominant in cuticular waxes and leaves among PAHs detected, accounting for 66.4–88.0% of the Σ_6PAHs. However, PYR, PHE, and BaA were dominant in roots, accounting for 33.2–48.1, 6.21–33.4, and 11.3–19.3% of the Σ_6PAHs, respectively. Physicochemical properties of

Fig. 4 Percentage distribution profiles of Σ_6 PAHs in cuticular wax (**a**), ▶ leaf (**b**) and root (**c**) of six varieties (CW, HD, JM, XY, YN, and ZM) of winter wheat under applying mixed PAHs solutions (0.25 mg L^{-1}) onto the leaf surface for 10 days

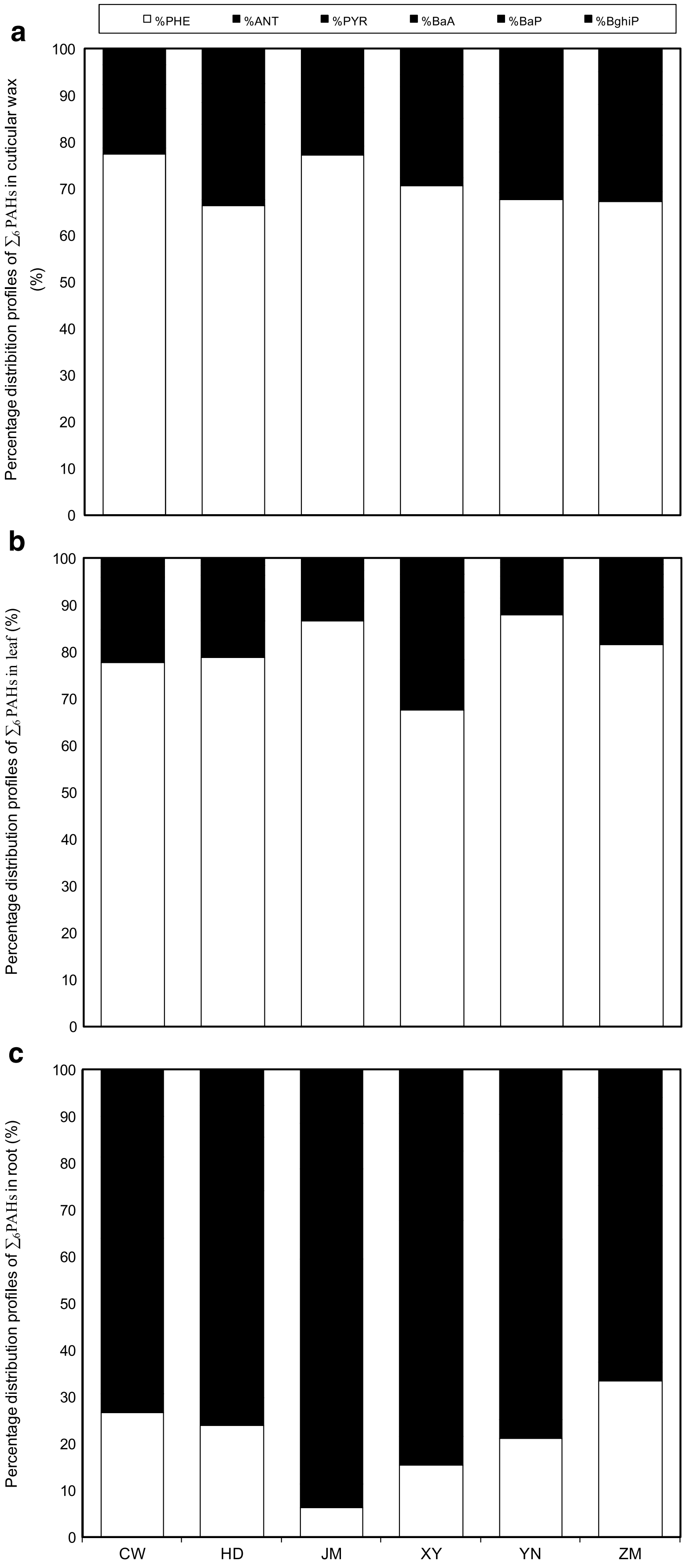
a
b
c
□ %PHE
■ %ANT
■ %PYR
■ %BaA
■ %BaP
■ %BghiP
Percentage distribution profiles of ∑6 PAHs in cuticular wax (%)
Percentage distribution profiles of ∑6 PAHs in leaf (%)
Percentage distribution profiles of ∑6 PAHs in root (%)
0
10
20
30
40
50
60
70
80
90
100
CW
HD
JM
XY
YN
ZM

Table 3 Pearson correlation coefficients between ΣPAH_6 concentrations in leaf of six varieties of winter wheat and physicochemical properties of PAHs ($n = 12$)

	Molecular weight	Log*Kow*	Log*Koa*	Log (water solubility)	log*H*
CW	NS	NS	NS	0.74**	NS
HD	NS	NS	NS	0.73**	NS
JM	NS	NS	NS	0.71**	NS
XY	NS	NS	NS	0.65*	NS
YN	NS	NS	NS	0.68*	NS
ZM	NS	NS	NS	0.68*	NS

NS indicates no significance

*$p < 0.05$, **$p < 0.01$

PAHs have been considered responsible for their foliar uptake, such as number of ring, molecular weight, solubility, octanol-water partition coefficient (K_{ow}), octanol-air partition coefficient (K_{oa}), partition between the particle and gasphases of the atmosphere and Henry's constant (Sun et al. 2016). As shown in Table 3, the present results indicated that the concentrations PAHs in leaves were positively ($p < 0.05$) correlated with the water solubility of the six selected PAHs. Both PHE and ANT contain a three-membered aromatic ring, but the mean concentrations of PHE were 6.16–25.08 times of ANT in wheat leaves, which seemed to be attributed to the apparent difference in solubility at 25 °C between PHE (1.65 mg L^{-1}) and ANT (0.075 mg L^{-1}). The LMW PAHs in the cuticular waxes and leaves was greater mainly due to their higher solubility. Gao and Collins (2009) showed that shoot uptake was driven by the transpiration stream flux which was related to the solubility of the individual PAH rather than the K_{ow}. In addition, the present study indicated that there were insignificant relationship between concentrations PAHs in leaves and logK_{ow} of the six selected PAHs (Table 3). Generally, lipophilic organic chemicals possess a greater tendency to partition into plant lipids than hydrophilic chemicals (Collins et al. 2006). Due to their lipophilic characteristic, PAHs were readily absorbed by leaf cuticle (Chen et al. 2005; Wang et al. 2005), which basically consists of a wax fraction (lipids extractable by organic solvents) and an insoluble cuticular matrix. Effects of lipophilicity on foliar uptake of PAHs in wheat need further research.

Table 4 Concentrations of PAHs in phloem sap collected from six varieties of winter wheat including Changwu 521 (CW), Hedong TX-006 (HD), Jiaomai 266 (JM), Xiaoyan 22 (XY), Yunong 949 (YN), and Zhongmai 175 (ZM) under spraying different level of mixed PAHs solutions onto the leaf surface for 10 days (mean, $n = 3$) (mg kg^{-1})

	PHE	ANT	PYR	BaA	BaP	BghiP
CW	0.089	0.012	0.03	0.012	ND	ND
HD	0.115	0.019	0.037	0.009	ND	ND
JM	0.311	0.019	0.039	0.009	ND	ND
XY	0.088	0.01	0.038	0.014	ND	ND
YN	0.306	0.019	0.039	0.009	ND	ND
ZM	0.016	0.014	0.025	0.012	ND	ND

ND not detectable

Basipetal translocation of PAHs in winter wheat

Once organic pollutants enter plant tissues, they can migrate from roots to leaves (acropetal) and vice versa (basipetal) depending on chemical processes (Korte et al. 2000). After 10 consecutive days of leaf exposure, all the six selected PAHs were recorded in the roots of the six varieties of winter wheat, while the corresponding Σ_6 PAHs concentrations were apparently lower than those in leaves (Table 2). PAHs in roots should be from two pathways, uptake from sands and translocation from leaves. Due to the six selected PAHs were undetectable in roots under the control, Σ_6 PAHs in roots should be mainly translocated from foliar uptake of PAHs. In addition, PHE, ANT, PYR, and BaA were detected in phloem exudates (Table 4). The present study indicated that there was basipetal translocation of PAHs in winter wheat after foliar application of PAHs. PAHs on the surface of plant leaves may be strongly bound into the waxy cuticle layer. Some can enter into the inner leaves and be translocated by the phloem. Using isotope tracing method, Zezulka et al. (2014) also indicated uptake and basipetal translocation of fluoranthene by pea plants (*Pisum sativum*). Similarly, Su and Liang (2013) found that organic pollutants such as richloroethylene (TCE) and 1,2,3-trichlorobenzene (TCB) could be taken up by wheat leaves and translocated from the leaves to roots.

Conclusion

In the present study, foliar uptake of atmospheric PAHs has been simulated by applying solvent solutions containing PAHs directly on leaves. Under actual conditions, both environmental variables such as temperature, humidity and light and the physicochemical properties of PAHs involved in the PAH partitioning between air and plants (Desalme et al. 2013). The present study attempted to report a pilot research focus on investigating intraspecific variations of foliar uptake of PAHs in the winter wheat. The cuticular waxes could play significant role in foliar uptake of PAHs in the winter wheat. The present results also showed that the concentrations PAHs in leaves were positively ($p < 0.05$) correlated with the water solubility of the six selected PAHs. The present study suggested that PAHs accumulation by winter wheat can be greatly reduced by minimizing the transfer of PAHs from air to the leaf via judicious selection of the appropriate variety.

Acknowledgements The financial support from National Natural Science Foundation of China (41571456), Program for Science & Technology Innovation Talents in Universities of Henan Province (14HASTIT048) and the Scientific Research Foundation for the Introduction of Talent, Northwest A&F University, China (2014) is gratefully acknowledged.

References

Bakker MI, Michel V, Dick THMS, Chris K (1999) Dry deposition of atmospheric polycyclic aromatic hydrocarbons in three plantago species. Environ Toxicol Chem 18:2289–2294

Barthlott W, Neinhuis C (1997) Purity of the sacred lotus, or escape from contamination in biological surfaces. Planta 202:1–8

Chen L, Yong R, Xing B, Mai B, He J, Wei X, Fu J, Sheng G (2005) Contents and sources of polycyclic aromatic hydrocarbons and organochlorine pesticides in vegetable soils of Guangzhou, China. Chemosphere 60:879–890

China statistical yearbook (2016) Beijing: China Statistical press p. 475–390

Collins C, Fryer M, Grosso A (2006) Plant uptake of non-ionic organic chemicals. Environ Sci Technol 40:45–52

Desalme D, Binet P, Chiapusio G (2013) Challenges in tracing the fate and effects of atmospheric polycyclic aromatic hydrocarbon deposition in vascular plants. Environ Sci Technol 47: 3967–3981

Dias APL, Rinaldi MCS, Domingos M (2016) Foliar accumulation of polycyclic aromatic hydrocarbons in native tree species from the Atlantic Forest (SE-Brazil). Sci Total Environ 544:175–184

Gao YZ, Collins CD (2009) Uptake pathways of polycyclic aromatic hydrocarbons in white clover. Environ Sci Technol 43:6190–6195

Hoagland DR, Arnon DI (1938) The water culture method for growing plants without soil. Circ Calif Agric Exp Sta 347:1–39

Howsam M, Jones KC, Ineson P (2000) PAHs associated with the leaves of three deciduous tree species. I-Concentrations and profiles. Environ Pollut 108:413–424

Jouraeva VA, Johnsona DL, Hassett JP, Nowak DJ (2002) Differences in accumulation of PAHs and metals on the leaves of Tiliaeuchlora and Pyrus calleryana. Environ Pollut 120:331–338

Keyte I, Wild E, Dent J, Jones KC (2009) Investigating the foliar uptake and within-leaf migration of phenanthrene by moss (*Hypnum Cupressiforme*) using two-photon excitation microscopy with autofluorescence. Environ Sci Technol 43:5755–5761

Kipopoulou AM, Manoli E, Samara C, Smith KEC, Thomas GO, Jones KC, Simonich SL, Hites RA (1999) Bioconcentration of PAHs in vegetables grown in an industrial area. Environ Pollut 106:369–380

Korte F, Kvesitadze G, Ugrekhelidze D, Gordeziani M, Khatisashvili G, Buadze O, Zaalishvili G, Coulston F (2000) Review: organic toxicants and plants. Ecotoxicol Environ Safety 47:1–26

Lehndorff E, Schwark L (2004) Biomonitoring of air quality in the Cologne Conurbation using pine needles as a passive sampler part II: polycyclic aromatic hydrocarbons (PAH). Atmos Environ 38: 3793–3808

Lin H, Tao S, Zuo Q, Coveney RM (2007) Uptake of polycyclic aromatic hydrocarbons by maize plants. Environ Pollut 148:614–619

Ma Y, Harrad S (2015) Spatiotemporal analysis and human exposure assessment on polycyclic aromatic hydrocarbons in indoor air, settled house dust, and diet: a review. Environ Int 17:7–16

Neinhuis C, Barthlott W (1997) Characterisation and distribution of water-repellent, self-cleaning pant surfaces. Ann Bot 79:667–677

Palmer LJ, Dias DA, Boughton B, Roessner U, Graham RD, Stangoulis JCR (2014) Metabolite profiling of wheat (*Triticum aestivum* L.) phloem exudate. Plant Methods 10:1–9

Phillips DH (1999) Polycyclic aromatic hydrocarbons in the diet. Mutat Res 443:139–147

Ratola N, Alves A, Lacorte S, Barcelo D (2012) Distribution and sources of PAHs using three pine species along the Ebro River. Environ Monit Assess 184:985–999

Su YH, Liang YC (2013) The foliar uptake and downward translocation of trichloroethylene and 1,2,3-trichlorobenzene in air-plant-water systems. J Hazard Mater 252:300–305

Sun HF, Shi J, Guo S, Zhang Y, Duan LS (2016) In situ determination of the depuration of three- and four-ringed polycyclic aromatic hydrocarbons co-adsorbed onto mangrove leaf surfaces. Environ Pollut 208:688–695

Tao S, Jiao XC, Chen SH, Liu WX, Coveney RM, Zhu LZ, Luo YM (2006) Accumulation and distribution of polycyclic aromatic hydrocarbons in rice (*Oryza sativa*). Environ Pollut 140:406–415

Tao YQ, Zhang SZ, Zhu YG, Christie P (2009) Uptake and acropetal translocation of polycyclic aromatic hydrocarbons by wheat (*Triticum aestivum* L.) grown in field-contaminated soil. Environ Sci Technol 43:3556–3560

Tian K, Bao HY, Zhang XC, Shi TR, Liu XP, Wu FY (2017) Residuals, bioaccessibility and health risk assessment of PAHs in winter wheat grains from areas influenced by coal combustion in China. Sci Total Environ. https://doi.org/10.1016/j.scitotenv.2017.08.174

USEPA (1996a) Method 3540C: Soxhlet extraction. US Environmental Protection Agency, Washington

USEPA (1996b) Method 3620B: Florisil cleanup. US Environmental Protection Agency, Washington

Wang D, Chen J, Xu Z, Qiao X, Huang L (2005) Disappearance of polycyclic aromatic hydrocarbons sorbed on surfaces of pine Pinua thunbergii needles under irradiation of sunlight: volatilization and photolysis. Atmos Environ 39:4583–4591

Wang YQ, Tao S, Jiao XC, Coveney RM, Wu SP, Xing BS (2008) Polycyclic aromatic hydrocarbons in leaf cuticles and inner tissues of six species of trees in urban Beijing. Environ Pollut 151:158–164

Wild E, Dent J, Thomas OG, Jones KC (2005) Direct observation of organic contaminant uptake, storage, and metabolism within plant roots. Environ Sci Technol 39:3695–3702

Wild SR, Jones KC (1995) Polynuclear aromatic hydrocarbons in the United-Kingdom environment—a preliminary source inventory and budget. Environ Pollut 88:91–108

Xia ZH, Duan XL, Qiu WX, Liu D, Wang B, Tao S, Jiang QJ, Lu B, Song YX, Hu XX (2010) Health risk assessment on dietary exposure to polycyclic aromatic hydrocarbons (PAHs) in Taiyuan, China. Sci Total Environ 408:5331–5337

Yang B, Liu S, Liu Y, Li XF, Lin XB, Liu M, Liu XR (2017) PAHs uptake and translocation in Cinnamomum camphora leaves from Shanghai, China. Sci Total Environ 574:358–368

Yin XM, Liang X, Xu GH, Zhan XH (2014) Effect of phenanthrene uptake on membrane potential in roots of soybean, wheat and carrot. Environ Exp Bot 99:53–58

Zezulka S, Klems M, Kummerova M (2014) Root and foliar uptake, translocation, and distribution of [C-14] fluoranthene in pea plants (*Pisum sativum*). Environ Toxicol Chem 33:2308–2312

Zhan XH, Liang X, Xu GH, Zhou LX (2013b) Influence of plant root morphology and tissue composition on phenanthrene uptake: stepwise multiple linear regression analysis. Environ Pollut 179:294–300

Zhan XH, Liang X, Jiang TH, Xu GH (2013a) Interaction of phenanthrene and potassium uptake by wheat roots: a mechanistic model. BMC Plant Biol 13:168

Zhan XH, Ma HL, Zhou LX, Liang JR, Jiang TH, Xu GH (2010) Accumulation of phenanthrene by roots of intact wheat (*Triticum acstivnm* L.) seedlings: passive or active uptake? BMC Plant Biol 10:52

Ecological Engineering 111 (2018) 22–30

Contents lists available at ScienceDirect

Ecological Engineering

journal homepage: www.elsevier.com/locate/ecoleng

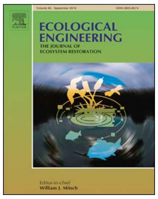

Dynamics of soil microbial biomass and enzyme activities along a chronosequence of desertified land revegetation

Jiao Li[a], Xiaogang Tong[a,*], Mukesh Kumar Awasthi[a,b], Fuyong Wu[a,*], Sier Ha[c], Jianye Ma[c], Xiaohan Sun[a], Chao He[c]

[a] College of Natural Resources and Environment, Northwest A&F University, Yangling, Shaanxi, 712100, China
[b] Department of Biotechnology, Amicable Knowledge Solution University, Satna, India
[c] Institute of Soil and Water Conservation, Northwest A&F University, Yangling Shaanxi, 712100, China

ARTICLE INFO

Keywords:
Desertified land revegetation
Soil nutrient availability
Microbial biomass
Soil enzyme activities
Mu Us Sandy land

ABSTRACT

Large-scale sand control and afforestation in the Mu Us Sandy land of China have greatly improved soil nutrients and physicochemical properties; however, little is known about their effects on soil biological properties. This study aimed to investigate the changes in soil microbial biomass and enzyme activities and their relationships with soil physicochemical properties during sand land rehabilitation. Soil samples were collected from the shrub and arbor plantations with an age sequence of 20, 30, and 51 years in Yulin at depths of 0–10 cm and 10–20 cm and with semi-fixed sand land selected as a control (0-year-old site). The soil physicochemical and biological properties in the 0–10 cm soil layer were significantly ($P < 0.001$) higher than in the 10–20 cm soil layer for all stand lands. The soil microbial biomass (e.g., microbial carbon and nitrogen) in the 0–10 cm and 10–20 cm layers greatly increased, by 1.58–5.59 times and 2.27–6.07 times, respectively, during the revegetation of shrub and arbor from 20 to 30 years on the control land. During the same period, the activities of soil catalase, urease, alkaline phosphatase and invertase also greatly increased, by 1.27–2.18, 0.59–1.23, 0.48–3.66 and 0.57–2.72 times in shrub land, respectively, whereas they increased by 1.51–2.73, 0.46–2.09, 0.97–2.79 and 2.00–6.65 times in arbor land, respectively, compared with the control land. However, during the 30–51 years of revegetation on the control land, the soil microbial biomass and all enzyme activities remained relatively stable or slightly increased in the arbor land, whereas they were reduced in the shrub land. The soil organic carbon (SOC), dissolved organic carbon (DOC), total nitrogen (TN) and available nitrogen (AN) contents also greatly increased after revegetation in the control land. Principal component analysis (PCA) also confirmed that most of the chemical and biological properties were influenced by the afforestation and showed coordinated variation between the analyzed parameters. Moreover, redundancy analysis (RDA) showed that the soil microbial biomass and enzyme activities were correlated with the changes of SOC, DOC and TN, whereas they were negatively correlated with the bulk density, pH and total potassium. Therefore, we concluded that revegetation by the establishment of both shrub and arbor plantations significantly improved soil biological properties. Moreover, SOC, DOC and TN were regarded as the key factors in the enhancement of soil biological activity during desertified land revegetation in the Mu Us Sandy land of China.

1. Introduction

The Mu Us Sandy land is one of the four major sandy lands in China; it has undergone oppressive desertification, mainly attributed to climate and anthropogenic activity such as overgrazing by livestock, excessive farming intensity, and vegetation devastation by fuel wood acquisition. These activities have resulted in a landscape of moving, semi-moving, and stabilized sand dunes in alternation (Cao et al., 2008). The desertification has not only resulted in an increase in bare soil and loss of soil resources (e.g., loss of nutrients and serious degradation of soil) but has also influenced the sustainable growth of the environment of China and the world (Liu and Diamond, 2005). Therefore, to control land desertification and mitigate its negative impacts on grassland and farmland, the government of China has adopted

---

Abbreviations: BD, bulk density; TP, total phosphorus; AP, available phosphorus; TK, total potassium; AK, available potassium; SOC, soil organic carbon; MBC, microbial biomass carbon; DOC , dissolved organic carbon; TN, total nitrogen; MBN, microbial biomass nitrogen; AN , available nitrogen; C:N, total carbon/nitrogen ratio; ANOVA , Analysis of variance; LSD, Least significance difference; PCA, principal component analysis; RDA, redundancy analysis

[*] Corresponding authors.

E-mail addresses: xiaogangtong@126.com (X. Tong), wfy09@163.com (F. Wu).

https://doi.org/10.1016/j.ecoleng.2017.11.006
Received 8 March 2017; Received in revised form 2 November 2017; Accepted 10 November 2017

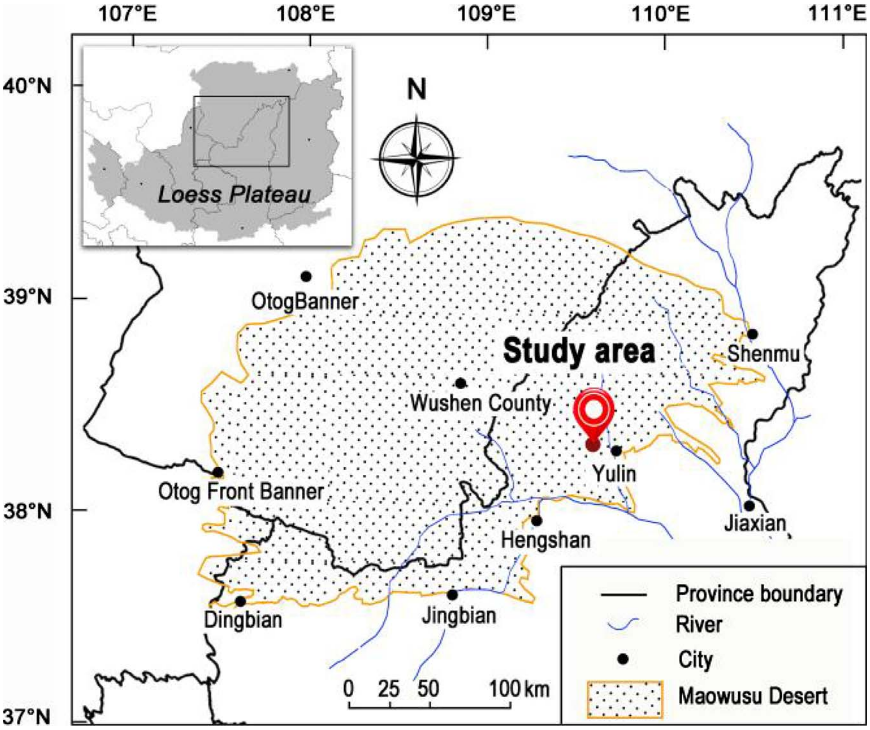

Fig 1. Location of the study area (Hongshixia Afforestation of Sands Experiment Station at Yulin) in the Loess Plateau of China.

many critical mechanical methods (such as the elimination of grazing via fencing, returning degraded farmland to forest and grassland, placing sand arresters and planting indigenous trees, shrubs and grasses) since the 1960s for the revegetation of desertified land in China such as the Mu Us Sandy land (Dai, 2010; Cao et al., 2011). During the past 50 years, the desertification management process on the Mu Us Sandy land has produced good ecological benefits and has significantly improved soil texture and physicochemical properties (Bolling and Walker, 2000; Zhang et al., 2008; Zuo et al., 2009). Nonetheless, very limited studies have focused on the progressive changes of soil biological properties during the reversion of desertification and the relationship among soil physicochemical properties, microbial biomass and enzyme activity along a chronosequence of desertification vegetation reconstruction.

The soil microbial biomass carbon, nitrogen and enzyme activities play an important role in nutrient cycling; they are more sensitive parameters than the physicochemical properties (Zhang et al., 2015) and thus potentially influence the element cycles of terrestrial ecosystems. Cai et al. (2013) observed that the soil microbial biomass and catalase, urease, phosphatase activities gradually increased with increasing stand age and successive rotation duration after farmland was returned to forestland. Moreover, soil biological characteristics, including soil microbial biomass and the activities of urease, invertase, alkaline phosphatase and catalase, decreased from slope farmland to an herbaceous community, significantly increased from an herbaceous community to a shrubby community, and slightly increased or stabilized from a shrubby community to an arboreal community (Cui, 2011). Current studies of microbial biomass and enzyme activity dynamics have mainly focused on the process of vegetation restoration and the conversion of cropland to forest and land degradation (Liu et al., 2007; Nunes et al., 2012; Wei et al., 2011). Most previous researchers were concerned with the study of urease, invertase, alkaline phosphatase and catalase activity because these enzymes are closely related to the transformation of soil carbon and nitrogen (Liu et al., 2007; Zhang et al., 2015); however, no systematic study has been reported on the microbial biomass and enzyme activity during desertification vegetation reconstruction.

Therefore, elucidating the relationship between carbon and nitrogen stock fractions with enzyme activities during vegetation reconstruction, especially for below-ground levels, is crucial in explaining the mechanisms of biogeochemical cycling processes. Li et al. (2008) observed that soil urease, alkaline phosphatase and invertase activities were closely related to soil nutrient levels and cycling. Additionally, Taylor et al. (2002) showed that there was a significant positive correlation between soil enzyme activity and soil organic matter. Baldrian (2008) reported that soil microbial biomass and enzyme activities correlated with the contents of C, N and P in the soil, and a previous study reported that the microbial biomass-related properties correlated with the content of organic C (Frouz and Nováková, 2005). Wang et al. (2010) then found that soil enzyme activity directly correlated with soil nutrient and microbial biomass during the process of vegetation recovery: urease activity was found to be mainly affected by total nitrogen, whereas alkaline phosphatase, catalase and invertase were closely influenced by available nitrogen, although alkaline phosphatase had no significant correlation with total phosphorus and available phosphorus. However, Wang et al. (2012) reported that enzyme activity and nutrient characteristics under different transformation modes of degraded forest land showed a close relation between phosphatase and urease activities with available phosphorus. To date, there has been no clear investigation that confirmed the co-relationship between soil microbial biomass, enzyme activity and soil nutrients under the process of vegetation reconstruction for desertified land.

The previous studies provided a good platform to understand the dynamics of soil physicochemical and biological properties and their relationships. Therefore, we explored the effects of vegetation reconstruction on soil fertility and its microbial biomass as well as enzymatic activities in the Mu Us Sandy land of China. We hypothesized that soil biological properties could be considerably changed by revegetation and that soil biological properties and soil nutrients are synergistically recovered and have significant interaction. The objectives of the present study were 1) to determine the dynamics of various soil physicochemical and biological properties along a chronosequence of 20, 30, and 51 years of desertified land revegetation, including soil nutrient contents, microbial biomass and enzyme activities, and 2) to identify the relationship between soil microbial biomass, enzyme activities and physicochemical properties, as well as find out the key factors that responsible for enhancement of soil biological activity during desertified land revegetation.

2. Materials and methods

2.1. Site description

Field sampling was conducted in September 2015 at the Hongshixia Afforestation of Sands Experiment Station (38 °20′N, 109 °44′E), which is located 8 km northwest of Yulin city, in the east edge of Mu Us Desert and the northern Shaanxi province (Fig. 1), China. The average elevation of the area is 1050–1500 m and it belongs to the typical continental monsoon arid and semi-arid climate. During the past 50 years, the annual average precipitation is 415 mm that 60%–70% primarily falls in summer; and the annual potential evaporation is 2014 mm, while the average wind speed is 1.9 $m^{-1}s^{-1}$ and strong wind frequently occurred in winter and spring. The average temperature is 8.1 °C, which reached maximum temperature of 23.2 °C in July and lowest temperature −8.9 °C during January (Yang et al., 2012). Soils in the study area are classified as aeolian sandy soil. Their sand content is 92.6%, and their silt and clay content is 7.4%, but groundwater is deep (–8 m) and that cannot be utilized by the natural vegetation. The area is a typical farming-pastoral ecotone, excessively reclaiming, cultivating and grazing brought serious desertification in history has led to form a dense, continuous and reticulate flow dune zone with less than 1.8% of vegetation cover in 1950s (Cheng et al., 2004). In order to choose effective silvicultural technique and psammophytes species for reversing desertification, the experimental stations established by Desert Control Research Institute of Shaanxi province in 1958 (Dang et al., 2003). At first, windbreaks (mechanical sand fences) were erected to reduce wind erosion, and then straw checkerboard barriers (1 m × 1 m in area) installed on shifting sand surfaces. In following 3 years, the natural pioneer plant invaded and changed shifting sand to semi-fixed sand. Then two-year-old seedlings of xerophytic shrubs (*Salix psammophila C.* Wang et Ch. Y. Yang, *Psammochloa villosa (Trin.)* Bor, and *Amorpha fruticosa* Linn.) or arbors (*Pinus sylvestris L. var. mongolica* Litv.) were planted inside the straw checkerboard barriers to stabilize the surface of the sand dunes. After several years of labor management, understory grass, legumes, and forbs colonized, and a shrubby-grass or arboreal-grass vegetation system was gradually established. Then vegetation system has gone into natural succession stage (Dang et al., 2003). More sand-binding shrub and arbor with the same species and similar density were planted every 10–15 years. Combined, the completed protective vegetation system was 33.3 km^2 and the vegetation coverage has been increased to 80% in the study area.

2.2. Experimental design and soil sampling

Using the space-for-time substitution (chronosequence) method, six tree stands were chosen based on years of afforestation in the study area; the stands included three shrub stands (*Salix psammophila C.* Wang et Ch. Y. Yang mixed with *Psammochloa villosa (Trin.)* Bor) and three arbor stands (*Pinus sylvestris L. var. mongolica* Litv.). Both types of forest land (shrub and arbor) were established in 1964 (the 51-year-old site), 1985 (the 30-year-old site) and 1995 (the 20-year-old site). Additionally, a semi-fixed sand land was selected as a control (0-year-old site). The site conditions and soil characteristics were relatively consistent for each forest stand year prior to revegetation. A description of each stand site is shown in Table 1. At each stand site, three 20 m × 20 m fields were randomly selected for the investigation of vegetation features such as coverage, plant density and plant height. In each field, three subplots (1 m × 1 m) were randomly selected for surveys of vegetation species. One soil sample was collected using a soil auger (5–cm diameter × 120–cm length) from 16 spots in an "S" shape at each field and then mixed to prepared composite sample. All soil cores were sectioned into two layers (0–10 cm and 10–20 cm), and the soils from the same layer were combined into one final soil sample. All soil samples were sieved through a 2-mm screen, and roots and other debris were removed and discarded. Half of each sample was kept field-moist in a freezer at 4 °C, and the other half was air-dried and stored at room temperature. Additionally, three soil profiles of −20 cm depth were dug in each stand field and in the semi-fixed sand land to estimate the bulk density (BD) in each soil layer from the soil cores (volume: 100 cm^3).

2.3. Soil analysis

Soil pH was measured in 1:2.5 soil-water suspensions (on a dry weight basis) using a pH meter with a glass electrode (Zhang et al., 2015). Part of the air-dried and sieved samples was ground and passed through a 0.25–mm screen and used for soil total carbon and total nitrogen analyses. The soil organic carbon (SOC) content was measured using the potassium dichromate method (Zhang et al., 2013), and total nitrogen (TN) was determined by the Kjedahl method (Fterich et al., 2012). The total phosphorus (TP), total potassium (TK) and available potassium (AK) concentrations were determined by the Keeney (1982) and Qi et al. (2012) methods, and available phosphorus (AP) was analyzed by the $NaHCO_3$ extraction–molybdenum antimony anti-colorimetric method. The content of available nitrogen (AN) (NH_4^+-N and NO_3^--N) was determined using the Continuous Flow Analyzer (Analytical AA3 Auto Analyzer 3HR, Germany) after extraction by the KCl (1 mol L^{-1}) (Zhang et al., 2010), whereas the soil microbial biomass carbon (MBC) and nitrogen (MBN) were estimated using the chloroform fumigation-incubation and extraction method (Jenkinson and Powlson, 1976; Hu et al., 2016).

2.4. Soil enzyme activity

The catalase activity was determined by back-titrating residual H_2O_2 with $KMnO_4$, and the enzymatic activity was expressed as ml 0.1 M $KMnO_4$ g^{-1} dw h^{-1} under the assay conditions (Lu et al., 2014). Soil urease activity was measured by using the urea solution as the substrate, and the released ammonium was assayed colorimetrically at 578 nm according to Kandeler and Gerber (1988); the activity was expressed as mg NH_3—N g^{-1} dw 24 h^{-1}. Alkaline phosphatase activity was estimated by *para*-nitrophenylphosphate (pNPP) as an orthophosphate monoester analog substrate, and the hydrolysis of *p*-nitrophenol phosphate was calculated by referring to a calibration curve obtained with standards containing 0, 10, 20, 30, 40 and 50 mg L^{-1} of *p*-nitrophenol; the activity was expressed as mg PNP (*p*-nitrophenol) g^{-1} dw 24 h^{-1} (Sardans et al., 2008). The invertase activity was determined according to Ye et al. (2015) using sucrose as the substrate, and the activity was expressed as mg glucose g^{-1} dw 24 h^{-1}.

2.5. Statistical analysis

All results are reported as the means + standard deviations. The soil physical, chemical properties, MBC, MBN and enzyme activities were analyzed by three-way Analysis of variance (ANOVA) with tree species, plantation age and soil depth as factors. Multiple comparison tests were also performed to compare the least significance difference (LSD) at $P = 0.05$ using SPSS 19.0 software for windows. Figures were drawn using Sigma-Plot 12.0 software. The principal component analysis (PCA) was performed by the R language v3.0 software with the prcomp function and the package ggbiplot, and redundancy analysis (RDA) was used to identify the relationship between the soil microbial biomass, enzymatic activities and soil physicochemical properties. RDA was performed using the Canoco v.5.0 software package.

Table 1
Vegetation characteristics in different stand ages of afforestation.

Sites	Height (m)	Coverage (%)	Stand density (plant·hm^{-2})	Main vegetation species
Semifixed sand	0	17d	–	Psammochloa villosa (Trin.), Bor; Poa sphondylodes Trin
Shrub$_{20yr}$	2.3 ± 0.4d	70 ± 11c	870 ± 56b	Hedysarum scoparium Fisch. et Mey; Artemisia ordosica Krasch; Setaria viridis (L.) Beauv.
Shrub$_{30yr}$	3.8 ± 0.5c	86 ± 8b	930 ± 45b	Hedysarum scoparium Fisch. et Mey; Artemisia ordosica Krasch; Setaria viridis (L.) Beauv.
Shrub$_{51yr}$	4.5 ± 0.9c	92 ± 7a	820 ± 76b	Hedysarum scoparium Fisch. et Mey; Artemisia ordosica Krasch; Elymus dahuricus Turcz; Tripolium vulgare Nees
Arbor$_{20yr}$	18.4 ± 2.6b	67 ± 6c	1231 ± 95a	Euphorbia humifusa Willd. ex Schlecht; Suaeda glauca (Bunge) Bunge; Dendranthema indicum (L.) Des Moul; Setaria viridis (L.) Beauv.
Arbor$_{30yr}$	24.3 ± 2.7a	85 ± 9b	1279 ± 101a	Suaeda glauca (Bunge) Bunge; Setaria viridis (L.) Beauv; Salsola collina Pall; Poa sphondylodes Trin
Arbor$_{51yr}$	22.2 ± 1.4a	95 ± 15a	1245 ± 122a	Setaria viridis (L) Beauv; Poa sphondylodes Trin

Multiple comparisons using the least significant difference (LSD) method, different letters indicate significant difference among different restoration ages at the 0.05 level.

3. Results

3.1. Soil physical and chemical properties

Soil physicochemical properties drastically changed with plantation age and soil depths (Table 2). In both layers (0–10 cm and 10–20 cm depth), soil bulk density and the soil pH values slightly decreased with plantation age, whereas soil bulk density and pH increased with soil depth. The AK contents in the 0–10 cm layer significantly increased after 20, 30, and 51 years of shrub and arbor growth, by 0.32, 2.14 and 3.89 times and 0.25, 1.71 and 2.63 times compared with the control, respectively; soil AP followed the same pattern as AK and increased by 1.98 times and 0.52 times after 51 years of shrub and arbor growth, respectively. Soil AK and AP declined sharply at 10–20 cm depth in the plantations of all ages.

During the shrub vegetation reconstruction process, the TP contents showed a consistent increase from 20 to 30 years in both layers (0–10 cm and 10–20 cm depth) and then decreased. After 30 years of revegetation with shrub, TP content increased by 1.05 times at 0–10 cm and 0.64 times at 10–20 cm soil depth, respectively, compared with that in the control site (0-year). In the case of arbor land, TP content at the 0–10 cm depth gradually increased from 20 to 51 years, whereas at 10–20 cm depth it increased from 20 to 30 years and then decreased. In contrast, TK contents did not show much variation with increasing plantation age at both depths. The C/N ratio decreased at 0–10 cm depth, whereas at 10–20 cm depth in shrub forest land the C/N ratio first increased up to 30 years and then suddenly decreased, although in arbor forest land, it gradually decreased with plantation age (Table 2).

3.2. Soil organic carbon, dissolved organic carbon, total nitrogen and available nitrogen

Significant differences were observed for SOC, DOC, TN and AN between shrub and arbor land of different ages as well as at different soil depths (Table 3). The SOC, DOC, TN and AN at 0–10 cm soil depth gradually increased along a chronosequence of 20, 30, and 51 years of desertified land revegetation. After 51 years of shrub vegetation reconstruction, SOC, TN, AN and DOC at 0–10 cm soil depth increased by 8.38, 7.88 and 3.30 times and by 81.8%, respectively, whereas for arbor land, SOC, TN, AN and DOC increased by 9.10, 7.96 and 2.38 times and by 72.0%, respectively, compared with that in the control site (0-year). Overall, SOC, DOC, TN and AN in the 10–20 cm soil layer followed the same pattern as in the 0–10 cm soil layer, whereas a very slowly increasing trend of SOC, DOC, TN and AN was observed at 10–20 cm depth for both forest land types. After 51 years of shrub growth, SOC, TN, AN and DOC in the 10–20 cm soil layer only increased by 2.58, 1.54 and 1.35 times and by 48.0%, respectively, whereas for arbor land, SOC, TN, AN and DOC increased by 2.10, 2.12 and 1.14 times and by 36.0%, respectively, compared with the control site (Fig. 2a and c and Fig. 3a and c).

3.3. Soil microbial biomass carbon and nitrogen

Soil MBC and MBN significantly differed between the different tree species, soil depths and plantation ages (Table 3). During the shrub and arbor vegetation reconstruction process, both MBC and MBN showed a consistent increase from 20 to 30 years in the 0–10 cm and 10–20 cm soil layers (Fig. 2b and Fig. 3b). After 30 years of revegetation with

Table 2
Changes of soil properties at 0–10 and 10–20 cm soil layers with 20, 30 and 51 years of shrub and arbor establishment on desertified land.

Soil properties	Soil depth (cm)	Semi-fixed sand	Stand age of shrub			Stand age of arbor		
		0yr	20yr <	30yr	51yr	20yr	30yr	51yr
pH	0–10	8.09 ± 0.08a	8.02 ± 0.16ab	7.80 ± 0.04b	7.54 ± 0.21c	8.00 ± 0.11ab	7.93 ± 0.04ab	7.90 ± 0.07ab
	10–20	8.12 ± 0.09a	8.08 ± 0.11a	8.04 ± 0.05ab	7.88 ± 0.17b	8.16 ± 0.14a	8.09 ± 0.02a	8.11 ± 0.08a
TP (mg kg^{-1})	0–10	63.94 ± 1.69d	96.27 ± 4.01b	130.83 ± 13.20a	73.55 ± 3.39cd	62.09 ± 3.37d	79.83 ± 1.11c	92.76 ± 8.08b
	10–20	40.48 ± 1.27de	57.38 ± 3.81b	66.53 ± 3.00a	42.42 ± 5.06de	35.76 ± 4.99e	50.73 ± 4.63bc	43.80 ± 4.26cd
AP (mg kg^{-1})	0–10	3.13 ± 0.25d	3.05 ± 0.49d	6.58 ± 1.26b	9.34 ± 0.63a	2.21 ± 0.22d	3.19 ± 0.45d	4.76 ± 0.36c
	10–20	2.09 ± 0.21a	1.16 ± 0.09d	1.32 ± 0.07d	1.77 ± 0.17ab	1.33 ± 0.24d	1.44 ± 0.09bc	1.77 ± 0.35ab
TK (g kg^{-1})	0–10	11.19 ± 0.14a	10.70 ± 0.22ab	10.17 ± 0.40ab	10.27 ± 1.11ab	9.79 ± 0.68b	10.23 ± 0.29ab	10.27 ± 0.57ab
	10–20	11.20 ± 0.52a	10.08 ± 0.61a	10.47 ± 0.64a	10.69 ± 1.32a	11.46 ± 0.99a	10.72 ± 0.26a	10.97 ± 0.50a
AK (mg kg^{-1})	0–10	32.64 ± 4.70e	43.00 ± 5.02e	102.64 ± 12.59c	159.83 ± 8.90a	40.81 ± 2.83e	88.41 ± 2.42d	118.47 ± 4.59b
	10–20	19.22 ± 3.63d	20.67 ± 2.92d	39.43 ± 3.47bc	68.14 ± 8.15a	25.10 ± 1.35d	34.40 ± 4.17c	45.03 ± 3.63b
C:N	0–10	13.27 ± 0.94c	23.86 ± 2.88a	20.51 ± 6.91ab	14.77 ± 3.80bc	20.86 ± 1.80ab	15.42 ± 2.15bc	15.03 ± 1.17bc
	10–20	17.51 ± 1.47d	20.79 ± 4.45abc	37.49 ± 1.12a	25.50 ± 5.18b	24.38 ± 3.19b	24.14 ± 0.94bc	17.97 ± 4.30cd
BD (g cm^{-3})	0–10	1.70 ± 0.09a	1.66 ± 0.05ab	1.58 ± 0.07bc	1.46 ± 0.04de	1.65 ± 0.01ab	1.53 ± 0.07cd	1.41 ± 0.02e
	10–20	1.70 ± 0.05a	1.69 ± 0.01ab	1.67 ± 0.03abc	1.65 ± 0.03abc	1.70 ± 0.05a	1.61 ± 0.04bc	1.58 ± 0.06c

TP (total phosphorus), AP (available phosphorus), TK (total potassium), AK (available potassium),C:N (total carbon/nitrogen ratio) and BD (bulk density), Multiple comparisons used the least significant difference (LSD) method; different letters indicate significant differences among different restoration ages in the same soil layer at the 0.05 level.

Table 3
Results of three-way ANOVA for soil chemical and biological properties in different tree species, in plantations of different age and at different soil depths.

Index	Tree species		Plantation age		Soil depth	
	F	P	F	P	F	P
SOC	1.85	0.18	823.96	< 0.001	1277.91	< 0.001
MBC	38.35	< 0.001	510.08	< 0.001	428.99	< 0.001
DOC	1.95	0.17	124.62	< 0.001	128.75	< 0.001
TN	1.80	0.19	66.99	< 0.001	142.06	< 0.001
MBN	13.41	0.001	586.80	< 0.001	513.82	< 0.001
AN	62.54	< 0.001	247.25	< 0.001	1476.78	< 0.001
Catalase	61.51	< 0.001	207.95	< 0.001	301.16	< 0.001
Urease	320.81	< 0.001	439.59	< 0.001	483.08	< 0.001
Alkaline phosphatase	42.20	< 0.001	212.43	< 0.001	555.45	< 0.001
Invertase	122.05	< 0.001	84.87	< 0.001	334.07	< 0.001

SOC (soil organic carbon), MBC (microbial biomass carbon), DOC (dissolved organic carbon), TN (total nitrogen), MBN (microbial biomass nitrogen), AN (available nitrogen); F and P values of three-way ANOVA compare the effects of tree species, plantation age and soil depth.

shrub and arbor, the MBC and MBN contents increased by 6.71 and 4.66 times, respectively, and by 6.89 and 5.07 times at 0–10 cm depth, respectively, compared with those in the control (0–year). From 30–51 years, the responses of MBC in the 0–10 cm and 10–20 cm soil layers gradually increased for arbor land but slightly decreased for shrub land, whereas no significance variation was observed in MBN for arbor and shrub land between 30 and 51 years. Overall, MBC and MBN in the 10–20 cm soil layers were only 45.1%–56.6% and 49.7%–55.8% of those at 0–10 cm, respectively.

3.4. Soil enzyme activities

The soil enzyme (catalase, urease, alkaline phosphatase and invertase) activities significantly differed among tree species, plantation ages and soil depths (Table 3). During the shrub and arbor vegetation reconstruction process, the activities of soil catalase, urease, alkaline phosphatase and invertase showed a consistent increase from 20 to 30 years in the 0–10 cm soil layers (Fig. 4). After 30 years of revegetation with shrub and arbor, soil catalase, urease, alkaline phosphatase and invertase activities increased by 3.01 and 4.21 times, 1.70 and 3.30 times, 6.53 and 4.52 times and 4.27 and 9.54 times, respectively, at 0–10 cm soil depth compared with that in the control site (0–year). From 30–51 years, the activities of soil catalase, urease and alkaline phosphatase in the 0–10 cm soil layers gradually increased for arbor land and were 6.76, 17.78 and 8.88 times higher than those of the control, respectively. In contrast, soil catalase, alkaline phosphatase and invertase activities sharply decreased in shrub land from 30 to 51 years at the sites but were still higher than those of the control; they increased by 2.84, 2.78 and 0.48 times at 0–10 cm, respectively, compared with the control.

At 10–20 cm soil depth, the activities of soil catalase, urease, alkaline phosphatase and invertase also significantly increased along a chronosequence of desertified land revegetation, although their increments were less than that at 0–10 cm; catalase, urease, alkaline phosphatase and invertase activities in the 10–20 cm soil layers were only 37.4%–86.5%, 23.5%–56.8%, 18.5%–78.2% and 8.2%–49.5% of those at 0–10 cm, respectively. Overall, soil enzyme activities were higher in the 0–10 cm soil layer and significantly decreased ($P < 0.001$) in the 10–20 cm soil layer. Therefore, our results indicated that revegetation significantly promoted activities of soil urease, invertase, alkaline phosphatase and catalase in the desertified land.

3.5. Variation and correlation analysis for restoration ages, soil properties and enzyme activities

PCA was performed on the correlation matrix of the data obtained for soil physicochemical properties, biological activities and the restoration ages of both forest land types to illustrate the variation of the data on the two most significant components (0–10 cm and 10–20 cm soil depth) (Fig. 5). In the top soil at 0–10 cm depth, factor 1 explained 58.40% of the total variability and was related to SOC, TN, DOC, AK, AN, MBC, MBN, catalase, alkaline phosphatase and urease activity. Factor 2 described only 13.84% of the total variance among the BD, pH, and TK values. A similar result of PCA analysis was also shown at 10–20 cm soil depth (Fig. 5b), where factor 1 represented almost all the changes in the chemical and biological properties of the soil. The results indicated that soil nutrients and the biological activity of the sand soils were improved together during desertified land revegetation. Moreover, the plot of PCA (Fig. 5) clearly identified variations of physicochemical properties and biological activities among the sites along a chronosequence of desertified land revegetation. The profiles of physicochemical properties and biological activities at the 20-, 30- and 51-year-old sites were clearly separated from each other. These factors discriminated among both soil depths and the restoration age of the vegetation showed that these parameters had been seriously affected by restoration. The relationships between soil physicochemical variables (i.e., BD, pH, TN, TP, TK, AN, AP, AK, SOC, DOC and C:N) and the

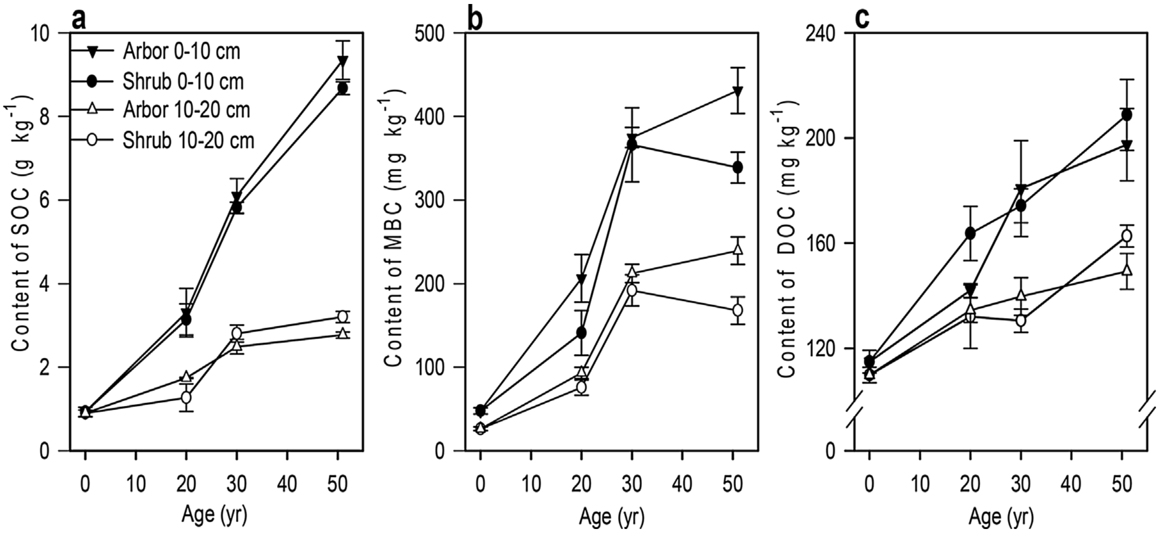

Fig. 2. Changes of organic carbon (a), microbial biomass carbon (b) and dissolved organic carbon (c)in soil with 20, 30, 51 years of shrub and arbor establishment on desertified land.

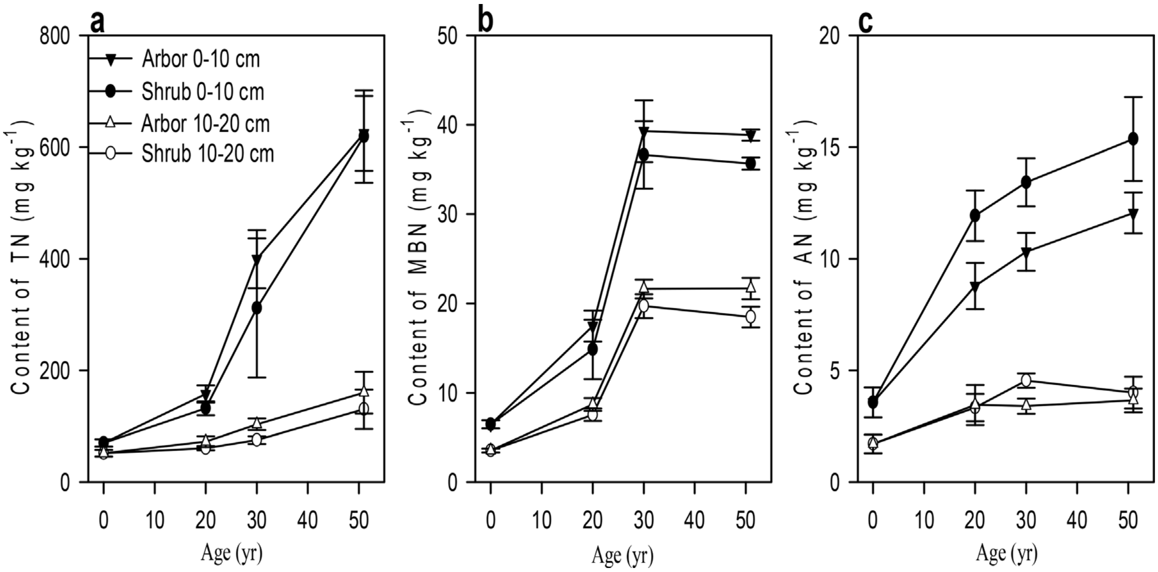

Fig. 3. Changes of total nitrogen (a), microbial biomass nitrogen (b) and available nitrogen (c) in soil with 20, 30, 51 years of shrub and arbor establishment on desertified land.

microbial biomass and enzyme activities were also examined based on redundancy analysis (Fig. 6). RDA showed that those variables significantly affected soil microbial biomass and enzyme activities in the 0–10 cm and 10–20 cm soil layers and together explained 83.14% and 77.64% of the total variation, respectively, especially for SOC, DOC and TN. Moreover, the soil microbial biomass and enzyme activities were positively correlated with the changes of SOC, DOC and TN and negatively correlated with BD, pH and TK.

4. Discussion

4.1. Dynamics of soil microbial biomass and enzyme activities

The soil microbial biomass and all enzyme activities in both soil layers (0–10 cm and 10–20 cm) greatly increased (by 1.58–5.59 times and 0.78–2.76 times in the shrub forest land, respectively) during the 20–50 years of revegetation at the Mu Us Sand Land, whereas they increased by 2.27–6.63 times and 1.58–7.29 times in the arbor forest

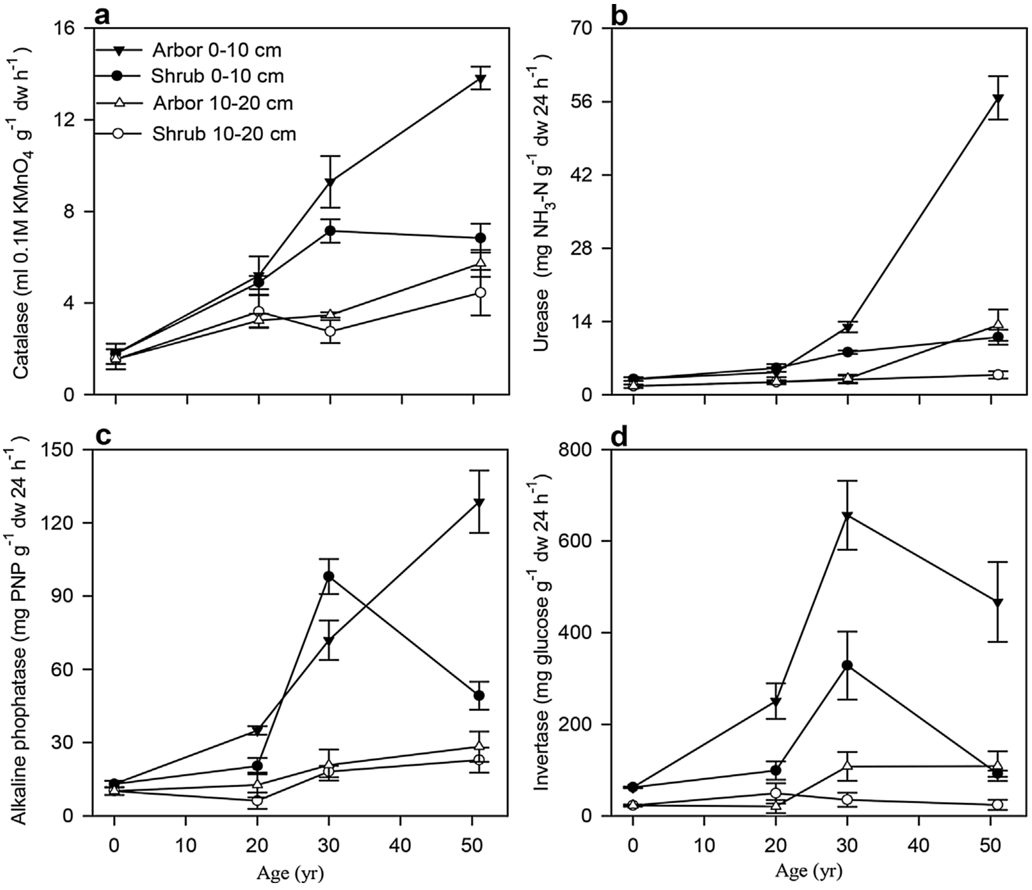

Fig. 4. Changes of soil enzyme activities (catalase (a), urease (b), alkaline phosphatase (c) and invertase (d)) with 20, 30 and 51 years of shrub and arbor establishment on desertified land.

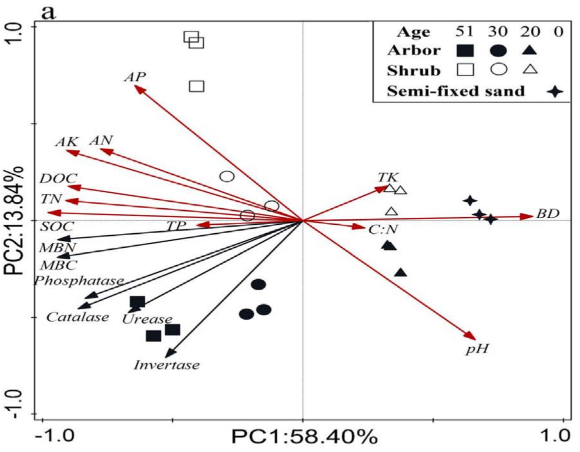

0-10cm

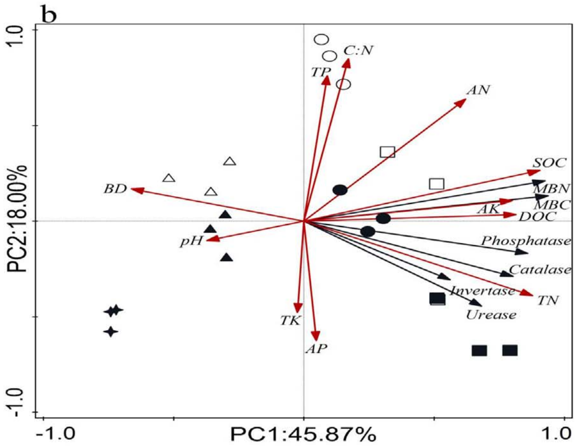

10-20cm

Fig. 5. Principal components analysis (PCA) of soil basic physicochemical characters and biological properties in the 0–10 cm soil layer (a) and 10–20 cm soil layer (b) with 20, 30 and 51 years of restoration and semi-fixed sand. TP (total phosphorus); AP (available phosphorus); TK (total potassium); AK (available potassium); C:N (total carbon/nitrogen ratio); BD (bulk density); SOC (soil organic carbon); MBC (microbial biomass carbon); DOC (dissolved organic carbon); TN (total nitrogen); MBN (microbial biomass nitrogen); AN (available nitrogen); Phosphatase (alkaline phosphatase).

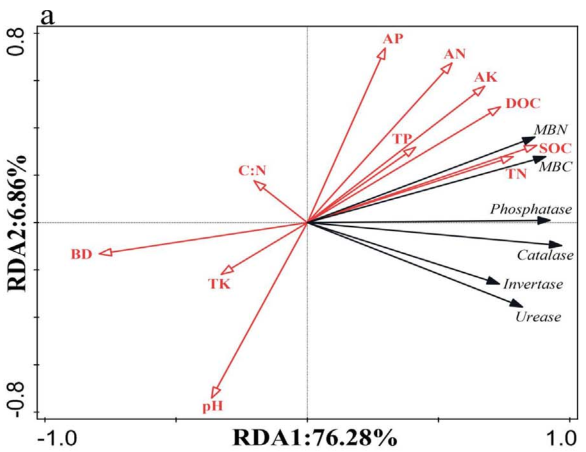

0-10cm

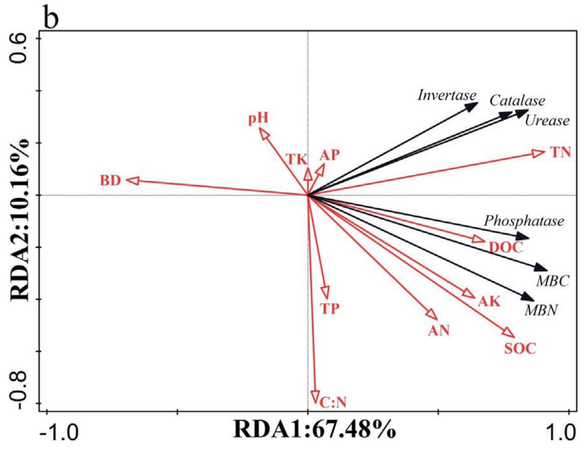

10-20cm

Fig. 6. Redundancy analysis (RDA) of soil basic physicochemical characters and biological properties in the 0–10 cm soil layer (a) and 10–20 cm soil layer (b) with 20, 30 and 51 years of restoration and semi-fixed sand. Ordination plots of the results from the RDA identifythe relationships among the soil biological properties (black arrows) and soil physicochemical characters (red arrows). TP (total phosphorus); AP (available phosphorus); TK (total potassium); AK (available potassium); C:N (total carbon/nitrogen ratio); BD (bulk density); SOC (soil organic carbon); MBC (microbial biomass carbon); DOC (dissolved organic carbon); TN (total nitrogen); MBN (microbial biomass nitrogen); AN (available nitrogen); Phosphatase (alkaline phosphatase). (For interpretation of the references to color in this figure legend, the reader is referred to the web version of this article).

land, respectively, compared with the semi-fixed sand land (Figs. 2b, 3b and 4). Cao et al. (2008) reported that sampling sites of 5, 10, and 23 years after *Caragana microphylla* Lam. revegetation showed an amelioration of plant leaf deposition and degradation, net primary productivity and electrical conductivity, thereafter gradually increased soil enzymatic activities, nutrients and microbial biomass. Additionally, Su et al. (2005) reported that the activities of catalase, urease, phosphatase in soils increased with time under progressive vegetation restoration in the Horqin sandy land of Northeast China. Moreover, several earlier scientists reported that vegetation restoration over time improved the important enzymatic activities, such as polyphenol oxidase, dehydrogenase, urease, protease, alkaline phosphatase and phosphomonoesterase (Dick et al., 1996; Consuelo and Teodoro, 2002; Nannipieri et al., 2002), which increased with time after vegetation restoration because of the C and N input from vegetation into the soil (Kaur et al., 2002). In this study, the vegetation reconstruction could elevate the soil MBC and MBN, which in turn raised the activities of soil catalase, urease, alkaline phosphatase and invertase. Several researchers have reported that increased soil microbial biomass and enzyme activities could be due to enhanced organic matter input and C and N immobilization during the process of organic matter decomposition (Plaza et al., 2004; Cao et al., 2008; Zhang et al., 2015). Consequently, earlier researchers also reported that revegetation had a strong impact on the alteration of C and N storage in bulk soil and increased soil particle-size fractions during a soil restoration time sequence measured at 3, 8, 20, 24 and 28 years from planting (He et al., 2009), which is consistent with our results. Meanwhile, the contents of SOC, DOC, TN and AN at both soil depths gradually increased along a chronosequence of 20, 30, and 51 years of desertified land revegetation.

Additionally, Petr et al. (2008) noticed that the microbial biomass increased when organic C and N were supplied to soil in the form of residues or roots. Normally, the microbial biomass growth depended on organic input, which is collectively involved to increase the bio-availability of C and N in sandy soil. Overall, the availability of organic inputs increased because of revegetation, and more enzymes were synthesized as soil microorganisms were enhanced (An et al., 2009). In this study area, the nutrient contents were increased during the process of revegetation in both soil layers by gradual litter deposition, which then changed the soil physicochemical properties such as pH and other nutrients contents (TP, AP, TK, AK and TN) (Table 2). Cao et al. (2008) reported that a chronosequence of *Caragana microphylla* Lam. plantations in the Horqin sandy land of Northeast China induced an increased input of plant residues into soil, which played a significant role in the enhancement of nutrient cycling and microbiological productivity in the tree-based systems. In general, our results demonstrated that soil microbial biomass, enzyme activities and soil nutrients were strongly altered by revegetation restoration in the arid Mu Us Sandy Land soils.

The soil nutrient content, microbial biomass and the activities in the four studied enzymes were significantly ($P < 0.001$) higher in the 0–10 cm soil layers than in the 10–20 cm layers. Similar results were widely observed by Chen (2003) and Sardans and Peñuelas (2005). Zaman et al. (2002) also observed that enzyme activities decreased in forest and agricultural soil profiles when there were organic inputs to the soil surface. The higher soil nutrient content, microbial biomass and enzyme activities in the soil upper surface layer (0–10 cm) in the plantations were probably because of the asymmetrical inputs of litter throughout the upper soil profile together with better soil aeration, which was attributed to the improved soil physical environment and the increased organic and inorganic materials released from plants. Consequently, the contents of SOC, TN, soil enzyme activities and microbial biomass in the arbor land were higher than those of shrub land, which was mainly related to higher litter inputs in the arbor land during the process of vegetation reconstruction. On the other hand, the carbon/nitrogen ratio (72) of the litter in the arbor land was significantly higher than in the shrub land (31); the microorganisms were relatively easy to decompose and used litter with low carbon/nitrogen ratios, which resulted in the accumulation of more organic matter in the arbor forest land and thus promoted the increase of soil microbial biomass and enzyme activity.

However, the soil MBC, MBN contents and enzyme activities in the 30–51 years recovery period remained stable or were enhanced in the arbor land, whereas they were reduced in the shrub land. The shrub apparently began to die with increasing age after 30 years, whereas in the case of the arbor, the biodiversity of the forest was reduced after the 30 years growth period (Table 1); the input of soil biomass decreased, which then resulted in the reduced microbial biomass and enzyme activities (Dang et al., 2003). Previous studies have shown that biodiversity has a significant correlation with soil microbial biomass and enzyme activity (Zhong and Han, 1999; Yang et al., 2001). Wang (2009) also reported that the activities of urease and phosphatase were positively correlated with biodiversity. Therefore, the revegetation process in the Mu Us Sandy land should update the shrub forest and increase the biodiversity under the arbor land for the continuous improvement of soil biological properties.

4.2. *The interaction between soil microbial biomass, enzyme activities and soil physicochemical properties*

Soil microbial biomass and enzyme activities in sandy land can generally be influenced by many physicochemical factors (e.g., season, geographic condition, soil depth, and anthropogenic factors (O_2 availability, pH, moisture content and nutrients content) because these factors could simultaneously influence the growth of soil microbes (Zhou et al., 2005). Soil microbial biomass and enzyme activities are closely related to soil nutrient transformations and soil fertility in rehabilitated sandy soils (Consuelo and Teodoro, 2002). The PCA results (Fig. 5) confirmed that most of the physicochemical and biological properties were influenced by the revegetation and showed coordinated variation between the analyzed parameters. On the other hand, the RDA (Fig. 6) showed that soil microbial biomass and enzyme activities were significantly correlated with the changes in soil physicochemical properties at both soil depths; they were positively correlated with SOC, DOC and TN but were negatively correlated with BD, pH and TK. Similar results were widely observed by Cao et al. (2008) and Zhang et al. (2015). In this study, urease and invertase are important functional hydrolyses enzymes that are directly related to carbon and nitrogen. Total nitrogen can increase the biomass of above-ground and underground roots and promote the growth of rhizosphere microorganisms, which then increases the activity of related enzymes in soil. Additionally, SOC can change soil porosity, air permeability and soil aggregate structure, which are collectively involved in buffering the soil and increasing the water holding capacity, which is an important carrier of various enzymes and provides suitable conditions for the soil enzymes. Subsequently, DOC is active soil organic matter that is easily decomposed by soil microbes and that plays an important role to improve soil nutrients, microbial biomass and enzyme activities. Consequently, Baldrian (2008) revealed that soil microbial biomass and enzyme activities were closely related to the contents of C and N in the soil.

Moreover, a previous study reported that the microbial biomass-related properties correlated with the content of organic C (Frouz and Nováková, 2005). In fact, the effects of microbial biomass, enzyme activity and soil nutrients have significant correlation because soil enzymes enhance macromolecular organic hydrolysis and then increase the contents of carbon and nitrogen. In summary, soil microbial biomass, enzyme activity and nutrient contents synergistically increased during the revegetation of desertified land, and SOC, DOC and TN were the key factors that enhanced soil biological activity.

5. Conclusions

The revegetation by establishment of shrub and arbor plantations on the Mu Us Sandy land, China, resulted in significant improvement in soil microbial biomass and enzyme activities, especially in the 0–10 cm layer, which was closely related to the increase of SOC, DOC, TN, TP, AN, AP and AK and the decrease of pH and soil bulk density. The significant increase of SOC, DOC and TN in the soil provided a source of carbon and nitrogen for the growth of microorganisms, which significantly increased the microbial biomass and then promoted the enzymes activities. Therefore, SOC, TN and DOC were the key factors that enhanced soil biological activity during the revegetation of desertified land. However, the soil MBC, MBN and enzyme activities in the 30–51 years recovery period tended to a stable state in the arbor land, whereas they decreased in the shrub land, which was related to the biodiversity of the forest; the biodiversity was reduced after 30 years of growth and the shrub began to die with increasing age after 30 years. Therefore, the revegetation process in the Mu Us Sandy land should update the shrub forest and increase the biodiversity in the arbor land for the continuous improvement of soil biological properties. Additionally, the soil enzyme activities and microbial biomass in the arbor land were higher than in the shrub land, which indicates that revegetation by the establishment of arbor plantations is a more effective and suitable measure to restore surface vegetation and soil biological properties and control desertification in the Mu Us Sandy land.

Acknowledgments

The authors are grateful for the financial support from National Natural Science Foundation of China (41301602), and the Fundamental Research Funds of the Central Universities (2452017105). We are also thanks to our all laboratory colleagues and research staff members for their constructive advice and help.

References

An, S.S., Huang, Y.M., Zheng, F.L., 2009. Evaluation of soil microbial indices along a revegetation chronosequence in grassland soils on the Loess Plateau, Northwest China. Appl. Soil Ecol. 41, 286–292.

Baldrian, P., 2008. Enzymes of Saprotrophic Basidiomycetes. In: Boddy, L., Frankland, J., van West, P. (Eds.), Academic Press, New York, pp. 19–41 (Ecol. Saprot Basidio).

Bolling, J.D., Walker, L.R., 2000. Plant and soil recovery along a series of abandoned desert roads. J. Arid Environ. 46, 1–24.

Cai, L.J., Xu, Y.G., Yu, W.T., 2013. Effects of continuous planting poplar on the soil nutrient contents, microbial biomass, and enzyme activities in lower reaches of Liaohe River Plain, Northeast China. Chin. J. Ecol. 32, 337–343 (in Chinese with English abstract).

Cao, C., Jiang, D., Teng, X., Jiang, Y., Liang, W., Cui, Z., 2008. Soil chemical and microbiological properties along a chronosequence of *Caragana microphylla* Lam. plantations in the Horqin sandy land of Northeast China. Appl. Soil Ecol. 40, 78–85.

Cao, C., Jiang, S., Ying, Z., Zhang, F., Han, X., 2011. Spatial variability of soil nutrients and microbiological properties after the establishment of leguminous shrub *Caragana microphylla* Lam. plantation on sand dune in the Horqin Sandy Land of Northeast China. Ecol. Eng. 37, 1467–1475.

Chen, H., 2003. Phosphatase activity and P fractions in soils of an 18-year-old Chinese fir (*Cunninghamia lanceolata*) plantation. For. Ecol. Manage. 178, 301–310.

Cheng, S.L., Ouyang, H., Niu, H.S., Wang, L., Zhang, F., Gao, J.Q., Tian, Y.Q., 2004. Spatial and temporal dynamics of soil organic carbon in reserved desertification area. Chin. Geogr. Sci. 14, 245–250.

Consuelo, Q., Teodoro, M., 2002. Dehydrogenase activity in Mediterranean forest soils. Biol. Fertil. Soils. 35, 102–107.

Cui, X.X., 2011. Study on Soil Biological Properties in Vegetation Restoration in Karst Region Master Thesis. Nanjing Forestry University, Nanjing.

Dai, Z., 2010. Intensive agropastoralism: dryland degradation, the Grain-to-Green Program and islands of sustainability in the Mu Us Sandy Land of China. Agric. Ecosyst Environ. 138, 249–256.

Dang, B., Sun, Z., Sun, Y., Zhao, X., 2003. Formation and succession of artificial plant community in Yulin Sandy Land. Inner Mongolia For. Sci. Technol. 2, 10–14 (in Chinese with English abstract).

Dick, R.P., Breakwell, D.P., Turco, R.F., 1996. Soil enzyme activities and biodiversity measurements as integrative microbiological indicators. Methods for Assessing Soil Quality. SSSA, Madison, pp. 247–272.

Frouz, J., Nováková, A., 2005. Development of soil microbial properties in topsoil layer during spontaneous succession in heaps after brown coal mining in relation to humus microstructure development. Geoderma 129, 54–64.

Fterich, A., Mahdhi, M., Mars, M., 2012. Impact of grazing on soil microbial communities along a chronosequence of Acacia tortilis subsp raddiana in arid soils in Tunisia. Eur. J. Soil Biol. 50, 56–63.

He, N., Wu, L., Wang, Y., Han, X., 2009. Changes in carbon and nitrogen in soil particle-size fractions along a grassland restoration chronosequence in northern China. Geoderma 150, 302–308.

Hu, N., Li, H., Tang, Z., Li, Z., Li, G., Jiang, Y., Hu, X., Lou, Y., 2016. Community size, activity and C: N stoichiometry of soil microorganisms following reforestation in a Karst region. Eur. J. Soil Biol. 73, 77–83.

Jenkinson, D.S., Powlson, D.S., 1976. The effects of biosidal treatments on metabolism in soil: a Method for measuring soil biomass. Soil Biol. Biochem. 8, 209–213.

Kandeler, E., Gerber, H., 1988. Short-term assay of soil urease activity using colorimetric determination of ammonium. Biol. Fert Soil. 6, 68–72.

Kaur, B., Gupta, S.R., Singh, G., 2002. Carbon storage and nitrogen cycling in silvopastoral systems on a sodic soil in northwestern India. Agrofor. Syst. 54, 21–29.

Keeney, D.R., 1982. Nitrogen—Availability indices. methods of soil analysis. part. Chem. Microbiol. Prop. 711–733.

Li, W., Yu, L.J., Li, T., Xiang, J., 2008. Seasonal and spatial dynamics of soil enzyme activities and its relationship to soil fertility in karst ecosystem–a case study of Guilin Yaji karst experimental site. J Agro-Environ. Sci. 27, 260–266.

Liu, J., Diamond, J., 2005. China's environment in a globalizing world. Nature 435, 1179–1186.

Liu, Z.F., Liu, G.H., Fu, B.J., Hu, H.F., Zheng, X.X., Wu, Y.Q., 2007. Dynamics of soil microbial biomass C, N along restoration chronosequences in pine plantations. Acta Ecol. Sin. 27, 1011–1018.

Lu, L., Huggins, T., Jin, S., Zuo, Y., Ren, Z.J., 2014. Microbial metabolism and community structure in response to bioelectrochemically enhanced remediation of petroleum hydrocarbon-contaminated soil. Environ. Sci. Technol. 48, 4021.

Nannipieri, P., Kandeler, E., Ruggiero, P., Burns, R.G., Dick, R.P., 2002. In: Burns, R.G., Dick, R. (Eds.), Enzyme Activities and Microbiological and Biochemical Processes in Soil. CRC Press. http://books.google.it/books?id=kuWv6ovE4qoC.

Nunes, J.S., Araujo, A.S.F., Nunes, L.A.P.L., Lima, L.M., Carneiro, R.F.V., Salviano, A.A.C., Tsai, S.M., 2012. Impact of land degradation on soil microbial biomass and activity in Northeast Brazil. Pedosphere 22, 88–95.

Petr, B., Josef, T., Jan, F., Jaroslav, S., Vendula, V., Vera, M., Cajthaml, T., Jana, H., 2008. Enzyme activities and microbial biomass in topsoil layer during spontaneous succession in spoil heaps after brown coal mining. Soil Biol. Biochem. 40, 2107–2115.

Plaza, C., Hernández, D., García-Gil, J.C., Polo, A., 2004. Microbial activity in pigslurry-amended soils under semiarid conditions. Soil Biol. Biochem. 36, 1577–1585.

Qi, L., Fan, S., Ai, W., Liu, G., Meng, Y., Du, M., Tang, X., 2012. Effects of Phyllostachy edulis and Cunninghamia lanceolata mixed forests on soil qualities in the hilly region, central Hunan. J. Mt. Sci. 30, 314–320.

Sardans, J., Peñuelas, J., 2005. Drought decreases soil enzyme activity in a Mediterranean Quercus ilex L forest. Soil Biol. Biochem. 37, 455–461.

Sardans, J., Peñuelas, J., Ogaya, R., 2008. Experimental drought reduced acid and alkaline phosphatase activity and increased organic extractable P in soil in a Quercus ilex Mediterranean forest. Eur. J. Soil Biol. 44, 509–520.

Su, Y.Z., Li, Y.L., Cui, J.Y., Zhao, W.Z., 2005. Influences of continuous grazing and livestock exclusion on soil properties in a degraded sandy grassland Inner Mongolia northern China. Catena 59, 267–278.

Taylor, J.P., Wilson, B., Mills, M.S., Burns, R.G., 2002. Comparison of microbial numbers and enzymatic activities in surface and subsoils using various techniques. Soil Biol. Biochem. 34, 387–401.

Wang, B., Liu, G.B., Xue, S., 2010. Effects of soil nutrient and soil microbial biomass on soil enzyme activities in abandoned croplands with different restoration age. China Environ Sci. 30, 1375–1382.

Wang, Q., Xia, J.B., Zhang, J.C., Zhang, J., Liu, J.T., 2012. Soil enzyme activities and nutrient charateristics of different improving patterns in the Yellow river Delta area. J. Soil Water Conserv. 26, 133–137 (in Chinese with English abstract).

Wang, Y.C., 2009. Study of Various Vegetative Restoration Patterns on Species Diversity and Soil Nutrients and Creature Factors in Iron Tailings Master Thesis. Agricultural University of Hebei, Hebei.

Wei, Y., Yu, L.F., Zhang, J.C., Yu, Y.C., Deangelis, D.L., 2011. Relationship between vegetation restoration and soil microbial characteristics in degraded Karst regions. A case study. Pedosphere 21, 132–138.

Yang, W.Q., Zhong, Z.C., Tao, J.P., He, W.M., 2001. Study on relationship between soil enzymic activities and plant species diversity in forest ecosystem of Mt. Jinyun. Sci. Silvae Sin. 37, 124–128 (in Chinese with English abstract).

Yang, Q., Qin, Z.H., Wang, T., Wang, Q.Q., 2012. Characteristics of climate factor change in Yulin Region during 1970–2010. Arid Land Geogr. 35, 695–707.

Ye, S., Yang, Y., Xin, G., Wang, Y., Lin, R., Ye, G., 2015. Studies of the Italian ryegrass–rice rotation system in southern China: arbuscular mycorrhizal symbiosis affects soil microorganisms and enzyme activities in the Lolium mutiflorum L. rhizosphere. Appl. Soil Ecol. 90, 26–34.

Zaman, M., Cameron, K.C., Di, H.J., Inubushi, K., 2002. Changes in mineral N, microbial biomass and enzyme activities in different soil depths after surface applications of dairy shed effluent and chemical fertilizer. Nutr. Cycl. Agroecosyst. 63, 275–290.

Zhang, Z.S., Liu, L.C., Li, X.R., Zhang, J.G., He, M.Z., Tan, H.J., 2008. Evaporation properties ofa revegetated area of the Tengger Desert, North China. J. Arid Environ. 72, 964–973.

Zhang, Y.L., Chen, L.J., Chen, Z.H., Sun, C.X., Wu, Z.J., Tang, X.H., 2010. Soil nutrient contents and enzymatic characteristics as affected by 7-year no tillage under maize cropping in a meadow brown soil. J. Soil Sci. Plant Nutr. 10, 150–157.

Zhang, H., Li, G., Song, X., Yang, D., Li, Y., Qiao, J., Zhang, J., Zhao, S., 2013. Changes in soil microbial functional diversity under different vegetation restoration patterns for Hulunbeier Sandy Land. Acta Ecol. Sin. 33, 38–44.

Zhang, Y.L., Chen, L.J., Chen, X.H., Tan, M.L., Duan, Z.H., Wu, Z.J., Li, X.J., Fan, X.H., 2015. Response of soil enzyme activity to long-term restoration of desertified land. Catena 133, 64–70.

Zhong, Z., Han, Y., 1999. Study on the distribution characteristics and seasonal dynamics of forest soil enzymatic activities and its relations with Gordonia Acuminata on Mt.Jinyun. J. Southwest China Normal Univ. 24 (3), 318–324 (in Chinese with English abstract).

Zhou, Q.H., Wu, Z.B., Cheng, S.P., He, F., Fu, G.P., 2005. Enzymatic activities in constructed wetlands and di-n-butyl phthalate (DBP) biodegradation. Soil Biol. Biochem. 37, 1454–1459.

Zuo, X., Zhao, X., Zhao, H., Zhang, T., Guo, Y., Li, Y., Huang, Y., 2009. Spatial heterogeneity of soil properties and vegetation-soil relationships following vegetation restoration of mobile dunes in Horqin Sandy Land. North. China Plant Soil 318, 153–167.

This article was downloaded by: [113.139.32.157]
On: 22 July 2015, At: 07:48
Publisher: Taylor & Francis
Informa Ltd Registered in England and Wales Registered Number: 1072954 Registered office: 5 Howick Place, London, SW1P 1WG

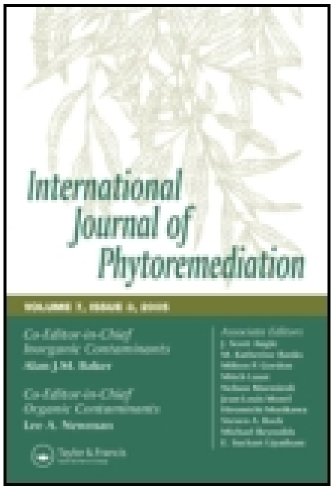

Click for updates

International Journal of Phytoremediation
Publication details, including instructions for authors and subscription information:
http://www.tandfonline.com/loi/bijp20

Effects of Phosphate on Arsenate Uptake and Translocation in Nonmetallicolous and Metallicolous Populations of Pteris Vittata L. Under Solution Culture

Fuyong Wu[ab], Shengchun Wu[c], Dan Deng[b] & Ming Hung Wong[bc]

[a] Key Laboratory of Plant Nutrition and the Agri-environment in Northwest China, Ministry of Agriculture, and College of Natural Resources and Environment, Northwest A&F University, Yangling, Shaanxi, PR China

[b] Croucher Institute for Environmental Sciences, and Department of Biology, Hong Kong Baptist University, Kowloon Tong, Hong Kong SAR, PR China

[c] School of Environmental and Resource Sciences, Zhejiang Agricultural and Forestry University, Linan, Zhejiang, PR China

Published online: 17 Jun 2015.

To cite this article: Fuyong Wu, Shengchun Wu, Dan Deng & Ming Hung Wong (2015) Effects of Phosphate on Arsenate Uptake and Translocation in Nonmetallicolous and Metallicolous Populations of Pteris Vittata L. Under Solution Culture, International Journal of Phytoremediation, 17:9, 841-846, DOI: 10.1080/15226514.2014.964848

To link to this article: http://dx.doi.org/10.1080/15226514.2014.964848

PLEASE SCROLL DOWN FOR ARTICLE

Taylor & Francis makes every effort to ensure the accuracy of all the information (the "Content") contained in the publications on our platform. However, Taylor & Francis, our agents, and our licensors make no representations or warranties whatsoever as to the accuracy, completeness, or suitability for any purpose of the Content. Any opinions and views expressed in this publication are the opinions and views of the authors, and are not the views of or endorsed by Taylor & Francis. The accuracy of the Content should not be relied upon and should be independently verified with primary sources of information. Taylor and Francis shall not be liable for any losses, actions, claims, proceedings, demands, costs, expenses, damages, and other liabilities whatsoever or howsoever caused arising directly or indirectly in connection with, in relation to or arising out of the use of the Content.

This article may be used for research, teaching, and private study purposes. Any substantial or systematic reproduction, redistribution, reselling, loan, sub-licensing, systematic supply, or distribution in any form to anyone is expressly forbidden. Terms & Conditions of access and use can be found at http://www.tandfonline.com/page/terms-and-conditions

International Journal of Phytoremediation, 17: 841–846, 2015
Copyright © Taylor & Francis Group, LLC
ISSN: 1522-6514 print / 1549-7879 online
DOI: 10.1080/15226514.2014.964848

Effects of Phosphate on Arsenate Uptake and Translocation in Nonmetallicolous and Metallicolous Populations of *Pteris Vittata* L. Under Solution Culture

FUYONG WU[1,2], SHENGCHUN WU[3], DAN DENG[2], and MING HUNG WONG[2,3]

[1]*Key Laboratory of Plant Nutrition and the Agri-environment in Northwest China, Ministry of Agriculture, and College of Natural Resources and Environment, Northwest A&F University, Yangling, Shaanxi, PR China*
[2]*Croucher Institute for Environmental Sciences, and Department of Biology, Hong Kong Baptist University, Kowloon Tong, Hong Kong SAR, PR China*
[3]*School of Environmental and Resource Sciences, Zhejiang Agricultural and Forestry University, Linan, Zhejiang, PR China*

An arsenic hyperaccumulator, *Pteris vittata* L., is common in nature and could occur either on As-contaminated soils or on uncontaminated soils. However, it is not clear whether phosphate transporter play similar roles in As uptake and translocation in nonmetallicolous and metallicolous populations of *P. vittata*. Five populations were used to investigate effects of phosphate on arsenate uptake and translocation in the plants growing in 1.2 L 20% modified Hoagland's nutrient solution containing either 100 μM phosphate or no phosphate and 10 μM arsenate for 1, 2, 6, 12, 24 h, respectively. The results showed that the nonmetallicolous populations accumulated apparently more As in their fronds and roots than the metallicolous populations at both P supply levels. Phosphate significantly ($P < 0.01$) decreased frond and root concentrations of As during short time solution culture. In addition, the effects of phosphate on As translocation in *P. vittata* varied among different time-points during time-course hydroponics (1–24 h). The present results indicated that the inhibitory effect of phosphate on arsenate uptake was larger in the three nonmetallicolous populations than those in the two metallicolous populations of *P. vittata*.

Keywords: Chinese brake fern, population variation, phytoremediation, As-contaminated soils

Introduction

Most hyperaccumulators are generally endemic to metalliferous soils, whereas some are also present on non-metalliferous soils (Assuncao, Schat and Aarts 2003). In some of these, the hyperaccumulation is a constitutive trait at species level, as shown in *Thlaspi caerulescens* (Assuncao *et al.* 2003) and *Arabidopsis halleri* (Bert *et al.* 2002) for Zn hyperaccumulation. In others, either Cd hyperaccumulation in *T. caerulescens* or Zn hyperaccumulation in *Sedum alfredii* is not a constitutive trait at species level, but only confined to metallicolous populations (those collected from metalliferous soils) (Assuncao *et al.* 2003; Yang *et al.* 2006). Escarre *et al*. (2013) also indicated that depending on the substrate used in the experiments, there was a large heterogeneity of responses to uptake of Zn, Ni and Cd among 18 populations of *T. caerulescens* from metalliferous, non metalliferous and serpentine soils. Moreover, *Pteris vittata* L. has received increasing attention due to its remarkable capacity for As hyperaccumulation (up to 2.3% in its fronds) since its identification (Ma *et al.* 2001). *P. vittata* can live either on As-contaminated soils (Ma *et al.* 2001; Chen *et al.* 2002; Wang *et al.* 2006) or on uncontaminated soils (Wang *et al.* 2007; Wu *et al.* 2014). It has been revealed that As hyperaccumulation is a constitutive property in *P. vittata* (Zhao, Dunham and McGrath 2002; Wang *et al.* 2007). Wu *et al.* (2009) further showed that nonmetallicolous populations (those collected from uncontaminated soils) of *P. vittata* possess more effective As hyperaccumulation than metallicolous populations,indicating that the former has great potential as appropriate candidature for phytoextraction of As from contaminated soils. Unfortunately, it is still not clear the mechanisms underlying variation in As hyperaccumulation among the nonmetallicolous and metallicolous populations of *P. vittata*, although this is vital for breaking through towards commercially attractive phytoextraction applications.

For almost all plants tested so far, including *P. vittata*, arsenate is taken up via phosphate transporters (Abedin, Feldmann and Meharg 2002; Wang *et al*. 2002; Poynton *et al.* 2004). Bleeker *et al.* (2003) found that mine population of *Cytisus striatus* from an As-enriched gold mine reduced arsenate uptake through the suppression of phosphate transporter activity compared with population from a nonmetalliferous site. Similarly, some plants from As-contaminated soils reduced uptake of As through suppression of the high-affinity

---

Address correspondence to Fuyong Wu, Key Laboratory of Plant Nutrition and the Agri-environment in Northwest China, Ministry of Agriculture, and College of Natural Resources and Environment, Northwest A&F University, Yangling, Shaanxi, PR China. E-mail: wfy09@163.com

phosphate uptake system (Meharg and Hartley-Whitaker 2002). Our preliminary investigation showed that the nonmetallicolous population of *P. vittata* had a greater capacity for uptake of P, which may result in significantly greater As concentrations in fronds and roots than those in the metallicolous populations (Wu *et al.* 2009). Wang *et al.* (2013) also observed that high As accumulation was observed in the populations of *P. vittata* at the low habitat As concentration, accompanied by efficient root As uptake. However, it is not clear whether phosphate transporter plays similar roles in As uptake and translocation in the nonmetallicolous and metallicolous populations of *P. vittata*.

The major objectives of the present study were to: (1) compare nonmetallicolous and metallicolous populations of *P. vittata* in terms of As uptake and translocation at different levels of P supply; and (2) assess effects of phosphate on arsenate uptake and translocation in the nonmetallicolous and metallicolous populations of *P. vittata*.

Materials and Methods

Collection of Spores of **P. vittata**

From November 2008 to February 2009, spores of *P. vittata* were collected from fertile fronds of 4–6 plants growing at As and Pb/Zn mining and/or smelting sites located in Dashunlong (DSL) and Yejiwei (YJW) of Hunan Province and at three uncontaminated sites [Tai Po Kau Nature Reserve, Hong Kong (HK), a botanical garden in Guangxi Academy of Forestry Sciences, Nanning City, Guangxi Province (NN) and Sun Yat-sen University campus, Guangdong Province (ZD)]. The spores were air-dried and reserved for the following plant culture. Total As, Pb, Zn, Cd and Cu concentrations in soils of the five sites were characterized in Wu *et al.* (2014). Both DSL and YJW were heavily contaminated by As (6,108-20,710 mg kg^{-1}), Pb (4,541-6,050 mg kg^{-1}) and Zn (4,799-9,523 mg kg^{-1}), while the corresponding metal concentrations at the three uncontaminated sites (HK, NN and ZD) were below the threshold of metal-contaminated soils (GB15618-1995).

Sporeling Culture

The spores of five populations of *P. vittata* (HK, NN, ZD, DSL and YJW) were germinated as described previously (Wu *et al.* 2009). Four month-old sporelings (with 3–4 fronds) of *P. vittata* were transplanted to polyethylene pots filled with 1.2 L 20% Hoagland's nutrient solution (Hoagland and Arnon 1938): 0.2 mM KH_2PO_4, 1.0 mM KNO_3, 1.0 mM $Ca(NO_3)_2·4H_2O$, 0.4 mM $MgSO_4·7H_2O$, 9 μM H_3BO_3, 1.8 μM $MnCl_2·4H_2O$, 0.15 μM $ZnSO_4·7H_2O$, 0.07 μM $CuSO_4·5H_2O$, 0.03 μM $H_2MoO·H_2O$, 4 μM Fe-EDTA. The pH of the nutrient solution was adjusted to 5.8 using dilute HCl or NaOH. The solution was aerated vigorously and renewed once every 4 days. Both spore germination and plant culture were performed in a greenhouse with temperature control (28/23°C, day/night). In addition to natural sunlight, a 12-h photon flux density of 380 μmol m^{-2} s^{-1} was supplied via an assembly of cool-white fluorescent lamps. After one month, the sporelings (with 5–7 fronds) were ready for subsequent experiments. There are little morphological difference among populations of *P. vittata*. Generally, vigorous growth were recorded in the three nonmetallicolous populations (HK, ZD and NN) of *P. vittata* compared with the two metallicolous populations (DSL and YJW).

Assessment of Phosphate on Arsenate Uptake and Translocation in Populations of **P. vittata** *Grown in Hydroponics*

The sporelings of the three nonmetallicolous populations of *P. vittata* and the two metallicolous populations were exposed to 10 μM arsenate ($Na_2HAsO_4·7H_2O$) for 1, 2, 6, 12, 24 h, respectively. Arsenate was added to the basal nutrient solution (20% modified Hoagland's nutrient solution) containing either 100 μM phosphate (+P) or no phosphate (−P). Potassium phosphate was replaced with potassium chloride in the −P treatment. The exposure to arsenate lasted for 24 h, from 09:00 (2 h after the light period started) to 09:00 next day. At each time-point, fronds were cut at the base of the stipe (*c.* 1 cm above the roots). The roots were separated from the fronds, rinsed with deionized water and incubated in an ice-cold, As-free medium [containing MES and $Ca(NO_3)_2$, and amended with 1 mM Na_2HPO_4] for 15 min to remove apoplastic As. There were four replicates for each treatment. The roots and fronds were blotted dry, weighed and oven-dried before being ground.

Chemical Analyses

Analyses of As concentrations in the plant tissues were conducted by digesting the plant tissues with an acid mixture [conc. HNO_3 + conc. $HClO_4$ (4:1, v/v)] and determined with Inductively Coupled Plasma – Mass Spectrometry (ICP-MS, Perkin–Elmer, Elan 9000). A standard reference, spinach leaves (SRM 1570a) from the U.S National Institute of Standards and Technology (NIST), was used to verify the accuracy of metal determination. The recovery rates for As were within 92 ± 9%.

Statistical Analysis

The translocation factor (TF) was expressed as the ratio of $[\text{As conc.}]_{\text{aboveground}}/[\text{As conc.}]_{\text{belowground}}$. The differences in plant biomass, As concentrations and As TF among populations of *P. vittata* were assessed using Fisher's protected least significant difference after ANOVA. All statistical procedures were carried out using SAS 8.1 software. Unless indicated otherwise, all treatment means were tested for significant difference at $P < 0.05$.

Results

Effects of Phosphate on As Concentrations in Populations of **P. vittata**

Regardless of nonmetallicolous or metallicolous populations of *P. vittata*, presence of phosphate in the uptake solution significantly ($P < 0.01$) decreased both frond and root

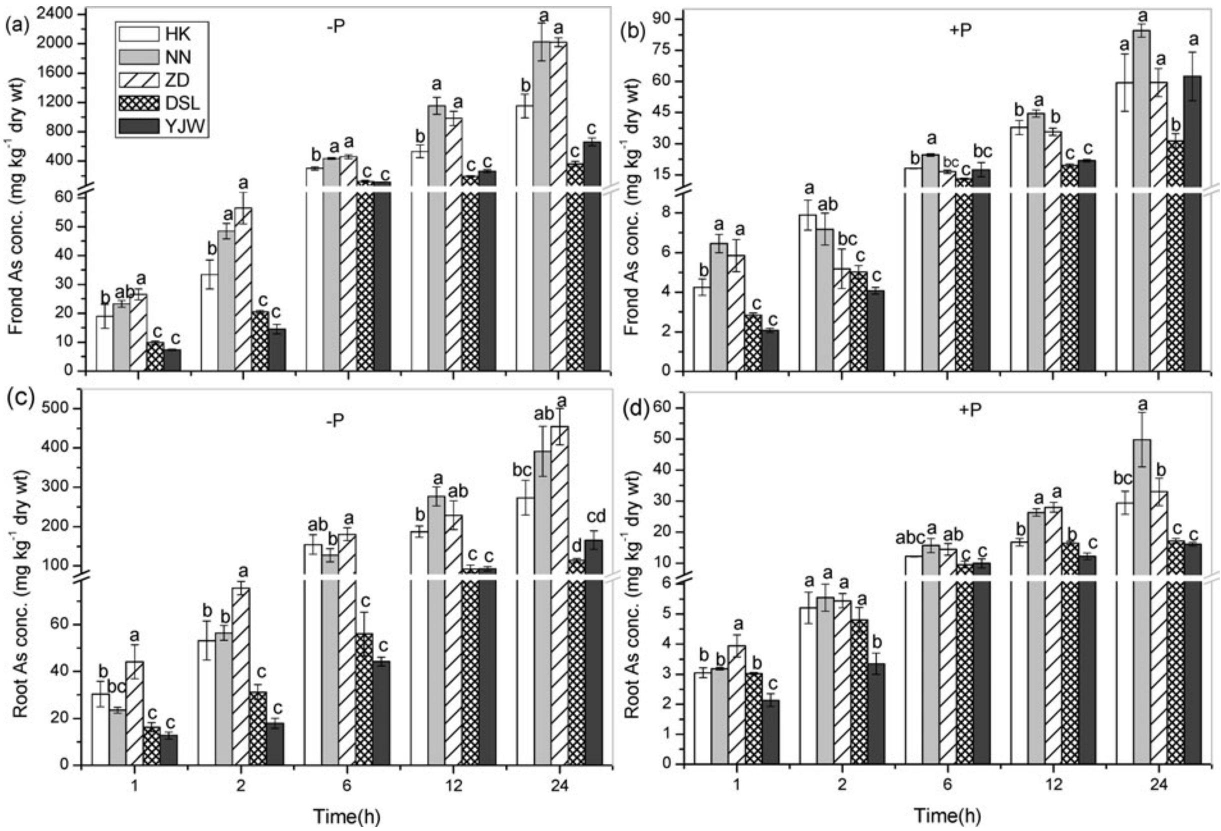

Fig. 1. Effects of phosphate [100 μM phosphate (+P) or no phosphate (−P)] on arsenic concentrations in fronds (**a, b**) and roots (**c, d**) of nonmetallicolous (HK, NN, and ZD) and metallicolous (DSL and YJW) populations of *Pteris vittata* L. growing in 20% Hoagland's nutrient solution containing 10 μM arsenate ($Na_2HAsO_4{\cdot}7H_2O$) for 1, 2, 6, 12, 24 h (mean ± S.E., n = 4).

concentrations of As during short time solution culture (Fig. 1, Table 1). Frond As concentration of *P. vittata* in the +P treatment were 22.0–29.0% and 4.2–9.4% of those in the −P treatment after 1 h and 24 h of exposure to arsenate, respectively. The inhibitory effect of phosphate on frond and root concentrations of As was larger in the three nonmetallicolous populations (HK, NN and ZD) than those in the two metallicolous populations (DSL and YJW). For example, presence of phosphate in the uptake solution decreased frond As concentration, on average, by 94.9% and 87.0% in the nonmetallicolous and metallicolous populations at 6 h, respectively. With solution culture time increasing, the inhibitory effect of phosphate on frond As concentrations increased steadily, but the effect on root As concentrations remained stable. In addition, at both P supply levels, the nonmetallicolous populations accumulated apparently more As in their fronds and roots than the metallicolous populations (Fig. 1). After 12 h of exposure to arsenate, As concentrations in fronds of the three non-

Table 1. Analysis of covariance frond As concentrations, root As concentrations, percent of frond As to total plant As and translocation factors of nonmetallicolous (HK,NN and ZD) and metallicolous populations (DSL and YJW) of *Pteris vittata* L. growing in nutrient solution containing 10 μM arsenate for 1,2,6,12, or 24 h

	Frond As conc.		Root As conc.		Percent of frond As to total plant As		Translocation factors (TF)	
	F	*P*	*F*	*P*	*F*	*P*	*F*	*P*
Phosphate treatment	813.03	<0.0001	647.97	<0.0001	3.01	0.08	82.20	<0.0001
Population	73.47	<0.0001	43.16	<0.0001	6.42	< 0.0001	10.93	<0.0001
P*Pop	67.55	<0.0001	32.68	<0.0001	1.12	0.35	7.69	<0.0001
Time	266.46	<0.0001	129.35	<0.0001	31.76	< 0.0001	124.70	<0.0001
P*Time	223.07	<0.0001	85.04	<0.0001	13.25	< 0.0001	47.47	<0.0001
Pop*Time	20.08	<0.0001	7.39	<0.0001	0.81	0.67	2.36	<0.01
P*Pop*Time	18.72	<0.0001	5.53	<0.0001	0.72	0.77	3.26	<0.0001

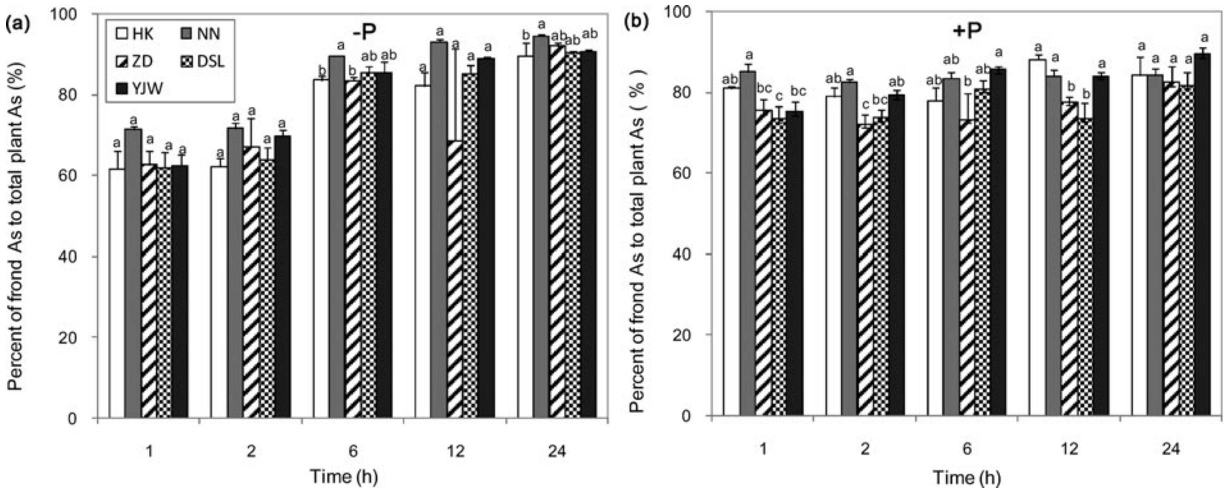

Fig. 2. Arsenic distribution in fronds of nonmetallicolous (HK, NN and ZD) and metallicolous (DSL and YJW) populations of *Pteris vittata* L. growing in 20% Hoagland's nutrient solution containing 10 μM arsenate ($Na_2HAsO_4 \cdot 7H_2O$) and 100 μM phosphate (−P) (**a**) or no phosphate (+P) (**b**) for 1, 2, 6, 12, 24 h, respectively (mean ± S.E., n = 4).

metallicolous populations were 3.9-times and 1.9-time higher than those in the two metallicolous populations at both P supply levels, respectively. At 24 h of exposure to arsenate, the highest As concentrations in fronds (2,025 and 84.6 mg kg^{-1}) were recorded in nonmetallicolous population (NN), while the lowest As concentrations in fronds (364 and 31.3 mg kg^{-1}) were recorded in metallicolous population (DSL) in the presence and absence of phosphate, respectively. This indicated that there were apparently variations in As concentrations among the nonmetallicolous and metallicolous populations and that the former had more effective capacity for As accumulation than the latter.

Influence of Phosphate on As Translocation and Distribution in Populations of P. vittata

The effects of phosphate in the uptake solution on As translocation in *P. vittata* varied in culture time (1–24 h) (Table 1 and Table 2). In detail, the presence of phosphate in the uptake solution significantly ($P < 0.05$) increased the translocation of As from roots to fronds at the early of the solution culture (1 and 2 h), but significantly ($p < 0.05$) decreased the translocation of As from roots to fronds at 12 and 24 h (Table 2). For example, As TFs of NN population were 4.18 and 5.30 in the presence of phosphate at 12 and 24 h, while the corresponding values were 1.70 and 1.93 in the absence of phosphate, respectively. In the +P treatment, on average, proportion of As (78%) taken up in the fronds of five populations was significantly ($P < 0.05$) higher than that (64%) in the −P treatment after 1 h of exposure to arsenate (Fig. 2). With culture time increasing, proportion of As taken up in the fronds increased steadily when no phosphate was supplied, but the proportion of As taken up in the fronds remained stable when phosphate was supplied, except for YJW populations. In addition, there was no significantly difference in As distribution between nonmetallicolous and metallicolous populations of *P. vittata*, regardless of presence of phosphate in the solution.

Discussion

Based on time-course hydroponics, the present study showed that there were apparently ecotypic variations in As uptake and translocations among five populations of *P. vittata* (Fig. 1). Regardless of the presence of phosphate in the solution, the three nonmetallicolous populations (HK, NN and ZD) exhibited higher As concentrations in fronds than the two metallicolous populations (DSL and YJW). In −P treatments, fond As concentrations up to 2,025 mg kg^{-1} recorded in the NN populations were 5.56 times of those in the DSL populations (364 mg kg^{-1}) at 24 h (Fig. 1). This is in line with our previous study based on pot trials (Wu *et al*. 2014). Intra-specific variation in Ni and Zn hyperaccumulation has also been shown in Ni-hyperaccumulator *Alyssum lesbiacum* (Adamidis *et al.* 2014) and in two Zn hyperaccumulators, *A. halleri* (Bert *et al.* 2000) and *T. caerulescens* (Assuncao *et al.* 2003b; Frerot *et al.* 2003), respectively. The present results suggested that selection of appropriate candidature for effective phytoremediation of As-contaminated soils should also be considered at the population level.

It is generally accepted that arsenate is taken up via phosphate transporters in almost all plants tested so far, including *P. vittata* (Abedin *et al.* 2002; Wang *et al*. 2002; Poynton *et al.* 2004). This means that arsenate and phosphate can compete for the same absorption sites in root apoplast and the same uptake carriers in root plasma membrane (Liu *et al.* 2004). This is further confirmed by a significantly ($P < 0.01$) inhibitory effect of phosphate on As accumulation by *P. vittata* in the present study (Fig. 1, Table 1). Previous studies also found apparent decrease of As uptake rates in roots of *P. vittata* with increasing P concentration in the solution (Poynton *et al.* 2004; Wang *et al.* 2002). It has been showed that arsenate influx in roots of *P. vittata* fitted well with Michaelis–Menten kinetics (Poynton *et al.* 2004; Lou, Ye and Wong 2009; Wu *et al.* 2014). Therefore, it can be concluded that the arsenate influx into roots of *P. vittata* is protein-mediated and arsenate binds active site.

Table 2. Effects of phosphate on translocation factors (TF) of nonmetallicolous (HK, NN and ZD)and metallicolous populations (DSLand YJW) of *Pteris vittata* L. growing in nutrient solution containing 10 μM arsenate for 1, 2, 6, 12 or 24 h (mean ± S.E., n = 4)

Time (h)	HK	NN	ZD	DSL	YJW
−P					
1	0.62 ± 0.11 cB	0.99 ± 0.03 cA	0.66 ± 0.11 cB	0.62 ± 0.04 cB	0.59 ± 0.05 cB
2	0.64 ± 0.04 cB	0.86 ± 0.04 cA	0.75 ± 0.09 cAB	0.68 ± 0.07 cAB	0.82 ± 0.05 cA
6	2.05 ± 0.23 bB	3.67 ± 0.62 bA	2.57 ± 0.12 bB	2.30 ± 0.19 bB	2.54 ± 0.15 bB
12	2.80 ± 0.32 bB	4.18 ± 0.26 abA	4.52 ± 0.64 aA	2.20 ± 0.30 bB	2.80 ± 0.07 bB
24	4.53 ± 0.82 aAB	5.30 ± 0.50 aA	4.56 ± 0.74 aAB	3.17 ± 0.22 aB	4.14 ± 0.36 aAB
+P					
1	1.39 ± 0.06 bBC	2.03 ± 0.17 aA	1.53 ± 0.25 abB	0.94 ± 0.03 cD	0.99 ± 0.05 bCD
2	1.53 ± 0.10 abA	1.31 ± 0.16 aAB	0.96 ± 0.18 cB	1.06 ± 0.10 cB	1.26 ± 0.14 bAB
6	1.48 ± 0.01 abAB	1.66 ± 0.21 aAB	1.21 ± 0.20 bcB	1.41 ± 0.15 bAB	1.72 ± 0.11 bA
12	2.26 ± 0.15 aA	1.70 ± 0.09 aB	1.28 ± 0.06 bcC	1.19 ± 0.07 bcC	1.82 ± 0.15 bB
24	2.18 ± 0.57 abB	1.93 ± 0.46 aB	1.87 ± 0.21 aB	1.81 ± 0.16 aB	3.90 ± 0.74 aA

The Fisher's protected least significant difference (LSD) was used to compare means after ANOVA. Different low letters within the samecolumn indicate significant difference at $P < 0.05$ among different time treatments and different capital letters within the same row indicate significant difference at $P < 0.05$ among populations of *P. vittata.*

Wu *et al.* (2014) demonstrated that there were higher values of V_{max} for arsenate in the nonmetallicolous populations of *P. vittata* compared with the metallicolous populations, which suggested that the former has more numbers of transport proteins per unit of root plasma membrane than the latter. This might be contributed to the inhibitory effect of phosphate was more pronounced in the nonmetallicolous populations than in the metallicolous populations in the present study (Fig. 1). Bleeker *et al.* (2003) indicated that at both 10 μM and 100 μM P supply levels, the nonmetallicolous populations of *C. striatus* accumulated significantly more As in their roots than the mine populations of *C. striatus* and that the arsenate uptake was reduced in the former through suppression of phosphate transporter activity. Some plants reduced uptake of As through constitutive suppression of the high-affinity phosphate uptake system and consequently achieved As tolerance (Meharg and Hartley-Whitaker 2002). Wu *et al.* (2009) found that the metallicolous population (DSL) of *P. vittata* was more tolerant to As than the nonmetallicolous population (HK). Whether the metallicolous populations of *P. vittata* used in the present study posses similar mechanisms with non hyperaccumulators is still not clear.

Su *et al.* (2008) indicated phosphate had no significant effect on As translocation from roots and fronds of *P. vittata* in time-course culture (1–24 h), mainly due to arsenate taken up by roots was rapidly reduced to arsenite and the arsenite as the predominant form of As transported in the xylem from roots to fronds of *P. vittata*. In comparison, the present study showed that regardless of nonmetallicolous or metallicolous populations of *P. vittata*, the presence of phosphate in the solution significantly ($P < 0.05$) decreased As translocation at 12 h and 24 h of exposure to arsenate (Table 2). This might be contributed to the inhibitory effect of phosphate on arsenate uptake in roots of *P. vittata* and a smaller pool of As in the roots available in the +P treatment for translocation to the fronds. At 24 h exposure of arsenate, As concentrations in roots of *P. vittata* in the +P treatment were 7.3–15.0% of those in the −P treatment (Fig. 1). Lou *et al.* (2010) also observed that increasing phosphate in the solution apparently inhibited As transportation from roots to fronds of *P. vittata* under hydroponic culture. Similarly, Huang *et al.* (2007) found that an increase in phosphate reduced As TFs in *P. vittata* treated with arsenate under sand culture. However, the present study also showed that the presence of phosphate in the uptake solution significantly ($P < 0.05$) increased the As translocation in *P. vittata* at the early of the solution culture (1 and 2 h). The reasons for effects of phosphate on As translocation in *P. vittata* varied in culture time and for the interaction of phosphate and arsenate in As uptake and translocation of *P. vittata* need further investigation.

Funding

The study was supported by Natural Science Basic Research Plan in Shaanxi Province of China, and the Mini-AoE Fund from Hong 310 Kong Baptist University (RC/AOE/08-09/01).

References

Abedin MJ, Feldmann J, Meharg A. 2002. Uptake kinetics of arsenic species in rice plants. Plant Physiol 128:1120–1128.

Adamidis GC, Aloupi M, Kazakou E, Dimitrakopoulos PG. 2014. Intra-specific variation in Ni tolerance, accumulation and translocation patterns in the Ni-hyperaccumulator *Alyssum lesbiacum*. Chemosphere 95:496–502.

Assuncao AGL, Bookum WM, Nelissen HJM, Vooijs R, Schat H, Ernst WHO. 2003. Differential metal-specific tolerance and accumulation patterns among Thlaspi caerulescens populations originating from different soil types. New Phytol 159:411–419.

Assuncao AGL, Schat H, Aarts MGM. 2003. *Thlaspi caerulescens*, an attractive model species to study heavy metal hyperaccumulation in plants. New Phytol 159:351–360.

Bert V, Bonnin I, Saumitou-Laprade P, de Laguerie P, Petit D. 2002. Do *Arabidopsis halleri* from nonmetallicolous populations accumulate zinc and cadmium more effectively than those from metallicolous populations? New Phytol 155:47–57.

Bert V, Macnair MR, Laguerie PD, Saumitou-Laprade P, Petit D. 2000. Zinc tolerance and accumulation in metallicolous and nonmetallicolous populations of *Arabidopsis halleri* (Brassicaceae). New Phytol 146:225–233.

Bleeker PM, Schat H, Vooijs R, Verkleij JAC, Ernst WHO. 2003. Mechanisms of arsenate tolerance in *Cytisus striatus*. New Phytol 157:33–38.

Chen TB, Wei CY, Huang ZC, Huang QF, Lu QG, Fan ZL. 2002. Arsenic hyperaccumulator *Pteris vittata* L. and its arsenic accumulation. Chin Sci Bull 47:902–905.

Escarre J, Lefebvre C, Frérot H, Mahieu S, Noret N. 2013. Metal concentration and metal mass of metallicolous, non metallicolous and serpentine Noccaea caerulescens populations, cultivated in different growth media. Plant Soil 370:197–221.

Frerot H, Petit C, Lefebvre C, Gruber W, Collin C, Escarre J. 2003. Zinc and cadmium accumulation in controlled crosses between metallicolous and nonmetallicolous populations of *Thlaspi caerulescens* (Brassicaceae). New Phytol 157:643–648.

GB15618-1995. Environmental quality standard for soils in P. R. China.

Hoagland DR, Arnon DI. 1938. The water culture method for growing plants without soil. Calif Agric Exp Stn Circ 347:1–39.

Huang ZC, An ZZ, Chen TB, Lei M, Xiao XY, Liao XY. 2007. Arsenic uptake and transport of *Pteris vittata* L. as influenced by phosphate and inorganic arsenic species under sand culture. J Environ Sci-China 19:714–718.

Liu WJ, Zhu YG, Smith FA, Smith SE. 2004. Do phosphorus nutrition and iron plaque alter arsenate (As) uptake by rice seedlings in hydroponic culture? New Phytol 162:481–488.

Lou LQ, Ye ZH, Lin AJ, Wong MH. 2010. Interaction of arsenic and phosphate on their uptake and accumulation in Chinese brake fern. Int J Phytoremediat 12:487–502.

Lou LQ, Ye ZH, Wong MH. 2009. A comparison of arsenic tolerance, uptake and accumulation between arsenic hyperaccumulator, *Pteris vittata* L. and non-accumulator, P. semipinnata L.—a hydroponic study. J Hazard Mater 171:436–442.

Ma LQ, Komar KM, Tu C, Zhang W, Cai Y, Kennelly ED. 2001. A fern that hyperaccumulates arsenic. Nature 409:579.

Meharg AA, Hartley-Whitaker J. 2002. Arsenic uptake and metabolism in arsenic- resistant and nonresistant plant species. New Phytol 154:29–43.

Poynton CY, Huang JWW, Blaylock MJ, Kochian LV, Elless MP. 2004. Mechanisms of arsenic hyperaccumulation in Pteris species: root as influx and translocation. Planta 219:1080–1088.

Su YH, McGrath SP, Zhu YG, Zhao FJ. 2008. Highly efficient xylem transport of arsenite in the arsenic hyperaccumulator *Pteris vittata*. New Phytol 180:434–441.

Wang HB, Wong MH, Lan CY, Baker AJM, Qin YR, Shu WS, Chen GZ, Ye ZH. 2007. Uptake and accumulation of arsenic by 11 Pteris taxa from southern China. Environ Pollut 145:225–233.

Wang HB, Ye ZH, Shu WS, Li WC, Wong MH, Lan CY. 2006. Arsenic uptake and accumulation in fern species growing at arsenic-contaminated sites of southern China: field survey. Int J Phytoremediat 8:1–11.

Wang JR, Zhao FJ, Meharg AA, Raab A, Feldmann J, McGrath SP. 2002. Mechanisms of arsenic hyperaccumulation in *Pteris vittata*: Uptake kinetics, interactions with phosphate, and arsenic speciation. Plant Physiol 130:1552–1561.

Wang XM, Lei M, Liu YR, Huang ZC, Chen TB, Gao D. 2013. A comparison of arsenic accumulation and tolerance among four populations of Pteris vittata from habitats with a gradient of arsenic concentration. Sci Total Environ 442:143–151.

Wu FY, Deng D, Wu SC, Lin XG, Wong MH. 2014. Arsenic tolerance, uptake and accumulation between nonmetallicolous and metallicolous populations of *Pteris vittata* L. Environ Sci Pollut Res DOI 10.1007/s 11356-013-1593-1.

Wu FY, Ye ZH, Wu SC, Leung HM, Wong MH. 2009. Variation in arsenic, lead and zinc tolerance and accumulation in six populations of *Pteris vittata* L. from China. Environ Pollut 157: 2394–2404.

Yang XE, Li TQ, Long XX, Xiong YH, He ZL, Stoffella PJ. 2006. Dynamics of zinc uptake and accumulation in the hyperaccumulating and nonhyperaccumulating ecotypes of *Sedum alfredii* Hance. Plant Soil 284:109–119.

Zhao FJ, Dunham SJ, McGrath SP. 2002. Arsenic hyperaccumulation by different fern species. New Phytol 156:27–31.

菌物学报

jwxt@im.ac.cn | 22 July 2017, 36(7): 933-941
Http://journals.im.ac.cn | Mycosystema ISSN1672-6472 CN11-5180/Q
Tel: +86-10-64807521 |

研究论文 Research paper Doi: 10.13346/j.mycosystema.170038

两种 AM 真菌对冬小麦根系锌吸收的影响

马晓娜 [1,2] 罗万清 [1,2] 许飞飞 [1,2] 吴福勇 [1,2*]

[1] 西北农林科技大学资源环境学院 陕西 杨凌 712100
[2] 农业部西北植物营养与农业环境重点实验室 陕西 杨凌 712100

摘 要：无论在温室还是在大田条件下，菌根（AM）真菌均能够侵染冬小麦，但其对冬小麦锌（Zn）吸收的效应及机制尚不明确。本研究将摩西管柄囊霉 *Funneliformis mosseae* 和根内根孢囊霉 *Rhizophagus intraradices* 分别接种于冬小麦 *Triticum aestivum*（品种：小偃 22）根围，10 周后分别利用菌根化幼苗进行短期（0–90min）Zn 吸收动力学试验和长期（0–210min）Zn 吸收积累试验，并研究 AM 真菌侵染对冬小麦根系形态特征的影响。结果表明，AM 真菌通过增加根系长度和根尖数量来扩大冬小麦根系 Zn 吸收的有效面积、Zn 最大吸收速度 V_{max} 和 Zn^{2+} 流入根系的速度 α，进而促进冬小麦根系对 Zn 的吸收。接种摩西管柄囊霉降低了 K_m 值而接种根内根孢囊霉增加了 K_m 值，这可能与不同 AM 真菌对冬小麦根系形态影响及对 Zn 转运蛋白基因表达的影响存在差异有关。

关键词：丛枝菌根真菌，吸收动力学，侵染率，根系形态

Effects of two AM fungi on zinc uptake of winter wheat roots

MA Xiao-Na [1,2] LUO Wan-Qing [1,2] XU Fei-Fei [1,2] WU Fu-Yong [1,2*]

[1] *College of Natural Resources and Environment, Northwest A & F University, Yangling, Shaanxi 712100, China*
[2] *Key Laboratory of Plant Nutrition and the Agri-environment in Northwest China, Ministry of Agriculture, Yangling, Shaanxi 712100, China*

Abstract: Arbuscular mycorrhizal (AM) fungi could colonize winter wheat either under greenhouse or field conditions. However, the effects of AM fungi on Zn uptake in the winter wheat are still not fully elucidated. In this study, *Funneliformis mosseae* and *Rhizophagus intraradices* were inoculated to rhizosphere of the winter wheat *Triticum aestivum* (cultivar: Xiaoyan 22) respectively. After ten weeks of growth, a short-term (0–90min) uptake kinetics experiment and a long-term (0–210min) Zn accumulation experiment were conducted using seedlings of winter wheat colonized by AM fungi. The effects of AM fungi on root morphology of winter wheat have also been investigated. The results showed that AM fungi could increase the effective

---

基金项目：国家自然科学基金（41571456）；中央高校基本科研业务费专项资金（2452016118）
Supported by the National Natural Science Foundation of China (41571456); Chinese Universities Scientific Fund (2452016118).
*Corresponding author. E-mail: wfy09@163.com
ORCID: MA Xiao-Na (0000-0002-4635-7406); WU Fu-Yong (0000-0002-9566-0698)
Received: 2017-03-02, accepted: 2017-04-13

area of Zn uptake in the winter wheat roots by increasing root length and root tip numbers, and the maximum absorption rate (V_{max}) and the rate of Zn^{2+} influx into roots (α), thereby promoted the absorption of Zn. Inoculation of *Funneliformis mosseae* reduced the K_m value but inoculation of *Rhizophagus intraradices* increased the K_m value, suggesting that there might bear a certain relationship with the difference of the effects of different AM fungi on the root morphology of winter wheat and Zn transporter gene expression in winter wheat roots.

Key words: AM fungi, absorption kinetic, colonization rate, root morphology

小麦籽粒 Zn 含量一般为 20–35mg/kg，为保证以小麦为主食的居民健康，籽粒 Zn 含量至少应达到 40mg/kg（Cakmak 2008）。小麦作为中国三大粮食作物之一，主要分布于黄淮海平原、华北平原、关中平原和河西走廊，冬小麦种植区往往和土壤缺 Zn 地区高度重合。最近调查结果显示：我国冬小麦籽粒平均含 Zn 量为 30.3mg/kg，87%的冬小麦籽粒 Zn 含量低于营养推荐量，其中土壤有效 Zn 含量不足是导致小麦籽粒 Zn 含量过低的主要环境因素（Liu *et al*. 2014）。截至目前，国内外许多学者报道了施用Zn肥改善小麦籽粒Zn含量方面的研究成果（Yilmaz *et al*. 1998；Hussain *et al*. 2012；李孟华等 2013），然而这些研究往往忽视了丛枝菌根（AM）真菌的作用。

AM真菌不仅能够增加寄主植物对土壤水分和矿质元素的吸收，而且还可以提高寄主植物的抗逆性和抗病性（曾秀华等 2011；王强等 2016；Eke *et al*. 2016）。AM 真菌尤其是对移动性较差、易在根围土壤形成亏空区的矿质养分（如 P、Zn 和铵态氮）的吸收发挥重要作用，高达 90%的 P、60%的 Cu、25%的Zn 可通过菌根吸收途径进入寄主植物（Marschner & Dell 1994；Cavagnaro 2008；Lehmann *et al*. 2014）。在 meta-分析的基础上，Lehmann *et al*.（2014）认为 AM 真菌能够明显增加农作物地上部分及籽粒 Zn 的浓度。小麦是一种菌根作物，在温室和大田条件下均能被 AM 真菌侵染（Cade-Menun *et al*. 1991；Talaat & Shawky 2011），大田条件下小麦根系菌根侵染率约为 24%–60%（Sharif *et al*. 2010）。菌根依赖性高的寄主植物形成共生菌根时往往会改变根系构型（Hetrick 1991）。此外，AM 真菌侵染对根系转运蛋白基因表达具有调控作用，水稻与 AM 真菌共生会影响水通道转运蛋白基因表达（Chen *et al*. 2012）。AM 真菌在土壤中普遍存在并有益于冬小麦对 P、Zn 的吸收，但 AM 真菌对冬小麦 Zn 吸收的机制尚不清楚。因此，本实验以冬小麦为研究对象，以摩西管柄囊霉 *Funneliformis mosseae* 和根内根孢囊霉 *Rhizophagus intraradices* 为试验材料，旨在查明 AM 真菌对冬小麦根系吸收 Zn 的影响及相关机制，为应用菌根技术促进冬小麦根系 Zn 吸收、增加籽粒含 Zn 量进而缓解人体 Zn 缺乏提供理论依据。

1 材料与方法

1.1 试验材料

供试菌种摩西管柄囊霉和根内根孢囊霉均由北京市农林科学院植物营养与资源环境研究所提供，以苜蓿和玉米为寄主于西北农林科技大学科研温室进行盆栽扩繁。以含有寄主植物根段、菌根真菌孢子和菌丝体的根围土壤为接种剂。

供试土壤采集于陕西省咸阳市杨凌区揉谷镇未污染农田，室内风干粉碎（<2mm）。供试土壤基本理化性状如下：pH 7.47（水:土=1:1），有机质为 10.18g/kg，全 N 为 4.19g/kg，有效 P 为 12.97mg/kg，速效 K 为 122.9mg/kg，全 Cu 为 20.68mg/kg，全 Pb 为 16.60mg/kg，全 Zn 为 50.93mg/kg，有效 Zn 为 0.31mg/kg。

1.2 方法

1.2.1 菌根化冬小麦幼苗培育：以陕西省关中地区

广泛种植的小麦品种小偃 22 为供试植物。小麦种子于 3% H_2O_2 浸泡 30min，去离子水清洗后，浸泡过夜。培养基质（土壤:河沙=3:1，*W*/*W*）蒸汽高温灭菌（121℃，2h），风干后装盆，每盆盛 3.0kg 培养基质。试验设置 3 个接种处理：未接种、接种摩西管柄囊霉和接种根内根孢囊霉，每个处理 30 盆。AM 真菌以穴播方法进行接种，每盆接种 250g 菌剂，未接种处理分别加入相应的 250g 灭菌菌剂（121℃，2h）和 50mL 菌剂滤液，以保持土壤中除 AM 真菌外其他微生物区系的一致性。每盆种植小麦种子 15–18 粒，出苗 3–4d 后间苗至 8–10 棵。小麦幼苗于 2016 年 7 月初至 9 月中旬于西北农林科技大学科研温室[(25±3)℃/(20±3)℃，白天/夜晚]培养，每周用称重法保持土壤含水量恒定（75%），第 1–8 周每周浇灌 1 次 200mL 50%的霍格兰营养液（Hoagland & Arnon 1950），第 9–10 周每周浇灌 1 次 200mL 50%缺 Zn 的霍格兰营养液。

1.2.2 短期 Zn 吸收动力学试验：温室生长 10 周后，自来水清洗不同接种处理小麦幼苗根部泥土，去离子水清洗数次后剪去地上部分，将剩余小麦根系置于 0℃的预处理液[0.5mmol/L $Ca(NO_3)_2$ 和 5mmol/L 2-(N-morpholino) ethanesul-fonic acid（MES），pH 5]中。预培养 30min 后将不同接种处理的小麦根系移至含有不同 Zn 浓度（0、2、4、8、12、40、80μmol/L）的上述处理液中继续培养，重复 4 次，分别在 0 和 90min 取 10mL Zn 处理液。同时在相同条件下设 4 个空白对照，对处理液进行体积矫正，90min 内溶液体积未发生明显变化。90min 后收集根系样品，为释放根部表面吸附 Zn，根系经去离子水清洗后，浸没于 0℃的预处理液中，10min 后再经去离子水清洗数次后烘干（70℃，72h）、称重、保存。吸收动力学试验开始前，随机选取不同接种处理的完整冬小麦根系，用于测定根系形态、AM 真菌侵染率和根系 P 浓度。

1.2.3 长期 Zn 吸收积累试验：不同接种处理小麦幼苗清洗后，利用泡沫板固定 4 株小麦幼苗于 0℃预处理液（同上）中，30min 后移入 Zn 浓度为 30μmol/L 的营养液中，营养液配方如下：2 000μmol/L $Ca(NO_3)_2$，500μmol/L $MgSO_4$，1 500μmol/L KNO_3，100μmol/L KCl，2 000μmol/L MES，2 000μmol/L KOH，100μmol/L $NH_4H_2PO_4$，10μmol/L H_3BO_3 和 0.1μmol/L Na_2MoO_4，pH 6.0（Rengel & Wheal 1997），重复 4 次，不间断充气，分别在第 0min、15min、60min、90min、120min、180min 和 210min 取 5mL 溶液。在相同条件下设 4 个空白对照，进行溶液体积矫正，在 150min 时向处理液中补充 3.6mL 未添加 Zn 处理的营养液。

1.3 测定方法

分别随机取少量不同接种处理根系冲洗干净，进行侵染率测定（Phillips & Hayman 1970），根段用 10% KOH 溶液浸泡，90℃水浴 30min，冲洗 3 次后，用碱性 H_2O_2（30mL 10% H_2O_2+3mL NH_4OH+567mL 去离子水）溶液漂白 20–60min，随后用 1% HCl 酸化（1–4min），然后直接加入 0.05%台盼蓝染色，90℃水浴 30min，水洗。置于盛有乳酸油溶液的培养皿中脱色。取 50 条根段制片，在 100×的显微镜下观察，并用 MYCOCALC 软件计算真菌的根段侵染率（McGonigle *et al*. 1990）。植物根系 P 浓度采用钒钼黄比色法测定，采用国家标准物质紫菜标样（GSB-14）进行植物分析质量控制，磷回收率为 (98±6)%。随机选取不同接种处理小麦根系，尽量避免根系受到损伤，清水冲洗干净后放到装有少量水的有机玻璃盘上，用镊子将每条根舒展开，尽量使根与根之间不要重叠，用根系分析系统 Epson Perfection V700 Photo 扫描和图像分析软件 WinRHIZO 进行根系分析，测定根长、根表面积、平均直径、根体积、根尖数，每个处理重复 4 次。处理液 Zn 浓度采用原子吸收分光光度计（日本日立，Z-2000）测定。

1.4 数据处理分析

数据方差分析采用 SPSS 19.0 多重比较，采用新

复极差测验（$P<0.05$），米氏方程用 SigmiaPlot12.5 拟合。

2 结果与分析

2.1 AM 真菌对冬小麦根系吸收 Zn 的影响

2.1.1 AM 真菌对冬小麦根系短期 Zn 吸收动力学影响：短期内（0–90min）不同接种处理下冬小麦根系对 Zn 吸收速度随溶液中 Zn^{2+}浓度的增加而大致呈增加趋势（图 1），且符合 Michalis-Menten 酶动力学模型（表 1）。接种摩西管柄囊霉的小麦根系 Zn 的吸收速度显著（$P<0.05$）高于未接种处理，Zn^{2+}浓度为 80μmol/L 时接种摩西管柄囊霉处理冬小麦根系 Zn 吸收速度约为未接种处理的 2.38 倍。接种根内根孢囊霉处理冬小麦根系 Zn 的吸收速度虽然在低浓度 Zn（2μmol/L 和 4μmol/L）时比未接种处理略低，但在其余 Zn^{2+}浓度下接种根内根孢囊霉的 Zn 吸收速度均明显高于未接种处理，Zn^{2+}浓度为 80μmol/L 时接种根内根孢囊霉的小麦根系 Zn 吸收速度是未接种处理的 2.07 倍，说明接种 AM 真菌短期内促进了冬小麦根系对 Zn 的吸收。接种摩西管柄囊霉处理冬小麦根系 Zn 的吸收速度明显高于接种根内根孢囊霉，这说明不同 AM 真菌对冬小麦根系 Zn 吸收的影响存在明显差异。

菌根化小麦根系 Zn 吸收速度随溶液中 Zn^{2+}浓度变化而变化（表 1）。接种摩西管柄囊霉和根内根孢囊霉处理冬小麦根系 Zn 的最大吸收速度 V_{max} 均高于未接种处理，分别是未接种处理的 2.28 倍、2.33 倍，这说明接种 AM 真菌增加了冬小麦根系对 Zn 的吸收潜力。接种摩西管柄囊霉处理冬小麦根系 Zn 吸收动力学米氏常数 K_m 比未接种处理低 8.99%，接种根内根孢囊霉处理冬小麦根系 Zn 吸收动力学米氏常数 K_m 则比未接种处理高 13.27%，这说明不同菌种处理对小麦根系 Zn^{2+}的亲和能力存在差异。通常用 V_{max} 和 K_m 的比值 α 来阐明离子流入根系速率大小，α 值越大离子流入根系的速度越快（蒋延惠等 1995；马检和樊卫国 2016）。接种 AM 真菌明显增加了 Zn^{2+}流入小麦根系中的速率，接种摩西管柄囊霉、根内根孢囊霉的 α 值分别为未接种处理的 2.51、2.05 倍，但接种摩西管柄囊霉和根内根孢囊霉之间 α 值差异不显著。

2.1.2 AM 真菌对冬小麦根系长期 Zn 吸收积累的影响：长期内（0–210min）不同接种处理对小麦根系 Zn 吸收积累的影响表明，接种摩西管柄囊霉的小麦根系 Zn 的吸收积累量在各个时间点均明显高于未接种处理，在 60min、90min 和 120min 时接种摩西管柄囊霉的冬小麦根系 Zn 积累量显著高于（$P<0.05$）未接种处理，前者分别是后者的 1.68、2.00 和 1.45 倍。在 15min 时，接种根内根孢囊霉处理小麦根系 Zn 的吸收积累量比未接种处理低，随着时间的增加，接种根内根孢囊霉的小麦根系 Zn 的积累量均高于未接种处理，210min 时接种根内根孢囊霉的小麦根系 Zn 吸收积累量是未接种处理的 1.36 倍（图 2），这说明接种 AM 真菌会影响冬小麦根系 Zn 的吸收积累量。

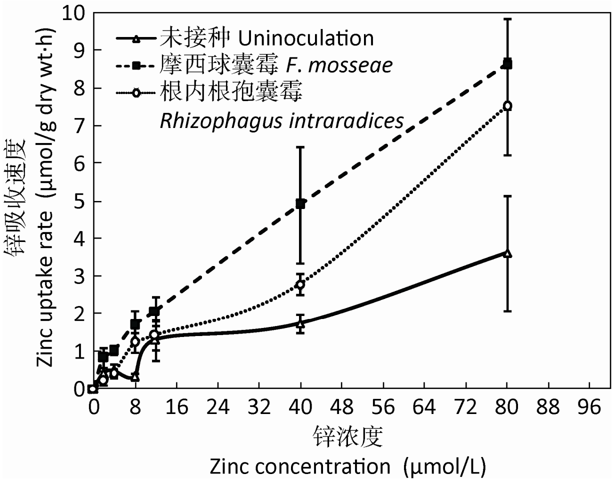

图 1 不同 AM 真菌对冬小麦根系 Zn 吸收动力学的影响（平均值±标准差，n=4）

Fig. 1 Concentration-dependent kinetics of zinc uptake of winter wheat roots inoculated with *Funneliformis mosseae* or *Rhizophagus intraradices* (mean±SE, n=4).

表 1 不同 AM 真菌对冬小麦根系 Zn 吸收动力学参数的影响（平均值，n=4）

Table 1 Effects of different AM fungus on zinc absorption kinetic parameters of winter wheat roots (mean, n=4)

接种处理 Inoculation treatments	最大吸收速率 V_{max} (μmol/g dry wt·h)	米氏常数 K_m (μmol/L)	α V_{max}/K_m	R^2
未接种 Uninoculation	10.74	164.48	0.0653	0.9399
摩西管柄囊霉 *F. mosseae*	24.49	149.69	0.1636	0.9912
根内根孢囊霉 *Rhizophagus intraradices*	24.99	186.31	0.1341	0.9982

注：R^2 表示 1/*V* 与 1/*C* 的相关系数. *V* 指小麦根系 Zn 吸收速率，*C* 指底物浓度

Note: R^2 indicates the correlation coefficient between 1/*C* and 1/*V*. *V* refers to the absorption rate of wheat roots, and *C* refers to the concentration of substrate.

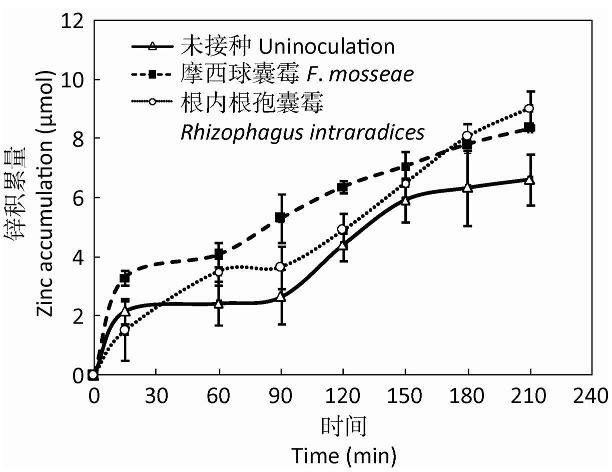

图 2 不同 AM 真菌对冬小麦根系 Zn 积累量的影响（平均值±标准差，n=4）

Fig. 2 Effects of different AM fungi on zinc accumulation of winter wheat roots (mean±SE, n=4).

2.2 不同 AM 真菌对冬小麦根系侵染率和含磷量的影响

接种 AM 真菌 10 周后，冬小麦根系分别与摩西管柄囊霉和根内根孢囊霉形成中等程度的侵染（54.7%–65.9%），未接种处理未被 AM 真菌侵染（表 2）。两种接种处理菌根侵染率显著（*P*<0.05）高于未接种处理，但接种摩西管柄囊霉和根内根孢囊霉之间菌根侵染率不存在显著性差异。接种 AM 真菌均显著（*P*<0.01）促进了冬小麦根系对 P 的吸收，接种摩西管柄囊霉和根内根孢囊霉处理冬小麦根系含 P 量分别是未接种处理的 2.00 和 1.88 倍，这说明温室条件下 AM 真菌能够与冬小麦形成菌根共生体。

2.3 不同 AM 真菌对冬小麦根系形态的影响

接种 AM 真菌能够显著影响冬小麦根系形态特征，但不同菌种处理之间存在明显差异。接种摩西管柄囊霉显著（*P*<0.01）增加了小麦根系根长、根表面积、根体积和根尖数量，其根长、根表面积、根体积和根尖分别是未接种处理的 2.54、1.60、1.42 和 2.19 倍。接种根内根孢囊霉对冬小麦根系形态特征的影响不明显，根长和根尖数量分别高于未接种处理，根表面积、根系平均直径和根体积则略小于未接种处理，但均未达到显著水平，这说明不同 AM 真菌对冬小麦根系形态特征的影响存在差异（表 3）。

表 2 不同 AM 真菌对冬小麦根系侵染率和含磷量的影响（平均值±标准差，n=4）

Table 2 Effects of different AM fungus on colonization rate and P concentration of winter wheat roots (mean±SE, n=4)

接种处理 Inoculation treatment	侵染率 Colonization rate (%)	根系含磷量 P concentration in root (%)
未接种 Uninoculation	0 b	0.17±0.01 b
摩西管柄囊霉 *F. mosseae*	54.69±2.91 a	0.34±0.06 a
根内根孢囊霉 *Rhizophagus intraradices*	65.86±5.71 a	0.32±0.02 a

注：同列不同字母表示达到 5%显著水平（*P*<0.05）

Note: Different letters of the column indicate significance at 0.05.

表 3 不同 AM 真菌对冬小麦根系形态的影响（平均值±标准差，n=4）

Table 3 Effects of different AM fungus on root morphology of winter wheat (mean±SE, n=4)

接种处理 Inoculation treatments	根长 Root length (cm)	根表面积 Root surface area (cm^2)	根平均直径 Root average diameter (mm)	根体积 Root volume (cm^3)	根尖 Root tips (N)
未接种 Uninoculation	866.9±65.4 b	79.03±4.81 b	0.29±0.01 a	0.57±0.13 b	3 169±278.8 b
摩西管柄囊霉 *F. mosseae*	1 570±118 a	126.1±5.97 a	0.26±0.01 a	0.81±0.03 a	6 928±249.2 a
根内根孢囊霉 *Rhizophagus intraradices*	889.8±130 b	77.34±9.26 b	0.28±0.01a b	0.54±0.05 b	3 188±433.7 b

注：同列不同字母表示达到 5%显著水平（$P<0.05$）

Note: Different letters of the column indicate significance at 0.05.

3 讨论

本研究结果表明，接种菌根处理冬小麦根系 Zn 吸收曲线符合 Michalis-Menten 酶动力学模型（表 1）。Hacisalihoglu *et al*.（2001）早期研究也发现，未接种处理冬小麦根系 Zn 吸收曲线符合 Michalis-Menten 酶动力学模型。在 0–80μmol/L Zn^{2+} 浓度范围内，未接种处理 V_{max} 值（10.74μmol/g dry wt·h）与 Hacisalihoglu *et al*.（2001）未接种处理冬小麦根系吸收动力学 V_{max}（0.521μmol/g fresh wt·h，根系含水量 80%–95%）结果大致相同。无论是短期（0–90min）Zn 吸收动力学试验（图 1）还是长期（0–210min）Zn 吸收积累试验（图 2）均显示：接种 AM 真菌均明显促进了冬小麦根系对 Zn 的吸收，增加了根系对 Zn 的最大吸收速度和 Zn^{2+}流入根系的速度。多数研究结果显示：低 Zn 条件下接种 AM 真菌明显促进了寄主 Zn 的吸收（Chen *et al*. 2003；Cavagnaro 2008）。

菌根化植物根系一般通过两种途径吸收矿质营养元素：一是直接通过根毛和根表皮细胞吸收（直接吸收途径），二是通过 AM 真菌菌丝吸收、再进入根系皮层细胞（菌根途径）（Smith & Read 1997；Smith & Smith 2011）。一方面，接种 AM 真菌对冬小麦根系对 Zn 吸收的促进作用与 AM 真菌侵染显著影响冬小麦根系形态特征（表 3）、改变直接吸收途径有关。接种摩西管柄囊霉和根内根孢囊霉均增加了冬小麦根系的长度和根尖的数量。黄京华（2013）发现玉米接种摩西管柄囊霉能显著增加根长，Berta *et al*.（2005）证实接种摩西管柄囊霉显著增加番茄根尖数。此外，接种摩西管柄囊霉和根内根孢囊霉均减少冬小麦根系的平均直径（表 3）。菌根化冬小麦根系形态的改变增加了根系 Zn 吸收的有效吸收面积，进而促进了 Zn 的吸收。Zhang *et al*.（2016）发现根长和根系表面积与小麦 Zn 吸收呈正相关。Li *et al*.（2005）研究发现东南景天对 Zn 的吸收与根长显著正相关。较细的根在能量的吸收与消耗平衡上更有优势（Fitter 1987；Hetrick 1991），细根比例高，增加根系比表面积，有利于促进小麦对土壤中 Zn 的吸收（Rengel & Graham 1995）。另一方面，接种 AM 真菌对冬小麦根系 Zn 吸收的促进作用可能是由于增加了菌根吸收途径对 Zn 的贡献。冬小麦是须根系作物，主根不明显，不定根发达，菌根化冬小麦不仅可以通过根表皮或根毛吸收养分，还可以通过 AM 真菌菌

丝体吸收养分。本试验中冬小麦根系的菌根侵染率为 54.7%–64.9%。根外菌丝不但有效地增加了根系的吸收面积，同时根内菌丝、丛枝和泡囊还可以较大幅度地提高植物根系活跃吸收面积（袁丽环等 2009）。Zn 能够通过外生菌丝直接吸收并转运至寄主（Smith & Read 1997）。近期研究（Watts-Williams *et al*. 2015）表明，在低 Zn 土壤中植物地上部分 24%的 Zn 来自菌根吸收途径。

本研究结果还表明不同 AM 真菌对冬小麦根系 Zn 吸收的影响存在差异，接种摩西管柄囊霉的效应优于根内根孢囊霉。类似地，Wu *et al.*（2015）发现接种摩西管柄囊霉和地表球囊霉菌 *G. versiforme* 对水稻根系砷酸盐和亚砷酸盐吸收的影响也存在差异。接种摩西管柄囊霉降低了米氏常数 K_m 而接种根内根孢囊霉增加 K_m（表 1）。不同 AM 真菌对 K_m 的影响不同可能是由于不同 AM 真菌对根系形态的影响存在差别所致（表3）。接种摩西管柄囊霉显著（$P<0.01$）增加了冬小麦根系根长、根表面积、根体积和根尖数量，而接种根内根孢囊霉对冬小麦根系形态特征的影响不明显。Wu *et al.*（2011）也发现玉米接种摩西管柄囊霉显著增加了根长、根表面积和根体积，但接种 *Paraglomus occultum* 却没有显著增加根长、根表面积和根体积。

根系对 Zn 的吸收是主动吸收过程，需要能量、结合位点和运输载体。吸收动力学参数 V_{max} 大小与载体数量有关。接种摩西管柄囊霉和根内根孢囊霉处理冬小麦根系 Zn 的 V_{max} 均高于未接种处理，说明菌根化小麦根系与未接种处理相比单位细胞质膜中具有更多的运输载体，AM 真菌侵染可能影响了冬小麦根系Zn转运蛋白基因的表达。Tamayo *et al.*（2014）研究显示：利用全基因组分析，*Rhizophagus irregularis* 形成菌根中的Zn转运蛋白基因 *RiZRT*、*RiZTR3.1* 和 *RiZTR3.2* 比发芽的孢子和根外菌丝上调了 420 倍、3.5 倍和 3 倍。不同 AM 真菌对玉米根系磷转运蛋白基因表达的调控能力存在差别（Tian *et al*. 2013）。类似地，不同 AM 真菌对冬小麦根系 Zn 转运蛋白基因表达的影响也可能不同。然而，接种 AM 真菌对冬小麦根系 Zn 转运蛋白基因的调控机制尚不清楚，还需进一步探究。

[REFERENCES]

Berta G, Sampo S, Gamalero E, Massa N, Lemanceau P, 2005. Suppression of *Rhizoctonia* root-rot of tomato by *Glomus mosseae* BEG12 and *Pseudomonas fluorescens* A6RI is associated with their effect on the pathogen growth and on the root morphogenesis. *European Journal of Plant Pathology*, 111(3): 279-288

Cade-Menun BJ, Berch SM, Bomke AA, 1991. Seasonal colonization of winter wheat in South Coastal British Columbia by vesicular-arbuscular mycorrhizal fungi. *Canadian Journal of Botany*, 69(1): 78-86

Cakmak I, 2008. Enrichment of cereal grains with zinc: agronomic or genetic biofortification? *Plant and Soil*, 302(1-2): 1-17

Cavagnaro TR, 2008. The role of arbuscular mycorrhzas in improving plant zinc nutrition under low soil zinc concentrations: a review. *Plant and Soil*, 304(1-2): 315-325

Chen BD, Li X, Tao HQ, Christie P, Wong MH, 2003. The role of arbuscular mycorrhiza in zinc uptake by red clover growing in a calcareous soil spiked with various quantities of zinc. *Chemosphere*, 50(6): 839-846

Chen X, Li H, Chan WF, Wu C, Wu F, Wu S, Wong MH, 2012. Arsenite transporters expression in rice (*Oryza sativa* L.) associated with arbuscular mycorrhizal fungi (AMF) colonization under different levels of arsenite stress. *Chemosphere*, 89(10): 1248-1254

Eke P, Chatue GC, Wakam LN, Kouipou RMT, Fokou PVT, Boyom FF, 2016. Mycorrhiza consortia suppress the fusarium root rot (*Fusarium solani* f. sp. *phaseoli*) in common bean (*Phaseolus vulgaris* L.). *Biological Control*, 103: 240-250

Fitter AH, 1987. An architectural approach to the comparative ecology of plant root systems. *New Phytologist*, 106(s1): 61-77

Hacisalihoglu G, Hart JJ, Kochian LV, 2001. High- and low-affinity zinc transport systems and their possible role in zinc efficiency in bread wheat. *Plant Physiology*, 125(1): 456-463

Hetrick BAD, 1991. Mycorrhizas and root architecture. *Cellular and Molecular Life Sciences*, 47(4): 355-362

Hoagland DR, Arnon DI, 1950. The water culture method for growing plants without soil. *California Agricultural Experiment Station*, 347: 1-39

Huang JH, Liu Q, Li XH, Zeng RS, Luo SM, 2013. Mechanism of maize root morphology change induced by arbuscular mycorrhizal fungi. *Journal of Maize Sciences*, 21(3): 131-135 (in Chinese)

Hussain S, Maqsood MA, Rengel Z, Aziz T, 2012. Biofortification and estimated human bioavailability of zinc in wheat grains as influenced by methods of zinc application. *Plant and Soil*, 361(1-2): 279-290

Jiang TH, Zheng SJ, Shi JQ, Hu AT, Shi RH, Xu M, 1995. Several considerations in kinetics research on nutrients uptake by plants. *Plant Nutrition and Fertilizer Science*, 1(2): 11-17 (in Chinese)

Lehmann A, Veresoglou SD, Leifheit EF, Rillig MC, 2014. Arbuscular mycorrhizal influence on zinc nutrition in crop plants-A meta-analysis. *Soil Biology & Biochemistry*, 69: 123-131

Li MH, Wang ZH, Wang WJ, Mao H, Dai J, Li Q, Zou CQ, 2013. Effect of Zn application methods on wheat grain yield and Zn utilization in Zn-deficient soils of dryland. *Journal of Plant Nutrition and Fertilizer*, 19(6): 1346-1355 (in Chinese)

Li TQ, Yang XE, He ZL, Yang JY, 2005. Root morphology and Zn^{2+} uptake kinetics of the Zn hyperaccumulator of *Sedum alfredii* Hance. *Journal of Integrative Plant Biology*, 47(8): 927-934

Liu H, Wang ZH, Li F, Li K, Yang N, Yang Y, Huang D, Liang D, Zhao H, Mao H, Liu J, Qiu W, 2014. Grain iron and zinc concentrations of wheat and their relationships to yield in major wheat production areas in China. *Field Crops Research*, 156: 151-160

Ma J, Fan WG, 2016. Effects of different ratios of nitrate and ammonium on the dynamic kinetic and growth for *Eriobotrya japonica* Lindl. seedlings*. Scientia Agricultura Sinica*, 49(6): 1152-1162 (in Chinese)

Marschner H, Dell B, 1994. Nutrient uptake in mycorrhizal symbiosis. *Plant and Soil*, 159(1): 89-102

McGonigle TP, Miller MH, Evans DG, Fairchild GL, Swan JA, 1990. A new method which gives an objective measure of colonization of roots by vesicular-arbuscular mycorrhizal fungi. *New Phytologist*, 115(3): 495-501

Phillips JM, Hayman DS, 1970. Improved procedures for clearing roots and staining parasitic and vesicular-arbuscular mycorrhizal fungi for rapid assessment of infection. *Transactions of the British Mycological Society*, 55(1): 158-161

Rengel Z, Graham RD, 1995. Wheat genotypes differ in Zn efficiency when grown in chelate-buffered nutrient solution. *Plant and Soil*, 176(2): 317-324

Rengel Z, Wheal MS, 1997. Kinetic parameters of Zn uptake by wheat are affected by the herbicide chlorsulfuron. *Journal of Experimental Botany*, 48(4): 935-941

Sharif M, Rubina K, Burni T, 2010. Occurrence and distribution of arbuscular mycorrhizal fungi in wheat and maize crops of Malakand division of North West Frontier Province. *Pakistan Journal of Botany*, 42(2): 1301-1312

Smith SE, Read DJ, 1997. Mycorrhizal symbiosis. Elsevie Ebsco Publishing, London. 1-605

Smith SE, Smith FA, 2011. Roles of arbuscular mycorrhizas in plant nutrition and growth: new paradigms from cellular to ecosystem scales. *Annual Review of Plant Biology*, 62: 227-250

Talaat NB, Shawky BT, 2011. Influence of arbuscular mycorrhizae on yield, nutrients, organic solutes, and antioxidant enzymes of two wheat cultivars under salt stress. *Journal of Plant Nutrition and Soil Science*, 174(2): 283-291

Tamayo E, Gómez-Gallego T, Azcón-Aguilar C, Ferrol N, 2014. Genome-wide analysis of copper, iron and zinc transporters in the arbuscular mycorrhizal fungus *Rhizophagus irregularis*. *Frontiers in Plant Science*, 5: 547

Tian H, Drijber RA, Li XL, Miller DN, Wienhold BJ, 2013. Arbuscular mycorrhizal fungi differ in their ability to regulate the expression of phosphate transporters in maize (*Zea mays* L.). *Mycorrhiza*, 23(6): 507-514

Wang Q, Wang X, Wang XJ, Zhang L, Zhang YF, Huang LC, Jin L, 2016. The application of arbuscular mycorrhizal fungi in organic farming systems. *Acta Ecologica Sinica*, 36(1): 11-21 (in Chinese)

Watts-Williams SJ, Smith FA, McLaughlin MJ, Patti AF, Cavagnaro TR, 2015. How important is the mycorrhizal pathway for plant Zn uptake? *Plant and Soil*, 390(1-2): 157-66

Wu F, Liu X, Wu S, Wong MH, 2015. Effects of mycorrhizal inoculation of upland rice on uptake kinetics of arsenate and arsenite. *Journal of Plant Nutrition and Soil Science*, 178(2): 333-338

Wu QS, Li GH, Zou YN, 2011. Improvement of root system architecture in peach (*Prunus persica*) seedlings by arbuscular mycorrhizal fungi, related to allocation of glucose/sucrose to root. *Notulae Botanicae Horti Agrobotanici Cluj-Napoca*, 39(2): 232

Yilmaz A, Ekiz H, Gültekin I, Torun B, Barut H, Karanlik S, Cakmak I, 1998. Effect of seed zinc content on grain yield and zinc concentration of wheat grown in zinc-deficient calcareous soils. *Journal of Plant Nutrition*, 21(10): 2257-2264

Yuan LH, Yan GQ, Zhu ZM, 2009. Effects of arbuscular mycorrhizal fungi on the seedling roots of *Elaeagnus mollis* Diel. *Acta Botanica Boreali-Occidentalia Sinica*, 29(3): 580-585 (in Chinese)

Zeng XH, Ye SP, Bai CJ, Xin GY, Luo RF, 2011. Effects of arbuscular mycorrhizal fungi (amf) on the drought resistance of bermudagrass under different phosphorus application rates. *Chinese Journal of Tropical Crops*, 32(6): 1069-1074 (in Chinese)

Zhang W, Liu D, Liu Y, Cui Z, Chen X, Zou C, 2016. Zinc uptake and accumulation in winter wheat relative to changes in root morphology and mycorrhizal colonization following varying phosphorus application on calcareous soil. *Field Crops Research*, 197: 74-82

［附中文参考文献］

黄京华，刘青，李晓辉，曾任森，骆世明，2013. 丛枝菌根真菌诱导玉米根系形态变化及其机制. 玉米科学，21(3): 131-135

蒋廷惠，郑绍建，石锦芹，胡霭堂，史瑞，徐茂，1995. 植物吸收养分动力学研究中的几个问题. 植物营养与肥料学报，1(2): 11-17

李孟华，王朝辉，王建伟，毛晖，戴健，李强，邹春琴，2013. 低锌旱地施锌方式对小麦产量和锌利用的影响. 植物营养与肥料学报，19(6): 1346-1355

马检，樊卫国，2016. 不同配比的硝态氮和铵态氮对枇杷实生苗氮素吸收动力学及生长的影响. 中国农业科学，49(6): 1152-1162

王强，王茜，王晓娟，张亮，张云飞，黄利春，金樑，2016. AM 真菌在有机农业发展中的机遇. 生态学报，36(1): 11-21

袁丽环，闫桂琴，朱志敏，2009. 丛枝菌根（AM）真菌对翅果油树幼苗根系的影响. 西北植物学报，29(3): 580-585

曾秀华，叶少萍，白昌军，辛国荣，罗仁峰，2011. 接种丛枝菌根真菌（AMF）及施磷量对狗牙根抗旱性的影响. 热带作物学报，32(6): 1069-1074

（本文责编：韩丽）

第30卷 第9期
2017年9月

环 境 科 学 研 究
Research of Environmental Sciences

Vol. 30, No. 9
Sep., 2017

石陶然,田凯,包环宇,等.多环芳烃在冬小麦体内的吸收与转运及富集研究进展[J].环境科学研究,2017,30(9):1398-1405.

SHI Taoran, TIAN Kai, BAO Huanyu, *et al*. Research advances in uptake, translocation and accumulation of polycyclic aromatic hydrocarbons in winter wheat [J]. Research of Environmental Sciences, 2017, 30(9):1398-1405.

多环芳烃在冬小麦体内的吸收与转运及富集研究进展

石陶然[1,2], 田 凯[1,2], 包环宇[1,2], 侯劭炜[1,2], 刘雪平[3], 吴福勇[1,2]*

1. 西北农林科技大学资源环境学院, 陕西 杨凌 712100
2. 农业部西北植物营养与农业环境重点实验室, 陕西 杨凌 712100
3. 河南城建学院市政与环境工程学院, 河南 平顶山 467036

摘要: 多年来以煤炭为主的能源消费结构和经济社会持续发展,导致我国PAHs(多环芳烃)排放量居高不下,直接造成土壤和大气PAHs严重污染.为了探明PAHs在冬小麦体内的积累过程和调控机制,在系统分析PAHs在冬小麦体内的吸收、转运和富集的基础上,重点阐述了冬小麦PAHs根系吸收和叶面吸收影响因素方面的最新研究进展.研究发现:①小麦根系对PAHs的吸收包括主动吸收和被动吸收两种方式,其中主动吸收是一个载体协助、消耗能量、PAHs与H^+共运的过程;被动吸收除了在高等植物中普遍存在的简单扩散外,水-甘油通道也参与了该过程.②PAHs通过气态、颗粒态沉降到小麦叶面角质层或直接通过气孔进入叶片.③影响PAHs根系和叶面吸收的主要因素包括PAHs理化性质、植物生理状况、环境因素等.④小麦根系吸收的PAHs可以向地上部转运,并且与辛醇-水分配系数(K_{OW})、蒸腾速率、土壤中氮的形态和浓度有关.主要问题:①对于小麦叶片吸收的PAHs向基运输机理有待进一步研究.②农田生态系统中冬小麦往往遭受土壤及大气双重污染,根系吸收及叶面吸收分别对其体内积累PAHs的贡献尚不清楚.因此,需关注韧皮部、木质部在PAHs转运中所起的作用;利用同位素示踪、双光子激发显微镜等先进技术观察和跟踪PAHs如何进入小麦以及在小麦叶中的转移和分布,阐明PAHs叶面吸收的微观机理;注重大田试验研究,为揭示冬小麦对PAHs的吸收、积累及调控机理,同时也为有机污染地区生产安全农产品提供重要依据.

关键词: 多环芳烃; 小麦; 根系吸收; 叶面吸收; 转运机理
中图分类号: X56　　**文章编号:** 1001-6929(2017)09-1398-08
文献标志码: A　　**DOI:** 10.13198/j.issn.1001-6929.2017.02.63

Research Advances in Uptake, Translocation and Accumulation of Polycyclic Aromatic Hydrocarbons in Winter Wheat

SHI Taoran[1,2], TIAN Kai[1,2], BAO Huanyu[1,2], HOU Shaowei[1,2], LIU Xueping[3], WU Fuyong[1,2]*

1. College of Natural Resources and Environment, Northwest A & F University, Yangling 712100, China
2. Key Laboratory of Plant Nutrition and the Agri-Environment in Northwest China, Ministry of Agriculture, Northwest A & F University, Yangling 712100, China
3. School of Municipal and Environment Engineering, Henan University of Urban Construction, Pingdingshan 467036, China

Abstract: Due to continuous economic and social development and the predominant use of coal in energy consumption, emissions of PAHs in China has maintained a high level for years, which has resulted in serious PAHs contamination in atmospheric and soil environments. To evaluate the processes and mechanisms contributing to accumulation and regulation of PAHs in wheat, based on systematic analysis of characteristics and mechanisms of uptake, translocation and accumulation of PAHs in wheat, the present work focused on the effects of root and foliar uptake of PAHs. Previous studies have found that wheat root uptake of PAHs mainly includes active and passive processes, of which active process is a carrier-mediated, energy-consuming and H^+-coupled symport process. Besides simple diffusion, which is especially prevalent for passive uptake in higher plants, PAHs could enter into roots via aquaglyceroporin. PAHs could enter into leaves by gas-phase and particle-phase deposition onto the waxy cuticle or via the stomata. Root and foliage uptake of PAHs are governed by the physicochemical properties of PAHs, plant species and

---

收稿日期: 2016-12-08　　**修订日期:** 2017-05-23
基金项目: 国家自然科学基金项目(41571456);河南省高校科技创新人才支持计划项目(14HASTIT048)

作者简介: 石陶然(1986-),女,山西忻州人,shitaoran@126.com.
* 责任作者,吴福勇(1973-),男,河南方城人,教授,博士,博导,主要从事土壤植物修复、PAHs毒性机理、健康风险评价及食品质量安全研究,wfy09@163.com

environmental conditions. Acropetal translocation of PAHs by root is associated with K_{OW}, transpiration rate, nitrogen form and concentration in soil. Current studies face some challenges. The mechanisms of PAHs translocating from leaves to root need further research. In addition, winter wheat always suffers from the double pollutions of soil and atmosphere under field conditions, and the role of root and foliar uptake of PAHs in the accumulation of PAHs in wheat has not been developed yet. Therefore, more efforts should be devoted to illustrating the effects of phloem and xylem in translocation of PAHs, using powerful techniques such as isotope trace and two-photon excitation microscopy to visualize and track how such compounds enter, move and distribute within wheat foliage, providing insight into PAHs foliar uptake. Paying more attention to field experiments to fully address root and foliar uptake of PAHs will provide logical proofs for revealing mechanisms of uptake, accumulation and regulation of PAHs in wheat and for the safety of agro-products growing in the PAHs-polluted areas.

Keywords: polycyclic aromatic hydrocarbons; wheat; root uptake; foliar uptake; transport mechanism

PAHs(多环芳烃)是一类具有“三致”(致癌、致畸、致突变)效应的持久性有机污染物,由于其在自然环境中无处不在、对人体危害大而备受关注. 我国是全球 PAHs 排放量最多的国家,2004 年高达 114 000 t,占全球 PAHs 排放总量的 29%[1],直接造成大气、土壤等自然环境中 PAHs 含量升高. 华北平原空气中 ρ(PAHs)高达 346 ng/m^3[2],分别为伦敦和芝加哥的 8.9 和 4.9 倍[3-4]. 自然界 90% 以上的 PAHs 存在于表层土壤[5]. PAHs 已经成为我国农田土壤中最为常见的污染物,无论是在东三省、京津地区,还是在长三角、珠三角地区,均发现农田遭受 PAHs 污染且呈持续恶化趋势[6-7]. 我国小麦种植面积约占农作物种植总面积的 1/4,华中、华北和西北地区既是小麦主产区也是煤炭生产和消费大区,相当面积的小麦种植区位于众多的燃煤发电厂、炼焦厂、城市供热厂等燃煤企业周边区域. 调查结果[8-12]显示,济南(7.6～495.2 μg/kg)、太原(161.5 μg/kg)和天津(177 μg/kg)小麦籽粒内 PAHs 含量均远高于美国加利福尼亚和西班牙加泰罗尼亚小麦籽粒内 PAHs 含量(10.3～27.9 μg/kg). 通常情况下,膳食摄入是人体暴露 PAHs 的主要途径[8-9]. 小麦是我国北方和中原地区大多数居民的主食,成人日均消耗 250 g 左右,其中河南省成年居民日均消耗量达 376～547 g[13]. 太原居民膳食暴露 PAHs 致癌风险较高,通过小麦摄入的 PAHs 占膳食摄入总量的 48.3%～53.5%[12]. 因此,进行野外采样和模型模拟探讨 PAHs 在环境-植物系统中的富集规律,以及利用显微镜、光谱、热重分析和元素分析等技术探明 PAHs 在植物体内的行为,对于研究 PAHs 从土壤、大气等自然环境到小麦的吸收、转运、积累过程的机理和影响因素,预测农产品有机污染、降低农作物污染风险、确保农产品安全生产至关重要.

1　小麦对 PAHs 的吸收和积累

PAHs 既可以通过土壤-根系也可以通过空气-叶面进入小麦体内[14],即根系从土壤中吸收 PAHs 进入木质部,随蒸腾流向茎叶传输的根系吸收;PAHs 通过叶面角质层或气孔进入小麦体内的叶面吸收[15]. 有研究[16]认为,与叶面吸收相比,根系对疏水性有机物(HOCs)的吸收是主要的;也有研究[17]认为,由于 PAHs 易与土壤有机质结合,并且根系吸收后很难转运至地上部分,因此植物暴露器官中的 PAHs 主要来自叶面吸收. 进一步探讨根系、叶片对 HOCs 的吸收以及在植物体内的积累、转移,对于治理 PAHs 污染土壤、确保食品安全、模拟潜在吸收量及进行风险评估等至关重要[18].

1.1　PAHs 的根系吸收

小麦根系对 PAHs 的吸收包括主动和被动吸收两种方式. 主动吸收量约占吸收总量的 40%,并且受 PAHs/H$^+$ 协同载体的影响[19]. PAHs 与 H$^+$ 形成共运对进入细胞内部后会导致细胞质 pH 降低[19],而细胞质 pH 通常呈中性或偏碱性,这就存在一个 pH 变化和稳定的过程. 进一步研究细胞内 pH 自我调控机制对农产品安全保障和 PAHs 污染土壤修复具有重要意义. 由于大多数有机污染物均系人工合成,植物体内没有相应的运输载体,因此大多数有机污染物进入植物体主要是通过被动运输. 被动运输除了简单扩散,还与水-甘油跨膜输送蛋白通道有关[20]. 小麦根系对菲的吸收过程可分为快速吸收和慢速吸收两个阶段. 当小麦根部浸到含有 PAHs 的营养液中,快速吸收立即进行,这一阶段主要受吸收作用、扩散作用和质量流量的影响. 随后是一个慢相循环阶段,以载体为媒介且受新陈代谢的影响[19]. 与快速吸收阶段的吸收速率相比,慢速吸收阶段的吸收速率要低 1 个数量级[21],但是对于其他种类 PAHs 是否具有与菲相同的吸收特征尚不明确. 用双光子激发显微镜

(TPEM)直接观察PAHs被小麦根系的吸收、存储和代谢,发现蒽和菲最初结合在根系表皮,随后穿过表皮细胞到达皮层. PAHs呈放射状进入表皮,然而一旦接触皮层细胞就变为缓慢的横向运输[22]. 这可能与PAHs进入表皮、皮层细胞的原生质,并且滞留在原生质中,然后通过胞间连丝进入内皮层、中柱和韧皮部有关.

1.2 PAHs的叶面吸收

空气中的PAHs以气态或颗粒态沉降至植物叶面,一部分结合在叶面角质层的脂质中,扩散穿过脂质层,最终被韧皮部运输至其他部位;另一部分向叶片内部迁移,扩散至细胞间隙,然后再分配到邻近组织的液相或脂相中[23]. 此外,叶片表面还分布着许多气孔,这些气孔为有机污染物进入植物体提供了另一个途径[15]. 污染物从空气到叶片吸收包括3个步骤[24](见图1):①污染物穿过大气和叶之间的湍流带;②污染物穿越边界层;③污染物与叶片表面反应. 植物叶片角质层对PAHs具有一定的屏障作用,PAHs在角质层上会发生团聚现象,表明角质层对PAHs的吸附并非是均匀的[25]. 但经过一段时间后PAHs可以渗透至角质层,跨过细胞膜进入叶肉细胞,累积在液泡组织内[26]. Wild等[27]在观察玉米叶片内荧蒽在96 h的运动轨迹时发现,叶片中的荧蒽穿过上表皮蜡质和角质层后到达表皮细胞的细胞质,在这一阶段,荧蒽存在于叶片的5个部位,即上表皮蜡质-薄扩散层(约5 μm)、从上表层蜡质穿过角质层到达表皮细胞的细胞壁-厚扩散带(约28 μm)、上表皮细胞壁外表面、上表皮细胞壁内表面及上表皮细胞的细胞质. PAHs在叶片中的存储位置影响其在植物体内的迁移转化和最终归趋. 如果滞留于表皮蜡质和角质层中,可能发生光降解、再挥发或从角质层脱落[28];如果进入到表皮细胞壁或者细胞质中,则易发生代谢作用[29]. 此外,Wild等[29]发现菲以气态沉降进入玉米叶片气孔,出现在气孔的保卫细胞,但是在气孔内表面和气孔下腔并没有检测到菲,因此推断菲没有通过气孔而是被叶蜡所吸收. Barber等[30]认为,当角质层较难穿透且气孔密度较大时,气孔吸收途径相对重要;而当角质层极易穿透时,气孔的作用几乎为零. 目前,对于活体小麦叶片吸收PAHs的可视化实时追踪研究相对较少. 小麦叶片对PAHs的吸收是角质层途径为主还是气孔途径为主,至今尚不清楚.

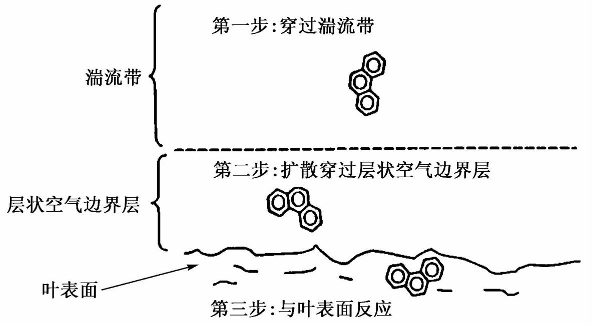

图1 疏水性有机污染物从大气到叶角质层的吸收过程[24]

Fig. 1 The uptake process of hydrophobic organic compounds from air onto leaf cuticles

1.3 籽粒对PAHs吸收

由于PAHs本身的疏水特性,Briggs等[31]认为小麦籽粒内的PAHs主要来源于大气而不是土壤. 然而,DU等[32]通过野外Lymimeter试验追踪^{14}C标记的菲在小麦体内的积累发现,根系吸收的PAHs可以通过向顶运输进入茎、叶、籽粒和颖壳. 有研究[33]发现,小麦籽粒内积累的主要为2~4环PAHs,并且萘含量最高. 裸露的小麦籽粒对PAHs吸收速率大于有外壳的籽粒,可能是外壳阻碍了PAHs向籽粒的扩散. 大田中的小麦籽粒从形成到收获大致需要一个月,对于气态PAHs的吸收处于动力学限制阶段且达不到平衡浓度[34]. 小麦籽粒PAHs浓度与接触大气的PAHs浓度有关,其关系受吸收时间和大田条件的影响[34],但是目前关于二者之间的关系缺乏定量研究,需要创建合适的动力学吸收模型,从而确定有效的途径降低籽粒引起的PAHs膳食暴露风险. 农田中的小麦经常遭受土壤及大气双重污染,因此叶面吸收及根系吸收PAHs分别对籽粒积累PAHs的贡献是当前亟待解决的科学问题.

2 小麦对PAHs的吸收和积累的影响因素

2.1 根系吸收PAHs的影响因素

2.1.1 PAHs理化性质

PAHs能否进入植物根系,依赖于其K_{OW}(辛醇-水分配系数)、水溶解度(S)、亨利系数(H)、分子量(M_W)等理化性质. 对于不同种类PAHs,根系对其吸收、转运速率不同[35]. Chiou等[36]提出了限制分配模型用于定量预测植物对有机物的积累:

$$C_{pt} = \alpha_{pt}[C_s/(f_{som}K_{som})][f_{pw} + f_{ch}K_{ch} + f_{lip}K_{OW}] \tag{1}$$

式中:C_{pt}为植物体内污染物的浓度,mg/kg;α_{pt}为准平衡因子;C_s为污染物在土壤中的浓度,mg/kg;f_{pw}为植物中无机组分的含量,%;f_{ch}为植物中碳水化合物的

含量，%；f_{lip}为植物中脂类的含量，%；f_{som}为土壤有机质的质量分数，%；K_{ch}为污染物在碳水化合物和水间的分配系数；K_{som}为污染物在土壤有机质和水间的分配系数.

由式（1）可知，K_{OW}是植物根系吸收有机污染物的主要限制因子. 有研究认为小麦根系对 PAHs 的吸收量随 K_{OW} 的增加而增加[31]，也有研究认为小麦根系 PAHs 富集系数与 K_{OW} 没有线性关系[14]，原因是大多数 lg K_{OW} > 4 的 PAHs 分配到根的表皮或土壤颗粒而不会被根系或木质部吸收. 因此，K_{OW}对小麦根系吸收 PAHs 的影响尚需深入系统研究. PAHs 随着分子量的增加其挥发性降低[37]. 植物根系对不同 M_w 的 PAHs 吸收转运能力不同. 小麦根系对 4 环 PAHs 吸收最多，其次是 2 环、3 环、5～6 环 PAHs[14]. Wild 等[22]观察同分异构体菲和蒽在小麦根系的迁移过程时发现，菲的吸收和迁移速率比蒽快. 这可能与二者不同的水溶性有关：在 25 ℃下菲和蒽在水中的溶解度分别为 1.65、0.075 mg/L[38].

然而，对于一些 PAHs 理化性质精确的测量非常困难. 定量结构-活性关系（quantitatives structure activity relationship QSAR）指化合物的分子结构与其活性之间的关系，目前已从个别的、定性的描述方式发展到一般的、定量的数学模型表达[39]. 利用定量结构-活性关系可以对 PAHs 理化性质、环境归趋和生物毒性进行预测，弥补数据的缺失，降低昂贵的测试费用. 目前对 PAHs 的定量结构-活性关系研究主要集中在光解活性[40]、生物可降解性[41]和生物毒性[42]等方面，对其吸附-解吸等环境行为的研究相对缺乏. 预测的理化性质参数代入多介质逸度模型，可得到理想环境状态下 PAHs 在多环境介质中的分配归趋，为了解 PAHs 在环境中的迁移转化提供了简便的途径.

2.1.2　植物生理状况

植物种类及其生理学特性（包括脂肪或水分含量及蒸腾速率等）都会影响植物对有机污染物的吸收[43]. 研究[44]表明，小麦根系对 PAHs 的吸收与根部脂肪含量、根表面积有关. 吸附剂的极性也会显著影响其对有机物的吸附能力，小麦根细胞的极性与 PAHs 吸收速率呈负相关[45]. 植物体主要由水、脂肪、碳水化合物、蛋白质、纤维素等物质构成，这些成分对有机污染物的亲和力不同[46]. 研究[47]表明，K_{OW} < 10 的有机污染物，根系水吸收占主导作用（85%以上）；K_{OW} = 10 的有机污染物，根系水和脂肪作用各占 50%；K_{OW} > 1 000的有机物，植物对有机污染物的吸收几乎都来自根系脂肪对有机物的分配. 植物不同生育期由于生命代谢活动强度不同，吸收污染物的能力也不同. 在不同生长期小麦各组织器官低环、中高环 PAHs 分布有显著差异[48]. 此外，不同的根系类型、根表面积、根系分泌物、菌根细菌等在种类和数量上的差异导致根际对 PAHs 的吸收、降解能力不同[49].

2.1.3　土壤理化性质

YANG 等[50]发现，土壤 DOM（可溶性有机质）不仅能明显地促进小麦对菲的吸收和富集，而且还能促进根系吸收的菲向地上部转运. 这可能是由于 DOM 改变了 PAHs 的理化性质，如水溶解度和 K_{OW}，从而提高了 PAHs 的生物有效性，进而促进了植物对菲的吸收[50]. 但是小麦根系吸收 PAHs 与土壤有机碳（SOC）含量呈负相关（$P < 0.01$）[14]. 低的 pH 促进根吸收 PAHs，研究[20]表明根系对菲的主动吸收是以 H^+共运方式进行的. K^+也会促进小麦根系对菲的吸收，K^+激活了质膜 H^+-ATPase[44]. 植物对 PAHs 的吸收与土壤中 PAHs 的浓度和植物组分有关[51]，研究表明[14]小麦根中 PAHs 浓度与土壤中 PAHs 的浓度呈正相关. 另外，阳离子表面活性剂能显著增强土壤对有机污染物的吸附[52]，而且能够抑制作物吸收土壤中的 PAHs[53]. 土壤粒径组成影响其对有机污染物的吸附和利用能力. 粗砂和黏粒对芘的吸附能力较大，细砂和粉砂相对较小[54]. 此外，土壤中氮的浓度和形态也会影响小麦根系对 PAHs 的吸收[55].

2.2　叶面吸收 PAHs 的影响因素

2.2.1　PAHs 理化性质

植物叶片对 PAHs 的吸收和转移与 PAHs 本身的理化性质有关，如环数、分子量、水溶解度、辛醇-水分配系数、辛醇-气分配系数、形态（气态/颗粒态）、亨利系数等. 气态的 PAHs 容易在叶片角质层扩散而被吸收，而大部分颗粒态 PAHs 只是嵌入到角质层，很容易被脱附[56]. 蒽和苯并[k]荧蒽混合喷施对生菜地上部分产生的积累效应和单独喷施有明显差异[57]. 车前草叶内部 PAHs 含量随 PAHs 分子量的增加而减少[58]；然而也有研究[59]认为，植物叶中 PAHs 以 5、6 环为主，根中以 2～4 环为主. 挥发性、半挥发性有机污染物在植物叶片和空气之间的分配与其辛醇-气分配系数密切相关[43].

2.2.2　植物生理状况

不同种类植物叶片性质存在差异,如形态、叶面积、角质层、叶片数量、气孔大小及密度、叶毛长度与密度、疏水性等[60]. 植物叶片拦截颗粒态PAHs与其叶向、叶面积、叶毛有关[24]. 研究表明,植物暴露器官中的PAHs主要来自叶的吸收[17],影响叶片角质层吸收PAHs的主要因素是暴露于大气中的叶面积[61]. 此外,叶毛可以提高叶片清除和黏附大气颗粒物的能力,因为它们具有更大的表面积并且会在叶表面的边缘形成相对静态空气[56]. 然而也有研究[62]表明,表面光滑的叶片比表面粗糙的叶片更易于吸附颗粒物. 因为叶子越粗糙,防水性能就越好,所以对叶子表面颗粒物的黏附作用减弱[56]. 因此,叶毛对叶片吸收大气颗粒物的影响还没有统一的结果. 叶脂含量也是影响植物吸收和滞留大气持久性有机污染物(POPs)的一个重要的因素[52]. 在这些因素中,哪些是影响PAHs穿过角质层被小麦吸收的主要因素有待进一步研究.

2.2.3 环境因素

植物从空气中吸收PAHs受温度、空气中污染物的浓度、暴露时间等影响. PAHs通过气孔在叶片和大气之间交换与大气温度有关[63],因为温度影响气孔的开启和闭合. 在温度较低的秋冬季节,PAHs由大气向植物迁移,而在温度较高的夏季,部分PAHs又通过挥发作用回到大气中[64]. 叶面对PAHs的吸收量还取决于叶面周围大气中PAHs的浓度[65]. 由于暴露时间的不同,老叶积累的PAHs量往往大于新叶[66].

3 PAHs在小麦体内的分布和迁移

3.1 向顶运输

植物根系吸收的有机污染物一部分固定在根的脂质中,一部分则穿过根系不透水硬组织带进入内表皮层到达管胞和导管组织,并通过木质部随蒸腾流向地上部分迁移,最终在茎叶中分布[43]. 小麦根系吸收的PAHs可以通过向顶运输进入茎叶[14]. 有研究[67]认为,蔬菜地上部大分子量PAHs主要来源于根系的转运. 小麦地上部不同环数的PAHs的分布特征与大气中的PAHs的分布有显著的差异,表明地上部PAHs来自于根系的转运[14].

小麦对PAHs的向顶运输与PAHs的理化性质有关,芴倾向于在小麦根部积累,而菲被转运到地上部分[68]. 有研究[14]表明小麦根吸收PAHs向地上部转运与$\lg K_{\mathrm{OW}}$呈负相关. $\lg K_{\mathrm{OW}} \leq 1$的有机物易溶于水,可以在木质部和韧皮部流动;$1 < \lg K_{\mathrm{OW}} \leq 4$的有机物易被根系吸收,可以在木质部流动,但不能在韧皮部流动;$\lg K_{\mathrm{OW}} > 4$的有机物可以在根部大量积累,但不能向顶运输. 因此,$1 < \lg K_{\mathrm{OW}} \leq 4$的有机污染物更适合于植物修复[69]. 向顶运输还与植物的蒸腾速率[70]及土壤中营养盐有关,如小麦根吸收PAHs后向地上部运输与土壤中氮的浓度和形态有关[55].

3.2 向底运输

由于PAHs较高的疏水性和较低的溶解性,植物根系表皮吸收后难以运输到根的内部或木质部[71],因此推断植物体内的PAHs可以通过地上部吸收后运输至根部. 在土壤菲浓度很低的情况下,三叶草和黑麦草根部检测到高浓度的菲,很大程度上证明地上部吸收的菲被转移至根部[72]. 然而也有研究[51]表明,植物(如大豆、空心菜等)地上部从大气中积累的菲和芘没有被运输到根部. 用同位素示踪法研究豌豆体内荧蒽的转运发现:荧蒽通过韧皮部存在向基、向顶运输,尤其是在植物新生部位如茎尖及根尖积累[73]. 目前,小麦叶面吸收PAHs是否会向根部运输还没有明确的结论,有待进一步的研究.

4 结论

a) 目前,关于小麦对PAHs吸收和转运的模型在风险评价、植物修复等方面应用得很多,然而,缺乏PAHs在小麦体内转运过程的直接证据. 研究韧皮部、木质部运输动力学对确定可食部分-小麦籽粒积累的PAHs主要来自根系吸收还是叶片吸收,从而采取有效的农艺措施阻控PAHs进入食物链是必要的.

b) 小麦处于自然状态下PAHs是如何进入其叶片,如何在叶片中转移和/或与叶肉组织结合尚不清楚. 采用先进技术探讨小麦叶面吸收、转运PAHs的微观机理,如利用同位素示踪法、双光子激发显微镜等技术跟踪和观察PAHs在小麦叶片的吸收和转移,有望为宏观调控植物吸收PAHs获得安全农产品提供科学依据.

c) 大多数研究致力于室内盆栽试验,因为受自然环境等不可控因素的影响小于田间试验而利于机理的研究,但是植物吸收PAHs的大田试验的经验对于完全理解植物-环境体系的宏观关系也是必要的. 探讨影响PAHs在小麦体内的吸收、转运和富集过程的因素,除了污染物性质、植物特征和土壤性质(尤其是土壤有机质)外,小麦生长环境的污染史也需要考虑在内.

参考文献(References):

[1] ZHANG Yanxu, TAO Shu, SHEN Huizhong, *et al.* Inhalation

exposure to ambient polycyclic aromatic hydrocarbons and lungcancer risk of Chinese population［J］. Proceedings of the National Academy of Sciences of the United States of America, 2009, 106(50): 21063-21067.

［2］ LIU Shuzhen, TAO Shu, LIU Wenxin, *et al.* Atmospheric polycyclic aromatic hydrocarbons in north China: a wintertime study［J］. Environmental Science & Technology, 2007, 41: 8256-8261.

［3］ DIMASHKI M, LIM L H, HARRISON R M, *et al.* Temporal trend, temperature dependence, and relative reactivity of atmospheric polycyclic aromatic hydrocarbons［J］. Environmental Science & Technology, 2001, 35(11): 2264-2267.

［4］ SUN Ping, BLANCHARD P, BRICE K A, *et al.* Trends in polycyclic aromatic hydrocarbon concentrations in the Great Lakes atmosphere［J］. Environmental Science & Technology, 2006, 40(20): 6221-6227.

［5］ WILD S R, JONES K C. Polycyclic aromatic hydrocarbons in the United Kingdom environment: a preliminary source in inventory and budget［J］. Environmental Pollution, 1995, 88(1): 91-108.

［6］ 姜永海，韦尚正，席北斗，等. PAHs 在我国土壤中的污染现状及其研究进展［J］. 生态环境学报，2009，18：1176-1181.
JIANG Yonghai, WEI Shangzheng, XI Beidou, *et al.* Polycyclic aromatic hydrocarbons (PAHs) pollution in soils in China: recent advances and future prospects［J］. Ecology and Environment, 2009, 18: 1176-1181.

［7］ WANG Wentao, SIMONICH S L M, XUE Miao, *et al.* Concentrations, sources and spatial distribution of polycyclic aromatic hydrocarbons in soils from Beijing, Tianjin and surrounding areas, North China［J］. Environmental Pollution, 2010, 158(5): 1245-1251.

［8］ 李新荣. 天津地区多环芳烃排放、扩散和人群暴露的空间分异［D］. 北京：北京大学，2007：104-116.

［9］ 薛海泉，崔兆杰，杜世勇，等. 加速溶剂萃取/气相色谱-质谱法测定小麦中多环芳烃［J］. 中国环境监测，2011，27：42-46.
XUE Haiquan, CUI Zhaojie, DU Shiyong, *et al.* Determination of PAHs in wheat by accelerated solvent extraction and gas chromatography-mass spectrometry［J］. Environmental Monitoring of China, 2011, 27: 42-46.

［10］ KOBAYASHI R, CAHILL T M, KAMOTO R O, *et al.* Controlled exposure chamber study of uptake and clearance of airborne polynuclear aromatic hydrocarbons by wheat grain［J］. Environmental Science & Technology, 2007, 41: 7934-7940.

［11］ ZHANG Yanyan, JOSEPH J P, TAO Shu, *et al.* Bioaccessibility of PAHs in fuel soot assessed by an in vitro digestive model with absorptive sink: effect of food ingestion［J］. Environmental Science & Technology, 2015, 49: 14641-14648.

［12］ XIA Zhonghuan, DUAN Xiaoli, QIU Wenxun, *et al.* Health risk assessment on dietary exposure to polynuclear aromatic hydrocarbons (PAHs) in Taiyuan, China［J］. Science of the Total Environment, 2010, 408: 5331-5337.

［13］ 朱宝玉，张书芳，詹宣. 河南省成年居民膳食结构变化分析［J］. 卫生研究，2004，33：615-617.

［14］ TAO Yuqiang, ZHANG Shuzhen, ZHU Yongguan, *et al.* Uptake and acropetal translocation of polycyclic aromatic hydrocarbons by wheat (*Triticum aestivum* L.) grown in field-contaminated soil［J］. Environmental Science & Technology, 2009, 43: 3556-3560.

［15］ DESALME D, BINET P, CHIAPUSIO G. Challenges in tracing the fate and effects of atmospheric polycyclic aromatic hydro carbon deposition in vascular plants［J］. Environmental Science & Technology, 2013, 47: 3967-3981.

［16］ LI Hui, SHENG Guangyao, CHIOU C T, *et al.* Relation of organic contaminant equilibrium sorption and kinetic uptake in plants［J］. Environmental Science & Technology, 2005, 39: 4864-4870.

［17］ TRAPP S. Modelling uptake into roots and subsequent translocation of neutral and ionisable organic compounds［J］. Pest Management Science, 2000, 56: 767-778.

［18］ INGRID L, SAHRAOUI A L H, LARUELLE F, *et al.* Arbuscular mycorrhizal wheat inoculation promotes alkane and polycyclic aromatic hydrocarbon biodegradation: microcosm experiment on aged-contaminated soil［J］. Environmental Pollution, 2016, 213: 549-560.

［19］ ZHAN Xinhua, MA Hengliang, ZHOU Lixiang, *et al.* Accumulation of phenanthrene by roots of intact wheat (*Triticum acstivnm* L.) seedlings: passive or active uptake?［J］. BMC Plant Biology, 2010, 10(1): 1-8.

［20］ ZHAN Xinhua, ZHANG Xiaobin, YIN Xiaoming, *et al.* H^+/phenanthrene symporter and aquaglyceroporin are implicated in phenanthrene uptake by wheat (*Triticum aestivum* L.) roots［J］. Journal of Environmental Quality, 2012, 41: 188-196.

［21］ 易修，袁嘉韩，顾锁娣，等. 小麦根系吸收萘、菲、芘的动力学特征［J］. 环境科学学报，2013，33(4)：1135-1140.
YI Xiu, YUAN Jiahan, GU Suodi, *et al.* Kinetic characteristics of naphthalene, phenanthrene and pyrene uptake by wheat roots［J］. Acta Scientiae Circumstantiae, 2013, 33(4): 1135-1140.

［22］ WILD E, DENT J, THOMAS G O, *et al.* Direct observation of organic contaminant uptake, storage, and metabolism within plant roots［J］. Environmental Science & Technology, 2005, 39: 3695-3702.

［23］ 李云桂. 典型有机污染物在植物角质层上的吸附行为与跨膜过程［D］. 杭州：浙江大学，2011：7-13.

［24］ BAKKER M I, VORENHOUT M, SIJM D, *et al.* Dry deposition of atmospheric polycyclic aromatic hydrocarbons in three Plantago species［J］. Environmental Toxicology and Chemistry, 1999, 18(10): 2289-2294.

［25］ KEYTE I, WILD E, DENT J, *et al.* Investigating the foliar uptake and within-leaf migration of phenanthrene by moss (*Hypnum cupressiforme*) using two-photon excitation microscopy with autofluorescence［J］. Environmental Science & Technology, 2009, 43: 5755-5761.

［26］ LI Qingqing, CHEN Baoliang. Organic pollutant clustered in the plant cuticular membranes: visualizing the distribution of phenanthrene in leaf cuticle using two-photon confocal scanning laser microscopy［J］. Environmental Science & Technology, 2014, 48:4774-4781.

[27] WILD E, DENT J, BARBER J L, *et al.* A novel analytical approach for visualizing and tracking organic chemicals in plants [J]. Environmental Science & Technology, 2004, 38: 4195-4199.

[28] WILD E, DENT J, THOMAS G O, *et al.* Real-time visualization and quantification of PAH photodegradation on and within plant leaves [J]. Environmental Science & Technology, 2005, 39: 268-273.

[29] WILD E, DENT J, THOMAS G O, *et al.* Visualizing the air-to-leaf transfer and within-leaf movement and distribution of phenanthrene: further studies utilizing two-photon excitation microscopy [J]. Environmental Science & Technology, 2006, 40 (3): 907-916.

[30] BARBER J L, KURT P B, THOMAS G O, *et al.* Investigation into the importance of the stomatal pathway in the exchange of PCBs between air and plants [J]. Environmental Science & Technology, 2002, 36: 4282-4287.

[31] BRIGGS G G, BROMILOW R H, EVANS A A. Relationship between lipophilicity and root uptake and translocation of non-ionised chemicals by barley [J]. Pesticide Science, 1982, 13: 495-504.

[32] DU Wenchao, SUN Yuanyuan, CAO Lu, *et al.* Environmental fate of phenanthrene in lysimeter planted with wheat and rice in rotation [J]. Journal of Hazardous Materials, 2011, 188: 408-413.

[33] REIKO K, ROBERT A O, RANDY L M, *et al.* Polycyclic aromatic hydrocarbons in edible grain: a pilot study of agricultural crops as a human exposure pathway for environmental contaminants using wheat as a model crop [J]. Environmental Research, 2008, 107: 145-151.

[34] REIKO K, THOMASM M C, ROBERT A O, *et al.* Controlled exposure chamber study of uptake and clearance of airborne polycyclic aromatic hydrocarbons by wheat grain [J]. Environmental Science & Technology, 2007, 41: 7934-7940.

[35] ESMAEIL S, ERIC M A, MOHAMED T, *et al.* Rhizoremediation of phenanthrene and pyrene contaminated soil using wheat [J]. Journal of Environmental Management, 2015, 155: 171-176.

[36] CHIOU C T, SHENG Guangyao, MANES M. A partition-limited model for the plant uptake of organic contaminants from soil and water [J]. Environmental Science & Technology, 2001, 35 (7): 1437-1444.

[37] AKYUZ M, CABUK H. Gas-particle partitioning and seasonal variation of polycyclic aromatic hydrocarbons in the atmosphere of Zonguldak, Turkey [J]. Science of the Total Environment, 2010, 408: 5550-5558.

[38] MACKAY D, WANYING S, MA K C. Illustrated handbook of physical-chemical properties and environmental fate for organic chemicals [J]. Lewis Publishers, 1992, 1 (7): 551-552.

[39] YUAN Quan, MA Guangcai, XU Ting, *et al.* Developing QSPR model of gas/particle partition coefficients of neutral poly-/perfluoroalkyl substances [J]. Atmospheric Environment, 2016, 143: 270-277.

[40] LU Guining, DANG Zhi, TAO Xueqin, *et al.* Modeling and prediction of photolysis half-lives of polycyclic aromatic hydrocarbons in aerosols by quantum chemical descriptors [J]. Science of the Total Environment, 2007, 373: 289-296.

[41] XU Peng, MA Wencheng, HAN Hongjun, *et al.* Quantitative structure-biodegradability relationships for biokinetic parameter of polycyclic aromatic hydrocarbons [J]. Journal of Environmental Sciences, 2015, 30: 180-185.

[42] 蔡啸宇,姜龙,曾娅玲,等.基于密度泛函理论的多环芳烃硝基衍生物的生物毒性预测[J].发光学报,2013,34(12):1667-1671.

CAI Xiaoyu, JIANG Long, ZENG Yaling, *et al.* Prediction of polycyclic aromatic hydrocarbon derivatives toxicity studies based on density functional Theory [J]. Chinese Journal of Luminescence, 2013, 34 (12): 1667-1671.

[43] 马恒亮.多环芳烃(菲)跨小麦根系界面的传输机制[D].南京:南京农业大学,2009:4.

[44] ZHAN Xinhua, LIANG Xiao, JIANG Tinghui, *et al.* Interaction of phenanthrene and potassium uptake by wheat roots: a mechanistic model [J]. BMC Plant Biology, 2013, 13: 168.

[45] LI Chen, ZHANG Shuzhen, HUANG Honglin, *et al.* Partitioning of phenanthrene by root cell walls and cell wall fractions of wheat (*Triticum aestivum* L.) [J]. Environmental Science & Technology, 2009, 43: 9136-9141.

[46] WEI Haiying, SONG Shanjuan, TIAN Hongling, *et al.* Effects of phenanthrene on seed germination and some physiological activities of wheat seedling [J]. Comptes Rendus Biologies, 2014, 337: 95-100.

[47] CHIOU C T, SHENG Guangyao, MANES M. A partition-limited model for the plant uptake of organic contaminants from soil and water [J]. Environmental Science & Technology, 2001, 35 (7): 1437-1444.

[48] 薛海全.农作物中多环芳烃和多氯联苯的分布、累积规律[D].济南:山东大学,2011:33-34.

[49] 阴启蓬.荧蒽在土壤-作物系统中的富集规律及对农产品质量的影响[D].南京:南京农业大学,2012:21.

[50] YANG Xiuhong, GARNIER P, WANG Shizhong, *et al.* PAHs sorption and desorption on soil influenced by pine needle litter-derived dissolved organic matter [J]. Pedosphere, 2014, 24 (5): 575-584.

[51] GAO Yanzhen, ZHU Lizhong. Plant uptake, accumulation and translocation of phenanthrene and pyrene in soils [J]. Chemosphere, 2004, 55 (9): 1169-1178.

[52] SUN Haifeng, SHI Jing, GUO Shuai, *et al.* In situ determination of the depuration of three- and four-ringed polycyclic aromatic hydrocarbons co-adsorbed onto mangrove leaf surfaces [J]. Environmental Pollution, 2016, 208: 688-695.

[53] 吕黎.阳离子表面活性剂对PAHs在土壤-作物间迁移的阻控作用及机制[D].杭州:浙江大学,2011:59.

[54] 李久海.多环芳烃(芘)在水稻土及其不同粒组中的吸附和老化效应[D].杭州:浙江大学,2003:4-6.

[55] ZHAN Xinhua, Yuan Jiahan, YUE Le, *et al.* Response of uptake

and translocation of phenanthrene to nitrogen form in lettuce and wheat seedlings [J]. Environmental Science and Pollution Research,2015,22:6280-6287.

[56] HOWSAM M,JONES K C,INESON P. PAHs associated with the leaves of three deciduous tree species:I. concentrations and profiles [J]. Environmental Pollution,2000,108:413-424.

[57] JOLANTA W, STANISLAW S, MONIKA P, *et al.* Uptake and phytotoxicity of anthracene and benzo[k]fluoranthene applied to the leaves of celery plants (*Apium graveolens* var. *Secalinum* L.) [J]. Ecotoxicology and Environmental Safety,2015,115:19-25.

[58] BAKKER M I,KOERSELMAN J W,TOLLS J,*et al.* Localization of deposited polycyclic aromatic hydrocarbons in leaves of Plantago [J]. Environmental Toxicology and Chemistry,2001,20(5):1112-1116.

[59] 匡少平. 中原油田周边土壤及玉米中 PAHs 的分布[J]. 环境化学,2008,27(6):845-846.

[60] BALDANTONI D,NICOLA F D,ALFANI A. Air biomonitoring of heavy metals and polycyclic aromatic hydrocarbons near a cement plant[J]. Atmospheric Pollution Research,2014,5:262-269.

[61] TERZAGHI E,ZACCHELLO G,SCACCHI M,*et al.* Towards more ecologically realistic scenarios of plant uptake modelling for chemicals: PAHs in a small forest [J]. Science of the Total Environment,2015,505:329-337.

[62] NEINHUIS C,BARTHLOTT W. Characterization and distribution of water-repellent,self-cleaning pant surfaces[J]. Annals of Botany,1997,79:667-677.

[63] 王雅琴,左谦,焦杏春,等. 北京大学及周边地区非取暖期植物叶片中的多环芳烃[J]. 环境科学,2004,25(4):23-27.
WANG Yaqin, ZUO Qian, JIAO Xingchun, *et al.* Polycyclic promatic pydrocarbons in plant leaves from Peking University Campus and nearby in summer season[J]. Environmental Science,2004,25(4):23-27.

[64] NAKAJIMA D,YOSHIDA Y,SUZUKI J,*et al.* Seasonal changes in the concentration of polycyclic aromatic hydrocarbons in Azalea leaves and relationship to atmospheric concentration [J]. Chemosphere,1995,30(3):409-418.

[65] DIAS A P L,RINALDI M C S,DOMINGOS M. Foliar accumulation of polycyclic aromatic hydrocarbons in native tree species from the Atlantic Forest (SE-Brazil)[J]. Science of the Total Environment,2016,544:175-184.

[66] 万开,江明,杨国义,等. 珠江三角洲典型城市蔬菜中多环芳烃分布特征[J]. 土壤,2009,41(4):583-587.

[67] FISMES J,PERRIN-GANIER C,EMPEREREUR-BISSONNET P,*et al.* Soil-to-root transfer and translocation of polycyclic aromatic hydrocarbon by vegetables grown on industrial contaminated soils [J]. Journal of Environmental Quality,2002,31:1649-1656.

[68] SALEHI-LISAR S Y,DELJOO S,HARZANDI A M. Fluorene and phenanthrene uptake and accumulation by wheat, alfalfa and sunflower from the contaminated soil[J]. International Journal of Phytoremediation,2015,17(12):1145-1152.

[69] 焦海华,潘建刚,徐圣君,等. 原位生物修复提高多环芳烃污染土壤农用安全性[J]. 环境科学,2015,36(8):3038-3044.
JIAO Haihua, PAN Jiangang, XU Shengjun, *et al.* Improving agricultural safety of soils contaminated with polycyclic aromatic hydrocarbons by in situ bioremediation[J]. Environmental Science,2015,36(8):3038-3044.

[70] GAO Yanzheng, COLLINS C D. Uptake pathways of polycyclic aromatic hydrocarbons in white clover[J]. Environmental Science & Technology,2009,43:6190-6195.

[71] KIPOPOULOU A M,MANOLIA E,SAMARA C. Bioconcentration of polycyclic aromatic hydrocarbons in vegetables grown in an industrial area[J]. Environmental Pollution,1999,106:369-380.

[72] DESALME D, BINET P, BERNARD N, *et al.* Atmospheric phenanthrene transfer and effects on two grassland species and their root symbionts: a microcosm study [J]. Environmental and Experimental Botany,2011,71:146-151.

[73] ZEZULKA S, KLEMS M, KUMMEROVA M. Root and foliar uptake,translocation,and distribution of [^{14}C] fluoranthene in pea plants fluoranthene in pea plants (*Pisum sativum*) [J]. Environmental Toxicology and Chemistry, 2014, 33(10): 2308-2312.

不同生态型蜈蚣草对砷富集的差异及其机理

许飞飞,马晓娜,罗万清,吴福勇

西北农林科技大学资源环境学院,农业部西北植物营养与农业环境重点实验室,杨凌 712100

摘要 土壤砷污染是全球尤其是东南亚和中国非常突出且亟需解决的环境问题。自砷超富集植物——蜈蚣草(*Pteris vittata* L.)发现以来,一直是国内外学者研究的一个热点。深入理解蜈蚣草体内砷代谢和富集机制是有效利用植物修复技术治理砷污染土壤的关键。在长期的自然进化过程中,蜈蚣草逐渐分化出不同生态型。已有研究结果显示:不同生态型蜈蚣草在砷富集和砷耐性等方面均存在明显差异。本文在系统分析蜈蚣草砷富集特征、机理的基础上,重点阐述了生态型差异对蜈蚣草砷富集的影响方面的最新研究进展。研究结果显示:非污染生态型与污染生态型蜈蚣草相比砷富集能力更为高效,说明通过选择性的利用合适的蜈蚣草生态型将明显改善植物修复的效率。不同生态型蜈蚣草砷富集与砷耐性差异的分子机理尚不清楚,相关关键功能基因及其过程尚需深入研究。

关键词 砷污染;蜈蚣草;生态型;种内差异

砷(As)在地壳中的含量约为1.8~2.1 mg·kg^{-1},广泛存在于自然环境中。尽管与磷同属于第Ⅴ族,但As及其化合物均被认为是致癌物质[1]。砷化合物分为无机砷(As(Ⅴ)和As(Ⅲ))和有机砷(主要为二甲基砷酸(dimethylarsinic acid,DMAA)和单甲基砷酸(monomethylarsonic acid,MMAA))两类[2],其毒性存在明显差别。As(Ⅲ)的毒性是As(Ⅴ)的60倍,无机砷的毒性远远高于有机砷,As(Ⅴ)的毒性约为DMAA和MMAA的70倍[3]。近年来,As污染成为全球特别是东南亚及中国局部地区非常突出且亟需解决的环境问题[4]。孟加拉国约8000万居民(占该国总人口的61.5%)饮用水As含量超过100 μg·L^{-1},远远高于WHO规定的饮用水砷含量标准(10 μg·L^{-1})[5]。2014年4月全国土壤污染状况调查结果显示:19.4%农田土壤遭受污染尤其是重金属污染,其中As点位超标率为2.7%[6]。2010年中国累计消耗煤炭33.8亿t,根据煤炭中As含量及其排放系数计算相当于排放9000 t As[7-8]。湖南郴州、甘肃白银等地铅、锌冶炼厂周边土壤中As含量达到133~24500 mg·kg^{-1}[9-11]。湖南省受金属开采及冶炼影响地区50%的水稻谷粒As含量超过国家标准(0.15 mg·kg^{-1},GB 2762—2005),最高达7.5 mg·kg^{-1}[12-13]。全球数百万居民正在遭受As污染危害,数10万居民死于慢性As中毒[14-15]。因此,亟需开发高效、切实可行的As污染土壤修复技术。

As污染土壤治理是世界各国面临的一个共同难题。传统的物理、化学治理技术由于存在工程量大、费用高、易造成二次污染、破坏土壤理化性质等缺点[16],不太适宜于大面积As污染土壤的治理。植物修复技术是指利用植物及其根际微生物原位修复污染土壤[17-19]。以超富集植物为基础的植物修复技术由于投资和维护成本低、环境扰动小、易于被接受等优点[19-21],一直是国内外学术界研究的热点。As超富集植物——蜈蚣草(*Pteris vittata* L.)的发现,大大增强了人们利用植物修复技术治理As污染土壤的信心和希望[22]。Wu等[23]室内试验研究结果显示:不同生态型蜈蚣草As富集能力存在明显差异。本文拟在系统分析蜈蚣草As富集特征、机理的基础上,综述不同生态型蜈蚣草对砷富集的差异及其富集机理的最新研究进展。

1 蜈蚣草As吸收、富集特征及其机理

超富集植物(Hyperaccumulator)是指植物地上部分能够吸收超过100 mg·kg^{-1}的Cd,或超过300 mg·kg^{-1}的Cu、Co、Cr,或超过1000 mg·kg^{-1}的As、Ni、Pb,或超过3000 mg·kg^{-1}的Zn,或超过10000 mg·kg^{-1}的Mn[24]。超富集植物只占植物界很少一部分,截至目前累计发现各类超富集植物500多种[24],其中As超富集植物14种[20,22,25-31]。与其他As超富集植物相比,蜈

收稿日期:2015-11-24;修回日期:2016-12-02

基金项目:陕西省自然科学基础研究计划项目(2016JM4004);中央高校基本科研业务费专项资金项目(2452015179)

作者简介:许飞飞,硕士研究生,研究方向为土壤污染修复,电子信箱:395091175@qq.com;吴福勇(通信作者),教授,研究方向为土壤植物修复、超富集植物重金属毒性机理及其根际过程,电子信箱:wfy09@163.com

引用格式:许飞飞, 马晓娜, 罗万清, 等. 不同生态型蜈蚣草对砷富集的差异及其机理[J]. 科技导报, 2017, 35(3): 86-91. doi: 10.3981/j.issn.1000-7857.2017.03.010

蜍草研究相对较为充分。

1.1 显著的超富集As能力

一般植物体内As含量小于10 mg·kg^{-1}，蜈蚣草与它们相比具有超强的As富集能力[31-32]，其地上部分As含量高达22600 mg·kg^{-1}[22]，生物富集系数(bioaccumulation factor：植物地上部分As含量与根际土壤As含量的比值)可达1450[33]。Zhao等[26]和Wang等[31]均发现超富集As是蜈蚣草的一种固有属性。Fayiga等[34]研究结果表明：相同时间内蜈蚣草吸收与转运到地上部分的As约为非超富集植物*Nephrolepis exaltata*的10倍。As(V)处理8 h后，蜈蚣草根系所吸收As中的76%被转运至地上部分，而非超富集植物*P. tremula*只有9%的As被转运至地上部分[32]。吸收动力学试验进一步证明：蜈蚣草吸收As(V)过程中的米氏常数K_m显著小于非As超富集植物*N. exaltata*，说明蜈蚣草对As(V)具有更强的亲和力[35]。蜈蚣草既能高效吸收As(V)也能高效吸收As(III)[36]。与其他植物相似，As(V)主要通过磷酸盐运输通道被蜈蚣草根系吸收[35,37]，As(III)则主要通过水通道蛋白进入蜈蚣草体内[38]，但是目前尚未有文献报道蜈蚣草具有如此强的As吸收和转运能力的原因。

1.2 独特的忍耐和富集As机制

蜈蚣草体内78%~96%的As分布于羽叶中[22,39-40]，储存于细胞液泡内[40-41]。羽叶中85%的As以As(III)形态存在，其余为As(V)、微量的甲基砷和二甲基砷[22,37]。蜈蚣草根内As(V)的含量占明显优势，As(III)只占根内总As量的10%~40%[35,40]。蜈蚣草体内As的生理作用尚不清楚。Rathinasabapathi等[42]和Mathews等[43]认为，蜈蚣草体内富集大量As的原因可能是为了防御食草类害虫。

大多数非超富集植物主要通过以下机制获得对As的耐性：一是通过抑制高亲和磷的吸收通道减少植物As的吸收，从而增加对As的耐性[44-45]；二是所吸收的As(V)在植物体内被还原为As(III)，毒性较高的As(III)再与硫醇(Thiols)尤其是植络素(PCs)络合为毒性较小的有机态As[45-46]。与以上机理完全不同，蜈蚣草拥有一些独特的耐As机制，最为显著的是蜈蚣草具有高效的还原As(V)的能力。As(V)处理1 h后，蜈蚣草根内便能够检测到As(III)的存在[47]，且其吸收的As(V)中有40%被还原为As(III)[35]。Tu等[48]将蜈蚣草离体的根和羽叶浸泡在含As(V)的营养液中24 h后发现：羽叶中90%以上的As为As(III)，根系中20%以上的As为As(III)。Duan等[49]研究结果显示：蜈蚣草根内As酸盐还原酶在As形态转化的过程中发挥着至关重要的作用，且其根内As酸盐还原酶的活性显著高于非超富集植物如水稻、拟南芥。As酸盐还原酶基因(*PvACR2*)已经从蜈蚣草的cDNA文库中克隆出，该基因与*ScACR2*具有较高的同源性[50]。在谷胱甘肽(GSH)等协同因子存在的条件下，纯化的*PvACR2*蛋白质表达产物在体外能够将As(V)还原为As(III)[50]。蜈蚣草体内的GSH等其他还原性物质也能将As(V)还原为As(III)[49]。其次是蜈蚣草羽叶中的砷主要存储于表皮细胞的液胞中，液泡的区隔化作用降低了砷的毒性。Indriolo等[51]发现：蜈蚣草液泡膜内亚砷酸盐转运蛋白基因*PvACR3*可将As(III)转运至液泡内。液泡中砷含量占羽叶总砷含量的91%[52]。此外，Zhao等[53]发现：蜈蚣草体内被植络素(PCs)络合的As只占总As的1%~3%，这说明PCs在蜈蚣草耐As的机制中作用有限，与大多数非超富集植物的耐As机制明显不同。

2 植物生态型的概念及分类

1922年瑞典遗传生态学家Turesson首次提出了生态型(ecotype)的概念：即同一物种因适应不同生境而表现出的、具有一定结构或功能差异的不同类群[54]。植物生态型是指同种植物长期生长在不同的生长环境中，因趋异适应而形成的在生态学上有差别的同种异地个体或种群[55]。根据形成生态型的主导生态因子不同，一般将植物划分为3种生态型：气候生态型，长期适应不同的光周期、气温和降水等气候因子而形成的各种生态型；土壤生态型，长期在不同的土壤水分、温度和肥力等自然和栽培条件的作用下而形成的生态型；生物生态型，主要在生物因子的作用下形成的生态型[56]。多数植物因地理分布广、气候和土壤条件差异大，生境异质性和自然选择往往导致单一物种存在多种生态型[57]。植物种群为适应环境选择的压力而诱导产生对胁迫的抗性、耐性、生理、生物化学特性更多样的基因，这可能会导致其适应性增强或减弱[58]。部分植物不同生态型在形态上表现出差异，部分只在生理或生化上有差异而在形态上并无明显差异。

3 不同生态型对蜈蚣草As富集的影响

蜈蚣草在自然界分布范围相当广泛，美国、英国、泰国和中国等地均有发现，无论是As污染土壤还是非污染土壤均能正常生长[20,22,25-26,30-31,59]。在长期进化过程中，为适应特殊立地条件下不利的自然环境，生长于As污染土壤的蜈蚣草(污染生态型)与生长于非污染土壤的蜈蚣草(非污染生态型)相比存在明显的生理差异。室内模拟As污染条件下，非污染生态型比污染生态型蜈蚣草生长更旺盛，前者(源自于香港大埔窖自然保护区)地上部分干重约为后者(大顺垄生态型)干重的2.1~2.5倍[23]。污染生态型蜈蚣草与其相应的非污染生态型相比，还具有显著高的As、Pb和Zn耐性[23,59]。无论是野外调查还是室内研究均证实：非污染生态型与污染生态型蜈蚣草对As的吸收与富集存在明显差异，前者与后者相比吸收、富集As能力更强(表1)。非污染生态型蜈蚣草(香港生态型)吸收As总量是另外2个污染生态型蜈蚣草(分别源于湖南省大顺垄As污染点和湖南省金川塘As污染点)的1.1~1.9倍[23]。Wan等[60]也发现：来源于不同As污染土壤中的蜈蚣草As吸收、As耐性存在明显差异。在其他重金属(如Pb,Zn)存在的情况下，非污染生态型蜈蚣草对砷的吸收效率依然高于污染生态型蜈蚣草[61]。非污染生态型与污染生态型蜈蚣草相比As吸收更为高效的主要机理为：1) 非污染生态型蜈蚣草地上部分生物量更大；2) 非污染生态型蜈蚣草根系无论是对

As(V)还是对As(III)的吸收速率均更高;3) 非污染生态型蜈蚣草地下部分向地上部分转移As的能力更强[59]。此外,不同生境下的丛枝菌根真菌菌株对蜈蚣草As的积累也能产生显著的影响,非污染型菌株比污染型菌株表现出更强的促进作用[62–63],这可能是导致不同生态型蜈蚣草As吸收差异的另一原因。

表1 不同生态型蜈蚣草砷富集特征

Table 1 Characteristics of arsenic accumulation of different ecotypes of *Pteris vittata* L.

生态类型	来源	野外土壤砷质量分数/(mg·kg^{-1})	室内试验		地上部分砷质量分数/(mg·kg^{-1})	参考文献
			土壤砷质量分数/(mg·kg^{-1})	培育时间		
非污染生态型	香港大浦滘	9.78	—	—	17.4	[9]
非污染生态型	广西南宁	10.7	—	—	48.5	[59]
非污染生态型	广州中大校园	13.3	—	—	54.4	[59]
非污染生态型	广西南丹	26.7	—	—	142	[59]
污染生态型	湖南大顺垄	20710	—	—	1373	[9]
污染生态型	湖南野鸡尾	6108	—	—	1130	[9]
污染生态型	浙江衢州	151	—	—	112	[59]
污染生态型	湖南 113°09′59″E 25°43′15″N	108	—	—	4650	[60]
污染生态型	湖南 113°09′05″E 25°48′04″N	1159	—	—	1003	[60]
污染生态型	湖南 113°09′39″E 25°43′25″N	3579	—	—	402	[60]
污染生态型	湖南 113°09′53″E 25°43′23″N	7527	—	—	4207	[60]
非污染生态型	广州中大校园	—	50	12周	1601	[31]
非污染生态型	香港大浦滘	—	50	12周	1659	[59]
非污染生态型	广西南宁	—	50	12周	1472	[59]
非污染生态型	广州中大校园	—	50	12周	1209	[59]
污染生态型	广东乐昌	—	50	12周	285	[31]
污染生态型	湖南大顺垄	—	50	12周	481	[59]
污染生态型	广西南丹	—	50	12周	1197	[59]
污染生态型	浙江衢州	—	50	12周	2546	[59]

室内研究结果初步显示:非污染生态型与污染生态型蜈蚣草相比还存在明显的基因差异。非污染生态型与污染生态型蜈蚣草根系对As(V)和As(III)的吸收均符合米氏吸收方程,前者根系对As(V)和As(III)的最大吸收速率($V_{\max}$)均明显高于后者,说明前者根系细胞膜内单位转运蛋白(磷酸转运蛋白和水通道蛋白)的数量要明显多于后者[59]。蜈蚣草既超富集As,也对As具有超耐性,但这2个特性可能分别受不同基因控制。来自低As污染区的生态型比高As污染区的蜈蚣草生态型积累的As含量高80%,然而后者展现出更强的As耐性,具有比前者高5倍的生物量[60]。Wu等[23]研究也发现:非污染生态型蜈蚣草有较高的As积累能力,但是在As耐性方面要比污染生态型差。这与另一超富集植物天蓝遏蓝菜(*Thlaspi caerulescens*)明显不同:源自法国南部的Ganges生态型比源自比利时的Prayon生态型不仅积累更多的Cd,而且对Cd的耐性也更强,表现出协同性[64]。然而也有研究表明:来自As污染区佛罗里达州、非As污染区牛津和法国奥隆扎克(Olonzac)3个地方的蜈蚣草并没有对As的积累产生显著性差异[65]。此外,源自于贵州省兴仁县回龙镇2处污染区蜈蚣草As积累也没有发现显著性差异[66],因此,不同生态型蜈蚣草As吸收及As耐性机理是否存在差异,尚需深入系统研究。

综上所述,尽管在蜈蚣草As吸收、转运、还原和富集方面取得了一些重要进展,但蜈蚣草As吸收和As耐性的种内差异机理仍不明晰,影响不同生态型蜈蚣草对As的吸收、积累与分布的因素尚不清楚。截至目前,国内外从不同生态型蜈蚣草对As吸收、转运、还原存在差异的角度去揭示蜈蚣草As富集和As耐性机理的文献报道仍十分少见。

4 展望

近30年来,随着工农业持续高速发展和城市化进程不断加快,中国土壤环境状况总体呈恶化态势,部分地区土壤污染形势相当严峻,采取以超富集植物——蜈蚣草为基础的植物修复技术治理As污染土壤,对于合理利用土地、确保农产品质量安全具有极其重要的意义。今后应重点在以下几个方向开展研究。

1) 理想As修复植物生态型的筛选和培育:中国幅员广阔,地域差别大,应广泛存在不同蜈蚣草生态型,筛选和培育适用范围更广、栽培更容易、生物量更大的生态型,为As污染土壤的植物修复技术走向产业化提供前提条件。

2) 不同生态型蜈蚣草As富集与As耐性差异的分子机理:不同生态型蜈蚣草对As富集、As耐性等方面存在显著性差异,但目前研究大多停留在宏观水平,而对不同生态型蜈蚣草As富集与As耐性差异的分子机理研究较少。深入研究蜈蚣草超富集As的机制,充分挖掘其关键功能基因,揭示相关过程和机理有利于提高植物修复效率。

3) 不同生态型蜈蚣草多基因组比对:蜈蚣草基因组很大且缺少有效的转基因手段,截至目前其基因组图谱尚不清楚。在全面了解蜈蚣草基因组图谱和序列分析的基础上,通过比对不同生态型蜈蚣草多基因组,有望对砷富集及砷耐性至关重要的基因结构及其调控作用有所了解。

参考文献(References)

[1] International Agency for Research on Cancer. Some drinking- water disinfectants and contaminants, including arsenic[R]. Geneva: WHO, 2004.

[2] Ng J C. Environmental contamination of arsenic and its toxicological impact on humans[J]. Environmental Chemistry, 2005, 2(3): 146-160.

[3] World Health Organization. Arsenic compounds, environmental health criteria 224[R]. Geneva: WHO, 1998.

[4] Meharg A A. Arsenic in rice-understanding a new disaster for South-East Asia[J]. Trends in Plant Science, 2004, 9(9): 415-417.

[5] Hossain M F. Arsenic contamination in Bangladesh- an overview[J]. Agriculture, Ecosystems & Environment, 2006, 113(1-4): 1-16.

[6] Zhao F J, Ma Y B, Zhu Y G, et al. Soil contamination in China: Current status and mitigation strategies[J]. Environmental Science & Technology, 2015, 49: 750-759.

[7]《中国环境年鉴》编辑委员会. 中国环境年鉴[M]. 北京: 中国环境科学出版社, 2011: 22.
The China Environment Yearbook Editing Committee. China´s environmental yearbook[M]. Beijing: China Environment Yearbook Publisher, 2011: 22.

[8] Luo L, Ma Y B, Zhang S Z, et al. An inventory of trace element inputs to agricultural soils in China[J]. Journal of Environmental Management, 2009, 90(8): 2524-2530.

[9] Wu F Y, Ye Z H, Wu S C, et al. Metal accumulation and arbuscular mycorrhizal status in metallicolous and nonmetallicolous populations of *Pteris vittata* L. and *Sedum alfredii* Hance[J]. Planta, 2007, 226(6): 1363-1378.

[10] Zhu Y G, Sun G X, Lei M, et al. High percentage inorganic arsenic content of mining impacted and nonimpacted Chinese rice[J]. Environmental Science & Technology, 2008, 42(13): 5008-5013.

[11] 曾希柏, 苏世鸣, 吴翠霞, 等. 农田土壤中砷的来源及调控研究与展望[J]. 中国农业科技导报, 2014, 16(2): 85-91.
Zeng Xibai, Su Shiming, Wu Cuixia, et al. Research and prospect of arsenic source and its regulation in arable land soil[J]. Journal of Agricultural Science and Technology, 2014, 16(2): 85-91.

[12] Liao X Y, Chen T B, Xie H, et al. Soil As contamination and its risk assessment in areas near the industrial districts of Chenzhou City, Southern China[J]. Environment International, 2005, 31: 791-798.

[13] Williams P N, Villada A, Deacon C, et al. Greatly enhanced arsenic shoot assimilation in rice leads to elevated grain levels compared to wheat and barley[J]. Environmental Science & Technology, 2007, 41 (19): 6854-6859.

[14] Chowdhury U K, Biswas B K, Roychowdhury T, et al. Groundwater arsenic contamination in Bangladesh and West Bengal, India[J]. Environmental Health Perspectives, 2000, 108(5): 393-397.

[15] Das D, Chatterjee A, Mandal B K, et al. Arsenic in ground-water in 6 districts of West Bengal, India- the biggest arsenic calamity in the world. 2. arsenic concentration in drinking- water, hair, nails, urine, skin-scale and liver-tissue (biopsy) of the affected people[J]. Analyst, 1995, 120(3): 917-924.

[16] Wenzel W W, Adriano D C, Salt D, et al. Phytoremediation: A plant-microbe- based remediation system[M]//Adriano D C, Bollag J M, Frankenberger W T J, Sims R C, eds. Bioremediation of Contaminated Soils. Agronomy Monograph No. 37. Madison, WI, USA, 1999: 456-508.

[17] Kramer U. Phytoremediation: novel approaches to cleaning up polluted soils[J]. Current Opinion in Biotechnology, 2005, 16(2): 133-141.

[18] Van Nevel L, Mertens J, Oorts K, et al. Phytoextraction of metals from soils: How far from practice? [J] Environmental Pollution, 2007, 150 (1): 34-40.

[19] Marques A P G C, Rangel A O S S, Castro P M L. Remediation of heavy metal contaminated soils: Phytoremediation as a potentially promising clean- up technology[J]. Critical Reviews in Environmental Science and Technology, 2009, 39(8): 622-654.

[20] Chen T B, Wei Z Y, Huang Z C, et al. Arsenic hyperaccumulator *Pteris Vittata* L. and its arsenic accumulation[J]. Chinese Science Bulletin, 2002, 47(11): 901-905.

[21] Leduc D L, Terry N. Phytoremediation of toxic trace elements in soil and water[J]. Journal of Industrial Microbiology & Biotechnology, 2005, 32(11/12): 514-520.

[22] Ma L Q, Komar K M, Tu C, et al. A fern that hyperaccumulates arsenic[J]. Nature, 2001, 409: 579.

[23] Wu F Y, Ye Z H, Wu S C, et al. Variation in arsenic, lead and zinc tolerance and accumulation in six populations of *Pteris vittata* L from China[J]. Environmental Pollution, 2009, 157: 2394-2404.

[24] Van Der Ent A, Baker A J M, Reeves R D, et al. Hyperaccumulators of metal and metalloid trace elements: facts and fiction[J]. Plant and Soil, 2013, 362(1/2): 319-334.

[25] Visoottiviseth P, Francesconi K, Sridokchan W. The potential of Thai indigenous plant species for the phytoremediation of arsenic contaminated land[J]. Environmental Pollution, 2002, 18(3): 453-461.

[26] Zhao F J, Durham S J, Mcgrath S P. Arsenic hyperaccumulation by different fern species[J]. New Phytologist, 2002, 156(1): 27-31.

[27] Meharg A A. Variation in arsenic accumulation-hyperaccumulation in

ferns and their allies[J]. New Phytologist, 2003, 157(1): 25-31.

[28] Du W B, Li Z A, Zou B, et al. *Pteris multifida* Poir., a new arsenic hyperaccumulator: Characteristics and potential[J]. International Journal Environment and Pollution, 2005, 23(4): 388-396.

[29] Srivastava M, Ma L Q, Santos J A G. Three new arsenic hyperaccumulating ferns[J]. Science of the Total Environment, 2006, 364(1-3): 24-31.

[30] Wang H B, Ye Z H, Shu W S, et al. Arsenic uptake and accumulation in fern species growing at arsenic- contaminated sites of southern China: Field survey[J]. International Journal of Phytoremediation, 2006, 8(1): 1-11.

[31] Wang H B, Wong M H, Lan C Y, et al. Uptake and accumulation of arsenic by 11 Pteris taxa from southern China[J]. Environmental Pollution, 2007, 145(1): 225-233.

[32] Caille N, Zhao F J, Mcgrath S P. Comparison of root absorption, translocation and tolerance of arsenic in the hyperaccumulator *Pteris vittata* and the nonhyperaccumulator *Pteris tremula*[J]. New Phytologist, 2005, 165(3): 755-761.

[33] Tu C, Ma L Q, Bondada B. Arsenic accumulation in the hyperaccumulator Chinese brake and its utilization potential for phytoremediation [J]. Journal of Environmental Quality, 2002, 31(5): 1671-1675.

[34] Fayiga A O, Ma L Q, Santos J, et al. Effects of arsenic species and concentrations on arsenic accumulation by different fern species in a hydroponic system[J]. International Journal of Phytoremediation, 2005, 7(3): 231-240.

[35] Poynton C Y, Huang J W W, Blaylock M J, et al. Mechanisms of arsenic hyperaccumulation in *Pteris* species: Root as influx and translocation[J]. Planta, 2004, 219(6): 1080-1088.

[36] Kertulis G M, Ma L Q, Macdonald G E, et al. Arsenic speciation and transport in *Pteris vittata* L. and the effects on phosphorus in the xylem sap[J]. Environmental and Experimental Botany, 2005, 54(3): 239-247.

[37] Wang J R, Zhao F J, Meharg A A, et al. Mechanisms of arsenic hyperaccumulation in *Pteris vittata*. Uptake kinetics, interactions with phosphate, and arsenic speciation[J]. Plant Physiology, 2002, 130(3): 1552-1561.

[38] Mathews S, Rathinasabapathi B, Ma L Q. Uptake and translocation of arsenite by *Pteris vittata* L.: Effects of glycerol, antimonite and silver [J]. Environmental Pollution, 2011, 159(12): 3490-3495

[39] Chen T B, Yan X L, Liao X Y, et al. Subcellular distribution and compartmentalization of arsenic in *Pteris vittata* L.[J]. Chinese Science Bulletin, 2005, 50(24): 2843-2849.

[40] Pickering I J, Gumaelius L, Harris H H, et al. Localizing the biochemical transformations of arsenate in a hyperaccumulating fern [J]. Environmental Science and Technology, 2006, 40(16): 5010-5014.

[41] Lombi E, Zhao F J, Fuhrmann M, et al. Arsenic distribution and speciation in the fronds of the hyperaccumulator *Pteris vittata*[J]. New Phytologist, 2002, 156(2): 195-203.

[42] Rathinasabapathi B, Rangasamy M, Froeba J, et al. Arsenic hyperaccumulation in the Chinese brake fern (*Pteris vittata*) deters grasshopper (*Schistocerca americana*) herbivory[J]. New Phytologist, 2007, 175(2): 363-369.

[43] Mathews S, Ma L Q, Rathinasabapathib B, et al. Arsenic reduced scale-insect infestation on arsenic hyperaccumulator *Pteris vittata* L. [J]. Environmental and Experimental Botany, 2009, 65(2-3): 282-286.

[44] Meharg A A, Hartley-Whitaker J. Arsenic uptake and metabolism in arsenic resistant and nonresistant plant species[J]. New Phytologist, 2002, 154(1): 29-43.

[45] Hartley-Whitaker J, Woods C, Meharg A A. Is differential phytochelatin production related to decreased arsenate influx in arsenate tolerant *Holcus lanatus*?[J]. New Phytologist, 2002, 155(2): 219-225.

[46] Hartley-Whitaker J, Ainsworth G, Vooijs R, et al. Phytochelatins are involved in differential arsenate tolerance in *Holcus lanatus*[J]. Plant Physiology, 2001, 126(1): 299-306.

[47] Su Y H, Mcgrath S P, Zhu Y G, et al. Highly efficient xylem transport of arsenite in the arsenic hyperaccumulator *Pteris vittata*[J]. New Phytologist, 2008, 180(2): 434-441.

[48] Tu S, Ma L Q, Macdonald G E, et al. Effects of arsenic species and phosphorus on arsenic absorption, arsenate reduction and thiol formation in excised parts of *Pteris vittata* L.[J]. Environmental and Experimental Botany, 2004, 51(2): 121-131.

[49] Duan G L, Zhu Y G, Tong Y P, et al. Characterization of arsenate reductase in the extract of roots and fronds of Chinese brake fern, an arsenic hyperaccumulator[J]. Plant Physiology, 2005, 138(1): 461-469.

[50] Ellis D R, Gumaelius L, Indriolo E, et al. A novel arsenate reductase from the arsenic hyperaccumulating fern *Pteris vittata*[J]. Plant Physiology, 2006, 141(4): 1544-1554.

[51] Indriolo E, Na G, Ellis D, et al. A vacuolar arsenite transporter necessary for arsenic tolerance in the arsenic hyperaccumulating fern *Pteris vittata* is missing in flowering plants[J]. Plant Cell, 2010, 22(6): 2045-2057.

[52] Yang X X, Chen H, Dai X J, et al. Evidence of vacuolar compartmentalization of arsenic in the hyperaccumulator *Pteris vittata*[J]. Chinese Science Bulletin, 2009, 54(22): 4229-4233.

[53] Zhao F J, Wang J R, Barker J H A, et al. The role of phytochelatins in arsenic tolerance in the hyperaccumulator *Pteris vittata*[J]. New Phytologist, 2003, 159(2): 403-410.

[54] Turesson G. The species and the variety as ecological units[J]. Hereditas, 1922, 3(1): 100-113.

[55] Briggs D, Walters S M. Plant variation and evolution[M]. Cambridge: Cambridge University Press, 1997.

[56] 骆世明. 农业生态学[M]. 北京: 中国农业出版社, 2001: 27-29.
Luo Shiming. Agricultural ecology[M]. Beijing: China Agriculture Press, 2001: 27-29.

[57] Kristina M H, Susan J M. Plant ecotypes: genetic differentiation in the age of ecological restoration[J]. Trends in Ecology and Evolution, 2003, 18(3): 147-155.

[58] John K M, Caroline E C, Susan H, et al. 'How Local Is Local?'—A review of practical and conceptual issues in the genetics of restoration [J]. Restoration Ecology, 2005, 13(3): 432-440.

[59] Wu F Y, Deng D, Wu S C, et al. Arsenic tolerance, uptake, and accumulation by nonmetallicolous and metallicolous population of *Pteris vittata* L.[J]. Environmental Science and Pollution Research, 2015, 22(12): 8911-8918.

[60] Wan X M, Lei M, Liu Y R, et al. A comparison of arsenic accumulation and tolerance among four populations of *Pteris vittata* from habitats with a gradient of arsenic concentration[J]. Science of the Total Environment, 2013, 442: 143-151.

[61] Wu F Y, Zhakypbek Y Z, Bi Y L, et al. Effects of Pb and Zn on As accumulation in nonmetallicolous and metallicolous populations of *Pteris vittata* L.[J]. Communications in Soil Science and Plant Analysis, 2013, 44(19): 2839-2851.

[62] Wu F Y, Ye Z H, Wong M H. Intraspecific differences of arbuscular mycorrhizal fungi in their impacts on arsenic accumulation by *Pteris*

vittata L.[J]. Chemosphere, 2009, 76(9): 1258-1264.

[63] 吴福勇, 毕银丽, 郭一飞, 等. 不同生态型摩西球囊霉菌株对蜈蚣草砷吸收的影响[J]. 生态学杂志, 2013, 32(6): 1539-1544.
Wu Fuyong, Bi Yinli, Guo Yifei, et al. Effects of different ecotype Glomus mosseae isolates on arsenic uptake by *Pteris vittata*[J]. Chinese Journal of Ecology, 2013, 32(6): 1539-1544.

[64] Lombi E, Zhao F J, Dunham S J, et al. Cadmium accumulation in populations of Thlaspi caerulescens and *Thlaspi goesingense*[J]. New Phytologist, 2000, 145(1): 11-20.

[65] Zhao F J, Dunham S J, McGrath S P. Arsenic hyperaccumulation by different fern species[J]. New Phytologist, 2002, 156(1): 27-31.

[66] Wei C Y, Sun X, Wang C, et al. Factors influencing arsenic accumulation by *Pteris vittata*: A comparative field study at two sites[J]. Environ Pollution, 2006, 141(3): 488-493.

Mechanisms and variations of arsenic accumulation in different ecotypes of *Pteris vittata* L.

XU Feifei, MA Xiaona, LUO Wanqing, WU Fuyong

College of Natural Resources and Environment, Northwest A&F University; Key Laboratory of Plant Nutrition and the Agri-environment in Northwest China, Ministry of Agriculture, Yangling 712100, China

Abstract Arsenic (As) contamination has become a global environmental issue for years, with the most severe problem occurring in Southeast Asia and China. There has been a particular research interest since the first As-hyperaccumulator, *Pteris vittata* L., was identified. The mechanism of accumulation and metabolism of As in *P. vittata* can contribute to the optimization of phytoremediation. *P. vittata* has developed different ecotypes during its long-term evolution process. It is shown that there are significant differences in As accumulation and tolerance among the ecotypes of *P. vittata*. Based on a systematic analysis of characteristic and mechanism of As accumulation in *P. vittata*, the present work reviews the latest progress in the effects of different ecotypes on As accumulation in *P. vittata*. The preliminary result shows that the nonmetallicolous ecotypes possess more effective As accumulation than the metallicolous ecotypes, suggesting that the efficiency of phytoextraction can be greatly enhanced by judicious selection of appropriate ecotypes of *P. vittata*. However, it is still not fully clear how molecular mechanisms are related to accumulation and tolerance of As in different ecotypes of *P. vittata*. Further studies should concentrate on key functional genes and the process involved in As hyperaccumulation in *P. vittata*.

Keywords arsenic contamination; *Pteris vittata* L.; ecotype; intraspecific variation

（责任编辑　王媛媛）

第40卷 第2期
2017年2月

环境科学与技术
Environmental Science & Technology

Vol. 40 No.2
Feb. 2017

石陶然，吴福勇，于涛，等. 分子量和浓度梯度对溶解性有机质结合重金属的影响[J].环境科学与技术，2017，40（2）：1-8. Shi Taoran，Wu Fuyong，Yu Tao, et al. Molecular weight and concentration influenced dissolved organic matter complexation with heavy metals[J]. Environmental Science & Technology，2017，40（2）：1-8.

分子量和浓度梯度对溶解性有机质结合重金属的影响

石陶然[1]， 吴福勇[1*]， 于涛[2]， 许飞飞[1]， 田凯[1]， 马晓娜[1]
（1.西北农林科技大学资源与环境学院，陕西 杨凌 712100；
2.中国环境科学研究院，环境基准与风险评估国家重点实验室，北京 100012）

摘 要：采用平衡渗析法和光谱分析等技术研究了滇池代表性湖区沉积物不同分子量溶解性有机质（DOM）与不同浓度Cu^{2+}、Pb^{2+}的结合特征。结果表明，与Cu、Pb结合后，M_w<1 000 u、1 000~2 000 u的DOM组分中总有机碳（TOC）含量最高，且TOC浓度随DOM分子量的增加而降低，但不受重金属浓度梯度的影响。M_w<1 000 u、1 000~2 000 u的DOM组分中总Cu、总Pb含量最高，且受重金属浓度梯度的影响。三维荧光光谱特征表明，与Cu、Pb结合后，M_w<1 000 u、1 000~2 000 u的DOM组分荧光强度最小，且都是与高浓度重金属结合的荧光强度较小。紫外光谱特征表明草海DOM的分子量在整体上大于外海，同一分子量DOM与Cu结合后在250 nm和365 nm处紫外吸光度之比（E2/E3）小于与Pb结合的情况。研究结果为湖泊沉积物有机质与重金属之间的相互作用特征提供理论基础。

关键词：平衡渗析； 重金属； 溶解性有机质； 分子量； 浓度梯度
中图分类号：X131 **文献标志码**：A doi：10.3969/j.issn.1003-6504.2017.02.001 **文章编号**：1003-6504(2017)02-0001-08

Molecular Weight and Concentration Influenced Dissolved Organic Matter Complexation with Heavy Metals

SHI Taoran[1]， WU Fuyong[1*]， YU Tao[2]， XU Feifei[1]， TIAN Kai[1]， MA Xiaona[1]
（1.College of Resource and Environmental Science，Northwest Agriculture and Forestry University，Yangling 712100，China；2.State Key Laboratory of Environment Criteria and Risk Assessment，Chinese Research Academy of Environmental Science，Beijing 100012，China）

Abstract：The equilibrium dialysis method and spectroscopy technology were performed to explore the interaction between different concentrations of heavy metal and different molecular weights DOM from Dianchi Lake sediment. Results indicated that TOC concentration was maximal in the DOM fraction with molecular weight lower than 1 000 u after different molecular weights DOM combined with total Cu，TOC concentration was maximal in the DOM fraction with molecular weight of 1 000 to 2 000 u after different molecular weights DOM combined with total Pb. TOC concentration decreased with increased molecular weight，and was not effected by concentration gradient of heavy metal. Total Cu concentration was maximal in the DOM fraction with molecular weight lower than 1 000 u，total Pb concentration was maximal in the DOM with molecular weight between 1 000 and 2 000 u. Total Cu and total Pb concentrations affected by concentration gradient of heavy metal were higher in Caohai individual DOM fractions than in Waihai. This research will provide the theory basis for the research on interaction of DOM and heavy metals in the lake sediments.

Key words：equilibrium dialysis；heavy metal；dissolved organic matter；molecular weight；concentration gradient

溶解性有机质（dissolved organic matter，DOM）在水环境中普遍存在，它是水环境中重要的配位体和吸附载体，能与重金属形成稳定的化合物，从而影响重金属的迁移转化、生物有效性和最终归宿[1]。DOM是物理上不均匀的、多分散性的、结构复杂的有机混合物，由相对高分子量的腐殖质、富里酸以及低分子

《环境科学与技术》编辑部：（网址）http://fjks.chinajournal.net.cn（电话）027-87643502（电子信箱）hjkxyjs@vip.126.com
收稿日期：2016-06-24；修回 2016-08-30
基金项目：国家自然科学基金项目资助（51278475）

作者简介：石陶然（1986-），女，博士研究生，研究方向为土壤污染修复，（电子信箱）shitaoran@126.com；* 通讯作者，教授，博士，（电子信箱）wfy09@163.com。

量的蛋白质、有机酸、糖类和其他化合物组成[2]。DOM的分子特征，尤其是分子量（M_w），在很大程度上影响其在自然和工程水系统中的反应[3]。不同分子量DOM的光反应活性、光学性质和生物有效性有很大的差异[4]。目前有很多技术能有效地将DOM按分子量分离成不同的组分，如平衡渗析法[5]、超滤膜法[6]、凝胶过滤色谱[7]、高效体积排阻色谱[8]等。平衡渗析法是被广泛应用的技术之一，基于成本低、使用方便、以及可以根据目的灵活选择分子量范围等优点，已经被成功地运用于许多关于自然体系中不同分子量的DOM对重金属影响的研究[9-10]。

国内外学者对DOM和重金属相互作用的研究主要有：不同分子量DOM对重金属的结合能力差异的研究[11]；不同分子量DOM对重金属的毒性和生物有效性的影响[12]；利用荧光激发发射光谱和平行因子分析研究DOM对重金属迁移的影响[13]、DOM对重金属活性的影响[14]、运用模型评估DOM对重金属形态的影响[15]等。这些研究涉及到土壤、天然水体或垃圾渗滤液中的DOM与重金属相互作用、结合前后的荧光特性及其结合机理的研究，然而对于湖泊沉积物不同分子量DOM与不同种类重金属的结合特征的差异，以及重金属浓度对其与DOM结合的影响方面的研究很少。

本研究以滇池沉积物中DOM为研究对象，选择Cu和Pb这2种环境中重要的重金属元素，应用平衡渗析实验，通过分析滇池草海和外海沉积物中不同分子量DOM对不同浓度重金属Cu和Pb的结合特性，探讨DOM分子量、重金属浓度对DOM与重金属相互作用的影响，对重金属的环境行为以及与湖泊沉积物DOM之间的作用特征提供理论依据。

1 材料与方法

1.1 样品的采集与处理

于2010年10月采集滇池表层（0~10 cm）沉积物样品，采样点位置见图1。由于滇池草海和外海在重金属污染水平、富营养化程度、有机质含量等方面存在显著差异[16-18]，因此采样点分布在这2个有代表性的湖区。用GPS定位分别在草海和外海用抓斗式采泥器采集表层沉积物样品，每个采样点采集3个重复样，代表典型湖区的沉积物特征。样品采集后保存在洁净的密封袋中，4 ℃环境下保存运回实验室。沉积物样品经真空冷冻干燥后研磨，过孔径为0.149 mm的尼龙筛后装密封袋保存。采样点表层沉积物的基本理化性质见表1。由表1可知，在空间分布上，除了pH，对于其他的理化性质都是在草海的浓度显著（$P<0.05$）高于外海。

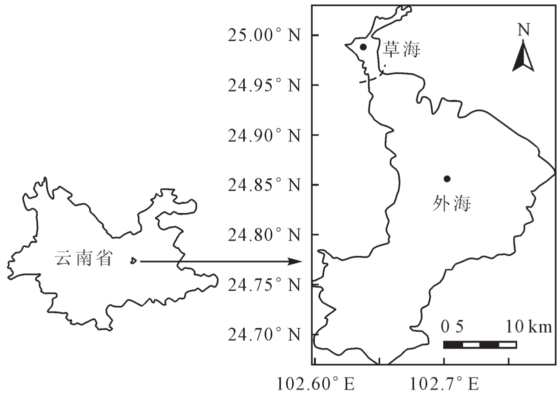

图1 滇池沉积物采样点位示意图
Fig.1 Location of sampling sites in Dianchi Lake

沉积物DOM的提取：取上述预处理的沉积物20 g混合到100 mL去离子水中（电阻率为18.2 Ω·cm）（水∶沉积物=5∶1），在振荡器250 r/min条件下连续振荡24 h，然后以8 000 r/min的速度离心5 min，上清液通过0.45 μm玻璃纤维滤膜（预先在450 ℃下灼烧，恒温5 h），滤液为实验用的DOM溶液。DOM溶液置于4 ℃避光保存备用。

表1 滇池沉积物的理化性质（平均值±标准差）
Table 1 Physiochemical properties of the sediments from Dianchi Lake（means ± standard）（$n=3$）

采样点位	pH	EC/μS·cm^{-1}	TN/mg·g^{-1}	TP/mg·g^{-1}	TOC/mg·L^{-1}	OM/mg·g^{-1}	Cu/mg·kg^{-1}	Pb/mg·kg^{-1}
草海	7.35±0.01	4 195±92	13.674±0.01	2.812±0.34	1.278±0.29	177.9±19.16	426.50±25.07	364.01±44.59
外海	7.67±0.01	955±63	10.912±1.35	2.958±0.11	0.687±0.01	53.00±4.10	80.64±11.45	70.17±16.72

1.2 平衡渗析实验方法

平衡渗析实验：选用M_w为1 000、2 000、5 000、10 000 u的渗透袋（Spectra/Por CE，Fisher Scientific），剪成若干截合适的长度（本研究确保能装下15 mL DOM为宜），置于去离子水中30 min去除渗透袋表面的保护液叠氮化钠，然后用去离子水反复冲洗后备用。用500 mL耐热玻璃烧杯作为渗析容器，加入处理溶液400 mL，设4种处理溶液：ρ(Cu)为1 mg/L、5 mg/L，ρ(Pb)为0.5 mg/L、1 mg/L 400 mL。空白实验为加入400 mL去离子水。取ρ(DOM)为30 mg/L的提取液15 mL放入渗透袋中，袋两端用渗析夹封闭，将其浸在已装入处理溶液的烧杯中。最后用保鲜膜密封烧杯，避免在实验过程中水分蒸发。整个实验过程在恒温振荡器（4 ℃）中进行，为了避免微生物活动和光氧

化[5]。所有实验均设 3 个重复样。根据已有文献[19]，DOM 分子量为 3 500 u 和 500 u 的渗透袋达到渗析平衡需要的时间分别是 7 和 14 d。因此，本研究以 14 d 作为平衡时间，确保使不同分子量的 DOM 都充分达到平衡。达到平衡后，M_w 为 1 000 u 渗透袋外部烧杯中的溶液就是 $M_w<1\ 000$ u 的 DOM 组分；然后将 M_w 为 1 000 u 渗透袋放置在 M_w 为 2 000 u 渗透袋所在的烧杯中达到渗透平衡以后，烧杯中的溶液就是 $1\ 000<M_w<2\ 000$ u 的 DOM 组分，以此类推，得到 $2\ 000<M_w<5\ 000$ u，$5\ 000<M_w<10\ 000$ u 和 $M_w>10\ 000$ u 的 DOM 组分。

1.3　分析仪器条件及参数

DOM 的三维荧光光谱测定：在高灵敏度荧光光谱分析仪（Hitachi F-4500）上进行。激发光源为 150 W 氙弧灯，PMT 电压 700 V，信噪比>110，带通（Bandpass）λ_{Ex} 为 5 nm，λ_{Em} 为 5 nm；响应时间为自动；扫描速度为 1 200 nm/min；扫描波长范围 λ_{Ex}=200~400 nm，λ_{Em}=220~600 nm；扫描光谱进行仪器自动校正。每个样品扫描 3 遍。TOC 测定：采用岛津 TOC-VCPH 仪测定，检出限为 0.01 mg/L。紫外吸收光谱测定：将滇池表层沉积物 DOM 样品置于 1 cm 光程石英比色皿中，采用 UV-1800 紫外可见分光光度计在 200~800 nm 范围内全扫描；总氮的测定：过硫酸钾消解，紫外分光光度法（GB11894-89）。总 Cu、总 Pb 测定：原子吸收光谱（AAS）（Perkin Elmer 603）。Cu、Pb 金属离子测定：离子选择性电极（ion selective electrodes，ISE）。

1.4　数据统计与分析

数据分析过程中通过统计检验剔除异常值。数据统计和分析工作在 SPSS 和 Excel 中完成。采样点位图用 surfer 8.0 绘制。

2　结果与讨论

2.1　与 Cu、Pb 结合后 DOM 中 TOC 含量

如表 2 所示，达到渗析平衡后，草海与外海各分子量 DOM 组分中 TOC 含量差别不大。Cu 浓度梯度对于不同分子量 DOM 组分 TOC 含量的影响不显著（$p>0.05$）。对比 2 个湖区、2 个浓度梯度，都是在 $M_w<1\ 000$ u 的 DOM 组分中 TOC 含量最高，在 $M_w>10\ 000$ u 的 DOM 组分中 TOC 含量最低，且随着DOM 分子量的增加 TOC 浓度有降低的趋势，TOC 大部分集中在 $M_w<5\ 000$ u 的 DOM 中。达到渗析平衡后，结合同一浓度的 Pb 后，草海各 DOM 组分中 TOC 含量略高于外海。同样的，与 Cu 浓度梯度对于 TOC 在不同分子量 DOM 组分分布的影响一样，Pb 浓度梯度的影响也不显著（$p>0.05$）。对比 2 个湖区、2 个浓度梯度，都是 $1\ 000<M_w<2\ 000$ u 的 DOM 组分中 TOC 含量最高，$M_w>10\ 000$ u 的组分 TOC 含量最低，且随着 DOM 分子量的增加 TOC 浓度有降低的趋势，与 Cu 结合 DOM 后 TOC 在各分子量 DOM 组分的分布相似。研究表明，真正影响重金属迁移的是低分子量的 DOM[20]。由表 2 看出，不同分子量 DOM 与相同浓度（即 1 mg/L）的 Cu、Pb 结合后，TOC 含量在与 Pb 结合的 DOM 组分中偏高（草海 5 000~10 000 u 除外），说明 Cu 比 Pb 结合了更多的有机质使得游离的 TOC 浓度较低。这可能是由于在所有的二价阳离子中，Cu 与有机质具有比较强的络合能力，且形成的化合物最稳定[21-22]。

表 2　DOM 与 Cu、Pb 结合后不同分子量范围的 TOC 测试值

Table 2　TOC concentrations in different molecular weights DOM combined with Cu，Pb

	ρ(Cu)/mg·L^{-1}	DOM 分子量/u				
		<1 000	1 000~2 000	2 000~5 000	5 000~10 000	>10 000
草海	1	2.480	2.259	2.195	1.201	0.365
	5	4.129	2.305	2.356	1.351	0.499
外海	1	2.423	2.080	2.181	1.159	0.256
	5	2.598	2.155	2.308	1.190	0.430
	ρ(Pb)/mg·L^{-1}	DOM 分子量/u				
		<1 000	1 000~2 000	2 000~5 000	5 000~10 000	>10 000
草海	0.5	3.338	6.002	4.139	2.577	0.437
	1	3.684	9.130	4.527	2.990	0.645
外海	0.5	2.561	3.230	2.486	2.807	0.459
	1	2.603	3.771	3.690	2.011	0.620

2.2　不同分子量 DOM 组分总 Cu、总 Pb 的含量

如表 3 所示，草海与外海各分子量 DOM 结合同一浓度 Cu 达到渗析平衡后，草海各 DOM 组分中总 Cu 含量高于外海，说明草海 DOM 对 Cu 的结合能力大于外海。有研究表明，pH 值和 DOM 浓度是 DOM 与 Cu 络合的最主要的影响因素[23]。草海靠近昆明市

区，受到周围严重的工业污水、城市排水的影响。同时草海湖区相对封闭，有机污染物分散很困难，大部分沉积到湖底，使底泥中有机质含量水平明显高于全湖[17]。1 mg/L Cu与两个湖区DOM结合后，各分子量DOM组分中总Cu含量低于5 mg/L Cu与DOM结合的情况。对于2个湖区、2个浓度梯度，都是在M_w<1 000 u的DOM中总Cu含量最高，说明该分子量组分对Cu具有较强的结合能力。与已有研究[24-26]结果一致，都是低分子量DOM组分与Cu形成最多的DOM-Cu化合物从而影响Cu的迁移。因为低分子量有机质较高分子量的有机质有更多的金属键合点位[27]。

表3 各分子量DOM组分中总Cu和总Pb的含量

Table 3 Total Cu,Pb concentrations in the different molecular weights DOM fractions

	ρ(Cu)/mg·L^{-1}	DOM分子量/u				
		<1 000	1 000~2 000	2 000~5 000	5 000~10 000	>10 000
草海	1	5.579	3.407	4.07	3.289	3.777
	5	6.427	5.116	95.235	5.291	5.093
外海	1	4.075	1.961	2.308	0.934	2.640
	5	4.129	2.155	3.984	3.462	2.159
	ρ(Pb)/mg·L^{-1}	DOM分子量/u				
		<1 000	1 000~2 000	2 000~5 000	5 000~10 000	>10 000
草海	0.5	1.382	1.392	1.050	0.812	1.008
	1	1.438	1.834	1.135	0.950	1.085
外海	0.5	0.713	1.084	0.316	0.183	0.588
	1	0.865	1.394	1.047	0.945	0.775

如表3所示，达到渗析平衡后，草海与外海各分子量DOM组分结合同一浓度Pb之后，草海各DOM组分总Pb含量高于外海，与Cu结合情况相似，可能是草海有机质含量较高，导致有机结合态铅含量的升高[28]。较高浓度（1 mg/L）的Pb与2个湖区DOM结合后，各分子量DOM组分中总Pb含量较高，与Cu的情况相似，说明低浓度的重金属并没有与DOM的全部暴露位点相结合[29]。对于2个湖区、2个浓度梯度，都是1 000<M_w<2 000 u的DOM组分中总Pb含量最高，说明该分子量组分对Pb具有较强的结合能力。对比表3，不同分子量DOM与相同浓度的重金属结合后，重金属含量在与Cu结合的组分中偏高。因为不同分子量有机质对重金属结合能力的差异除了与吸附点位有关之外，还与重金属本身的特征有关，如与有机质的结合能力、内层和/或外层配位化合物的形成[26]。此外，M_w<500 u范围DOM主要成分是小分子有机酸，如草酸、柠檬酸、苹果酸和甲酸等可以与金属离子形成稳定的化合物[30]，是影响重金属迁移及生物有效性的主要组分。而且Cu比Pb对小分子有机酸有更强的结合能力[31]。

2.3 不同分子量DOM结合Cu、Pb后的三维荧光光谱特征

利用三维荧光光谱研究不同分子量的DOM与不同浓度Cu、Pb的结合特征。有研究[32]表明，湖泊沉积物DOM荧光峰主要表现为类富里酸荧光峰（A、C）和类蛋白荧光峰（B、D）。其中紫外区类富里酸荧光峰A的中心位置：$\lambda_{Ex}/\lambda_{Em}$=（230~260） nm/（420~450） nm；可见光区类富里酸荧光峰C的中心位置：$\lambda_{Ex}/\lambda_{Em}$=（300~320） nm/（400~420） nm类蛋白荧光峰B出现在$\lambda_{Ex}/\lambda_{Em}$=（275~285） nm/（300~320） nm，类蛋白荧光峰D出现在$\lambda_{Ex}/\lambda_{Em}$=（220~230） nm/（330~340） nm。这些荧光峰的荧光强度主要与有机质浓度有关，同时还受到pH、金属离子的影响[20]。

由表4、表5可以看出，草海DOM和外海DOM结合Cu、Pb后只呈现出类2种荧光峰——类蛋白荧光峰B和D，而没有出现类富里酸荧光峰A和C。可能是由于类蛋白的激发波长都处于UV范围内，光子产率较高，荧光强度值相对较高。Baker[33]研究表明，受工业废水污染的河流中DOM的类蛋白峰荧光强度非常高。滇池是一个典型的受工业废水和生活污水污染的湖泊，而农业污染只占总污染负荷的40%[34]。此外，DOM中可见光区类富里酸物质对Cu配位能力最强，可能也是导致C峰消失的原因[35]。

由表4可知，2个湖区不同分子量DOM结合相同浓度的Cu后，同一分子量范围同一荧光峰在草海和外海的荧光强度没有显著差异（P>0.05）。对于不同湖区、不同Cu浓度梯度，都是M_w<1 000 u的DOM荧光强度最小，表明M_w<1 000 u的DOM组分更容易结合Cu，与2.1、2.2节得出的结果一致。这可能与水体中50%的有机配体分布在M_w<1 000 u的DOM组分中有关[36]。对于同一湖区、不同Cu浓度梯度，都是与较高浓度Cu（5 mg/L）结合的DOM荧光峰B的荧光强度小，而且荧光峰D没有出现，说明高浓度更易发生荧光猝灭效应。有研究根据紫外吸光度曲线变

表 4　不同分子量 DOM 与 Cu 结合后三维荧光特征

Table 4　Three-dimensional fluorescence characteristics of different molecular weights DOM combined with Cu

分子量/u	草海			草海			外海			外海		
	ρ(Cu)1 mg/L			ρ(Cu)5 mg/L			ρ(Cu)1 mg/L			ρ(Cu)5 mg/L		
	$\lambda_{Ex}/\lambda_{Em}$	荧光强度	峰	$\lambda_{Ex}/\lambda_{Em}$	荧光强度	峰	$\lambda_{Ex}/\lambda_{Em}$	荧光强度	峰	$\lambda_{Ex}/\lambda_{Em}$	荧光强度	峰
<1 000	285/315	79.12	B	275/300	70.09	B	285/315	74.1	B	280/305	67.07	B
	225/335	92.63	D	–	–	–	230/335	90.02	D	–	–	–
1 000~2 000	285/315	89.9	B	275/300	82.46	B	285/315	86.78	B	285/315	80.03	B
	230/335	131.9	D	–	–	–	230/335	80.8	D	–	–	–
2 000~5 000	285/315	99.32	B	275/300	83.27	B	285/315	89.97	B	275/300	82.18	B
	230/335	206.1	D	–	–	–	225/330	87.6	D	–	–	–
5 000~10 000	275/300	95.71	B	275/300	94.29	B	285/315	91.25	B	285/315	96.63	B
	230/335	124.2	D	–	–	–	230/330	88.48	D	–	–	–
>10 000	285/315	95.29	B	285/315	91.29	B	285/315	96.32	B	275/300	91.13	B
	225/335	141.9	D	–	–	–	225/330	101	D	–	–	–

注：–表示未检出。

表 5　不同分子量 DOM 与 Pb 结合后三维荧光特征

Table 5　Three-dimensional fluorescence characteristics of different molecular weights DOM combined with Pb

分子量/u	草海			草海			外海			外海		
	ρ(Pb)0.5 mg/L			ρ(Pb)1 mg/L			ρ(Pb)0.5 mg/L			ρ(Pb)1 mg/L		
	$\lambda_{Ex}/\lambda_{Em}$	荧光强度	峰	$\lambda_{Ex}/\lambda_{Em}$	荧光强度	峰	$\lambda_{Ex}/\lambda_{Em}$	荧光强度	峰	$\lambda_{Ex}/\lambda_{Em}$	荧光强度	峰
<1 000	275/300	122.5	B	285/315	110.9	B	285/315	223.7	B	285/320	128.6	B
	230/335	167.2	D	230/335	75.12	D	225/340	284.2	D	225/335	255.3	D
1 000~2 000	280/310	77.95	B	285/315	70.16	B	285/315	77.69	B	285/315	77.98	B
	230/330	75.12	D	–	–	–	230/340	210	D	230/335	171.2	D
2 000~5 000	285/315	120.6	B	285/315	115.8	B	285/315	113.8	B	285/315	105.7	B
	225/335	231.2	D	230/340	167.1	D	225/335	373.2	D	230/340	241.6	D
5 000~10 000	285/315	108.2	B	285/315	110.1	B	285/315	100.4	B	285/315	93.98	B
	230/340	124.2	D	–	–	–	225/340	202.8	D	–	–	–
>10 000	285/315	122.2	B	285/315	109.6	B	285/315	109.6	B	285/315	116.3	B
	230/335	141.4	D	230/335	141.3	D	230/335	336.2	D	225/335	288.1	D

注：–表示未检出。

化得出 Cu 与 DOM 络合的过饱和浓度为 ρ（Cu）12.8 mg/L，选取 ρ（Cu）6.4 mg/L 为与湖泊水体 DOM 络合的最大离子络合浓度进行研究[37]。

由表 5 可知，2 个湖区不同分子量 DOM 结合相同浓度 Pb 后，同一 DOM 分子量、同一荧光峰在草海的荧光强度小于外海（M_w>10 000 ρ（Pb）0.5 mg/L 的荧光峰 B 除外）。DOC 含量与有机结合态 Pb 含量有良好的线性关系，这可能是草海高浓度有机质与 Pb络合较多使荧光强度低于外海的原因[38]。对于不同湖区不同浓度梯度，都是 1 000<M_w<2 000 u 的 DOM 荧光强度最小，表明 1 000<M_w<2 000 u 的 DOM 更容易结合 Pb。对于同一湖区不同浓度梯度，都是与高浓度 Pb（1 mg/L）结合的荧光峰 B、D 荧光强度小，与已有研究 Pb^{2+}浓度的增加导致 DOM 荧光峰强不断降低的结论一致[39]。对比表 4、表 5，相同分子量 DOM 与相同浓度（ρ=1 mg/L）的 Cu、Pb 结合后，基本上都是与 Cu 结合的荧光强度小于与 Pb 结合的情况，这可能由于顺磁性金属离子 Cu 和 Pb 加入含有类蛋白物质的 DOM 溶液后会使类蛋白荧光强度急剧下降，而且 Cu 的荧光猝灭效果更强[40]。

2.4　不同分子量 DOM 结合 Cu、Pb 后的紫外吸收光谱特征

特定波长的紫外/可见（UV/VIS）吸收比常被用来指示腐殖酸的腐殖化、团聚化程度和分子量的大小，通常用 250 nm 和 365 nm 处吸光度之比（E2/E3）表征 DOM 分子量大小[41–42]。研究表明，随着 E2/E3 的减小，腐殖质腐殖化程度、芳香性及分子量相对增大[43]。本研究空白实验 E2/E3 范围在 2.06~9.41，因此推断滇池 DOM 腐殖化程度比较高、芳香性较大，且随着分子量的增加，DOM 腐殖化程度以及芳香性等逐渐增大。研究表明样品的相对平均分子量与紫外/可见光比值成负相关关系[20]。由表 6 可知，滇池草海 DOM E2/E3 范围在 2.06~3.69，平均值为 3.119，外海 DOM E2/E3 范围在 2.97~9.41，平均值为 5.569，可以推断滇池草海表层沉积物 DOM 的分子量在整体上大于外海，而且芳环上羟基、羧基等取代基较多为重金属提供了更多结合点位[44]。由表 6 看出，相同分子量 DOM 与相同浓度（即 ρ=1 mg/L）的 Cu、Pb 结合后，基本上

表6 不同分子量DOM与Cu、Pb结合后在250、365 nm处的紫外吸光度之比

Table 6 Ratio of absorbance at 250 nm and 365 nm of different molecular weights DOM combined with Cu,Pb

	ρ(Cu)/mg·L^{-1}	DOM分子量/u				
		<1 000	1 000~2 000	2 000~5 000	5 000~10 000	>10 000
草海	空白	3.69	3.5	3.353	2.99	2.06
	0.5	2.636	2	1.917	2.625	2
	1	2.202	2.077	2.333	1.667	1.341
外海	空白	9.41	6.667	4.75	4.03	2.97
	0.5	3.4	2.903	2.75	2.857	2.464
	1	3.333	2.833	2.673	3	2.333

	ρ(Pb)/mg·L^{-1}	DOM分子量/u				
		<1 000	1 000~2 000	2 000~5 000	5 000~10 000	>10 000
草海	空白	3.69	3.5	3.353	2.99	2.06
	1	3.375	2.583	2.6	2.556	2.375
	5	2.75	2.41	2.250	1.9	2.286
外海	空白	9.41	6.667	4.75	4.03	2.97
	1	3.69	3.1	3	2.75	2.589
	5	3.167	2.675	2.071	2.1	2.13

都是与Cu结合的E2/E3小于与Pb结合的情况，即Cu–DOM的分子量大于Pb–DOM的分子量。这可能由于Cu^{2+}半径比Pb^{2+}小，更易进入有机质胶体内层与之结合[45]，使得Cu^{2+}与有机质结合的几率高于Pb^{2+}，而且Cu与DOM主要是以2:1的计量形成DOM–Cu–DOM的形式[46]，而Pb有可能是以1:1的计量形成Pb–DOM的形式。

3 结论

⑴ 各分子量DOM与Cu结合后M_{w}<1 000 u的DOM组分TOC含量最高，与Pb结合后，1 000<M_{w}<2 000 u的DOM中TOC含量最高，而且TOC浓度随DOM分子量的增加而降低，不受重金属浓度梯度的影响。M_{w}<1 000 u的DOM组分总Cu含量最高，1 000<M_{w}<2 000 u的DOM总Pb含量最高。草海各分子量DOM组分总Cu、总Pb含量高于外海，且各分子量DOM组分重金属总量随重金属浓度增加而增加。

⑵ 三维荧光光谱特征表明Cu趋向于和M_{w}<1 000 u的DOM结合，而Pb趋向于和1 000<M_{w}<2 000 u的DOM结合，而且都是高浓度重金属与DOM结合后，DOM的荧光峰荧光强度较小。紫外光谱特征表明草海表层沉积物DOM的分子量在整体上大于外海。同一分子量DOM与相同浓度的Cu、Pb结合后，与Cu结合的E2/E3小于与Pb结合的情况，这可能与重金属和有机质形成的配位化合物的结构不同有关。

⑶ 富营养化湖泊中Cu和Pb与DOM中不同分子量组分的结合特征有显著差异，重金属的浓度也是DOM与重金属结合特性的影响因素。

[参考文献]

[1] Tipping E. Modeling the competition between alkaline earth cations and trace metal species for binding by humic substance[J]. Environmental Science and Technology，1993(27)：520–529.

[2] Leenheer J A，Croue J P. Characterizing aquatic dissolved organic matter[J]. Environmental Science and Technology，2003(37)：18–26.

[3] Korshin G，Chow C W K，Fabris R，et al. Absorbance spectroscopy based examination of effects of coagulation on the reactivity of fractions of natural organic matter with varying apparent molecular weights[J]. Water Research，2009(43)：1541–1548.

[4] Gao H，Zepp R G. Factors influencing photoreactions of dissolved organic matter in a coastal river of the southeastern United States[J]. Environmental Science and Technology，1998(32)：2940–2946.

[5] Chen Guang，Lin Chao，Chen Liang，et al. Effect of size-fractionation dissolved organic matter on the mobility of prometryne in soil[J]. Chemosphere，2010(79)：1046–1055.

[6] 陈雪霜，江韬，卢松，等. 三峡库区消落带水体DOM不同分子量组分三维荧光特征[J]. 环境科学，2016，37(3)：884–891.
Chen Xueshuang，Jiang Tao，Lu Song，et al. Three-dimensional fluorescence spectral characteristics of different molecular weight fractionations of dissolved organic matter in the water-level fluctuation zones of Three Gorges reservoir areas[J]. Environmental Science，2016，37(3)：884–891. (in Chinese)

[7] Wang Zhiwei，Wu Zhichao. Distribution and transformation of molecular weight of organic matters in membrane bioreactor and conventional activated sludge process[J]. Chemical Engineering Journal，2009，150(2/3)：396–402.

[8] Wu Fengchang，Evans R D，Dillon P J. High-performance liquid chromatographic fractionation and characterization of

fulvic acid[J]. Analytica Chimica Acta，2002（464）：47–55.

[9] Truitt R E，Weber J H. Determination of complexing capacity of fulvic acid for copper（Ⅱ）and cadmium（Ⅱ）by dialysis titration[J]. Analytical Chemistry，1981（53）：337–342.

[10] Pan B，Qiu M Y，Wu M，et al. The opposite impacts of Cu and Mg cations on dissolved organic matter–ofloxacin interaction[J]. Environmental Pollution，2012（161）：76–82.

[11] Maharaa Y，Kubotaa T，Wakayamab R，et al. Effects of molecular weight of natural organic matter on cadmium mobility in soil environments and its carbon isotope characteristics[J]. Science of the Total Environment，2007，387（1/2/3）：220–227.

[12] Brandt K K，Holm P E，Nybroe O. Evidence for bioavailable copper–dissolved organic matter complexes and transiently increased copper bioavailability in manure–amended soils as determined by bioluminescent bacterial biosensors[J]. Environmental Science and Technology，2008，42（8）：3102–3108.

[13] Wu Jun，Zhang Hua，He Pinjing. Insight into the heavy metal binding potential of dissolved organic matter in MSW leachate using EEM quenching combined with PARAFAC analysis[J]. Water Research，2011，45（4）：1711–1719.

[14] **李廷强，杨肖娥. 土壤中水溶性有机质及其对重金属化学与生物行为的影响**[J]. **应用生态学报**，2004，15（6）：1083–1087.

Li Tingqiang，Yang Xiao´e. Soil dissolved organic matter and its effect on chemical and biological behaviors of soil heavy metals[J]. Journal of Applied Ecology，2004，15（6）：1083–1087.（in Chinese）

[15] Ponthieu M，Pourret O，Marin B，et al. Evaluation of the impact of organic matter composition on metal speciation in calcareous soil solution：comparison of model VI and NICA–Donnan[J]. Journal of Geochemical Exploration，2016（165）：1–7.

[16] **陈云增，杨浩，张振克，等. 滇池沉积物金属污染及环境质量评价**[J]. **湖泊科学**，2008，20（4）：492–499.

Chen Yunzeng，Yang Hao，Zhang Zhenke，et al. Metal contamination and quality assessment of Lake Dianchi sediment [J]. Journal of Lake Science，2008，20（4）：492–499.（in Chinese）

[17] **卢少勇，金相灿，张烨，等. 滇池内湖滨带底泥的有机质分布规律**[J]. **湿地科学**，2009，7（2）：135–141.

Lu Shaoyong，Jin Xiangcan，Zhang Ye，et al. Distribution of organic matter in sediment of inner lakeside belt in Dianchi Lake[J]. Wetland Science，2009，7（2）：135–141.（in Chinese）

[18] Du Lina，Li Yuan，Chen Xiaoyong，et al. Effect of eutrophication on molluscan community composition in the Lake Dianchi（China，Yunnan）[J]. Limnologica，2011（41）：213–219.

[19] Chen Zhangrong，Cai Yong，Helena S G，et al. Interactions of arsenic and the dissolved substances derived from turf soils [J]. Environmental Science and Technology，2006（40）：4659–4665.

[20] **张甲，曹军，陶澍. 土壤水溶性有机物的紫外光谱特征及地域分异**[J]. **土壤学报**，2003，40（1）：118–122.

Zhang Jia，Cao Jun，Tao Shu. Spatial variation of UV–VIS spectroscopy of water soluble organic carbon in eastern China [J]. Acta Pedologica Sinica，2003，40（1）：118–122.（in Chinese）

[21] Pandey A K，Pandey S D，Misri V. Stability constants of metal–humic acid complexes and its role in environmental detoxification[J]. Ecotoxicology and Environmental Safety，2000（47）：195–200.

[22] Evans L J. Chemistry of metal retention by soils[J]. Environmental Science and Technology，1989（23）：1046–1056.

[23] **赵婧，吴敏，王万宾，等. 铜与 DOM 络合稳定常数的影响因子测定**[J]. **上海环境科学集**，2015（1）：110–114.

Zhao Jing，Wu Min，Wang Wanbin，et al. Determination of impact factors on complexing stability constant of copper with DOM[J]. Journal of Shanghai Environment Science，2015（1）：110–114.（in Chinese）

[24] Knoth De Azrruk K，Scholer G，Dudal Y. Fluorescence fingerprints and Cu^{2+}–complexing ability of individual molecular size fractions in soil–and waste–borne DOM[J]. Chemosphere，2007（69）：540–548.

[25] Wang X D，Chen X N，Liu S，et al. Effect of molecular weight of dissolved organic matter on toxicity and bioavailability of copper to lettuce[J]. Journal of Environmental Sciences，2010，22（12）：1960–1965.

[26] Calace N，Liberatori A，Petronio B M，et al. Characteristics of different molecular weight fractions of organic matter in landfill leachate and their role in soil sorption of heavy metals [J]. Environmental Pollution，2001（113）：331–339.

[27] Guggenberger G，Glaser B，Zeeh W. Heavy metal binding by hydrophobic and hydrophilic dissolved organic fractions in a spodosol A and B horizon[J]. Water，Air & Soil Pollution，1994（72）：111–127.

[28] **范春辉，张颖超，王家宏. 黄土区秸秆腐殖化溶解性有机质对土壤铅赋存形态的影响机制**[J]. **光谱学与光谱分析**，2015，35（11）：3146–3150.

Fan Chunhui，Zhang Yingchao，Wang Jiahong. Influence mechanism of dissolved organic matter（DOM）from straw humification on chemical speciation of lead in loess region[J]. Spectroscopy and Spectral Analysis，2015，35（11）：3146–3150.（in Chinese）

[29] Merckx R，Brans K，Smolders E. Decomposition of dissolved organic carbon after soil drying and rewetting as an indicator of metal toxicity in soils[J]. Soil Biology & Biochemistry，2001，33（2）：235–240.

[30] Wu L H，Luo Y M，Christie P，et al. Effects of EDTA and

low molecular weight organic acids on soil solution properties of a heavy metal polluted soil[J]. Chemosphere，2003 (50):819–822.

[31] Martell A E，Smith R M. Critical Stability Constants in Other Organic Ligands[M]. vol 3. New York：Plenum Press，1977.

[32] **宋晓娜，于涛，张远，等. 利用三维荧光技术分析太湖水体溶解性有机质的分布特征及来源**[J]. **环境科学学报**，2010，30 (11):2321–2331.
Song Xiaona，Yu Tao，Zhang Yuan，et al. Distribution characterization and source analysis of dissolved organic matter in Taihu Lake using a three dimensional fluorescence excitation–emission matrix[J]. Acta Scientiae Circumstantiae，2010，30 (11):2321–2331. (in Chinese)

[33] Baker A. Fluorescence excitation–emission matrix characterization of some sewage–impacted rivers[J]. Environmental Science and Technology，2001，35 (5):948–953.

[34] Liu Yanfang，Li Yangang，Yang Xiaohong，et al. Analysis of pollution in Dianchi Lake and consideration of its application in crop planting[J]. Procedia Environmental Sciences，2012 (12):174–183.

[35] **赵萱，成杰民. 白洋淀沉积物中溶解有机质荧光特性及其与铜的相互作用**[J]. **农业环境科学学报**，2012 (6):1217–1222.
Zhao Xuan，Cheng Jiemin. Fluorescence characteristics of dissolved organic matter and interaction between Cu (II) and DOM in sediments of Baiyangdian Lake[J]. Journal of Agro–environment Science，2012 (6):1217–1222. (in Chinese)

[36] Midorikawa T，Tanoue E. Molecular masses and chromophoric properties of dissolved organic ligands for copper (II) in oceanic water[J]. Marine Chemistry，1998 (62):219–239.

[37] **朱先辰. 淡水环境中溶解性有机物及其与** Cu^{2+}**相互作用：荧光光谱学研究**[D]. **武汉：华中科技大学**，2014：34–35.
Zhu Xianchen. Dissolved Organic Matter in Natural Aquatic Environments and Its Complexation with Cu^{2+}：a Study Based on Fluorescence Spectroscopy[D]. Wuhan：Huazhong University of Science and Technology，2014：34–35. (in Chinese)

[38] **方盛荣，徐颖，魏晓云，等. 典型城市污染水体底泥中重金属形态分布和相关性**[J]. **生态环境学报**，2009，18 (6):2066–2070.
Fang Shengrong，Xu Ying，Wei Xiaoyun，et al. Morphological distribution and correlation of heavy metals in sediment of typical urban polluted water bodies[J]. Ecology and Environmental Science，2009，18 (6):2066–2070. (in Chinese)

[39] **范春辉，张颖超，王家宏. 温度和铅离子对秸秆腐殖化溶解性有机质三维荧光光谱的干扰效应**[J]. **光谱学与光谱分析**，2015，35 (11):3117–3122.
Fan Chunhui，Zhang Yingchao，Wang Jiahong. Effect of temperatures and lead ions on 3D–EEMs of dissolved organic matter (DOM) derived from straw humification[J]. Spectroscopy and Spectral Analysis，2015，35 (11):3117–3122. (in Chinese)

[40] Mcintyre A M，Gueguen C. Binding interactions of algal–derived dissolved organic matter with metal ions[J]. Chemosphere，2013 (90):620–626.

[41] Peuravuori J，Pihlaja K. Molecular size distribution and spectroscopic properties of aquatic humic substances [J]. Analytica Chimica Acta，1997，337 (2):133–149.

[42] De Haan H，De Boer T. Applicability of light absorbance and fluorescence as measures of concentration and molecular size of dissolved organic carbon in humic Lake Tjeukemeer[J]. Water Research，1987，21 (6):731–734.

[43] Battin T J. Dissolved organic matter and its optical properties in a blackwater tributary of the upper Orinoco River，Venezuela[J]. Organic Geochemistry，1998，28 (9/10):561–569.

[44] **傅平青，刘丛强，吴丰昌. 三维荧光光谱研究溶解有机质与汞的相互作用**[J]. **环境科学**，2004，25 (6):140–144.
Fu Pingqing，Liu Congqiang，Wu Fengchang. Three–dimensional excitation emission matrix fluorescence spectroscopic characterization of the complexation between mercury (II) and dissolved organic matter[J]. Environment Science，2004，25 (6):140–144. (in Chinese)

[45] **于波，何江，吕昌伟，等. 基于水生植物分区的湖泊 DOM 与重金属离子的结合特性研究**[J]. **农业环境科学学报**，2015，34 (12):2343–2348.
Yu Bo，He Jiang，Lyv Changwei，et al. Binding characteristics of heavy metals with DOM from different aquatic macrophyte zones[J]. Journal of Agro–environment Science，2015，34 (12):2343–2348. (in Chinese)

[46] Klass G J N，Boris J，Jasper A V，et al. Copper complexation by dissolved organic matter and uncertainty assessment of their stability constants[J]. Chemosphere，2002 (49):1191–1200.

第35卷 第11期　　环 境 化 学　　Vol. 35，No. 11
2016年　11月　　ENVIRONMENTAL CHEMISTRY　　November 2016

DOI: 10.7524/j.issn.0254-6108.2016.11.2016032904
石陶然，吴福勇，于涛，等.平衡渗析-多种光谱法研究太湖不同分子量溶解性有机质及其与铜的相互作用［J］.环境化学，2016，35(11)：2386-2393.
SHI Taoran，WU Fuyong，YU Tao，et al. Determination of Cu complexed with individual molecular size fractions of dissolved organic matter from the Taihu Lake，China by equilibrium dialysis and multiple spectroscopic methods［J］.Environmental Chemistry，2016，35(11)：2386-2393.

平衡渗析-多种光谱法研究太湖不同分子量溶解性有机质及其与铜的相互作用*

石陶然^{1,2,3}　吴福勇^{1,2**}　于　涛^{3}　马晓娜^{1,2}　田　凯^{1,2}　许飞飞^{1,2}

（1. 西北农林科技大学资源与环境学院，杨凌，712100； 2. 农业部西北植物营养与农业环境重点实验室，杨凌，712100；
3. 中国环境科学研究院，环境基准与风险评估国家重点实验室，北京，100012）

摘　要　采用平衡渗析技术将太湖沉积物溶解性有机质(DOM)按分子量分成不同的组分.利用光谱技术和离子选择电极(ISE)分析了不同分子量溶解性有机质的光谱特征及对Cu的结合，进一步探讨分子量对DOM特性和对金属结合能力的影响.结果表明，南太湖DOM分子量以高于10000 Da为主，然而北太湖分子量以低于3500 Da为主.三维荧光光谱(3DEEM)表明太湖沉积物DOM呈现出4种特征荧光峰.类富里酸荧光峰的荧光强度随着DOM分子量的增加而增强，然而类蛋白质荧光峰的荧光强度随着DOM分子量的增加而降低.南太湖DOM碳氮比(C/N)(20.30)显著高于北太湖(7.58)，表明了DOM不同的来源.对于南北湖区，DOM-Cu浓度最大值都是在DOM分子量低于1000 Da组分，大约50%的DOM-Cu在分子量低于3500 Da的组分中.结合容量表明南太湖DOM分子量低于3500 Da的组分和北太湖分子量在1000—3500 Da的组分对于Cu结合起主要的作用，表明低分子量DOM对于结合重金属的重要性.

关键词　分子量，溶解性有机质，平衡渗析，太湖.

Determination of Cu complexed with individual molecular size fractions of dissolved organic matter from the Taihu Lake，China by equilibrium dialysis and multiple spectroscopic methods

SHI Taoran^{1,2,3}　*WU Fuyong*^{1,2**}　*YU Tao*^{3}　*MA Xiaona*^{1,2}　*TIAN Kai*^{1,2}　*XU Feifei*^{1,2}

（1.College of Natural Resource and Environmental Sciences，North West Agriculture and Forestry University，Yangling，712100，China；
2. Key Laboratory of Plant Nutrition and the Agri-environment in Northwest China，Ministry of Agriculture，Yangling，712100，China；
3. State Key Laboratory of Environment Criteria and Risk Assessment，Chinese Research Academy of Environmental Sciences，Beijing，100012，China）

Abstract: Dissolved organic matter (DOM) from Taihu Lake sediment was separated into different molecular weight fractions with equilibrium dialysis. Spectroscopic methods and ion selective electrode (ISE) were employed to analyze spectral characteristics of different molecular weight DOM and the interaction with Cu，and to further examine metal-binding abilities and fluorescence signals in connection with molecular weight. The results indicated that in South Lake DOM was dominated

---

2016年3月29日收稿(Received: March 29，2016).

* 国家自然科学基金(51278475)，陕西省自然科学基础研究计划(2016JM4004)资助.

Supported by the National Natural Science Foundation of China (Grant 51278475)，Natural Science Basic Research Plan in Shaanxi Province of China (2016JM4004).

**通讯联系人，E-mail: wfy09@163.com

Corresponding author，E-mail: wfy09@163.com

with molecular weight higher than 10000 Da, while in the North Lake DOM was dominated with molecular weight lower than 3500 Da. Three-dimensional fluorescence excitation-emission matrix (3DEEM) showed that DOM from Taihu sediment displayed four distinct fluorophores peaks. Fluorescence intensity of humic-like fluorescence peak increased with the DOM molecular weight, while the fluorescence intensity of protein-like fluorescence peak decreased with the molecular weight. C/N of DOM in South Lake (20.30) was significantly higher than that in North Lake (7.58), indicating their different source. DOM-Cu complex concentration was maximal in the fractions with molecular weight lower than 1000 Da in both South Lake and North Lake, and around 50% of the total DOM-Cu in the fractions with molecular weight lower than 3500 Da. Complexing capacity showed that DOM with molecular weight lower than 3500 Da in the South Lake and molecular weight between 1000 and 3500 Da in the North Lake were largely responsible for Cu complexing, indicating the importance of low molecular weight fractions in heavy metal binding.

Keywords: molecular weight, dissolved organic matter, equilibrium dialysis, Taihu Lake.

重金属的生物有效性和毒性一直被认为与水环境中水化学因素的作用有关，如溶解性有机质(DOM)、pH，氧化还原电位(ORP)、离子强度等[1].在这些因素中，DOM 被认为是控制重金属迁移转化和归趋的主要因素之一[2].例如，形成有机结合态重金属虽然没有减少重金属的含量，但是可以降低重金属对生物的毒性[3].DOM 对于重金属迁移和生物有效性的影响与 DOM 以及重金属-DOM 复合物的性质有关，如官能团的种类和分子组成.DOM 分子量被认为是控制重金属迁移、毒性和生物有效性的重要因素之一[4].近年来，关于土壤和沉积物孔隙水中 DOM 分子量分布的研究已经引起了很大的关注[5-7].有研究表明，江河中 89%的结合态 Cu 在 DOM 分子量高于 45 kDa 的组分中[8].相反，Smith[9]认为 DOM 结合 Cu 的能力与其分子量的大小没有联系.此外，有研究[5]发现 DOM 分子量低于 500 Da 的组分能够形成最多的 DOM-Cu 复合物，表明低分子量组分结合重金属的重要性.目前还没有统一的结论关于 DOM 分子量对于重金属结合能力的影响.DOM 是含有大量有机组分的复杂的混合物，主要有氨基酸和有机酸、腐殖质、糖类、多酚以及高分子酶[10].按照分子量将 DOM 分成不同的组分，测定各组分结构组成和化学性质对于研究各组分对重金属的作用十分重要.因此，本研究应用平衡渗析膜技术探讨太湖 DOM 各分子量组分对 Cu 的结合能力，以期为重金属的生物有效性及我国水质基准的制定提供基础资料.

太湖是中国第三大淡水湖位于长江下游，湖泊面积为 2428 km^2，平均深度为 2 m[11].太湖是一个典型的浅水富营养化湖泊，根据本课题组 2011 年调查 TOC 浓度范围为 15.35—69.02 $mg \cdot L^{-1}$，平均值为 26.96 $mg \cdot L^{-1}$[12].近几年，北太湖蓝藻爆发的频率一直增加，尤其是竺山湾和梅梁湾，这主要是由于水体的富营养化.有研究表明，DOM 的增加是湖泊富营养化的结果[13]，它对 Cu 的溶解度产生很大的影响[14].然而，南太湖大量的水生植物是 DOM 的主要来源.除了富营养化，太湖重金属污染也是一个重大的环境污染问题[15].有研究表明，太湖沉积物 Cu 浓度最高值在漕桥河(121.8—180.5 $mg \cdot kg^{-1}$)，其次是在竺山湾(35.2—110.7 $mg \cdot kg^{-1}$)，最低值在东太湖(18.48 $mg \cdot kg^{-1}$)，在其他湖区没有显著差异，从漕桥河到太湖有明显的浓度梯度.与当地土壤背景值(15.4 $mg \cdot kg^{-1}$)相比，富集指数为 2.6，属于Ⅱ级污染[12].因此，研究沉积物 DOM 与 Cu 的作用规律很重要，其中，DOM 分子量作为最重要的影响因素之一，值得深入探讨.

因此，本研究探讨太湖沉积物 DOM 不同分子量组分对 Cu 的结合能力.旨在研究太湖沉积物 DOM 分子量分布，以及探讨分子量对重金属和 DOM 相互作用的影响.

1　材料与方法(Materials and methods)

1.1　样品的采集与处理

2011 年 9 月采集太湖表层沉积物(0—10 cm)样品.采样过程中采用 GPS 导航定位，采样点分布在两个典型的湖区(图 1)，一个采样点位于竺山湾，经常蓝藻爆发[16]；另一个位于太湖北部，生长有大量的水生植物.用抓斗采样器采集 2 个采样点的表层沉积物，每个采样点采集 3 个重复样，当场保存在洁

净的密封袋中，4 ℃下保存运回实验室，经真空冷冻干燥后研磨，过孔径为 0.149 mm 的尼龙筛后装密封袋保存待分析.

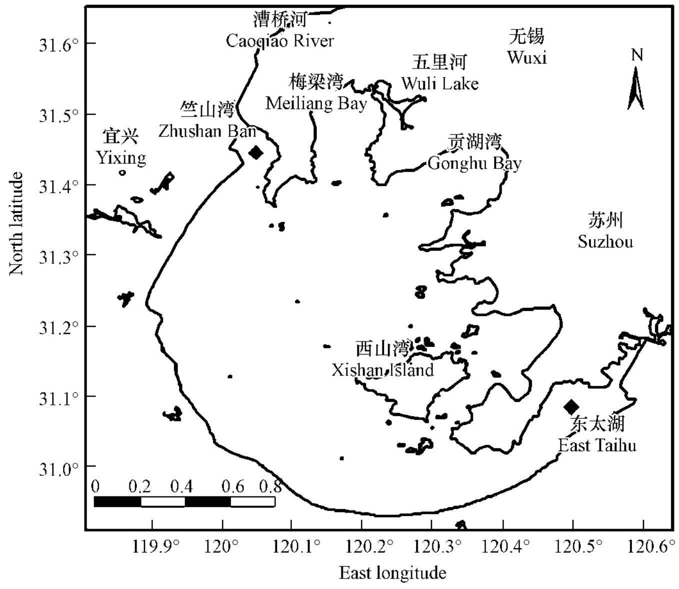

图 1 太湖沉积物采样点位示意图

Fig.1 The location of sampling sites in Taihu Lake

沉积物 DOM 的提取：混合 20 g 沉积物样品和 100 mL 去离子水（电阻率为 18.2 $\Omega\cdot$cm）（水∶沉积物=5∶1），然后在振荡器转速为 250 r·min^{-1}条件下振荡 24 h.提取物以 8000 r·min^{-1}的速度离心 10 min，上清液通过 0.45 μm 玻璃纤维滤膜，滤液即为实验用的 DOM 溶液.DOM 溶液储存在棕色玻璃瓶 4 ℃避光保存，最长不超过 12 h.沉积物 DOC 浓度稀释到 30 mg·L^{-1}.

1.2 平衡渗析试验

采用平衡渗析试验研究太湖沉积物 DOM 的分子量分布以及 DOM 和 Cu 的相互作用.将分子量为 1000、3500、7000、10000 Da 的渗析袋(Spectra/Por CE，Fisher Scientific)剪下适当的长度，置于去离子水中 30 min 去除渗析袋表面的保护液叠氮化钠，然后用去离子水反复冲洗.在渗析袋中装入 15 mL DOM 提取液(30 mg·L^{-1})后用渗析夹封闭，放入烧杯中.将 400 mL Cu^{2+}溶液(2 mg·L^{-1})加到烧杯中，空白实验为等量的超纯水.最后用保鲜膜密封烧杯，避免在实验过程中水分蒸发.为了避免微生物活动和光氧化，整个实验过程在恒温振荡器(4 ℃)中进行.根据已有文献[17]，5 d 可以达到渗析平衡.达到平衡后，取渗析袋内部和外部的的溶液测定相关参数.所有实验均设 3 个重复样.

渗析过程从最小的分子量(1000 Da)开始.达到渗析平衡后，分子量为 1000 Da 渗析袋外部的溶液就是分子量 <1000 Da 组分.将分子量为 1000 Da 的渗析袋转移到 3500 Da 的烧杯中，达到渗析平衡后，该烧杯中溶液就是 1000—3500 Da 组分.以此类推，最后得到 5 个分子量组分：<1000 Da、1000—3500 Da、3500—7000 Da、7000—10000 Da 和 >10000 Da.

1.3 分析仪器条件及参数

溶解性有机碳(DOC)用 TOC 仪(Shimadzu-VCPH)测定，样品过 0.45 μm 滤膜，检出限为 0.01 mg·L^{-1}.总氮的测定用过硫酸钾消解，紫外分光光度法(GB11894—89)测定.总 Cu(Total-Cu)浓度用火焰原子吸收光谱(Perkin Elmer 603)测定，检出限低于 0.007 mg·L^{-1}.自由态 Cu(Free-Cu)用离子选择性电极(ISE)测定，检出限为 6.4×10^{-4}—6.4×10^{4} mg·L^{-1}(校准曲线的绘制用 Cu 标准溶液，浓度为 0.001、0.01、0.1 mg·L^{-1}).

三维荧光光谱测定用荧光光谱分析仪(Hitachi F-4500).激发光源为 150 W 氙弧灯，PMT 电压700 V，信噪比(SNR)>110，带通(Bandpass) Ex 为 5 nm，Em 为 5 nm；响应时间为自动；扫描速率为1200 nm·min^{-1}；激发波长范围为 200—400 nm，发射波长为 220—600 nm；扫描光谱进行仪器自动校正.每个样品扫描 3 遍.紫外吸收波长采用紫外可见 UV/VIS 分光光度计(Shimadzu，UV-2300) 200—800 nm范围内全扫描测定.

用预先过滤的去离子水（0.2 μm）装入 1 cm 光程石英比色皿作为样品的参照.

结合容量被用来评估不同分子量组分 DOM 结合 Cu 的能力，通过 DOM-Cu 浓度除以各分子量组分 DOM 浓度计算得出. DOM-Cu 浓度为总 Cu（Total-Cu）浓度减去自由态 Cu（Free-Cu）浓度，公式为：

$$结合容量=(C_{\mathrm{T\text{-}Cu}}-C_{\mathrm{F\text{-}Cu}})/C_{\mathrm{DOM}}$$

1.4　质量控制与数据处理

样品处理和分析使用分析纯化学药品和去离子水. 所有的玻璃器皿用稀硝酸浸泡，去离子水冲洗 3 遍. 3 个重复的相对偏差低于 10%，标准样品回收率在 85%—110%.

数据分析过程中通过统计检验剔除异常值. 显著性水平为 0.05. 分析结果表示为平均值±标准差. 数据计算和统计在 SPSS 和 Excel 中完成. 采样点位图用 surfer 8.0. 绘制.

2　结果与讨论（Results and discussion）

2.1　分子量分布

空白实验达到渗析平衡后，太湖沉积物各分子量组分 DOM 的浓度（TOC 浓度代替）如图 2 所示. 对于所有的 DOM 浓度都是渗析袋外部溶液远远低于渗析袋内的溶液. 此外，渗析袋外部溶液 DOM 的浓度没有显著差异. 因此，本研究只列出渗析袋内 DOM 的浓度.

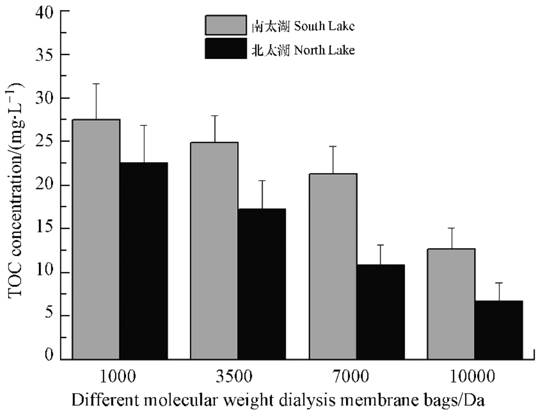

图 2　空白实验达到渗析平衡不同分子量渗析袋内 DOM 的浓度

Fig.2　DOM concentrations in individual dialysis bags after blank experiment reaching dialysis equilibrium

DOM 的浓度在低分子量渗析袋高于高分子量，且随着分子量的增加而减小. 对于同一分子量，DOM 的浓度在南太湖高于北太湖. 太湖的东南区面积为 131 km²，漂浮的叶片和水生植物占了 97% 的面积[18]，当它们死亡腐烂沉到湖底导致沉积物有机质的增加.

达到渗析平衡后，对各组分 DOM 浓度进行测定. 如表 1 所示，在南太湖 DOM 浓度随着分子量的增加而增加. 低分子量（<3500 Da）DOM 占总量的 17.06%，中等分子量组分（3500—10000 Da）占 40.70%，高分子量组分（>10000 Da）占 42.20%. 推断出南太湖沉积物 DOM 以高分子量为主. 然而，北太湖沉积物 DOM 分子量分布没有呈现出明显的特征，每个组分大约占 20%. 整体上，低分子量（<3500 Da）占总量的 42.43%，中等分子量组分（3500—10000 Da）占 35.27%，然而高分子量组分（>10000 Da）只占 22.30%.

表 1　太湖沉积物不同分子量组分 DOM 的浓度和所占的比例（平均值±标准差）（$n=3$）

Table 1　Concentration and proportion of different molecular weight DOM fractions in the Taihu Lake sediment (means ± standard) ($n=3$)

	Mw/Da	<1000	1000—3500	3500—7000	7000—10000	>10000
南太湖	**浓度** Concentration/(mg·L⁻¹)	2.49±0.07	2.63±0.13	3.56±0.04	8.65±0.59	12.66±1.02
	比例 Proportion/%	8.30±0.21	8.76±0.06	11.87±0.32	28.83±1.01	42.20±0.04
北太湖	**浓度** Concentration/(mg·L⁻¹)	7.47±0.43	5.26±0.24	6.44±0.45	4.14±0.20	6.69±0.09
	比例 Proportion/%	24.90±0.04	17.53±0.89	21.47±1.07	13.80±0.06	22.30±0.53

根据已有文献[19]，DOM 分子量主要集中在 300—10^6 Da 范围内.DOM 分子量在 300—2000 Da 范围主要是富里酸（FA）；2000—10^4 Da 主要是腐殖酸（HA）；10^4—10^6 Da 主要是腐黑物（HM）.因此可以推断南太湖沉积物 DOM 腐黑物含量较高，北太湖沉积物 DOM 含有大量的富里酸和腐殖酸.

2.2 三维荧光光谱特征

通常，水体中腐殖质和类蛋白物质用三维荧光光谱表征.南北太湖沉积物 DOM 三维荧光光谱一共呈现出 4 种特征峰.类富里酸紫外区荧光峰 A（$\lambda_{Ex}/\lambda_{Em}$ = 230—260 nm/420—450 nm）和可见区峰 C（$\lambda_{Ex}/\lambda_{Em}$ = 300—320 nm/400—420 nm）代表腐殖酸物质，类蛋白荧光峰 B（$\lambda_{Ex}/\lambda_{Em}$ = 275—285 nm/300—320 nm）和峰 D（$\lambda_{Ex}/\lambda_{Em}$ = 220—230 nm/330—340 nm）代表类蛋白物质[20].图 3 显示了南北太湖沉积物不同分子量 DOM 三维荧光峰的荧光强度.可以看出，峰 A 和峰 C 的荧光强度随着 DOM 分子量的增加而增加，然而峰 B 和峰 D 的荧光强度随着 DOM 分子量的增加而降低.Wang[4]等发现不同分子量 DOM 的组成不同.可以推断出低分子量的 DOM 主要成分是类蛋白物质，高分子量的 DOM 主要成分是类腐殖质物质.此外，图 3 显示尤其对于小分子 DOM，B、D 峰荧光强度较高，高于 A、C 峰.这可能是类蛋白物质的激发波长在紫外和可见范围内，产生更多的光子，因此具有较高的荧光强度.另一方面，太湖表层沉积物严重的污染是由于城市未处理的或处理不完全的工业废水排放[14].有研究发现工业废水污染的湖泊 DOM 类蛋白物质荧光强度特别强[21].

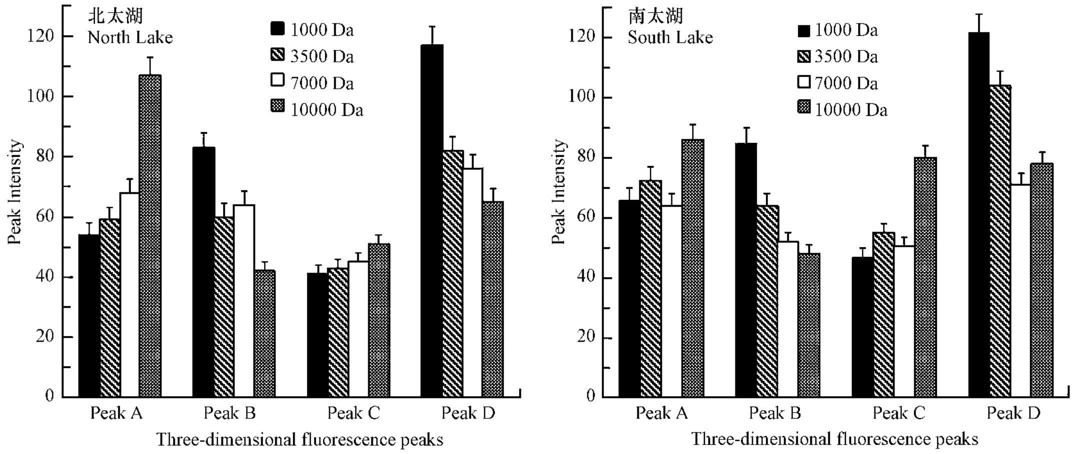

图 3 不同分子量 DOM 三维荧光峰强度

Fig.3 Three-dimensional fluorescence intensities of different molecular weight DOM

2.3 碳氮比（C/N）

除了用三维荧光光谱分析不同分子量的组成外，C/N 被广泛用来反映湖泊沉积物不同类型有机质的来源.由表 2 可知，南太湖 DOM 的 C/N 远远高于北太湖.根据表 2 中各分子量组分的碳氮比值和表 1 中各分子量组分所占的比例，可以计算出南部湖区和北部湖区 DOM 的 C/N 平均值，南部湖区为 20.30，北部湖区为 7.58.高等水生植物的 C/N 值在 13—30 范围，然而藻类和细菌的 C/N 值低于 10[22-23].由此可以推出，南太湖 DOM 主要来自水生植物或陆源生物输入，北太湖 DOM 主要来自外源有机质如藻类.在太湖中，类蛋白物质是 DOM 主要的组分，尤其是北部湖区[24]，因此相对碳而言氮含量上升.而在南部和东部湖区生长着大量的高等水生植物，含有较低的蛋白质.此外，对于南北湖区都是 C/N 值随 DOM 分子量的增加而减小.高的 C/N 表明 DOM 含有更多的与碳有关的官能团，如羧基和酚基，它们常常作为重金属的结合位点[25-26].因此有必要进一步验证低分子量 DOM 组分对于结合重金属的重要性.

表 2 太湖不同分子量 DOM 组分碳氮比（平均值±标准差）

Table 2 C/N ratio of different molecular weight DOM in Taihu Lake (means ± standard) ($n=3$)

Mw/Da	<1000	1000—3500	3500—7000	7000—10000	>10000
南太湖	23.65±0.51	21.36±1.03	16.54±0.94	12.63±0.04	13.56±0.29
北太湖	14.85±0.35	8.54±0.20	4.63±0.04	5.21±0.31	4.75±0.14

2.4　DOM-Cu

不同分子量 DOM 的来源和组成不同，势必会影响其结合 Cu 的能力. 为了明确能够被 DOM 迁移的潜在 Cu 的含量，通过从总 Cu 浓度中减去 Cu 离子的浓度计算不同分子量 DOM 组分 DOM-Cu 的浓度，结果如表 3 所示.

表 3　太湖不同分子量 DOM 组分 DOM-Cu 的浓度 (平均值±标准差) ($n=3$)

Table 3　DOM-Cu complexe concentrations in different molecular weight fractions in Taihu Lake (means ± standard) ($n=3$)

	Mw/Da	<1000	1000—3500	3500—7000	7000—10000	>10000
南太湖	浓度 Concentration/(mg·L^{-1})	0.65±0.01	0.58±0.02	0.45±0.01	0.38±0.03	0.31±0.02
	比例 Proportion/%	27.60±1.33	24.47±1.56	19.09±0.45	15.88±0.94	12.96±0.48
北太湖	浓度 Concentration/(mg·L^{-1})	0.55±0.01	0.48±0.03	0.43±0.02	0.32±0.01	0.27±0.02
	比例 Proportion/%	26.70±0.14	23.67±0.97	20.78±0.11	15.45±0.70	13.40±0.66

DOM-Cu 的浓度随 DOM 分子量的增加而减小，浓度值在 0.27 mg·L^{-1}(>10000 Da，北太湖) 到 0.65 mg·L^{-1}(<1000 Da，南太湖) 范围. DOM-Cu 的最大值在分子量低于 1000 Da，分子量低于 3500 Da 的 DOM-Cu 约占总 DOM-Cu 的 50%. 因此可以得出 Cu 趋向于和低分子量的 DOM 结合，这与已有文献 [27-28] 一致，低分子量的有机酸影响重金属的迁移. 对比不同湖区看出对于相同分子量组分南太湖 DOM-Cu 浓度高于北太湖，表明南太湖 DOM 有较强的 Cu 结合能力. 有机质与重金属的结合与结合点位有关，结合点位又与官能团有关[29]. 结合容量和结合强度与含氧组分有关，如羧基、羟基、酚醛基、酮基，这些官能团主导重金属的结合[30]. 不同 DOM 组分的红外光谱显示分子量高于 14 kD 的 DOM 由腐殖质组成，具有相对高的芳香性有共轭键官能团[31]. 此外，不同分子量 DOM 吸附 Cu 的差异反映了不同分子量 DOM 的组成不同. C/N 的结果也揭示了南太湖 DOM 有更多的腐殖酸物质，南太湖 DOM 较强的结合 Cu 能力可能归因于更多的腐殖酸物质，它们可以提供更多的活性结合点位[32].

2.5　结合容量

DOM-Cu 浓度与 DOM 结合 Cu 的能力以及 DOM 的浓度有关. 结合容量被用来评估不同分子量组分 DOM 结合 Cu 的能力，通过 DOM-Cu 浓度除以各分子量组分 DOM 浓度计算得出，结果列于表 4 中.

表 4　不同分子量 DOM 组分对 Cu 的结合容量 (mg·g^{-1}) (平均值±标准差) ($n=3$)

Table 4　Complexing capacity of different molecular weight DOM for Cu (mg·g^{-1}) (means ± standard) ($n=3$)

Mw/Da	<1000	1000—3500	3500—7000	7000—10000	>10000
南太湖	261.85±7.24	219.77±10.04	126.69±6.01	43.35±0.44	24.17±1.77
北太湖	73.09±4.55	92.02±2.36	65.99±5.53	76.33±1.21	40.96±0.23

太湖沉积物不同分子量 DOM 对 Cu 的结合容量具有显著差异($P<0.05$). 南太湖 DOM 的结合容量随着分子量的增加而减小，而且最大值在分子量低于 1000 Da 组分，最小值在分子量高于 10000 Da 组分. 北太湖也是低分子量组分对于 Cu 的结合有很大优势，且 DOM 分子量低于 3500 Da 对 Cu 的结合贡献最大. Cu 结合容量最大值为 92.02 mg·g^{-1}在 DOM 分子量 1000—3500 Da 范围，分子量高于 10000 Da 结合容量为 40.96 mg·g^{-1}，表明该组分结合 Cu 的能力较弱. 对比不同湖区显示南太湖 DOM 低分子量结合容量较北太湖大. DOM 分子量低于 1000 Da、1000—3500 Da、3500—7000 Da 组分的结合容量在南太湖分别是北太湖的 3.58、2.38 和 1.92 倍. 然而，南太湖 DOM 高分子量结合容量较北太湖小. 可能是太湖中 DOM 组成不同，北太湖 55%的 DOM 是蛋白质，在南太湖是 47.37%[24]. 蛋白质在高分子量组分对于结合重金属也起很重要的作用.

3　结论 (Conclusion)

南太湖沉积物 DOM 以高分子量为主，而北太湖以低分子量、中等分子量为主. 根据各湖区 DOM 的 C/N 值推测南太湖 DOM 主要来自外源有机质，北太湖 DOM 主要来自内源有机质. 对于南北湖区

DOM-Cu浓度最大值在DOM分子量低于3500 Da组分，且南太湖DOM具有较强的Cu结合能力.不同分子量DOM对Cu的结合容量显示南太湖分子量低于3500 Da组分和北太湖分子量在1000—3500Da对于结合Cu的贡献最大.

参考文献(References)

[1] 利锋，张学先，戴睿志. 重金属有效态与土壤环境质量标准制订[J]. 广东微量元素科学，2008，15(1)：7-10.
LI F, ZHANG X X, DAI R Z. The bioavailability of heavy metal and environmental quality standard for soil [J]. Guangdong Trace Elements Science, 2008, 15(1): 7-10(in Chinese).

[2] 冯精兰，胡鹏抟，刘群，等.黄河中下游干流沉积物中重金属的赋存形态及其生态风险[J]. 环境化学，2015，34(1)：178-185.
FENG J L, HU P T, LIU Q, et al. Chemical speciation and risk assessment of heavy metals in the sediments from the mainstream of middle and lower reaches of Yellow River [J]. Environmental Chemistry, 2015, 34(1): 178-185(in Chinese).

[3] 曾希柏，杨佳波，李莲芳，等.溶解性有机物对土壤中铜生物有效性的影响[J].农业环境科学学报，2009，28(5)：883-889.
ZENG X, YANG J B, LI L F, et al. Influence of dissolved organic matter (DOM) on bioavailability of copper in soils [J]. Journal of Agro-Environment Science, 2009, 28(5): 883-889(in Chinese).

[4] WANG X D, CHEN X N, LIU S, et al. Effect of molecular weight of dissolved organic matter on toxicity and bioavailability of copper to lettuce [J]. Journal of Environmental Sciences, 2010, 22(12): 1960-1965.

[5] KNOTH DE Z K G, SCHOLER Y D. Fluorescence fingerprints and Cu^{2+}-complexing ability of individual molecular size fractions in soil- and waste-borne DOM [J]. Chemosphere, 2007, 69(4): 540-548.

[6] 岳兰秀，刘丛强，吴丰昌.水环境中天然溶解有机质分子量的研究现状及意义[J]. 环境科学与管理，2010，35(4)：29-34.
YUE L X, LIU C Q, WU F C. Development of studies on molecular weight of humic substances in natural environment [J]. Environmental Science and Management, 2010, 35(4): 29-34(in Chinese).

[7] 乔春光，魏群山，王东升，等.典型南方水源溶解性有机物分子量分布变化及去除特性[J]. 环境科学学报，2007，27(2)：195-200.
QIAO C G, WEI Q S, WANG D S, et al. Molecular weight distribution and removal characters of DOM in the typical source water in south of China [J]. Acta Scientiae Circumstantiae, 2007, 27(2): 195-200(in Chinese).

[8] RAMAMOORTHY S, KUSHNER D J. Heavy metal binding sites in river water [J]. Nature, 1975, 256: 399-401.

[9] SMITH R G. Evaluation of combined applications of ultrafiltration and complexation capacity techniques to natural waters [J]. Analytical Chemosphere, 1976, 48: 74-76.

[10] 郭旭晶，席北斗，谢森，等.乌梁素海沉积物孔隙水中溶解有机质的荧光及紫外光谱研究[J]. 环境工程学报，2012，6(2)：440-444.
GUO X J, XI B D, XIE S, et al. Study on fluorescence spectra and UV-vis spectra of dissolved organic matter collected from sediment pore water inWuliangsuhai Lake [J]. Chinese Journal of Environmental Engineering, 2012, 6(2): 440-444(in Chinese).

[11] 张路，范成新，王建军.太湖草藻型湖区间隙水理化特性比较[J]. 中国环境科学，2004，24(5)：556-560.
ZHANG L, FAN C X, WANG J J. Comparison of physicochemical characters of pore water in grass/algae type zone in Lake Taihu [J]. China Environmental Science, 2004, 24(5): 556-560(in Chinese).

[12] YU T, ZHANG Y, MENG W, et al. Characterization of heavy metals in water and sediments in Taihu Lake, China [J]. Environment Monitoring and Assessment, 2012, 184: 4367-4382.

[13] KOELMANS A A, VANDERHEIJDE A, KNIJFF L M, et al. Integrated modelling of eutrophication and organic contaminant fate & effects in aquatic ecosystems: A review [J]. Water Research, 2001, 35(15): 3517-3536.

[14] 石陶然，张远，于涛，等.滇池沉积物不同分子量溶解性有机质分布及其与Cu、Pb的相互作用[J].环境科学研究，2013，26(2)：137-144.
SHI T R, ZHANG Y, YU T, et al. Distribution of different molecular weight fractions of dissolved organic matters and their complexation with Cu and Pb in the sediment from Dianchi Lake, China [J].Research of Environmental Science, 2013, 26(2): 137-144(in Chinese).

[15] 郑乐平，刘玉梅，钱显文，等.太湖、巢湖沉积物中重金属污染的总量特征及其区域性差异[J].环境化学，2009，28(6)：883-887.
ZHENG L P, LIU Y M, QIAN X W, et al.The characteristics and regional differences of heavy metal contents in the sediments of Taihu Lake and Chaohu Lake [J]. Environmental Chemistry, 2009, 28(6): 883-887(in Chinese).

[16] 王钦，丁明玉，张志洁，等.太湖不同湖区沉积物重金属含量季节变化及其影响因素[J].生态环境，2008，17(4)：1362-1368.
WANG Q, DING M Y, ZHANG Z J. Seasonal varieties and influential factors of heavy metals in sediments of Taihu Lake [J]. Ecology and Environment, 2008, 17(4): 1362-1368(in Chinese).

[17] CHEN Z R, CAI Y, SOLO-GABRIELE H G, et al. Interactions of arsenic and the dissolved substances derived from Turf Soils [J]. Environmental Science and Technology, 2006, 40: 4659-4665.

[18] 袁和忠，沈吉，刘恩峰.太湖重金属和营养盐污染特征分析[J].环境科学，2011，32(3)：649-657.
YUAN H Z, SHEN J, LIU E F. Assessment and characterization of heavy metals and nutrients in sediments from Taihu Lake [J]. Environmental Science, 2011, 32(3): 649-657(in Chinese).

[19] 曾宪成，成绍鑫.腐殖酸的主要类别[J].腐殖酸，2002，4(2)：4-10.

ZENG X C, CHENG S X. Category of humic acid [J] .Humic Acid, 2002,4(2):4-10(in Chinese).

[20] 傅平青,吴丰昌,刘丛强,等.高原湖泊溶解有机质的三维荧光光谱特性初步研究 [J]. 海洋与湖沼,2007,38(6):512-520.
FU P Q, WU F C, LIU C Q, et al. Three-dimensional imensional excitation emission matrix fluorescence spectroscopy of dissolved organic matter from Chinese highland Lakes [J]. Akes, Oceanologia Et Limnologia Sinica, 2007,38(6):512-520(in Chinese).

[21] BAKER A. Fluorescence excitation-emission matrix characterization of some sewage-impacted rivers [J]. Environmental Science and Technology, 2001,35(5):948-953.

[22] SALM C R, SAROS J E, FRITZ S C, et al. Phytoplankton productivity across prairie saline lakes of the Great Plains (USA): A step toward deciphering patterns through lake classification models [J]. Canadian Journal of Fisheries and Aquatic Sciences, 2009,66(9):1435-1448.

[23] NOBUYASU I, SHU J T, MICHIO K. Distributions of polycyclic aromatic hydrocarbons in a sediment core from the north basin of Lake Biwa, Japan [J]. Organic Geochemistry,2010, 41(8):845-852.

[24] ZHANG Y, ZHANGY, YU T, et al. Characterization and environmental significance of degradation of DOM from Taihu Lake under different conditions using multiple analytical techniques [J]. Fresenius Environmental Bulletin, 2012,21(5):1118-1126.

[25] FU P Q, WU F C, LIU C Q, et al. Fluorescence characterization of dissolved organic matter in an urban river and its complexation with Hg(Ⅱ) [J]. Applied Geochemistry, 2007,22(8):1668-1679.

[26] 耿安朝,章申.腐殖酸与稀土元素的结合点位及其表征研究 [J].厦门大学学报(自然科学版),2006,45(2):238-242.
GENG A C, ZHANG S. Study on the binding sites of humic acids with rare earth elements and its characterization [J].Journal of Xiamen University(Natural Science),2006,45(2):238-242(in Chinese).

[27] VAN HEES P A W, LUNDSTROM U S, GIESLER R. Low molecular weight organic acids and their Al-complexes in soil solution-composition, distribution and seasonal variation in three podzolized soils [J]. Geoderma,2000,94: 173-200.

[28] WU L H, LUO Y M, CHRISTIE P, et al. Effects of EDTA and low molecular weight organic acids on soil solution properties of a heavy metal polluted soil [J]. Chemosphere, 2003,50: 819-822.

[29] NIEROP K G J, JANSEN B, VRUGT J A, et al. Copper complexation by dissolved organic matter and uncertainty assessment of their stability constants [J]. Chemosphere,2002,49:1191-1200.

[30] CALACE N, LIBERATORI A, PETRONIO B M, et al. Characteristics of different molecular weight fractions of organic matter in landfill leachate and their role in soil sorption of heavy metals [J]. Environmental Pollution, 2001,113: 331-339.

[31] YAN M Q, KORSHIN G, WANG D S. Characterization of dissolved organic matter using high-performance liquid chromatography (HPLC)-size exclusion chromatography (SEC) with a multiple wavelength absorbance detector [J]. Chemosphere,2012, 87:879-885.

[32] 范文宏,陈俊,王琼.胡敏酸对沉积物中重金属形态分布的影响 [J]. 环境化学,2007,26(2):224-227.
FAN W H, CHEN J, WANG Q. Influence of humic acid on species of heavy metals in sediments [J]. Environmental Chemistry, 2007,26(2):224-227 (in Chinese).